TRINITY COLLEGE DUBLIN
COLÁISTE NA TRÍONÓIDE, BAILE ÁTHA CLIATH
THE UNIVERSITY OF DUBLIN

Applying geogenic methods and decision-making tools to model radon at local and regional scales.

A thesis submitted to the University of Dublin for the degree of Doctorate of Philosophy

Department of Geology, University of Dublin, Trinity College.

2023.

Author:

Méabh Hughes Banríon

Declaration

I declare that this thesis has not been submitted as an exercise for a degree at this or any other university and it is entirely my own work.

I agree to deposit this thesis in the University's open access institutional repository or allow the library to do so on my behalf, subject to Irish Copyright Legislation and Trinity College Library conditions of use and acknowledgement.

Méabh H Banríon

Summary

Radon is an environmental health hazard for indoor environments, caves and underground mines exposure to which is related to an increased probability of developing lung cancer. Globally, radon is the second leading cause of lung cancer after tobacco smoking, and the leading cause of lung cancer in non-smokers. Radon is geogenic, in that it primarily originates from beneath the Earth's surface. Specifically, radon has several isotopes which form intermediate decay products from the radioactive decay of uranium and thorium (^{238}U, ^{235}U and ^{232}Th). From a radiological protection perspective ^{222}Rn is the main isotope of interest, given its relatively longer half-life compared to the other radon isotopes. Ireland has a geographically weighted average indoor radon concentration (77 Bq m^{-3}) and population weighted average indoor radon (98 Bq m^{-3}) which is over twice that of the global average (39 Bq m^{-3}), and a disproportionally high number of radon-related lung cancer cases occur here (ca. 300 - 350 cases per year, which equates to 14% of the total lung cancer cases, compared to the global range of between 3% to 15%) (Elío et al., 2018, p. 20; Fuente et al., 2020; Long, 2018; Murphy et al., 2021; World Health Organization, 2009). The high average radon concentrations, geological diversity, and availability of open access data relating to natural and built environments make Ireland an ideal case study to better understand the factors contributing to the concentration and spatial variation of radon.

Although the connection between local geology and radon is widely known, radon maps seldom utilise information relating to the radon source or pathway through the natural environment; both factors govern the distribution of indoor radon. For instance, the first national radon map of Ireland (S.G Fennell et al., 2002) although a major achievement in that it estimated the probability of indoor radon exceeding a threshold value from 10 x 10 km grids, it had several

shortcomings in that it utilised a limited number of indoor radon measurements, and did not contain any geological data.

Not only does Ireland have a high average indoor radon concentration, some exceptionally high indoor radon concentrations have also been found here. In 2003, the highest single measurement of indoor radon (65,000 Bq m^{-3}) was reported in a house in Castleisland Co. Kerry after several occupants tragically died of lung cancer, despite being non-smokers. No previous geological studies have been implemented to investigate the cause of high radon occurring in the area.

This research sets out to investigate the use of geological datasets to map radon. This thesis also aims to provide decision-making tools that will aid with efficiently choosing appropriate methods for mapping radon depending on the intended purpose. The primary data collected in this thesis includes (a) subsoil radon gas concentration, (b) subsoil permeability and (c) topsoil geochemistry. A number of additional pre-existing data types have been used as part of this research (e.g. geological maps, geophysical data, geochemical data, indoor radon data).

The work presented here utilizes a background knowledge of geological processes and applies it to model radon distribution.

Within this thesis, a range of case studies are presented for different spatial scales, and utilising a range of different datasets. Castleisland in Co. Kerry was chosen as a case study due to the geologically unexplained high indoor radon occurring in the area. More than one hundred soil-gas radon and subsoil permeability measurements were collected in a systematic and representative manner over several geology types. Analysis of major and trace elements is completed for 92 topsoil samples and compared with soil-gas radon samples collected from the same locations. In addition, the geochemical data from the topsoils are investigated for covariance and correlation to determine if certain elements are commonly associated with geogenic radon. The general geostatistical methodology developed for Castleisland is scaled and repeated for the Irish Midlands. In this instance various modelling approaches are applied

to 4,131 topsoil samples obtained from the Geological Survey Ireland TELLUS Midlands, and combined with a previously published national radon potential map, which was derived from TELLUS radiometric data, and a national subsoil permeability model (Elío et al., 2020).

The main findings demonstrate that geology and geological attributes can offer useful insights to the distribution and expected concentration of radon. From this research, it is apparent that different spatial scales of sampling and modelling can result in significantly different radon risk maps even if the same dataset is used. Soil-gas radon and soil permeability mapping can act as a rapid method for quantifying the radon risk in relatively small (i.e. 10 km^2) areas, but are not practical for considerably larger areas.

Regardless of spatial scale, integration of topsoil geochemistry into radon models shows covariance occurring between elements correlated with geogenic radon, thus demonstrating that chemistry of soils can be indicative of radon prone areas. In this way legacy soil geochemistry data and geological map data can be utilised to assist efforts to highlight radon prone areas, without the need to directly measure radon indoors or in soil gas.

7.3 Extra supplementary materials for Chapter 5

Table 7.3.1 PCA loading summary of Clr transformed topsoil geochemistry from Castleisland Co. Kerry, Ireland

Loading	PC 1	PC 2	PC 3	PC 4	PC 5	PC 6	PC 7	PC 8	PC 9	PC 10	PC 11	PC 12	PC 13	PC 14	PC 15	PC 16	PC 17	PC 18	PC 19	PC 20	PC 21	PC 22	PC 23	PC 24	PC 25	PC 26
Mg	-0.29	0.1	-0.07	-0.03	-0.03	-0.21	-0.21	0.07	0.13	-0.11	-0.01	0.21	0.06	-0.25	0.23	-0.21	-0.06	0.19	0.21	0.28	0.01	0.41	0.14	0.46	0.08	0.08
Ga	-0.23	0.07	0.3	0.25	0.09	0.15	0.18	0.03	-0.09	-0.39	0.06	-0.07	0.26	0.2	-0.01	-0.12	-0.31	-0.01	-0.48	0.2	0.04	0.24	-0.03	-0.12	0.09	0.02
Co	-0.27	0.06	-0.27	-0.1	0.02	-0.02	-0.03	0.14	-0.16	0.21	0.17	0.04	0.04	0.01	0.04	0.12	-0.29	0.04	-0.14	0.01	0.03	-0.08	0.2	0	-0.13	-0.74
Fe	-0.28	0.05	-0.08	-0.07	0.29	-0.14	0.12	0.05	0.14	-0.05	-0.08	-0.06	-0.22	0.31	0.06	-0.12	0.11	0.17	0.07	-0.48	-0.14	0.15	0.2	-0.17	0.45	-0.03
Na	-0.21	0.04	0.19	0.37	-0.03	-0.17	-0.02	0.03	0.39	0.61	0.14	0.12	0.08	0.08	-0.3	-0.05	0	-0.01	-0.08	0.06	0.15	-0.05	-0.14	0.04	0.14	0.04
Sc	-0.3	0.04	-0.09	0.04	-0.07	-0.06	-0.08	-0.29	-0.17	0	-0.02	-0.13	-0.16	-0.07	-0.1	0.19	0.25	0	-0.15	-0.26	0.53	0.37	0	-0.04	-0.32	0.09
Ni	-0.27	0.03	-0.26	-0.1	-0.14	-0.02	-0.12	0.08	-0.13	0.07	0.2	0.18	0.29	-0.03	0.08	-0.1	0.11	-0.05	0.13	0.21	-0.01	-0.06	0.14	-0.65	0.02	0.31
Th	-0.28	0.01	0.14	-0.09	-0.06	-0.1	-0.22	-0.3	0.09	0.03	-0.19	-0.4	-0.24	-0.22	0.2	0.15	0.07	0.18	-0.26	0.32	-0.15	-0.3	-0.05	-0.12	0.2	-0.03
Al	-0.29	0	0.09	0.2	0.07	-0.05	0.02	-0.1	-0.32	-0.1	-0.01	-0.02	0.09	0.08	-0.04	-0.17	-0.15	0.15	0.2	-0.18	0.14	-0.61	0.22	0.28	-0.12	0.22

Appendix A continued

Mn	**-0.22**	**0**	**-0.24**	**-0.26**	**-0.09**	**0.32**	**0.35**	**0.24**	**-0.04**	**0.21**	**0**	**-0.28**	**-0.1**	**-0.23**	**-0.18**	**0.11**	**-0.34**	**0.03**	**0.01**	**-0.02**	**-0.01**	**0.07**	**-0.13**	**0.15**	**0.12**	**0.35**
K	**-0.23**	**-0.05**	**0.34**	**-0.04**	**-0.17**	**0.13**	**-0.02**	**-0.2**	**0.3**	**-0.06**	**0.07**	**0.12**	**0.15**	**-0.02**	**0.19**	**0.47**	**-0.27**	**-0.13**	**0.28**	**-0.28**	**-0.24**	**0.07**	**0.09**	**-0.07**	**-0.17**	**0.03**
Zn	**-0.27**	**-0.07**	**-0.15**	**-0.04**	**-0.2**	**0.07**	**-0.07**	**0.27**	**0.23**	**-0.19**	**-0.05**	**0.27**	**-0.05**	**-0.09**	**0.01**	**-0.13**	**0.28**	**-0.19**	**-0.46**	**-0.26**	**-0.25**	**-0.21**	**-0.12**	**0.17**	**-0.2**	**0.06**
Ca	**0.04**	**-0.1**	**-0.43**	**0.08**	**-0.41**	**-0.27**	**0.18**	**-0.35**	**0.23**	**-0.13**	**-0.34**	**0**	**0.04**	**0.23**	**-0.1**	**-0.16**	**-0.32**	**0.04**	**0.04**	**0.03**	**-0.01**	**-0.01**	**-0.11**	**-0.07**	**-0.07**	**-0.03**
Pb	**-0.02**	**-0.12**	**-0.27**	**0.38**	**0.21**	**0.6**	**-0.32**	**-0.04**	**0.12**	**0**	**-0.18**	**0.22**	**-0.27**	**0.08**	**0.1**	**0.06**	**-0.13**	**0.16**	**0.06**	**0.09**	**0.08**	**-0.01**	**-0.02**	**-0.09**	**-0.01**	**0.03**
Hg	**0.08**	**-0.12**	**-0.37**	**0.46**	**0.11**	**0**	**0.11**	**-0.16**	**0.11**	**-0.07**	**0.38**	**-0.36**	**0.3**	**-0.29**	**0.15**	**0.05**	**0.17**	**0**	**-0.01**	**-0.14**	**-0.18**	**0.02**	**0.05**	**0.09**	**0.08**	**-0.03**
As	**-0.23**	**-0.13**	**-0.14**	**-0.17**	**0.36**	**0**	**0.19**	**-0.22**	**0.02**	**0**	**0.17**	**0.03**	**-0.04**	**0.43**	**-0.12**	**0.17**	**0.23**	**-0.09**	**0.09**	**0.39**	**-0.25**	**0.02**	**-0.13**	**0.2**	**-0.24**	**0.06**
Cr	**-0.25**	**-0.15**	**0.06**	**0.21**	**0.07**	**-0.09**	**-0.05**	**0.29**	**-0.24**	**-0.04**	**-0.37**	**-0.14**	**0.2**	**-0.07**	**-0.02**	**0.04**	**0.11**	**0.01**	**0.33**	**-0.04**	**-0.11**	**0.08**	**-0.56**	**-0.1**	**-0.05**	**-0.2**
La	**-0.11**	**-0.26**	**0.1**	**-0.08**	**-0.39**	**0.32**	**0.09**	**-0.31**	**-0.23**	**-0.06**	**0.18**	**0.24**	**0.03**	**-0.03**	**-0.16**	**-0.08**	**0.23**	**0.07**	**0.09**	**0**	**0.03**	**0.02**	**-0.12**	**0.12**	**0.46**	**-0.23**
Sb	**0.02**	**-0.28**	**-0.03**	**-0.3**	**0.21**	**0.11**	**-0.47**	**-0.21**	**-0.02**	**0.21**	**-0.18**	**-0.18**	**0.42**	**0.06**	**-0.13**	**-0.23**	**-0.13**	**-0.21**	**-0.14**	**-0.17**	**-0.05**	**0.1**	**0.06**	**0.12**	**0.06**	**0.05**
Mo	**-0.07**	**-0.29**	**0.06**	**-0.25**	**0.36**	**-0.02**	**0.19**	**-0.04**	**0.41**	**-0.24**	**0.1**	**0.08**	**0.03**	**-0.31**	**0.01**	**-0.17**	**-0.06**	**0**	**0.11**	**0.02**	**0.43**	**-0.19**	**-0.16**	**-0.16**	**-0.04**	**-0.15**
U	**0.05**	**-0.31**	**-0.09**	**0.09**	**0.19**	**-0.42**	**-0.14**	**-0.05**	**-0.28**	**-0.08**	**0.15**	**0.34**	**-0.22**	**-0.19**	**-0.14**	**0.28**	**-0.31**	**-0.11**	**-0.17**	**-0.06**	**-0.12**	**0.02**	**-0.14**	**-0.03**	**0.21**	**0.17**

Appendix A continued

Ba	**-0.12**	**-0.31**	**0.14**	**0.18**	**-0.1**	**0**	**0.07**	**0.02**	**-0.08**	**0.1**	**0.06**	**-0.19**	**-0.42**	**-0.05**	**0.11**	**-0.4**	**-0.08**	**-0.54**	**0.16**	**0.09**	**-0.09**	**0.12**	**0.2**	**-0.07**	**-0.12**	**-0.06**
Cu	**0.01**	**-0.31**	**-0.02**	**-0.01**	**-0.25**	**-0.08**	**-0.34**	**0.39**	**0.18**	**-0.3**	**0.22**	**-0.31**	**-0.05**	**0.28**	**-0.27**	**0.22**	**0.02**	**0.08**	**0.11**	**0.1**	**0.17**	**-0.03**	**0.15**	**0.05**	**0.07**	**0.01**
Sr	**0.08**	**-0.34**	**0.08**	**-0.1**	**-0.12**	**-0.05**	**0**	**0.06**	**-0.07**	**0.23**	**0.28**	**-0.03**	**-0.05**	**0.24**	**0.53**	**-0.16**	**-0.1**	**0.4**	**-0.13**	**-0.13**	**0.04**	**0.05**	**-0.29**	**0.01**	**-0.18**	**0.11**
P	**0.01**	**-0.35**	**-0.03**	**0.06**	**-0.01**	**-0.05**	**0.29**	**0.15**	**-0.03**	**0.14**	**-0.39**	**0.11**	**0.2**	**0.08**	**0.35**	**0.32**	**0.16**	**-0.18**	**-0.13**	**0.13**	**0.27**	**-0.05**	**0.3**	**0.12**	**0.2**	**0.05**
V	**0.04**	**-0.36**	**0.15**	**0.05**	**0.03**	**0**	**0.17**	**0.02**	**-0.01**	**0.08**	**-0.17**	**0.06**	**0.02**	**-0.23**	**-0.35**	**-0.06**	**0.1**	**0.49**	**-0.07**	**0.04**	**-0.28**	**0.14**	**0.37**	**-0.15**	**-0.29**	**-0.02**
Standard deviation	**3.12**	**2.58**	**1.61**	**1.28**	**1.09**	**0.94**	**0.81**	**0.78**	**0.63**	**0.56**	**0.5**	**0.44**	**0.41**	**0.37**	**0.32**	**0.31**	**0.29**	**0.27**	**0.23**	**0.21**	**0.19**	**0.16**	**0.15**	**0.12**	**0.1**	**0.06**
Proportion of Variance	**0.37**	**0.26**	**0.1**	**0.06**	**0.05**	**0.03**	**0.03**	**0.02**	**0.02**	**0.01**	**0.01**	**0.01**	**0.01**	**0.01**	**0**	**0**	**0**	**0**	**0**	**0**	**0**	**0**	**0**	**0**	**0**	**0**
Cumulative Proportion	**0.37**	**0.63**	**0.73**	**0.79**	**0.84**	**0.87**	**0.9**	**0.92**	**0.94**	**0.95**	**0.96**	**0.97**	**0.97**	**0.98**	**0.98**	**0.99**	**0.99**	**0.99**	**0.99**	**1**	**1**	**1**	**1**	**1**	**1**	**1**

Table 7.3.2 PCA Score of Castleisland, Co. Kerry topsoil (Clr transformed)

Score	X.ITM	Y.ITM	PC1	PC2	PC3	PC4	PC5	PC6	PC7	PC8	PC9	PC10	PC11	PC12	PC13	PC14	PC15	PC16	PC17	PC18	PC19	PC20	PC21	PC22	PC23	PC24	PC25	PC26
x.4	499445	610436	1.18	-0.79	-1.27	0.77	1.63	-0.47	-0.44	-0.31	-0.35	-0.54	0.1	0.37	0.19	0.47	-0.67	0.07	-0.4	-0.41	-0.08	-0.14	0.16	-0.05	-0.04	-0.16	-0.08	-0.04
x.1	498457	609929	-4.75	-1.03	-0.31	0.88	-1.28	1.2	2.44	-0.15	-0.77	0.15	-0.17	0.36	0.42	-0.34	-0.2	-0.52	0.32	-0.46	-0.07	-0.1	0.12	-0.04	0.06	-0.04	-0.11	-0.04
x.2	499852	611939	0.54	1.57	1.7	-1.24	1.77	0.93	1.03	0.03	0.22	-0.69	-0.62	0.16	-0.42	-0.04	0.42	0.26	0.06	-0.12	-0.18	-0.37	-0.09	-0.31	0.15	-0.02	0.05	-0.03
x.3	498915	611909	1.79	-0.57	-1.16	-2.15	1.74	1.97	-1.48	-0.35	0.26	-0.3	-0.11	-0.35	0.82	-0.12	-0.4	-0.31	-0.08	-0.21	-0.05	-0.16	-0.22	0.23	-0.04	0.16	-0.03	0.04
x.5	500457	610437	0.76	2.07	1.93	0.65	0.29	0.36	-0.12	-0.98	0.39	0.34	0.13	-0.48	-0.22	0.34	0.07	-0.17	0.23	-0.18	0.08	0.26	-0.17	0.18	0.26	-0.18	0.03	-0.04
x.6	499956	610918	-1.6	0.92	0.87	1.92	0.47	0.24	0.57	1.8	0.69	-0.92	0.76	0.12	-0.34	0.61	-0.11	-0.38	-0.03	0.1	0.53	0.11	0.35	0.13	0.07	0.05	-0.16	0.09

Appendix A continued

x.7	**500452**	**611439**	**-1.54**	**3.73**	**1.83**	**0.82**	**-1.15**	**-1.24**	**0.15**	**0.13**	**0.22**	**0.14**	**0.13**	**0.35**	**0.62**	**0.06**	**0.46**	**0.32**	**-0.22**	**0.37**	**0.17**	**0**	**-0.02**	**0.1**	**-0.19**	**-0.16**	**0.06**	**0.07**
x.8	**500291**	**611248**	**-3.33**	**3.07**	**0.9**	**-1.54**	**-0.29**	**-0.62**	**-0.64**	**0.5**	**-0.57**	**-0.51**	**-0.26**	**-0.63**	**0.31**	**-0.06**	**-0.01**	**-0.07**	**0.15**	**0.44**	**0.48**	**-0.13**	**-0.07**	**-0.09**	**-0.19**	**0.1**	**-0.01**	**-0.04**
x.9	**499579**	**610965**	**-2.22**	**-0.6**	**-2.27**	**1.74**	**-1.8**	**0.97**	**-0.89**	**-0.53**	**1.79**	**0.03**	**0.2**	**0.1**	**0.06**	**0.39**	**0.47**	**0.16**	**-0.47**	**-0.16**	**-0.01**	**-0.4**	**-0.18**	**0.11**	**0.02**	**0.13**	**-0.07**	**0**
x.10	**500537**	**609463**	**0.43**	**1.5**	**-0.95**	**-0.52**	**0.56**	**-1.42**	**0.38**	**-1.16**	**-0.05**	**-0.1**	**-0.05**	**-0.09**	**0.02**	**0.39**	**-0.12**	**0.6**	**0.52**	**0.06**	**0.26**	**0.04**	**-0.45**	**0.05**	**-0.11**	**0.02**	**-0.06**	**0**
x.11	**498720**	**609181**	**-1.33**	**3.6**	**1.29**	**-0.61**	**-0.84**	**-0.44**	**-0.57**	**-0.03**	**-0.78**	**0.25**	**-0.32**	**0.28**	**-0.32**	**0.61**	**0.01**	**0.03**	**0**	**0.18**	**-0.2**	**0.3**	**0.07**	**0**	**0**	**0.07**	**-0.1**	**0.07**
x.12	**499209**	**609183**	**-3.02**	**0.8**	**-0.41**	**0.57**	**-1.83**	**-1.29**	**0.09**	**-1.03**	**-0.54**	**0.5**	**-0.41**	**-0.09**	**-0.07**	**0.89**	**-0.49**	**-0.37**	**-0.13**	**-0.01**	**-0.31**	**0.08**	**-0.04**	**-0.03**	**-0.13**	**-0.02**	**0.02**	**-0.12**
x.13	**499203**	**609685**	**5.64**	**2.06**	**-0.86**	**1**	**-0.11**	**0.55**	**0.75**	**-0.05**	**-0.62**	**0.76**	**-0.74**	**-0.71**	**0.62**	**-0.17**	**0.23**	**0.14**	**-0.46**	**0.13**	**-0.13**	**0.08**	**-0.01**	**0.17**	**0.06**	**-0.28**	**-0.04**	**0.15**
x.14	**499203**	**609685**	**-1.53**	**2.21**	**-0.73**	**-1.39**	**1.02**	**0.21**	**-1.76**	**0.68**	**-0.01**	**0.48**	**-0.66**	**0.65**	**-0.52**	**0.1**	**0.19**	**0.1**	**0.34**	**-0.3**	**0.1**	**0.03**	**0.15**	**0.09**	**0.01**	**0.02**	**-0.06**	**-0.02**

Appendix A continued

x.15	**498957**	**609921**	**6.28**	**1.85**	**-3.24**	**-0.33**	**-0.6**	**-0.39**	**0.31**	**0.84**	**0.56**	**1.21**	**-0.07**	**-0.83**	**-0.1**	**-0.44**	**-0.24**	**0.01**	**-0.02**	**0.07**	**0.24**	**-0.15**	**0.2**	**-0.29**	**0.04**	**-0.03**	**-0.08**	**-0.06**
x.21	**499702**	**610679**	**1.17**	**-1.42**	**-1.56**	**2.01**	**2.28**	**-0.62**	**0.35**	**0.18**	**-1.05**	**-0.42**	**-0.02**	**0.84**	**0.01**	**0.2**	**-0.28**	**-0.07**	**-0.32**	**0.03**	**0.35**	**-0.32**	**-0.32**	**-0.04**	**-0.02**	**-0.08**	**0.12**	**0.05**
x.22	**499452**	**608950**	**-3.12**	**0.89**	**-0.3**	**0.25**	**-0.48**	**0.61**	**-0.39**	**-0.42**	**0.28**	**0.05**	**-0.41**	**-0.09**	**-0.04**	**0.11**	**0.03**	**-0.2**	**-0.16**	**-0.01**	**0.09**	**-0.16**	**-0.18**	**-0.05**	**-0.24**	**-0.04**	**-0.09**	**-0.03**
x.23	**500327**	**611939**	**1.29**	**2.61**	**2.08**	**-2.02**	**1.07**	**-0.34**	**1.21**	**-0.37**	**0.16**	**-0.77**	**-0.44**	**-0.8**	**-0.37**	**0.43**	**-0.13**	**-0.07**	**0.15**	**-0.27**	**-0.29**	**-0.25**	**0.1**	**0.07**	**-0.06**	**-0.04**	**-0.01**	**0.1**
x.25	**499967**	**610434**	**-0.77**	**2.19**	**1.98**	**1.32**	**1.04**	**-0.65**	**-0.59**	**-0.49**	**-0.08**	**0.75**	**0.4**	**0.27**	**0.38**	**-0.53**	**0**	**-0.25**	**0.27**	**-0.29**	**0.26**	**0.09**	**-0.02**	**-0.21**	**-0.06**	**-0.04**	**-0.01**	**0.03**
x.28	**500218**	**609463**	**-1.13**	**2.18**	**0.58**	**-0.61**	**-0.46**	**-0.45**	**-1.27**	**0.08**	**0.3**	**-0.21**	**-0.47**	**-0.07**	**-0.03**	**-0.05**	**0.09**	**-0.16**	**-0.12**	**-0.11**	**0.14**	**-0.05**	**0.13**	**-0.33**	**0.21**	**-0.11**	**-0.09**	**-0.05**
x.32	**500537**	**609464**	**-3.26**	**-0.16**	**-0.4**	**1.16**	**0.47**	**0.38**	**-0.02**	**0.27**	**-0.05**	**0.12**	**-0.69**	**-0.33**	**0.02**	**-0.3**	**0.13**	**-0.04**	**-0.17**	**-0.11**	**-0.37**	**0.18**	**0.09**	**0**	**-0.23**	**0.13**	**0.02**	**0.05**
x.16	**498861**	**608891**	**-3.16**	**1.18**	**-0.29**	**0.92**	**0.47**	**3.16**	**-0.82**	**-0.6**	**-0.08**	**0.93**	**-0.24**	**0.4**	**-0.64**	**0.02**	**0.1**	**0.28**	**0.12**	**0.34**	**0.09**	**0**	**0.13**	**-0.05**	**0.04**	**-0.16**	**0.02**	**0.02**

Appendix A continued

x.17	**498681**	**610686**	**0.33**	**0.61**	**0.11**	**-1.58**	**0.27**	**-0.21**	**-0.02**	**0.57**	**0.03**	**-0.3**	**-0.45**	**0.39**	**0.15**	**0**	**-0.04**	**-0.44**	**-0.09**	**0.33**	**-0.36**	**0.29**	**0.1**	**-0.01**	**0.11**	**0.1**	**-0.03**	**-0.01**
x.18	**500136**	**610766**	**-2.71**	**1.68**	**0.79**	**0.87**	**0.36**	**0.08**	**-0.13**	**0.53**	**0.37**	**-0.2**	**0.23**	**-0.36**	**-0.21**	**-0.33**	**-0.11**	**0.13**	**0.02**	**-0.1**	**0.12**	**0.12**	**-0.01**	**0.01**	**0.01**	**-0.07**	**0.26**	**-0.08**
x.19	**499697**	**609188**	**-3.5**	**-0.02**	**-3.3**	**-2.64**	**-2.74**	**1.06**	**0.05**	**-1.56**	**-0.9**	**-0.88**	**0.63**	**0.12**	**0.05**	**-0.18**	**-0.14**	**0.06**	**0.3**	**0.07**	**0.27**	**-0.05**	**0.2**	**0.01**	**0.13**	**-0.06**	**0.16**	**0.1**
x.20	**498441**	**610459**	**2.27**	**1.44**	**-1.27**	**-1.58**	**-0.55**	**-2.13**	**-0.8**	**-0.37**	**0.38**	**0.44**	**0.23**	**0.72**	**-0.19**	**-0.22**	**0.03**	**-0.28**	**-0.5**	**-0.21**	**-0.17**	**-0.06**	**0.07**	**0.1**	**0.15**	**0.04**	**0.11**	**0.02**
x.24	**500481**	**610939**	**-3.02**	**0.68**	**0.41**	**0.43**	**-0.82**	**-0.56**	**1.03**	**0.65**	**0.68**	**-0.21**	**-0.47**	**-0.37**	**0.3**	**0.18**	**0.02**	**0.29**	**-0.38**	**-0.21**	**0.04**	**-0.2**	**0.31**	**-0.03**	**0.09**	**0.19**	**0.23**	**0.02**
x.26	**498694**	**609723**	**-2.29**	**1.26**	**0.75**	**-1.56**	**0.15**	**-0.74**	**-0.21**	**1.08**	**-0.25**	**0.77**	**0.6**	**0.06**	**0.01**	**-0.64**	**-0.22**	**0.06**	**-0.12**	**-0.31**	**0.03**	**0.1**	**-0.26**	**0.11**	**0.12**	**0.13**	**0.04**	**0.06**
x.27	**498714**	**610184**	**0.12**	**0.09**	**-1.78**	**0.01**	**-0.24**	**-0.01**	**0.25**	**0.79**	**-0.57**	**-0.94**	**-0.24**	**-0.4**	**-0.01**	**-0.38**	**0.08**	**-0.3**	**-0.31**	**0.37**	**0.16**	**0.19**	**-0.23**	**0.31**	**0.32**	**-0.06**	**-0.13**	**-0.12**
x.29	**499441**	**611393**	**0.32**	**-2.68**	**1.12**	**0.85**	**-0.18**	**0.3**	**0.45**	**0.05**	**0.11**	**0.67**	**-0.56**	**0.55**	**-0.1**	**-0.24**	**-0.68**	**0.11**	**0.1**	**0.86**	**-0.16**	**-0.26**	**0.01**	**0.16**	**-0.06**	**0.19**	**0.01**	**-0.01**

Appendix A continued

x.30	**498643**	**609431**	**-4.59**	**1.14**	**0.28**	**0.07**	**0.32**	**0.04**	**0.37**	**0.77**	**-0.54**	**0.25**	**0.55**	**0.07**	**-0.59**	**-0.78**	**-0.3**	**0.06**	**-0.24**	**-0.11**	**-0.17**	**-0.14**	**0.01**	**0.03**	**-0.24**	**-0.07**	**-0.04**	**0**
x.31	**499811**	**611122**	**-0.33**	**0.18**	**1.38**	**-0.5**	**0.87**	**-0.46**	**-0.23**	**0.02**	**-0.3**	**-0.17**	**0.66**	**0.14**	**0.72**	**-0.22**	**0.76**	**0.1**	**0.38**	**0.26**	**-0.32**	**-0.45**	**0.28**	**0.35**	**-0.07**	**-0.07**	**-0.05**	**-0.13**
x.33	**499201**	**610705**	**-0.93**	**-1.49**	**-0.9**	**-0.94**	**0.3**	**0.46**	**0.9**	**0.12**	**1.07**	**-0.54**	**-0.51**	**0.47**	**0.69**	**-0.21**	**0.02**	**0.38**	**0**	**0.07**	**0.09**	**0.58**	**-0.13**	**-0.25**	**-0.15**	**0.1**	**-0.07**	**0.03**
x.34	**499439**	**609942**	**-1.27**	**1.53**	**-1.26**	**2.33**	**1.04**	**-0.41**	**0.5**	**-1.4**	**0.62**	**0.05**	**0.6**	**-0.54**	**-0.32**	**-0.28**	**0.36**	**-0.7**	**0.37**	**-0.09**	**-0.17**	**0.18**	**-0.14**	**0.06**	**-0.07**	**0.18**	**0.02**	**0.03**
x.35	**499706**	**610203**	**-1.59**	**-1.25**	**-0.38**	**2.48**	**0.24**	**-0.65**	**-0.4**	**0.33**	**-0.54**	**-0.07**	**-0.21**	**-0.05**	**-0.03**	**0.01**	**-0.14**	**0.76**	**0.43**	**-0.04**	**-0.29**	**0.07**	**-0.05**	**0.05**	**0.51**	**0.16**	**0.01**	**0.03**
x.36	**499095**	**610262**	**6.65**	**0.19**	**-4.05**	**-0.53**	**0.47**	**-0.49**	**1.02**	**0.75**	**0.47**	**0.52**	**-0.14**	**0.38**	**-0.36**	**0.36**	**0.18**	**-0.24**	**0.73**	**0.12**	**0.09**	**-0.06**	**0.16**	**0.1**	**-0.14**	**0.02**	**0.1**	**0**
x.37	**499039**	**610999**	**-0.55**	**-1.44**	**-0.79**	**-0.92**	**0.41**	**0.1**	**0.93**	**0.2**	**0.75**	**0.02**	**0.22**	**0.87**	**0.64**	**0.15**	**0.34**	**0.04**	**-0.02**	**-0.08**	**-0.17**	**0.31**	**-0.11**	**-0.08**	**0.06**	**-0.19**	**0.06**	**-0.09**
x.38	**500077**	**611689**	**3.91**	**-1.02**	**0.12**	**1.85**	**0.58**	**1.03**	**-1.4**	**0.12**	**-0.68**	**-0.4**	**0.02**	**-0.58**	**0.6**	**0.24**	**-0.14**	**-0.04**	**0.09**	**0.03**	**0.01**	**0.27**	**0.26**	**-0.1**	**-0.12**	**0.07**	**0.23**	**-0.09**

Appendix A continued

x.39	**498979**	**610434**	**1.69**	**-1.08**	**-2.64**	**0.9**	**-0.02**	**-0.83**	**-0.66**	**-0.45**	**-0.26**	**-1.31**	**0.72**	**-0.21**	**-0.72**	**-0.49**	**0.2**	**0.48**	**-0.13**	**0.18**	**-0.44**	**0.16**	**0.13**	**-0.18**	**-0.19**	**-0.07**	**-0.11**	**0.02**
x.40	**498498**	**611514**	**7.9**	**-0.22**	**3.14**	**0.05**	**-0.71**	**0.6**	**-0.2**	**-1.1**	**-0.23**	**-0.05**	**0.7**	**0.58**	**0.36**	**-0.05**	**-0.12**	**0**	**-0.08**	**-0.14**	**0.05**	**0.1**	**0.28**	**-0.01**	**-0.01**	**0.13**	**-0.09**	**0.04**
x.41	**499139**	**611189**	**4.56**	**-2.82**	**2.46**	**0.25**	**-2.67**	**0.22**	**-0.48**	**0.97**	**1.05**	**-0.64**	**-0.36**	**0.06**	**-0.37**	**-0.35**	**-0.6**	**0.3**	**0.41**	**-0.43**	**-0.04**	**0.05**	**-0.16**	**0.27**	**-0.18**	**-0.2**	**0.01**	**-0.02**
x.42	**498874**	**610968**	**2.46**	**-1.07**	**2.64**	**-0.39**	**0.26**	**0.01**	**0.35**	**-1.36**	**1.11**	**-0.15**	**0.48**	**-0.04**	**-0.34**	**-0.24**	**-0.39**	**-0.32**	**-0.18**	**0.68**	**-0.04**	**-0.11**	**-0.1**	**-0.22**	**0.19**	**-0.03**	**0.04**	**-0.01**
x.43	**499208**	**611551**	**4.06**	**-4.13**	**1.37**	**-0.49**	**-1.16**	**0.87**	**-0.07**	**1**	**-1.06**	**-0.12**	**-0.08**	**0.17**	**-0.77**	**0.2**	**0.77**	**-0.52**	**-0.28**	**-0.03**	**0.02**	**0.08**	**-0.33**	**-0.06**	**-0.11**	**0.05**	**0.13**	**0.02**
x.44	**499405**	**611904**	**5.13**	**1**	**0.95**	**0.76**	**-1.67**	**0.37**	**0.43**	**0.16**	**-1.1**	**0.16**	**0.34**	**-0.05**	**0.14**	**0.12**	**0.3**	**0.34**	**0.06**	**-0.28**	**0.1**	**-0.23**	**-0.2**	**-0.22**	**0.04**	**0.25**	**-0.12**	**-0.06**
x.45	**499886**	**611419**	**-3.58**	**-7.53**	**0.1**	**-0.48**	**-0.34**	**-0.65**	**-1.05**	**1.49**	**0.15**	**0.51**	**0.65**	**-0.54**	**0.54**	**0.49**	**0.01**	**-0.28**	**0.46**	**0.16**	**-0.32**	**-0.2**	**-0.14**	**-0.29**	**0.08**	**-0.17**	**-0.03**	**0.11**
x.46	**498681**	**611653**	**-1.65**	**-2.54**	**0.24**	**-2.42**	**1.17**	**0.94**	**1.11**	**0.16**	**-0.13**	**1.05**	**1.3**	**-0.57**	**-0.31**	**0.62**	**-0.11**	**0.61**	**-0.46**	**-0.02**	**0.04**	**0.24**	**0.04**	**0.11**	**-0.07**	**0.04**	**-0.02**	**-0.07**

Appendix A continued

x.47	**4997 26**	**6116 73**	**-1.72**	**-10.39**	**1.09**	**-0.45**	**0.71**	**-1.57**	**-0.03**	**-1.55**	**-0.15**	**0.33**	**-0.97**	**-0.3**	**-0.29**	**-0.32**	**0.4**	**0.06**	**-0.13**	**-0.16**	**0.52**	**0.05**	**0.3**	**0.12**	**0**	**0.01**	**-0.06**	**0**

Table 7.3.3 PCA Score of deeper topsoil from Castleisland, Co. Kerry, Ireland (Clr transformed).

PCAScore	X.ITM	Y.ITM	PC1	PC2	PC3	PC4	PC5	PC6	PC7	PC8	PC9	PC10	PC11	PC12	PC13	PC14	PC15	PC16	PC17	PC18	PC19	PC20	PC21	PC22	PC23	PC24	PC25	PC26
x.1	499405	611904	0.74	-0.2	-0.03	-0.08	0.31	0.09	0.08	0.11	-0.22	-0.19	0.05	0.18	0.05	-0.1	-0.02	-0.09	0.01	0.03	0.05	0.03	0.03	0.05	0.02	0	-0.01	0
x.2	499441	611393	0.08	0.97	-0.1	0.26	-0.18	0.3	0.15	-0.19	0.04	0.17	0.15	0.03	-0.07	-0.02	0.03	0	0.11	-0.09	0.02	-0.01	0.07	0.03	-0.01	-0.01	0	-0.01
x.3	499886	611419	-0.83	2.38	0.22	0.15	0.63	0.2	-0.01	-0.04	0.04	-0.15	0.09	0.09	0	0.08	0	0.02	-0.08	0.04	-0.01	0	-0.01	-0.01	-0.02	-0.01	0	0
x.4	500077	611689	0.35	-0.04	-0.41	0.48	0.16	-0.07	-0.34	0.13	-0.01	-0.03	-0.07	-0.11	-0.01	0.17	-0.02	-0.14	0.04	-0.01	-0.06	0.05	0	0.01	0.02	-0.02	0	0
x.5	500327	611939	0.31	-0.28	-0.28	-0.04	-0.55	0.34	-0.11	-0.17	0.15	-0.11	-0.04	0.11	0	0.09	0.1	0.01	-0.07	-0.03	-0.04	0.02	0.01	-0.04	0	0	-0.02	0.02
x.6	499852	611939	-0.01	-0.1	-0.51	-0.08	-0.46	0.26	-0.03	-0.05	0.13	-0.06	-0.06	0.08	-0.05	0.09	0.03	-0.04	-0.06	0	0.06	0.02	-0.02	0.03	0.01	0.02	0.03	-0.02

Appendix A continued

x.7	**498874**	**610968**	**1**	**0.73**	**-0.74**	**0.42**	**-0.32**	**-0.44**	**-0.14**	**0.04**	**-0.13**	**-0.04**	**0.06**	**-0.01**	**-0.17**	**-0.11**	**0.07**	**0.04**	**0.01**	**0.05**	**0**	**-0.03**	**-0.03**	**-0.02**	**-0.01**	**0**	**0**	**0**
x.8	**499039**	**610999**	**-0.67**	**0.62**	**0.02**	**0.17**	**0.04**	**-0.17**	**-0.07**	**-0.09**	**-0.19**	**0.12**	**-0.01**	**0.07**	**0.17**	**0.06**	**-0.03**	**-0.01**	**-0.01**	**-0.03**	**0.02**	**-0.02**	**-0.01**	**-0.01**	**0**	**0.05**	**-0.01**	**0**
x.9	**499579**	**610965**	**-0.01**	**0.37**	**-0.19**	**-0.03**	**0**	**0.36**	**-0.09**	**0.07**	**-0.18**	**-0.09**	**-0.24**	**0.05**	**0**	**-0.01**	**-0.05**	**0.05**	**0.1**	**-0.01**	**0.05**	**-0.04**	**-0.04**	**-0.03**	**0.01**	**0**	**0.01**	**-0.01**
x.10	**499956**	**610918**	**-0.17**	**-0.1**	**0.12**	**-0.49**	**-0.19**	**0.47**	**-0.02**	**0.37**	**0**	**-0.07**	**0.3**	**-0.06**	**-0.04**	**0.01**	**-0.02**	**-0.03**	**0.05**	**0.02**	**0.02**	**-0.02**	**-0.04**	**-0.03**	**0.02**	**0.02**	**0**	**0.01**
x.11	**500481**	**610939**	**-0.86**	**-0.32**	**-0.07**	**-0.27**	**0.02**	**0.2**	**-0.06**	**0.21**	**0.02**	**0.08**	**-0.01**	**0.07**	**-0.02**	**0**	**0**	**0.09**	**-0.01**	**-0.06**	**-0.03**	**0**	**0**	**0.03**	**0.06**	**-0.02**	**-0.01**	**0**
x.12	**498498**	**611514**	**1.58**	**0.79**	**-0.47**	**-0.23**	**0.2**	**0.18**	**0.62**	**0.03**	**0.08**	**0.03**	**-0.1**	**-0.15**	**0.07**	**-0.07**	**-0.03**	**0.03**	**-0.02**	**-0.01**	**-0.02**	**0.06**	**0**	**-0.02**	**0.01**	**0.01**	**0**	**0**
x.13	**500291**	**611248**	**-0.49**	**0.15**	**-0.14**	**-0.49**	**-0.07**	**0.13**	**-0.1**	**-0.15**	**0**	**0.14**	**-0.09**	**-0.14**	**-0.15**	**-0.1**	**-0.14**	**-0.11**	**-0.07**	**0.03**	**-0.02**	**-0.05**	**0.03**	**-0.01**	**-0.01**	**-0.01**	**0**	**0**
x.14	**500452**	**611439**	**0.07**	**-0.94**	**0.04**	**-0.01**	**0.68**	**0.31**	**-0.18**	**-0.02**	**-0.13**	**0.07**	**0.01**	**-0.05**	**-0.08**	**-0.07**	**0.12**	**-0.01**	**0**	**-0.05**	**0.03**	**0.01**	**0.01**	**-0.04**	**-0.05**	**0**	**0**	**0**

Appendix A continued

x.15	**498441**	**610459**	**0.45**	**-0.15**	**0.5**	**0.19**	**0.38**	**0.01**	**0.07**	**-0.07**	**0.17**	**-0.05**	**-0.13**	**-0.08**	**-0.17**	**0.05**	**0.07**	**0.03**	**0.02**	**0.04**	**0**	**-0.07**	**0.01**	**0.05**	**0.04**	**0.03**	**0**	**0.01**
x.16	**498681**	**610686**	**-0.15**	**0.03**	**-0.3**	**0.23**	**0.03**	**-0.14**	**-0.12**	**-0.02**	**-0.06**	**0.13**	**0.06**	**0.02**	**0.01**	**-0.01**	**-0.01**	**0.03**	**-0.01**	**0.01**	**0.07**	**0**	**0**	**-0.03**	**0.05**	**-0.02**	**0.03**	**0.01**
x.17	**498714**	**610184**	**1.39**	**-0.36**	**0.02**	**-0.69**	**0.28**	**-0.44**	**-0.17**	**-0.04**	**0.11**	**-0.08**	**0.12**	**0.02**	**-0.01**	**0.19**	**-0.07**	**0.06**	**0.02**	**-0.01**	**0**	**-0.02**	**0.04**	**-0.01**	**-0.02**	**0**	**0.01**	**0**
x.18	**498979**	**610434**	**0.69**	**1.01**	**0.92**	**-0.13**	**-0.3**	**-0.24**	**-0.33**	**0.3**	**0.25**	**0.18**	**-0.11**	**0.08**	**0.06**	**-0.13**	**0.06**	**-0.04**	**0**	**0.01**	**0.01**	**0.02**	**0.01**	**-0.01**	**0**	**0**	**0**	**-0.01**
x.19	**499201**	**610705**	**-0.18**	**0.36**	**-0.27**	**-0.29**	**-0.33**	**-0.12**	**-0.01**	**-0.04**	**-0.11**	**0.1**	**0.15**	**-0.19**	**0.18**	**0.04**	**0.08**	**-0.03**	**0**	**0.04**	**-0.03**	**-0.02**	**0**	**0.05**	**-0.02**	**0**	**0**	**0**
x.20	**499445**	**610436**	**0.92**	**-0.54**	**0.32**	**0.09**	**-0.21**	**-0.05**	**0.38**	**0.09**	**-0.14**	**0.05**	**-0.07**	**0.19**	**0.05**	**0.08**	**-0.01**	**-0.07**	**-0.03**	**-0.02**	**0.01**	**-0.08**	**-0.02**	**-0.01**	**-0.03**	**-0.02**	**0**	**0**
x.21	**499702**	**610679**	**0**	**-0.39**	**0.16**	**0.4**	**-0.11**	**0.14**	**0.09**	**-0.14**	**0**	**0.18**	**-0.01**	**-0.05**	**0.09**	**0.07**	**-0.08**	**0.04**	**-0.01**	**0.05**	**0.04**	**-0.03**	**0.01**	**-0.02**	**0.02**	**-0.01**	**-0.01**	**0**
x.22	**499706**	**610203**	**-0.32**	**-0.65**	**0.5**	**0.35**	**-0.05**	**-0.17**	**0.25**	**0.14**	**-0.12**	**0.08**	**0.15**	**0.03**	**-0.17**	**0.02**	**-0.03**	**0.02**	**-0.06**	**0.01**	**-0.07**	**0.05**	**0.03**	**-0.02**	**0.01**	**0.02**	**0**	**-0.02**

Appendix A continued

x.23	**499967**	**610434**	**-0.25**	**-0.4**	**0.04**	**0.54**	**-0.02**	**0.07**	**0.03**	**0.27**	**0.27**	**-0.02**	**0**	**-0.07**	**0.04**	**-0.01**	**-0.13**	**0.03**	**0.01**	**-0.03**	**0**	**0**	**-0.04**	**0.03**	**-0.06**	**0**	**0.01**	**0.01**
x.24	**500457**	**610437**	**0.01**	**-0.32**	**-0.38**	**0.32**	**-0.04**	**-0.08**	**-0.2**	**-0.05**	**0.06**	**-0.07**	**0.04**	**-0.01**	**0**	**-0.09**	**-0.1**	**0.04**	**-0.04**	**-0.02**	**0.06**	**0**	**0**	**0.02**	**0**	**0.01**	**-0.03**	**0**
x.25	**498643**	**609431**	**-1.09**	**0.06**	**0.05**	**-0.29**	**0**	**-0.19**	**0.25**	**-0.01**	**0.01**	**0.1**	**-0.12**	**-0.02**	**-0.1**	**0.07**	**0.07**	**-0.08**	**0.04**	**0**	**0.05**	**0.04**	**-0.04**	**0.01**	**-0.02**	**0**	**0**	**0.01**
x.26	**498694**	**609723**	**-0.8**	**-0.01**	**-0.08**	**-0.01**	**-0.02**	**-0.39**	**0.21**	**0.22**	**-0.09**	**0**	**-0.1**	**-0.02**	**-0.02**	**0.09**	**0.02**	**0.09**	**0.02**	**0.02**	**0.03**	**0.04**	**0.03**	**-0.02**	**0**	**0**	**0**	**0**
x.27	**498861**	**608891**	**-0.78**	**-0.44**	**-0.32**	**-0.04**	**0.15**	**-0.12**	**-0.05**	**0.03**	**0.07**	**-0.14**	**-0.1**	**0.04**	**0.12**	**-0.09**	**-0.01**	**-0.05**	**0.03**	**0.01**	**0**	**-0.01**	**0.08**	**-0.03**	**0**	**0.03**	**0.01**	**0**
x.28	**498957**	**609921**	**0.41**	**-0.81**	**-0.03**	**0.05**	**0.53**	**0.18**	**-0.15**	**-0.06**	**0.06**	**0.16**	**0.01**	**-0.05**	**0.13**	**0**	**0.08**	**0.02**	**-0.02**	**0.05**	**0.01**	**0**	**-0.04**	**0**	**0.01**	**-0.01**	**-0.01**	**-0.02**
x.29	**499439**	**609942**	**-0.21**	**-0.24**	**0.75**	**0.18**	**-0.5**	**0.2**	**-0.02**	**-0.01**	**-0.16**	**-0.27**	**-0.06**	**-0.2**	**0.05**	**-0.01**	**0.05**	**0.06**	**-0.01**	**0.03**	**0.02**	**0**	**0.04**	**0.01**	**-0.02**	**-0.02**	**0**	**0**
x.30	**499452**	**608950**	**-0.71**	**-0.32**	**-0.28**	**-0.13**	**0.15**	**-0.42**	**0.15**	**0.09**	**0.05**	**-0.12**	**0.02**	**-0.05**	**0.05**	**-0.1**	**0.08**	**0**	**-0.07**	**-0.08**	**-0.04**	**-0.06**	**-0.02**	**0.01**	**0.02**	**-0.01**	**0.01**	**0**

Appendix A continued

x.31	**499952**	**608939**	**-0.57**	**-0.18**	**0.31**	**0.03**	**-0.03**	**-0.29**	**0.18**	**-0.36**	**0.22**	**-0.18**	**0.1**	**-0.01**	**0.03**	**-0.04**	**-0.01**	**-0.07**	**0.08**	**0**	**0.01**	**0.01**	**-0.04**	**-0.04**	**0.02**	**-0.01**	**-0.01**	**-0.01**
x.32	**500537**	**609463**	**0.21**	**-0.68**	**0.24**	**0.23**	**-0.02**	**0.08**	**0.04**	**-0.23**	**0.04**	**0.04**	**0.1**	**0.13**	**0.03**	**-0.09**	**-0.01**	**0.03**	**0.01**	**0.04**	**-0.08**	**0.03**	**-0.02**	**0.01**	**0**	**0**	**0.02**	**0.01**
x.33	**498528**	**608891**	**-0.65**	**-0.31**	**-0.27**	**-0.5**	**-0.07**	**-0.05**	**-0.04**	**-0.09**	**0.01**	**0.07**	**-0.06**	**0.15**	**-0.03**	**-0.04**	**-0.02**	**0.08**	**0.03**	**0.07**	**-0.02**	**0.03**	**-0.01**	**0.03**	**-0.04**	**-0.01**	**-0.01**	**0**
x.34	**499095**	**610262**	**0.56**	**0.32**	**0.68**	**-0.31**	**-0.09**	**-0.14**	**-0.22**	**-0.26**	**-0.23**	**-0.03**	**-0.04**	**-0.07**	**-0.03**	**-0.02**	**-0.07**	**0.03**	**-0.02**	**-0.08**	**0.02**	**0.04**	**-0.04**	**0.02**	**0.01**	**0.01**	**0.01**	**0**

Table 7.3.4 Topsoil Castleisland Co. Kerry Clr transformed

sample	X.ITM	Y.ITM	Mo	Cu	Pb	Zn	Ni	Co	Mn	Fe	As	U	Th	Sr	Sb	V	Ca	P
L40AS234A	498457	609929	0.091387	-0.23611	0.000474	0.369525	0.360096	0.381147	0.928126	0.162993	0.22487	-0.26728	0.046004	-0.10323	-0.29636	0.132861	0.193037	0.224
L67AS221A	499852	611939	0.272441	-0.3541	-0.03334	-0.07138	-0.27763	-0.19961	0.016842	0.171334	0.043546	-0.26728	0.017976	-0.22133	-0.12027	-0.04693	-0.53396	-0.02
L65AS202	498915	611909	0.291746	0.02649	0.167248	-0.05435	-0.04192	-0.07237	0.187848	-0.08488	0.119425	-0.11601	-0.11672	-0.06373	0.921122	-0.01474	-0.23293	-0.13
S209L47A	499445	610436	0.134139	0.046128	0.122966	-0.1076	-0.04879	0.003355	-0.3811	0.008606	0.132487	0.510875	-0.20387	-0.12442	0.247706	-0.00452	0.165009	-0.00
S212AL49A	500457	610437	-0.22488	-0.23437	-0.02636	-0.25184	-0.18307	-0.29192	-0.4947	-0.0253	-0.05833	-0.39222	0.097157	-0.195	-0.12027	-0.08169	-0.28408	-0.20
001AL53	499956	610918	0.076147	0.21329	0.080467	0.098878	0.013509	-0.01437	-0.03276	0.195436	0.019187	-0.23251	-0.15812	-0.12442	-0.59739	-0.05821	-0.31211	-0.09
L61A	500452	611439	-0.41677	-0.25217	-0.21119	-0.04608	0.119529	0.047372	-0.30249	0.047966	-0.22699	-0.34646	0.120638	-0.22133	-0.59739	-0.22302	-0.10799	-0.20
L23AS206A	500291	611248	-0.16689	-0.06827	-0.21652	0.092969	0.248758	0.307271	0.303148	0.261584	0.019187	-0.44337	0.273248	-0.31151	-0.12027	-0.22302	-0.31211	-0.30
L52AS207A	499579	610965	-0.16689	0.230371	0.295773	0.366367	0.223592	0.277513	0.242807	0.067884	-0.00662	-0.17037	0.072333	0.036945	0.004668	-0.13284	0.696487	-0.00
L34AS215A	500537	609463	-0.14056	-0.20732	-0.13157	-0.13689	0.001331	-0.00838	-0.26136	0.124	0.237682	0.084906	0.046004	-0.22133	-0.12027	-0.10651	0.259984	-0.09
L1AS225A	498720	609181	-0.52591	-0.22745	-0.14048	-0.02217	0.098653	0.145327	-0.12353	0.041649	-0.07357	-0.34646	0.164104	-0.24936	-0.29636	-0.24005	-0.20945	-0.25
L2AS219A	499209	609183	-0.41677	-0.05653	-0.11641	0.138131	0.236956	0.329691	0.057607	0.155714	0.102524	-0.04543	0.222096	-0.08303	-0.12027	-0.08169	0.612167	-0.06
L6AS239A	499203	609685	-0.52591	-0.3361	0.031844	-0.4916	-0.30592	-0.38034	-0.17184	-0.42139	-0.44154	-0.23251	-0.31302	-0.08303	-0.12027	-0.04693	0.219366	0.009
S239AL6A	499203	609685	-0.11574	-0.14201	0.096407	0.148724	0.214868	0.321418	0.074834	0.200982	0.081335	-0.14234	0.097157	-0.31151	0.180759	-0.25778	-0.37426	-0.15
L41AS238A	498957	609921	-0.32962	-0.02851	-0.0178	-0.30796	-0.20901	-0.13931	0.136579	-0.36109	-0.41806	-0.17037	-0.37996	-0.06373	-0.12027	-0.13284	0.507431	-0.06
L31AS223A	498861	608891	-0.19492	-0.27073	0.417195	0.127273	0.202094	0.315814	0.533891	0.144562	0.135693	-0.44337	0.184307	-0.22133	0.004668	-0.08169	-0.40902	-0.13
L13AS229A	498681	610686	0.134139	-0.0451	-0.08361	0.042559	0.013509	0.036779	0.058861	0.015419	-0.01558	-0.09119	-0.01199	-0.01048	0.101578	0.015221	-0.05684	-0.02
L16AS237A	500136	610766	-0.02859	-0.03178	0.010125	0.092969	0.105184	0.177512	0.178447	0.206459	0.014991	-0.20033	0.184307	-0.34627	-0.29636	-0.11948	-0.34208	-0.15
L3AS218A	499697	609188	-0.04879	0.082925	-0.02464	0.340236	0.657507	0.583139	1.062847	0.084052	0.255007	-0.20033	0.184307	-0.08303	0.101578	-0.17559	0.682058	-0.12
S233AL45A	498441	610459	-0.09226	-0.09275	-0.18799	-0.08911	0.038777	0.062792	-0.33534	-0.08702	-0.18493	0.306755	-0.07893	-0.01048	0.101578	-0.17559	0.414886	-0.15
L15AS210A	499702	610679	0.076147	-0.09909	0.193056	-0.13689	-0.06288	-0.02045	-0.37088	0.118704	0.142033	0.739902	-0.31302	-0.02751	0.004668	0.125437	0.09158	0.112

Appendix A continued

L32AS222A	**499452**	**608950**	**-0.09226**	**-0.10037**	**0.08851**	**0.211917**	**0.202094**	**0.258628**	**0.328091**	**0.184125**	**0.092059**	**-0.26728**	**0.203612**	**-0.17018**	**0.004668**	**-0.10651**	**0.12458**	**-0.13**
L68AS214A	**500327**	**611939**	**0.134139**	**-0.28617**	**-0.27991**	**-0.21405**	**-0.33618**	**-0.35319**	**-0.07154**	**0.147065**	**0.02746**	**-0.39222**	**0.046004**	**-0.24936**	**-0.12027**	**-0.13284**	**-0.31211**	**-0.17**
L54AS205A	**500481**	**610939**	**0.026929**	**0.0614**	**-0.10797**	**0.179036**	**0.090349**	**0.214654**	**0.468409**	**0.235914**	**0.006475**	**-0.23251**	**0.120638**	**-0.195**	**-0.29636**	**-0.08169**	**0.174554**	**0.112**
L48AS211A	**499967**	**610434**	**-0.11574**	**-0.35872**	**-0.06243**	**-0.1471**	**0.001331**	**-0.09355**	**-0.60066**	**-0.0125**	**-0.06843**	**-0.0677**	**0.097157**	**-0.27932**	**-0.12027**	**-0.10651**	**-0.53396**	**-0.20**
L51AS235	**498694**	**609723**	**0.0092**	**-0.05653**	**-0.21119**	**0.116137**	**0.230932**	**0.368843**	**0.490734**	**0.130531**	**0.062852**	**-0.00404**	**0.120638**	**-0.12442**	**0.004668**	**-0.06979**	**-0.4882**	**-0.13**
008AL9	**498714**	**610184**	**-0.06998**	**0.096162**	**0.03636**	**0.035826**	**0.113212**	**0.192752**	**0.324711**	**0.018786**	**-0.06335**	**0.01527**	**-0.07893**	**-0.08303**	**-0.12027**	**0.04325**	**0.259984**	**-0.02**
L4aS217A	**500218**	**609463**	**-0.14056**	**-0.02311**	**-0.06055**	**0.068495**	**0.119529**	**0.110565**	**-0.18921**	**0.058804**	**-0.15275**	**-0.26728**	**0.184307**	**-0.27932**	**0.004668**	**-0.19083**	**-0.07323**	**-0.20**
S203AL59A	**499441**	**611393**	**0.147503**	**0.095346**	**0.081818**	**0.000498**	**-0.22604**	**-0.21849**	**-0.03122**	**-0.0641**	**-0.05336**	**0.255602**	**-0.04417**	**0.298823**	**0.101578**	**0.422706**	**0.003158**	**0.211**
L36AS236A	**498643**	**609431**	**0.060352**	**-0.14627**	**-0.03159**	**0.26307**	**0.284504**	**0.527967**	**0.771869**	**0.280347**	**0.142033**	**0.033753**	**0.203612**	**-0.22133**	**-0.29636**	**-0.06979**	**-0.40902**	**-0.15**
L22AS207A	**499811**	**611122**	**0.173057**	**-0.10423**	**-0.12284**	**-0.04608**	**0.005429**	**-0.00247**	**-0.37767**	**0.066384**	**-0.02012**	**0.033753**	**0.017976**	**0.218**	**0.101578**	**-0.01474**	**-0.4882**	**-0.00**
L39AS220A	**500537**	**609464**	**0.026929**	**-0.07426**	**0.136255**	**0.211917**	**0.133415**	**0.274422**	**0.423247**	**0.166587**	**0.116097**	**-0.02424**	**0.203612**	**-0.1467**	**0.004668**	**-0.01474**	**-0.02581**	**0.082**
007AL14A	**499201**	**610705**	**0.480247**	**0.056963**	**0.046719**	**0.179036**	**0.10356**	**0.057713**	**0.404457**	**0.00516**	**0.264605**	**-0.02424**	**0.017976**	**-0.02751**	**0.101578**	**0.117883**	**0.252159**	**0.222**
L42AS231A	**499439**	**609942**	**-0.04879**	**-0.3541**	**0.106717**	**-0.00693**	**0.015505**	**0.042108**	**-0.19367**	**0.181827**	**0.169471**	**-0.09119**	**0.120638**	**-0.24936**	**-0.29636**	**-0.14663**	**0.201992**	**-0.17**
L11AS230A	**499706**	**610203**	**-0.22488**	**0.190948**	**0.125412**	**0.104707**	**0.049961**	**0.123929**	**-0.26398**	**0.067884**	**0.066612**	**0.385936**	**0.072333**	**-0.10323**	**-0.12027**	**0.132861**	**-0.02581**	**0.220**
L10AS232A	**499095**	**610262**	**-0.06998**	**-0.0659**	**0.065324**	**-0.21405**	**-0.20901**	**-0.28064**	**-0.15513**	**-0.18233**	**-0.11703**	**0.11594**	**-0.55606**	**0.154331**	**-0.12027**	**-0.05821**	**0.608706**	**0.139**
L51AS228A	**499039**	**610999**	**0.40714**	**-0.01778**	**0.003715**	**0.138131**	**0.176736**	**0.157678**	**0.196138**	**0.069379**	**0.232603**	**0.084906**	**-0.07893**	**0.165612**	**0.101578**	**0.086284**	**0.145265**	**0.213**
L72AS213A	**500077**	**611689**	**-0.19492**	**0.237491**	**0.218401**	**-0.30796**	**-0.28552**	**-0.44034**	**-0.74111**	**-0.39451**	**-0.25748**	**0.130663**	**-0.20387**	**0.093061**	**0.305698**	**0.034106**	**-0.16598**	**0.027**
L46A06A	**498979**	**610434**	**0.043962**	**0.247381**	**0.130265**	**0.014976**	**-0.01332**	**0.020388**	**-0.25358**	**-0.15899**	**-0.02472**	**0.62667**	**-0.01199**	**0.093061**	**-0.12027**	**-0.04693**	**0.461186**	**-0.03**
L57AS201A	**498498**	**611514**	**-0.11574**	**-0.04964**	**-0.0997**	**-0.59426**	**-0.66019**	**-1.02661**	**-1.27735**	**-0.78173**	**-0.50648**	**0.068516**	**-0.37996**	**0.322735**	**0.101578**	**0.117883**	**-0.25776**	**-0.06**
004AL21	**499139**	**611189**	**0.0092**	**0.601668**	**-0.0681**	**-0.00693**	**-0.44214**	**-0.87171**	**-0.64262**	**-0.55566**	**-0.52073**	**0.11594**	**-0.15812**	**0.306941**	**0.004668**	**0.311399**	**0.09158**	**0.160**
L20005A	**498874**	**610968**	**0.384863**	**-0.00525**	**-0.08165**	**-0.2652**	**-0.43086**	**-0.57068**	**-0.56239**	**-0.13444**	**-0.10575**	**0.033753**	**0.046004**	**0.246645**	**0.101578**	**0.270494**	**-0.10799**	**-0.10**
L70A010A	**499208**	**611551**	**0.043962**	**0.357101**	**0.046719**	**-0.11714**	**-0.33172**	**-0.50998**	**-0.25875**	**-0.39019**	**-0.28184**	**0.369546**	**-0.20387**	**0.84406**	**0.247706**	**0.291428**	**-0.09026**	**0.282**
009AL66	**499405**	**611904**	**-0.59286**	**-0.05307**	**-0.0997**	**-0.30796**	**-0.35916**	**-0.45673**	**-0.52723**	**-0.53119**	**-0.45378**	**-0.09119**	**-0.31302**	**0.154331**	**-0.29636**	**-0.04693**	**-0.04105**	**-0.00**

03AL60	499886	611419	0.61576	0.908511	0.02112	0.449754	0.35007	0.261833	0.272879	0.194318	0.332567	0.622025	0.184307	0.970746	0.833972	0.47928	-0.04105	0.486
L69AS227A	498681	611653	0.49822	0.152623	-0.04583	-0.07138	0.064439	0.373806	0.964757	0.167779	0.527199	0.11594	0.046004	0.483032	0.35685	0.125437	-0.37426	0.137
002AL71A	499726	611673	1.117539	0.562837	0.04231	-0.01448	-0.12705	-0.24846	-0.2143	0.057272	0.439904	1.224085	0.289042	1.065909	1.083849	0.729365	0.441215	0.788

Table 7.3.4 continued: Topsoil Castleisland Co. Kerry Clr transformed, with log10Soil-gas radon, radon potential class and bedrock groups.

sample	X.ITM	Y.ITM	Cr	Mg	Ba	Al	Na	K	Hg	Sc	Ga	log10RnConc	SoilPerm_1	Radon Pote	soil permeabilitys	RPclass	SGRnclass	Sgclass.1	Bedrock class	Quaternary Geology
L40AS234A	498457	609929	0.14	0.09	0.26	0.24	0.09	0.12	0.06	0.24	0.2	4.11	h	9.912805	Medium	22.5-35	10 -- 30	a	WaulsortianLimestones	Tillderivedfrom Limestones
L67AS221A	499852	611939	-0.06	-0.13	-0.11	-0.01	-0.11	0.07	-0.24	-0.1	0.08	4.3	h	15.69528	Medium	22.5-35	10 -- 30	a	ClooneFlagstones	Tillderivedfrom Namurian sandstonessiltstones andshales
L65AS202	498915	611909	-0.08	-0.1	-0.17	-0.15	-0.19	-0.08	0.03	-0.12	-0.1	4.36	h	18.25608	Medium	22.5-35	10 -- 30	a	DirtogeLimestones	Tillderivedfrom Namurian sandstonessiltstones

Appendix A continued

																				andshales
S209L47A	499445	610436	0	-0.13	-0.04	0.01	-0.04	-0.13	0.16	-0.02	0	4.36	l	8.553076	Low	10-22.5	10 -- 30	a	RockfieldLimestones	Tillderivedfrom Limestones
S212AL49A	500457	610437	-0.08	-0.07	0.01	-0.02	0.07	0.07	-0.06	-0.02	0.08	4.38	m	12.45174	Moderately Low	22.5-35	10 -- 30	a	RockfieldLimestones	Tillderivedfrom Limestones
001AL53	499956	610918	0.07	0.14	0.1	0.12	0.12	0.03	0.03	-0.02	0.2	4.41	h	21.06471	Medium	22.5-35	10 -- 30	a	CracoeanReefMember	Tillderivedfrom Namurian sandstonessiltstones andshales
L61A	500452	611439	0.03	0.23	-0.17	0.09	0.16	0.18	-0.17	0.06	0.14	4.43	h	21.39514	Medium	22.5-35	10 -- 30	a	DirtogeLimestones	Tillderivedfrom Namurian sandstonessiltstones andshales
L23AS206A	500291	611248	0.1	0.31	-0.16	0.16	-0.01	0.1	-0.32	0.16	0.08	4.53	e	27.02616	Medium	22.5-35	30-50	b	DirtogeLimestones	Tillderivedfrom Namurian sandstonessiltstones

Appendix A continued

																				andshales
L52AS207A	499579	610965	0	0.17	0.08	0.02	0.12	0.18	0.31	0.13	0	4.53	m	18.02225	Moderately Low	22.5-35	30-50	b	CracoeanReefMember	Tillderivedfrom Namurian sandstonessiltstones andshales
L34AS215A	500537	609463	-0.04	0	-0.18	-0.04	-0.04	-0.04	0.06	0.06	-0.1	4.56	l	13.40236	Moderately Low	22.5-35	30-50	b	WaulsortianLimestones	Tillderivedfrom Limestones
L1AS225A	498720	609181	-0.02	0.15	-0.14	0.08	0.05	0.03	-0.41	0.11	0.08	4.58	l	14.05148	Low	22.5-35	30-50	b	WaulsortianLimestones	Tillderivedfrom Limestones
L2AS219A	499209	609183	0.06	0.14	0.08	0.16	0.14	0.03	-0.11	0.24	0.08	4.58	h	30.56448	Medium	22.5-35	30-50	b	WaulsortianLimestones	Alluvium
L6AS239A	499203	609685	-0.12	-0.37	-0.21	-0.21	-0.11	-0.23	0.21	-0.24	-0.1	4.6	h	32.21662	Medium	22.5-35	30-50	b	WaulsortianLimestones	Alluvium
S239AL6A	499203	609685	0.01	0.23	-0.14	-0.02	-0.01	-0.04	-0.32	0.1	-0.1	4.6	h	32.21662	Medium	22.5-35	30-50	b	WaulsortianLimestones	Alluvium

Appendix A continued

L41AS238A	**498957**	**609921**	**-0.19**	**-0.32**	**-0.25**	**-0.33**	**-0.11**	**-0.38**	**0.29**	**-0.27**	**-0.4**	**4.62**	**h**	**33.45572**	**Medium**	**22.5-35**	**30-50**	**b**	**WaulsortianLimestones**	**Tillderivedfrom Limestones**
L31AS223A	**498861**	**608891**	**0.03**	**0.07**	**0.01**	**0.13**	**0.09**	**0.12**	**-0.06**	**0.21**	**0.08**	**4.64**	**h**	**35.93392**	**Medium**	**35+**	**30-50**	**b**	**WaulsortianLimestones**	**Tillderivedfrom Limestones**
L13AS229A	**498681**	**610686**	**-0.04**	**0.09**	**-0.12**	**-0.05**	**-0.07**	**-0.08**	**-0.24**	**-0.08**	**0**	**4.69**	**h**	**39.56862**	**Medium**	**35+**	**30-50**	**b**	**RockfieldLimestones**	**Tillderivedfrom Limestones**
L16AS237A	**500136**	**610766**	**0.07**	**0.19**	**0.03**	**0.11**	**0.12**	**0.1**	**-0.02**	**0.1**	**0.14**	**4.71**	**h**	**41.63378**	**Medium**	**35+**	**50-70**	**c**	**CracoeanReefMember**	**Tillderivedfrom Namurian sandstonessiltstones andshales**
L3AS218A	**499697**	**609188**	**-0.06**	**0.21**	**-0.06**	**0.08**	**-0.19**	**0.07**	**-0.02**	**0.35**	**-0.1**	**4.72**	**h**	**43.28592**	**Medium**	**35+**	**50-70**	**c**	**WaulsortianLimestones**	**Tillderivedfrom Limestones**
S233AL45A	**498441**	**610459**	**-0.16**	**0.1**	**-0.16**	**-0.17**	**-0.04**	**-0.13**	**-0.11**	**-0.08**	**-0.22**	**4.76**	**h**	**46.42497**	**Medium**	**35+**	**50-70**	**c**	**RockfieldLimestones**	**Tillderivedfrom Limestones**
L15AS210A	**499702**	**610679**	**0.07**	**-0.1**	**0.02**	**0.08**	**-0.04**	**-0.18**	**0.31**	**-0.1**	**0**	**4.78**	**l**	**22.33727**	**V.Low**	**22.5-35**	**50-70**	**c**	**RockfieldLimestones**	**Tillderivedfrom Limestones**

Appendix A continued

L32AS222A	499452	608950	0.07	0.17	0.03	0.12	0.07	0.12	-0.06	0.16	0.08	4.79	l	23.40641	Low	22.5-35	50-70	c	WaulsortianLimestones	Tillderivedfrom Limestones
L68AS214A	500327	611939	-0.1	-0.16	-0.14	-0.07	-0.11	0	-0.32	-0.04	0.08	4.8	l	21.8299	Low	22.5-35	50-70	c	ClareShales	Tillderivedfrom Namurian sandstonessiltstones andshales
L54AS205A	500481	610939	0.09	0.17	0.04	0.13	0.12	0.15	-0.06	0.11	0.14	4.81	h	52.37266	Medium	35+	50-70	c	CracoeanReefMember	Tillderivedfrom Namurian sandstonessiltstones andshales
L48AS211A	499967	610434	0.03	0.1	-0.01	0.12	0.18	0.07	-0.02	0.03	0.08	4.83	l	25.27739	Low	22.5-35	50-70	c	RockfieldLimestones	Tillderivedfrom Limestones
L51AS235	498694	609723	0.03	0.23	0.01	0.03	0.07	0.07	-0.24	0.04	0	4.88	h	61.21157	Medium	35+	70-100	d	WaulsortianLimestones	Alluvium
008AL9	498714	610184	0.03	0.1	-0.01	-0.01	-0.14	-0.13	0.13	-0.02	0	4.88	h	62.20285	Medium	35+	70-100	d	RockfieldLimestones	Tillderivedfrom Limestones

Appendix A continued

L4aS217A	**500218**	**609463**	**0**	**0.17**	**-0.08**	**0.06**	**0.02**	**0.07**	**-0.24**	**0.06**	**0**	**4.89**	**l**	**28.98118**	**Low**	**22.5-35**	**70-100**	**d**	**WaulsortianLimestones**	**Tillderivedfrom Limestones**
S203AL59A	**499441**	**611393**	**0.06**	**-0.1**	**0.08**	**0.01**	**0.09**	**0.03**	**-0.02**	**-0.02**	**0**	**4.91**	**h**	**66.08537**	**Medium**	**35+**	**70-100**	**d**	**ClareShales**	**Tillderivedfrom Namurian sandstonessiltstones andshales**
L36AS236A	**498643**	**609431**	**0.11**	**0.24**	**0.1**	**0.18**	**0.12**	**0.1**	**-0.11**	**0.24**	**0.14**	**4.93**	**h**	**70.1331**	**Medium**	**35+**	**70-100**	**d**	**WaulsortianLimestones**	**Alluvium**
L22AS207A	**499811**	**611122**	**0.01**	**0.07**	**-0.08**	**0.01**	**-0.01**	**0.07**	**-0.02**	**0.06**	**0.08**	**4.94**	**e**	**72.28087**	**Medium**	**35+**	**70-100**	**d**	**CracoeanReefMember**	**Tillderivedfrom Namurian sandstonessiltstones andshales**
L39AS220A	**500537**	**609464**	**0.14**	**0.17**	**0.1**	**0.14**	**0.09**	**0.03**	**0.06**	**0.16**	**0.14**	**4.98**	**h**	**77.98074**	**Moderately Low**	**22.5-35**	**70-100**	**d**	**WaulsortianLimestones**	**Tillderivedfrom Limestones**
007AL14A	**499201**	**610705**	**0.03**	**0.07**	**-0.06**	**-0.04**	**-0.04**	**0.07**	**0.03**	**-0.08**	**0**	**5.02**	**h**	**85.08491**	**Medium**	**35+**	**100-150**	**e**	**RockfieldLimestones**	**Tillderivedfrom Limestones**

Appendix A continued

L42AS231A	499439	609942	-0.02	0.14	0.07	0.09	0.12	-0.08	0.43	0.14	0.08	5.05	h	105.49	Medium	35+	100-150	e	WaulsortianLimestones	Tillderivedfrom Limestones
L11AS230A	499706	610203	0.11	0.07	0.12	0.13	0.09	0	0.24	0.15	0.08	5.1	l	47.72922	V.Low	35+	100-150	e	RockfieldLimestones	Tillderivedfrom Limestones
L10AS232A	499095	610262	-0.19	-0.32	-0.24	-0.39	-0.19	-0.48	0.31	-0.3	-0.4	5.12	m	54.84152	Low	35+	100-150	e	RockfieldLimestones	Tillderivedfrom Limestones
L51AS228A	499039	610999	-0.02	0.02	-0.02	-0.06	-0.01	0.03	0.03	-0.1	0	5.17	m	67.83768	Low	35+	100-150	e	CracoeanReefMember	Tillderivedfrom Limestones
L72AS213A	500077	611689	0	-0.28	-0.03	-0.07	-0.07	-0.18	0.26	-0.19	0	5.2	h	131.3447	Medium	35+	150-300	f	ClareShales	Tillderivedfrom Namurian sandstonessiltstones andshales
L46A06A	498979	610434	-0.06	-0.05	-0.03	-0.06	-0.14	-0.18	0.38	0.04	-0.1	5.28	l	72.93024	V.Low	35+	150-300	f	RockfieldLimestones	Tillderivedfrom Limestones
L57AS201A	498498	611514	-0.24	-0.5	-0.09	-0.26	-0.11	-0.04	-0.06	-0.38	-0.1	5.32	l	85.56022	Low	35+	150-300	f	DirtogeLimestones	Tillderivedfrom Namurian

Appendix A continued

																			sandstonessiltstonesandshales
004AL21	499139	611189	-0.04	-0.32	0.17	-0.31	-0.04	0.07	-0.11	-0.27	-0.1	5.43	l	110.3017	Low	35+	150-300	f	ClareShales	Tillderivedfrom Namurian sandstonessiltstonesandshales
L20005A	498874	610968	-0.14	-0.2	0.02	-0.06	0.02	0.1	-0.06	-0.16	0	5.47	l	100.4295	V.Low	35+	150-300	f	CracoeanReefMember	Tillderivedfrom Limestones
L70A010A	499208	611551	-0.02	-0.32	0.28	-0.15	-0.19	-0.08	-0.11	-0.34	-0.1	5.5	m	170.9383	Moderately Low	35+	300-600	g	ClareShales	Tillderivedfrom Namurian sandstonessiltstonesandshales
009AL66	499405	611904	-0.12	-0.37	-0.06	-0.13	-0.11	-0.08	0.06	-0.24	-0.1	5.55	l	133.6418	Low	35+	300-600	g	ClareShales	Tillderivedfrom Namurian sandstonessiltstonesandshales

03AL60	499886	611419	0.22	0.05	0.42	0.12	0.09	0.1	0.1	0.06	0	5.59	l	160.3374	V.Low	35+	300-600	g	ClareShales	Tillderivedfrom Namurian sandstonessiltstones andshales
L69AS227A	498681	611653	-0.02	-0.13	0.13	-0.02	-0.01	0.1	-0.11	0.01	0	5.67	E	479.9752	High	35+	300-600	g	DirtogeLimestones	Tillderivedfrom Namurian sandstonessiltstones andshales
002AL71A	499726	611673	0.22	-0.05	0.63	0.11	-0.01	0.18	0.1	0.11	-0.1	6.16	h	1778.419	High	35+	1200-1400+	h	ClareShales	Tillderivedfrom Namurian sandstonessiltstones andshales

Table 7.3.5 Deeper topsoil geochemistry from Castleisland Co. Kerry Ireland (Clr transformed)

sample	X.ITM	Y.ITM	Mo	Cu	Pb	Zn	Ni	Co	Mn	Fe	As	U	Th	Sr	Sb	V
009SL66S	499405	611904	-0.24778	-0.14065	-0.02921	-0.08092	-0.11445	-0.17576	-0.49862	-0.33828	-0.30919	-0.19803	-0.08552	0.2891	-0.21748	-0.04482
L59SS203S	499441	611393	0.47713	0.117756	0.054952	-0.08092	-0.15203	-0.17576	-0.17126	0.244989	0.283112	0.324845	-0.08552	0.38601	0.384579	0.540467
03SL60	499886	611419	0.713828	0.814638	0.170795	0.375008	0.454908	0.236906	0.389803	0.168178	0.414176	0.875073	0.064245	1.23849	0.928647	0.588952

L72SS213S	**500077**	**611689**	**0.143431**	**0.031646**	**-0.03195**	**-0.06072**	**0.026506**	**0.069415**	**-0.42399**	**-0.20126**	**-0.19897**	**-0.16327**	**0.026456**	**-0.01193**	**0.384579**	**-0.01927**
L68SS214S	**500327**	**611939**	**0.069645**	**-0.11499**	**-0.15142**	**-0.25702**	**-0.3101**	**-0.31594**	**-0.25172**	**0.255824**	**0.094504**	**-0.32297**	**0.115397**	**-0.31296**	**-0.04139**	**-0.04482**
L67SS221S	**499852**	**611939**	**0.143431**	**-0.00823**	**-0.06924**	**-0.08092**	**-0.24772**	**-0.26709**	**0.011168**	**0.25044**	**0.144809**	**-0.32297**	**0.099007**	**-0.23378**	**0.083549**	**-0.00703**
05SL20S	**498874**	**610968**	**0.572779**	**-0.11677**	**-0.09388**	**-0.36175**	**-0.38717**	**-0.43404**	**-0.47873**	**-0.1439**	**0.010727**	**0.023815**	**-0.13988**	**0.320508**	**0.595432**	**0.160939**
L51SS228S	**499039**	**610999**	**0.354284**	**0.071651**	**0.022248**	**0.204311**	**0.341146**	**0.372568**	**0.347444**	**0.131776**	**0.342951**	**0.227935**	**-0.06069**	**0.205554**	**0.326587**	**0.108761**
S207SL52S	**499579**	**610965**	**0.16976**	**0.059913**	**0.007441**	**-0.03208**	**-0.02526**	**-0.06995**	**-0.1089**	**0.067982**	**0.006082**	**-0.02194**	**-0.08552**	**0.178402**	**0.180459**	**0.070132**
001SL53S	**499956**	**610918**	**0.069645**	**0.459515**	**0.045856**	**0.073978**	**-0.09898**	**-0.12627**	**0.087895**	**0.146934**	**-0.00816**	**-0.19803**	**-0.13988**	**-0.10884**	**-0.51851**	**-0.04482**
L54SS205S	**500481**	**610939**	**-0.13127**	**0.2364**	**-0.0105**	**0.220106**	**0.182058**	**0.264935**	**0.495227**	**0.262022**	**0.078992**	**-0.27721**	**0.045761**	**-0.19902**	**-0.21748**	**-0.11618**
L57SS201S	**498498**	**611514**	**0.085439**	**-0.07425**	**0.145972**	**-0.66278**	**-0.60761**	**-0.98494**	**-0.51947**	**-0.69931**	**-0.29964**	**0.254264**	**-0.13988**	**0.63643**	**0.25964**	**0.427889**
L23SS206S	**500291**	**611248**	**0.053254**	**0.117756**	**0.349178**	**0.121901**	**-0.08194**	**-0.02011**	**0.474794**	**0.162688**	**0.082922**	**-0.16327**	**-0.03721**	**-0.10884**	**0.083549**	**-0.07198**
L61SS204S	**500452**	**611439**	**-0.58357**	**-0.13877**	**0.050428**	**0.134676**	**0.283042**	**0.102207**	**-0.23292**	**-0.08535**	**-0.64018**	**-0.49906**	**-0.01494**	**-0.10884**	**-0.21748**	**-0.10094**
L45SS233S	**498441**	**610459**	**-0.28254**	**-0.09584**	**-0.02378**	**-0.09139**	**-0.02343**	**0.005297**	**-0.35541**	**-0.17643**	**-0.4061**	**0.335569**	**0.161155**	**0.118404**	**-0.04139**	**-0.00703**
L13SS229S	**498681**	**610686**	**0.100679**	**-0.01951**	**-0.05163**	**0.073978**	**0.119823**	**0.060815**	**0.043503**	**0.059657**	**0.078992**	**-0.13109**	**-0.06069**	**0.029463**	**0.25964**	**-0.00703**
L9S008S	**498714**	**610184**	**-0.51662**	**0.04907**	**-0.09073**	**-0.47372**	**-0.46551**	**-0.43404**	**-0.35541**	**-0.70743**	**-0.60067**	**-0.10112**	**-0.23679**	**-0.03421**	**-0.21748**	**-0.26231**
L46S06S	**498979**	**610434**	**0.47713**	**0.428569**	**-0.03195**	**-0.07071**	**-0.28942**	**-0.14679**	**-0.44747**	**-0.30785**	**0.050436**	**0.980464**	**0.026456**	**0.178402**	**-0.04139**	**-0.00703**
007SL14S	**499201**	**610705**	**0.409133**	**0.127029**	**0.052696**	**-0.0052**	**-0.12585**	**-0.06995**	**0.387163**	**-0.01175**	**0.233499**	**-0.10112**	**-0.13988**	**-0.08251**	**0.083549**	**0.108761**
L47SS209S	**499445**	**610436**	**-0.18563**	**-0.473**	**-0.11333**	**-0.32396**	**-0.26967**	**-0.17576**	**-0.58053**	**-0.21952**	**-0.20653**	**0.214147**	**-0.06069**	**-0.08251**	**-0.51851**	**-0.14836**
L15SS210S	**499702**	**610679**	**-0.08297**	**-0.24711**	**-0.03471**	**-0.01398**	**0.080002**	**0.065136**	**-0.22202**	**0.120963**	**0.109481**	**0.065208**	**0.026456**	**-0.16683**	**-0.04139**	**-0.01927**
S230SL11S	**499706**	**610203**	**-0.18563**	**-0.25934**	**-0.0053**	**0.102006**	**0.245417**	**0.409119**	**0.006952**	**0.142326**	**0.050436**	**0.137758**	**0.081973**	**-0.16683**	**-0.51851**	**-0.11618**
L48SS211S	**499967**	**610434**	**-0.13127**	**0.104001**	**-0.0105**	**0.081156**	**0.203139**	**0.15072**	**-0.18095**	**0.137669**	**0.11678**	**0.065208**	**0.161155**	**-0.23378**	**-0.04139**	**-0.05819**
L49SS212S	**500457**	**610437**	**-0.08297**	**-0.07425**	**-0.01842**	**0.01183**	**0.074211**	**-0.0307**	**-0.14947**	**0.106114**	**0.066983**	**-0.32297**	**0.064245**	**-0.13687**	**0.180459**	**-0.10094**
L36SS236S	**498643**	**609431**	**0.018492**	**4.69E-05**	**0.072591**	**0.352731**	**0.177487**	**0.370445**	**0.907386**	**0.226306**	**0.15487**	**0.102996**	**0.045761**	**-0.13687**	**-0.04139**	**0.004865**
S235SL5S	**498694**	**609723**	**0.036221**	**0.006822**	**-0.06625**	**0.204311**	**0.225307**	**0.350849**	**0.702519**	**0.094634**	**0.17432**	**0.102996**	**0.026456**	**-0.03421**	**-0.04139**	**-0.05819**

L31SS223S	498861	608891	-0.24778	0.014816	0.024667	0.220106	0.28214	0.330327	0.493158	0.137669	0.086817	-0.43212	0.115397	-0.23378	0.083549	-0.13197
L41SS238S	498957	609921	-0.51662	-0.11145	-0.04591	-0.03208	0.107851	-0.04709	-0.38052	-0.27942	-0.5	-0.37413	0.026456	-0.16683	-0.04139	-0.11618
L42SS231S	499439	609942	0.182349	-0.15603	-0.05451	0.140924	0.081437	0.110033	-0.08209	0.258491	0.230724	0.254264	0.115397	-0.23378	-0.51851	-0.08622
S222SL32S	499452	608950	-0.1576	-0.00407	0.024667	0.128335	0.264637	0.253939	0.685537	0.035163	0.041921	-0.27721	0.115397	-0.16683	-0.04139	-0.11618
S216SL33S	499952	608939	-0.21559	-0.15996	-0.03748	0.165058	0.187706	0.259472	0.404468	0.169268	0.268048	0.084513	0.131191	-0.23378	-0.04139	-0.01927
S215SL34S	500537	609463	-0.36172	-0.32629	-0.09073	-0.07071	0.016635	0.065136	-0.36032	0.052595	0.001387	-0.16327	0.045761	-0.23378	-0.21748	-0.07198
L30SS224S	498528	608891	-0.24778	0.012168	-0.0105	0.159149	-0.03079	0.15072	0.606888	0.191544	0.11678	-0.37413	-0.03721	-0.27157	-0.04139	-0.14836
S232SL10S	499095	610262	0.100679	-0.13131	0.050428	-0.07071	-0.12354	-0.15386	-0.2441	-0.25273	-0.07031	0.394883	-0.16984	0.118404	-0.21748	-0.08622

Table 7.3.6 Deeper topsoil geochemistry and associated soil-gas radon, radon potential and bedrock group from Castleisland Co. Kerry Ireland

(Clr transformed)

sample	X.ITM	Y.ITM	Ca	P	La	Cr	Mg	Ba	Al	Na	K	Hg	Sc	Ga	Radon Conce.1	Radon Pote
009SL66S	499405	611904	-0.02911	-0.05094	0.0861	-0.13949	-0.20456	0.016272	-0.09323	-0.01732	0.046877	0.041941	-0.10573	-0.03611	351000	133.6418
L59SS203S	499441	611393	0.067804	0.2694	0.15865	0.073116	-0.04966	0.085353	0.020708	-0.01732	-0.01527	-0.02501	-0.0361	0.043071	81000	66.08537
03SL60	499886	611419	0.258135	0.921562	0.406435	0.194538	-0.04966	0.423105	0.114745	-0.18005	0.046877	0.310786	0.088841	-0.13302	393000	160.3374
L72SS213S	500077	611689	-0.33014	-0.21727	-0.0522	0.058875	0.029526	-0.21568	-0.00132	-0.22144	-0.05003	-0.02501	-0.18871	-0.03611	160000	131.3447
L68SS214S	500327	611939	-0.05714	-0.01315	-0.17714	0.073116	-0.20456	-0.13437	0.061667	0.009007	0.101234	0.099933	-0.0203	0.110018	63000	21.8299
L67SS221S	499852	611939	-0.27898	0.111792	-0.11019	0.028912	-0.14657	-0.07506	0.032479	-0.04535	0.126058	-0.02501	-0.00506	0.16801	20000	15.69528
05SL20S	498874	610968	-0.38813	-0.0816	0.123888	-0.24215	-0.30929	-0.11369	-0.44002	-0.37634	-0.28412	-0.10419	-0.35352	-0.43405	295000	100.4295
L51SS228S	499039	610999	0.045527	0.2694	0.0861	0.028912	0.064288	-0.03959	-0.02985	-0.01732	0.046877	-0.02501	0.037689	-0.03611	148000	67.83768
S207SL52S	499579	610965	-0.19183	0.377494	-0.00105	0.028912	0.080678	0.030995	0.011057	0.057312	0.193005	0.276024	-0.05249	0.043071	34000	18.02225

Appendix A continued

001SL53S	**499956**	**610918**	**0.022046**	**0.168935**	**-0.0522**	**0.100268**	**-0.00826**	**0.207086**	**0.061667**	**0.176498**	**0.126058**	**0.099933**	**-0.0203**	**0.16801**	**26000**	**21.06471**
L54SS205S	**500481**	**610939**	**-0.15405**	**0.22469**	**-0.11019**	**0.125822**	**0.282783**	**0.008719**	**0.165471**	**0.176498**	**0.171815**	**-0.10419**	**0.145323**	**0.110018**	**64000**	**52.37266**
L57SS201S	**498498**	**611514**	**-0.11928**	**0.125156**	**0.29998**	**-0.16297**	**-0.4476**	**0.144938**	**-0.17867**	**-0.04535**	**0.149539**	**-0.02501**	**-0.29137**	**-0.03611**	**209000**	**85.56022**
L23SS206S	**500291**	**611248**	**0.088993**	**0.419556**	**-0.0522**	**0.044152**	**0.096472**	**0.045235**	**0.063833**	**0.079588**	**-0.01527**	**0.041941**	**0.00966**	**0.110018**	**34000**	**27.02616**
L61SS204S	**500452**	**611439**	**0.109196**	**-0.21727**	**-0.17714**	**0.113233**	**0.292767**	**-0.06592**	**0.17561**	**0.120981**	**0.126058**	**-0.10419**	**-0.0203**	**0.110018**	**27000**	**21.39514**
L45SS233S	**498441**	**610459**	**0.258135**	**-0.24723**	**-0.00105**	**-0.02031**	**0.111712**	**0.110176**	**0.061667**	**-0.01732**	**-0.12921**	**0.099933**	**0.100741**	**0.043071**	**57000**	**46.42497**
L13SS229S	**498681**	**610686**	**-0.15405**	**-0.06092**	**-0.00105**	**-0.02031**	**0.080678**	**-0.11369**	**-0.01925**	**-0.04535**	**-0.05003**	**-0.2011**	**-0.06952**	**-0.03611**	**49000**	**39.56862**
L9S008S	**498714**	**610184**	**0.357838**	**-0.0816**	**-0.0522**	**-0.3043**	**-0.50559**	**-0.21568**	**-0.23936**	**-0.2672**	**-0.28412**	**-0.02501**	**-0.26334**	**-0.13302**	**76000**	**62.20285**
L46S06S	**498979**	**610434**	**0.482777**	**0.287883**	**-0.00105**	**-0.13949**	**-0.30929**	**-0.03115**	**-0.24373**	**0.297072**	**-0.43024**	**0.276024**	**0.088841**	**-0.43405**	**192000**	**72.93024**
007SL14S	**499201**	**610705**	**0.067804**	**0.15071**	**0.044707**	**-0.07582**	**-0.12024**	**-0.03115**	**-0.12542**	**-0.04535**	**0.101234**	**-0.02501**	**-0.14524**	**-0.03611**	**104000**	**85.08491**
L47SS209S	**499445**	**610436**	**-0.00278**	**-0.35197**	**-0.0522**	**-0.21413**	**-0.2715**	**-0.02288**	**-0.03254**	**0.100777**	**0.046877**	**-0.10419**	**-0.06952**	**0.043071**	**23000**	**8.553076**
L15SS210S	**499702**	**610679**	**0.045527**	**-0.35197**	**-0.11019**	**0.044152**	**0.193382**	**-0.06592**	**0.099093**	**0.120981**	**0.074905**	**-0.10419**	**-0.0203**	**0.219162**	**60000**	**22.33727**
S230SL11S	**499706**	**610203**	**-0.02911**	**-0.46394**	**-0.17714**	**0.044152**	**0.205617**	**0.150471**	**0.097097**	**0.057312**	**-0.12921**	**-0.2011**	**0.100741**	**0.043071**	**126000**	**47.72922**
L48SS211S	**499967**	**610434**	**-0.33014**	**-0.43912**	**-0.00105**	**0.149956**	**0.262098**	**-0.03115**	**0.091051**	**0.033831**	**0.074905**	**-0.10419**	**0.166007**	**0.043071**	**67000**	**25.27739**
L49SS212S	**500457**	**610437**	**-0.23323**	**-0.24723**	**-0.00105**	**0.028912**	**0.111712**	**-0.20309**	**-0.07501**	**-0.14226**	**-0.05003**	**-0.10419**	**-0.0361**	**-0.03611**	**24000**	**12.45174**
L36SS236S	**498643**	**609431**	**-0.0871**	**0.250095**	**0.044707**	**0.113233**	**0.111712**	**0.166658**	**0.127993**	**0.057312**	**0.046877**	**-0.10419**	**0.204637**	**0.110018**	**86000**	**70.1331**
S235SL5S	**498694**	**609723**	**-0.33014**	**-0.02229**	**-0.00105**	**-0.02031**	**0.126436**	**0.038174**	**-0.00637**	**-0.01732**	**0.016914**	**-0.10419**	**0.076607**	**-0.03611**	**75000**	**61.21157**
L31SS223S	**498861**	**608891**	**-0.27898**	**-0.05094**	**0.0861**	**0.044152**	**0.126436**	**-0.07506**	**0.076607**	**0.057312**	**0.101234**	**-0.02501**	**0.155788**	**0.043071**	**44000**	**35.93392**
L41SS238S	**498957**	**609921**	**0.164714**	**-0.31418**	**-0.11019**	**0.028912**	**0.154464**	**-0.12391**	**0.089017**	**0.120981**	**0.149539**	**-0.2011**	**-0.08725**	**0.110018**	**42000**	**33.45572**
L42SS231S	**499439**	**609942**	**0.243895**	**-0.27941**	**-0.17714**	**0.028912**	**0.180793**	**0.052184**	**0.086973**	**0.120981**	**0.016914**	**0.519062**	**0.123603**	**0.043071**	**111000**	**105.49**
S222SL32S	**499452**	**608950**	**-0.23323**	**-0.09233**	**0.190835**	**-0.03803**	**0.096472**	**0.001032**	**0.03015**	**-0.1075**	**0.046877**	**-0.2011**	**0.134599**	**-0.13302**	**62000**	**23.40641**

Appendix A continued

S216SL33S	**499952**	**608939**	**0.243895**	**-0.16291**	**0.220798**	**0.100268**	**0.011042**	**0.127905**	**0.10699**	**-0.1075**	**-0.17497**	**0.041941**	**0.222735**	**0.043071**	**35000**	**27.83846**
S215SL34S	**500537**	**609463**	**0.198137**	**-0.35197**	**-0.11019**	**0.028912**	**0.080678**	**0.023696**	**0.061667**	**0.079588**	**-0.01527**	**-0.10419**	**0.088841**	**0.043071**	**36000**	**13.40236**
L30SS224S	**498528**	**608891**	**-0.05714**	**0.296838**	**-0.11019**	**0.013118**	**0.047254**	**0.001032**	**-0.00132**	**0.079588**	**0.101234**	**-0.10419**	**0.076607**	**0.043071**	**25500**	**13.38016**
S232SL10S	**499095**	**610262**	**0.630097**	**0.22469**	**-0.11019**	**-0.11722**	**-0.12024**	**-0.07506**	**-0.14946**	**-0.07531**	**-0.28412**	**0.342971**	**-0.0361**	**-0.13302**	**131000**	**54.84152**

Appendix A continued

Table 7.3.7 TELLUS Midlands topsoil (Clr transformed) correlation table

	Al	Ba	Ca	Cr	Cu	Fe	K	Li	Mg	Mn	Na	Ni	P
Al	1	0.675703	-0.03039	0.925849	0.556965	0.821952	0.862857	0.944509	0.689075	0.615059	0.100849	0.723053	0.488768
Ba	0.675703	1	0.209561	0.682677	0.532908	0.72563	0.669882	0.649655	0.56551	0.569931	0.11272	0.625827	0.489074
Ca	-0.03039	0.209561	1	0.100346	0.192978	0.085051	-0.08897	0.008017	0.181769	0.109314	-0.19571	0.272758	0.305814
Cr	0.925849	0.682677	0.100346	1	0.615897	0.809476	0.799203	0.877219	0.695484	0.644203	0.039298	0.818653	0.536829
Cu	0.556965	0.532908	0.192978	0.615897	1	0.593122	0.538514	0.531671	0.381015	0.53526	-0.13751	0.677219	0.658448
Fe	0.821952	0.72563	0.085051	0.809476	0.593122	1	0.749324	0.77311	0.60284	0.723484	0.045402	0.756448	0.553495
K	0.862857	0.669882	-0.08897	0.799203	0.538514	0.749324	1	0.852809	0.649754	0.645979	0.10987	0.689401	0.470354
Li	0.944509	0.649655	0.008017	0.877219	0.531671	0.77311	0.852809	1	0.717675	0.604576	0.058632	0.710421	0.491019
Mg	0.689075	0.56551	0.181769	0.695484	0.381015	0.60284	0.649754	0.717675	1	0.412886	0.347252	0.580139	0.376268
Mn	0.615059	0.569931	0.109314	0.644203	0.53526	0.723484	0.645979	0.604576	0.412886	1	-0.14994	0.744108	0.522275
Na	0.100849	0.11272	-0.19571	0.039298	-0.13751	0.045402	0.10987	0.058632	0.347252	-0.14994	1	-0.12306	-0.19126
Ni	0.723053	0.625827	0.272758	0.818653	0.677219	0.756448	0.689401	0.710421	0.580139	0.744108	-0.12306	1	0.538622
P	0.488768	0.489074	0.305814	0.536829	0.658448	0.553495	0.470354	0.491019	0.376268	0.522275	-0.19126	0.538622	1
S	-0.50965	-0.25887	0.361627	-0.48655	-0.34057	-0.36083	-0.6016	-0.50583	-0.1677	-0.50538	0.200243	-0.44685	-0.07587
Sr	-0.22389	0.019881	0.761362	-0.07505	0.082904	-0.09479	-0.28455	-0.21646	0.102948	-0.09603	0.034548	0.126811	0.114068
Ti	0.505633	0.42973	-0.06625	0.56636	0.329239	0.462359	0.470685	0.483188	0.366995	0.451097	0.013726	0.411231	0.322778
V	0.88324	0.636827	0.056253	0.937219	0.617091	0.788546	0.745903	0.803708	0.593712	0.623618	0.022682	0.773947	0.52985
Zn	0.666329	0.617608	0.161326	0.742552	0.602934	0.668066	0.664506	0.661569	0.565451	0.749247	-0.03532	0.83668	0.547703
Zr	0.60653	0.581382	0.386915	0.662526	0.596438	0.624825	0.587917	0.608673	0.454377	0.643078	-0.22015	0.817318	0.502816
Ag	0.558135	0.460589	0.094699	0.613176	0.529958	0.487196	0.478564	0.506277	0.303128	0.547718	-0.10516	0.615708	0.480662
As	0.543969	0.583023	0.227705	0.579829	0.60961	0.732392	0.544822	0.538431	0.369744	0.669356	-0.14467	0.685379	0.532577
Be	0.834424	0.672666	0.191782	0.839019	0.628324	0.784097	0.757051	0.796959	0.58017	0.712629	-0.00247	0.854156	0.529595
Bi	0.593821	0.403442	-0.09399	0.555571	0.368427	0.550651	0.521012	0.543069	0.474188	0.399427	0.330922	0.457157	0.337057
Cd	0.370814	0.4523	0.456417	0.519004	0.559742	0.434818	0.309095	0.345688	0.257795	0.565568	-0.2456	0.722495	0.495715
Ce	0.862413	0.639035	0.061528	0.833158	0.523771	0.752654	0.826955	0.834385	0.615711	0.658726	-0.023	0.726643	0.489105
Co	0.805171	0.665263	0.079639	0.827669	0.645205	0.84807	0.786008	0.784508	0.594207	0.833647	-0.05416	0.899449	0.516658
Cs	0.810355	0.585262	-0.16744	0.733376	0.396987	0.627484	0.764977	0.799945	0.469666	0.591914	-0.00524	0.546225	0.359905
Ga	0.971263	0.66538	-0.08007	0.900904	0.525637	0.794022	0.856721	0.931532	0.675112	0.580125	0.120227	0.666554	0.469086
Ge	0.67997	0.57312	0.176911	0.705743	0.48171	0.709917	0.594692	0.629171	0.577716	0.532671	0.161811	0.668983	0.45988
Hf	0.644349	0.596345	0.332923	0.679279	0.583807	0.635222	0.626095	0.650823	0.483851	0.642813	-0.18771	0.80434	0.500262
Hg	-0.07335	0.161674	0.237827	-0.02715	0.088361	0.060748	-0.15444	-0.09011	0.02293	-0.0181	0.115572	0.035481	0.185127
In	0.795851	0.545937	-0.00224	0.759844	0.483907	0.719868	0.687565	0.737767	0.592071	0.528895	0.167532	0.658095	0.424204
La	0.798327	0.600778	0.181308	0.808489	0.526321	0.692363	0.745301	0.771401	0.566708	0.643252	-0.09899	0.743066	0.512169
Mo	0.466028	0.486376	0.124713	0.532901	0.534654	0.672536	0.453901	0.42369	0.274537	0.651614	-0.08991	0.65886	0.452388
Nb	0.760345	0.593985	0.032137	0.797203	0.463117	0.660849	0.677277	0.731397	0.548103	0.577658	0.022178	0.638102	0.451821
Pb	0.351828	0.423075	-0.0065	0.358057	0.257673	0.369023	0.337106	0.316806	0.343722	0.319653	0.334959	0.319669	0.227596
Rb	0.880112	0.607833	-0.14775	0.808226	0.515516	0.749862	0.942436	0.872952	0.608232	0.695649	0.042819	0.674548	0.478302
Sb	0.332336	0.452866	0.145124	0.432732	0.485897	0.447469	0.370896	0.289984	0.367842	0.495716	0.148656	0.574211	0.342933
Sc	0.83416	0.659189	0.198064	0.843957	0.596755	0.774575	0.755544	0.799219	0.59304	0.671774	-0.04846	0.863678	0.45294
Se	-0.23215	0.078021	0.308622	-0.16076	0.014798	-6.84E-05	-0.32761	-0.27557	0.003177	-0.18326	0.23837	-0.04219	0.007714
Sn	0.53384	0.436313	-0.02403	0.511296	0.464853	0.486766	0.45993	0.500469	0.406962	0.37993	0.199885	0.415945	0.428691
Te	0.65159	0.57252	0.15765	0.685305	0.628958	0.744663	0.614639	0.616213	0.502419	0.715979	-0.04281	0.821872	0.518853
Th	0.80089	0.615113	0.079643	0.748548	0.495608	0.711586	0.785461	0.779489	0.519885	0.601037	-0.04252	0.71661	0.35778
Tl	0.752522	0.533701	0.062407	0.788842	0.547547	0.642258	0.692213	0.719871	0.440331	0.696517	-0.12926	0.784622	0.455352
U	0.364985	0.432737	0.327328	0.417834	0.541459	0.439065	0.239126	0.338479	0.162423	0.295609	-0.18253	0.432368	0.499618
W	0.477533	0.398382	0.043187	0.534346	0.35893	0.440308	0.417894	0.444671	0.338959	0.392828	0.044816	0.441321	0.399673
Y	0.573462	0.462336	0.405443	0.660521	0.550763	0.551906	0.495659	0.552864	0.351671	0.656347	-0.31966	0.78853	0.508157

	S	Sr	Ti	V	Zn	Zr	Ag	As	Be	Bi	Cd	Ce	Co	Cs	Ga	Ge	Hf	Hg	In
Al	-0.50965	-0.22389	0.505633	0.88324	0.666329	0.60653	0.558135	0.543969	0.834424	0.593821	0.370814	0.862413	0.805171	0.810355	0.971263	0.67997	0.644349	-0.07335	0.795851
Ba	-0.25887	0.019881	0.42973	0.636827	0.617608	0.581382	0.460589	0.583023	0.672666	0.403442	0.4523	0.639035	0.665263	0.585262	0.66538	0.57312	0.596345	0.161674	0.545937
Ca	0.361627	0.761362	-0.06625	0.056253	0.161326	0.386915	0.094699	0.227705	0.191782	-0.09399	0.456417	0.061528	0.079639	-0.16744	-0.08007	0.176911	0.332923	0.237827	-0.00224
Cr	-0.48655	-0.07505	0.56636	0.937219	0.742552	0.662526	0.613176	0.579829	0.839019	0.555571	0.519004	0.833158	0.827669	0.733376	0.900904	0.705743	0.679279	-0.02715	0.759844
Cu	-0.34057	0.082904	0.329239	0.617091	0.602934	0.596438	0.529958	0.60961	0.628324	0.368427	0.559742	0.523771	0.645205	0.396987	0.525637	0.48171	0.583807	0.088361	0.483907
Fe	-0.36083	-0.09479	0.462359	0.788546	0.668066	0.624825	0.487196	0.732392	0.784097	0.550651	0.434818	0.752654	0.84807	0.627484	0.794022	0.709917	0.635222	0.060748	0.719868
K	-0.6016	-0.28455	0.470685	0.745903	0.664506	0.587917	0.478564	0.544822	0.757051	0.521012	0.309095	0.826955	0.786008	0.764977	0.856721	0.594692	0.626095	-0.15444	0.687565
Li	-0.50583	-0.21646	0.483188	0.803708	0.661569	0.608673	0.506277	0.538431	0.796959	0.543069	0.345688	0.834385	0.784508	0.799945	0.931532	0.629171	0.650823	-0.09011	0.737767
Mg	-0.1677	0.102948	0.366995	0.593712	0.565451	0.454377	0.303128	0.369744	0.58017	0.474188	0.257795	0.615711	0.594207	0.469666	0.675112	0.577716	0.483851	0.02293	0.592071
Mn	-0.50538	-0.09603	0.451097	0.623618	0.749247	0.643078	0.547718	0.669356	0.712629	0.399427	0.565568	0.658726	0.833647	0.591914	0.580125	0.532671	0.642813	-0.0181	0.528895
Na	0.200243	0.034548	0.013726	0.022682	-0.03532	-0.22015	-0.10516	-0.14467	-0.00247	0.330922	-0.2456	-0.023	-0.05416	-0.00524	0.120227	0.161811	-0.18771	0.115572	0.167532
Ni	-0.44685	0.126811	0.411231	0.773947	0.83668	0.817318	0.615708	0.685379	0.854156	0.457157	0.722495	0.726643	0.899449	0.546225	0.666554	0.668983	0.80434	0.035481	0.658095
P	-0.07587	0.114068	0.322778	0.52985	0.547703	0.502816	0.480662	0.532577	0.529595	0.337057	0.495715	0.489105	0.516658	0.359905	0.469086	0.45988	0.500262	0.185127	0.424204
S	1	0.460343	-0.38715	-0.47899	-0.4441	-0.35456	-0.35846	-0.30332	-0.41445	-0.13328	-0.1834	-0.45896	-0.53854	-0.57076	-0.50595	-0.14342	-0.39031	0.43554	-0.30996
Sr	0.460343	1	-0.211	-0.07583	0.041501	0.198877	0.030387	0.063538	0.025068	-0.0562	0.362787	-0.19011	-0.09226	-0.38268	-0.26659	0.06087	0.140286	0.307209	-0.0859
Ti	-0.38715	-0.211	1	0.536185	0.395908	0.236603	0.39697	0.273392	0.417196	0.300889	0.267682	0.548518	0.449776	0.512152	0.533024	0.392617	0.233959	-0.02021	0.329446
V	-0.47899	-0.07583	0.536185	1	0.701097	0.621444	0.651148	0.583321	0.809595	0.55033	0.538927	0.761788	0.789577	0.694663	0.861902	0.668824	0.628528	-0.02092	0.733621
Zn	-0.4441	0.041501	0.395908	0.701097	1	0.710578	0.656455	0.637022	0.762235	0.484062	0.710743	0.633751	0.813554	0.590556	0.628637	0.606356	0.728534	0.076799	0.620512
Zr	-0.35456	0.198877	0.236603	0.621444	0.710578	1	0.588095	0.683601	0.806476	0.356997	0.724972	0.659867	0.716911	0.488555	0.547174	0.59195	0.973393	0.062622	0.568051
Ag	-0.35846	0.030387	0.39697	0.651148	0.656455	0.588095	1	0.555819	0.67552	0.50728	0.686532	0.532875	0.558068	0.512791	0.537182	0.547866	0.584745	0.196471	0.582063
As	-0.30332	0.063538	0.273392	0.583321	0.637022	0.683601	0.555819	1	0.694086	0.439138	0.618356	0.559013	0.704753	0.48252	0.513596	0.569188	0.671695	0.160067	0.555528
Be	-0.41445	0.025068	0.417196	0.809595	0.762235	0.806476	0.67552	0.694086	1	0.591988	0.67273	0.824698	0.838145	0.689534	0.779438	0.744578	0.807843	0.061446	0.757982
Bi	-0.13328	-0.0562	0.300889	0.55033	0.484062	0.356997	0.50728	0.439138	0.591988	1	0.304983	0.505824	0.510777	0.485398	0.600948	0.633507	0.38386	0.28319	0.732042
Cd	-0.1834	0.362787	0.267682	0.538927	0.710743	0.724972	0.686532	0.618356	0.67273	0.304983	1	0.419341	0.562577	0.302954	0.314755	0.529426	0.684305	0.259443	0.431535
Ce	-0.45896	-0.19011	0.548518	0.761788	0.633751	0.659867	0.532875	0.559013	0.824698	0.505824	0.419341	1	0.777881	0.733649	0.834869	0.741094	0.674385	-0.04698	0.719288
Co	-0.53854	-0.09226	0.449776	0.789577	0.813554	0.716911	0.558068	0.704753	0.838145	0.510777	0.562577	0.777881	1	0.665645	0.762546	0.651058	0.729324	-0.03023	0.70334
Cs	-0.57076	-0.38268	0.512152	0.694663	0.590556	0.488555	0.512791	0.48252	0.689534	0.485398	0.302954	0.733649	0.665645	1	0.822499	0.508802	0.526717	-0.09652	0.60485
Ga	-0.50595	-0.26659	0.533024	0.861902	0.628637	0.547174	0.537182	0.513596	0.779438	0.600948	0.314755	0.834869	0.762546	0.822499	1	0.646998	0.589928	-0.05402	0.77396
Ge	-0.14342	0.06087	0.392617	0.668824	0.606356	0.59195	0.547866	0.569188	0.744578	0.633507	0.529426	0.741094	0.651058	0.508802	0.646998	1	0.588338	0.239807	0.739518
Hf	-0.39031	0.140286	0.233959	0.628528	0.728534	0.973393	0.584745	0.671695	0.807843	0.38386	0.684305	0.674385	0.729324	0.526717	0.589928	0.588338	1	0.045465	0.602193
Hg	0.43554	0.307209	-0.02021	-0.02092	0.076799	0.062622	0.196471	0.160067	0.061446	0.28319	0.259443	-0.04698	-0.03023	-0.09652	-0.05402	0.239807	0.045465	1	0.12589
In	-0.30996	-0.0859	0.329446	0.733621	0.620512	0.568051	0.582063	0.555528	0.757982	0.732042	0.431535	0.719288	0.70334	0.60485	0.77396	0.739518	0.602193	0.12589	1
La	-0.39412	-0.07416	0.522036	0.742616	0.625503	0.714635	0.585132	0.568869	0.831027	0.472622	0.520306	0.96124	0.733877	0.669029	0.764554	0.752083	0.712126	0.007131	0.683479
Mo	-0.30619	0.089741	0.292536	0.589799	0.637361	0.528164	0.500889	0.675188	0.587839	0.349816	0.583734	0.405266	0.665002	0.36636	0.429523	0.439179	0.513216	0.076712	0.451156
Nb	-0.42637	-0.13992	0.794052	0.781898	0.604914	0.482951	0.552146	0.452924	0.698772	0.49439	0.429048	0.747449	0.659499	0.705243	0.766572	0.589648	0.486642	0.017228	0.590533
Pb	-0.03058	0.016895	0.222203	0.344113	0.475946	0.277426	0.456215	0.402024	0.427411	0.631299	0.34682	0.328591	0.361307	0.359198	0.363023	0.508306	0.293797	0.458308	0.502374
Rb	-0.62641	-0.35613	0.487162	0.755021	0.676711	0.564288	0.48796	0.53231	0.751772	0.519828	0.290654	0.835215	0.797893	0.835035	0.875733	0.581639	0.605034	-0.19158	0.691115
Sb	-0.18612	0.189683	0.199771	0.462036	0.634873	0.46646	0.515928	0.562704	0.494682	0.523667	0.598731	0.278747	0.527654	0.272273	0.309572	0.521127	0.4641	0.326287	0.477905
Sc	-0.47743	0.035656	0.346486	0.804486	0.754386	0.865666	0.620733	0.663186	0.904491	0.50174	0.633946	0.798294	0.840061	0.652257	0.787513	0.692167	0.87628	0.006833	0.752715
Se	0.629444	0.511597	-0.19459	-0.10902	-0.06555	-0.00663	0.032545	0.058254	-0.04852	0.15298	0.213447	-0.25871	-0.14639	-0.34459	-0.24389	0.118427	-0.05223	0.550504	-0.00196
Sn	-0.17259	-0.02965	0.326339	0.509111	0.488797	0.345679	0.47344	0.411765	0.492176	0.674254	0.312906	0.428318	0.45243	0.442136	0.549451	0.533285	0.36802	0.314912	0.592927
Te	-0.33423	0.082029	0.306816	0.692219	0.759765	0.708526	0.635631	0.70595	0.780593	0.6084	0.660681	0.612688	0.808507	0.517323	0.611805	0.664941	0.701715	0.196957	0.693498
Th	-0.52793	-0.10784	0.327121	0.702588	0.635613	0.818356	0.511421	0.603463	0.822781	0.461594	0.474063	0.795344	0.751258	0.695867	0.764324	0.599844	0.844753	-0.1033	0.676673
Tl	-0.54766	-0.08443	0.428779	0.790194	0.782793	0.691323	0.705829	0.626989	0.816077	0.472396	0.66112	0.715412	0.774529	0.732888	0.71838	0.598	0.700981	-0.03991	0.635303
U	-0.04169	0.249311	0.241686	0.457888	0.310964	0.43142	0.381212	0.463803	0.468123	0.178103	0.502977	0.344192	0.372614	0.254619	0.338495	0.347984	0.395647	0.186591	0.27627
W	-0.24705	-0.00604	0.493874	0.601561	0.448356	0.358163	0.518808	0.396299	0.500205	0.507215	0.410157	0.448536	0.418698	0.451143	0.486119	0.491696	0.350088	0.146661	0.47389
Y	-0.31972	0.182791	0.350702	0.632003	0.66508	0.840873	0.651949	0.626993	0.817758	0.317924	0.798053	0.715439	0.670842	0.476771	0.502858	0.629426	0.803303	0.086962	0.539847

	La	Mo	Nb	Pb	Rb	Sb	Sc	Se	Sn	Te	Th	Tl	U	W	Y
Al	0.798327	0.466028	0.760345	0.351828	0.880112	0.332336	0.83416	-0.23215	0.53384	0.65159	0.80089	0.752522	0.364985	0.477533	0.573462
Ba	0.600778	0.486376	0.593985	0.423075	0.607833	0.452866	0.659189	0.078021	0.436313	0.57252	0.615113	0.533701	0.432737	0.398382	0.462336
Ca	0.181308	0.124713	0.032137	-0.0065	-0.14775	0.145124	0.198064	0.308622	-0.02403	0.15765	0.079643	0.062407	0.327328	0.043187	0.405443
Cr	0.808489	0.532901	0.797203	0.358057	0.808226	0.432732	0.843957	-0.16076	0.511296	0.685305	0.748548	0.788842	0.417834	0.534346	0.660521
Cu	0.526321	0.534654	0.463117	0.257673	0.515516	0.485897	0.596755	0.014798	0.464853	0.628958	0.495608	0.547547	0.541459	0.35893	0.550763
Fe	0.692363	0.672536	0.660849	0.369023	0.749862	0.447469	0.774575	-6.84E-05	0.486766	0.744663	0.711586	0.642258	0.439065	0.440308	0.551906
K	0.745301	0.453901	0.677277	0.337106	0.942436	0.370896	0.755544	-0.32761	0.45993	0.614639	0.785461	0.692213	0.239126	0.417894	0.495659
Li	0.771401	0.42369	0.731397	0.316806	0.872952	0.289984	0.799219	-0.27557	0.500469	0.616213	0.779489	0.719871	0.338479	0.444671	0.552864
Mg	0.566708	0.274537	0.548103	0.343722	0.608232	0.367842	0.59304	0.003177	0.406962	0.502419	0.519885	0.440331	0.162423	0.338959	0.351671
Mn	0.643252	0.651614	0.577658	0.319653	0.695649	0.495716	0.671774	-0.18326	0.37993	0.715979	0.601037	0.696517	0.295609	0.392828	0.656347
Na	-0.09899	-0.08991	0.022178	0.334959	0.042819	0.148656	-0.04846	0.23837	0.199885	-0.04281	-0.04252	-0.12926	-0.18253	0.044816	-0.31966
Ni	0.743066	0.65886	0.638102	0.319669	0.674548	0.574211	0.863678	-0.04219	0.415945	0.821872	0.71661	0.784622	0.432368	0.441321	0.78853
P	0.512169	0.452388	0.451821	0.227596	0.478302	0.342933	0.45294	0.007714	0.428691	0.518853	0.35778	0.455352	0.499618	0.399673	0.508157
S	-0.39412	-0.30619	-0.42637	-0.03058	-0.62641	-0.18612	-0.47743	0.629444	-0.17259	-0.33423	-0.52793	-0.54766	-0.04169	-0.24705	-0.31972
Sr	-0.07416	0.089741	-0.13992	0.016895	-0.35613	0.189683	0.035656	0.511597	-0.02965	0.082029	-0.10784	-0.08443	0.249311	-0.00604	0.182791
Ti	0.522036	0.292536	0.794052	0.222203	0.487162	0.199771	0.346486	-0.19459	0.326339	0.306816	0.327121	0.428779	0.241686	0.493874	0.350702
V	0.742616	0.589799	0.781898	0.344113	0.755021	0.462036	0.804486	-0.10902	0.509111	0.692219	0.702588	0.790194	0.457888	0.601561	0.632003
Zn	0.625503	0.637361	0.604914	0.475946	0.676711	0.634873	0.754386	-0.06555	0.488797	0.759765	0.635613	0.782793	0.310964	0.448356	0.66508
Zr	0.714635	0.528164	0.482951	0.277426	0.564288	0.46646	0.865666	-0.00663	0.345679	0.708526	0.818356	0.691323	0.43142	0.358163	0.840873
Ag	0.585132	0.500889	0.552146	0.456215	0.48796	0.515928	0.620733	0.032545	0.47344	0.635631	0.511421	0.705829	0.381212	0.518808	0.651949
As	0.568869	0.675188	0.452924	0.402024	0.53231	0.562704	0.663186	0.058254	0.411765	0.70595	0.603463	0.626989	0.463803	0.396299	0.626993
Be	0.831027	0.587839	0.698772	0.427411	0.751772	0.494682	0.904491	-0.04852	0.492176	0.780593	0.822781	0.816077	0.468123	0.500205	0.817758
Bi	0.472622	0.349816	0.49439	0.631299	0.519828	0.523667	0.50174	0.15298	0.674254	0.6084	0.461594	0.472396	0.178103	0.507215	0.317924
Cd	0.520306	0.583734	0.429048	0.34682	0.290654	0.598731	0.633946	0.213447	0.312906	0.660681	0.474063	0.66112	0.502977	0.410157	0.798053
Ce	0.96124	0.405266	0.747449	0.328591	0.835215	0.278747	0.798294	-0.25871	0.428318	0.612688	0.795344	0.715412	0.344192	0.448536	0.715439
Co	0.733877	0.665002	0.659499	0.361307	0.797893	0.527654	0.840061	-0.14639	0.45243	0.808507	0.751258	0.774529	0.372614	0.418698	0.670842
Cs	0.669029	0.36636	0.705243	0.359198	0.835035	0.272273	0.652257	-0.34459	0.442136	0.517323	0.695867	0.732888	0.254619	0.451143	0.476771
Ga	0.764554	0.429523	0.766572	0.363023	0.875733	0.309572	0.787513	-0.24389	0.549451	0.611805	0.764324	0.71838	0.338495	0.486119	0.502858
Ge	0.752083	0.439179	0.589648	0.508306	0.581639	0.521127	0.692167	0.118427	0.533285	0.664941	0.599844	0.598	0.347984	0.491696	0.629426
Hf	0.712126	0.513216	0.486642	0.293797	0.605034	0.4641	0.87628	-0.05223	0.36802	0.701715	0.844753	0.700981	0.395647	0.350088	0.803303
Hg	0.007131	0.076712	0.017228	0.458308	-0.19158	0.326287	0.006833	0.550504	0.314912	0.196957	-0.1033	-0.03991	0.186591	0.146661	0.086962
In	0.683479	0.451156	0.590533	0.502374	0.691115	0.477905	0.752715	-0.00196	0.592927	0.693498	0.676673	0.635303	0.27627	0.47389	0.539847
La	1	0.383069	0.722009	0.302274	0.749616	0.284368	0.802778	-0.21283	0.394045	0.607532	0.765974	0.723348	0.372601	0.456986	0.821574
Mo	0.383069	1	0.420629	0.288133	0.462341	0.575607	0.566708	0.167586	0.34432	0.691304	0.471252	0.607524	0.481609	0.358106	0.478395
Nb	0.722009	0.420629	1	0.337686	0.692349	0.307708	0.617498	-0.17403	0.45852	0.535589	0.573012	0.65854	0.358625	0.640563	0.559212
Pb	0.302274	0.288133	0.337686	1	0.315544	0.632308	0.33911	0.229611	0.616389	0.447022	0.29956	0.360221	0.111445	0.373703	0.228615
Rb	0.749616	0.462341	0.692349	0.315544	1	0.318012	0.735507	-0.40276	0.474717	0.611252	0.76163	0.733297	0.231548	0.417317	0.507086
Sb	0.284368	0.575607	0.307708	0.632308	0.318012	1	0.468917	0.259348	0.513791	0.656353	0.338097	0.474334	0.247543	0.391092	0.371466
Sc	0.802778	0.566708	0.617498	0.33911	0.735507	0.468917	1	-0.08382	0.425651	0.756357	0.906979	0.789761	0.403662	0.403323	0.796127
Se	-0.21283	0.167586	-0.17403	0.229611	-0.40276	0.259348	-0.08382	1	0.089106	0.137067	-0.18524	-0.1704	0.298859	0.007076	-0.07084
Sn	0.394045	0.34432	0.45852	0.616389	0.474717	0.513791	0.425651	0.089106	1	0.498275	0.367085	0.407898	0.233823	0.468515	0.263628
Te	0.607532	0.691304	0.535589	0.447022	0.611252	0.656353	0.756357	0.137067	0.498275	1	0.634064	0.701938	0.386159	0.478327	0.65287
Th	0.765974	0.471252	0.573012	0.29956	0.76163	0.338097	0.906979	-0.18524	0.367085	0.634064	1	0.727562	0.358162	0.351267	0.679325
Tl	0.723348	0.607524	0.65854	0.360221	0.733297	0.474334	0.789761	-0.1704	0.407898	0.701938	0.727562	1	0.406535	0.475725	0.74017
U	0.372601	0.481609	0.358625	0.111445	0.231548	0.247543	0.403662	0.298859	0.233823	0.386159	0.358162	0.406535	1	0.308927	0.451794
W	0.456986	0.358106	0.640563	0.373703	0.417317	0.391092	0.403323	0.007076	0.468515	0.478327	0.351267	0.475725	0.308927	1	0.392539
Y	0.821574	0.478395	0.559212	0.228615	0.507086	0.371466	0.796127	-0.07084	0.263628	0.65287	0.679325	0.74017	0.451794	0.392539	1

7.3.8 Castleisland topsoil plots

Appendix A continued

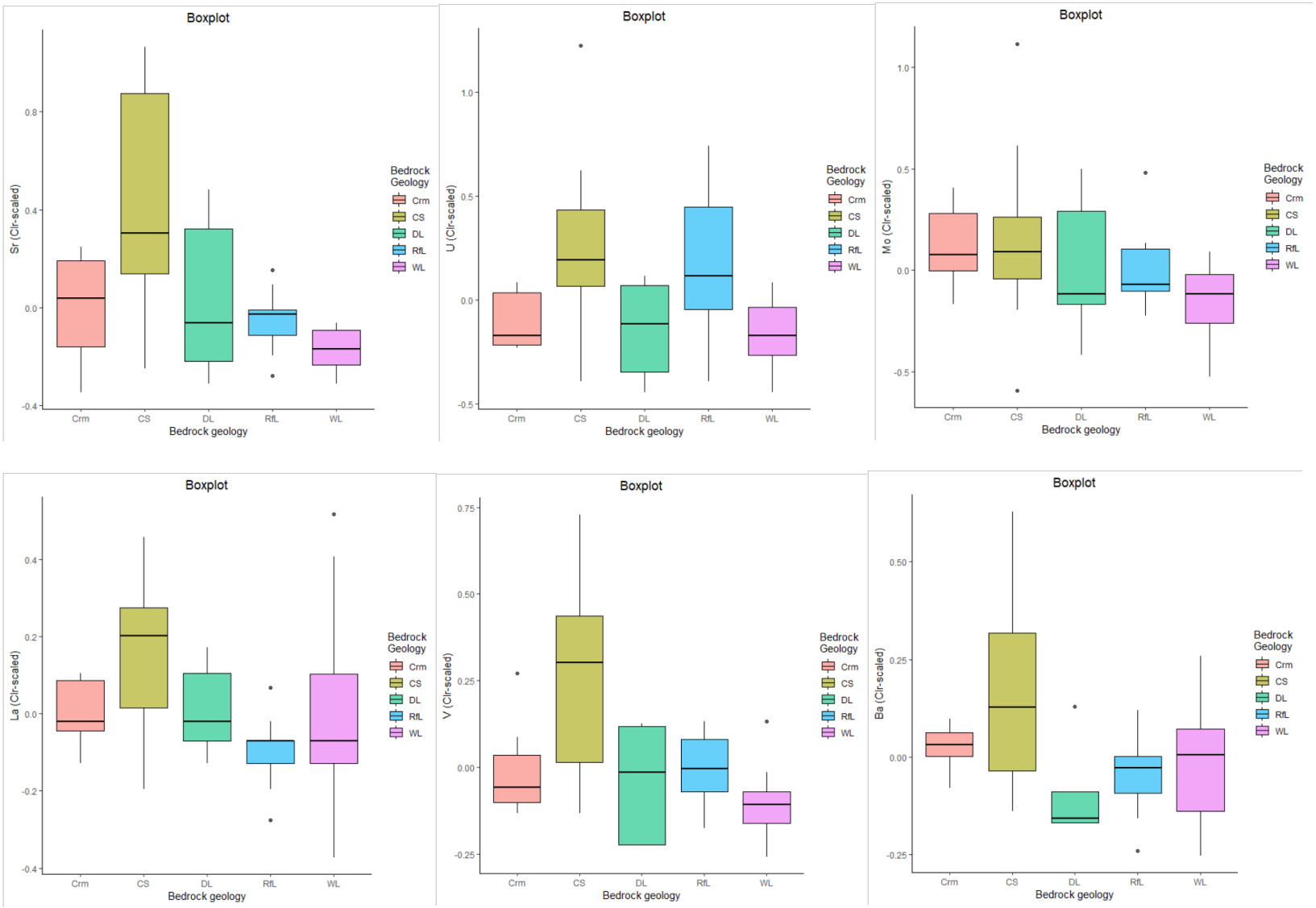

Appendix A continued

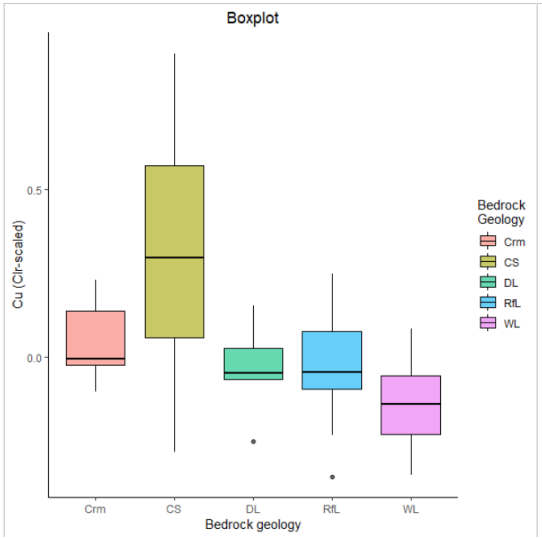

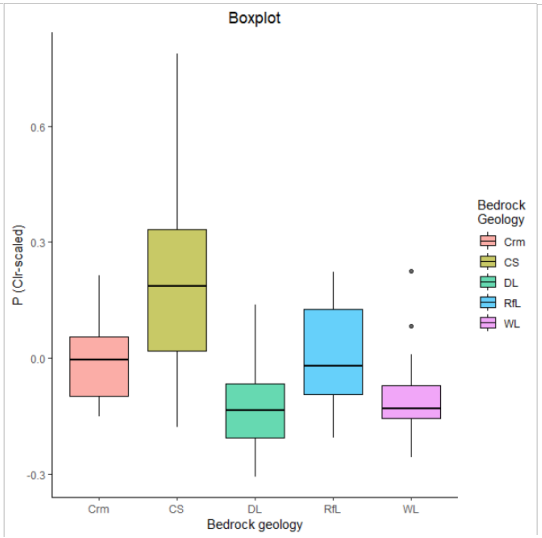

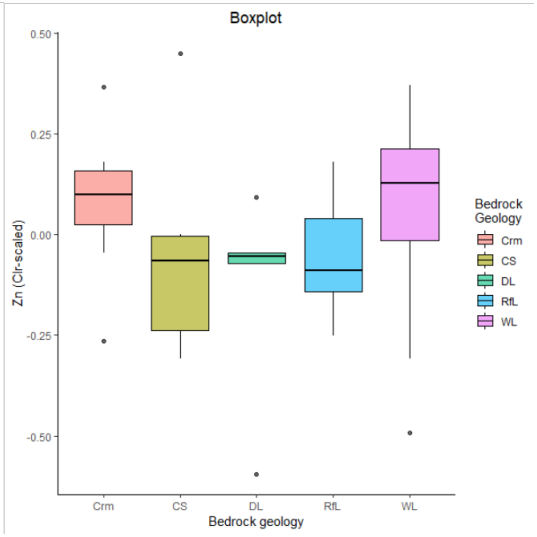

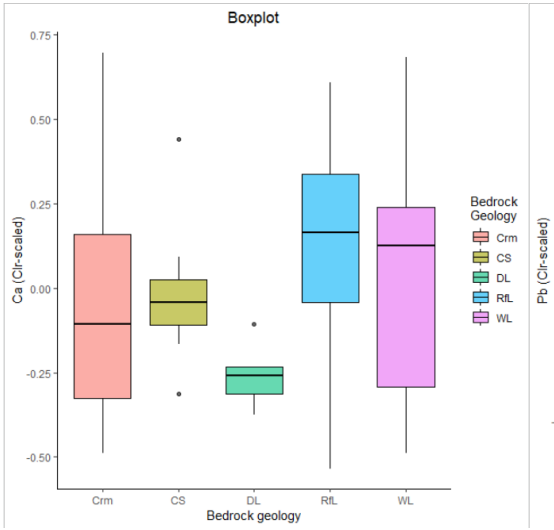

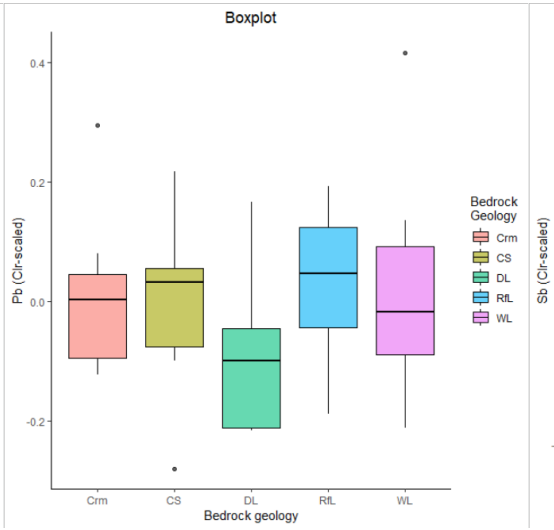

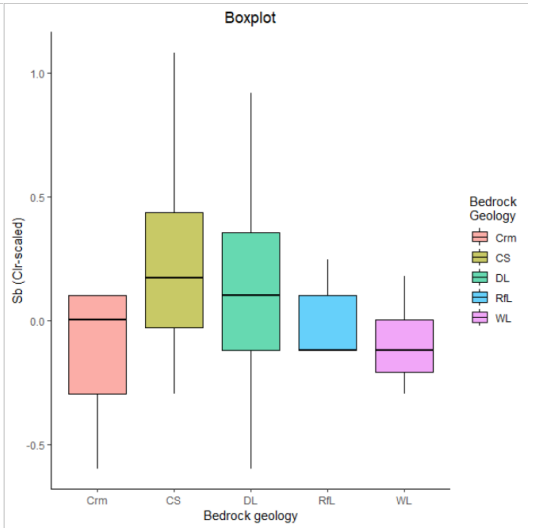

Appendix A continued

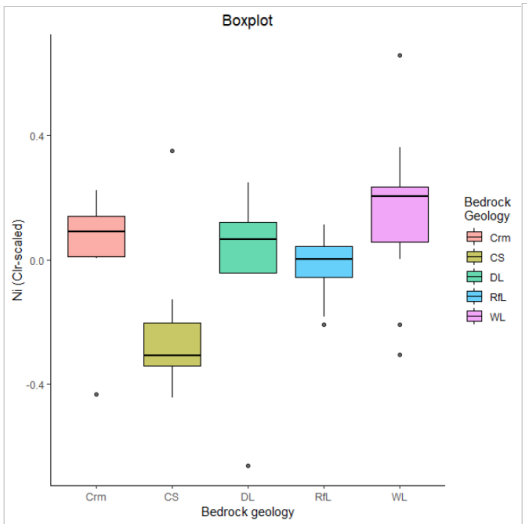

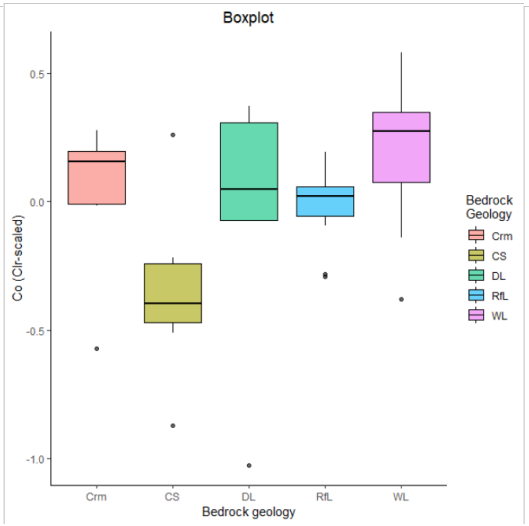

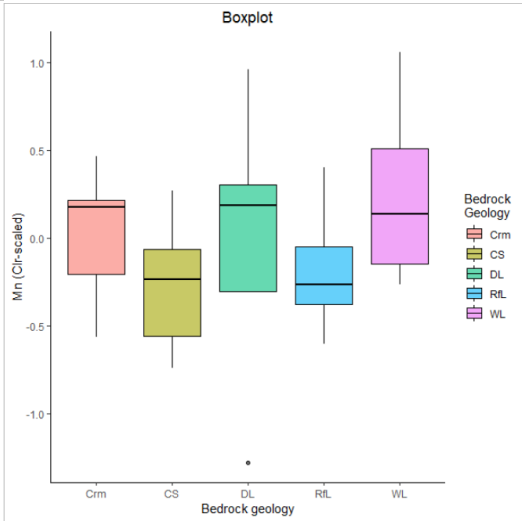

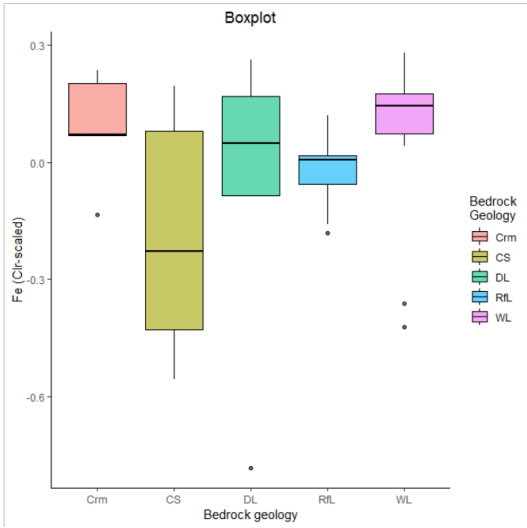

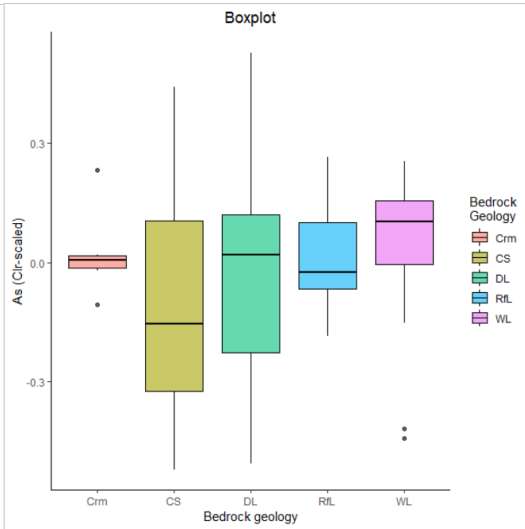

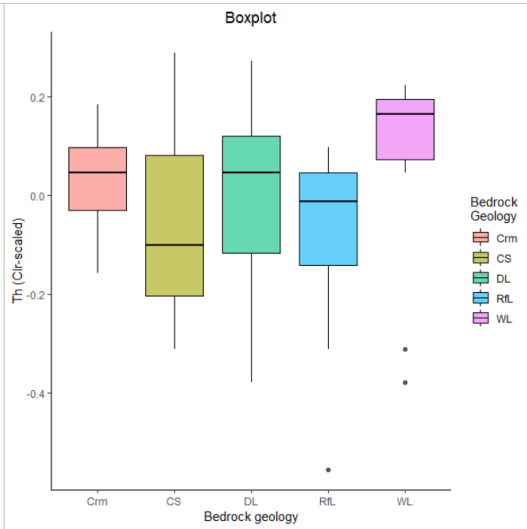

Appendix A continued

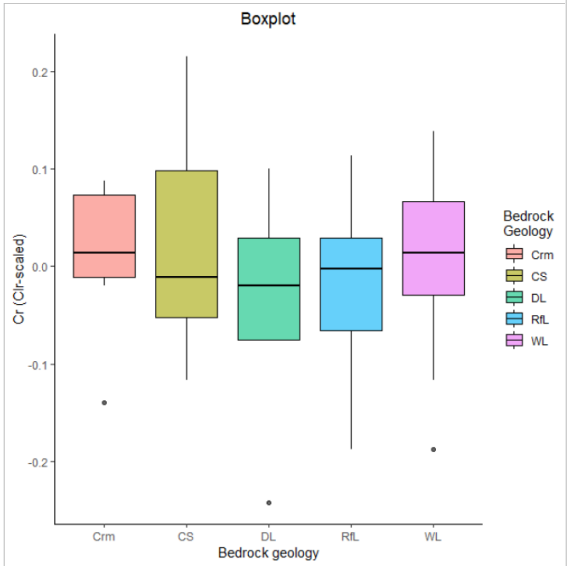

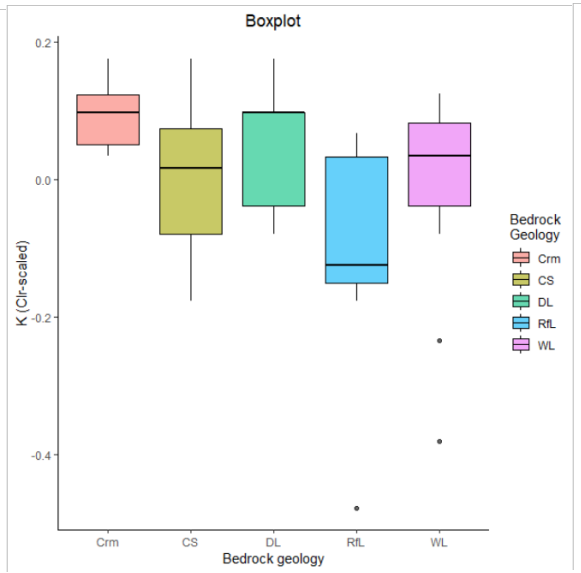

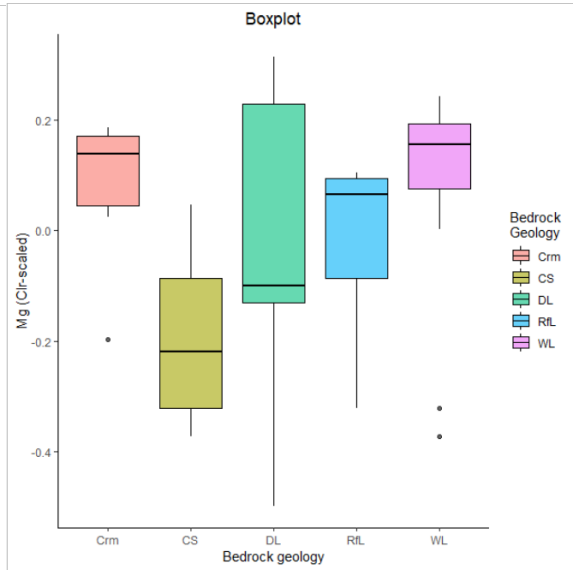

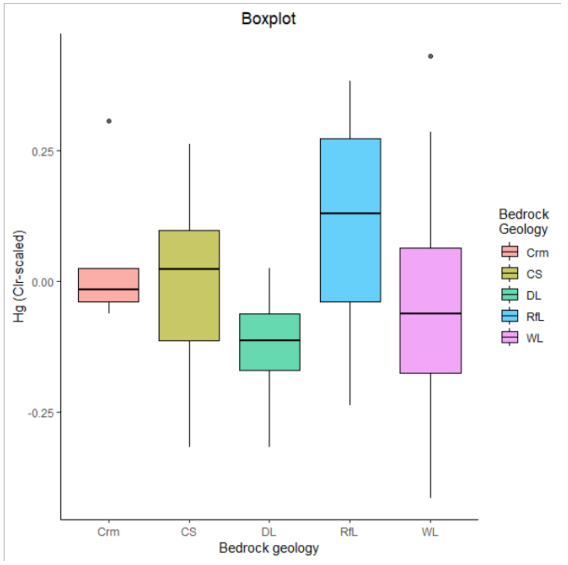

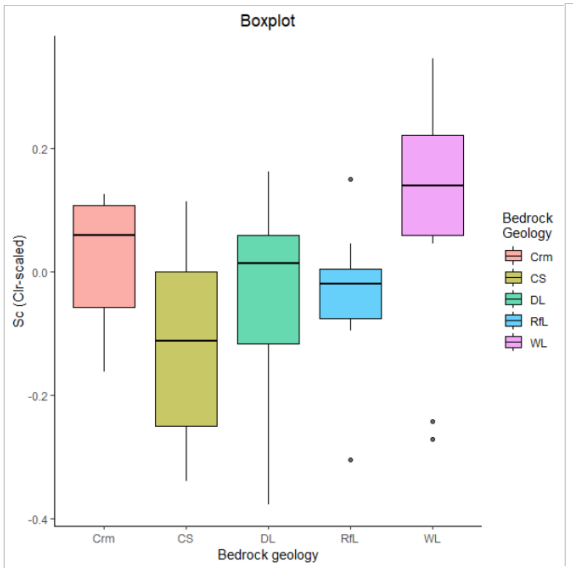

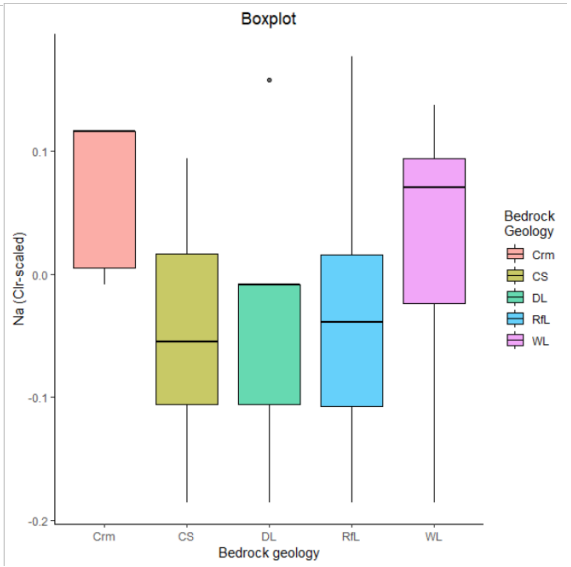

Appendix A continued

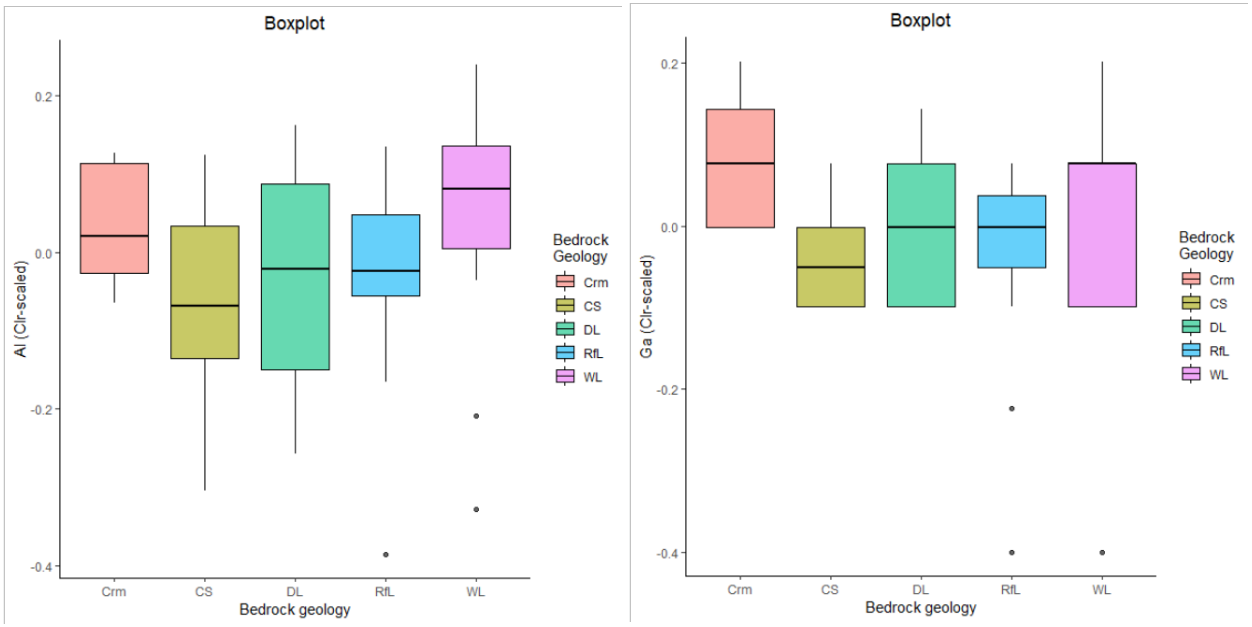

Appendix A continued

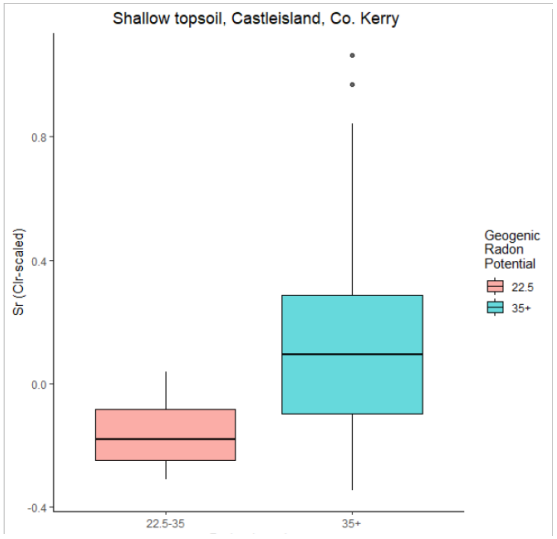

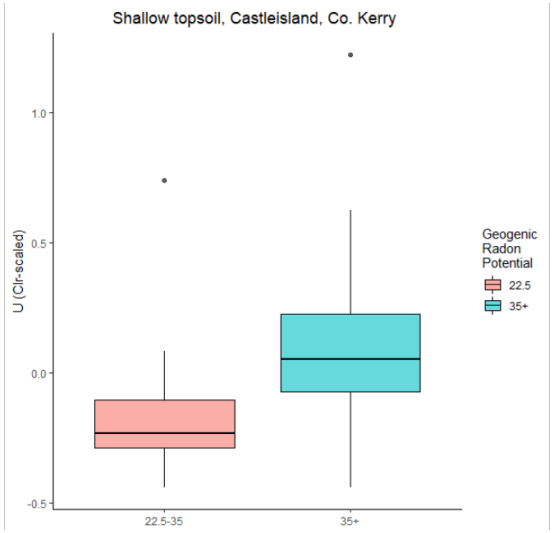

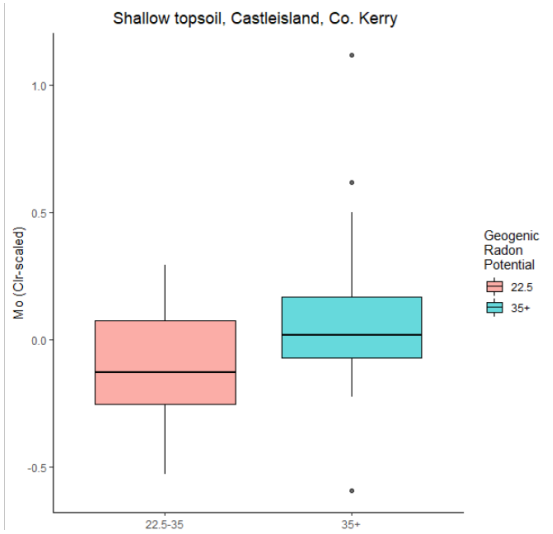

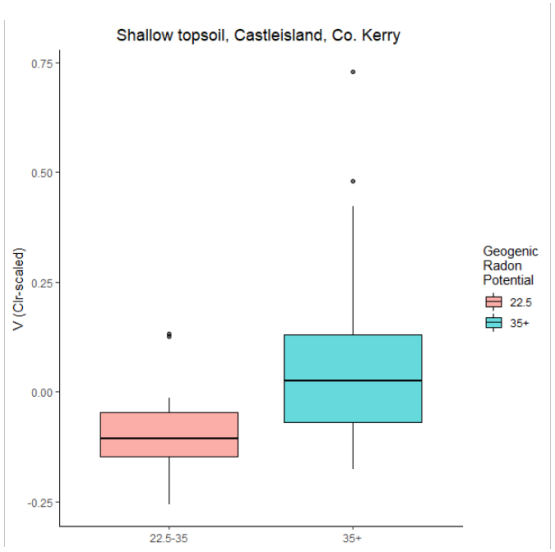

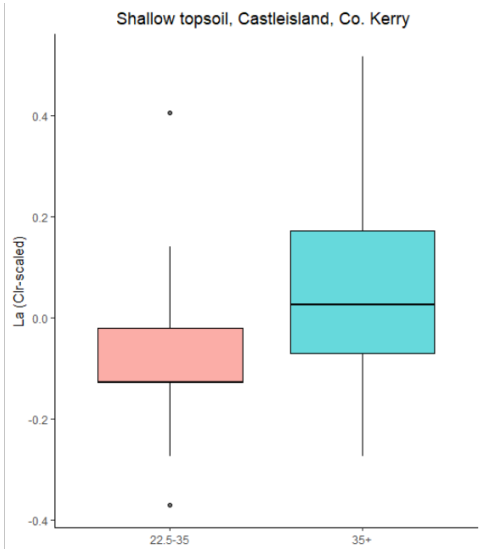

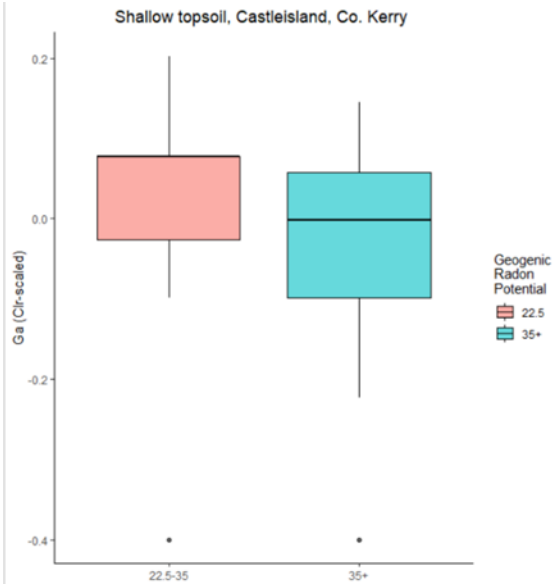

Appendix A continued

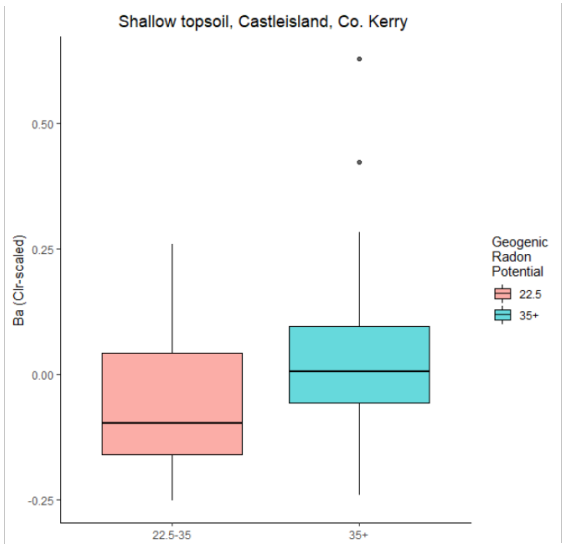

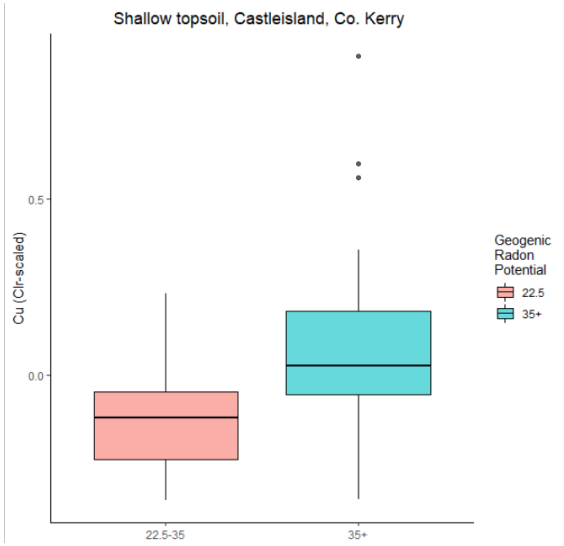

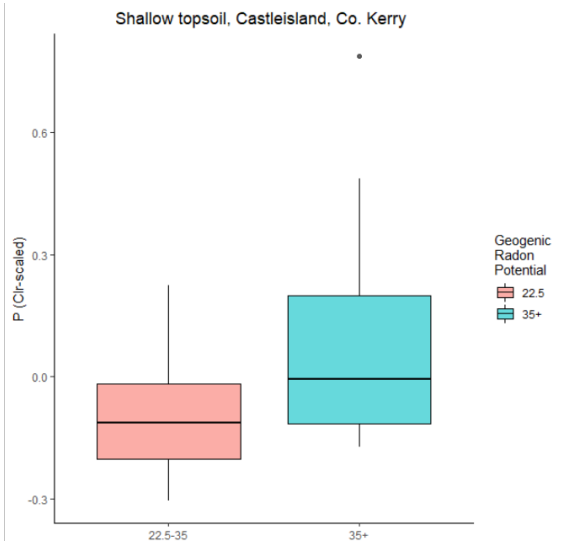

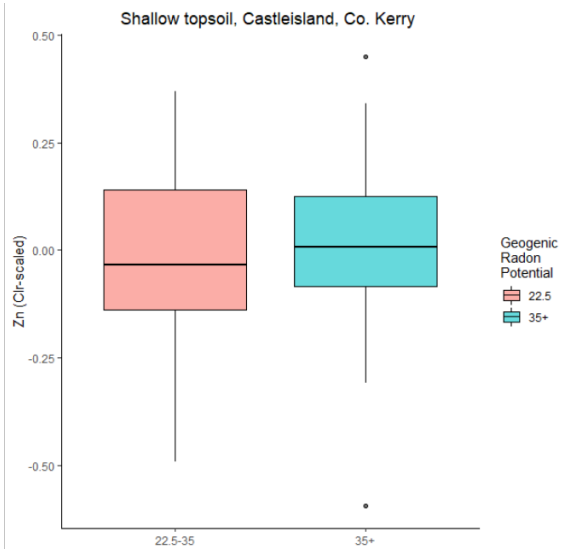

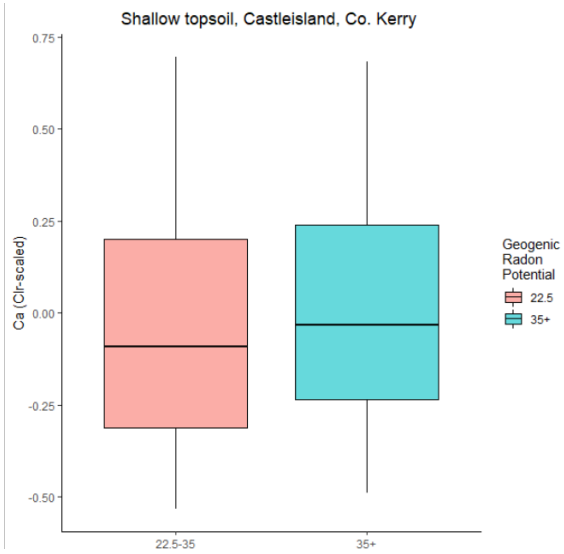

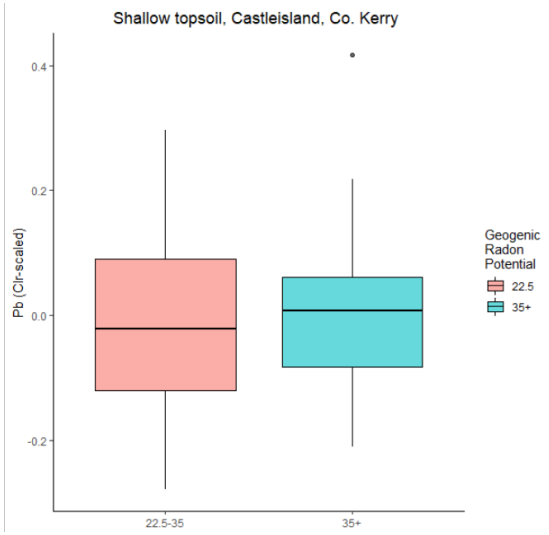

Appendix A continued

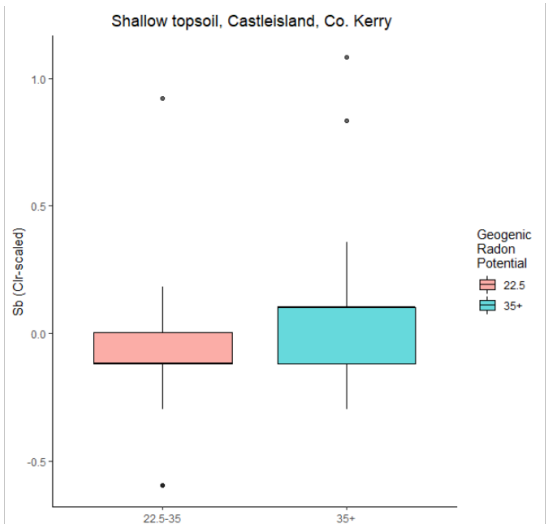

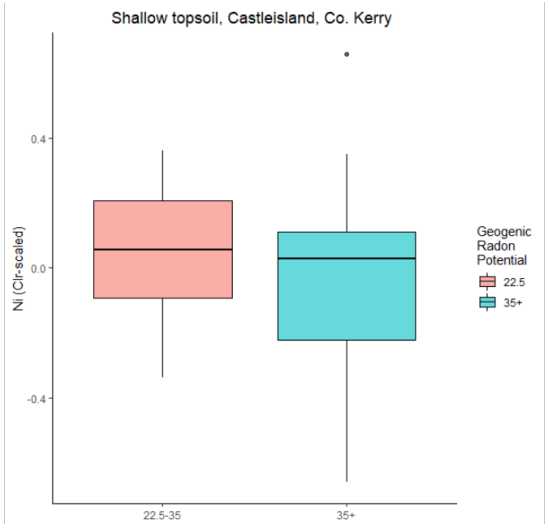

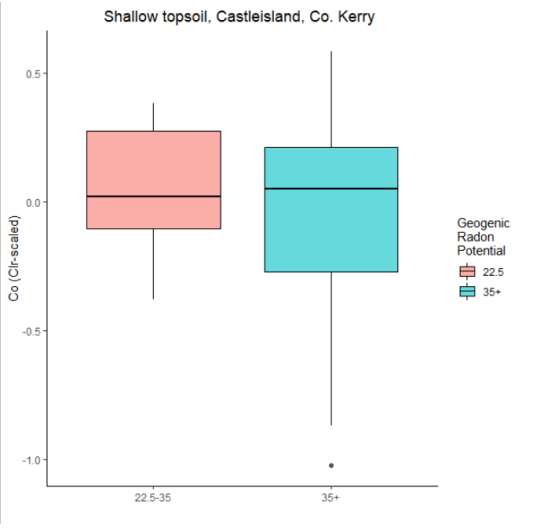

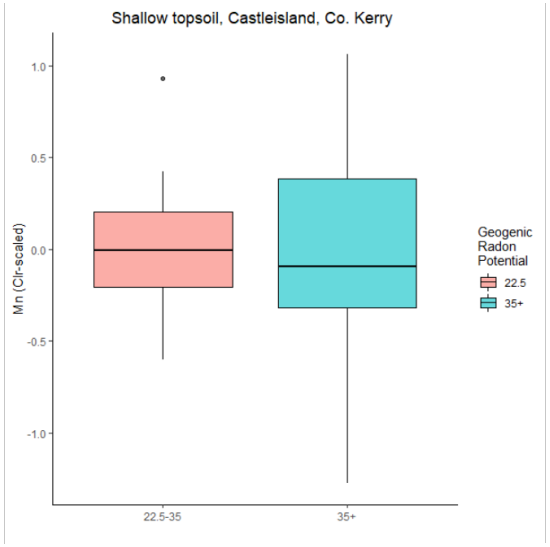

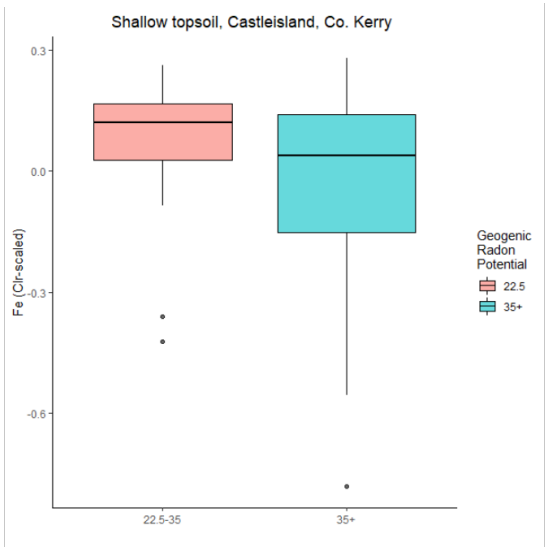

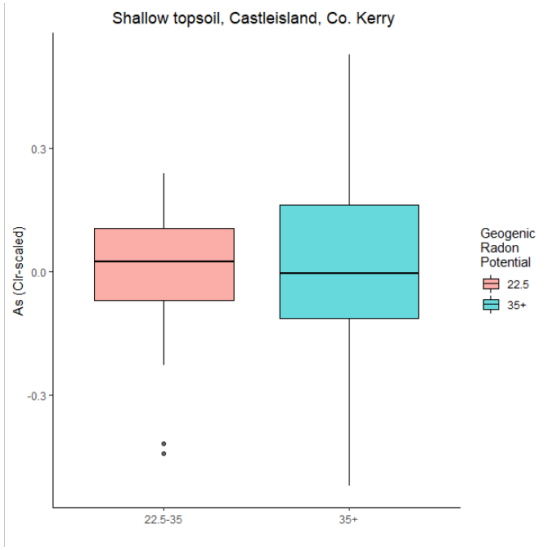

Appendix A continued

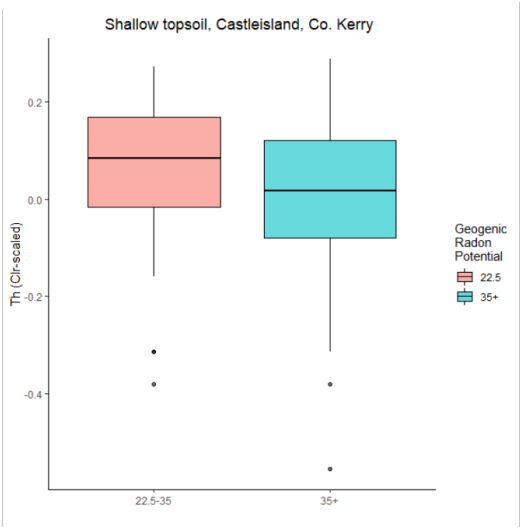

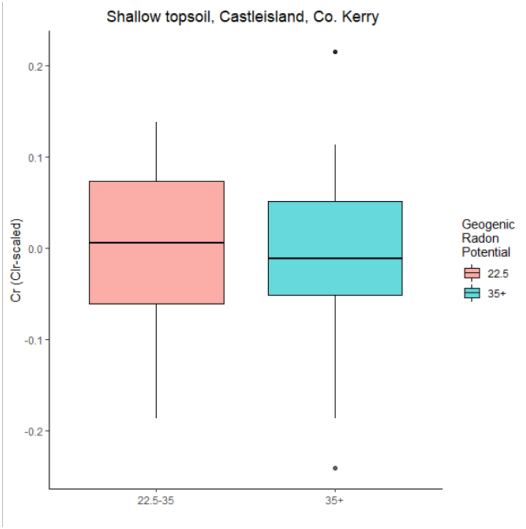

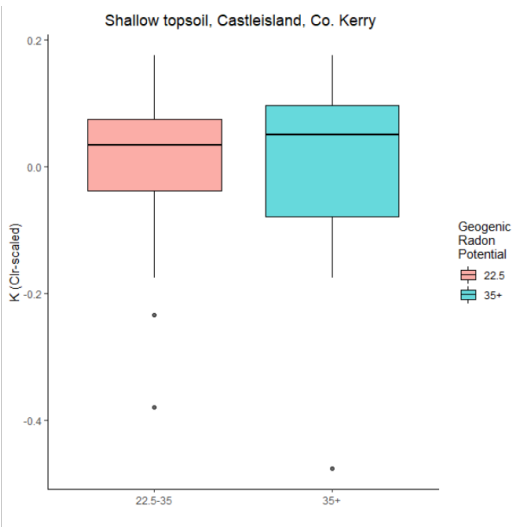

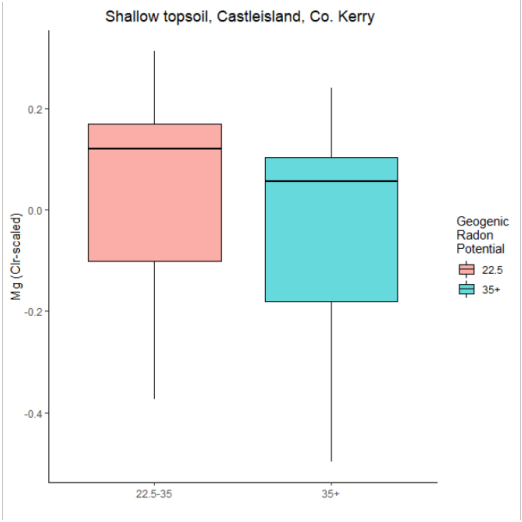

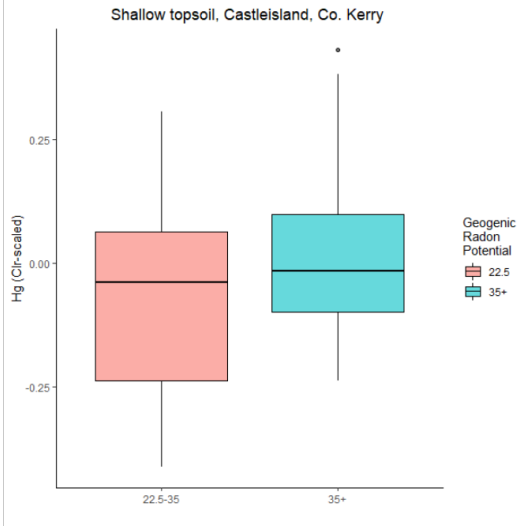

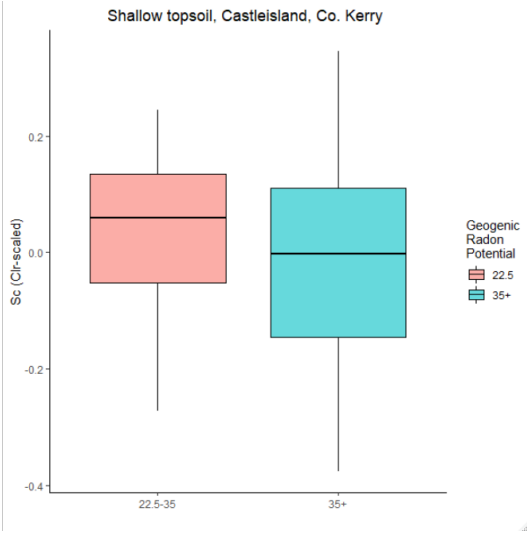

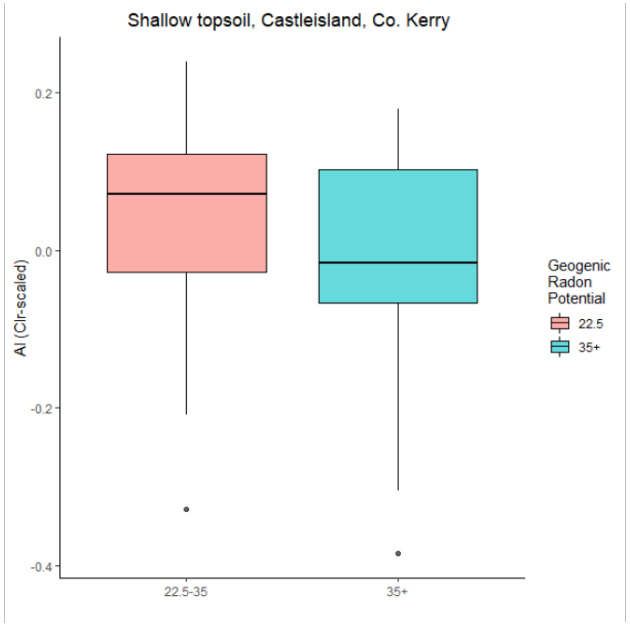
Shallow topsoil, Castleisland, Co. Kerry
Al (Clr-scaled)
0.2
0.0
-0.2
-0.4
22.5-35
35+
Geogenic Radon Potential
22.5
35+

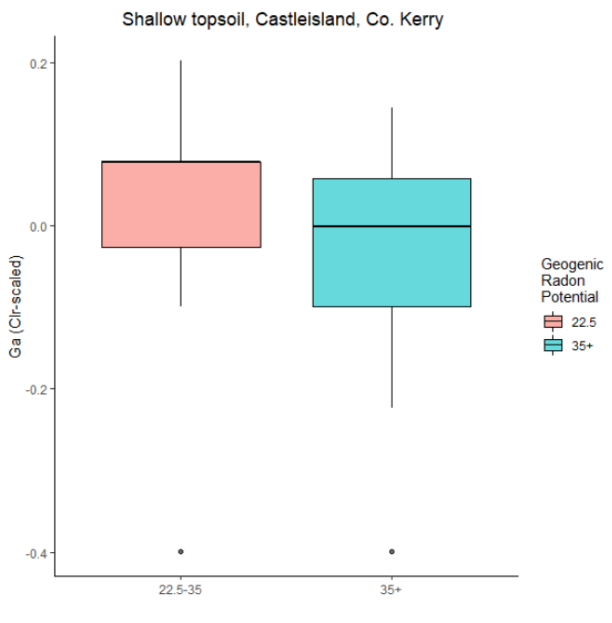
Shallow topsoil, Castleisland, Co. Kerry
Ga (Clr-scaled)
0.2
0.0
-0.2
-0.4
22.5-35
35+
Geogenic Radon Potential
22.5
35+

Appendix A continued

7.3.9 Python Script modified depending on which machine leaning algo rhythm used (Random Forest, Gaussian process regression, Logistic regression)

```
import numpy as np

import matplotlib.pyplot as plt

import pandas as pd

from sklearn.manifold import TSNE

from sklearn.cluster import KMeans

from sklearn.ensemble import RandomForestClassifier

from sklearn.gaussian_process.kernels import RBF

from sklearn.decomposition import PCA

from sklearn.metrics import confusion_matrix, classification_report

from sklearn.linear_model import LogisticRegression

from sklearn.inspection import permutation_importance

import json

def balanced_sample(compositions, radon_cat, coordinates):

    N = np.min([len(radon_cat[radon_cat==0]), len(radon_cat[radon_cat==1])])

    X = []

    y = []

    coo = []

    indexes = np.arange(0, len(compositions))
```

```
print(len(compositions))

np.random.shuffle(indexes)

n = 0

while len(y) < N:

    if radon_cat[indexes[n]] == 0:

        X.append(compositions.iloc[indexes[n]])

        y.append(radon_cat[indexes[n]])

        coo.append(coordinates[indexes[n]])

    n += 1

print(len(y))

n = 0

while len(y) < 2 * N:

    if radon_cat[indexes[n]] == 1:

        X.append(compositions.iloc[indexes[n]])

        y.append(radon_cat[indexes[n]])

        coo.append(coordinates[indexes[n]])

    n += 1

y = np.asarray(y)

print("n 0 class:", len(y[y == 0]))

print("n 1 class:", len(y[y == 1]))
```

```
    return X, y, coo

###

n_clusters = 5

n_fold = 10

data = pd.read_csv("../data/TELLUS_Midlands_mgkg_RP_clr.csv")

compositions = data.iloc[:, 5:-5]

elements = data.iloc[:, 5:-5].columns

coordinates = np.asarray([data.iloc[:, 3].values, data.iloc[:, 4].values]).T

### convert radon classes into 2 classes

radon_cat = list(data["RPClass"])

for i in range(len(radon_cat)):

    if radon_cat[i] == 1:

        radon_cat[i] = 0

    elif radon_cat[i] == 2 or radon_cat[i] == 3 or radon_cat[i] == 4:

        radon_cat[i] = 1

radon_cat = np.asarray(radon_cat)

print(len(radon_cat[(radon_cat == 0)]), len(radon_cat[(radon_cat == 1)]))

d = {

    "split_index": [],

    "precision_class1": [],
```

"recall_class1": [],

"f1-score_class1": [],

"support_class1": [],

"precision_class2": [],

"recall_class2": [],

"f1-score_class2": [],

"support_class2": [],

"precision_weighted_avg": [],

"recall_weighted_avg": [],

"f1-score_weighted_avg": [],

"support_weighted_avg": [],

"precision_macro_avg": [],

"recall_macro_avg": [],

"f1-score_macro_avg": [],

"support_macro_avg": [],

"accuracy": [],

"T_class1": [],

"T_class2": [],

"F_class1": [],

"F_class2": [],

```
}

importance = {'mean':[], 'std':[]}

scores = {'target':[], 'predicted':[], 'scores':[]}

### Spacial cross validation

for j in range(n_fold):

    ### Spatial separation

    kmeans = KMeans(n_clusters=n_clusters, init="random", max_iter=1, n_init=1)

    kmeans.fit(coordinates)

    labels = kmeans.predict(coordinates)

    X = []

    y = []

    coo = []

    indexes = []

    for i in range(n_clusters):

        class_i_indexes = np.where(labels==i)



        X_i = compositions.iloc[class_i_indexes]

        y_i = radon_cat[class_i_indexes]

        coordinates_i = coordinates[class_i_indexes]

        X_i, y_i, coordinates_i = balanced_sample(X_i, y_i, coordinates_i)
```

```
    X.append(X_i)

    y.append(y_i)

    coo.append(coordinates_i)

    indexes.append(np.asarray([i for _ in range(len(y_i))]))

for i in range(n_clusters):



    X_train = np.concatenate([X[ii] for ii in range(n_clusters) if ii!=i])

    y_train = np.concatenate([y[ii] for ii in range(n_clusters) if ii!=i])

    X_test = X[i]

    y_test = y[i]

    ### Randon Forest

    model = RandomForestClassifier(class_weight="balanced")

    model.fit(X_train, y_train)

    pred_train = model.predict(X_train)

    pred_test = model.predict(X_test)

    print("support", len(y_test[y_test == 0]), len(y_test[y_test == 1]))

    ### Confusion matrix

    c_m = confusion_matrix(y_test, pred_test)

    print("### RF ### ", str(j), "###")

    print(
```

```
    "accuracy",
    (c_m[0][0] + c_m[1][1])
    / (c_m[0][0] + c_m[1][1] + c_m[0][1] + c_m[1][0])
    * 100,
    "%",
)
print("confusion_matrix:")
print(c_m)

report = classification_report(
    y_test,
    pred_test,
    digits=4,
    target_names=["class 1", "class 2"],
    output_dict=True,
)
# print(report)

scores['target'].append(y_test.tolist())
scores['predicted'].append(y_test.tolist())
```

```
scores['scores'].append(model.predict_proba(X_test).tolist())

d["split_index"].append(str(j+1))

d["precision_class1"].append(report["class 1"]["precision"])

d["recall_class1"].append(report["class 1"]["recall"])

d["f1-score_class1"].append(report["class 1"]["f1-score"])

d["support_class1"].append(report["class 1"]["support"])

d["precision_class2"].append(report["class 2"]["precision"])

d["recall_class2"].append(report["class 2"]["recall"])

d["f1-score_class2"].append(report["class 2"]["f1-score"])

d["support_class2"].append(report["class 2"]["support"])

d["accuracy"].append(report["accuracy"])

d["precision_weighted_avg"].append(report["weighted avg"]["precision"])

d["recall_weighted_avg"].append(report["weighted avg"]["recall"])

d["f1-score_weighted_avg"].append(report["weighted avg"]["f1-score"])

d["support_weighted_avg"].append(report["weighted avg"]["support"])

d["precision_macro_avg"].append(report["macro avg"]["precision"])

d["recall_macro_avg"].append(report["macro avg"]["recall"])

d["f1-score_macro_avg"].append(report["macro avg"]["f1-score"])

d["support_macro_avg"].append(report["macro avg"]["support"])
```

```
d["T_class1"].append((c_m[0][0]) * 100)

d["T_class2"].append((c_m[1][1]) * 100)

d["F_class1"].append((c_m[0][1]) * 100)

d["F_class2"].append((c_m[1][0]) * 100)



print("train", len(y_train), "test", len(y_test))

### Features importance

result = permutation_importance(

    model, X_train, y_train, n_repeats=10, random_state=42, n_jobs=2

  )



result = permutation_importance(

    model, X_train, y_train, n_repeats=10, random_state=42, n_jobs=4

  )

importance['mean'].append(result.importances_mean)

#importance['std'].append(result.importances_std)

fig = plt.figure(figsize=(15, 8), dpi=200)

ax = fig.add_subplot(1, 1, 1)

pd.Series(result.importances_mean, index=elements).plot.bar(ax=ax)
```

```
        fig.savefig("f_importance/f_importance_"+str(j+1)+"_"+str(i+1)+".png",
bbox_inches="tight")
        plt.close('all')
        ###
    fig = plt.figure(figsize=(15, 10), dpi=200)
    ax = fig.add_subplot(1, 1, 1)
    coo = np.concatenate([coo[_] for _ in range(n_clusters)])
    indexes = np.concatenate([indexes[_] for _ in range(n_clusters)])
    plt.scatter(np.asarray(coo)[:, 0], np.asarray(coo)[:, 1], c=indexes, alpha=1)
    ax.set_ylabel("northing", fontsize="large")
    ax.set_xlabel("easting", fontsize="large")
    # ax.set_title('PCA TS ICPMS')


    cbar = plt.colorbar()
    cbar.set_label("Radon cat")
    ax.tick_params("x")
    ax.tick_params("y")
    # plt.xlim(np.min(coordinates[1]), np.max(coordinates[1]))
    # plt.ylim(np.min(coordinates[1]), np.max(coordinates[1]))
    fig.savefig("splits/split_"+str(j+1)+".png", bbox_inches="tight")
```

```
d = pd.DataFrame.from_dict(d)

d.to_csv("random_forest.csv", index=False)

importance['mean'] = np.asarray(importance['mean'])

importance['std'] = np.asarray(importance['std'])

importance_dict = {elements[i]:importance['mean'][:,i] for i in range(len(elements))}

importance = pd.DataFrame.from_dict(importance_dict)

importance.to_csv("features_importance_mean.csv", index=False)

#importance_dict = {elements[i]:importance['std'][:,i] for i in range(len(elements))}

#importance = pd.DataFrame.from_dict(importance_dict)

#importance.to_csv("features_importance_std.csv", index=False)

with open('scores.json', 'w') as f:

    json.dump(scores, f, indent=4)
```

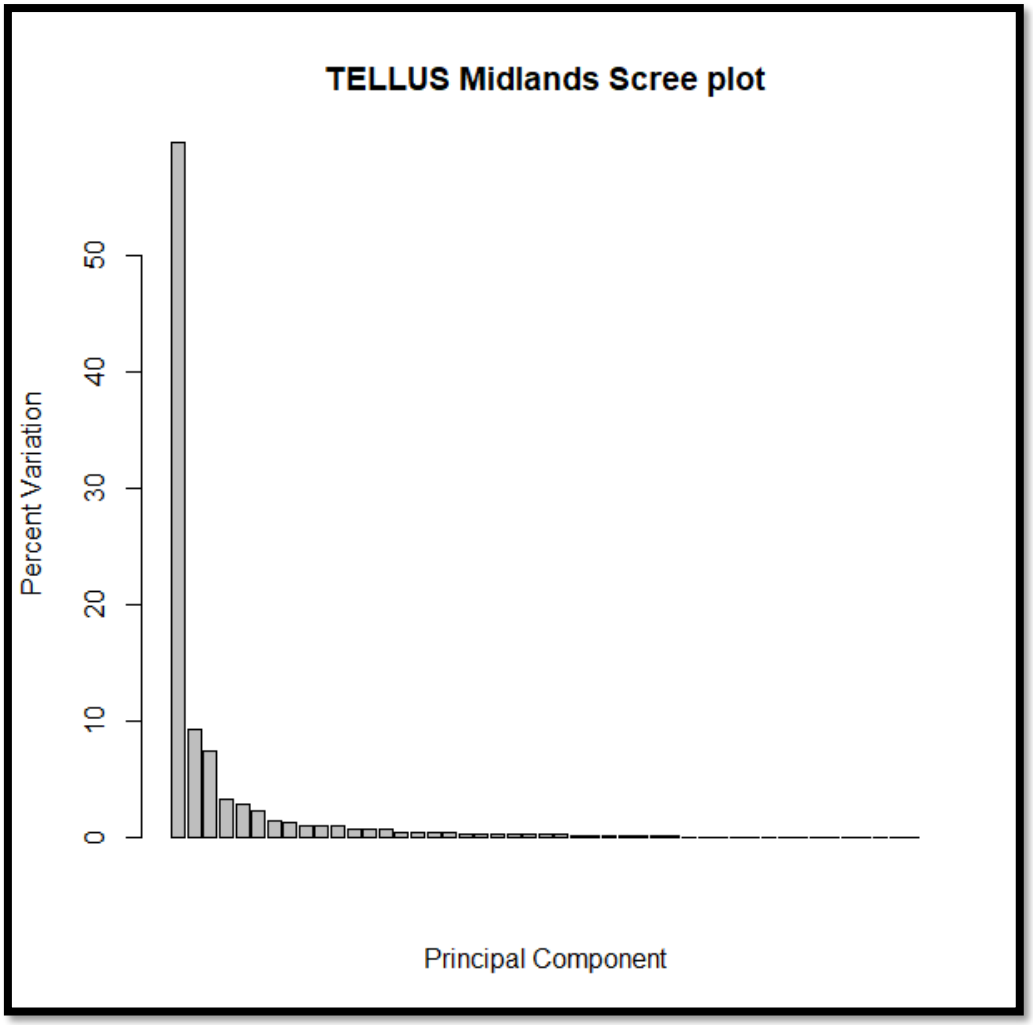

Figure 10 Scree plot of TELLUS Midlands PCA

Table 12 PCA Summary of TELLUS Midlands topsoil (Clr transformed) geochemistry

Loadings	PC 1	PC 2	PC 3	PC 4	PC 5	PC 6	PC 7	PC 8	PC 9	PC10	PC11	PC12	PC13	PC14	PC15	PC16	PC17	PC18	PC19	PC20	PC21	PC22	PC23
Al	-0.18	-0.1	-0.05	0.02	-0.09	0	-0.09	0.03	-0.01	0.08	-0.03	0.02	-0.05	0.05	-0.03	-0.03	0.03	0.02	0.01	0.01	-0.01	-0.08	0.05
Ba	-0.14	0.05	0.04	0.19	-0.12	-0.26	-0.19	-0.22	0.01	-0.14	0.49	-0.16	0.1	-0.05	0.01	-0.41	-0.26	0.08	-0.08	-0.01	-0.06	-0.23	-0.23
Ca	-0.02	0.21	0.38	0.19	-0.1	0.34	0.05	-0.1	-0.02	-0.1	0.1	0.22	0.09	-0.05	-0.07	-0.08	0.02	0.04	-0.07	-0.06	0	0.08	0
Cr	-0.18	-0.07	0.03	0.04	-0.06	0.02	0.01	-0.01	0.02	0.02	-0.05	-0.1	0.03	0.1	0.07	-0.03	0.11	0.07	-0.03	0.05	-0.03	-0.13	0.15
Cu	-0.16	0.07	0.07	-0.06	0.04	-0.02	0.06	-0.29	-0.03	0.31	-0.21	-0.19	0.16	0.01	0.29	-0.14	0.05	-0.38	0.08	-0.24	0.03	-0.16	-0.31
Fe	-0.17	-0.02	0.06	0.03	-0.07	-0.25	-0.01	-0.09	-0.12	-0.18	-0.01	0.17	-0.02	-0.05	0.03	0.01	0.01	-0.04	0.09	0.06	-0.07	-0.06	0.19

Appendix A continued

K	**-0.17**	**-0.1**	**-0.12**	**0.12**	**0.03**	**0**	**-0.07**	**-0.1**	**-0.06**	**0.13**	**0.05**	**0.02**	**0.02**	**-0.04**	**-0.18**	**-0.05**	**-0.03**	**-0.16**	**-0.21**	**0.17**	**0.03**	**0.15**	**-0.12**
Li	**-0.18**	**-0.12**	**0.02**	**0.03**	**-0.04**	**0.05**	**-0.05**	**-0.06**	**-0.04**	**0.05**	**-0.04**	**-0.01**	**-0.06**	**0.08**	**0**	**0.01**	**0.11**	**0.15**	**0**	**-0.06**	**0.13**	**0.04**	**0.04**
Mg	**-0.09**	**0.06**	**-0.09**	**0.63**	**-0.02**	**0.13**	**-0.01**	**-0.11**	**-0.05**	**-0.02**	**-0.17**	**-0.11**	**-0.02**	**0.36**	**-0.1**	**0.1**	**0.13**	**0.06**	**0.08**	**0.23**	**0.12**	**-0.02**	**0.06**
Mn	**-0.16**	**-0.04**	**0.1**	**0.04**	**0.1**	**-0.14**	**0.13**	**-0.16**	**0.01**	**-0.27**	**0.07**	**0.07**	**-0.13**	**-0.12**	**-0.12**	**0.09**	**-0.2**	**0.04**	**-0.08**	**-0.35**	**-0.16**	**0.08**	**0.39**
Na	**0.05**	**0.13**	**-0.27**	**0.47**	**-0.06**	**-0.19**	**-0.02**	**0.11**	**0.05**	**0.36**	**0.17**	**-0.04**	**-0.1**	**-0.52**	**0.08**	**0.17**	**0.12**	**-0.1**	**0.08**	**-0.2**	**0.06**	**0.06**	**0.17**
Ni	**-0.17**	**0**	**0.13**	**0.07**	**0.12**	**0.02**	**0.05**	**0**	**0.03**	**-0.03**	**-0.07**	**-0.11**	**-0.02**	**0.1**	**0.08**	**0.07**	**0.09**	**0.03**	**0.03**	**-0.04**	**-0.07**	**-0.09**	**0.02**
P	**-0.15**	**0.09**	**0.05**	**-0.08**	**-0.07**	**0.08**	**0.06**	**-0.45**	**-0.19**	**0.12**	**-0.32**	**-0.12**	**0.04**	**-0.32**	**-0.31**	**-0.09**	**-0.12**	**-0.07**	**0.03**	**0.21**	**-0.11**	**0.22**	**0.14**

Appendix A continued

S	**0.12**	**0.27**	**0.1**	**0.03**	**-0.25**	**-0.06**	**-0.14**	**-0.02**	**-0.1**	**-0.08**	**-0.13**	**0**	**0.09**	**-0.05**	**-0.25**	**0.07**	**-0.1**	**0.05**	**0.2**	**-0.02**	**0.01**	**0.06**	**-0.06**
Sr	**0.01**	**0.28**	**0.32**	**0.19**	**-0.06**	**0.3**	**0.11**	**0.04**	**-0.01**	**0.17**	**0.05**	**0.35**	**-0.1**	**-0.05**	**0.11**	**-0.11**	**0.06**	**0.05**	**-0.25**	**-0.07**	**-0.01**	**-0.16**	**-0.05**
Ti	**-0.12**	**-0.05**	**-0.12**	**0.08**	**-0.4**	**-0.05**	**0.45**	**-0.01**	**0.46**	**-0.21**	**-0.09**	**0.09**	**0.02**	**0**	**0.14**	**-0.08**	**-0.06**	**-0.15**	**0.12**	**0.04**	**-0.01**	**0.21**	**-0.06**
V	**-0.18**	**-0.04**	**0**	**-0.01**	**-0.06**	**-0.01**	**0.06**	**0.04**	**0**	**0.07**	**-0.06**	**-0.06**	**0.01**	**0.07**	**0.06**	**-0.06**	**0.11**	**0.07**	**-0.08**	**0.08**	**-0.05**	**-0.16**	**0.19**
Zn	**-0.15**	**0.09**	**0**	**0.11**	**0.29**	**0.08**	**0.12**	**-0.09**	**0.13**	**-0.06**	**-0.04**	**-0.31**	**-0.1**	**-0.05**	**-0.04**	**0.13**	**-0.12**	**0.35**	**0.17**	**-0.08**	**0.12**	**0.06**	**-0.25**
Zr	**-0.17**	**-0.02**	**0.17**	**0**	**0.08**	**0.09**	**-0.13**	**0.09**	**-0.02**	**0.05**	**0.15**	**0.01**	**-0.04**	**0.02**	**0.08**	**0.13**	**-0.1**	**-0.15**	**0.17**	**0.1**	**-0.03**	**0.18**	**0**
Ag	**-0.16**	**0.09**	**-0.1**	**-0.21**	**0.02**	**0.13**	**0.01**	**0.11**	**0.14**	**0.14**	**-0.03**	**-0.03**	**-0.1**	**-0.18**	**-0.09**	**-0.34**	**0.04**	**0.01**	**-0.03**	**0.15**	**0.18**	**-0.2**	**0.32**

Appendix A continued

As	**-0.15**	**0.11**	**0.06**	**-0.07**	**0.15**	**-0.16**	**-0.01**	**-0.13**	**-0.15**	**-0.27**	**0.04**	**0.22**	**0.18**	**-0.13**	**0.2**	**-0.1**	**0.42**	**-0.04**	**0.34**	**0.03**	**0.43**	**0.05**	**0.05**
Be	**-0.18**	**-0.01**	**0.03**	**0**	**-0.05**	**-0.01**	**-0.07**	**0.11**	**0.01**	**0.05**	**0.01**	**0.04**	**-0.04**	**-0.07**	**-0.08**	**0.09**	**-0.02**	**-0.01**	**0.05**	**-0.09**	**-0.04**	**-0.04**	**-0.07**
Bi	**-0.11**	**0.19**	**-0.31**	**-0.1**	**-0.03**	**0.1**	**-0.05**	**0.07**	**-0.12**	**0.05**	**-0.09**	**0.33**	**0.01**	**0.02**	**-0.14**	**-0.02**	**-0.09**	**0**	**-0.03**	**-0.21**	**0.18**	**0.13**	**-0.21**
Cd	**-0.13**	**0.2**	**0.16**	**-0.1**	**0.18**	**0.13**	**0.13**	**0.24**	**0.24**	**0.04**	**0**	**-0.25**	**-0.05**	**-0.22**	**-0.06**	**-0.07**	**-0.11**	**0.06**	**0.16**	**0.07**	**0.07**	**-0.07**	**-0.04**
Ce	**-0.18**	**-0.1**	**0**	**-0.03**	**-0.13**	**0.03**	**-0.09**	**0.04**	**0.02**	**0**	**-0.01**	**0.05**	**0.02**	**-0.01**	**-0.1**	**0.06**	**0.02**	**-0.15**	**0**	**0.04**	**-0.03**	**-0.11**	**-0.02**
Co	**-0.18**	**-0.05**	**0.08**	**0.06**	**0.07**	**-0.09**	**0.02**	**-0.08**	**-0.01**	**-0.12**	**-0.02**	**0**	**-0.07**	**0.06**	**0.01**	**0.07**	**0.05**	**0.02**	**0.03**	**-0.15**	**-0.05**	**-0.11**	**0.08**
Cs	**-0.17**	**-0.12**	**-0.08**	**-0.08**	**-0.08**	**0.02**	**-0.07**	**-0.01**	**0.02**	**0.03**	**0.13**	**0.07**	**-0.01**	**0.01**	**-0.11**	**-0.08**	**0**	**0.21**	**-0.1**	**-0.15**	**0.26**	**0.19**	**-0.12**

Appendix A continued

Ga	**-0.18**	**-0.08**	**-0.11**	**0.03**	**-0.1**	**0.01**	**-0.09**	**0.01**	**-0.02**	**0.07**	**-0.04**	**0.01**	**-0.03**	**0.07**	**0.02**	**-0.07**	**0.07**	**0.09**	**-0.06**	**0**	**0.04**	**-0.05**	**0.04**
Ge	**-0.13**	**0.18**	**-0.13**	**0.09**	**0.01**	**0.02**	**-0.13**	**0.23**	**-0.05**	**-0.32**	**-0.18**	**-0.12**	**0.55**	**-0.18**	**0.15**	**0.25**	**-0.15**	**-0.08**	**-0.36**	**0.09**	**0.04**	**-0.1**	**0**
Hf	**-0.17**	**-0.03**	**0.15**	**0.01**	**0.11**	**0.1**	**-0.15**	**0.08**	**-0.05**	**0.03**	**0.16**	**-0.01**	**-0.03**	**0.02**	**0.15**	**0.12**	**-0.15**	**-0.1**	**0.17**	**0.14**	**-0.02**	**0.37**	**-0.05**
Hg	**-0.03**	**0.36**	**-0.05**	**-0.2**	**-0.21**	**0**	**-0.28**	**-0.18**	**0.11**	**-0.24**	**0.06**	**-0.23**	**-0.48**	**-0.06**	**0.14**	**0.17**	**0.35**	**-0.05**	**-0.28**	**0.11**	**-0.05**	**0.13**	**-0.11**
In	**-0.14**	**0.09**	**-0.19**	**0.09**	**0.08**	**0.02**	**-0.2**	**0.26**	**-0.12**	**-0.1**	**-0.28**	**0.09**	**-0.03**	**-0.08**	**0.15**	**-0.41**	**0.11**	**0.25**	**0.18**	**-0.08**	**-0.54**	**0.15**	**-0.11**
La	**-0.18**	**-0.08**	**0.03**	**-0.04**	**-0.13**	**0.07**	**-0.08**	**0.06**	**0.04**	**-0.01**	**-0.01**	**0.03**	**0.03**	**-0.03**	**-0.1**	**0.06**	**0.03**	**-0.15**	**-0.02**	**0.04**	**-0.03**	**-0.11**	**0.02**
Mo	**-0.12**	**0.12**	**0.09**	**-0.03**	**0.18**	**-0.47**	**0.3**	**0.05**	**-0.09**	**0.13**	**-0.07**	**0.29**	**-0.13**	**-0.1**	**-0.06**	**0.18**	**0**	**0.18**	**-0.14**	**0.4**	**-0.08**	**-0.16**	**-0.29**

Appendix A continued

Nb	**-0.16**	**-0.05**	**-0.07**	**0.03**	**-0.27**	**0.01**	**0.21**	**0.06**	**0.16**	**-0.08**	**-0.04**	**0.03**	**-0.05**	**0.02**	**0**	**0.01**	**-0.02**	**0.03**	**0.01**	**-0.01**	**0.01**	**0.03**	**-0.22**
Pb	**-0.08**	**0.26**	**-0.28**	**-0.12**	**0.06**	**0.13**	**-0.05**	**-0.11**	**0.19**	**-0.01**	**0.26**	**0.13**	**0.16**	**0.14**	**-0.38**	**0.19**	**0.13**	**0.01**	**0.31**	**-0.02**	**-0.17**	**-0.29**	**-0.02**
Rb	**-0.17**	**-0.14**	**-0.08**	**0.02**	**0.02**	**0.02**	**-0.05**	**-0.06**	**-0.03**	**0.07**	**0.01**	**0.03**	**-0.03**	**0**	**-0.12**	**-0.03**	**-0.02**	**0.03**	**-0.14**	**0.02**	**0.08**	**0.07**	**-0.06**
Sb	**-0.1**	**0.28**	**-0.1**	**-0.01**	**0.34**	**-0.1**	**0.16**	**-0.03**	**0.21**	**0.12**	**0.2**	**0**	**0.23**	**0.28**	**-0.04**	**-0.15**	**0.15**	**-0.18**	**-0.24**	**0.05**	**-0.19**	**0.35**	**0.17**
Sc	**-0.18**	**-0.04**	**0.05**	**0.06**	**0.01**	**0.01**	**-0.13**	**0.15**	**0.02**	**0.05**	**0.07**	**0.04**	**-0.1**	**0.02**	**0.05**	**0.04**	**-0.01**	**-0.1**	**0.07**	**0.13**	**-0.07**	**-0.08**	**0.03**
Se	**0.02**	**0.37**	**0.13**	**-0.02**	**-0.22**	**-0.31**	**-0.11**	**0.24**	**0.01**	**0.11**	**-0.09**	**-0.12**	**-0.03**	**0.28**	**-0.04**	**-0.16**	**-0.26**	**0.01**	**0.13**	**0.09**	**0.26**	**0.06**	**0.21**
Sn	**-0.11**	**0.19**	**-0.26**	**-0.13**	**-0.03**	**0.15**	**-0.03**	**-0.31**	**-0.01**	**0.15**	**0.01**	**0.19**	**-0.05**	**0.11**	**0.49**	**0.2**	**-0.42**	**0.2**	**0.05**	**0.05**	**-0.02**	**-0.09**	**0.19**

Appendix A continued

Te	**-0.15**	**0.15**	**-0.02**	**0.05**	**0.19**	**-0.12**	**0**	**0.11**	**-0.1**	**-0.11**	**-0.21**	**0.03**	**-0.32**	**0.21**	**-0.13**	**0**	**-0.17**	**-0.34**	**-0.11**	**-0.37**	**0.11**	**-0.08**	**-0.05**
Th	**-0.17**	**-0.11**	**0.07**	**-0.03**	**-0.07**	**-0.03**	**-0.13**	**0.12**	**-0.02**	**0.09**	**0.15**	**0.15**	**-0.02**	**0.01**	**0.03**	**0.07**	**-0.1**	**-0.12**	**0.07**	**0.11**	**-0.01**	**0.14**	**-0.05**
Tl	**-0.17**	**-0.05**	**0.02**	**-0.09**	**0.06**	**0.04**	**0.01**	**0.09**	**0.02**	**0.01**	**0**	**-0.07**	**0.11**	**-0.06**	**0.01**	**0.01**	**0.04**	**0.29**	**-0.24**	**-0.08**	**0.24**	**0.13**	**0.07**
U	**-0.12**	**0.07**	**0.23**	**-0.15**	**-0.28**	**-0.22**	**0**	**0.01**	**-0.01**	**0.33**	**0**	**-0.11**	**0.26**	**0.13**	**-0.03**	**0.23**	**0.21**	**0.24**	**-0.02**	**-0.3**	**-0.18**	**0.12**	**0.01**
W	**-0.1**	**0.11**	**-0.16**	**-0.09**	**-0.18**	**0.17**	**0.48**	**0.19**	**-0.64**	**-0.06**	**0.32**	**-0.27**	**-0.07**	**0.05**	**0.02**	**0**	**0.04**	**-0.06**	**0.04**	**0.01**	**-0.06**	**-0.01**	**0.01**
Y	**-0.17**	**-0.02**	**0.16**	**-0.06**	**-0.01**	**0.13**	**-0.03**	**0.13**	**0.09**	**-0.06**	**-0.01**	**-0.02**	**0**	**-0.11**	**-0.06**	**0.16**	**0.03**	**-0.12**	**0.05**	**-0.03**	**-0.09**	**-0.14**	**0.02**
Center	**0**	**0**	**-0.01**	**0**	**0**	**0**	**0**	**-0.01**	**-0.01**	**0**	**-0.01**	**0**	**0**	**0**	**-0.01**	**-0.01**	**0**	**0**	**0**	**0**	**0**	**-0.01**	**0**

scale	0.5	0.4	0.47	0.51	0.36	0.46	0.35	0.79	0.28	0.68	0.18	0.51	0.23	0.35	0.28	0.3	0.46	0.34	0.52	0.3	0.36	0.49	0.31
Standard deviation	5.3	2.11	1.88	1.24	1.17	1.03	0.85	0.81	0.72	0.7	0.68	0.6	0.57	0.56	0.5	0.5	0.47	0.47	0.46	0.45	0.43	0.4	0.38
Proportion of Variance	0.6	0.09	0.07	0.03	0.03	0.02	0.02	0.01	0.01	0.01	0.01	0.01	0.01	0.01	0.01	0.01	0	0	0	0	0	0	0
Cumulative Proportion	0.6	0.69	0.77	0.8	0.83	0.85	0.87	0.88	0.89	0.9	0.91	0.92	0.93	0.93	0.94	0.94	0.95	0.95	0.96	0.96	0.97	0.97	0.97

Table 22 Continued: PCA Summary of TELLUS Midlands topsoil geochemistry (Clr transformed)

Loadings	PC 24	PC 25	PC 26	PC 27	PC 28	PC 29	PC 30	PC 31	PC 32	PC 33	PC 34	PC 35	PC 36	PC 37	PC 38	PC 39	PC 40	PC 41	PC 42	PC 43	PC 44	PC 45	PC 46	PC 47
Al	0.07	0.06	-0.07	-0.07	-0.02	-0.04	-0.03	-0.17	0.11	0.01	0.02	0.01	-0.12	-0.14	-0.03	-0.21	-0.26	0.28	0.04	0	0.33	-0.24	-0.66	0.14
Ba	-0.03	0.02	0.11	-0.23	0.09	0.04	-0.01	0	-0.14	0.02	0.03	0.04	-0.07	0.01	-0.02	0.02	0.05	0	0.02	0.02	-0.01	-0.04	0	0

Appendix A continued

Ca	**-0.07**	**0.24**	**-0.07**	**0.02**	**-0.23**	**0.2**	**0.18**	**0.17**	**0.41**	**0.08**	**0.15**	**0.29**	**-0.03**	**0.09**	**-0.01**	**-0.05**	**-0.11**	**0**	**0**	**-0.03**	**-0.07**	**0.01**	**-0.02**	**-0.01**
Cr	**0.21**	**-0.02**	**-0.12**	**-0.12**	**0.08**	**0.12**	**0.03**	**0.07**	**0.03**	**-0.04**	**0.24**	**0.02**	**0.2**	**0**	**0.07**	**-0.16**	**0.29**	**-0.05**	**-0.21**	**0.09**	**0.22**	**0.65**	**-0.13**	**-0.01**
Cu	**-0.17**	**-0.14**	**-0.32**	**0.09**	**-0.22**	**0**	**-0.02**	**0.02**	**0.07**	**0.04**	**-0.04**	**-0.08**	**0.05**	**-0.07**	**-0.02**	**0.03**	**0.01**	**0**	**0**	**0**	**0**	**0**	**0.01**	**0.01**
Fe	**0.18**	**-0.08**	**-0.06**	**0.01**	**0.07**	**0.02**	**0.28**	**-0.04**	**0.27**	**0.06**	**-0.4**	**0**	**0.22**	**-0.42**	**0.17**	**0.33**	**-0.04**	**0.05**	**0.05**	**0.1**	**-0.02**	**0.01**	**0.06**	**0.01**
K	**-0.01**	**0.02**	**0.19**	**0.49**	**0.13**	**0.24**	**0.15**	**0.23**	**0.06**	**-0.29**	**-0.02**	**-0.17**	**-0.09**	**-0.16**	**-0.09**	**-0.08**	**0.03**	**-0.15**	**-0.02**	**-0.14**	**0.28**	**-0.02**	**0.05**	**-0.02**
Li	**-0.01**	**0.08**	**-0.03**	**-0.04**	**-0.13**	**-0.02**	**-0.09**	**-0.35**	**0.17**	**-0.18**	**0.01**	**0.03**	**-0.58**	**-0.05**	**0.06**	**0.32**	**0.41**	**-0.17**	**0.06**	**-0.04**	**-0.03**	**0.01**	**0**	**0.01**
Mg	**-0.39**	**-0.03**	**0.03**	**-0.13**	**-0.02**	**0.01**	**-0.02**	**0**	**-0.14**	**0.16**	**-0.12**	**-0.1**	**0.12**	**-0.02**	**0.02**	**0.03**	**-0.01**	**0**	**0.03**	**0**	**0**	**-0.02**	**0.02**	**0**
Mn	**-0.34**	**-0.22**	**-0.2**	**0.14**	**-0.01**	**-0.01**	**-0.16**	**0.03**	**0.02**	**0.05**	**0.14**	**-0.25**	**-0.04**	**0.01**	**-0.05**	**-0.08**	**0.09**	**0.12**	**-0.16**	**-0.08**	**0.02**	**-0.04**	**-0.01**	**-0.02**
Na	**0.11**	**0.06**	**-0.04**	**-0.03**	**-0.05**	**0.04**	**-0.03**	**0.04**	**0.02**	**-0.02**	**0.04**	**0.11**	**0.02**	**0.06**	**0.06**	**0.05**	**0.01**	**-0.01**	**-0.01**	**0.02**	**-0.01**	**0**	**-0.01**	**0**
Ni	**0.13**	**0.02**	**-0.02**	**-0.06**	**0.07**	**0.07**	**0.18**	**0.02**	**-0.11**	**-0.5**	**-0.13**	**0.2**	**0.14**	**0.25**	**0.01**	**-0.02**	**0.2**	**0.28**	**-0.35**	**-0.05**	**-0.06**	**-0.38**	**0.06**	**-0.07**

Appendix A continued

P	**0.19**	**-0.04**	**0.12**	**-0.13**	**0.07**	**0.05**	**-0.13**	**-0.19**	**-0.11**	**0.13**	**-0.06**	**0.14**	**0.03**	**0.17**	**-0.09**	**-0.01**	**0**	**-0.01**	**0.01**	**-0.02**	**-0.01**	**-0.01**	**0.02**	**-0.01**
S	**0.14**	**0.28**	**-0.27**	**-0.09**	**-0.16**	**-0.29**	**0.15**	**0.19**	**-0.18**	**-0.26**	**0.05**	**-0.42**	**-0.08**	**-0.08**	**0.04**	**-0.01**	**0.03**	**-0.02**	**-0.02**	**0.02**	**0.05**	**0.01**	**-0.01**	**-0.01**
Sr	**0.22**	**-0.28**	**0.1**	**0.14**	**0.13**	**-0.2**	**-0.15**	**-0.2**	**-0.25**	**-0.04**	**-0.09**	**-0.18**	**0.02**	**-0.1**	**0.04**	**0**	**0.03**	**0**	**-0.01**	**0.02**	**0.05**	**0.01**	**0**	**0**
Ti	**0.01**	**-0.07**	**0.1**	**0.01**	**-0.12**	**0.01**	**0.23**	**-0.15**	**-0.19**	**-0.07**	**0.17**	**0.05**	**-0.03**	**-0.09**	**-0.08**	**-0.05**	**0.02**	**-0.02**	**0.08**	**0.03**	**-0.01**	**-0.01**	**0**	**-0.01**
V	**0.25**	**0.01**	**-0.15**	**-0.09**	**0.12**	**0.13**	**-0.04**	**0.14**	**0.08**	**0.1**	**0.32**	**-0.2**	**0.12**	**-0.09**	**0.09**	**-0.17**	**0.09**	**-0.32**	**0.28**	**-0.18**	**-0.27**	**-0.43**	**0.04**	**-0.02**
Zn	**0.21**	**-0.17**	**0.04**	**0.17**	**0.13**	**-0.4**	**0.16**	**0.14**	**0.17**	**0.17**	**0.11**	**0.14**	**-0.06**	**-0.11**	**0**	**-0.04**	**0**	**-0.02**	**0.01**	**-0.01**	**0.03**	**-0.01**	**0**	**0.01**
Zr	**0.02**	**-0.08**	**0.06**	**-0.08**	**-0.02**	**-0.03**	**-0.12**	**0.12**	**0**	**-0.14**	**0.15**	**-0.04**	**0.14**	**0.02**	**-0.14**	**0.18**	**0.18**	**0.42**	**0.57**	**-0.17**	**0.04**	**0.12**	**0.03**	**0.02**
Ag	**-0.27**	**-0.16**	**0.23**	**-0.19**	**-0.23**	**-0.32**	**0.13**	**0.24**	**0.15**	**-0.18**	**-0.08**	**-0.03**	**0.03**	**0.02**	**-0.01**	**0.01**	**-0.01**	**-0.05**	**-0.01**	**-0.01**	**0.02**	**0.02**	**0.01**	**-0.02**
As	**0**	**0.11**	**0.18**	**0.1**	**0.13**	**-0.01**	**-0.12**	**0.05**	**-0.1**	**0.06**	**0.08**	**-0.08**	**-0.06**	**0.06**	**-0.06**	**-0.13**	**0.01**	**0.02**	**-0.06**	**0**	**-0.01**	**-0.02**	**-0.04**	**0**
Be	**-0.13**	**0.21**	**-0.03**	**-0.06**	**0.06**	**-0.11**	**-0.07**	**-0.2**	**0.05**	**-0.07**	**-0.31**	**0.15**	**0.01**	**-0.29**	**-0.21**	**-0.62**	**0.11**	**-0.02**	**0.08**	**-0.12**	**-0.21**	**0.14**	**0.2**	**-0.02**

Appendix A continued

Bi	**-0.16**	**-0.24**	**-0.21**	**-0.32**	**0.46**	**0.13**	**0.2**	**0.04**	**0.03**	**-0.06**	**0.09**	**0.08**	**-0.03**	**0.03**	**-0.01**	**0.05**	**0.05**	**0**	**0.02**	**0.01**	**-0.03**	**0**	**-0.03**	**0**
Cd	**-0.16**	**0.25**	**-0.02**	**0.04**	**0.2**	**0.37**	**0.07**	**-0.27**	**-0.01**	**0.05**	**-0.07**	**-0.32**	**0.01**	**0.02**	**0.25**	**0.09**	**-0.08**	**0.08**	**0**	**-0.02**	**-0.01**	**0.07**	**-0.02**	**0**
Ce	**-0.06**	**0.08**	**-0.04**	**0.14**	**0.09**	**-0.18**	**-0.07**	**0.07**	**-0.17**	**0.1**	**0.09**	**0.21**	**-0.09**	**-0.05**	**0.34**	**0.11**	**-0.13**	**0.09**	**-0.06**	**-0.24**	**-0.12**	**0.08**	**-0.1**	**-0.67**
Co	**0.02**	**-0.06**	**-0.1**	**0.04**	**0.06**	**-0.03**	**0.07**	**-0.05**	**-0.1**	**-0.32**	**-0.14**	**0.08**	**-0.07**	**0.39**	**0.11**	**-0.05**	**-0.46**	**-0.34**	**0.39**	**0.01**	**0.07**	**0.2**	**0.01**	**0.07**
Cs	**-0.02**	**0.18**	**-0.1**	**0.09**	**-0.19**	**-0.13**	**-0.11**	**-0.29**	**0**	**-0.01**	**0.04**	**0**	**0.59**	**0.08**	**-0.04**	**0.17**	**-0.02**	**-0.16**	**-0.06**	**-0.19**	**0.17**	**-0.07**	**0.03**	**-0.01**
Ga	**0.14**	**0.01**	**-0.06**	**-0.05**	**-0.03**	**0**	**0**	**-0.12**	**0.14**	**0.07**	**0.21**	**-0.15**	**-0.16**	**0.05**	**-0.04**	**-0.07**	**-0.33**	**0.36**	**-0.05**	**0.2**	**0.19**	**-0.02**	**0.63**	**-0.11**
Ge	**0.01**	**-0.1**	**0.09**	**0.01**	**-0.08**	**-0.09**	**-0.03**	**-0.17**	**0.15**	**-0.04**	**0.02**	**-0.04**	**0.02**	**0.08**	**-0.01**	**0**	**0.02**	**-0.01**	**0.02**	**-0.02**	**0**	**0**	**-0.03**	**0.01**
Hf	**0.02**	**-0.24**	**0.05**	**-0.27**	**-0.16**	**0.07**	**-0.18**	**-0.01**	**-0.01**	**-0.18**	**0.11**	**-0.03**	**-0.01**	**-0.24**	**0.2**	**-0.08**	**-0.26**	**-0.27**	**-0.32**	**0.09**	**-0.05**	**-0.04**	**0.02**	**-0.01**
Hg	**-0.08**	**-0.06**	**-0.06**	**0.02**	**0**	**0.04**	**0.03**	**-0.02**	**0.02**	**0.03**	**0**	**0**	**0.02**	**0**	**0.01**	**-0.03**	**0.02**	**0.02**	**0.02**	**0**	**-0.02**	**-0.01**	**-0.02**	**0**
In	**-0.07**	**0.01**	**0.04**	**0.16**	**-0.11**	**0.03**	**-0.06**	**0.04**	**-0.06**	**0.03**	**0.02**	**0.05**	**0.02**	**0.01**	**0.02**	**0.04**	**0.05**	**-0.02**	**0.02**	**-0.01**	**0.01**	**0.01**	**-0.01**	**0**

Appendix A continued

La	**-0.08**	**0.1**	**-0.04**	**0.12**	**0.11**	**-0.16**	**-0.05**	**0.11**	**-0.2**	**0.09**	**0.15**	**0.21**	**-0.05**	**-0.06**	**0.26**	**0.13**	**-0.05**	**0.07**	**-0.15**	**-0.17**	**-0.08**	**0.02**	**0.16**	**0.7**
Mo	**-0.15**	**0.04**	**-0.08**	**-0.08**	**-0.19**	**0.01**	**-0.05**	**0**	**0**	**-0.02**	**0.16**	**0.07**	**-0.02**	**0.02**	**0**	**0.02**	**0**	**0.02**	**-0.01**	**-0.02**	**0.05**	**0.02**	**0.01**	**0.01**
Nb	**0.14**	**0.05**	**0.01**	**-0.09**	**0.1**	**0.02**	**-0.53**	**0.36**	**0.29**	**0**	**-0.35**	**-0.16**	**-0.05**	**0.2**	**-0.01**	**0.09**	**-0.03**	**0.03**	**-0.11**	**-0.03**	**-0.04**	**0.04**	**-0.04**	**0.03**
Pb	**0.15**	**-0.22**	**0.03**	**0.12**	**-0.28**	**0.2**	**-0.09**	**-0.09**	**0**	**-0.01**	**-0.01**	**0**	**0.02**	**0**	**-0.01**	**-0.01**	**0.04**	**-0.01**	**-0.01**	**0.01**	**-0.03**	**-0.01**	**0.01**	**0.01**
Rb	**-0.02**	**0.07**	**0.03**	**0.23**	**-0.04**	**-0.05**	**-0.01**	**-0.01**	**-0.01**	**-0.13**	**0.1**	**-0.09**	**0.1**	**0.04**	**0.05**	**-0.01**	**-0.01**	**0.15**	**0.07**	**0.61**	**-0.57**	**0.07**	**-0.2**	**0.04**
Sb	**0.07**	**0.25**	**-0.16**	**-0.08**	**0.11**	**-0.25**	**-0.04**	**-0.01**	**0.01**	**0.04**	**-0.09**	**0.02**	**-0.07**	**-0.02**	**0.03**	**0.04**	**-0.02**	**0.01**	**0**	**0.04**	**0.02**	**0.02**	**0**	**0**
Sc	**0.1**	**0**	**-0.11**	**0.03**	**0.06**	**-0.06**	**0.22**	**-0.06**	**-0.02**	**0.15**	**0.02**	**-0.15**	**-0.08**	**0.15**	**-0.63**	**0.23**	**-0.18**	**-0.12**	**-0.26**	**-0.18**	**-0.26**	**0.12**	**-0.11**	**0**
Se	**0.02**	**-0.17**	**-0.12**	**0.33**	**0.05**	**0.08**	**-0.17**	**-0.04**	**0.06**	**-0.02**	**0.02**	**0.27**	**-0.01**	**0.05**	**-0.06**	**-0.03**	**0.01**	**-0.02**	**-0.01**	**0.06**	**-0.01**	**-0.03**	**0.01**	**0**
Sn	**-0.05**	**0.3**	**0.1**	**0.08**	**0.02**	**0.01**	**0**	**0.08**	**-0.08**	**0**	**-0.04**	**0**	**-0.01**	**0**	**0.02**	**0.02**	**-0.01**	**-0.03**	**-0.02**	**0**	**0.02**	**0.01**	**-0.01**	**0**
Te	**0.21**	**0.2**	**0.4**	**-0.14**	**-0.21**	**0.08**	**0.03**	**0.04**	**-0.05**	**0.14**	**0.07**	**-0.03**	**0.01**	**-0.02**	**0.03**	**0.01**	**0.03**	**-0.04**	**-0.02**	**-0.01**	**0**	**0.03**	**-0.01**	**0.01**

Appendix A continued

Th	**0.02**	**-0.1**	**-0.05**	**0.06**	**-0.11**	**-0.1**	**0.28**	**-0.01**	**0**	**0.38**	**-0.21**	**-0.14**	**-0.06**	**0.44**	**0.26**	**-0.24**	**0.29**	**-0.06**	**0.01**	**0.11**	**0.14**	**-0.11**	**0.01**	**0.01**
Tl	**0.14**	**-0.09**	**-0.2**	**-0.05**	**-0.3**	**0.29**	**0.06**	**0.27**	**-0.45**	**0.16**	**-0.26**	**0.09**	**-0.15**	**-0.15**	**-0.09**	**0.02**	**-0.05**	**0.1**	**0.08**	**-0.03**	**-0.03**	**0.04**	**-0.01**	**0**
U	**-0.17**	**-0.04**	**0.44**	**-0.05**	**0.1**	**0.01**	**0.13**	**0.05**	**0.02**	**0.06**	**0.04**	**-0.09**	**0.02**	**0**	**-0.02**	**0.06**	**-0.08**	**0**	**-0.02**	**-0.01**	**-0.03**	**0.02**	**-0.04**	**0**
W	**-0.03**	**0.02**	**-0.02**	**0.07**	**-0.04**	**-0.05**	**0.05**	**-0.04**	**-0.03**	**-0.02**	**-0.01**	**0.02**	**-0.02**	**0**	**-0.01**	**0**	**-0.01**	**0.02**	**-0.01**	**0.02**	**0.02**	**0.01**	**0**	**0**
Y	**-0.13**	**0.16**	**-0.06**	**-0.02**	**0.14**	**-0.03**	**-0.14**	**0.13**	**-0.14**	**0.08**	**0.03**	**0.18**	**0.04**	**-0.1**	**-0.26**	**0.16**	**0.11**	**-0.26**	**0.07**	**0.52**	**0.35**	**-0.22**	**0.07**	**-0.11**
Center	**0**	**0**	**0**	**-0.01**	**0**	**0**	**0**	**0**	**0**	**-0.01**	**0**	**-0.01**	**0**	**0**	**0**	**0**	**0**	**0**	**0**	**-0.01**	**0**	**0**	**-0.01**	**0**
scale	**0.38**	**0.53**	**0.55**	**0.55**	**0.45**	**0.24**	**0.61**	**0.2**	**0.29**	**0.53**	**0.34**	**0.39**	**0.29**	**0.58**	**0.29**	**0.48**	**0.32**	**0.28**	**0.31**	**0.77**	**0.53**	**0.44**	**0.4**	**0.58**
Standard deviation	**0.36**	**0.36**	**0.34**	**0.33**	**0.33**	**0.3**	**0.28**	**0.27**	**0.27**	**0.25**	**0.24**	**0.23**	**0.2**	**0.2**	**0.18**	**0.17**	**0.16**	**0.15**	**0.14**	**0.12**	**0.12**	**0.11**	**0.09**	**0.06**
Proportion of Variance	**0**	**0**	**0**	**0**	**0**	**0**	**0**	**0**	**0**	**0**	**0**	**0**	**0**	**0**	**0**	**0**	**0**	**0**	**0**	**0**	**0**	**0**	**0**	**0**

Appendix A continued

Cumulative Proportion	**0.97**	**0.98**	**0.98**	**0.98**	**0.98**	**0.99**	**0.99**	**0.99**	**0.99**	**0.99**	**0.99**	**0.99**	**1**	**1**	**1**	**1**	**1**	**1**	**1**	**1**	**1**	**1**	**1**

.2.17.10 Machine learning outputs

Gaussian Process Regression (GPR)

(a) TELLUS Midlands 47 elements

Feature importance for each model

split_inde	Al	Ba	Ca	Cr	Cu	Fe	K	Li	Mg	Mn	Na	Ni
1	0.013568	0.013857	0.022055	0.012587	0.011374	0.001848	-0.00064	-5.77E-05	0.008025	0.034296	0.005196	0.002771
1	0.004286	0.017357	0.003857	0.008429	0.002	0.006	-0.00064	0.001071	0.003929	0.0255	0.001714	0.004286
1	-0.0002	0.002895	0.015197	0.001842	0.008026	0.004211	0.000197	0.002763	0.002105	0.026118	-0.00171	0.005855
1	0.000923	0.009656	0.015867	0.014514	0.007565	0.000246	-0.00018	0.000246	0.004121	0.015252	0.001538	0.003014
1	0.001445	0.007293	0.005519	0.005585	0.004074	0.003811	-0.00033	0.002497	0.000723	0.040473	0.002628	0.000197
2	0.00507	0.014044	0.028613	0.011305	0.017133	0.00542	0.012296	0.002506	0.006876	0.033566	0.015618	0.007343
2	0.001349	0.00045	0.008096	0.000375	0.006672	0.003598	0.01057	0.005172	0.004423	0.008621	0.005472	0.002399
2	0.017532	0.012532	0.010325	0.000325	0.008442	0.001104	-0.00221	0.008506	0.000909	0.055779	-0.00162	0.002338
2	0.002781	0.001164	0.01229	0.000453	0.012225	0.000259	0.006727	0.000906	0.000388	0.022186	0.002523	0.006016
2	0.004808	0.004988	0.022175	0.01845	0.009675	-0.00174	-0.00655	0.000901	0.001563	0.021334	-0.00114	0.011478
3	-0.00104	0.005901	0.005024	-0.00399	0.000718	0.0063	-0.00199	0.009569	0.000558	0.014753	-0.00128	-0.00048
3	0.012792	0.01474	0.027078	0.039091	0.01526	-0.00065	-0.00058	0.001364	0.002987	0.026948	0.00039	0.013117
3	-0.00231	-0.00149	0.017187	-0.00143	0.015082	-0.00109	0.003601	0.000272	-0.00285	0.019633	-0.00149	-0.00177
3	-0.00591	0.006407	0.013527	0.001752	0.005038	0.000383	-0.00285	0.000931	-0.00011	0.019989	-0.004	-0.00159
3	0.001288	0.004918	0.02178	0.003981	0.00767	0.000937	-0.00123	0.001347	0.001815	0.016979	-0.0024	0.000995
4	-0.00056	0.007438	0.017002	0.019128	0.008837	0.002685	-0.00073	0.017785	0.007662	0.038311	0.002461	0.00123
4	0.014501	0.008295	0.017285	0.02123	0.011485	0.00232	0.00261	0.023144	0.006555	0.05348	0.002668	0.001856
4	0.006138	0.008312	0.016688	0.05179	0.008248	0.004092	-0.0009	0.025512	0.003772	0.022954	0.00243	0.009015
4	-0.00211	0.0109	0.003376	0.000844	0.008579	-0.00155	-0.00331	0.011603	0.004993	0.05661	0.003797	0.001758
4	-0.002	0.007143	0.009063	0.000461	0.010829	0.001767	-0.002	0.015975	0.000614	0.03725	0.002151	0.003379
5	-0.00039	0.016427	0.021626	-0.00205	0.009513	0.004314	-0.00061	-0.00033	0.005973	0.033186	0.003595	0.006471
5	-0.00194	0.012313	0.017015	-0.00157	0.015746	0.004701	0.005	0.004104	-0.00127	0.020896	-0.00209	0.000821
5	-0.00127	0.006951	0.00441	-0.00045	0.002392	0.000822	-0.0009	0.01009	0.00142	0.020478	0.00142	0.001943
5	0.011481	0.015442	0.014122	0.002698	0.011424	0.002354	0.002239	0.002526	0.003789	0.017107	5.74E-05	0.002526
5	0.025127	0.01374	0.020356	0.01902	0.012723	0.006807	0.001145	0.007252	0.003753	0.049936	-0.00108	0.009097
6	0.000107	0.013583	0.015508	0.018021	0.008824	0.002513	0.000749	0.000267	0.004706	0.018877	-0.00064	0.00016
6	0.001302	0.013958	0.02151	0.021719	0.01099	0.004427	-0.00052	0.003385	0.004062	0.021094	0.001979	0.001198
6	0.00689	0.01278	0.020789	0.02662	0.013074	0.006949	0.005889	0.003239	0.004122	0.015371	0.003475	0.005124
6	0.00605	0.010274	0.000342	-0.00114	0.01016	0.003082	-0.0016	0.001256	0.003311	0.015525	0.001142	-0.00103
6	0.007799	0.016435	0.026671	0.033217	0.018315	0.002855	0.002646	0.007939	0.008357	0.044011	0.001532	0.014067
7	-0.00246	0.00892	0.013322	-0.00059	0.013732	-0.00305	-0.00076	0.01115	0.00493	0.00446	-0.00182	-0.00141
7	0.002313	0.010463	-0.00088	0.001982	0.0087	-0.0022	0.003965	0.009251	0.000661	0.009581	0.003304	-0.00088
7	-0.00085	0.003748	0.012164	0.006223	0.007921	0.003819	-0.00106	0.01082	0.006011	0.01471	0.001414	0.001556
7	0.000856	0.012246	0.013957	0.002246	0.013743	0.001337	0.000535	0.009947	0.006791	0.016952	0.003155	0.000481
7	0.001523	0.01229	0.010504	0.00063	0.011029	0.002574	-0.00121	0.01166	0.006828	0.017542	0.003571	0.00063
8	0.002812	0.005562	0.009719	0.01412	0.000428	-0.00397	-0.00642	0.014487	-0.0022	0.004829	-0.00092	0.001589
8	0.000948	0.007726	0.01844	0.000729	0.026749	0.003207	0.013921	0.005029	0.000729	0.016399	0.007945	-7.29E-05
8	0.005063	0.014813	0.026438	0.00925	0.011	0.00275	6.25E-05	0.0095	0.0045	0.010438	0.008188	0.000938
8	0.02289	0.018926	0.003197	0.006394	0.008951	0.010038	0.002685	0.020972	0.003133	0.044437	0.000639	0.003133
8	0.003317	0.008047	0.009889	0.002273	0.010258	0.003993	-0.00098	0.017629	0.001413	0.01683	0.002396	0.001413
9	0.001329	0.013608	0.017405	0.003165	0.017278	0.003671	0.002722	0.00981	0.008797	0.028608	0.004747	0.00481
9	0.003561	0.004399	0.00817	0.000628	0.006983	0.005028	0.000978	0.020112	0.001606	0.039246	0.002025	0.000349
9	-0.00312	0.009738	0.018914	-0.001	0.011548	0.000499	-0.00268	0.005306	0.002871	0.022534	-0.00019	-0.00094
9	0.003012	0.010964	0.005181	0.000843	0.01006	0.005663	-0.00048	0.004699	-6.02E-05	0.046024	-0.0038	0.003072
9	0.009961	0.006815	0.008388	0.022739	0.005767	0.005505	0.002556	0.004522	0.004194	0.015138	6.55E-05	0.006619
10	0.016748	0.013325	0.016443	0.007885	0.010147	-0.00122	-0.00202	0.004951	0.000428	0.044377	-0.00134	0.004401
10	0.00768	0.016285	0.015196	0.008007	0.013453	0.001198	0.001198	0.0061	0.004956	0.03573	0.005447	0.011819
10	-0.00431	0.00861	0.001813	-0.00068	0.009366	-0.00453	-0.00453	-0.00219	-0.00015	0.018505	-0.00098	0.002341
10	0.004545	0.003977	0.003815	0.003815	0.003653	0.009416	0.001218	0.010877	0.001867	0.019643	0.00487	0.009334
10	0.016986	0.015463	0.018849	0.020147	0.014898	0.002652	-0.0013	0.002032	0.007731	0.032449	0.004515	0.016986

split_inde	P	S	Sr	Ti	V	Zn	Zr	Ag	As	Be	Bi	Cd	Ce	Co	Cs	Ga	Ge	Hf
1	-0.0011	0.002483	0.010508	0.004042	0.00052	0.00664	0.003522	0.006062	0.002483	0.01582	0.006293	0.004619	0.010566	0.018591	0.005254	0.001732	-0.00202	0.005947
1	-0.00029	-0.00086	0.004929	0.002	-0.00079	0.004929	-0.00186	0.005714	-0.00136	0.007643	0.004286	0.0025	-0.00093	0.007929	-0.00093	0.002214	-0.001	0.007857
1	0.001184	-0.00145	0.007434	-0.00053	0.001184	-0.00066	0.000395	0.002039	0.001184	0.010066	0.00375	-0.00026	0.000987	0.010789	0.002434	0.001513	6.58E-05	0.002697
1	-0.00185	0.001968	0.005289	0.001599	-0.00092	0.00123	-0.00148	0.006581	0.000738	0.005658	0.00369	0.00369	0.006027	0.009102	-0.00178	-0.00105	-0.00197	0.000369
1	0.000986	0.001248	0.003482	0.00092	-0.00125	0.003219	0.004074	0.003548	0.004796	0.00703	0.006767	0.002168	-0.00059	0.004731	0.00046	0.001314	0.001183	0.001577
2	0.008392	0.003846	0.014627	0.006002	0.006352	0.003963	0.003263	0.011946	0.004196	0.010023	0.01521	0.008392	0.016725	0.024592	0.027273	0.006235	0.000758	0.007576
2	0.011319	-0.0003	0.000525	0.001424	0.000825	0.008321	0.005097	0.014843	-0.00052	0.003973	0.013718	0.017241	0.002249	0.003523	0.014918	0.005247	0.001724	0.005397
2	0.002987	0.002403	0.002987	0.00013	-0.00117	0.004091	0.00026	0.002597	0.000779	0.004351	0.012727	0.007922	0.012208	0.037078	6.49E-05	0.002273	-0.00013	0.006494
2	0.008862	0.000647	0.003428	0.001746	0.000388	0.001552	-0.00058	0.002652	-0.00291	0.008991	0.022639	0.000129	0.004722	0.022186	0.003881	-0.00142	0.002587	0.00194
2	0.004267	0.005048	0.005589	0.000901	0.014543	0.000601	-0.00325	0.007873	0.002704	0.018269	0.003125	-0.00036	0.005108	0.017849	0.004327	-0.0021	-0.00168	0.005228
3	-0.00191	-0.00247	0.000159	-0.00112	-0.00215	0.003429	-0.00223	-0.00032	-0.0004	-0.00016	0.000239	0.006539	-0.0051	0.000319	-0.00144	0.005742	-0.00175	7.97E-05
3	0.00013	-0.00058	0.010649	0.00487	0.021818	0.006883	0.000584	-0.00032	0.006753	0.015455	0.00961	0.008312	0.002013	0.01961	0.002727	0.001429	-0.00234	0.004545
3	-0.00211	-0.0017	0.001155	-0.00299	-0.00313	-0.0034	0.000883	-0.00129	-0.00156	0.004008	0.009783	0.001766	-0.00061	0.001902	0.003601	-0.00299	-0.00326	0.000204
3	-0.00509	-0.00214	-0.00159	-0.00246	-0.00767	-0.00142	-0.00225	-0.0029	-0.00246	0.002957	0.005203	-0.00186	-0.00131	0.004655	-0.00126	-0.00449	-0.0035	-0.00115
3	-0.00381	-0.00029	0.008724	-0.00053	-0.00375	0.000176	0.00041	0.000878	0.000234	0.003279	0.003923	0.003162	-0.00041	0.01089	0.014286	-0.00035	-0.00035	0.001464
4	-0.00235	-0.0038	0.004754	0.000112	0.00179	-0.00067	-0.00034	0.007047	0.00481	0.010235	0.007998	0.002461	0.005984	0.012584	-0.00084	0.005984	-0.00067	0.003579
4	-0.00041	0.00232	0.004466	0.001972	0.016415	0.004292	0.00348	0.008817	0.002552	0.015603	0.007193	0.007483	0.006148	0.02819	-0.00058	0.005916	0.004002	0.006206
4	2.22E-17	0.003389	0.01266	0.001087	0.013043	0.003069	-0.00192	-0.00128	0.001471	0.021611	0.002877	0.005115	0.007545	0.017519	0.005115	-0.00147	0.003581	2.22E-17
4	0.001406	-0.00373	0.004641	-0.00148	-7.03E-05	0.000281	-0.00127	-0.0012	0.004008	0.007876	0.002813	0.002883	0.003235	0.011885	-0.00492	0.007032	-0.00084	0.000352
4	0.002304	0.00553	-0.002	0.0053	0.00553	0.001536	0.005069	0.036098	0.001382	0.003226	0.012826	0.00023	-0.00161	0.005684	0.011444	0.005453	0.001459	0.006068
5	-0.0005	-2.22E-17	0.01615	0.001991	0.004259	0.004923	-0.00232	0.007135	0.003429	0.006361	0.003042	0.001327	0.010454	0.007743	0.015653	0.000664	0.002378	-0.00072
5	0.005	0.001269	0.006194	0.000373	-0.00157	-0.00022	0.001269	0.004701	0.000672	0.00306	0.00291	0.001045	0.00597	-0.00134	0.003358	-0.00231	0.000522	0.004403
5	-0.00149	-3.33E-17	0.00157	0.002093	0.000149	-0.0003	-0.0006	0.002093	0.002915	0.004858	-7.47E-05	0.010613	-0.00336	0.003961	0.008744	0.005157	0.000299	0.013976
5	-0.00103	0.000287	0.01659	0.004822	0.0031	0.002985	-0.00023	0.003846	0.00333	0.007979	0.004478	0.001091	0.005339	0.005224	0.010218	-0.0008	0.000976	-0.00172
5	-0.00064	-0.0014	0.011578	0.003181	0.017303	0.007952	0.001081	0.011705	0.007952	0.01673	0.007125	0.008588	0.011768	0.009606	0.015267	0.002672	-0.0014	0.003944
6	-0.00235	0.000267	0.003529	0.005455	-2.22E-17	0.004171	-0.0007	0.008075	0.002086	0.017861	0.007326	0.00369	0.010321	0.007807	0.030535	0.004545	-0.00064	0.000588
6	-0.00214	-0.00047	0.005469	0.005625	0.000365	0.006146	0.000781	0.005625	0.002135	0.02224	0.01125	0.005052	0.00875	0.009792	0.031094	0.002031	-0.00245	0.002448
6	0.00053	0.002768	0.009364	0.007774	0.003475	0.006243	0.003357	0.005241	0.004711	0.027915	0.012603	0.004417	0.014488	0.014959	0.039105	0.00477	0.001001	0.005536
6	3.33E-17	-0.0016	0.001598	0.000114	0.005708	0.012329	0.000913	0.002283	0.000342	0.011073	0.007192	0.002169	-0.00194	0.002055	0.03105	0.014498	0.003767	-0.00046
6	0.005501	0.002646	0.004318	0.006964	0.012047	0.004735	0.000487	0.004387	0.007103	0.026532	0.008983	0.00968	0.011142	0.029178	0.030223	0.000557	0.004109	0.009471
7	-0.0037	0.000822	0.005692	-0.00129	-0.00153	0.000704	-0.00217	-0.00147	0.000176	0.001585	0.00669	0.000411	-0.00246	0.00534	0.002113	0.003873	-0.00252	0.001643
7	-0.00154	0.009031	-0.00419	0.000881	0.002203	-0.00165	0.001762	-0.00099	-0.00088	0.000661	0.000441	0.000661	-0.00363	0.00011	0.008921	0.014207	0.000991	0
7	0.000778	0.006365	0.004314	0.003041	0.001132	0.00198	0.000636	-7.07E-05	0.006011	0.003819	0.008699	-0.00028	0.000636	0.011528	-7.07E-05	0.001061	0.000778	0.00587
7	-0.00064	0.002299	0.005401	0.002995	0.000856	0.001016	0.001765	0.002246	0.002086	0.003476	0.015615	0.000802	0.002299	0.009572	0.006096	0.006364	0.00139	0.00508
7	-0.00221	0.000788	0.004307	0.001628	5.25E-05	0.001208	0.000158	0.001996	0.002363	0.001786	0.012658	0.000788	0.000105	0.008666	0.008088	0.00709	0.00021	0.003782
8	-0.00031	0.000244	0.002812	-0.00043	0.030012	-0.00086	0.001467	-0.0033	-0.00165	0.004768	0.004401	-0.00196	0.004279	0.005196	-0.00251	-0.00367	0.0011	0.00055
8	0.01137	0.003353	0.006122	0.003499	0.004883	0.00656	0.001895	0.002041	0.000146	0.008892	0.017638	0.000875	0.00328	0.009038	0.002041	0.004738	0.003207	0.004155
8	0.00175	6.25E-05	0.025	0.004313	0.003313	0.002875	0.00275	-0.00025	0.001313	0.005125	0.005313	0.0015	0.001563	0.018625	0.004188	0.004938	-0.00106	0.0055
8	-0.0016	0.001662	0.00179	0.001215	0.002366	0.007609	-0.00198	0.000639	0.000448	0.007992	0.005818	0.003836	0.005051	0.032673	0.005371	0.007928	-0.00243	0.004028
8	0.00817	0.001044	0.006634	0.000246	0.006757	0.010074	0.003563	0.002211	0.004054	0.002518	0.012592	0.003378	-0.00018	0.00516	-0.00025	0.011057	0.00172	0.00473
9	-0.00177	0.00057	0.011646	0.001962	0.002405	0.004114	0.005759	0.002532	0.005443	0.009051	0.001266	0.007089	0.001203	0.027785	0.010823	0.004114	0.000759	0.003671
9	0.005517	0.000419	0.006006	0.003422	0.003911	0.013687	0.004399	0.006983	0.004888	0.007821	0.009218	0.004469	0.007472	0.013198	0.001885	0.012081	0.002723	0.002514
9	0.003184	0.00025	-0.00019	6.24E-05	0.001748	-0.001	-0.002	-0.0015	-0.00056	0.00774	0.003308	0.000624	-0.00268	0.015044	-0.00056	-6.24E-05	-0.00181	0.002934
9	0.001205	-0.00217	0.000482	-0.00024	0.000422	0.00759	0.000602	-0.0012	0.002229	0.001687	0.004699	0.000602	-0.00157	0.017229	0.000181	0.006807	-0.00211	0.003675
9	0.00616	0.004915	0.003342	0.000328	0.027392	0.004587	0.003014	-0.00026	0.003932	0.00498	0.002883	0.004128	0.00249	0.01671	0.002556	0.004128	0.000262	0.00118
10	-0.00153	0.000672	0.014548	0.004156	0.001956	0.005929	-0.00098	-0.00049	-0.00116	0.015281	0.003178	0.000795	0.001345	0.01143	0.001589	0.002628	0.002078	0.002506
10	0.002015	0.001198	0.010893	0.004248	0.004466	0.010675	0.003322	0.0061	0.001525	0.019717	0.007789	0.00207	0.010403	0.013508	0.005991	0.001906	0.002015	0.008551
10	-0.00491	0.000302	-0.00453	-0.00053	-0.00038	0.001284	0.002946	-0.00415	-0.00295	0.004834	-0.00483	-0.00234	-0.00106	-0.00211	-0.00498	0.004758	-0.00242	-0.00128
10	0.001542	0.002922	0.002435	0.002029	0.006331	0.007224	0.003003	0.003734	0.001948	0.012013	0.006088	0.009903	0.002597	0.008929	0.021429	-0.00122	0.002273	0.003084
10	0.003725	0.00553	0.014729	0.003668	0.004402	0.01219	0.008691	0.007393	0.003894	0.031264	0.002765	0.003555	0.013093	0.014221	0.007111	-0.00034	0.00237	0.00965

split_inde	Hg	In	La	Mo	Nb	Pb	Rb	Sb	Sc	Se	Sn	Te	Th	Tl	U	W	Y
1	0.008776	-0.00167	0.000924	0.002656	0.004619	0.003811	0.009527	0.011316	0.027483	0.004734	0.003984	0.002021	0.010277	0.054215	0.004908	0.002483	0.060508
1	0.001214	0.003357	-0.0005	0.001571	0.002357	0.000214	0.0345	0.002929	0.017143	-0.00029	0.005429	-0.00093	0.0055	-7.14E-05	0.004857	0.0035	0.056071
1	0.009079	0.001447	0.001908	0.001974	0.002763	0.000724	0.024737	0.009803	0.013684	0.00125	0.003816	0.000263	0.011645	0.027961	0.005197	0.001645	0.062039
1	0.006335	0.004244	-0.00215	6.15E-05	-0.00062	0.002645	0.009717	0.004797	0.013899	0.002583	0.0008	-0.0024	0.011255	0.052276	0.001722	0.00326	0.058057
1	0.003285	0.00092	0.006045	0.002497	-0.00039	0.00138	0.000197	0.002365	0.011892	0.002037	0.001117	0.001774	0.003679	0.015046	-0.00112	0.0023	0.031932
2	0.015093	0.007401	0.002972	0.004779	0.025408	0.009266	0.011072	0.022203	0.026748	0.010431	0.010956	0.008974	0.028613	0.055594	0.017657	0.006352	0.08514
2	0.004723	0	0	0.003298	0.001124	0.001499	0.012369	0.008246	0.015817	0.003073	0.001049	0.00075	0.028861	0.04078	0.023088	0.004423	0.032234
2	0.00526	-0.00273	-0.00175	0.003182	0.00487	0.001494	0.000909	0.012143	0.022727	0.004545	-0.00019	0.002143	0.032727	0.046753	0.04039	0.003896	0.091234
2	0.004204	0.003881	-0.00233	0.000453	0.004075	0.001811	0.01533	0.03053	0.027038	0.000841	0.004722	0.005692	0.003816	0.034994	0.025485	0.001552	0.083829
2	0.007512	0.007632	-0.00024	0.003666	-0.00252	0.003185	0.005108	0.016106	0.022476	0.002704	0.004327	0.001022	0.001563	0.037861	0.002885	0.002464	0.08095
3	0.002632	0.000159	-0.0004	-0.00239	-0.00223	-0.0012	0.000478	7.97E-05	0.011244	0.000957	-0.00064	-7.97E-05	-0.00096	0.020893	0.007496	-0.00263	0.0189
3	0.011429	0.006688	0.013182	-0.00149	0.003701	0.001364	-0.00247	0.015649	0.028312	0.004545	0.006169	0.00539	0.007013	0.059026	0.006104	0.003701	0.094675
3	0.002514	0.000204	0.008152	-0.00177	0.001359	0.000408	-0.00088	0.017391	0.018614	0.002921	0.000408	-0.00048	0.007337	0.050611	0.008628	0.000408	0.055435
3	0.000767	0.000164	0.004436	-0.00367	-0.00104	-0.0006	0.001205	0.005093	0.023713	0.003669	-0.00038	-0.00164	-0.00082	0.048959	0.000383	-0.00038	0.059091
3	0.005972	-0.00152	0.010773	-0.00222	0.00082	0.000117	-0.0017	0.005621	0.013173	-0.0007	0.000527	0.001464	0.010656	0.037939	0.005679	0.00041	0.067155
4	0.002964	0.000336	-0.0014	0.004027	0.016387	0.002517	0.029586	0.005089	0.031488	0.009396	0.002908	0.002461	0.002013	0.057438	0.004642	0.003356	0.062584
4	0.006265	0.001508	0.006845	0.005626	0.005278	0.00116	0.018155	0.004408	0.032831	0.006961	0.005336	0.005452	0.005278	0.063399	0.012529	0.007077	0.0721
4	0.009015	0.009079	0.004859	0.002302	-0.00051	0.001279	0.005051	0.003261	0.026279	0.003325	0.001535	0.00211	0.00454	0.055691	0.004028	0.006714	0.085997
4	0.005626	-0.00127	-0.00527	0.003305	0.00218	0.000211	-0.0026	0.003516	0.009775	0.005415	7.03E-05	0.001195	-0.00021	0.041561	0.005556	0.00654	0.038889
4	-0.00046	0.003072	0.013441	0.001767	0.008372	0.004455	0.022965	0.00361	0.032335	0.000538	0.001767	0.002304	0.003072	0.042857	0.021659	0.002919	0.049539
5	0.000719	-0.001	-0.0021	0.006084	0.002157	0.001715	0.013164	0.010398	0.021571	0.007412	0.004038	0.004701	0.006637	0.026881	0.001991	0.000608	0.083241
5	-0.00112	0.002612	0.000448	0.000896	0.00209	0.001866	0.018433	0.015522	0.005	0.003806	0.002164	-0.00104	0.003433	0.009403	0.00209	0.001045	0.080149
5	0.002093	0.003288	-0.00262	-0.00142	0.000299	0.003662	0.000972	0	0.012706	0.00157	-7.47E-05	0.001271	0.007324	0.005755	0.008296	-0.0012	0.039761
5	0.005166	0.001435	-0.00316	0.003157	0.004018	-0.00029	0.00178	0.006544	0.018255	0.002698	0.002181	0.00023	0.024053	0.037371	0.000459	0.004018	0.08938
5	0.009478	0.005153	-0.00401	0.005598	0.002481	0.004071	0.001845	0.011132	0.023537	0.002863	0.003944	0.008524	0.013868	0.03416	0.001781	0.00388	0.100509
6	0.003743	0.002086	-0.00043	0.003209	0.002139	0.004385	0.00754	0.005134	0.029305	0.006845	0.001551	0.001337	0.004599	0.056952	0.007861	0.001551	0.090802
6	0.00474	0.000885	0.00526	0.004948	0.003281	0.003125	0.004062	0.005417	0.03651	0.011146	0.001615	-0.00016	0.004583	0.063594	0.010885	0.002708	0.089323
6	0.008009	0.00742	0.005713	0.002709	0.008657	0.004888	0.006302	0.008716	0.038398	0.007067	0.005359	0.001413	0.008716	0.066784	0.011661	0.008363	0.089517
6	0.002968	0.001027	-0.00103	0.002283	-0.00205	-0.00011	-0.00194	0.009361	0.013014	0.00411	0.002055	-0.00126	0.000457	0.028082	0.014155	0.005594	0.018037
6	0.012674	0.009262	-0.0016	0.008635	0.002368	0.006407	0.001114	0.005432	0.035515	0.012744	0.005501	0.005014	0.010655	0.058008	0.010655	0.005641	0.086003
7	0.00135	-0.00112	-0.0037	-0.00123	0.007981	0.001291	-0.00106	0.000587	0.017136	0.002641	0.000822	-0.00112	0.005399	0.032746	-0.00335	0.001467	0.048826
7	-0.00121	-0.00033	-0.00044	-0.00198	0.005837	0.00011	0.00033	0.002313	0.001652	0.002863	0.000441	-0.00319	-0.00022	0.000661	0.012445	-0.0022	0.038656
7	0.002617	0.003324	-0.00113	0.000141	-0.00113	0.002687	-0.00339	0.005375	0.016054	0.004668	0.000212	0.003041	0.005304	0.03819	0.005233	0.00396	0.060184
7	0.002674	0	0.001925	-0.00123	0.008021	0.000214	0.008449	0.006096	0.019733	0.002995	-0.00011	0.001818	0.005561	0.041337	0.003583	0.002834	0.068021
7	0.001471	-0.00037	0	0.000105	0.007248	0.000735	0.002101	0.002363	0.018225	0.001996	0.00021	0.000525	0.007458	0.034769	0.002311	0.002048	0.062658
8	0.005929	-0.00043	-0.00489	-0.00489	-0.00183	-0.00275	-0.0022	0.005562	0.026467	0.000122	-0.00122	0.000917	0.017054	0.032641	-0.00177	-0.00153	0.062836
8	0.006122	0.002405	0.001093	0.001531	0.005539	0.007362	0.018586	0.02981	0.018367	0.008163	0.001822	0.010641	0.013776	0.034329	0.003863	0.004082	0.065671
8	0.000813	0.001563	0.000313	0.00075	0.014938	0.007125	0.00625	0.004313	0.038563	0.00225	0.002625	0.001813	0.017563	0.037938	0.004875	0.00175	0.063563
8	0.001151	0.000959	-0.00288	0.002941	0.0039	0.003069	0.002749	0.004923	0.031522	0.005179	0.002046	0.005307	0.01867	0.030371	0.003261	0.005179	0.08344
8	0.001597	-0.0019	0.004177	0.000921	0.002027	0.002826	0.006327	0.005405	0.03317	0.006327	0.001966	0.008968	0.009459	0.041339	0.003256	0.003563	0.04312
9	0.002215	0.001013	0.001646	0.00057	0.008608	0.001772	0.008228	0.005253	0.026709	0.006329	0.001519	0.002405	0.008291	0.052722	0.005759	0.006139	0.040127
9	0.002584	0.001606	0.011872	0.002235	0.005726	0.00412	0.023813	0.002863	0.025838	0.005936	0.003212	0.001816	0.002374	0.050559	0.01243	0.010335	0.017318
9	0.003683	-0.00144	0.00181	-0.00243	0.004557	-0.00019	0.014107	0.010986	0.018165	0.001436	0.000687	0.003059	0.006242	0.048564	0.004557	0.000499	0.03764
9	-1.11E-17	-0.00151	-0.00127	-0.0012	0.004759	-0.00163	0.011446	0.002349	0.018554	0.005542	-0.00036	0.000542	0.003373	0.061807	0.011506	0.002952	0.051084
9	0.003473	0.002818	0.008388	0.001442	0.004128	0.001573	0.009043	0.004194	0.019332	0.004194	0.003145	0.005898	0.003211	0.038925	0.007274	0.004915	0.047379
10	0.005746	0.001711	0.004401	-0.00037	0.003912	0.001834	-0.00226	0.012897	0.015342	0.003729	0.003729	0.000856	0.005685	0.058191	0.012042	0.002751	0.104095
10	0.007734	0.005882	-0.00153	0.010839	0.00659	0.004793	0.016013	0.020044	0.025054	0.009205	0.001198	0.010621	0.011057	0.056046	0.007462	0.006754	0.09951
10	0.00136	-0.00264	-0.00461	0.000151	-0.00023	-0.0006	-0.00181	0.016616	0.001586	-0.0031	0.000755	-0.00045	0.010952	0.026511	0.001813	-0.00234	0.075
10	0.007549	0.004545	0.00276	0.005682	0.001299	0.004383	0.006494	0.001623	0.020049	0.003734	0.000731	0.007062	0.00211	0.00487	0.013474	0.004058	0.052597
10	0.012754	0.006772	-0.00034	0.005079	0.001467	0.006659	0.004966	0.013883	0.028217	0.004402	0.002032	0.002314	0.013883	0.069074	0.008409	0.005926	0.108973

Appendix A continued

Spatial cross-validation splits

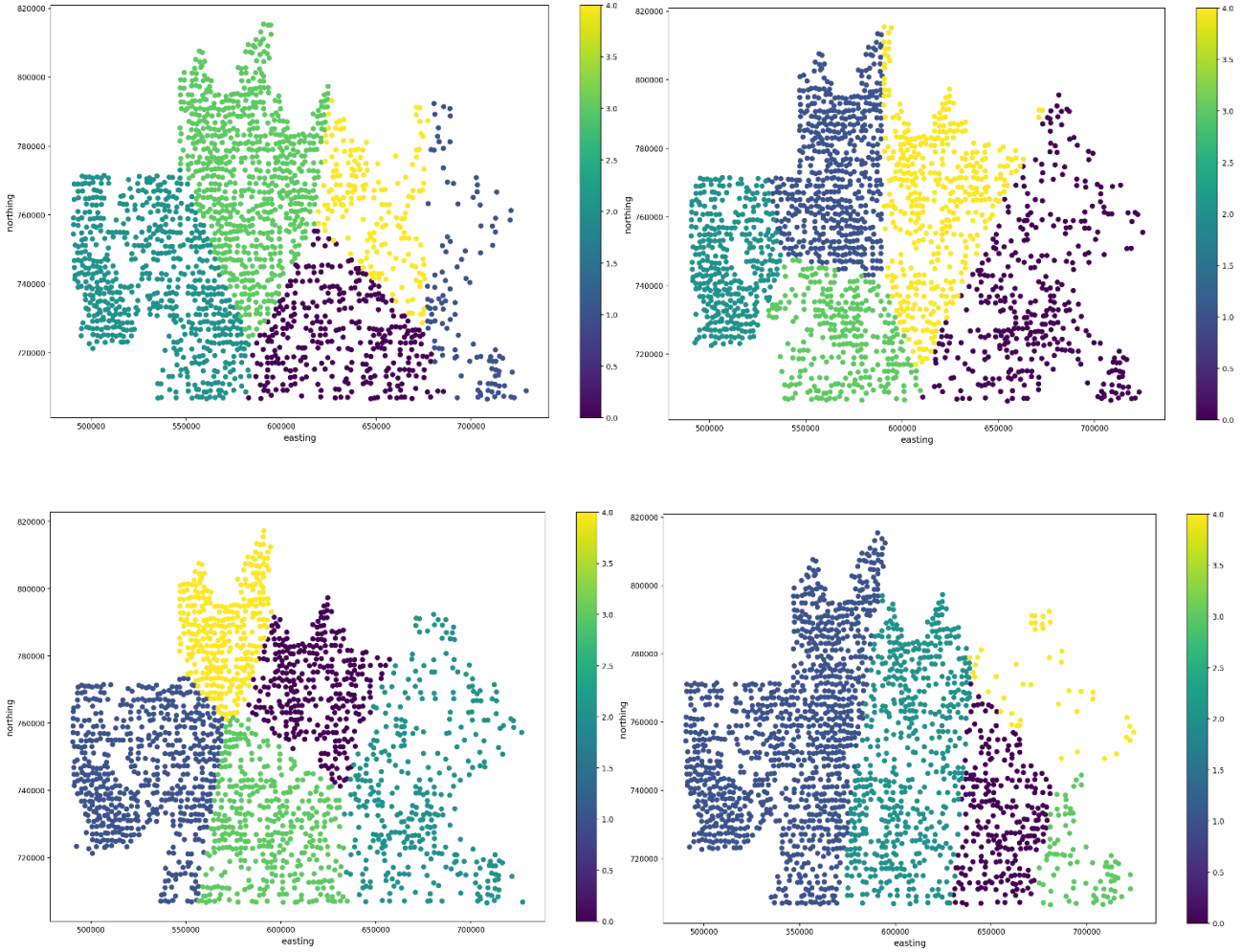

Appendix A continued

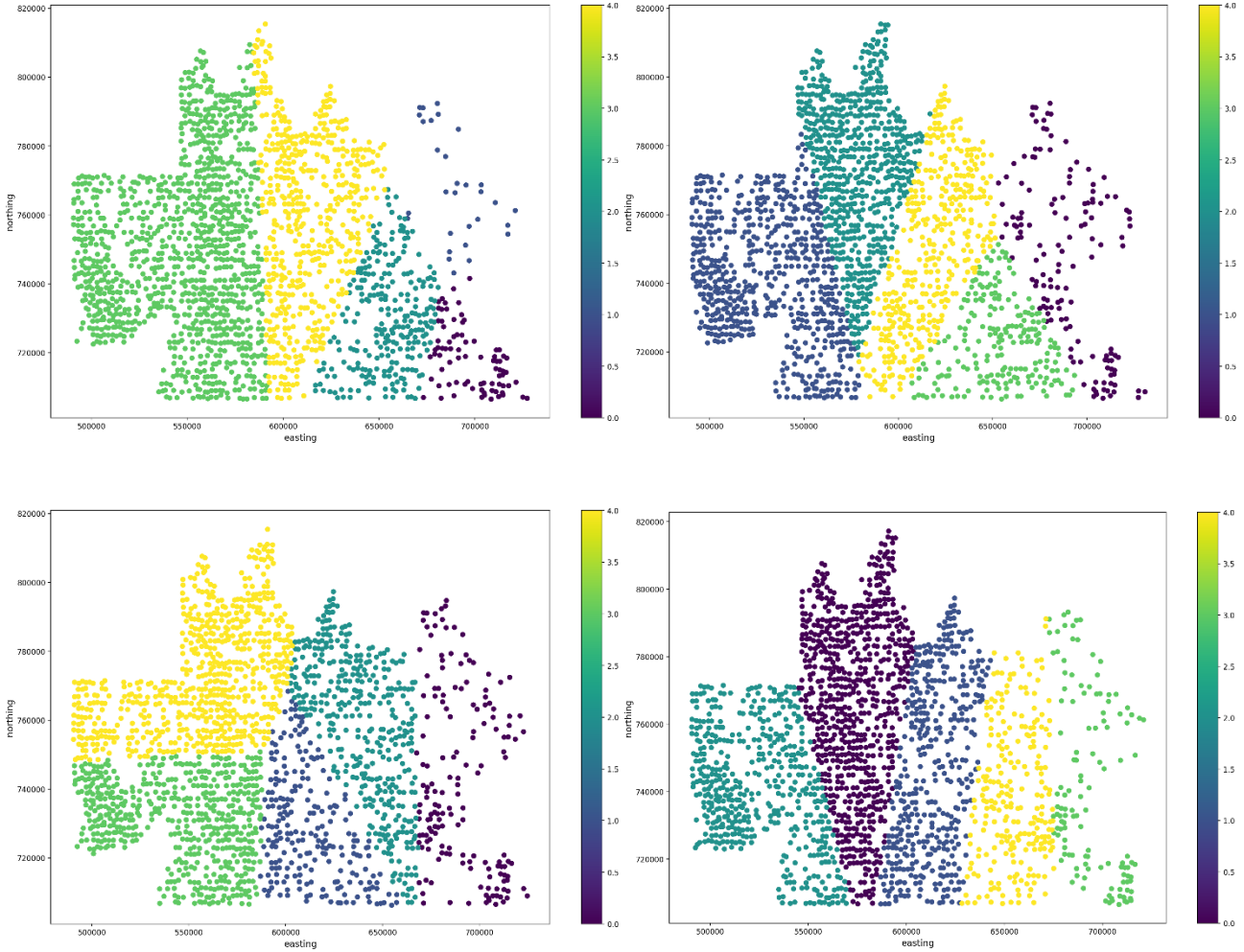

Appendix A continued

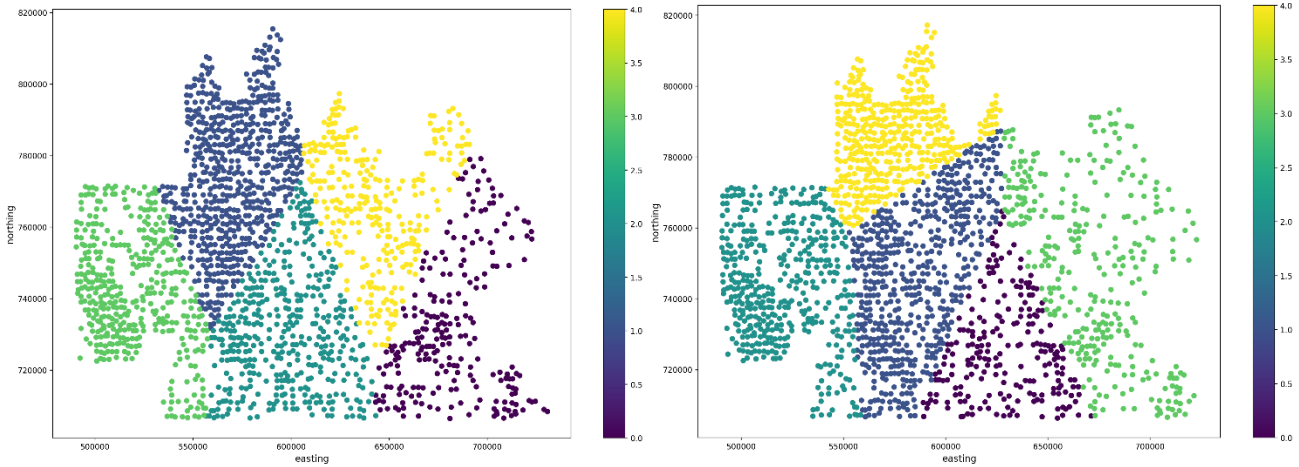

Model performance

split_inde	precision_	recall_clas	f1-score_c	support_c	precision_	recall_clas	f1-score_c	support_c	precision_	recall_wei	f1-score_v	support_v	precision_	recall_ma	f1-score_r	support_n	accuracy	T_class1	T_class2	F_class1	F_class2
1	0.755556	0.623853	0.683417	109	0.679688	0.798165	0.734177	109	0.717622	0.711009	0.708797	218	0.717622	0.711009	0.708797	218	0.711009	6800	8700	4100	2200
1	0.757009	0.589091	0.662577	275	0.66369	0.810909	0.729951	275	0.71035	0.7	0.696264	550	0.71035	0.7	0.696264	550	0.7	16200	22300	11300	5200
1	0.733607	0.832558	0.779956	215	0.806452	0.697674	0.74813	215	0.770029	0.765116	0.764043	430	0.770029	0.765116	0.764043	430	0.765116	17900	15000	3600	6500
1	0.893805	0.623457	0.734545	162	0.7109	0.925926	0.80429	162	0.802353	0.774691	0.769417	324	0.802353	0.774691	0.769417	324	0.774691	10100	15000	6100	1200
1	0.681159	0.658879	0.669834	214	0.669683	0.691589	0.68046	214	0.675421	0.675234	0.675147	428	0.675421	0.675234	0.675147	428	0.675234	14100	14800	7300	6600
2	0.939024	0.65812	0.773869	117	0.736842	0.957265	0.832714	117	0.837933	0.807692	0.803292	234	0.837933	0.807692	0.803292	234	0.807692	7700	11200	4000	500
2	0.743682	0.668831	0.704274	308	0.699115	0.769481	0.732612	308	0.721399	0.719156	0.718443	616	0.721399	0.719156	0.718443	616	0.719156	20600	23700	10200	7100
2	0.84375	0.658537	0.739726	205	0.72	0.878049	0.791209	205	0.781875	0.768293	0.765467	410	0.781875	0.768293	0.765467	410	0.768293	13500	18000	7000	2500
2	0.776824	0.89604	0.832184	202	0.877193	0.742574	0.80429	202	0.827009	0.819307	0.818237	404	0.827009	0.819307	0.818237	404	0.819307	18100	15000	2100	5200
2	0.902439	0.517483	0.657778	143	0.661765	0.944056	0.778098	143	0.782102	0.730769	0.717938	286	0.782102	0.730769	0.717938	286	0.730769	7400	13500	6900	800
3	0.807018	0.528736	0.638889	348	0.649573	0.873563	0.745098	348	0.728295	0.701149	0.691993	696	0.728295	0.701149	0.691993	696	0.701149	18400	30400	16400	4400
3	0.795031	0.62439	0.699454	205	0.690763	0.839024	0.757709	205	0.742897	0.731707	0.728581	410	0.742897	0.731707	0.728581	410	0.731707	12800	17200	7700	3300
3	0.759259	0.857741	0.805501	239	0.836538	0.728033	0.778523	239	0.797899	0.792887	0.792012	478	0.797899	0.792887	0.792012	478	0.792887	20500	17400	3400	6500
3	0.808511	0.612903	0.697248	62	0.688312	0.854839	0.76259	62	0.748411	0.733871	0.729919	124	0.748411	0.733871	0.729919	124	0.733871	3800	5300	2400	900
3	0.778846	0.669421	0.72	121	0.710145	0.809917	0.756757	121	0.744496	0.739669	0.738378	242	0.744496	0.739669	0.738378	242	0.739669	8100	9800	4000	2300
4	0.877193	0.617284	0.724638	81	0.704762	0.91358	0.795699	81	0.790977	0.765432	0.760168	162	0.790977	0.765432	0.760168	162	0.765432	5000	7400	3100	700
4	0.775701	0.734513	0.754545	113	0.747899	0.787611	0.767241	113	0.7618	0.761062	0.760893	226	0.7618	0.761062	0.760893	226	0.761062	8300	8900	3000	2400
4	0.856061	0.585492	0.695385	193	0.685039	0.901554	0.778523	193	0.77055	0.743523	0.736954	386	0.77055	0.743523	0.736954	386	0.743523	11300	17400	8000	1900
4	0.861751	0.708333	0.777547	264	0.752412	0.886364	0.813913	264	0.807081	0.797348	0.79573	528	0.807081	0.797348	0.79573	528	0.797348	18700	23400	7700	3000
4	0.686567	0.709877	0.698027	324	0.699681	0.675926	0.687598	324	0.693124	0.692901	0.692813	648	0.693124	0.692901	0.692813	648	0.692901	23000	21900	9400	10500
5	0.821429	0.647887	0.724409	71	0.709302	0.859155	0.77707	71	0.765365	0.753521	0.75074	142	0.765365	0.753521	0.75074	142	0.753521	4600	6100	2500	1000
5	0.733138	0.819672	0.773994	305	0.795539	0.701639	0.745645	305	0.764338	0.760656	0.759819	610	0.764338	0.760656	0.759819	610	0.760656	25000	21400	5500	9100
5	0.746667	0.54902	0.632768	306	0.643411	0.813725	0.718615	306	0.695039	0.681373	0.675692	612	0.695039	0.681373	0.675692	612	0.681373	16800	24900	13800	5700
5	0.842697	0.721154	0.777202	104	0.756303	0.865385	0.807175	104	0.7995	0.793269	0.792188	208	0.7995	0.793269	0.792188	208	0.793269	7500	9000	2900	1400
5	0.78169	0.587302	0.670695	189	0.669492	0.835979	0.743529	189	0.725591	0.71164	0.707112	378	0.725591	0.71164	0.707112	378	0.71164	11100	15800	7800	3100
6	0.828571	0.725	0.773333	40	0.755556	0.85	0.8	40	0.792063	0.7875	0.786667	80	0.792063	0.7875	0.786667	80	0.7875	2900	3400	1100	600
6	0.777778	0.466667	0.583333	15	0.619048	0.866667	0.722222	15	0.698413	0.666667	0.652778	30	0.698413	0.666667	0.652778	30	0.666667	700	1300	800	200
6	0.815534	0.666667	0.733624	126	0.718121	0.849206	0.778182	126	0.766827	0.757937	0.755903	252	0.766827	0.757937	0.755903	252	0.757937	8400	10700	4200	1900
6	0.741573	0.73743	0.739496	537	0.738889	0.743017	0.740947	537	0.740231	0.740223	0.740221	1074	0.740231	0.740223	0.740221	1074	0.740223	39600	39900	14100	13800
6	0.822115	0.66537	0.735484	257	0.718954	0.856031	0.781528	257	0.770535	0.7607	0.758506	514	0.770535	0.7607	0.758506	514	0.7607	17100	22000	8600	3700
7	0.844444	0.617886	0.713615	123	0.698718	0.886179	0.781362	123	0.771581	0.752033	0.747489	246	0.771581	0.752033	0.747489	246	0.752033	7600	10900	4700	1400
7	0.756539	0.721689	0.738703	521	0.733945	0.767754	0.750469	521	0.745242	0.744722	0.744586	1042	0.745242	0.744722	0.744586	1042	0.744722	37600	40000	14500	12100
7	0.799043	0.623134	0.70021	268	0.691131	0.843284	0.759664	268	0.745087	0.733209	0.729937	536	0.745087	0.733209	0.729937	536	0.733209	16700	22600	10100	4200
7	0.866667	0.65	0.742857	40	0.72	0.9	0.8	40	0.793333	0.775	0.771429	80	0.793333	0.775	0.771429	80	0.775	2600	3600	1400	400
7	0.714286	0.652174	0.681818	23	0.68	0.73913	0.708333	23	0.697143	0.695652	0.695076	46	0.697143	0.695652	0.695076	46	0.695652	1500	1700	800	600
8	0.858586	0.541401	0.664062	157	0.665116	0.910828	0.768817	157	0.761851	0.726115	0.71644	314	0.761851	0.726115	0.71644	314	0.726115	8500	14300	7200	1400
8	0.734756	0.83391	0.781199	289	0.808	0.698962	0.749536	289	0.771378	0.766436	0.765368	578	0.771378	0.766436	0.765368	578	0.766436	24100	20200	4800	8700
8	0.901639	0.628571	0.740741	175	0.714912	0.931429	0.808933	175	0.808276	0.78	0.774837	350	0.808276	0.78	0.774837	350	0.78	11000	16300	6500	1200
8	0.693122	0.678756	0.685864	193	0.685279	0.699482	0.692308	193	0.6892	0.689119	0.689086	386	0.6892	0.689119	0.689086	386	0.689119	13100	13500	6200	5800
8	0.666667	0.720497	0.692537	161	0.695946	0.639752	0.666667	161	0.681306	0.680124	0.679602	322	0.681306	0.680124	0.679602	322	0.680124	11600	10300	4500	5800
9	0.841379	0.659459	0.739394	185	0.72	0.875676	0.790244	185	0.78069	0.767568	0.764819	370	0.78069	0.767568	0.764819	370	0.767568	12200	16200	6300	2300
9	0.720472	0.706564	0.71345	259	0.712121	0.725869	0.718929	259	0.716297	0.716216	0.71619	518	0.716297	0.716216	0.71619	518	0.716216	18300	18800	7600	7100
9	0.704846	0.91954	0.798005	174	0.884298	0.614943	0.725424	174	0.794572	0.767241	0.761714	348	0.794572	0.767241	0.761714	348	0.767241	16000	10700	1400	6700
9	0.861702	0.558621	0.677824	145	0.673469	0.910345	0.774194	145	0.767586	0.734483	0.726009	290	0.767586	0.734483	0.726009	290	0.734483	8100	13200	6400	1300
9	0.80292	0.518868	0.630372	212	0.644599	0.872642	0.741483	212	0.72376	0.695755	0.685928	424	0.72376	0.695755	0.685928	424	0.695755	11000	18500	10200	2700
10	0.813953	0.66879	0.734266	157	0.718919	0.847134	0.777778	157	0.766436	0.757962	0.756022	314	0.766436	0.757962	0.756022	314	0.757962	10500	13300	5200	2400
10	0.871795	0.596491	0.708333	57	0.693333	0.912281	0.787879	57	0.782564	0.754386	0.748106	114	0.782564	0.754386	0.748106	114	0.754386	3400	5200	2300	500
10	0.757962	0.760383	0.759171	313	0.759615	0.757188	0.7584	313	0.758789	0.758786	0.758785	626	0.758789	0.758786	0.758785	626	0.758786	23800	23700	7500	7600
10	0.759857	0.590529	0.664577	359	0.665148	0.81337	0.73183	359	0.712502	0.70195	0.698203	718	0.712502	0.70195	0.698203	718	0.70195	21200	29200	14700	6700
10	0.809524	0.573034	0.671053	89	0.669565	0.865169	0.754902	89	0.739545	0.719101	0.712977	178	0.739545	0.719101	0.712977	178	0.719101	5100	7700	3800	1200

Appendix A continued

Logistic regression

Feature importance for each model

split_inde	Al	Ba	Ca	Cr	Cu	Fe	K	Li	Mg	Mn	Na	Ni	P	S	Sr	Ti	V	Zn	Zr	Ag	As	Be	Bi	Cd	Ce	Co	Cs	Ga	Ge	Hf	Hg	In	La	Mo	Nb	Pb	Rb	Sb	Sc	Se	Sn	Te	Th	Tl	U	W	Y
1	0.055804	0.003567	0.005623	0.00659	0.01445	0.003325	0.000605	0.0211	-0.00115	0.008464	0.000181	0.001572	0.003144	0.007437	0.004172	-0.00067	0.000605	0.002297	0.003023	0.000846	0.002237	0.00792	0.009794	0.00399	0.012878	0.005925	0.00127	0.013241	0.000967	0.002056	0.010641	3.33E-17	0.001874	0.000302	0.00127	0.003023	0.03942	0.005562	0.032346	-0.00048	0.009432	0.002721	0.005985	0.001451	0.004111	0.000907	0.219
1	0.085538	0.004355	0.003118	0.00043	0.014247	0.002204	0.003333	0.019839	-0.00172	0.016022	0.000591	0.00086	0.001935	0.002473	0.006022	-0.0021	0.000914	0	0.003495	-0.00075	0.014301	0.009785	0.015968	0.000591	0.013065	0.001022	0.002097	0.013441	-0.00081	0.004462	0.008011	-0.00086	-0.00183	0.001505	0.00371	-0.00075	0.081828	0.009677	0.032849	-0.00011	0.010591	0.000806	0.009462	0.00629	0.001989	-0.00231	0.208
1	0.074483	0.002944	0.003616	0.000362	0.01281	0.001498	-0.00015	0.019112	-0.00429	0.012603	-0.00021	0.000775	-0.00103	0.000775	0.003616	-0.00351	0.001033	0.000465	-0.00026	-0.00046	0.004339	0.004959	0.01405	-3.33E-17	0.012448	0.003461	-0.0015	0.013998	5.17E-05	0.000258	0.007593	-0.00021	-0.00077	-0.00108	-0.00279	0.000826	0.055888	0.00749	0.029442	-0.00155	0.005682	5.17E-05	0.006663	0.003461	0.003926	-0.0016	0.218
1	0.107503	0.003206	0.00075	0.03472	0.003411	-0.00068	0.001228	0.007913	0.003411	0.02558	-0.00027	0.002251	0.002797	0.005252	0.002729	0.002729	0.001432	0.002046	-0.00048	-0.0015	0.006139	0.004434	0.013438	0.001091	0.008799	0.004502	0.004366	0.002319	0.000477	0.001501	0.005457	-0.00164	0.001432	0.002387	0.000409	0.008322	0.067667	0.003274	0.019168	0.006344	0.000136	0	0.005935	-0.00075	0.004843	0.001432	0.224
1	0.008258	0.009389	0.006674	0.001923	0.02138	0.012217	0.044344	0.002715	0.001584	0.01776	-0.00147	0.013122	0.010633	0.013688	0.005543	0.004977	0.001584	0.005995	0.001131	0.002602	0.003054	0.01233	0.01595	0.001697	0.007014	0.006787	0.021041	0.028959	0.005995	0.070362	-0.00079	0.0069	0.001018	-0.00079	0.011991	0.001018	0.029864	0.031561	0.020701	0.000792	0.003281	0.005995	0.020475	0.052376	0.044118	0.000905	0.066
2	0.001871	0.013306	0.001247	0.000416	0.015593	-0.00229	0.043659	0.04158	-0.00166	0.007692	0	-0.00062	0.003638	0.006549	0.003119	-0.0027	-0.00042	0.001351	0.019751	0.005301	-0.00146	0.011954	-0.00218	-0.00187	-0.0001	-0.00218	0.014033	0.01237	-0.00114	-0.00405	-0.00249	-0.0027	-0.00281	0.001143	-0.00281	-0.00073	0.034511	0.024428	0.002807	-0.00052	0.003534	-0.00468	-0.0001	-0.00343	0.019439	-0.00125	0.122
2	0.041447	0.010348	0.0151	0.001848	0.010507	0.006336	0.000898	0.013992	-0.0009	0.021964	0.001267	-0.00042	0.003115	-0.00074	0.008553	0.000158	0.008606	0.009504	-0.00042	0.001267	0.006547	0.010612	0.011932	0.001056	0.014361	0.013886	0.017001	0.018743	-0.00084	0.009029	0.009081	0.000898	-2.22E-17	-2.22E-17	0.000106	-0.00016	0.071014	0.005755	0.025238	0.005649	0.008131	-0.00169	-0.00063	0.000634	0.003643	-1.11E-17	0.247
2	0.055024	0.011804	0.016223	0.0023	0.013438	0.00908	-0.0003	0.018947	0.000908	0.010472	0.001513	0.0023	-0.00115	-0.0003	0.00563	-0.00145	0.003208	0.006538	-0.00054	0.001877	0.0023	0.01132	0.006598	0.002785	0.012591	0.01477	0.034806	0.020218	-0.0003	0.00914	0.010169	0.000182	-0.00061	-0.00194	0.001816	0.000303	0.072458	0.004903	0.020339	0.0046	0.007869	-0.00061	-0.0003	0.000787	0.003329	-0.00048	0.246
2	0.029303	0.00915	0.017048	0.002179	0.01122	0.008007	0.003377	0.017484	-0.00098	0.015686	0.003758	-0.00076	0.000871	-0.00049	0.009314	0.000871	0.004303	0.007734	0.000163	-0.0006	0.007571	0.015359	0.009314	0.003159	0.014706	0.011166	0.02756	0.021405	0.001035	0.006536	0.008824	-0.00033	0.004466	-0.0006	0.005556	0.000272	0.065523	0.004521	0.025926	0.006373	0.008279	-0.00098	-0.00163	-0.00185	0.002179	-0.00022	0.238
2	0.058242	-0.00103	0.002266	0.008654	-0.00082	-0.00199	-0.00048	0.007761	0.001168	0.003571	0.000962	-0.00343	-0.0022	-0.00021	0.000412	6.87E-05	0.029258	-0.00137	-0.00206	0.000687	0.003571	0.002335	0.009409	-0.00034	0.005632	0.005975	0.013874	0.004464	-0.00261	-0.00014	0.005014	0.000824	-0.00124	0.000343	-0.0022	0.002953	0.038187	-0.00021	0.017445	-0.00124	0.000206	-0.00185	-0.0013	-0.00192	-0.00192	0.000412	0.223
3	0.001727	0.008771	0.010912	-0.00152	0.019475	-0.00055	0.042541	0.000552	0.004144	0.02058	-0.00193	0.014848	0.002072	0.005663	0.014365	0.008149	0.009807	-0.00159	-0.00214	-0.00173	-0.00062	0.002417	-6.91E-05	-0.00124	0.011257	-0.00193	-0.00014	-0.00311	-6.91E-05	-0.00207	-0.00214	-0.00138	-0.00256	0.000276	0.030939	-0.0029	0.002555	0.032251	0.001519	-0.00041	-0.00028	-0.00055	0.008771	0.001727	0.014917	1.11E-17	0.197
3	0.079097	0.013211	0.01388	0.026533	0.011538	0.011148	0.009197	0.016722	0.007692	0.020234	0.007414	0.013434	0.00524	0.003512	0.011761	0.004627	0.000836	0.006355	0.001895	0.002899	0.001951	0.010312	0.006856	0.008807	0.014604	0.011817	0.002899	0.011873	0.001561	0.002062	0.007135	0.004849	0.001115	0.00864	0.010089	0.002899	0.029933	0.01243	0.01505	0.004905	0.004571	0.001003	0.004292	0.005964	0.014827	0.005518	0.215
3	0.021378	0.009517	0.008665	0.040625	0.009517	0.00696	0.015412	0.012358	0.010298	0.013352	0.000994	0.00902	0.008026	0.007244	0.007457	0.00419	0.001349	0.005895	0.007315	0.001989	0.003551	0.012287	0.003409	0.006605	0.010298	0.000639	0.00483	0.002415	0.003693	0.022514	0.006534	0.001136	0.020739	0.010227	0.008097	0.007955	0.014276	0.007173	0.024645	0.003622	0.000426	0.001918	0.00206	7.10E-05	0.017685	0.00071	0.140
3	0.047529	0.010988	0.002536	0.030169	0.007737	0.005007	0.007542	0.005657	0.00052	0.016905	0.003576	0.001951	0.003576	0.005072	0.002796	0.003446	0.001756	0.007477	0.002211	0.002601	0.000585	0.008062	0.004486	0.004746	0.008388	0.006372	0.007087	0.014954	0.000455	0.005007	0.003186	0.001365	0.001105	0.008127	0.005397	0.000325	0.018791	0.002601	0.010793	-0.00059	0.00104	0.00117	0.003056	0.001625	0.020741	0.00065	0.154
3	0.026241	0.000993	0.007196	0.013524	0.005831	0.005025	-0.00465	0.009181	-0.00192	-0.00453	-0.00025	0.004156	-0.00558	0.000806	0.006141	-0.00155	-0.0031	-0.00118	-0.0036	-0.00627	0.002792	0.006948	-0.00484	-0.00335	0.010546	0.004156	-0.00459	-0.00124	-0.00509	-0.00242	0.005087	-0.00174	6.20E-05	0	-0.00043	-0.00416	0.033747	-0.00112	0.008809	0.001675	-0.00081	-0.00596	0.002543	-0.00267	-0.00447	-0.00037	0.218
4	0.031898	0.002692	-0.00135	-0.00296	0.010363	-0.00155	0.014872	0.002894	-0.00559	0.034993	-0.00168	0.004105	0.011978	0.00572	-0.00094	-0.0041	0.000673	-0.00067	-0.00249	-0.00162	-0.00195	0.001413	0.006729	-0.00061	0.009354	0.005384	0.000808	0.011642	-0.00081	0	-0.00121	-0.00289	-0.00471	-0.00222	-0.00336	-0.00431	0.038762	0.002759	0.000404	0.008479	-0.00074	-0.0002	-0.0004	0.06245	0.005114	-0.00108	0.137
4	0.029139	-0.00105	0.009437	-0.00182	0.009216	0.001159	-0.00348	0.012472	-0.00039	0.024834	-0.00287	-0.00138	-0.00292	-0.00099	0.003477	0	0.001049	-0.00237	0.00011	-5.52E-05	0.001821	0.006236	0.011479	5.52E-05	0.016611	0.008609	-0.0011	0.011976	-0.00055	0.000717	0.002759	-0.0005	-0.00276	-0.00221	0.001435	-0.00397	0.069757	0.002208	0.0133	0.003642	-0.00232	-0.00033	-0.00044	0.010375	5.52E-05	-0.00055	0.165
4	0.001765	0.000588	0.012269	0.007143	0.010168	0.003361	0.005294	0.016975	0.008908	0.032353	0.001429	0.018571	0.00958	0.033697	0.001008	0.003445	-0.00118	0.004874	0.001597	0.022101	0.000924	0.001597	0.024202	0.003277	0.002017	0.004286	0.00916	0.017227	0.002437	0.002941	0.003277	0.003529	0.002521	0.002605	0.056303	-0.00076	0.043866	0.004706	0.018319	-0.00134	0.004538	0.001176	0.001849	0.008739	0.036555	8.40E-05	0.102
4	0.07954	-0.00031	0.006779	0.000808	0.003047	-6.22E-05	0.000622	0.00796	0.003172	0.0074	-0.001	-0.001	0.000187	-0.00031	0.003172	-0.001	-0.00012	-1.11E-17	-0.00056	-0.00168	0.000124	0.007152	0.007152	-0.00137	0.008022	0.003794	-0.00081	-0.00087	-0.00056	-0.00081	0.002612	-0.00044	0.010945	-0.00087	-0.00118	-0.00243	0.048694	0.006592	0.006841	-0.00075	-0.00243	-0.00124	-0.00124	0.001368	-0.00131	0.000187	0.194
4	0.098709	-0.00141	0.011092	0.013674	0.01561	0.00358	-0.00417	0.015258	0.002171	0.025528	-0.0027	-0.00211	-0.0017	-0.0027	0.00088	-0.00164	-0.00047	-0.00106	-0.00082	0.000235	0.000117	0.003052	0.013204	0	0.015376	0.014261	-0.00094	0.011326	-0.00176	0.002582	0.003697	0	-0.00047	-0.0017	-0.00205	-0.002	0.065552	0.008392	0.018897	0.000704	-0.00405	-0.00094	-0.00182	0.014965	0.000646	-0.00182	0.1
5	0.00414	0.013885	0.00707	-0.00051	0.011338	0.002484	0.01293	0.008153	0.00121	0.022675	-0.00032	0.011783	0.000255	-0.00121	0.007707	0.001783	0.001592	0.001338	0.002548	0.001656	0.004586	0.008662	0.003121	0.001529	0.006051	0.010828	0.003439	0.003694	0.000955	-0.00057	0.003885	0.001338	0.007325	0.001911	0.026688	0.001274	0.031465	0.024586	0.011465	0.001847	0.001146	0.002293	0.010764	0.027261	0.005032	0.002357	0.172
5	0.08178	0.001553	-0.00305	0.004182	-5.97E-05	0.002688	0.003286	0.007467	-0.00293	0.034229	-0.00215	5.97E-05	-0.00084	-0.00054	-0.00108	-0.00514	-0.00245	-0.00131	-0.00221	-0.00376	0.002628	0.005137	0.012007	0.001912	0.005675	0.011649	-0.00293	0.00233	-0.00466	-0.00078	0.005615	-0.00012	0.000358	0.006392	-0.00502	-0.00161	0.018459	-0.00143	0.012246	-0.00209	-0.00233	-0.00227	-0.00454	0.008244	-0.00472	-0.00108	0.111
5	0.071613	-0.00219	-0.00232	0.000452	0.000194	0.000581	-0.0031	0.002452	-0.00219	0.009806	-0.00103	-0.00297	-0.00374	0.00129	0.001161	0.000516	0.01071	-0.0009	0.00071	0.000968	0.002516	-0.00129	-0.00181	-0.00348	0.001548	0.003806	-0.00123	-0.00013	-0.00116	-0.00084	-0.00142	0.00071	0.002581	-0.00168	-0.00213	-0.00039	0.023613	-0.00226	0.005097	-0.00277	-0.00077	0.00071	-0.00026	-0.00071	-0.00123	-0.00013	0.116
5	0.005853	0.005712	-0.00042	0.005712	0.003244	0.003667	0.012976	0.008745	-0.00169	0.009097	0.001269	-0.00092	0.004654	-0.00085	0.003526	-0.00162	0.005571	0.001834	7.05E-05	0.001693	0.002821	0.000987	0.001058	0.010508	0.000353	0.001763	-0.00254	0.000141	-0.00021	-0.00035	-0.00113	0.000282	0.001058	0.002186	-0.00028	-0.00197	0.073977	0.003385	0.010437	-0.00028	0.001199	0.000353	0.007193	0.000564	0.012412	-0.00197	0.02
5	0.043451	0.006927	0.017884	0.002897	0.008816	0.005479	0.004093	0.018262	-0.00057	0.008627	0.008375	0.000693	0.000504	0.006738	0.009761	0.004849	-0.00031	-0.00044	0.00403	0.003275	0.014043	0.002204	0.002519	0.011398	0.011083	0.014106	0.00932	0.004534	0.007053	0.002645	0.00573	6.30E-05	0.001511	0.008438	0.007305	0.002834	0.08961	0.008627	0.014861	0.000378	0.010202	0.005793	0.001826	0.002582	0.002708	0.001448	0.117
6	0.069478	0.004552	0.004254	0.015075	0.006493	0.011791	0.013134	0.017612	-0.00254	0.031716	-0.00134	0.004179	-0.00448	-0.00306	-0.00209	0.000224	-0.00239	-0.00201	0.005448	-0.00336	-0.00284	-0.00067	0.002164	0.014254	-0.00284	-0.0056	0.001642	0.008209	0.000896	-0.00299	0.004179	0.003433	-0.00209	-4.44E-17	-0.00037	-0.00082	0.002985	-0.00224	0.017239	-0.0006	-0.00015	0.000149	0.008507	-0.00082	0.003134	-0.00328	0.120
6	0.086369	0.001319	-0.00308	0.00892	0.003141	0.00892	0.000251	0.005025	-0.00308	0.057035	-0.00245	-0.00289	-0.00226	-0.00069	-0.0017	-0.00163	-0.0017	-0.00038	-0.00025	-0.00302	-0.0022	0.003455	0.008731	-0.00101	-0.0022	0.003957	0.007224	0.008668	0.000565	-0.00396	0.003455	-0.00214	6.28E-05	-0.00258	-0.00333	-0.0022	0.028769	-0.00239	0.00358	-0.00396	-0.00283	-0.00239	-0.00314	0.002827	-0.00339	-0.00352	0.218
6	0.033766	0.005	0.002403	6.49E-05	0.008182	0.002792	0.032273	0.006364	-0.00084	0.021688	-6.49E-05	0.011429	0.001104	0.008636	0.005455	-0.00182	0.002273	1.11E-17	0.000195	0.001169	0.001039	0.006104	0.002792	0.000455	0.006688	0.001558	1.11E-17	0.001623	0.000195	-0.00143	0.002662	0.000649	0.001623	6.49E-05	0.011104	1.11E-17	0.003701	0.016623	0.00487	0.00013	0.000195	0.001364	0.003506	0.005714	0.001234	0.00013	0.238
6	0.089874	0.000801	0.005892	0.015275	0.003661	0.007151	-0.0028	0.011384	-0.0032	0.032323	-0.00017	0.004176	-0.00338	-0.00069	-0.00172	-0.00069	-0.00263	-0.0004	-0.00195	-0.00252	-0.00343	0.000572	-0.00137	-0.0028	0.003261	-0.00057	-0.00412	0.004805	-0.00097	-0.00229	0.002689	0.000858	0.000286	-0.0036	-0.00189	-0.00097	0.026373	-0.00189	0.006693	-0.00366	-0.00086	-0.00126	-0.0028	-0.0012	-5.72E-05	-0.00257	0.192
6	0.123987	0.005127	-0.00171	0.027468	-0.00013	0.006266	-0.00101	0.010253	0.001203	0.014114	-0.0031	0.006013	0.000443	-0.0031	0.00057	0.001646	0.001646	-0.00228	-0.00468	-0.00089	-0.0012	0.006203	-0.00127	-0.00051	0.006772	0.001709	0.000696	-0.00127	-0.00165	-0.00032	0.007975	0.001835	-0.00101	0.000253	-0.00139	-0.00158	0.018228	0.004747	0.00538	0.00038	-0.00063	-0.00316	-0.00013	-0.00335	-0.0019	-0.00044	0.227
7	0.017532	0.001052	0.002454	0.007644	0.011921	0.008696	0.012973	0.018864	0.007644	0.059537	0.001403	0.004067	0.007153	0.002665	0.002945	0.004418	0.003787	0.008415	0.001052	0.008485	0.006171	0.003576	0.014586	0.007363	0.003717	0.003576	0.014586	0.015919	0.002034	0.004488	0.002174	0.003436	0.004558	0.000281	0.005891	0.002945	0.013184	0.008275	0.020617	0.001753	0.003366	0.004769	0.004488	0.004418	0.001683	0.005049	0.132
7	0.067594	0.001035	-0.00058	0.002717	0.007891	0.002264	-0.00116	0.008668	-0.00479	0.04088	0.002135	-0.0022	-0.00019	-0.00045	0.000906	0.001682	0.00207	0.004851	-0.00078	0.000129	0.003105	-0.00162	0.00815	0.003234	0.002652	0.008409	0.012484	0.019211	0.001617	0.002717	-0.00058	0.007891	0.004851	-1.11E-17	0.002652	0.001876	0.034282	0.000388	0.017012	0.002975	-1.11E-17	0.000517	0.001358	0.002587	0.002846	-0.00065	0.120
7	0.047812	0.001875	0.005062	0.002562	0.012937	0.000187	0.013687	0.002187	-0.00206	0.030437	0.00075	0.0095	0.005937	0.017937	0.00775	0.001312	0.0015	0.000875	0.028125	0.00175	0.000437	0.003062	0.016125	0.001625	0.011375	0.003562	-0.00025	0.00575	-0.00038	0.00325	0.005437	0.002125	0.012188	0.0005	0.034312	0.005437	0.008375	0.025375	0.01675	0.002375	-0.00012	0.006375	0.0035	0.007312	0.008312	0.0005	0.231
7	0.091872	-0.00154	0.002401	0.023768	0.006219	0.001293	-0.00228	0.006958	0.000924	0.01718	-0.00462	0.002401	0.00117	0.004988	0.00782	0.001047	-0.00296	0.000185	-0.00185	-0.00037	0.003325	-0.00339	0.004126	-0.00129	0.002278	0.003448	-0.00345	0.001786	0.001478	0.002709	-0.00259	0.000246	0.002094	-0.00025	-0.00012	-6.16E-05	0.031342	0.003387	0.010099	-0.00603	0.000369	0.001416	-0.00191	-0.00166	-0.00228	-0.00037	0.169
7	0.066771	0.001247	0.006546	0.012594	0.015524	0.006983	-0.00243	0.019514	-0.00237	0.020449	-0.00056	0.000249	-0.00143	-0.00168	0.008229	0.000436	-0.00243	0.006484	-0.00175	-0.00069	0.006608	0.00106	0.00798	0.001122	0.008416	0.008541	0.001559	0.013466	-0.00118	0.009476	0.006858	0.000561	0.014526	-0.00274	0.009476	0.000623	0.040524	0.007357	0.02419	-0.00069	0.001122	0.003928	0.017519	-4.44E-17	-0.00162	-0.00231	0.190
8	0.000628	-0.00188	0.001508	0.001508	0.007286	-0.00138	0.038442	0.004648	-0.00063	0.001256	-0.00113	-0.00138	0.002889	0.010302	-0.00075	0.009548	-0.00063	0.001131	-0.00038	-0.00075	0.00402	0.000628	0.007161	0.004397	0.001759	-0.00013	-0.00101	0.011935	0.002764	-0.00364	-0.00176	0.001508	-0.00176	0.000377	0.007412	0.000251	0.091834	0.01495	0.002638	-0.00251	-0.00239	-0.00025	0.000126	0.017462	0.023492	0.001884	0.048
8	0.090237	0.008014	0.019865	0.021163	0.011005	0.005869	0.008747	0.017551	0.002088	0.021388	-0.00102	0.001298	0.005135	-0.00056	0.012754	0.001975	0.006603	0.005813	0.010722	-0.00017	0.009199	0.010102	0.011738	0.00553	0.010609	0.00474	0.018228	0.006998	0.00158	-0.00023	0.009594	0.004007	0.001354	0.004515	0.023702	-5.64E-05	0.0443	0.016986	0.021163	0.004233	0.004345	0.004458	0.006772	0.027709	0.001467	0.002878	0.205
8	0.116249	0.003421	0.002281	0.023318	0.000969	-0.00046	-0.00011	0.010205	-0.00091	0.016249	0.000456	-0.00148	0.007298	-0.00182	0.003193	0	-0.00245	0.00114	0.008438	-0.00114	0.00496	0.004561	0.003877	-0.00011	0.010034	0.003706	0.015051	-0.00051	-0.00017	-0.00302	0.002395	0.001482	0.000684	-0.00057	-0.00125	-0.00046	0.012543	0.015564	0.016249	0.000228	-0.00125	0.001254	-0.00074	0.007868	-0.00051	0.000912	0.229
8	0.114983	0.007856	0.013973	0.021829	0.013131	0.007576	0.007071	0.019865	0.003367	0.03165	0.000561	0.002806	0.005556	-0.00017	0.005387	0.000393	0.003648	0.006341	0.009652	0	0.00679	0.010606	0.013692	0.002076	0.013805	0.015208	0.010382	0.009877	0.000617	0.002694	0.006173	0.003816	0.00073	0.007744	0.008474	0.000337	0.018519	0.023232	0.026319	-0.00028	0.004097	0.003928	0.002189	0.014759	0.003704	0.001235	0.208
8	0.113679	-0.00147	-5.90E-05	0.014328	0.003715	0.001238	-0.00035	0.010142	-0.00071	0.049882	-0.00088	0.003243	0.006132	5.90E-05	0.002535	-0.0013	0.001533	0.002535	0.003774	5.90E-05	-0.001	0.002064	0.016156	-0.00012	0.008903	0.007724	0.004776	0.003184	0.00059	0.001179	0.00283	0.000177	-5.90E-05	0.00112	0.000943	-0.00106	0.01191	0.006781	0.019222	-0.00065	-0.00147	-0.00189	0.001002	0.017099	-0.00159	0.000708	0.229
9	0.092454	0.006299	0.002625	0.022375	0.009514	0.001115	-0.00013	0.007874	-6.56E-05	0.043898	-3.33E-17	0.004068	-0.00046	0.000984	0.004331	0.000853	-0.00033	0.002887	0.010105	0.003609	-0.00098	0.016601	0.002887	-0.00085	0.005052	0.011286	-0.00217	0.01647	-0.00079	0.003871	0.003478	-0.00085	0.000131	0.003478	0.006759	-2.22E-17	0.036155	-3.33E-17	0.023753	0.001115	-0.0021	0.004396	0.008465	0.013517	0.007546	-0.00033	0.150
9	0.104394	0.005074	0.00953	0.05625	0.008787	0.000681	0.003032	0.012871	0.00625	0.008416	0.003651	0.013181	0.003218	0.002475	0.006559	0.004641	0.004146	0.001547	0.004146	0.005507	0.005879	0.016646	-0.00056	0.001609	0.008601	0.004889	0.006559	0.001485	0.004208	0.004332	0.009158	0.006807	0.006188	0.006312	0.000495	0.000681	0.007983	0.015656	0.024381	0.003403	0.004394	0.003094	0.001795	0.000681	0.000248	0.000186	0.217
9	0.013161	0.012687	0.005224	0.001221	0.019607	0.003053	0.020896	0.015536	0.009091	0.03365	0.002849	0.022524	0.006716	0.003392	0.01194	0.007598	0.004274	0.004478	0.04118	0.003256	0.003053	0.012076	0.000611	0.002239	0.005699	0.003189	0.001696	0.004342	0.008752	0.011533	0.006784	0.001221	0.004071	0.005427	0.02171	0.004071	0.025509	0.039484	0.009837	0.013569	-0.00041	0.000204	0.000882	0.004138	0.005902	0.000814	0.185
9	0.033474	0.004524	0.011761	0.016828	0.01345	0.004825	0.002413	0.01731	0.002352	0.012304	0.004162	0.012786	0.002473	0.006092	0.011339	0.004222	0.002232	0.001809	0.001568	0.000543	0.00579	0.016948	0.000543	0.003438	0.010374	0.00392	0.012063	0.008866	0.001568	0.003197	0.004162	0.000784	0.006212	0.000362	0.031001	0.003016	0.021834	0.005127	0.023522	0.001749	0.006031	3.33E-17	0.003257	0.003136	0.002352	0	0.205
9	0.021859	0.009031	0.000393	0.02055	0.017147	0.003861	0.007134	0.014202	0.008835	0.04555	-0.00111	-6.54E-05	0.003207	0.004319	0.00216	0.003403	-0.00013	0.000916	-0.00262	0.000851	0.002618	0.013874	0.002029	0.003207	-0.00203	0.00373	0.039529	0.013482	0.003207	-0.00059	0.00373	-0.00059	0.001047	-0.00308	0.01551	0.000785	0.010209	0.004647	0.025654	0.000458	0.003272	-2.22E-17	-0.00046	0.000524	0.010929	0.000589	0.162
10	0.05183	0.007497	0.002479	-0.00277	0.005903	0.000826	-0.00207	0.003129	0.000236	0.02438	0.001476	0.000295	-0.00201	-0.0003	0.00124	0.000413	0.004841	-0.00148	0.002125	-0.00189	-0.00112	0.008678	0.000945	0.00059	0.003955	0.001063	0.015407	0.008914	0.000945	0.001358	-0.00236	0.001181	0.005136	-0.00041	-0.00012	0.000945	-0.0039	0.005549	0.012161	-0.00018	0.000767	-0.00012	-0.00053	-0.00171	0.001299	1.11E-17	0.224
10	0.007903	0.003661	0.002163	0.035441	0.003744	8.32E-05	0.013311	0.008652	0.00391	0.003411	0.000582	0.001913	0.002995	0.000499	0.003078	0.000166	0.000915	0.001747	-0.00083	0.008236	8.32E-05	0.010899	0.009651	0.018968	0.003245	0.002329	0.013644	0.005657	0.001165	0.003078	0.000915	0.005241	0.000499	0	0.002496	0.005657	0.002912	0.00624	0.022296	-0.00175	0.004077	0.002829	0.001747	0.003744	0.016972	0.001747	0.145
10	0.057688	0.000411	0.012793	-0.00511	-0.00018	0.000763	-0.00417	0.002523	0.00135	-0.00335	-0.00417	-0.00029	0.001467	0.000293	0.000293	-0.00129	0.000411	-0.00211	-0.00211	-0.00217	-0.00376	-0.00094	0.000235	0.000117	-0.00164	0.001291	0.004871	-0.00106	0.002171	-0.00282	-0.0061	-0.00305	-0.001	-0.00153	-0.00065	-0.00047	0.018486	0.005458	0.00939	0.000411	-0.00258	0.000646	0.001056	0.000235	-0.0017	0.001526	0.233
10	0.104657	0.007567	0.010652	0.00454	0.014552	0.004366	0.004773	0.01135	0.005763	0.007683	-0.00064	0.008556	0.00099	0.002037	0.003551	0.002794	-0.00081	0.002328	0.002037	0.001513	0.003958	0.015367	0.003667	0.008556	0.005879	0.008033	0.011118	0.010768	0.002037	0.001222	0.00518	0.0039	0.004715	0.001281	0.003667	0.00163	0.003725	0.015367	0.022584	0.000349	0.002037	0.000407	0.003201	0.000931	0.002736	0.000582	0.245
10	0.003846	0.003576	0.004858	0.001282	0.008907	0.001417	0.034885	0.000405	-0.00108	-6.75E-05	0.00027	0.003374	-0.00108	-0.00297	0.00776	0.004791	0.001147	0.002024	0.004116	-0.00155	0.00135	0.008097	-0.00169	0.00135	0.001484	-0.00121	-0.00459	-0.00358	-0.00061	0.001012	0.000877	0.000337	0.00027	0.001147	0.000202	-0.00047	-0.00175	0.032794	0.002497	-0.00081	-0.00182	6.75E-05	0.006343	-0.00175	0.011269	-0.00061	0.198

Appendix A continued

Spatial cross validation splits

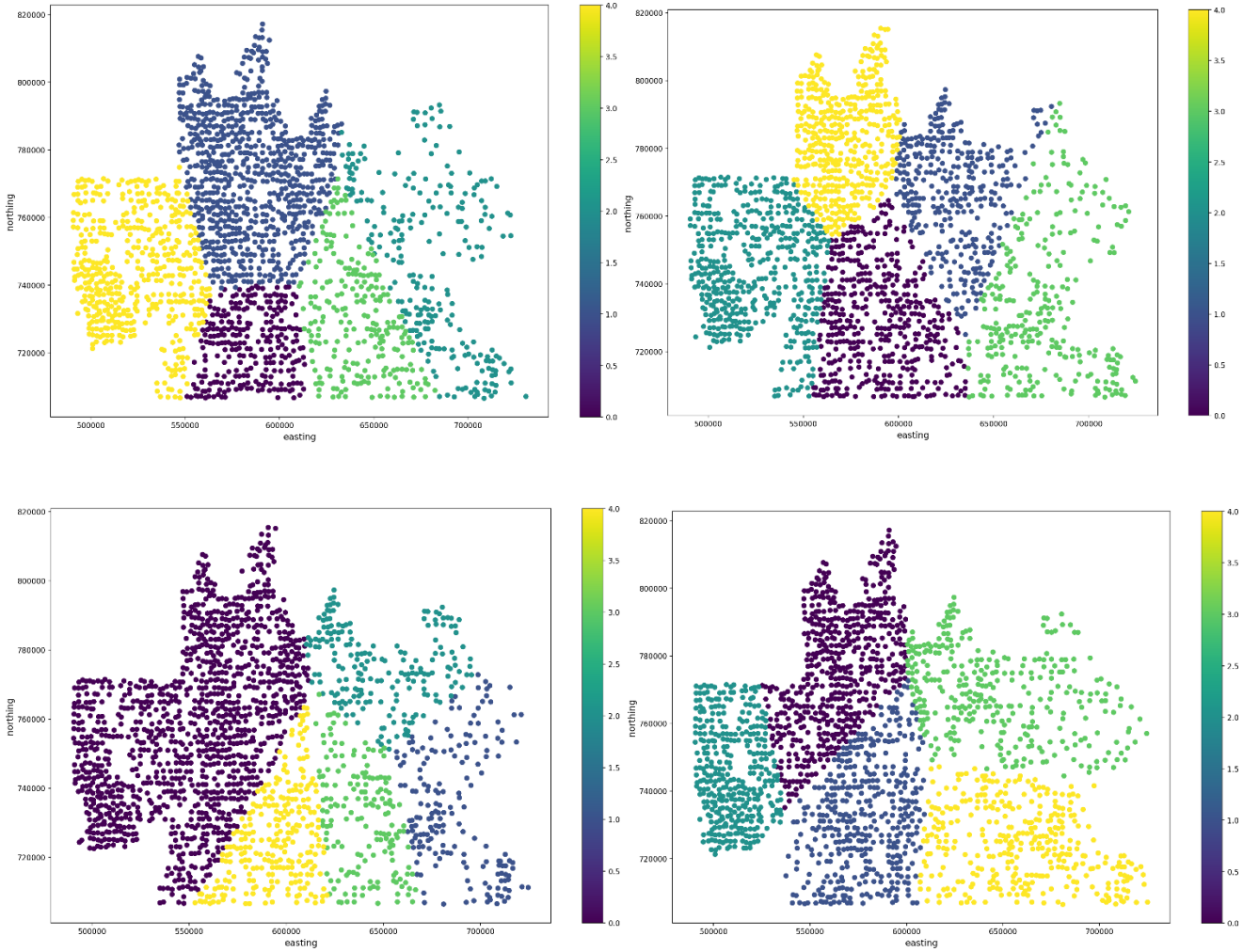

Appendix A continued

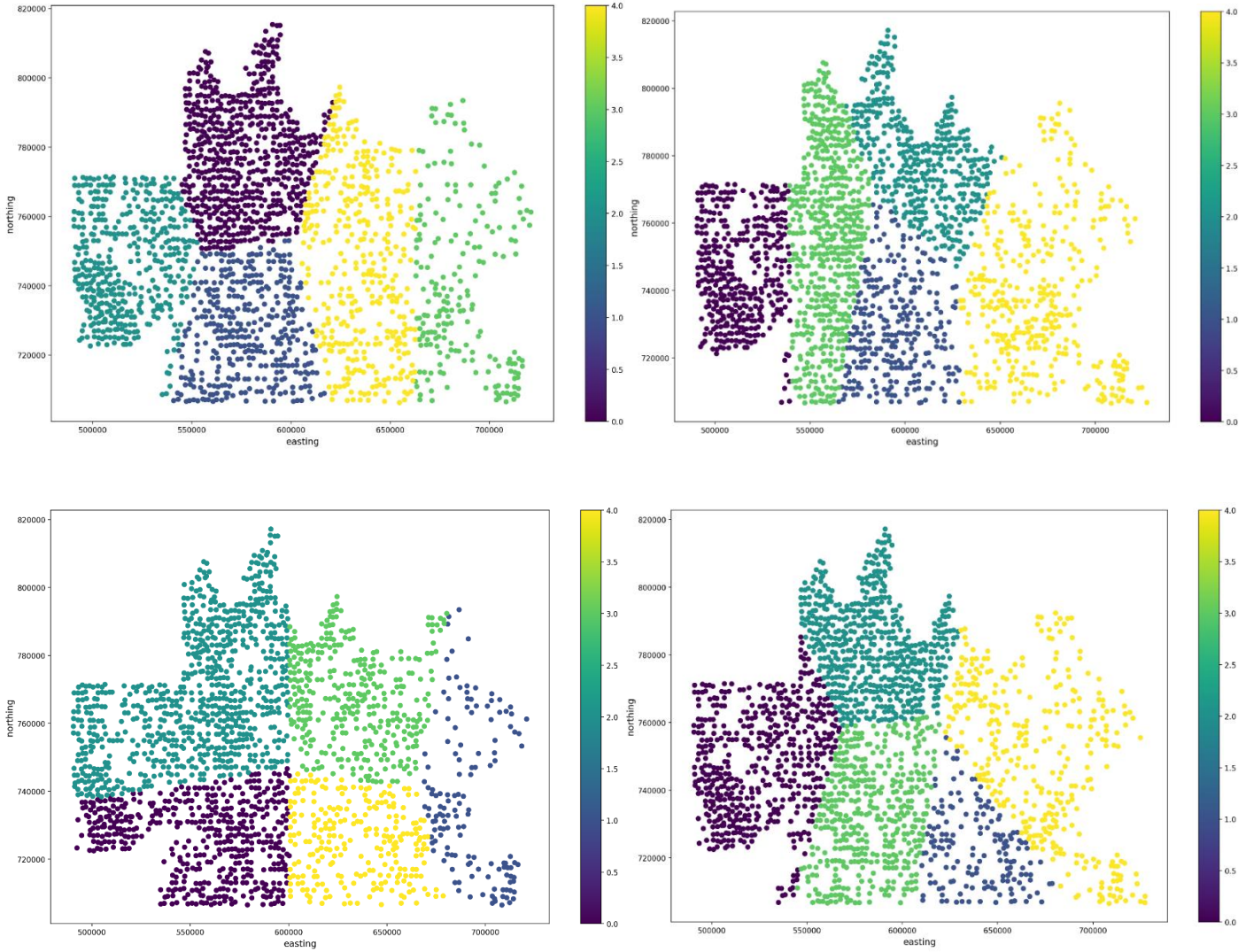

Appendix A continued

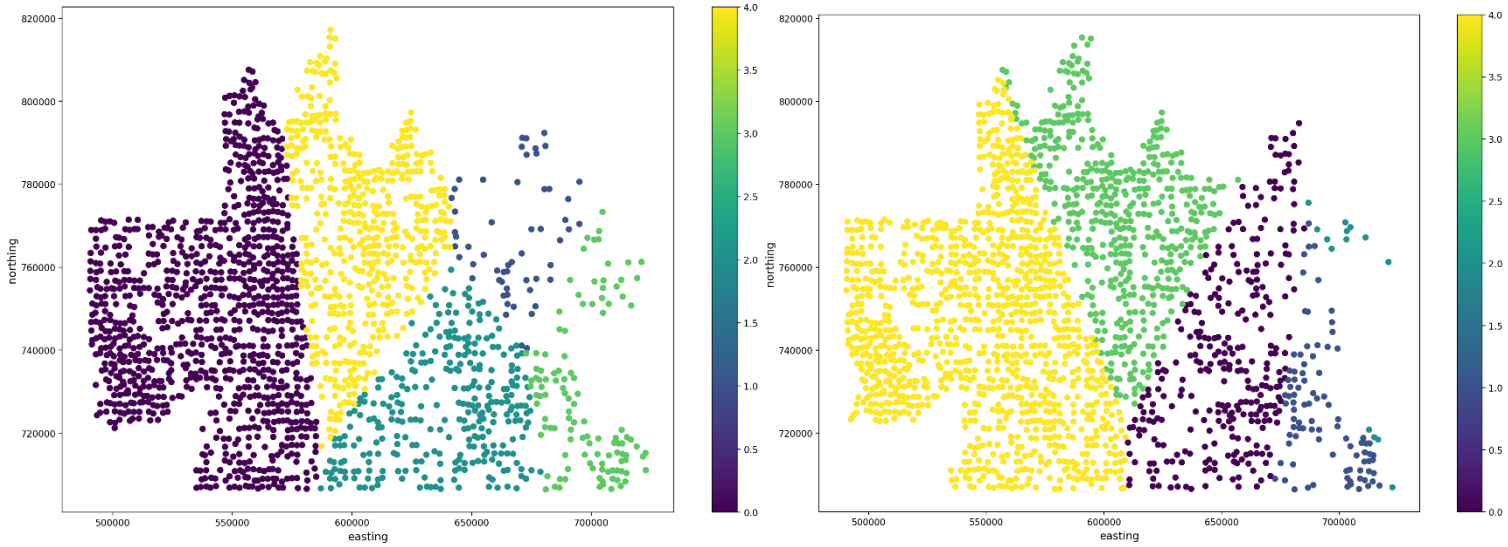

Model performance

split_inde	precision_	recall_clas	f1-score_c	support_c	precision_	recall_clas	f1-score_c	support_c	precision_	recall_wei	f1-score_v	support_v	precision_	recall_ma	f1-score_r	support_n	accuracy	T_class1	T_class2	F_class1	F_class2
1	0.84466	0.587838	0.693227	148	0.683938	0.891892	0.774194	148	0.764299	0.739865	0.73371	296	0.764299	0.739865	0.73371	296	0.739865	8700	13200	6100	1600
1	0.852941	0.644444	0.734177	45	0.714286	0.888889	0.792079	45	0.783613	0.766667	0.763128	90	0.783613	0.766667	0.763128	90	0.766667	2900	4000	1600	500
1	1	0.428571	0.6	7	0.636364	1	0.777778	7	0.818182	0.714286	0.688889	14	0.818182	0.714286	0.688889	14	0.714286	300	700	400	0
1	0.906977	0.483471	0.630728	242	0.647887	0.950413	0.770519	242	0.777432	0.716942	0.700624	484	0.777432	0.716942	0.700624	484	0.716942	11700	23000	12500	1200
1	0.71637	0.829268	0.768696	533	0.797327	0.67167	0.729124	533	0.756848	0.750469	0.74891	1066	0.756848	0.750469	0.74891	1066	0.750469	44200	35800	9100	17500
2	0.734737	0.706478	0.72033	494	0.717349	0.744939	0.730884	494	0.726043	0.725709	0.725607	988	0.726043	0.725709	0.725607	988	0.725709	34900	36800	14500	12600
2	0.75	0.535714	0.625	28	0.638889	0.821429	0.71875	28	0.694444	0.678571	0.671875	56	0.694444	0.678571	0.671875	56	0.678571	1500	2300	1300	500
2	0.818182	0.604027	0.694981	149	0.68617	0.865772	0.765579	149	0.752176	0.734899	0.73028	298	0.752176	0.734899	0.73028	298	0.734899	9000	12900	5900	2000
2	0.918919	0.596491	0.723404	57	0.701299	0.947368	0.80597	57	0.810109	0.77193	0.764687	114	0.810109	0.77193	0.764687	114	0.77193	3400	5400	2300	300
2	0.809816	0.534413	0.643902	247	0.652568	0.874494	0.747405	247	0.731192	0.704453	0.695654	494	0.731192	0.704453	0.695654	494	0.704453	13200	21600	11500	3100
3	0.727273	0.860558	0.788321	251	0.829268	0.677291	0.745614	251	0.778271	0.768924	0.766968	502	0.778271	0.768924	0.766968	502	0.768924	21600	17000	3500	8100
3	0.857143	0.615385	0.716418	78	0.7	0.897436	0.786517	78	0.778571	0.75641	0.751467	156	0.778571	0.75641	0.751467	156	0.75641	4800	7000	3000	800
3	0.773399	0.579336	0.662447	271	0.663717	0.830258	0.737705	271	0.718558	0.704797	0.700076	542	0.718558	0.704797	0.700076	542	0.704797	15700	22500	11400	4600
3	0.828571	0.563107	0.67052	206	0.669118	0.883495	0.761506	206	0.748845	0.723301	0.716013	412	0.748845	0.723301	0.716013	412	0.723301	11600	18200	9000	2400
3	0.891892	0.585799	0.707143	169	0.69163	0.928994	0.792929	169	0.791761	0.757396	0.750036	338	0.791761	0.757396	0.750036	338	0.757396	9900	15700	7000	1200
4	0.842932	0.693966	0.761229	232	0.739927	0.87069	0.8	232	0.791429	0.782328	0.780615	464	0.791429	0.782328	0.780615	464	0.782328	16100	20200	7100	3000
4	0.93617	0.637681	0.758621	69	0.725275	0.956522	0.825	69	0.830722	0.797101	0.79181	138	0.830722	0.797101	0.79181	138	0.797101	4400	6600	2500	300
4	0.727494	0.786842	0.756005	380	0.767908	0.705263	0.735254	380	0.747701	0.746053	0.745629	760	0.747701	0.746053	0.745629	760	0.746053	29900	26800	8100	11200
4	0.887755	0.508772	0.64684	171	0.655738	0.935673	0.771084	171	0.771746	0.722222	0.708962	342	0.771746	0.722222	0.708962	342	0.722222	8700	16000	8400	1100
4	0.776699	0.650407	0.707965	123	0.699301	0.813008	0.75188	123	0.738	0.731707	0.729922	246	0.738	0.731707	0.729922	246	0.731707	8000	10000	4300	2300
5	0.762136	0.826316	0.792929	190	0.810345	0.742105	0.774725	190	0.78624	0.784211	0.783827	380	0.78624	0.784211	0.783827	380	0.784211	15700	14100	3300	4900
5	0.758333	0.65942	0.705426	138	0.698718	0.789855	0.741497	138	0.728526	0.724638	0.723461	276	0.728526	0.724638	0.723461	276	0.724638	9100	10900	4700	2900
5	0.912088	0.415	0.570447	200	0.621359	0.96	0.75442	200	0.766724	0.6875	0.662434	400	0.766724	0.6875	0.662434	400	0.6875	8300	19200	11700	800
5	0.80203	0.593985	0.682505	266	0.677612	0.853383	0.755408	266	0.739821	0.723684	0.718957	532	0.739821	0.723684	0.718957	532	0.723684	15800	22700	10800	3900
5	0.846774	0.58011	0.688525	181	0.680672	0.895028	0.77327	181	0.763723	0.737569	0.730897	362	0.763723	0.737569	0.730897	362	0.737569	10500	16200	7600	1900
6	0.772926	0.580328	0.662921	305	0.664042	0.829508	0.737609	305	0.718484	0.704918	0.700265	610	0.718484	0.704918	0.700265	610	0.704918	17700	25300	12800	5200
6	0.852459	0.581006	0.69103	179	0.682203	0.899441	0.775904	179	0.767331	0.740223	0.733467	358	0.767331	0.740223	0.733467	358	0.740223	10400	16100	7500	1800
6	0.725869	0.917073	0.810345	205	0.887417	0.653659	0.752809	205	0.806643	0.785366	0.781577	410	0.806643	0.785366	0.781577	410	0.785366	18800	13400	1700	7100
6	0.942029	0.643564	0.764706	101	0.729323	0.960396	0.82906	101	0.835676	0.80198	0.796883	202	0.835676	0.80198	0.796883	202	0.80198	6500	9700	3600	400
6	0.824	0.556757	0.664516	185	0.665306	0.881081	0.75814	185	0.744653	0.718919	0.711328	370	0.744653	0.718919	0.711328	370	0.718919	10300	16300	8200	2200
7	0.685393	0.698473	0.691871	262	0.692607	0.679389	0.685934	262	0.689	0.688931	0.688903	524	0.689	0.688931	0.688903	524	0.688931	18300	17800	7900	8400
7	0.8	0.613861	0.694678	202	0.686747	0.846535	0.758315	202	0.743373	0.730198	0.726496	404	0.743373	0.730198	0.726496	404	0.730198	12400	17100	7800	3100
7	0.698276	0.925714	0.796069	175	0.889831	0.6	0.716724	175	0.794053	0.762857	0.756396	350	0.794053	0.762857	0.756396	350	0.762857	16200	10500	1300	7000
7	0.939024	0.472393	0.628571	163	0.647541	0.969325	0.776413	163	0.793283	0.720859	0.702492	326	0.793283	0.720859	0.702492	326	0.720859	7700	15800	8600	500
7	0.866142	0.635838	0.733333	173	0.712329	0.901734	0.795918	173	0.789235	0.768786	0.764626	346	0.789235	0.768786	0.764626	346	0.768786	11000	15600	6300	1700
8	0.710731	0.792028	0.74918	577	0.765166	0.677643	0.71875	577	0.737949	0.734835	0.733965	1154	0.737949	0.734835	0.733965	1154	0.734835	45700	39100	12000	18600
8	0.895522	0.674157	0.769231	89	0.738739	0.921348	0.82	89	0.817131	0.797753	0.794615	178	0.817131	0.797753	0.794615	178	0.797753	6000	8200	2900	700
8	0.891304	0.418367	0.569444	98	0.62	0.94898	0.75	98	0.755652	0.683673	0.659722	196	0.755652	0.683673	0.659722	196	0.683673	4100	9300	5700	500
8	0.852459	0.619048	0.717241	84	0.700935	0.892857	0.78534	84	0.776697	0.755952	0.751291	168	0.776697	0.755952	0.751291	168	0.755952	5200	7500	3200	900
8	0.769912	0.685039	0.725	127	0.716312	0.795276	0.753731	127	0.743112	0.740157	0.739366	254	0.743112	0.740157	0.739366	254	0.740157	8700	10100	4000	2600
9	0.754286	0.619718	0.680412	213	0.677291	0.798122	0.732759	213	0.715788	0.70892	0.706585	426	0.715788	0.70892	0.706585	426	0.70892	13200	17000	8100	4300
9	0.932432	0.413174	0.572614	167	0.623077	0.97006	0.758782	167	0.777755	0.691617	0.665698	334	0.777755	0.691617	0.665698	334	0.691617	6900	16200	9800	500
9	0.803347	0.806723	0.805031	238	0.805907	0.802521	0.804211	238	0.804627	0.804622	0.804621	476	0.804627	0.804622	0.804621	476	0.804622	19200	19100	4600	4700
9	0.894231	0.636986	0.744	146	0.718085	0.924658	0.808383	146	0.806158	0.780822	0.776192	292	0.806158	0.780822	0.776192	292	0.780822	9300	13500	5300	1100
9	0.688372	0.701422	0.694836	211	0.695652	0.682464	0.688995	211	0.692012	0.691943	0.691915	422	0.692012	0.691943	0.691915	422	0.691943	14800	14400	6300	6700
10	0.73913	0.53125	0.618182	128	0.634146	0.8125	0.712329	128	0.686638	0.671875	0.665255	256	0.686638	0.671875	0.665255	256	0.671875	6800	10400	6000	2400
10	0.771626	0.596257	0.6727	374	0.671024	0.823529	0.739496	374	0.721325	0.709893	0.706098	748	0.721325	0.709893	0.706098	748	0.709893	22300	30800	15100	6600
10	0.948052	0.593496	0.73	123	0.704142	0.96748	0.815068	123	0.826097	0.780488	0.772534	246	0.826097	0.780488	0.772534	246	0.780488	7300	11900	5000	400
10	0.846154	0.568966	0.680412	116	0.675325	0.896552	0.77037	116	0.760739	0.732759	0.725391	232	0.760739	0.732759	0.725391	232	0.732759	6600	10400	5000	1200
10	0.757143	0.905983	0.824903	234	0.882979	0.709402	0.78673	234	0.820061	0.807692	0.805816	468	0.820061	0.807692	0.805816	468	0.807692	21200	16600	2200	6800

Random Forest

Feature importance for each model

split_inde	Al	Ba	Ca	Cr	Cu	Fe	K	Li	Mg	Mn	Na	Ni	P	S	Sr	Ti	V	Zn	Zr	Ag	As	Be	Bi	Cd	Ce	Co	Cs	Ga	Ge	Hf	Hg	In	La	Mo	Nb	Pb	Rb	Sb	Sc	Se	Sn	Te	Th	Tl	U	W	Y
1	0	0.00174	0.000644	0.000451	0.000258	0.000193	0.000451	0.000129	6.44E-05	0.002577	0	0.000451	0.000322	0.000515	0.000515	0.000322	0.000451	0.00116	0.000387	0.000709	0.001289	0.000322	0.000129	0.000322	0.001546	0.000387	0.00116	0.000193	0.000451	0.000129	0.001031	0	0.001611	0.000838	0.000451	0.003802	0.000129	0.000709	0.001482	0.000644	0.00058	0.000451	0.000451	0.003995	0.000773	0.001095	0.001224
1	0.000231	0.002543	0.000231	0.000983	0	0.002543	0	0	0.000578	0.001618	0.000289	0.000116	0.000462	0	0	0	0.000462	0.000578	0.000751	0.001098	5.78E-05	0	0.000578	0.000289	0	0.000347	5.78E-05	0	0.00052	0	0.000636	0	0.000173	0.000925	0.000751	0.003526	0.000636	0.000578	0.000116	5.78E-05	0.000347	0	0.001503	0.007341	0.002197	0.000751	0.001618
1	5.74E-05	0.001435	0.00023	0.000804	0	0	0	0	0	0.001206	5.74E-05	0.000746	0.00023	0.000172	0.000172	0	0	0.001148	0	0.001033	0.000804	5.74E-05	0	0	0	5.74E-05	0.000402	0	0.000804	0.000115	0.000402	0.000287	0.000344	0.001435	0.000517	0.003387	0.000689	0.000746	0.002181	0.000402	0	0	0.000115	0.00597	0.000861	0.000574	0.001378
1	0.000232	0.001623	0	0	0.000309	0	0	0	0.000541	0.000541	0	7.73E-05	0.001236	0	7.73E-05	0	0	0.000773	0.000386	0.00085	0.000773	0	0.000155	0	7.73E-05	0	0	0	0	0	0.000386	0.000309	0.000464	0	0.000155	0.000927	0.000773	0.000927	0.001932	0.000618	0.000155	0.000773	0.001005	0.00796	0.000155	0.001468	0.002396
1	0.000135	0.00108	0	0	0.00027	0.000675	0	0.000405	0	0.000472	0	0.00054	0.000675	0	0.000337	0.000337	0.001754	0.00027	6.75E-05	6.75E-05	0	0	0	0.000472	0	0.000607	0.000135	0	0.000675	0	0	0	0.000675	0.000607	0	0.003576	0.000337	0.00027	0.001282	0	0.00027	0	0	0.00081	0.000877	0.000742	0
2	0	0.000375	0	0	0.000375	0.000501	0	0	0.000375	6.26E-05	0.000438	0	0.000313	0	0	0	0.000188	0.000751	0.00025	0.001627	0.000313	0.000375	0	0.00025	0	0	0.000438	0	0.000313	0.000626	0.000313	0	0.00025	0	0	0.001189	0.000125	0.002753	0	0	0	6.26E-05	0.010075	6.26E-05	0	0.001252
2	0.000266	0.000333	0	0	0.000466	0.0002	0.0002	0	0	0.000133	0	0	0.000266	0.000533	0.000399	0	0	0.000599	0	0.000799	0.000533	6.66E-05	0.000266	0	0.000466	0.0002	0.000333	0.000599	0	0	0	0.000533	0.000666	0	0.000999	0.001332	0.001598	0.000333	0.001265	0.000533	0	0	0.001465	0.003462	0.000333	0	0.001664
2	0	0.000187	0	0	0	0	0	0	0	0.000684	0	0	0.001493	0	0.000498	0.000311	0.000249	0	6.22E-05	0.001866	0.000933	0	0	0	0.000187	0	0.000498	0	0.000187	0	0	0.000124	0.001119	6.22E-05	6.22E-05	0.000622	0.000249	0.001866	0.00056	6.22E-05	0	0	0.000187	0.005846	0.00056	0	0.000435
2	0	0	0	0	0.000304	0	0.000457	0.000381	0	0	0	0	0.000989	0	0	0	0.000381	0.000685	0	0	0.000457	0	0	0	0	0	0.000533	0	0	0	0.000989	0	7.61E-05	0	0	0.003577	0.000228	0.001903	0	0	0	0	0.001598	0.000381	0.000152	0.000609
2	0	0.001462	0	0	0	0	0	0.000112	0	0	0	0.000169	0.000562	0	0	0.000169	0.000112	0.000281	0	0.001181	0	0	0	0.000562	0.000112	0	0.000112	0	0	0	0.000169	0	0.000225	0	0	0.002193	0.000281	0.002531	0	0.000675	0	0	0.00748	0.000394	5.62E-05	0.001406
3	0.000195	0.002727	0.000649	0.00026	6.49E-05	0.001039	0.00026	0	0	0.001234	0.000584	0.00026	0.000519	0	0.000455	0.000195	0.000844	0.002013	0	0.001104	0.000974	0.000195	0	0.000584	0.00013	0.001364	0.000714	0.000455	0	0.000455	0	0	0	6.49E-05	0	0.000909	0.001234	0.000519	0	0.000779	0.000714	0.000584	0.000519	0.003052	0.002208	0.000844	0.005519
3	0	0.002378	0.00074	0	0.000423	0.000951	0	0	0	0.00037	5.29E-05	0.00037	0.000529	0	0.000423	0	0	0.000211	0.000476	0.000106	0	0	0	0.000634	0	0.00037	0	0.000159	0	0.000106	0	5.29E-05	0	0.000529	0	0.000211	0.000687	0.000211	0.000793	0.001057	0.000634	0	0	5.29E-05	0.004387	0.001797	0.000793	0.00111
3	0	0.000794	0.000556	0	0	0	0.000794	0	0	0.000635	7.94E-05	0.000714	0.000317	0.001032	0.000317	0	0.000873	0.000714	0	0	0	0	0	7.94E-05	0.000397	0	0.000397	0.000238	0	0	0	7.94E-05	0	0	0.00381	0.000238	0.000714	0.000794	0.000556	0	0.000159	0.000635	0.002619	0.002778	0	0.000556
3	0	0.000721	0	8.01E-05	0.000321	0	0	0.000481	0	0.000401	0	0.000721	0	0	0	0	0	0	0.000401	8.01E-05	0	0	0.000481	0.001202	0	0	0	0.000401	0	0	0.000721	0	0.000321	0.000801	0.000721	0	0.000721	0	8.01E-05	0	0	0	0.000481	0.000801	0.000641	0.000801	0.00016
3	0	0.000645	0.002151	5.38E-05	0.000108	0.000161	0.000323	0	0	0.000215	0	0	0.000484	5.38E-05	0.001022	0.00043	0.000376	0.000914	0	0.000215	0.00043	5.38E-05	0.000108	0	0.00086	0.001344	5.38E-05	0	0.000108	0	0.000376	0	0.000645	0.000323	0.000108	0.001237	0.000699	0.000376	0.001022	0	0.000108	0.000484	0.00086	0.005538	0.001183	0.000645	0.001774
4	0.0002	0.000866	0.000666	0.000666	0.000133	0.000666	0	0.000599	0.000666	0.001531	0.000533	0.0002	0.000599	6.66E-05	0.000666	0.000399	0	0.001065	0.000866	6.66E-05	0.001664	0.001132	0.000666	0.000666	0.000732	0.000666	0.000666	0.000266	0.000333	6.66E-05	0.000732	6.66E-05	0.000666	0.000999	0.000732	0.002064	0.001531	0.000333	0.000666	0.000666	0	0.000732	0.000732	0.005526	0.002397	0.001132	0.000266
4	0	0.001818	0.00049	0.000699	0.000839	0.001119	0.00042	0.000629	6.99E-05	0.00042	0	0.000629	0	0.00028	0.003077	0	0.00014	0.001678	0.00014	0.00021	0.000559	0	0.000979	0.00028	0.000629	0.000559	6.99E-05	0	0.00035	0	0.000559	0.00021	0.00028	0.001329	0.000629	0.002517	0.001748	0.00021	0.001329	0.00049	6.99E-05	0.000699	0.000909	0.00979	0.001399	0.001049	0.002028
4	0.000312	0.002372	0.000499	0	0.000499	0.001061	0.000499	0	0.000624	0.000624	0.000125	0.000562	0.000437	0	0.000624	0	0.000562	0.001561	0.001311	0	0.00025	0.000749	0	0.000936	0.000312	0	0.000499	0.000562	0.000499	0	0.001311	0.000125	0.000562	0	0.000499	0.002559	0.001623	0.000687	0.000437	0	0	0.000562	6.24E-05	0.008427	0.002622	0.000624	0.001685
4	0.000307	0.001227	0	0.000245	0	0	0	0	0.000307	0.000307	0	0	0.000552	0.001227	0	0	0.00092	0.002515	0.001227	6.13E-05	0	0.000491	0	0.001104	0	0	0.000798	0	0	0	0.000552	0.000552	0.001184	0.000982	0.001184	0.000491	0.000613	0.000736	0	0	6.13E-05	0.001902	0.001534	0	0.000245
4	0.000244	0.002751	6.11E-05	0.000306	0	0.000611	0	0	0	0.001345	0.000306	0.000489	0.000306	0	0	0	0	0.00055	0.000306	0.000672	0	0.000183	0	0.000122	0.000122	0	0.000611	0	0.000489	0.000428	0.00055	0.000367	0.000428	0	0	0.00324	0	0.000183	0.000489	6.11E-05	0	0.000306	0	0.00599	0.0011	0	0.000611
5	0.00076	0.00152	0	0	0	0	0	0	0	0.000152	0	0	0.000608	0	0	0	0	0	0	7.60E-05	0.000304	0	0	0	0	0	7.60E-05	0	0	0	0	0	0.000228	0.000608	0	0.000608	0.000152	0.001444	0.000608	0	0	0	0.00076	7.60E-05	0.001748	0.000988	0	0
5	0.000146	0.00146	0.000146	0	0.000146	0.001022	0	0.000365	0.000146	0.000803	0	0.000365	0	0.000292	0.000949	0	0.001168	0	0.001825	0.000511	0.001168	7.30E-05	0	0	0.000365	0	0	0	0	0	0	0	0.000219	0	0.000511	0.000511	0	0.001679	0	0.000292	0.00073	0.000803	0	0.000803	0.007518	0.00073	0.000438	7.30E-05
5	0.000512	0.002617	0	0.000739	0.000398	0.000569	0	0	0.000284	0.000341	5.69E-05	0.002048	0.000341	0.000171	0.000341	0.000455	0.00091	0.000569	0.000228	0.001422	0.001138	5.69E-05	0.000512	0.000228	0.000739	0.000455	0.000512	0.000114	0.000114	0.000114	0.001479	0.000114	0.000569	0.000569	0.000796	0.002446	0.001081	0.00091	0.001024	0.001365	0.000853	0	0.000114	0.00438	0.002787	0.000455	0.002105
5	0	0.000545	0.001515	0	0.000606	0.000545	0	0	0	0.000424	0	0.001273	0.00097	0	0.00103	0	0.001455	0.000727	0.001152	0	0.000545	0.000424	0	0	0.000545	0.000303	0	0.000424	0	0	0.001333	0	6.06E-05	0.000485	0.000182	0.001455	0.000424	0.000424	0.001152	0.000667	0.000606	0.000545	0.000606	0.002667	0.00103	0	0.000485
5	0.000176	0.001524	0	0.000117	5.86E-05	0.000586	0.000293	0	0.000352	0.000293	0	0.002227	0	0	0	0.000469	0.000879	0	0.001172	0.000703	0	0.000528	0.000821	0	0	0.000117	0.000234	0	0	0	0	0	0.000293	0.000586	0.000996	0.000352	0.000762	0.000938	0.000469	0.000586	0.000117	0	0.000176	0.003341	0.000645	0.000528	0.001114
6	0	0.002125	0.000413	0.000531	0.000236	0.001476	0	0	0	0.000177	0	0.000413	0.001004	0	0.000236	0.001181	0	0.001535	0.001535	0.000767	0.000236	0.000413	5.90E-05	0.000767	5.90E-05	0.000236	0	0	0.000531	0	0.000413	0	0.00242	0.000354	0.000708	0.000531	0.001177	0.000531	0	0.000295	0	0	0.000177	0.002479	0.001004	0.00059	0.000826
6	5.71E-05	0.004224	-0.00017	0.000114	0.000114	0	-0.00011	0.000228	-5.71E-05	0.001826	0	0	0.000285	0	0.001199	0.000228	0	0.001142	0.000571	0.000342	5.71E-05	0	0.000114	5.71E-05	0	-0.0004	0	0	0	0.000457	0.000571	-0.00023	0.000457	0.000457	0.000342	0.001541	0.000742	0.000913	0	0.000457	0	0.000171	0.000742	0.011815	0.00137	0.000571	0.001427
6	0	0.002391	0	0.000104	0	0	0	0	0	0.001247	0	0	0	0	0	0	0	0	0	0.001455	0.001247	0	0	0	0	0	0	0	0	0	0	0	0	0.000104	0.00104	0.000208	0	0	0.000936	0	0.000728	0	0.001871	0.000208	0.000832	0
6	0	0.001645	0.000526	0.000855	0.000526	0.000526	6.58E-05	0	0	0.000329	0	0.000658	0.001316	0	0.001447	0.000658	0.000329	0.000658	0	0.000855	6.58E-05	6.58E-05	0	0.000658	0.000987	0.000921	0.000329	0.000526	0.000197	0.000197	0.000592	0.000263	0.003355	0.000592	0.000658	0.002105	0.000263	0.001184	0.001053	0.000987	0	0	6.58E-05	0.001513	0.000658	0.000987	0.000855
6	0	0.003739	0.000214	0	0.001229	0	0	0	0.000534	0.000641	0	0.000267	0.000267	0.000427	0.000427	0	0.000962	0.000694	0.001068	0.000801	0	0.000374	0	0.000427	5.34E-05	0.000214	0.000267	0.000267	0	5.34E-05	0.000641	0	0.001442	0.000855	0.000748	0.002511	5.34E-05	0.001442	0	0.001282	0.000534	0.000534	0.000321	0.00406	0.000641	0.000534	0.00235
7	5.73E-05	0.00126	0.000172	0	0.000515	0.000515	0	0	0.00063	0.002291	0.000229	0.000115	0.000115	0	0.004696	0	0	0.000745	0.000401	0.000344	0	0.000229	0.000573	0.000458	0.000229	0.001088	0.000229	0	0	0.000286	0.000172	5.73E-05	0.00315	0.001145	0	0.000515	0.000573	0.000515	0	0	0.000401	0	0.000172	0.009164	0.000458	0.000515	0.00126
7	0	0.001014	0	0	0	0	0	0	0	0.00117	0	0	0.000624	0.000546	0	0	0	0.000702	0.000156	0	7.80E-05	0	0	0.000468	0	0	0.000156	0.000156	0	0	0	0	0.001248	0	0	0.000858	0	0	0.00078	0	0	0	0.004836	7.80E-05	0	0.001014
7	0	0.00117	6.16E-05	0	0.000308	0.001108	0	0	0	0.001416	0.000123	6.16E-05	0.001293	0.000739	0	0	0.000123	6.16E-05	0.003941	0	0.000862	0	0.000369	0.000246	0.000616	0	0	0	6.16E-05	0.000369	0	0	0.001663	0	0.000308	0.000616	0.000369	6.16E-05	0.000924	0.000308	0	0	0.000369	0.007081	0.000246	0.000862	0.000616
7	0	0.000627	0	0	0	0.000705	0	0.000392	0	0.002273	0	0	0.000235	0.000157	0	0	0.002586	0	7.84E-05	0.000157	0	0	7.84E-05	0	0.000235	0.000549	0	0	0	0	0.001332	0	0.000313	0.000784	0.00094	0.000549	0.000313	0.000392	0.000549	0	0.000313	0	0.000157	0.002821	0.001724	0.001097	0.00094
7	0	0.000748	0	0.000427	0.000374	0.00016	0	0	0	0.000908	0.000214	0	0.000855	0	0.001709	0	0	0.00016	0.000694	0.000962	0.000321	0.000427	5.34E-05	0.000374	5.34E-05	0	0	0	5.34E-05	0.000481	0.000908	0	0.001122	0.000321	0	0.001389	0	0.000694	0.000908	0.000267	0	0	0.000799	5.34E-05	0.000374	0.001335
8	0	0.00089	0.000356	0.00083	0.000593	0	5.93E-05	0	0	0.001186	0.000119	0	0.000178	0	0.001127	0	0.000237	0.001601	0.001661	0.000712	0	0	0	0.000474	0	0.000949	0	0.000237	0.000237	0	0	0	0.000949	0.00083	0.00083	0	0	5.93E-05	0.000593	0.000534	0	0	0.000119	0.001601	0.001957	0	0.00089
8	7.52E-05	7.52E-05	0.000376	0	0	0	7.52E-05	0	0	0.00188	0	0	0.000301	0	0.001504	0	0.000301	0.000677	0.000602	7.52E-05	0.000602	0	0	0.000526	0	0	0.000677	0	0	0	0.000451	0	0.000301	0	0.000376	0	0.00015	0.000526	0	0	0	0	0.001278	0.001353	0	0
8	0.00058	0.00174	0	0	0.000387	0.001224	0	0	0.000451	0.000709	0	0.000193	0.001095	0	0	0	0	0.001353	0.000644	0.000322	6.44E-05	0.000451	0	0.000644	0	0	0.000515	0	0	0	0.000838	0.000129	0.000773	0	0.00058	0.000258	0.000644	0	0	0	0	6.44E-05	0.006572	0.000902	0	0.000451
8	0	0.007713	0.000532	0.000133	0.000199	0.00133	0	6.65E-05	0.000731	0.000798	0.000133	0.000133	0.000199	0.000598	0.00133	6.65E-05	0.000133	0.002327	0.000399	0.000731	0	0.000399	0.000665	0.000133	0.000532	0.000665	0.00133	0.000133	0	0.000399	0.000133	0	0.001529	0.000665	0.000532	0.000133	0.002266	0.000598	0	0.000532	0	0	0.000465	0.006117	0.001662	0.000598	0.001064
8	0.00081	0.001968	0.000579	0.000174	0.00081	0.000926	0	0	0	0.001505	0.000174	0	0.000521	5.79E-05	0.001157	0	0	0.001447	0.000521	0.000579	0.000116	0.000463	0.000231	0	0	0.000289	0.001563	0	0.000289	0.000521	0.000289	0	0.000637	0	0	0.001116	0.000174	0.000694	0.000868	0	0	0	0	0.003067	0.002141	0	0.001447
9	0	0.001258	0.000472	0.000419	0.000943	0	0	0	0	0.000524	0	0.000419	0.000629	0	0	0	0.000262	0.000472	0	0	0.000157	0	0.000367	0	0.001625	5.24E-05	0	0	5.24E-05	5.24E-05	5.24E-05	0.000367	0.00131	0	0.000157	0.002987	0.000996	0.000577	0	0.000105	0	0	0.003249	0.000419	0	0.001887
9	0	0.001936	0	0	0.000134	0.000334	0	0	0.000601	0.000868	0	0.0002	0.000668	6.68E-05	0.000601	0	0.000935	0.002069	0.000401	6.68E-05	6.68E-05	0	0	0.001135	0	0.000534	0.000401	0.000334	0	0.0002	0	0	0.0002	0	0.000467	0.002403	0.000868	0.002267	0.000401	0.000668	0.000334	0	0	0.003204	0.000334	0.000935	0.003204
9	0	0.000174	0.000696	0.000261	0.000261	8.70E-05	0.00087	0.000174	0.001043	0.000435	0.000348	0.000957	8.70E-05	0	0.001391	0.00087	0.000174	0.001217	0.00087	0.000696	0.00087	0	0.00087	0.001043	0.000348	0.000435	0.001652	0.001391	0.00087	0.000174	0.00087	0.00087	0.000957	0.000174	0.000174	0.001217	0.000609	0.000783	0	0.002	0.00087	0.000522	0.000957	0.005565	0.001217	0.002957	0.001217
9	0	0	0	0	0	0	0	0	0	0.001229	0	0	0.000194	0	0	0	0	0.000129	0.000129	0	0.000647	0	0.000841	0	0.001294	0	0	0	0	6.47E-05	0.000453	6.47E-05	0.000388	0.000517	0.000453	0	0.000259	0.000776	0	0.000129	0	0	0.005045	6.47E-05	0	0.000453
9	0	0.001826	0	0	0.000353	0	0	0	0	0.000824	0	0	0	0	0	0	0	0.000589	0	0.000942	0	0	0	0.000412	0.000353	0.000412	0	0	0.000471	0	0.000118	0.000471	0.000412	0	0.000236	5.89E-05	0.0053	0.000294	0.000471	0	0.000883	0	0	0	0.003475	0	0.000353	0.001001
10	0	0.000474	0	0.000711	0	0	0	0	0	0.000711	0.000592	0.000237	0.000474	0.000948	0.001066	0	0	0.000118	0	0.000118	0	0	0	0	0.000355	0	0	0	0	0	0	0	0	0.000474	0	0	0	0	0	0	0	0.001185	0.001185	0	0.002844	0.000355	0	0.000711
10	0	0.001874	0.000351	0	0.000351	0.000234	0	0	0	0.000585	0	0	0.001639	0.00041	0.001171	0	0.000351	0.001464	0.000527	0	0	0	0	5.85E-05	0	0.000117	0.001639	0	0	0	0	0	0.000176	0.000761	0.000995	0.000117	0.000234	0.000878	0.001171	0	0	0.000585	0.001112	0.005562	0.001347	0	0.001171
10	0	0.001559	0.000468	0.000468	0.000156	0.000468	0	0.00026	0	0.000104	0.000104	5.20E-05	0.000572	0	0.000364	0	0	0.000624	0.001247	0.000104	0	0.000468	0.000104	0.000416	0.000468	0	0.00026	0	0	5.20E-05	0.000468	0	0.001403	0.000676	0.000728	0.000884	0	0	0.000364	0.00104	0.003742	0.000364	0.000416	0.001611
10	0	0.000671	0.00047	6.71E-05	0	0.001477	0.000336	0.000268	0	0.00094	0	0	0.000537	0	0.000134	0	0.000268	0.001678	0.001342	6.71E-05	0	0	0	0.000604	6.71E-05	0	0	0	0	0	0.000336	0	0.000268	0.000201	0.000671	0.000336	0.000403	0	0.001611	0.001745	0	0	0	0.001141	0.002617	0.001275	0	0.000671
10	0	0.002454	0	0.000218	0.000273	0	0	0	0	0.000491	0	0	0.001145	0	0	0	0.000327	0.000927	0.000654	5.45E-05	0	0	0	0.000382	5.45E-05	0.0006	0.000164	0	0	0.000218	0	0.000436	0.000327	0	0	0.002617	0.000382	0.000545	0	0	0.000327	0	0.001145	0.007961	0.000763	0	0.000927

Appendix A continued

Spatial cross validation splits

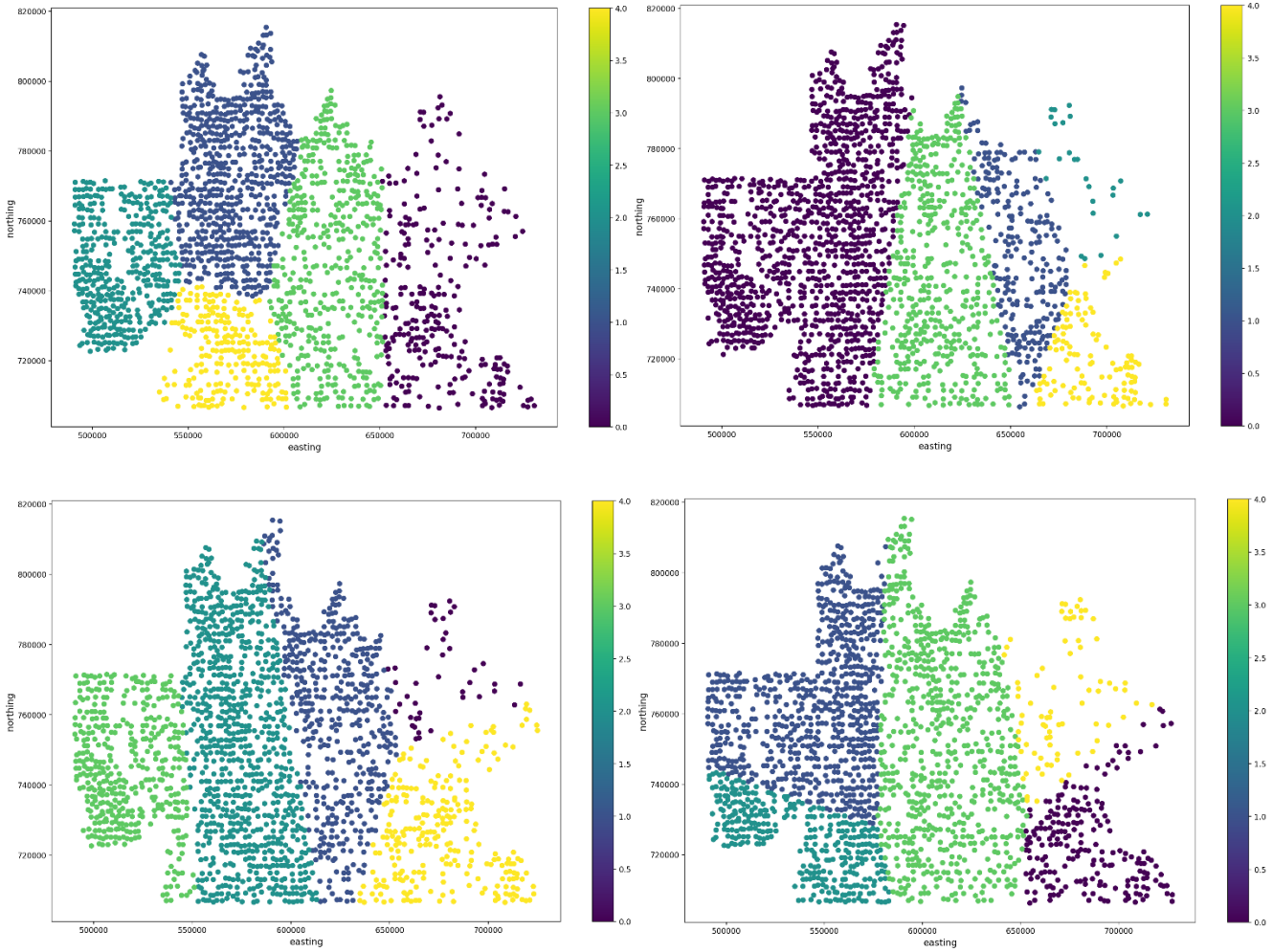

Appendix A continued

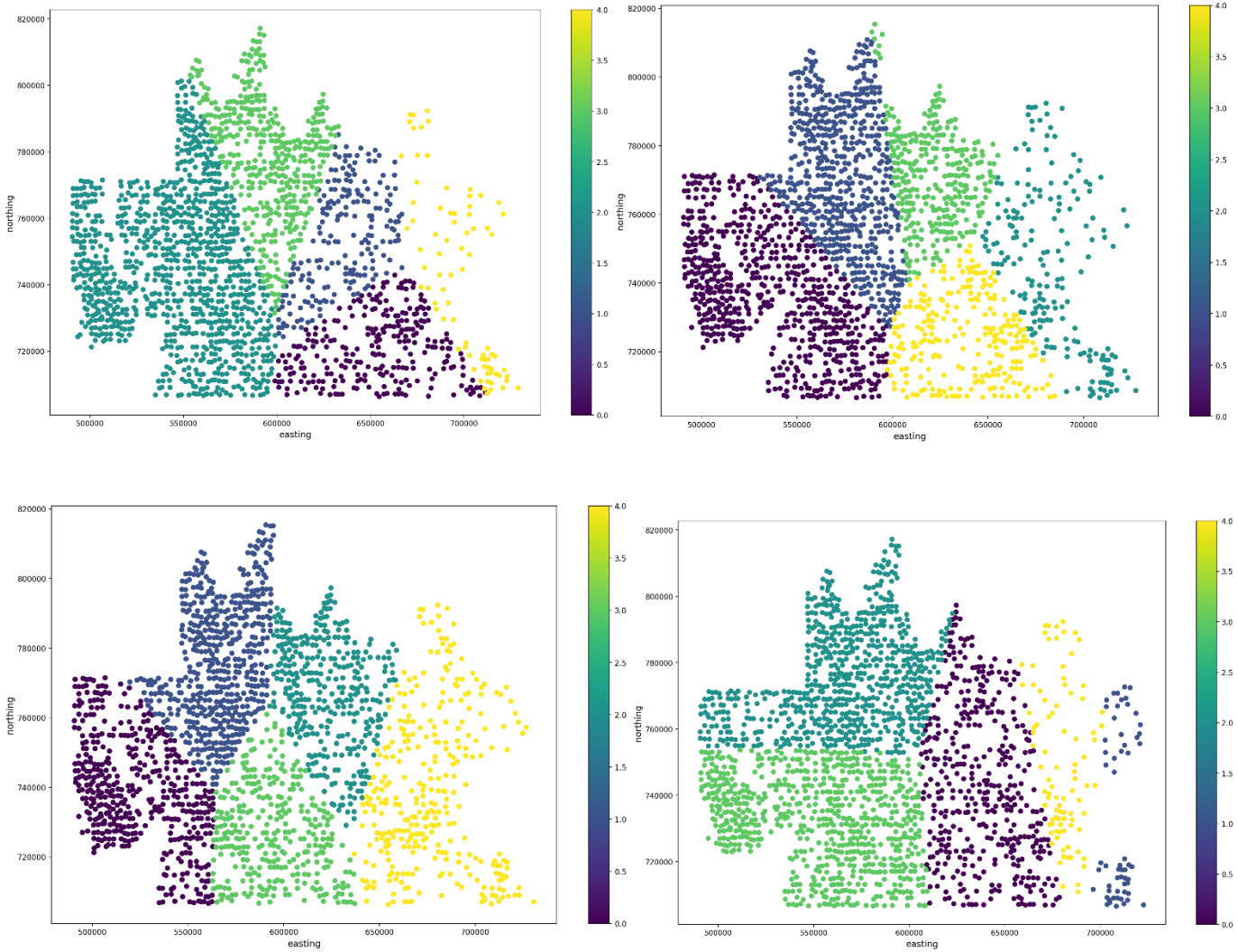

Appendix A continued

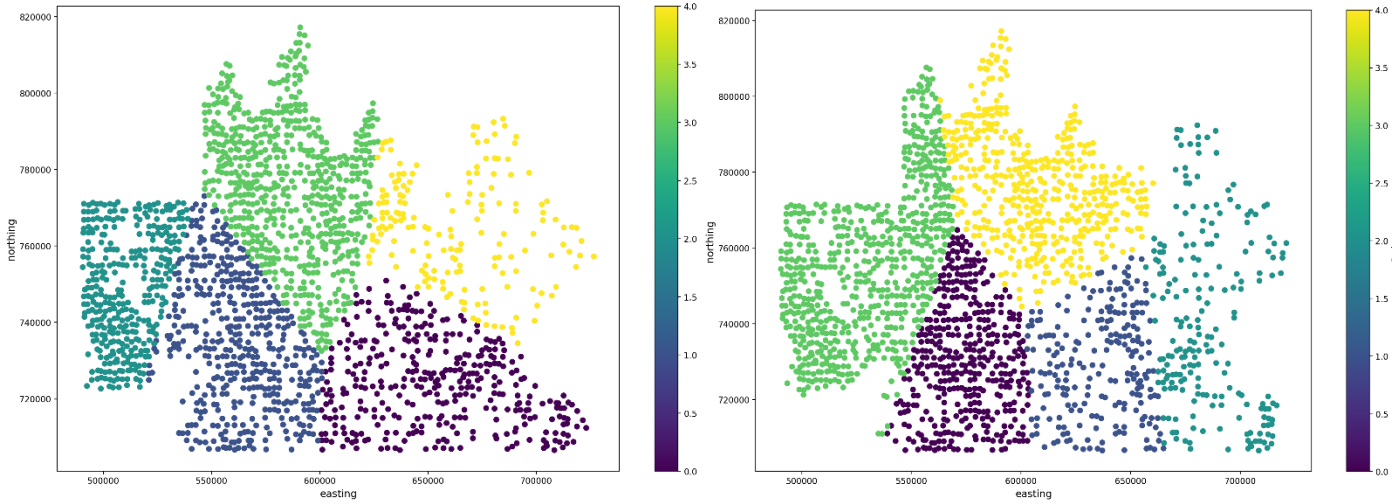

Model performance

split_inde	precision_	recall_clas	f1-score_c	support_c	precision_	recall_clas	f1-score_c	support_c	precision_	recall_wei	f1-score_v	support_v	precision_	recall_ma	f1-score_r	support_n	accuracy	T_class1	T_class2	F_class1	F_class2
1	0.793103	0.577889	0.668605	199	0.667984	0.849246	0.747788	199	0.730544	0.713568	0.708196	398	0.730544	0.713568	0.708196	398	0.713568	11500	16900	8400	3000
1	0.774194	0.654545	0.70936	110	0.700787	0.809091	0.751055	110	0.73749	0.731818	0.730207	220	0.73749	0.731818	0.730207	220	0.731818	7200	8900	3800	2100
1	0.891892	0.634615	0.741573	104	0.716418	0.923077	0.806723	104	0.804155	0.778846	0.774148	208	0.804155	0.778846	0.774148	208	0.778846	6600	9600	3800	800
1	0.68018	0.920732	0.782383	328	0.877358	0.567073	0.688889	328	0.778769	0.743902	0.735636	656	0.778769	0.743902	0.735636	656	0.743902	30200	18600	2600	14200
1	0.80137	0.5	0.615789	234	0.636646	0.876068	0.73741	234	0.719008	0.688034	0.6766	468	0.719008	0.688034	0.6766	468	0.688034	11700	20500	11700	2900
2	0.847826	0.664773	0.745223	176	0.724299	0.880682	0.794872	176	0.786063	0.772727	0.770047	352	0.786063	0.772727	0.770047	352	0.772727	11700	15500	5900	2100
2	0.761905	0.642857	0.697337	224	0.69112	0.799107	0.741201	224	0.726512	0.720982	0.719269	448	0.726512	0.720982	0.719269	448	0.720982	14400	17900	8000	4500
2	0.634241	0.953216	0.761682	171	0.905882	0.450292	0.601562	171	0.770062	0.701754	0.681622	342	0.770062	0.701754	0.681622	342	0.701754	16300	7700	800	9400
2	0.736842	0.616352	0.671233	318	0.67027	0.779874	0.72093	318	0.703556	0.698113	0.696082	636	0.703556	0.698113	0.696082	636	0.698113	19600	24800	12200	7000
2	0.859649	0.569767	0.685315	86	0.678261	0.906977	0.776119	86	0.768955	0.738372	0.730717	172	0.768955	0.738372	0.730717	172	0.738372	4900	7800	3700	800
3	0.768362	0.663415	0.712042	205	0.703863	0.8	0.748858	205	0.736112	0.731707	0.73045	410	0.736112	0.731707	0.73045	410	0.731707	13600	16400	6900	4100
3	0.862069	0.862069	0.862069	29	0.862069	0.862069	0.862069	29	0.862069	0.862069	0.862069	58	0.862069	0.862069	0.862069	58	0.862069	2500	2500	400	400
3	0.692073	0.657971	0.674591	345	0.674033	0.707246	0.69024	345	0.683053	0.682609	0.682416	690	0.683053	0.682609	0.682416	690	0.682609	22700	24400	11800	10100
3	0.779104	0.74359	0.760933	351	0.754768	0.789174	0.771588	351	0.766936	0.766382	0.76626	702	0.766936	0.766382	0.76626	702	0.766382	26100	27700	9000	7400
3	0.757576	0.555556	0.641026	45	0.649123	0.822222	0.72549	45	0.703349	0.688889	0.683258	90	0.703349	0.688889	0.683258	90	0.688889	2500	3700	2000	800
4	0.743494	0.892857	0.811359	224	0.865922	0.691964	0.769231	224	0.804708	0.792411	0.790295	448	0.804708	0.792411	0.790295	448	0.792411	20000	15500	2400	6900
4	0.735294	0.673077	0.702811	260	0.698582	0.757692	0.726937	260	0.716938	0.715385	0.714874	520	0.716938	0.715385	0.714874	520	0.715385	17500	19700	8500	6300
4	0.828829	0.528736	0.645614	174	0.654008	0.890805	0.754258	174	0.741419	0.70977	0.699936	348	0.741419	0.70977	0.699936	348	0.70977	9200	15500	8200	1900
4	0.712329	0.65	0.679739	160	0.678161	0.7375	0.706587	160	0.695245	0.69375	0.693163	320	0.695245	0.69375	0.693163	320	0.69375	10400	11800	5600	4200
4	0.888889	0.66242	0.759124	157	0.730964	0.917197	0.813559	157	0.809927	0.789809	0.786342	314	0.809927	0.789809	0.786342	314	0.789809	10400	14400	5300	1300
5	0.721557	0.760252	0.740399	317	0.746667	0.706625	0.726094	317	0.734112	0.733438	0.733247	634	0.734112	0.733438	0.733247	634	0.733438	24100	22400	7600	9300
5	0.728155	0.775862	0.751252	290	0.760148	0.710345	0.734403	290	0.744151	0.743103	0.742827	580	0.744151	0.743103	0.742827	580	0.743103	22500	20600	6500	8400
5	0.723077	0.489583	0.583851	96	0.614173	0.8125	0.699552	96	0.668625	0.651042	0.641701	192	0.668625	0.651042	0.641701	192	0.651042	4700	7800	4900	1800
5	0.870588	0.493333	0.629787	150	0.646512	0.926667	0.761644	150	0.75855	0.71	0.695716	300	0.75855	0.71	0.695716	300	0.71	7400	13900	7600	1100
5	0.776699	0.655738	0.711111	122	0.702128	0.811475	0.752852	122	0.739413	0.733607	0.731981	244	0.739413	0.733607	0.731981	244	0.733607	8000	9900	4200	2300
6	0.80531	0.710938	0.755187	128	0.741259	0.828125	0.782288	128	0.773284	0.769531	0.768737	256	0.773284	0.769531	0.768737	256	0.769531	9100	10600	3700	2200
6	0.753086	0.616162	0.677778	99	0.675214	0.79798	0.731481	99	0.71415	0.707071	0.70463	198	0.71415	0.707071	0.70463	198	0.707071	6100	7900	3800	2000
6	0.733068	0.744939	0.738956	494	0.740741	0.728745	0.734694	494	0.736904	0.736842	0.736825	988	0.736904	0.736842	0.736825	988	0.736842	36800	36000	12600	13400
6	0.773585	0.572093	0.657754	215	0.660517	0.832558	0.736626	215	0.717051	0.702326	0.69719	430	0.717051	0.702326	0.69719	430	0.702326	12300	17900	9200	3600
6	0.785714	0.564103	0.656716	39	0.66	0.846154	0.741573	39	0.722857	0.705128	0.699145	78	0.722857	0.705128	0.699145	78	0.705128	2200	3300	1700	600
7	0.780488	0.627451	0.695652	102	0.688525	0.823529	0.75	102	0.734506	0.72549	0.722826	204	0.734506	0.72549	0.722826	204	0.72549	6400	8400	3800	1800
7	0.704348	0.727545	0.715758	334	0.718266	0.694611	0.70624	334	0.711307	0.711078	0.710999	668	0.711307	0.711078	0.710999	668	0.711078	24300	23200	9100	10200
7	0.812121	0.822086	0.817073	163	0.819876	0.809816	0.814815	163	0.815998	0.815951	0.815944	326	0.815998	0.815951	0.815944	326	0.815951	13400	13200	2900	3100
7	0.764706	0.578635	0.658784	337	0.661098	0.821958	0.732804	337	0.712902	0.700297	0.695794	674	0.712902	0.700297	0.695794	674	0.700297	19500	27700	14200	6000
7	0.805556	0.74359	0.773333	39	0.761905	0.820513	0.790123	39	0.78373	0.782051	0.781728	78	0.78373	0.782051	0.781728	78	0.782051	2900	3200	1000	700
8	0.894737	0.643939	0.748899	132	0.721893	0.924242	0.810631	132	0.808315	0.784091	0.779765	264	0.808315	0.784091	0.779765	264	0.784091	8500	12200	4700	1000
8	0.703448	0.658065	0.68	310	0.678788	0.722581	0.7	310	0.691118	0.690323	0.69	620	0.691118	0.690323	0.69	620	0.690323	20400	22400	10600	8600
8	0.690566	0.919598	0.788793	199	0.879699	0.58794	0.704819	199	0.785133	0.753769	0.746806	398	0.785133	0.753769	0.746806	398	0.753769	18300	11700	1600	8200
8	0.739583	0.636771	0.684337	223	0.681102	0.775785	0.725367	223	0.710343	0.706278	0.704852	446	0.710343	0.706278	0.704852	446	0.706278	14200	17300	8100	5000
8	0.822581	0.459459	0.589595	111	0.625	0.900901	0.738007	111	0.72379	0.68018	0.663801	222	0.72379	0.68018	0.663801	222	0.68018	5100	10000	6000	1100
9	0.875	0.666667	0.756757	21	0.730769	0.904762	0.808511	21	0.802885	0.785714	0.782634	42	0.802885	0.785714	0.782634	42	0.785714	1400	1900	700	200
9	0.858209	0.50885	0.638889	226	0.650943	0.915929	0.761029	226	0.754576	0.712389	0.699959	452	0.754576	0.712389	0.699959	452	0.712389	11500	20700	11100	1900
9	0.749311	0.68	0.712975	400	0.707094	0.7725	0.738351	400	0.728203	0.72625	0.725663	800	0.728203	0.72625	0.725663	800	0.72625	27200	30900	12800	9100
9	0.726236	0.945545	0.821505	202	0.921986	0.643564	0.758017	202	0.824111	0.794554	0.789761	404	0.824111	0.794554	0.789761	404	0.794554	19100	13000	1100	7200
9	0.828283	0.650794	0.728889	126	0.712418	0.865079	0.781362	126	0.770351	0.757937	0.755125	252	0.770351	0.757937	0.755125	252	0.757937	8200	10900	4400	1700
10	0.760915	0.661844	0.70793	553	0.7008	0.792043	0.743633	553	0.730857	0.726944	0.725782	1106	0.730857	0.726944	0.725782	1106	0.726944	36600	43800	18700	11500
10	0.877778	0.652893	0.748815	121	0.723684	0.909091	0.805861	121	0.800731	0.780992	0.777338	242	0.800731	0.780992	0.777338	242	0.780992	7900	11000	4200	1100
10	0.75	0.461538	0.571429	13	0.611111	0.846154	0.709677	13	0.680556	0.653846	0.640553	26	0.680556	0.653846	0.640553	26	0.653846	600	1100	700	200
10	0.678733	0.652174	0.665188	230	0.665272	0.691304	0.678038	230	0.672002	0.671739	0.671613	460	0.672002	0.671739	0.671613	460	0.671739	15000	15900	8000	7100
10	0.863636	0.655172	0.745098	58	0.722222	0.896552	0.8	58	0.792929	0.775862	0.772549	116	0.792929	0.775862	0.772549	116	0.775862	3800	5200	2000	600

7.2.17.10 TELLUS Ireland midlands topsoil geochemistry 26 elements

Chapter 5 extra supplementary materials

TELLUS Midlands dataset limited to elements/variables in Castleisland dataset and clr transformed including Kerry data.

GPR: 5-fold splitting repeated 10 times

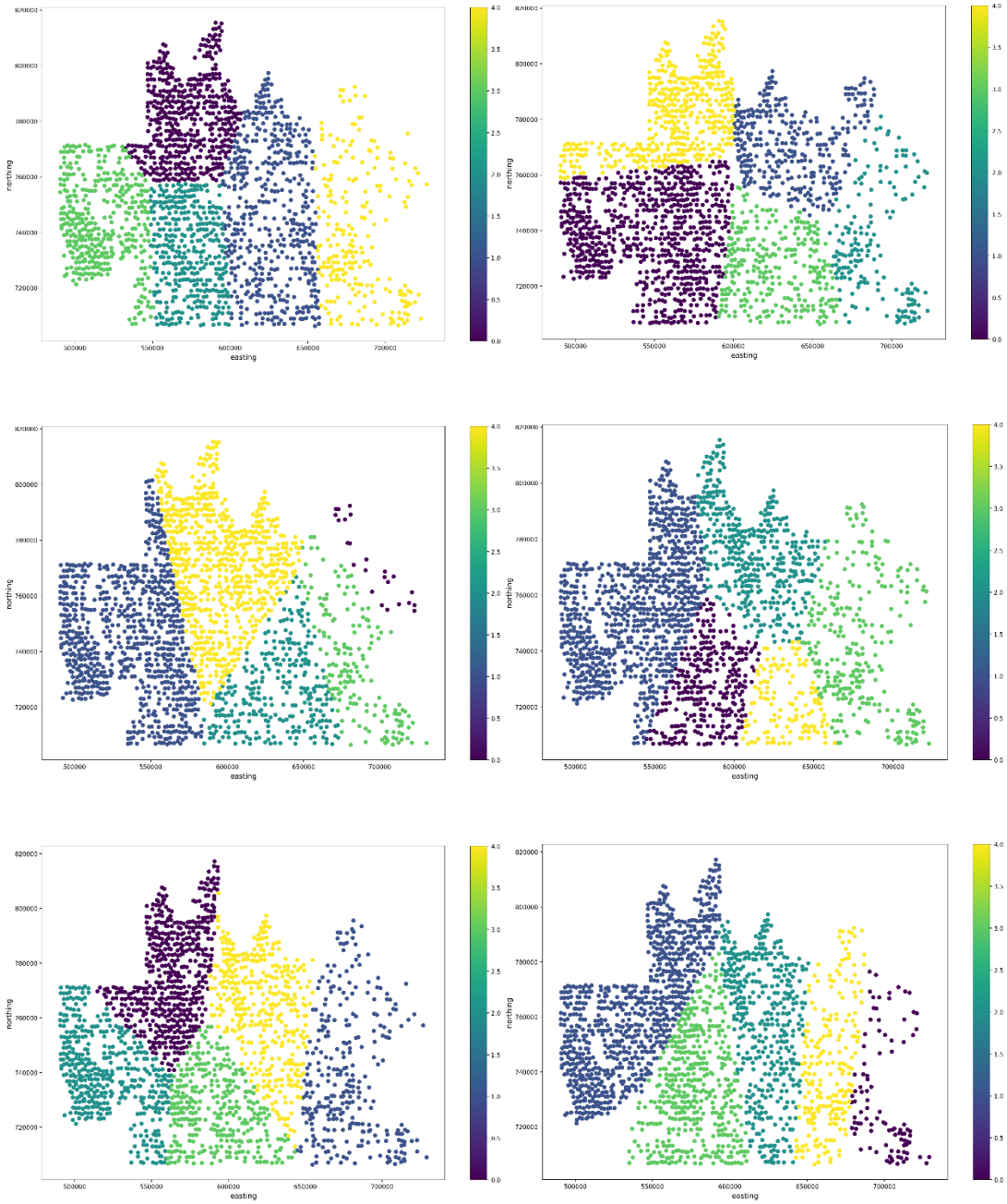

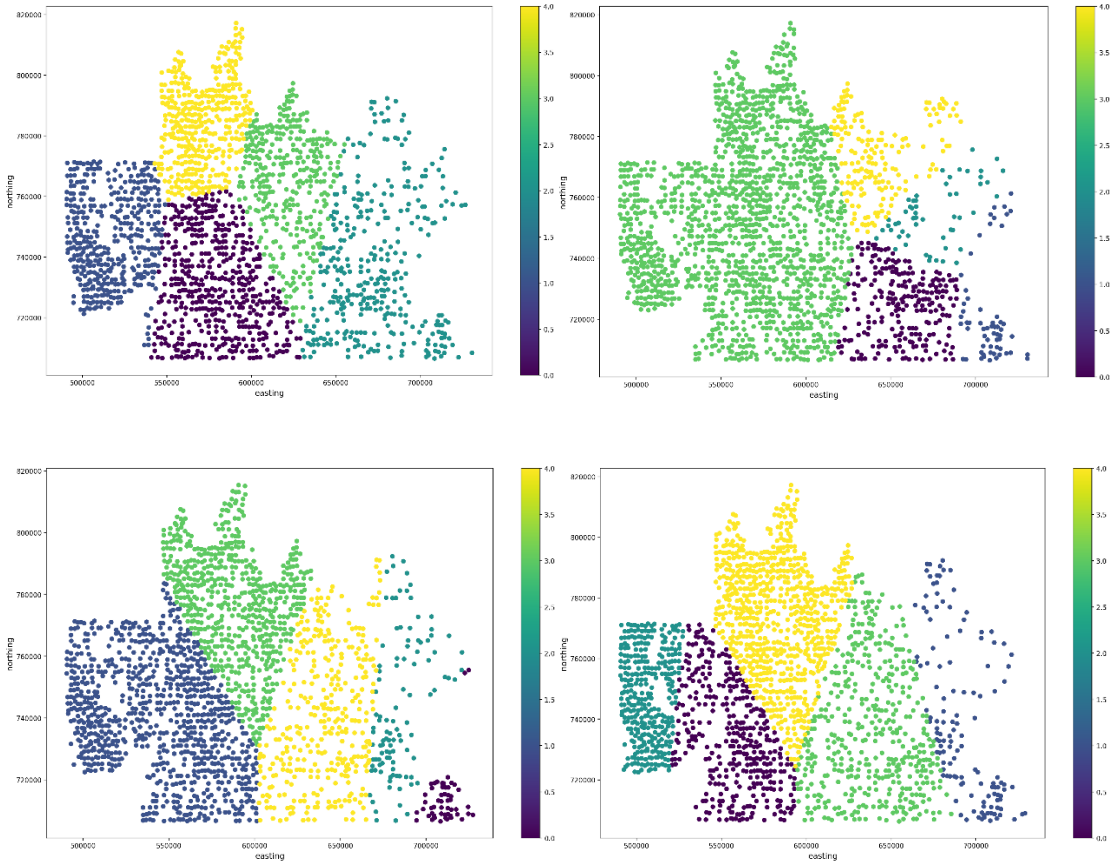

Feature importance

Al_mgkg_I	Ba_mgkg_	Ca_mgkg_	Cr_mgkg_	Cu_mgkg_	Fe_mgkg_	K_mgkg_I(	Mg_mgkg	Mn_mgkg	Na_mgkg_	Ni_mgkg_	P_mgkg_I(	Sr_mgkg_I(	V_mgkg_I(	Zn_mgkg_	As_mgkg_	Co_mgkg_	Ga_mgkg_	Hg_mgkg_	La_mgkg_	Mo_mgkg	Pb_mgkg_	Sb_mgkg_	Sc_mgkg_	Th_mgkg_	U_mgkg_I(
0.010013	0.013267	0.003942	0.003066	0.010826	0.001439	0.008698	0.004193	0.086733	0.000939	0.00169	-0.0005	0.009199	-0.0005	0.007447	0.000125	0.00826	0.010013	0.002065	0.057947	0.003129	0.002753	0.003755	0.004506	0.00363	0.022215
0.034396	0.020604	0.033571	0.056758	0.026758	0.00989	0.006429	0.017967	0.096484	0.009011	0.007143	0.006099	0.023956	0.028681	0.006429	0.010549	0.02544	0.008626	0.008462	0.063956	0.01467	0.008956	0.017363	0.02522	0.010385	0.023187
0.026442	0.008466	0.016074	0.009325	0.018098	0.00454	0.010245	0.01227	0.079018	0.003313	0.00184	0.006503	0.009939	0.01092	0.00589	0.012393	0.005767	0.000675	0.007546	0.052945	0.006748	0.003926	0.017914	0.008344	0.028282	0.015644
0.040278	0.025661	0.025463	0.043849	0.019709	0.010516	0.004696	0.008862	0.075661	0.004233	0.010714	0.008069	0.025132	0.036243	0.01078	0.014616	0.025926	0.008598	0.004034	0.061839	0.005688	0.005489	0.012698	0.017659	0.014484	0.022619
0.019839	0.010645	0.015	0.046532	0.014032	0.0175	0.014677	0.007419	0.091452	0.003871	0.01621	0.015161	0.003468	0.027903	0.008548	0.007903	0.016532	0.007742	0.007419	0.062097	0.003629	0.014435	0.001855	0.024113	0.070968	0.030968
0.028767	0.021286	0.018493	0.04215	0.01254	0.001897	0.00922	0.004004	0.061644	0.003741	0.003267	-0.00205	0.012434	0.03725	0.003899	0.004636	0.013488	0.004478	0.000474	0.068757	0.002529	0.003372	0.011907	0.033614	0.011117	0.025237
0.002883	0.022973	0.009189	0.004505	0.024324	0.00018	0.02973	0.005946	0.043964	0.00027	0.001712	-0.00189	0.016036	0.001261	0.00036	0.000721	0.002342	0.004054	0.000541	0.02982	0.006486	0.005135	0.048468	0.001081	0.011982	0.024144
0.03346	0.018113	0.021095	0.062852	0.014696	0.007701	0.013666	0.004826	0.068004	0.003471	0.004772	0.000271	0.010087	0.040184	0.011226	0.009219	0.014046	0.006996	-0.00038	0.075	0.004881	0.009056	0.017028	0.039588	0.016269	0.026681
0.031278	0.017905	0.01523	0.029049	0.010624	0.015676	0.011144	0.005869	0.074368	0.005052	0.006464	0.007652	0.002526	0.042273	0.005275	0.007652	0.020059	0.004383	0.009435	0.089896	0.002377	0.011664	0.008841	0.051263	0.072288	0.030461
0.049875	0.024969	0.031024	0.055056	0.018539	0.011735	0.000499	0.005805	0.052871	0.001935	0.008739	-0.00069	0.022097	0.043446	0.003433	0.008552	0.024782	0.005306	0.002871	0.084207	0.002372	0.005368	0.018414	0.046692	0.035705	0.027341
0.01907	0.00936	0.027558	0.021686	0.01314	0.002733	0.016163	0.010523	0.040407	-0.00169	0.028256	-0.00221	0.016977	0.015988	0.00814	0.006802	0.015349	-0.00047	-0.00227	0.058314	0.000407	0.004128	0.007849	0.025872	0.021453	0.007442
0.024339	0.01545	0.027672	0.047407	0.018413	0.005926	0.027672	0.015026	0.067196	0.003545	0.029418	0.002434	0.017725	0.029524	0.007302	0.008624	0.019101	0.004815	0.001005	0.064762	0.006825	0.006614	0.010317	0.029524	0.010582	0.023968
0.01308	0.009757	0.024314	0.043776	0.013766	0.000686	0.020095	0.01403	0.062658	0.000633	0.023787	-0.00137	0.011445	0.027373	0.000949	0.005327	0.017827	0.002268	0.000422	0.061603	0.000633	0.000949	0.003639	0.030854	0.018671	0.023365
0.009339	0.001751	0.003307	0.008366	0.023152	0.002918	0.032685	0.006615	0.094747	0.000389	-0.00136	0.004669	-0.00175	0.001751	0.006809	0.006031	0.001946	0.0064	0.005253	-0.00019	0.008366	0.02607	0.001167	0.009922	0.065564	0.064008
0.025674	0.009831	0.023146	0.063034	0.009326	0.000337	0.012022	0.004101	0.03236	0.00118	0.014719	0.002921	0.009494	0.021292	0.002809	0.005056	0.013596	-0.00051	-0.00028	0.075843	0.003146	0.001236	0.02118	0.026798	0.010562	0.008258
0.063297	0.00943	0.001764	0.03365	0.00536	0.009362	-0.00197	0.002442	0.067096	0.000678	0.01479	0.001425	0.005767	0.00095	0.001967	0.005156	0.020828	0.00882	0.000136	0.066689	0.002985	0.004342	0.008141	0.011398	0.007395	0.028833
0.021012	0.004086	0.011479	0.027756	0.019131	0.0107	0.01083	0.006615	0.062711	-0.00032	0.004929	0.007134	0.006485	0.03048	0.004604	0.012257	0.018418	0.00201	0.001427	0.069131	0.00668	-0.00032	0.022503	0.016861	0.024578	0.016602
0.03646	0.017702	0.03	0.073727	0.011491	0.013975	0.001801	0.014658	0.048634	0.000932	0.021739	-0.00037	0.020248	0.048385	0.00764	0.011615	0.022484	0.005217	0.001863	0.080559	0.003602	0.006087	0.005342	0.034286	0.014286	0.013478
0.03677	0.013789	0.020994	0.068634	0.006087	0.00913	0.000124	0.00118	0.031366	-0.00205	-0.00143	0.007391	0.01236	0.062484	0.001677	0.006832	0.010062	-0.00193	0.010559	0.087019	0.002174	0.004596	0.011925	0.024596	0.023043	0.012733
0.039194	0.012724	0.011957	0.050384	0.014834	0.019054	0.011253	0.004604	0.077494	0.004028	0.024872	0.010102	0.005627	0.040601	0.011189	0.01298	0.014258	0.016496	0.000384	0.092008	0.009719	0.001471	0.00876	0.034591	0.020077	0.040665
0.037433	0.019256	0.029288	0.028263	0.013053	0.011381	0.012783	0.015804	0.085005	0.005771	0.011327	0.004477	0.015264	0.03247	0.008252	0.01165	0.02589	0.012999	0.006472	0.075297	0.015912	0.004153	0.017907	0.037001	0.027994	0.037433
0.043554	0.009756	0.010192	0.000784	0.023519	0.009843	0.023868	0.006359	0.098519	0.00662	0.002613	0.010801	0.008275	0.011237	0.007753	0.001045	0.007404	0.003223	0.006882	0.049652	0.001307	0.001568	0.031882	0.00993	0.039983	0.019599
0.03044	0.015803	0.020661	0.051813	0.005052	0.010881	0.004858	0.009197	0.035492	-0.00058	0.011917	0.000324	0.010492	0.052202	0.005052	0.015544	0.018199	-0.00194	0.007837	0.081541	0.007189	0.007189	0.017876	0.030052	0.03886	0.019106
0.045586	0.020949	0.014559	0.003162	0.012451	0.022266	0.00863	0.010343	0.093412	0.004545	0.052964	0.000593	0.004348	0.00527	0.005204	0.003491	0.030105	0.012121	0.003689	0.077997	0.010935	0.003557	0.011989	0.033729	0.046377	0.063241
0.032776	0.023848	0.040092	0.026094	0.015092	0.018721	0.017396	0.015553	0.083122	0.006509	0.008583	0.005645	0.01947	0.02379	0.005933	0.018318	0.026498	0.007488	0.010714	0.079954	0.011578	0.006221	0.01371	0.044124	0.046832	0.033756
0.010824	0.015992	0.022975	0.056145	0.015573	0.013617	0.012151	0.006774	0.088897	0.003561	0.012849	0.002584	0.010754	0.017458	0.003282	0.00412	0.016061	0.001397	0.000768	0.080936	0.003142	0.003492	0.013408	0.03317	0.048464	0.024581
0.030181	0.024036	0.046265	0.089759	0.021566	0.007349	0.008795	0.018614	0.078313	0.010542	0.005783	0.001084	0.022892	0.013193	0.007952	0.004759	0.040843	0.008614	0.005361	0.085241	0.013855	0.009277	0.01506	0.054759	0.035964	0.018434
0.041656	0.014586	0.030486	0.034757	0.030486	0.015309	0.01958	0.005256	0.063141	0.008279	0.003548	0.004139	0.007687	0.007162	0.003154	0.00703	0.033443	0.009198	0.004008	0.057359	0.015112	0.00887	0.043758	0.04862	0.050788	0.03042
0.054377	0.017263	0.008508	0.043527	0.009864	0.006905	0.003822	0.009248	0.084649	0.003514	0.036991	0.002959	0.00672	0.002158	0.005857	0.006104	0.033107	0.005734	0.000247	0.074044	0.002158	0.0082	0.006967	0.037978	0.051171	0.03471
0.030179	0.01624	0.017647	0.085102	0.011573	0.007928	0.005691	0.009271	0.041624	0.005499	0.003708	0.001023	0.010806	0.030115	-4.44E-17	0.010422	0.027046	0.010486	0.015026	0.088491	0.005818	0.005499	0.023465	0.037084	0.043606	0.009463
0.044626	0.013466	0.012379	0.024336	0.01872	6.04E-05	0.001932	0.006824	0.08901	0.00157	0.052174	0.003442	0.005737	0.010266	0.003925	0.002959	0.020471	0.005495	0.0065	0.083575	0.00314	0.003261	0.012077	0.032609	0.019143	0.042512
0.001721	0.011232	0.014674	0.025453	0.035054	0.021649	0.038134	0.006612	0.064583	0.009239	0.012409	0.022373	0.013225	0.022736	0.001268	0.008514	0.001902	0.003442	0.009239	0.047373	0.016486	0.001721	0.061685	0.024457	0.049638	0.034058
0.016127	0.001554	0.010557	0.052202	0.006541	0.000324	-0.00466	-0.00065	0.020531	-0.00356	0.003821	-0.00583	0.001231	0.050648	0.002915	0.006088	0.003174	-0.00343	0.004598	0.056477	-0.00194	0.001878	0.002915	0.024676	0.024223	0.006606
0.016627	0.014593	0.030921	0.053648	0.019916	0.000478	0.002871	0.014593	0.060287	0.002751	0.013636	-0.0006	0.011722	0.045455	0.005502	0.003529	0.017883	0.006579	0.004067	0.079605	0.001316	0.004007	0.009091	0.041687	0.011065	0.010227
0.023355	0.016283	0.021985	0.040844	0.020066	0.000603	0.004441	0.004002	0.044408	0.002029	0.007072	-0.00104	0.008279	0.030702	0.00455	0.004496	0.009978	0.003015	0.003509	0.078509	0.002796	0.004715	0.013377	0.040461	0.021546	0.024397
0.043666	0.017601	0.029543	0.032555	0.01215	0.010125	0.003998	0.010177	0.049533	0.000156	0.003531	0.003634	0.017601	0.050467	0.003167	0.005815	0.01028	0.002804	0.005088	0.083593	0.004984	0.003946	0.019107	0.037227	0.020665	0.047612
-0.00316	0.01843	0.003925	-0.00392	0.014846	0.003072	0.004437	0.002816	0.023123	-0.00674	0.008703	-0.00256	-2.22E-17	-0.0023	-0.00239	0.001536	-0.00469	0.002816	-0.00034	0.043174	-0.00068	0.001195	0.02756	0.000171	0.008106	0.042918
0.052758	0.026439	0.023381	0.039269	0.019185	0.014928	0.003297	0.010552	0.06229	0.001079	0.013669	0.001379	0.019604	0.039568	0.007134	0.006295	0.019724	0.004736	0.009173	0.093645	0.003237	0.004017	0.016487	0.041487	0.020144	0.043225
0.019045	0.024213	0.039101	0.043708	0.011404	0.012247	0.005393	0.01573	0.033596	0.001966	0.004438	0.000899	0.022022	0.038764	0.00118	0.006461	0.011517	0.009607	0.010056	0.074045	0.004438	0.004831	0.011011	0.038146	0.015112	0.031966
0.030542	0.002951	0.002392	0.014833	-0.00016	0.011005	-0.00654	0.004226	0.027273	0.002632	0.00933	-0.00391	-0.00207	0.049601	-0.00303	0.00638	0.008612	-0.00088	0.000638	0.064274	0.000558	-6.66E-17	-0.00255	0.030383	0.042424	0.017225
0.011532	0.018287	0.006013	0.00313	0.032208	0.005601	0.017545	0.007414	0.05453	0.008155	0.002883	0.011038	0.007743	0.002224	0.006425	0.002471	0.016227	0.016969	0.00626	0.019687	0.001483	0.007249	0.037232	0.012191	0.078913	0.052554
0.020946	0.020823	0.032002	0.095946	0.021253	0.013882	0.005528	0.010504	0.022359	0.003563	0.004115	0.017015	0.031388	0.046744	0.010012	0.004423	0.013882	0.011671	0.016155	0.098464	0.0043	0.006388	0.034644	0.04441	0.037285	0.015971
0.013258	0.014157	0.028539	0.085843	0.02764	0.015843	0.001573	0.006742	0.056011	0.001404	0.011348	0.006685	0.021573	0.021573	0.008315	0.00736	0.016348	0.008427	0.003315	0.059607	0.002921	0.003989	0.023315	0.036461	0.018989	0.029607
0.062005	0.013325	0.022449	0.070108	0.023649	0.018007	0.008764	0.005822	0.084034	0.001561	0.032713	0.006242	0.021909	0.030792	0.005822	0.010504	0.019388	0.006783	0.005462	0.070408	0.002581	0.005642	0.016567	0.033493	0.028691	0.027131
0.010913	0.011839	0.018188	0.062698	0.023876	0.017791	0.002976	0.003373	0.084722	0.00172	0.033267	0.019577	0.009656	0.010847	-1.11E-17	0.010847	0.01164	0.005952	0.004034	0.070701	0.005225	0.007606	0.016997	0.041468	0.044775	0.040807
0.007934	0.007456	0.018947	0.022914	0.008755	0.007729	0.001163	0.007387	0.054446	0.001436	0.02223	-0.00185	0.008276	0.004104	0.004036	0.010534	0.00643	0.005746	0.008824	0.081122	-0.00027	0.004172	0.00342	0.039535	0.009508	0.048564
0.070572	0.022548	0.041417	0.096866	0.013488	0.009673	0.008515	0.014373	0.042439	0.007561	0.01049	0.00361	0.022343	0.037875	0.00654	0.00688	0.022003	0.008787	0.020232	0.094891	0.006335	0.007357	0.020163	0.052044	0.026907	0.019346
0.033985	0.010404	0.015889	0.017276	0.009142	0.008386	0.011475	0.007188	0.06797	0.003657	0.021942	6.31E-05	0.015069	0.004161	0.001639	0.002459	0.014502	0.010277	0.007377	0.065132	0.002459	0.004161	0.007692	0.018979	0.009332	0.044641
0.026343	0.00422	0.019693	0.011829	0.01624	0.004668	0.006138	0.005882	0.060678	0.004731	-0.00019	0.002941	0.005691	0.010102	0.003453	0.011445	0.005179	0.002621	0.006266	0.049233	0.001535	0.003453	0.024872	0.020844	0.019629	0.020141
0.032093	0.010581	0.039826	0.062733	0.014128	0.003721	0.004884	0.007093	0.04343	0.003023	0.005349	0.000407	0.022384	0.010756	0.007093	0.011279	0.010523	0.002267	0.005698	0.072616	0.008721	0.003953	0.007616	0.038023	0.01064	0.025523

GPR model results

split_inde	precision_	recall_clas	f1-score_c	support_c	precision_	recall_clas	f1-score_c	support_c	precision_	recall_wei	f1-score_v	support_v	precision_	recall_ma	f1-score_r	support_r	accuracy	T_class1	T_class2	F_class1	F_class2
1	0.766129	0.539773	0.633333	176	0.644737	0.835227	0.727723	176	0.705433	0.6875	0.680528	352	0.705433	0.6875	0.680528	352	0.6875	9500	14700	8100	2900
1	0.787234	0.569231	0.660714	65	0.662651	0.846154	0.743243	65	0.724942	0.707692	0.701979	130	0.724942	0.707692	0.701979	130	0.707692	3700	5500	2800	1000
1	0.659292	0.93125	0.772021	160	0.882979	0.51875	0.653543	160	0.771135	0.725	0.712782	320	0.771135	0.725	0.712782	320	0.725	14900	8300	1100	7700
1	0.865169	0.703196	0.775819	219	0.75	0.890411	0.814196	219	0.807584	0.796804	0.795007	438	0.807584	0.796804	0.795007	438	0.796804	15400	19500	6500	2400
1	0.723906	0.605634	0.659509	355	0.661017	0.769014	0.710938	355	0.692461	0.687324	0.685223	710	0.692461	0.687324	0.685223	710	0.687324	21500	27300	14000	8200
2	0.757576	0.961538	0.847458	26	0.947368	0.692308	0.8	26	0.852472	0.826923	0.823729	52	0.852472	0.826923	0.823729	52	0.826923	2500	1800	100	800
2	0.720455	0.754762	0.737209	420	0.7425	0.707143	0.72439	420	0.731477	0.730952	0.7308	840	0.731477	0.730952	0.7308	840	0.730952	31700	29700	10300	12300
2	0.862069	0.471698	0.609756	53	0.636364	0.924528	0.753846	53	0.749216	0.698113	0.681801	106	0.749216	0.698113	0.681801	106	0.698113	2500	4900	2800	400
2	0.738197	0.569536	0.642991	302	0.649596	0.798013	0.716196	302	0.693897	0.683775	0.679593	604	0.693897	0.683775	0.679593	604	0.683775	17200	24100	13000	6100
2	0.817568	0.695402	0.751553	174	0.735	0.844828	0.786096	174	0.776284	0.770115	0.768825	348	0.776284	0.770115	0.768825	348	0.770115	12100	14700	5300	2700
3	0.845238	0.617391	0.713568	115	0.69863	0.886957	0.781609	115	0.771934	0.752174	0.747589	230	0.771934	0.752174	0.747589	230	0.752174	7100	10200	4400	1300
3	0.892857	0.833333	0.862069	30	0.84375	0.9	0.870968	30	0.868304	0.866667	0.866518	60	0.868304	0.866667	0.866518	60	0.866667	2500	2700	500	300
3	0.8	0.592593	0.680851	27	0.676471	0.851852	0.754098	27	0.738235	0.722222	0.717475	54	0.738235	0.722222	0.717475	54	0.722222	1600	2300	1100	400
3	0.73487	0.710306	0.72238	718	0.719677	0.743733	0.731507	718	0.727273	0.727019	0.726943	1436	0.727273	0.727019	0.726943	1436	0.727019	51000	53400	20800	18400
3	0.810811	0.352941	0.491803	85	0.586466	0.917647	0.715596	85	0.698638	0.635294	0.6037	170	0.698638	0.635294	0.6037	170	0.635294	3000	7800	5500	700
4	0.803109	0.651261	0.719258	238	0.706714	0.840336	0.767754	238	0.754911	0.745798	0.743506	476	0.754911	0.745798	0.743506	476	0.745798	15500	20000	8300	3800
4	0.722656	0.906863	0.804348	204	0.875	0.651961	0.747191	204	0.798828	0.779412	0.775769	408	0.798828	0.779412	0.775769	408	0.779412	18500	13300	1900	7100
4	0.838235	0.670588	0.745098	170	0.72549	0.870588	0.791444	170	0.781863	0.770588	0.768271	340	0.781863	0.770588	0.768271	340	0.770588	11400	14800	5600	2200
4	0.858696	0.464706	0.603053	170	0.633065	0.923529	0.751196	170	0.74588	0.694118	0.677125	340	0.74588	0.694118	0.677125	340	0.694118	7900	15700	9100	1300
4	0.669903	0.715026	0.691729	193	0.694444	0.647668	0.670241	193	0.682174	0.681347	0.680985	386	0.682174	0.681347	0.680985	386	0.681347	13800	12500	5500	6800
5	0.878788	0.604167	0.716049	48	0.698413	0.916667	0.792793	48	0.7886	0.760417	0.754421	96	0.7886	0.760417	0.754421	96	0.760417	2900	4400	1900	400
5	0.689162	0.840399	0.757303	401	0.795527	0.620948	0.697479	401	0.742344	0.730673	0.727391	802	0.742344	0.730673	0.727391	802	0.730673	33700	24900	6400	15200
5	0.836066	0.502463	0.627692	203	0.644366	0.901478	0.75154	203	0.740216	0.70197	0.689616	406	0.740216	0.70197	0.689616	406	0.70197	10200	18300	10100	2000
5	0.825	0.611111	0.702128	216	0.691176	0.87037	0.770492	216	0.758088	0.740741	0.73631	432	0.758088	0.740741	0.73631	432	0.740741	13200	18800	8400	2800
5	0.793814	0.719626	0.754902	107	0.74359	0.813084	0.776786	107	0.768702	0.766355	0.765844	214	0.768702	0.766355	0.765844	214	0.766355	7700	8700	3000	2000
6	0.738776	0.698842	0.718254	259	0.714286	0.752896	0.733083	259	0.726531	0.725869	0.725668	518	0.726531	0.725869	0.725668	518	0.725869	18100	19500	7800	6400
6	0.846154	0.682759	0.755725	145	0.734104	0.875862	0.798742	145	0.790129	0.77931	0.777234	290	0.790129	0.77931	0.777234	290	0.77931	9900	12700	4600	1800
6	0.760684	0.831776	0.794643	214	0.814433	0.738318	0.77451	214	0.787558	0.785047	0.784576	428	0.787558	0.785047	0.784576	428	0.785047	17800	15800	3600	5600
6	0.766423	0.640244	0.697674	164	0.691099	0.804878	0.743662	164	0.728761	0.722561	0.720668	328	0.728761	0.722561	0.720668	328	0.722561	10500	13200	5900	3200
6	0.79661	0.487047	0.604502	193	0.630597	0.875648	0.733189	193	0.713604	0.681347	0.668845	386	0.713604	0.681347	0.668845	386	0.681347	9400	16900	9900	2400
7	0.764706	0.619048	0.684211	147	0.68	0.809524	0.73913	147	0.722353	0.714286	0.71167	294	0.722353	0.714286	0.71167	294	0.714286	9100	11900	5600	2800
7	0.699234	0.862884	0.772487	423	0.820988	0.628842	0.712182	423	0.760111	0.745863	0.742334	846	0.760111	0.745863	0.742334	846	0.745863	36500	26600	5800	15700
7	0.873684	0.408867	0.557047	203	0.614148	0.940887	0.743191	203	0.743916	0.674877	0.650119	406	0.743916	0.674877	0.650119	406	0.674877	8300	19100	12000	1200
7	0.821429	0.661871	0.733068	139	0.716867	0.856115	0.780328	139	0.769148	0.758993	0.756698	278	0.769148	0.758993	0.756698	278	0.758993	9200	11900	4700	2000
7	0.763636	0.666667	0.711864	63	0.704225	0.793651	0.746269	63	0.733931	0.730159	0.729067	126	0.733931	0.730159	0.729067	126	0.730159	4200	5000	2100	1300
8	0.75	0.25	0.375	12	0.55	0.916667	0.6875	12	0.65	0.583333	0.53125	24	0.65	0.583333	0.53125	24	0.583333	300	1100	900	100
8	0.716019	0.758355	0.736579	389	0.743169	0.699229	0.72053	389	0.729594	0.728792	0.728555	778	0.729594	0.728792	0.728555	778	0.728792	29500	27200	9400	11700
8	0.755906	0.680851	0.716418	141	0.709677	0.780142	0.743243	141	0.732791	0.730496	0.729831	282	0.732791	0.730496	0.729831	282	0.730496	9600	11000	4500	3100
8	0.852941	0.682353	0.75817	85	0.735294	0.882353	0.802139	85	0.794118	0.782353	0.780154	170	0.794118	0.782353	0.780154	170	0.782353	5800	7500	2700	1000
8	0.799127	0.525862	0.634315	348	0.646681	0.867816	0.741104	348	0.722904	0.696839	0.68771	696	0.722904	0.696839	0.68771	696	0.696839	18300	30200	16500	4600
9	0.743869	0.741848	0.742857	368	0.742547	0.744565	0.743555	368	0.743208	0.743207	0.743206	736	0.743208	0.743207	0.743206	736	0.743207	27300	27400	9500	9400
9	0.833333	0.496894	0.622568	161	0.641593	0.900621	0.749354	161	0.737463	0.698758	0.685961	322	0.737463	0.698758	0.685961	322	0.698758	8000	14500	8100	1600
9	0.875	0.658824	0.751678	85	0.726415	0.905882	0.806283	85	0.800708	0.782353	0.77898	170	0.800708	0.782353	0.77898	170	0.782353	5600	7700	2900	800
9	0.762295	0.65493	0.704545	142	0.697531	0.795775	0.743421	142	0.729913	0.725352	0.723983	284	0.729913	0.725352	0.723983	284	0.725352	9300	11300	4900	2900
9	0.682203	0.73516	0.707692	219	0.712871	0.657534	0.684086	219	0.697537	0.696347	0.695889	438	0.697537	0.696347	0.695889	438	0.696347	16100	14400	5800	7500
10	0.674603	0.696721	0.685484	244	0.686441	0.663934	0.675	244	0.680522	0.680328	0.680242	488	0.680522	0.680328	0.680242	488	0.680328	17000	16200	7400	8200
10	0.784431	0.543568	0.642157	241	0.650794	0.850622	0.73741	241	0.717612	0.697095	0.689783	482	0.717612	0.697095	0.689783	482	0.697095	13100	20500	11000	3600
10	0.804878	0.543956	0.64918	182	0.655602	0.868132	0.747045	182	0.73024	0.706044	0.698113	364	0.73024	0.706044	0.698113	364	0.706044	9900	15800	8300	2400
10	0.763393	0.88601	0.820144	193	0.864198	0.725389	0.788732	193	0.813795	0.805699	0.804438	386	0.813795	0.805699	0.804438	386	0.805699	17100	14000	2200	5300
10	0.873563	0.66087	0.752475	115	0.727273	0.904348	0.806202	115	0.800418	0.782609	0.779338	230	0.800418	0.782609	0.779338	230	0.782609	7600	10400	3900	1100

Logistic regression

5-fold spatial cross validation repeated 10 times

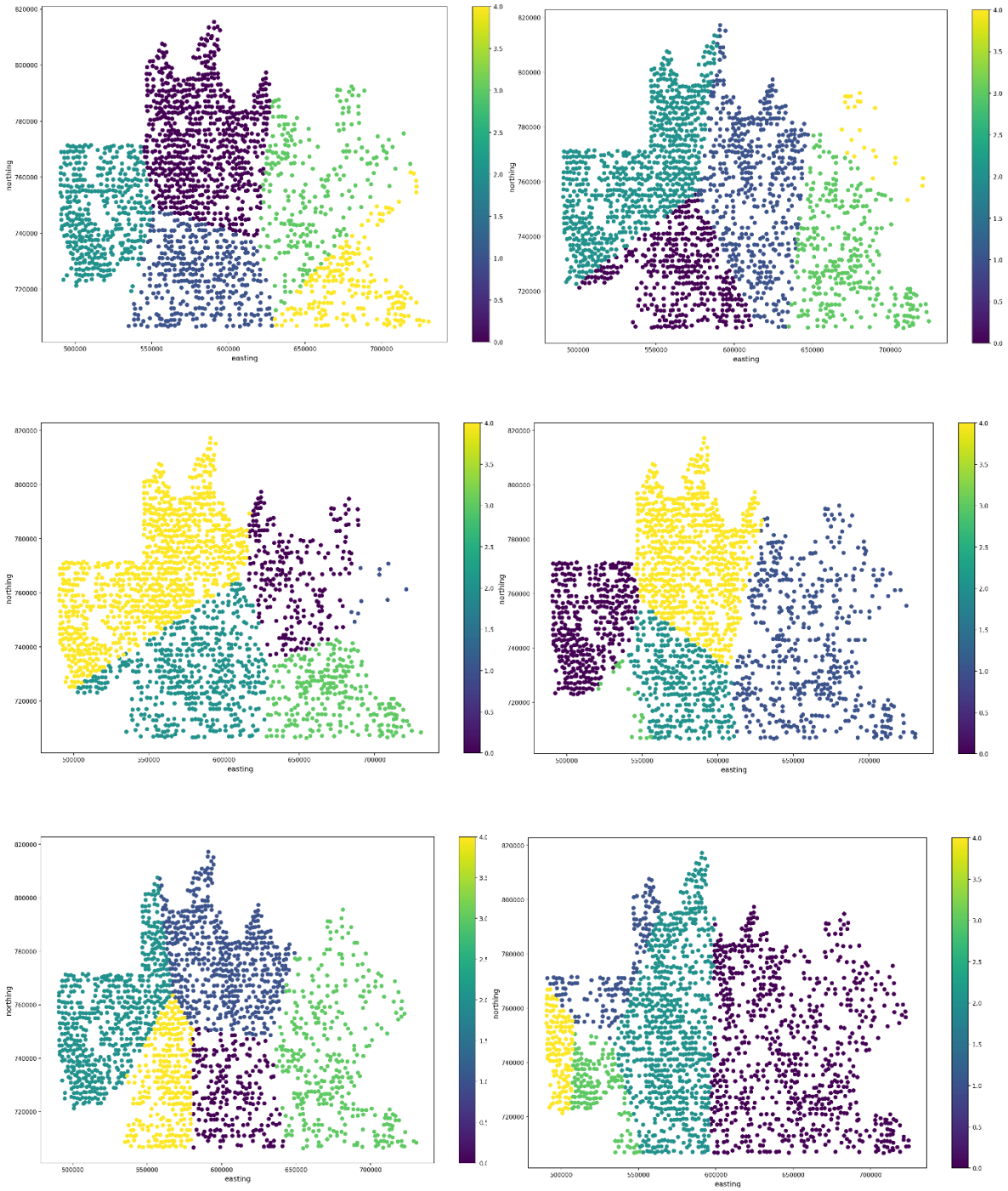

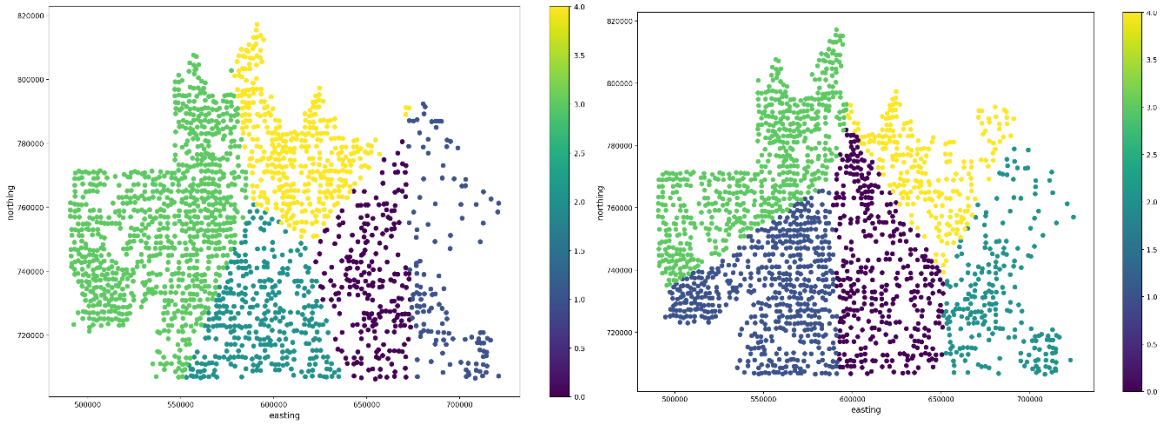
northing
easting
820000
800000
780000
760000
740000
720000
500000
550000
600000
650000
700000
4.0
3.5
3.0
2.5
2.0
1.5
1.0
0.5
0.0

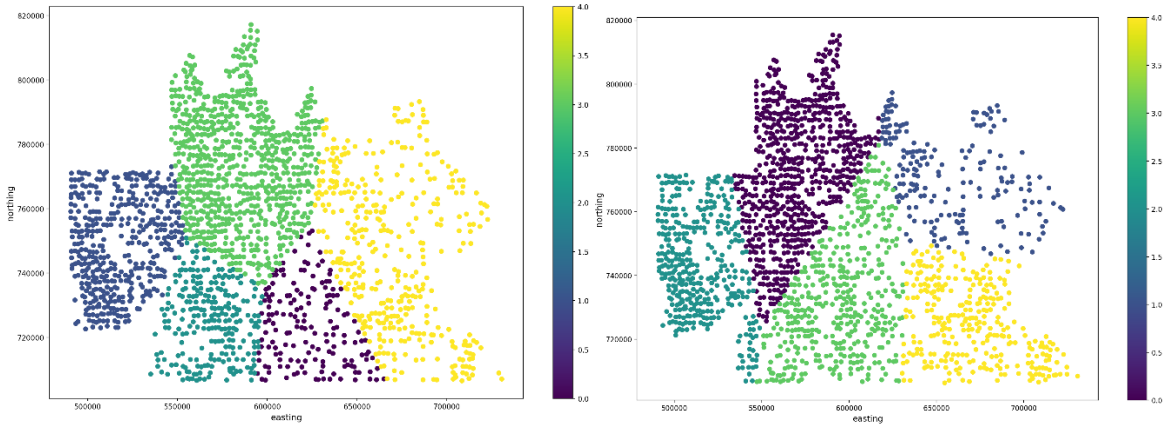
northing
easting
820000
800000
780000
760000
740000
720000
500000
550000
600000
650000
700000
4.0
3.5
3.0
2.5
2.0
1.5
1.0
0.5
0.0

ROC

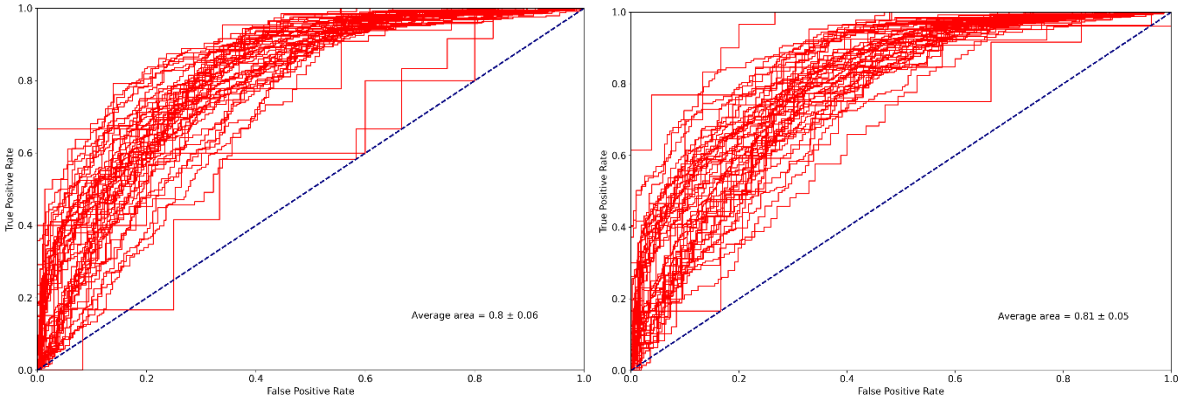
True Positive Rate
False Positive Rate
Average area = 0.8 ± 0.06
Average area = 0.81 ± 0.05
0.0
0.2
0.4
0.6
0.8
1.0

Feature importance

Al_mgkg_I	Ba_mgkg_	Ca_mgkg_	Cr_mgkg_	Cu_mgkg_	Fe_mgkg_	K_mgkg_I(	Mg_mgkg	Mn_mgkg	Na_mgkg_	Ni_mgkg_I	P_mgkg_I(	Sr_mgkg_I	V_mgkg_I(	Zn_mgkg_	As_mgkg_	Co_mgkg_	Ga_mgkg_	Hg_mgkg_	La_mgkg_	Mo_mgkg	Pb_mgkg_	Sb_mgkg_	Sc_mgkg_I	Th_mgkg_	U_mgkg_I(
0.06072	0.002113	0.009859	0.001095	0.000704	-0.0018	0.004617	0	0.029421	-0.00164	-0.00094	0.004773	0.003991	-0.00188	-0.0011	-0.00063	7.82E-05	0.002191	0.003521	0.061659	0.001017	0.006182	0.008764	0.005634	0.007042	0.001252
0.115511	0.018693	0.016364	0.041932	0.008807	0.001989	0.002159	0.000625	0.043352	-4.44E-17	0.006307	0.006193	0.009659	0.003239	0.00142	0.004659	0.008864	0.00375	0.009375	0.052273	0.002045	0.001477	0.0225	0.013352	0.004773	-0.0004
0.084557	0.025949	0.011392	-0.00114	0.012468	0.003481	0.002278	0.007089	0.055127	0.000823	0.001456	0.000633	0.004114	-0.0007	0.005253	-0.0012	0.005127	0.006392	0.000823	0.041013	-0.00025	0.001013	0.048101	0.005063	0.00019	0.00057
0.156365	0.020932	0.012008	0.005315	0.007021	0.004199	-0.00171	0.003871	0.097966	0.003018	0.037533	0.000262	-0.00236	-0.00125	0.000853	0.002165	0.015092	0.011417	0.003609	0.022113	-0.00059	0.003937	0.00374	0.009449	-0.00066	0.001247
0.071773	0.013269	0.025935	0.014053	0.008926	0.005428	-0.00036	0.000844	0.031001	-0.00084	0	-0.00012	0.014837	0.000543	0.002352	-0.00012	0.007238	0.004885	0.010856	0.069119	0.007901	0.002835	0.018758	0.011399	0.002533	0.000603
0.078547	0.008436	0.009553	0.047877	0.01095	0.017598	0.008883	0.003408	0.071732	-2.22E-17	0.001117	0.011061	0.011676	0.026313	0.001676	0.000559	0.015084	0.019497	0.014749	0.075251	0.008324	0.007933	0.013017	0.014581	0.000615	0.003017
0.023047	0.00931	0.012956	0.008203	0.013086	0.013672	0.038542	0.005924	0.049609	0.002409	0.003906	0.015104	0.007227	0.016146	0.000781	-0.00033	0.010352	0.012109	0.006706	0.039648	0.004167	-0.00124	0.038216	0.000781	0.001628	0.005078
0.054338	0.008324	0.003224	0.021395	0.010551	0.009789	0.026612	0.004045	0.069637	0.001114	0.002814	0.001993	0.002579	0.005393	0.003869	0.002579	0.007913	0.015768	0.0051	0.0466	0.004455	0.005979	0.010961	0.00592	-0.00035	0.008441
0.030366	0.000749	-0.00033	0.036855	0.001581	0.005324	0.025957	0.000166	0.015391	-0.00075	-0.00233	0.003827	-0.001	0.0297	0.003993	0.001581	0.000749	0.009651	0.010899	0.06223	-0.00324	0.012063	0.000666	0.018136	0.003078	0.002829
0.034036	0.001596	0.012644	0.072031	0.012069	0.009579	-0.00734	-0.00211	0.042337	-0.00115	-0.00287	-0.00192	0.014559	0.016475	-0.00587	0.00083	0.010345	0.014304	0.010983	0.068327	0.006194	-0.00492	0.011494	0.008621	-0.00453	-0.00319
0.075031	0.009748	0.008239	0.019308	0.007547	0.010252	0.000755	0.004025	0.018302	0.00283	0.001887	0.005535	0.001887	0.010566	-6.29E-05	6.29E-05	0.01327	0.010189	0.012767	0.073019	0.011069	0.005535	0.007421	0.016415	-0.00258	0.000692
0.040085	0.00949	0.000921	0.004887	0.008853	0.003612	0.061969	0.003824	0.018909	0.010552	0.015297	0.005878	0.005028	0.001275	0.002833	-0.00085	0.009207	0.011261	0.007295	0.039943	0.002337	0.003329	0.010198	0.001912	0.000142	0.011969
0.054408	0.019606	0.014095	0.0279	0.009223	0.007135	0.011079	0.003016	0.021288	0.005162	0.000406	5.80E-05	0.001682	0.001682	0.000812	0.00609	0.009397	0.007715	0.009223	0.07326	0.005858	0.001276	0.013225	0.010383	0.001392	-0.00046
0.06305	0.020015	0.007698	0.02654	0.017962	0.006452	0.032478	0.001466	0.08673	0.0011	-0.00015	0.006305	-0.00037	0.009677	0.000147	-7.33E-05	0.006598	0.000953	0.004472	0.092595	-0.00103	0.003006	0.025513	0.016642	0.015762	0.01437
0.075673	0.010643	0.006608	0.068596	0.008187	-0.00064	0.000702	0.000643	0.008538	0.001754	0.000292	0.007953	0.00193	-0.00164	0	0.006199	0.010175	0.006784	0.010994	0.082982	0.002398	-0.00146	0.017719	0.01462	0.004854	-0.00123
0.056481	0.010243	0.017419	0.04647	0.014873	0.008275	0.005093	-0.00017	0.055903	0.000463	-0.00046	0.000984	0.00787	0.000984	0.000926	0.001968	0.014236	0.005266	0.008565	0.09375	0.011053	-3.33E-17	0.01059	0.010069	0.003356	0.000174
0.064011	0.013791	0.011264	0.033516	0.013297	0.007692	0.006264	0.003297	0.059835	0.001209	0.000769	0.001758	0.005659	0.00022	0.000385	0.00544	0.008242	0.004396	0.006538	0.082802	0.006703	0.002692	0.017198	0.013626	-0.00137	0.001154
0.098522	0.007143	0.001047	0.045505	0.009483	0.007512	0.004187	6.16E-05	0.097783	0.001293	0.008251	0.002956	0.001416	-0.00055	-0.00025	-0.00135	0.015394	0.004618	0.003818	0.065394	0.007328	0.004433	0.002155	0.005111	0.000431	0.0008
-0.00019	0.010417	0.005682	-0.00218	0.025095	0.001231	0.040909	0.000379	0.00322	0.000284	0.000284	0.006061	0.005587	0.000852	-0.00066	-0.0036	0.002652	0.003788	-0.00199	0.061364	-0.00123	-0.00038	0.044697	-0.00019	0.004356	0.035322
0.06743	0.003817	0.012532	0.075509	0.007824	0.006934	0.001908	0.001081	0.020865	0.0007	0.003435	0.004389	0.006361	-6.36E-05	0.000891	0.005852	0.005916	0.003435	0.011196	0.049936	0.000891	0.002608	0.009351	0.015204	-0.00191	-0.00025
0.033891	0.005986	0.01831	0.059419	0.017606	0.010035	0.005282	0.001761	0.015405	-0.00484	0.014877	-0.00106	0.027465	0.017165	-0.00423	0.01382	0.010123	-0.0007	0.012148	0.083363	0.019806	0.009859	0.00669	0.017165	-0.00255	-2.22E-17
0.046818	0.021648	0.002898	0.0025	0.011989	0.008239	0.001534	-0.00477	0.085852	-0.00239	-0.00284	-0.00102	-0.00312	0.014432	-0.00511	-0.00267	0.005227	-0.00153	-0.0017	0.097045	0.009659	-0.00091	0.010909	0.008466	0.00875	-0.00148
0.054461	0.017677	-0.00017	0.000505	0.006566	0.00968	0.030976	0.000253	0.100253	0.002189	0.003704	-0.0016	-0.00152	0.00101	0.002862	0.006313	0.006818	0.007744	0.002273	0.068182	0.002946	0.003788	-0.00168	0.004293	-0.00177	0.003704
0.044148	0.027045	0.00125	0.00375	0.015795	0.008864	0.006875	0.000625	0.085398	-0.00148	0.005852	0.002784	0.005682	0.010455	-0.00159	0.003523	0.010909	0.003295	0.006364	0.125227	0.012727	0.002898	0.021307	0.003295	0.00017	0.003011
0.068454	0.019018	0.005474	0.00965	0.016704	0.009989	0.007054	-0.00226	0.07912	-0.00096	0.000282	-0.00152	0.001072	0.01377	0.001975	5.64E-05	0.013713	0.002427	0.007449	0.113262	0.003499	0.001919	0.017381	0.005079	-0.0004	0.001185
0.102653	0.015052	0.007728	0.006747	0.013552	0.012457	0.003576	0.001615	0.081949	-0.00069	5.77E-05	0.006055	0.003749	0.007151	-0.00179	-0.00219	0.019608	0.012803	0.012572	0.067589	0.005652	0.001788	0.001788	0.014129	0.001845	0.005248
0.083381	0.000142	0.007031	0.036577	0.001349	0.004759	-0.00057	-0.00071	0.02777	-0.00085	0.005966	0.007102	-0.00071	0.023864	-0.00149	-0.00078	0.005966	0.006818	0.005327	0.03196	-0.00021	0.005753	-0.00021	0.0125	-0.00078	0.000994
0.031628	0.025144	0.019885	0.020461	0.032349	0.022695	0.069885	0.014841	0.059222	0.001945	0.012176	0.01268	0.014697	0.004683	0.001225	0.004035	0.008429	0.00951	0.016787	0.066354	0.001225	0.000504	0.037608	0.010086	0.001009	0.01866
0.06702	0.01303	0.015773	0.012656	0.014214	0.007232	0.003554	-0.00069	0.051496	0.000374	0.00081	0.001247	0.010848	0.005923	0.002805	0.001683	0.015898	0.010723	0.00904	0.078429	0.006359	0.001185	0.004988	0.012282	0.004115	0.002057
0.055942	0.009784	-0.00372	-0.00246	0.008163	0.003962	0.020468	-0.00072	0.05054	0.001681	-0.00138	0.0012	0.003361	0.002341	-0.00138	-0.00024	0.007803	0.007443	0.002701	0.066026	0.001741	0.002701	0.00066	0.006122	-0.0015	0.009124
0.022949	0.010385	0.015128	0.0075	0.011154	0.005	0.061667	0.000577	0.046731	-0.00077	0.001538	-0.00071	0.002885	0	-6.41E-05	0.003974	0.004103	0.005705	6.41E-05	0.012885	0.001667	0.001218	0.031987	0.002564	0.004872	0.01359
0.060082	0.004733	0.015158	0.016187	0.008505	0.005007	-0.00309	0.001989	0.028464	-0.00158	0.001989	-0.00075	0.008711	-0.00405	-0.00021	0.000206	0.007956	0.006516	0.002469	0.032647	0.003361	0.000274	0.011043	0.006379	-0.00288	0.000137
0.079582	0.007073	0.003998	0.015621	0.004551	0.000185	0.021095	0.002337	0.047601	0.000738	0.006642	-0.00148	-0.00203	0.001538	-6.15E-05	0.000615	0.004244	0.005351	-0.00443	0.021464	0.00203	0.002153	0.009533	-0.00252	0.000308	0.008364
0.078416	0.00383	0.007971	0.012836	0.004555	-0.00104	0.021894	-0.00104	0.037319	-0.00166	0.002122	-0.00243	0.000776	0.000155	-0.00248	0.000673	0.000104	0.004969	-0.00285	0.037371	-0.00217	-0.00031	0.013199	0.002484	-0.00176	0.005538
0.059967	-0.0067	0.007843	0.05384	-0.00547	-0.00294	0.008333	-0.0031	0.004984	-0.00188	-0.00016	0.002696	-0.00743	-0.00131	-0.004	-0.004	-0.00114	0.002042	-0.00376	0.034886	0.001471	0.006127	0.001307	0.008824	0.010784	0.005637
0.021645	0.008343	0.008343	0.056943	0.005484	0.002684	4.44E-17	3.33E-17	0.041249	-0.00198	-0.00018	0.003676	0.004142	0.003851	0.000758	0.00245	0.005601	0.000817	0.002975	0.040548	0.003792	0.001575	0.009568	0.010035	0.002684	-0.00029
0.018866	0.011546	0.010052	0.023454	0.009072	0.001804	0.00299	0.003093	0.06701	0.001186	-0.00026	0.002629	0.004485	0.010412	0.001495	0.003144	0.005876	0.004381	0.005	0.035	0.000773	0.003196	0.008454	0.009021	0.000722	0.000412
0.050414	0.01331	0.000276	0.016897	0.006897	-0.00124	0.003586	0.004759	0.109448	-0.00055	0.011724	0.002828	0.002621	0.017448	-0.0011	-0.00076	0.013862	0.004483	-0.002	0.012207	0.000414	0.009172	0.006621	0.003034	0.005517	0.005724
0.00071	0.005089	0.004793	0.028225	0.003905	0.001479	-0.00024	-0.00148	0.048166	0.000296	0.000769	-0.00201	0.002663	0.009822	-0.00036	0.001598	0.003018	0.00142	0.000592	0.032485	-0.00107	0.000178	0.002781	0.005444	0.000296	0.000237
0.00169	-0.0003	0.002883	0.007058	0.011829	0.000199	0.015209	-0.00169	0.050497	0.000497	-0.00268	0.005964	-0.00487	-0.0003	0.025149	0	0.002584	0.002087	0.004771	0.072664	-0.00149	0.012525	0.006561	0.008946	0.024851	0.010934
0.030623	0.016074	0.001652	0.008513	0.00845	0.005527	0.013088	0.000445	0.060038	0.001779	0.010864	-0.00241	-0.00426	-0.00019	-0.00076	0.000445	0.006163	0.007687	-0.0007	0.05972	-0.0026	0.000254	0.002033	0.004638	0.011055	0.004511
0.097668	-0.00014	0.002401	0.078875	0.007888	0.003841	-0.00034	0.00144	0.033059	-0.00151	0.004458	0.003498	0.003841	0.005213	0.002675	0.002058	0.007956	-0.00075	0.007202	0.029218	0.006516	0.009053	-0.00014	0.012003	-0.0011	-0.00158
0.040266	0.023128	0.016972	0.007238	0.027953	0.017055	0.038519	0.008153	0.051664	0.003744	0.006572	0.002413	0.005158	0.00183	0.004493	0.000416	0.00624	0.006572	0.005408	0.097504	0.002496	0.004742	0.032779	0.01614	0.022296	0.012063
0.037195	0.01	0.009939	0.009634	0.012134	0.005122	0.002073	-0.00128	0.02189	-0.00098	-0.00537	-0.0014	0.000427	-0.00512	-0.00378	-0.00457	0.007012	0.000305	0.003537	0.095366	0.002805	-0.00451	-0.00067	0.006707	0.002012	-0.00695
0.068276	0.013344	0.005607	0.022793	0.013136	0.010748	0.009034	0.001506	0.048131	0.005244	0.000675	0.000312	0.001973	0.001038	0.002285	0.001194	0.010332	0.00893	0.007425	0.080426	0.002077	0.001142	0.009034	0.016407	0.004777	0.002388
0.018494	-0.00033	0.006792	0.00491	0.002537	0.011211	0.010638	-0.00025	0.010065	-0.00065	-0.00188	0.007119	0.004992	0.033142	0.002291	-0.00172	-0.00049	0.008429	0.005155	0.056056	-0.00049	0.020867	0.000982	0.01473	0.036088	0.004092
0.133166	0.003518	-0.0005	-0.00082	0.004962	0.011746	0.009925	-0.0005	0.083103	-0.00226	-0.00063	-0.00138	-0.0032	-0.00069	6.28E-05	-0.00151	0.003706	0.007601	0.000251	0.009359	-0.00151	0.005025	0.00044	0.003141	-0.0022	0.002764
0.083074	0.017575	0.024319	0.004215	0.009533	0.009339	0.042088	0.005383	0.070298	0.001038	0.002853	0.014527	0.009468	0.003891	0.005058	0.001492	0.005577	0.007847	0.007004	0.012711	-0.0011	0.005253	0.028016	0.001946	0.001102	0.007782
0.116549	0.008568	0.011209	0.006984	0.007864	0.008509	-0.0007	-0.00088	0.052406	0.000528	-0.00147	-0.00176	0.005399	0.01162	3.33E-17	0.000528	0.007453	0.00757	0.005751	0.030634	-0.00065	0.006925	0.011444	0.006984	0.000763	0.001526
0.075172	0.01454	0.020632	0.017241	0.015747	0.015977	0.009943	0.006207	0.037874	0.007874	0.003793	0.003218	0.01046	0.011667	0.003046	0.001437	0.011897	0.011264	0.012414	0.05477	0.006667	0.008448	0.008736	0.012414	0.001494	0.002069

Logistic regression model results

split_inde	precision_	recall_clas	f1-score_c	support_c	precision_	recall_clas	f1-score_c	support_c	precision_	recall_wei	f1-score_v	support_v	precision_	recall_ma(	f1-score_r	support_n	accuracy	T_class1	T_class2	F_class1	F_class2
1	0.766284	0.595238	0.670017	336	0.6691	0.818452	0.736278	336	0.717692	0.706845	0.703148	672	0.717692	0.706845	0.703148	672	0.706845	20000	27500	13600	6100
1	0.973684	0.389474	0.556391	95	0.618421	0.989474	0.761134	95	0.796053	0.689474	0.658762	190	0.796053	0.689474	0.658762	190	0.689474	3700	9400	5800	100
1	0.726872	0.891892	0.800971	185	0.86014	0.664865	0.75	185	0.793506	0.778378	0.775485	370	0.793506	0.778378	0.775485	370	0.778378	16500	12300	2000	6200
1	0.791411	0.605634	0.68617	213	0.680608	0.840376	0.752101	213	0.73601	0.723005	0.719136	426	0.73601	0.723005	0.719136	426	0.723005	12900	17900	8400	3400
1	0.878788	0.59589	0.710204	146	0.694301	0.917808	0.79056	146	0.786544	0.756849	0.750382	292	0.786544	0.756849	0.750382	292	0.756849	8700	13400	5900	1200
2	0.814286	0.7125	0.76	80	0.744444	0.8375	0.788235	80	0.779365	0.775	0.774118	160	0.779365	0.775	0.774118	160	0.775	5700	6700	2300	1300
2	0.719368	0.879227	0.791304	207	0.84472	0.657005	0.73913	207	0.782044	0.768116	0.765217	414	0.782044	0.768116	0.765217	414	0.768116	18200	13600	2500	7100
2	0.802632	0.5	0.616162	122	0.636905	0.877049	0.737931	122	0.719768	0.688525	0.677046	244	0.719768	0.688525	0.677046	244	0.688525	6100	10700	6100	1500
2	0.806818	0.569519	0.667712	374	0.667355	0.863636	0.752914	374	0.737087	0.716578	0.710313	748	0.737087	0.716578	0.710313	748	0.716578	21300	32300	16100	5100
2	0.897436	0.546875	0.679612	192	0.674157	0.9375	0.784314	192	0.785797	0.742188	0.731963	384	0.785797	0.742188	0.731963	384	0.742188	10500	18000	8700	1200
3	0.851064	0.666667	0.747664	180	0.726027	0.883333	0.796992	180	0.788546	0.775	0.772328	360	0.788546	0.775	0.772328	360	0.775	12000	15900	6000	2100
3	0.830189	0.654275	0.731809	269	0.714724	0.866171	0.783193	269	0.772456	0.760223	0.757501	538	0.772456	0.760223	0.757501	538	0.760223	17600	23300	9300	3600
3	0.917808	0.59292	0.72043	113	0.699346	0.946903	0.804511	113	0.808577	0.769912	0.762471	226	0.808577	0.769912	0.762471	226	0.769912	6700	10700	4600	600
3	0.7	0.692833	0.696398	293	0.695946	0.703072	0.699491	293	0.697973	0.697952	0.697944	586	0.697973	0.697952	0.697944	586	0.697952	20300	20600	9000	8700
3	0.96	0.4	0.564706	120	0.621053	0.983333	0.76129	120	0.790526	0.691667	0.662998	240	0.790526	0.691667	0.662998	240	0.691667	4800	11800	7200	200
4	0.915493	0.585586	0.714286	111	0.695364	0.945946	0.801527	111	0.805429	0.765766	0.757906	222	0.805429	0.765766	0.757906	222	0.765766	6500	10500	4600	600
4	0.972973	0.553846	0.705882	65	0.688172	0.984615	0.810127	65	0.830573	0.769231	0.758004	130	0.830573	0.769231	0.758004	130	0.769231	3600	6400	2900	100
4	0.772727	0.625767	0.691525	163	0.685567	0.815951	0.745098	163	0.729147	0.720859	0.718312	326	0.729147	0.720859	0.718312	326	0.720859	10200	13300	6100	3000
4	0.717742	0.796421	0.755037	447	0.771357	0.686801	0.726627	447	0.744549	0.741611	0.740832	894	0.744549	0.741611	0.740832	894	0.741611	35600	30700	9100	14000
4	0.869048	0.386243	0.534799	189	0.605442	0.941799	0.73706	189	0.737245	0.664021	0.635929	378	0.737245	0.664021	0.635929	378	0.664021	7300	17800	11600	1100
5	0.9	0.515625	0.655629	384	0.660584	0.942708	0.776824	384	0.780292	0.729167	0.716227	768	0.780292	0.729167	0.716227	768	0.729167	19800	36200	18600	2200
5	0.670588	0.791667	0.726115	72	0.745763	0.611111	0.671756	72	0.708175	0.701389	0.698935	144	0.708175	0.701389	0.698935	144	0.701389	5700	4400	1500	2800
5	0.820408	0.561453	0.666667	358	0.666667	0.877095	0.757539	358	0.743537	0.719274	0.712103	716	0.743537	0.719274	0.712103	716	0.719274	20100	31400	15700	4400
5	0.797297	0.819444	0.808219	72	0.814286	0.791667	0.802817	72	0.805792	0.805556	0.805518	144	0.805792	0.805556	0.805518	144	0.805556	5900	5700	1300	1500
5	0.648352	0.893939	0.751592	66	0.829268	0.515152	0.635514	66	0.73881	0.704545	0.693553	132	0.73881	0.704545	0.693553	132	0.704545	5900	3400	700	3200
6	0.78	0.722222	0.75	108	0.741379	0.796296	0.767857	108	0.76069	0.759259	0.758929	216	0.76069	0.759259	0.758929	216	0.759259	7800	8600	3000	2200
6	0.90625	0.428044	0.581454	271	0.625604	0.95572	0.756204	271	0.765927	0.691882	0.668829	542	0.765927	0.691882	0.668829	542	0.691882	11600	25900	15500	1200
6	0.667582	0.864769	0.753488	281	0.808081	0.569395	0.668058	281	0.737832	0.717082	0.710773	562	0.737832	0.717082	0.710773	562	0.717082	24300	16000	3800	12100
6	0.943396	0.578035	0.716846	173	0.695833	0.965318	0.808717	173	0.819615	0.771676	0.762781	346	0.819615	0.771676	0.762781	346	0.771676	10000	16700	7300	600
6	0.896552	0.549296	0.681223	142	0.675127	0.93662	0.784661	142	0.785839	0.742958	0.732942	284	0.785839	0.742958	0.732942	284	0.742958	7800	13300	6400	900
7	0.687747	0.892308	0.776786	195	0.846715	0.594872	0.698795	195	0.767231	0.74359	0.73779	390	0.767231	0.74359	0.73779	390	0.74359	17400	11600	2100	7900
7	0.906667	0.552846	0.686869	246	0.678363	0.943089	0.789116	246	0.792515	0.747967	0.737992	492	0.792515	0.747967	0.737992	492	0.747967	13600	23200	11000	1400
7	0.785714	0.54321	0.642336	162	0.650943	0.851852	0.737968	162	0.718329	0.697531	0.690152	324	0.718329	0.697531	0.690152	324	0.697531	8800	13800	7400	2400
7	0.666667	0.444444	0.533333	9	0.583333	0.777778	0.666667	9	0.625	0.611111	0.6	18	0.625	0.611111	0.6	18	0.611111	400	700	500	200
7	0.816901	0.479339	0.604167	363	0.631579	0.892562	0.739726	363	0.72424	0.68595	0.671946	726	0.72424	0.68595	0.671946	726	0.68595	17400	32400	18900	3900
8	0.959184	0.398305	0.562874	118	0.620321	0.983051	0.760656	118	0.789752	0.690678	0.661765	236	0.789752	0.690678	0.661765	236	0.690678	4700	11600	7100	200
8	0	0	0	5	0.5	1	0.666667	5	0.25	0.5	0.333333	10	0.25	0.5	0.333333	10	0.5	0	500	500	0
8	0.820652	0.604	0.695853	250	0.686709	0.868	0.766784	250	0.753681	0.736	0.731318	500	0.753681	0.736	0.731318	500	0.736	15100	21700	9900	3300
8	0.87	0.669231	0.756522	130	0.73125	0.9	0.806897	130	0.800625	0.784615	0.781709	260	0.800625	0.784615	0.781709	260	0.784615	8700	11700	4300	1300
8	0.720322	0.758475	0.738906	472	0.744966	0.705508	0.724701	472	0.732644	0.731992	0.731803	944	0.732644	0.731992	0.731803	944	0.731992	35800	33300	11400	13900
9	0.869565	0.531915	0.660066	188	0.662835	0.920213	0.770601	188	0.7662	0.726064	0.715334	376	0.7662	0.726064	0.715334	376	0.726064	10000	17300	8800	1500
9	0.788462	0.5	0.61194	246	0.633929	0.865854	0.731959	246	0.711195	0.682927	0.67195	492	0.711195	0.682927	0.67195	492	0.682927	12300	21300	12300	3300
9	0.709906	0.804813	0.754386	374	0.774691	0.671123	0.719198	374	0.742299	0.737968	0.736792	748	0.742299	0.737968	0.736792	748	0.737968	30100	25100	7300	12300
9	0.914286	0.619355	0.738462	155	0.712195	0.941935	0.811111	155	0.81324	0.780645	0.774786	310	0.81324	0.780645	0.774786	310	0.780645	9600	14600	5900	900
9	1	0.166667	0.285714	12	0.545455	1	0.705882	12	0.772727	0.583333	0.495798	24	0.772727	0.583333	0.495798	24	0.583333	200	1200	1000	0
10	0.846154	0.483516	0.615385	364	0.638462	0.912088	0.751131	364	0.742308	0.697802	0.683258	728	0.742308	0.697802	0.683258	728	0.697802	17600	33200	18800	3200
10	0.785185	0.592179	0.675159	179	0.672646	0.837989	0.746269	179	0.728915	0.715084	0.710714	358	0.728915	0.715084	0.710714	358	0.715084	10600	15000	7300	2900
10	0.728745	0.882353	0.798226	204	0.850932	0.671569	0.750685	204	0.789838	0.776961	0.774456	408	0.789838	0.776961	0.774456	408	0.776961	18000	13700	2400	6700
10	0.895522	0.487805	0.631579	123	0.648045	0.943089	0.768212	123	0.771784	0.715447	0.699895	246	0.771784	0.715447	0.699895	246	0.715447	6000	11600	6300	700
10	0.864198	0.666667	0.752688	105	0.728682	0.895238	0.803419	105	0.79644	0.780952	0.778053	210	0.79644	0.780952	0.778053	210	0.780952	7000	9400	3500	1100

Appendix A

Appendix B: extra materials not included in thesis

8.1 GT-40 Survey

The handheld GT-40 spectrometer is an instrument designed for the measurement of radioactive elements (^{40}K, ^{238}U and ^{232}Th). The spectrometer is based in a two-inch BGO ($Bi_4Ge_3O_{12}$) detector allowing accurate measurements on flat surfaces with at least one meter diameter (Skupio et al., 2018). The GT-40 has a five-minute measurement time and contains an inbuilt calibration system in accordance with EU standards.

The June 2021 field survey involved collecting GT-40 samples at the same locations where the soil-gas radon, soil permeability and physical soil samples were collected. A total of 60 samples were collected, 19 samples were extra and 41 were used for analysis.

Table 8.1.1 Pearson r correlation of GT-40 results and Log10 goil-gas radon.

Pearson correlation	log10RnConc	Log10U	Radon_Pote	U	Dose.rate	Th	K	Th/U
log10RnConc	1	0.67	0.63	0.57	0.44	-0.23	-0.29	-0.7
Log10U	0.67	1	0.8	0.89	0.85	0.17	0.11	-0.65
Radon_Pote	0.63	0.8	1	0.95	0.9	0.21	0.12	-0.43
U	0.57	0.89	0.95	1	0.96	0.26	0.17	-0.45
Dose.rate	0.44	0.85	0.9	0.96	1	0.5	0.42	-0.25
Th	-0.23	0.17	0.21	0.26	0.5	1	0.92	0.59
K	-0.29	0.11	0.12	0.17	0.42	0.92	1	0.59
Th/U	-0.7	-0.65	-0.43	-0.45	-0.25	0.59	0.59	1

Appendix B

Table 8.1.2 ANOVA table for GT-40 results vs bedrock geology and Quaternary geology categories

Anova eta	Bedrock geology (1: 100k)		Quaternary (1: 500 k)	
	(Pr >f)	Effect size	(Pr >f)	Effect size
Log10U	0.0113	0.33	0.0166	0.19
U	0.159	0.2	0.184	0.09
Th	0.0292	0.29	0.0443	0.15
Th/U	0.00131	0.42	0.0234	0.18
K	0.0722	0.24	0.21	0.08

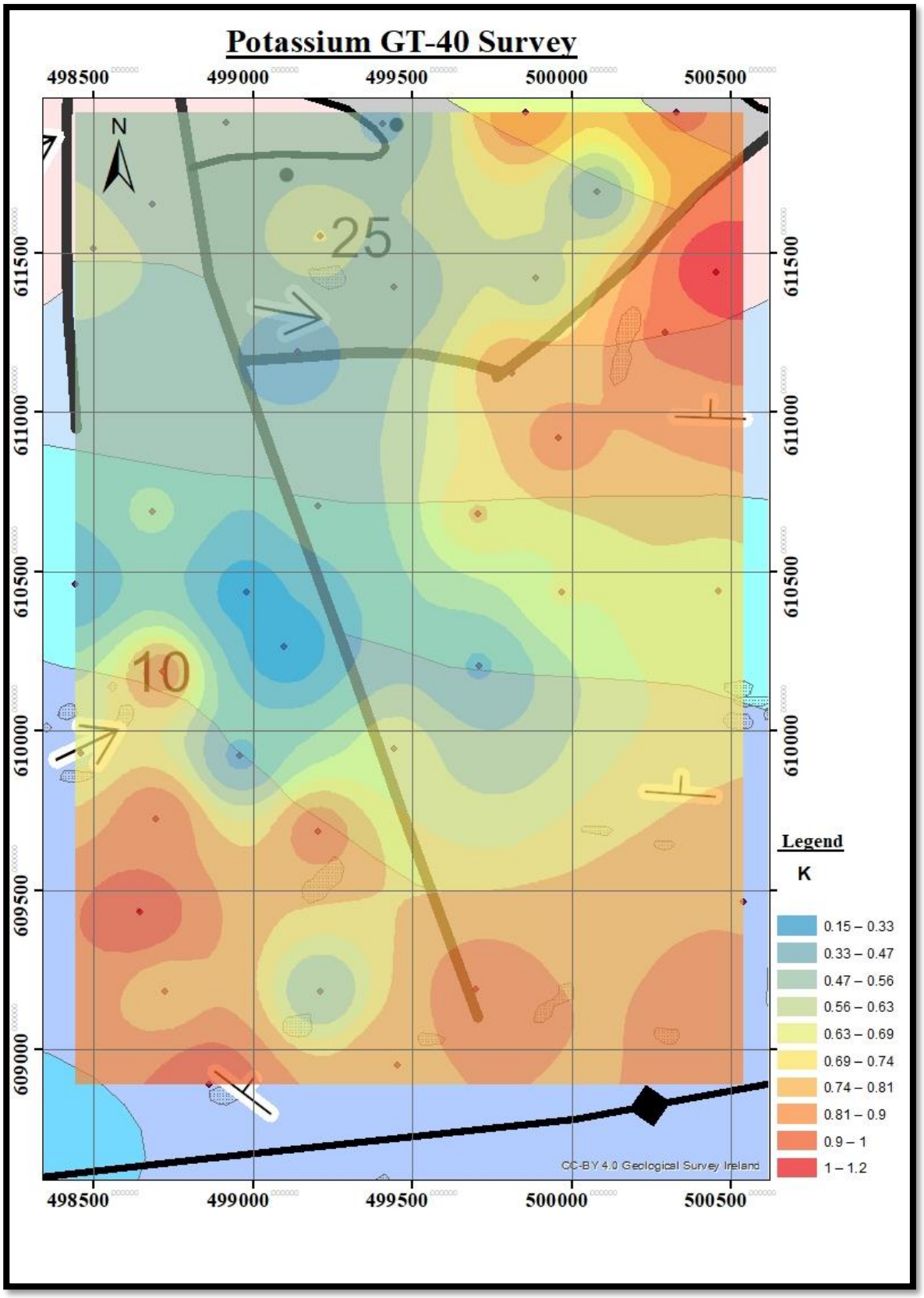

Figure 8.1.1 Ordinary kriging of GT-40 K results. Produced using ARC-GIS inverse distance weighted function.

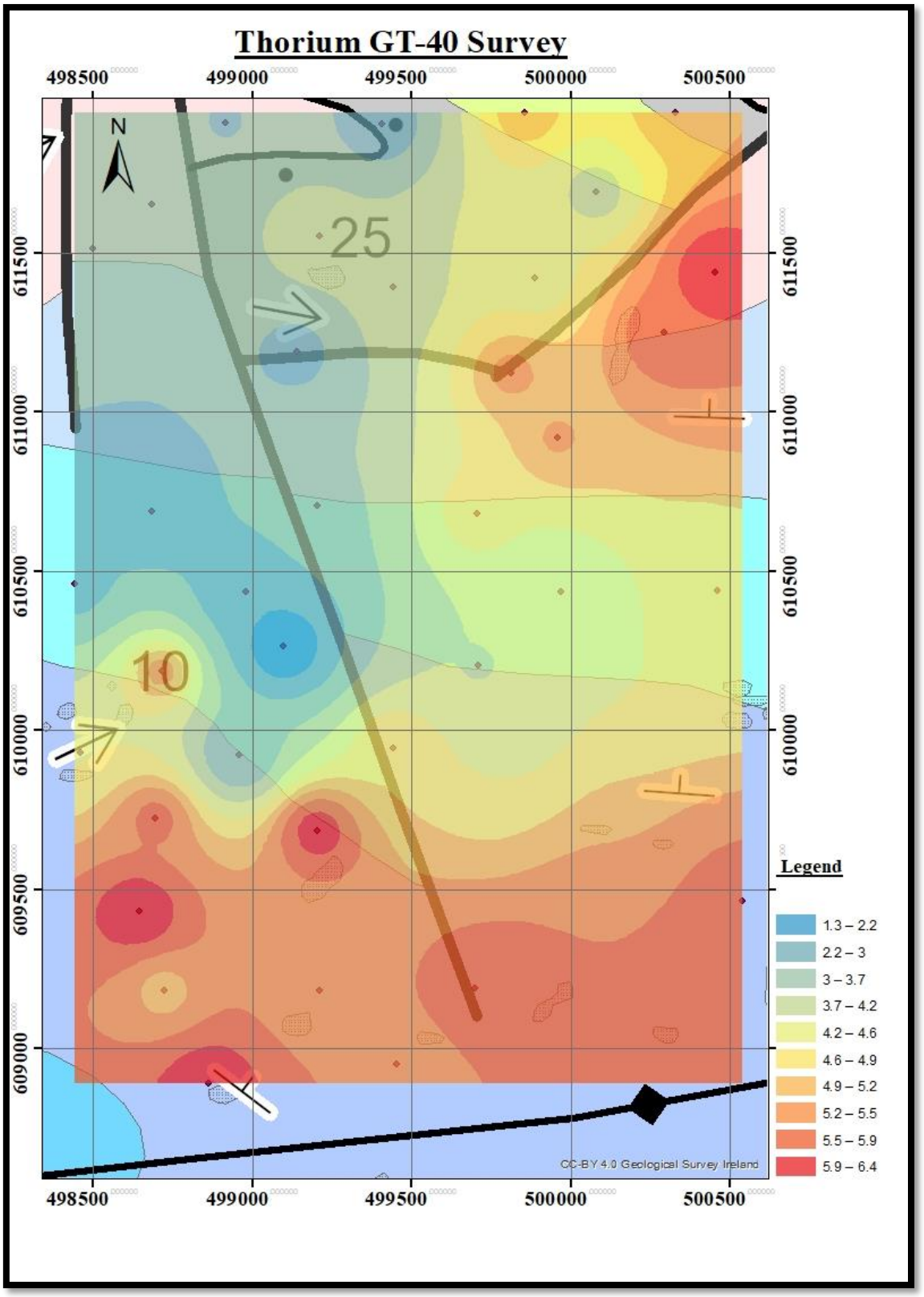

Figure 8.1.2 Ordinary kriging of GT-40 Th results. Produced using ARC-GIS inverse distance weighted function.

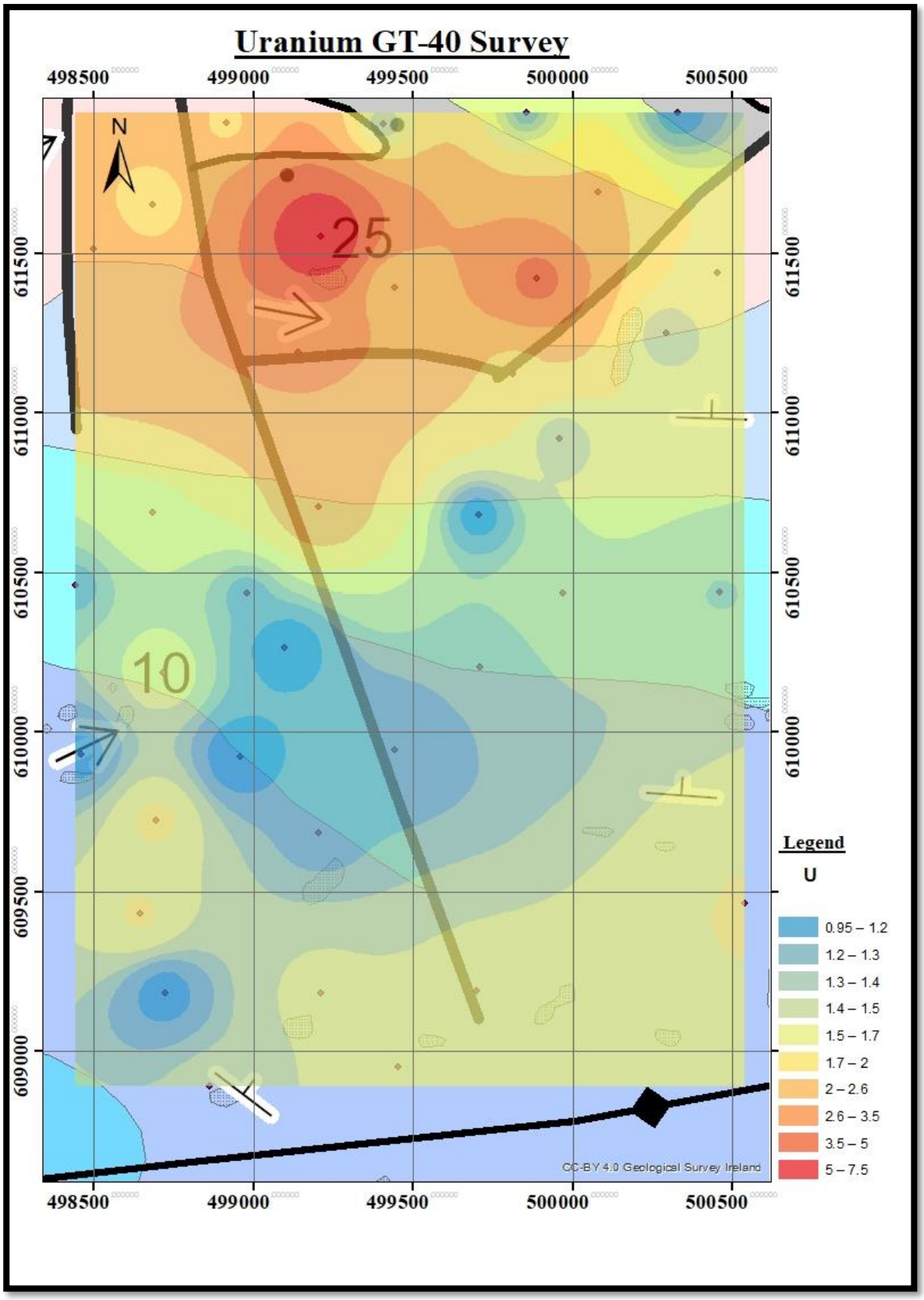

Figure 8.1.3 Ordinary kriging of GT-40 U results. Produced using ARC-GIS inverse distance weighted function.

Appendix B

Overall, the preliminary results showed that there was potential for gamma ray surveys to be an alternative for mapping geogenic radon. However, local scale data comes with the disadvantage of not being relevant to other geological areas. As such, the approach of utilizing regional scale data as outlined in chapter 5 was deemed higher impact. Explicitly, the geogenic radon modelling community would benefit more from the results presented in chapter 5 opposed to data limited to local scales. Especially considering that the research presented in chapter 4 already validated the use of local scale data for mapping radon. As such, we decided the best approach was to utilize the freely available TELLUS midlands data to reiterate the method and approach of using topsoil geochemistry to model radon.

8.2 Topsoil major oxides XRF

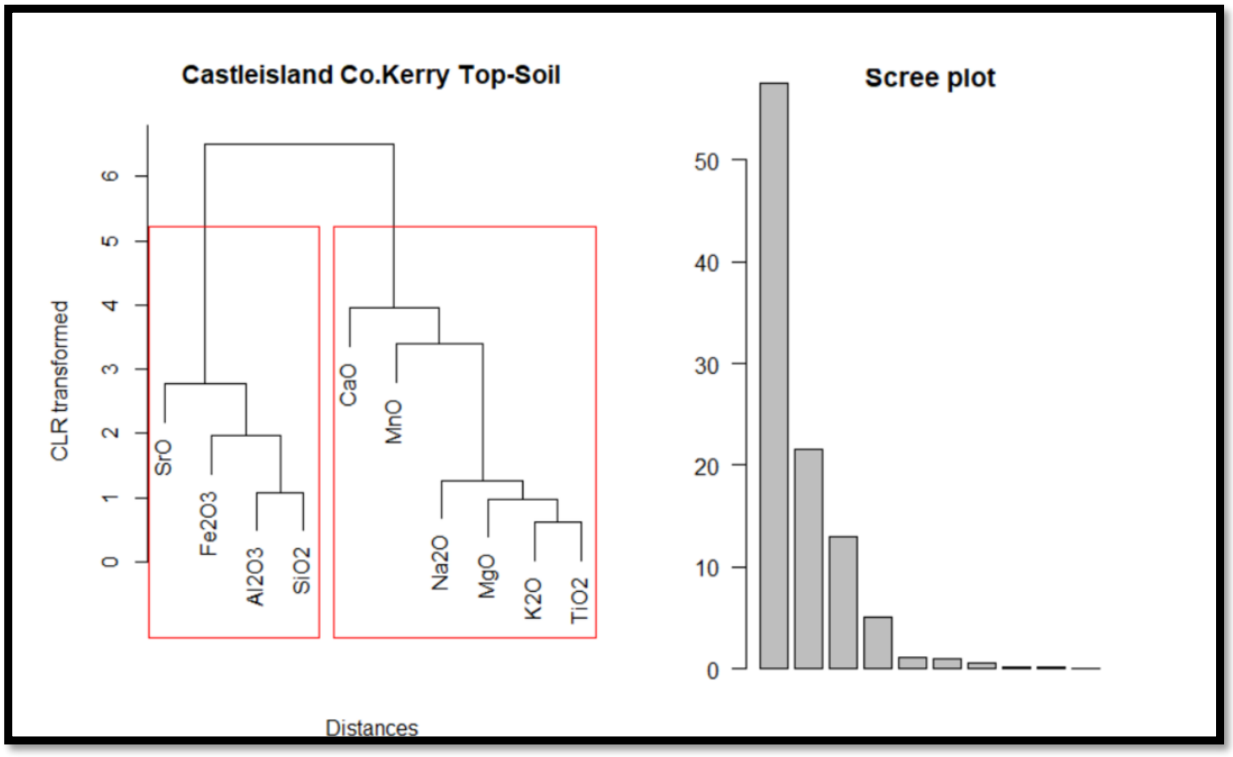

Figure 8.2.1 (left) cluster analysisamd (right) scree plot of major oxides clr transformed measured by XRF in Castleisland Co. Kerry.

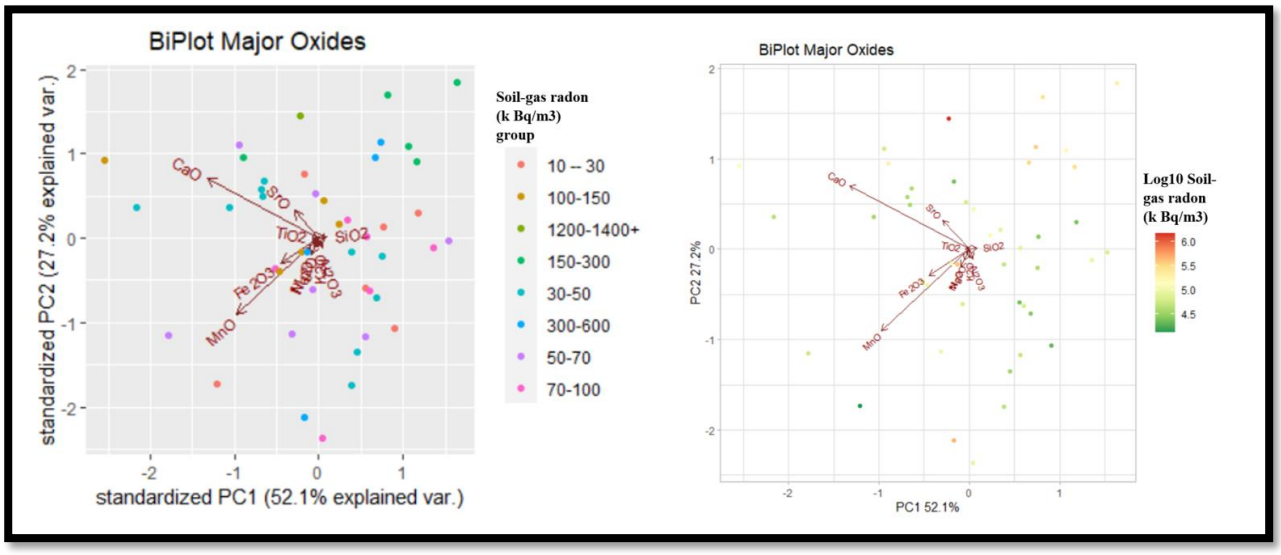

Figure 8.2.2 PC1 vs PC2 biplots of major oxides (clr transformed shallow topsoil Castleisland co. Kerry samples) with scores plotted as (left) soil-gas radon categorey and (right) log_{10} soil-gas radon (k Bq m^{-3}).

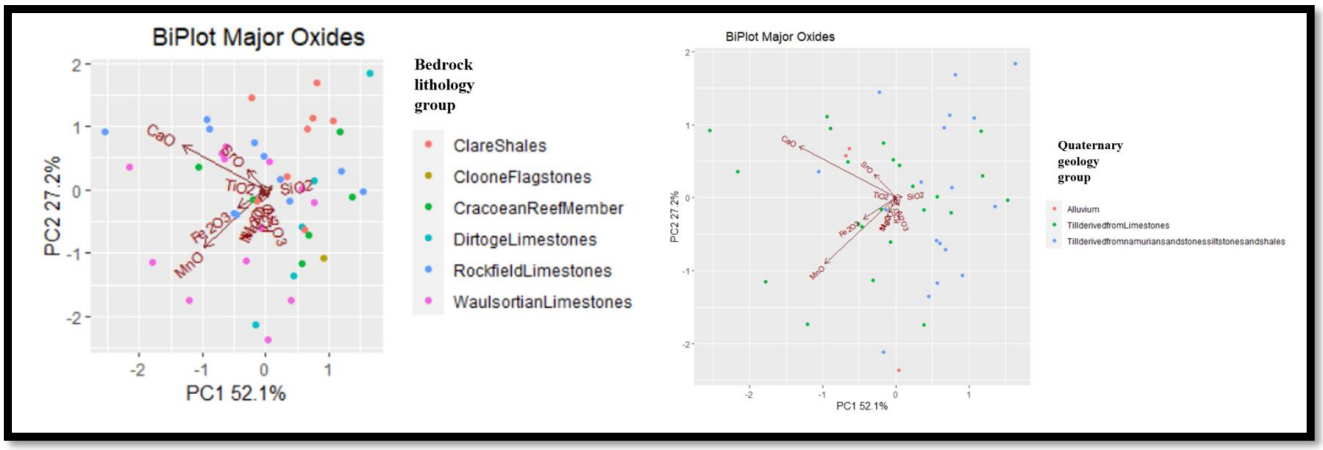

Figure 8.2.3 PC1 vs PC2 biplots of major oxides (clr transformed shallow topsoil Castleisland Co. Kerry samples) with scores plotted as (left) bedrock lithology group and (right) Quaternary geology type.

Table 8.2.1 Principle component loadings for first three PC's of clr transformed major oxides sampled from Castleisland, Co. Kerry.

Loadings	PC1	PC2	PC3
Na2O	-0.03091	-0.0966	**0.540248**
MgO	-0.05295	-0.15283	0.222787
Al2O3	**0.021056**	-0.08942	0.297035
SiO2	**0.051583**	0.010431	-0.10329
K2O	-6.23E-05	-0.07262	**0.320802**
CaO	-0.764	**0.561426**	0.07187
TiO2	-0.02661	0.006299	0.255055
MnO	-0.56013	-0.71953	-0.34473
Fe2O3	-0.25766	-0.23294	**0.497044**
SrO	-0.16912	**0.258296**	-0.14344
Standard deviation	0.523477	0.378597	0.237515
Proportion of Variance	0.52058	0.2723	0.10717
Cumulative Proportion	0.52058	0.79287	0.90004

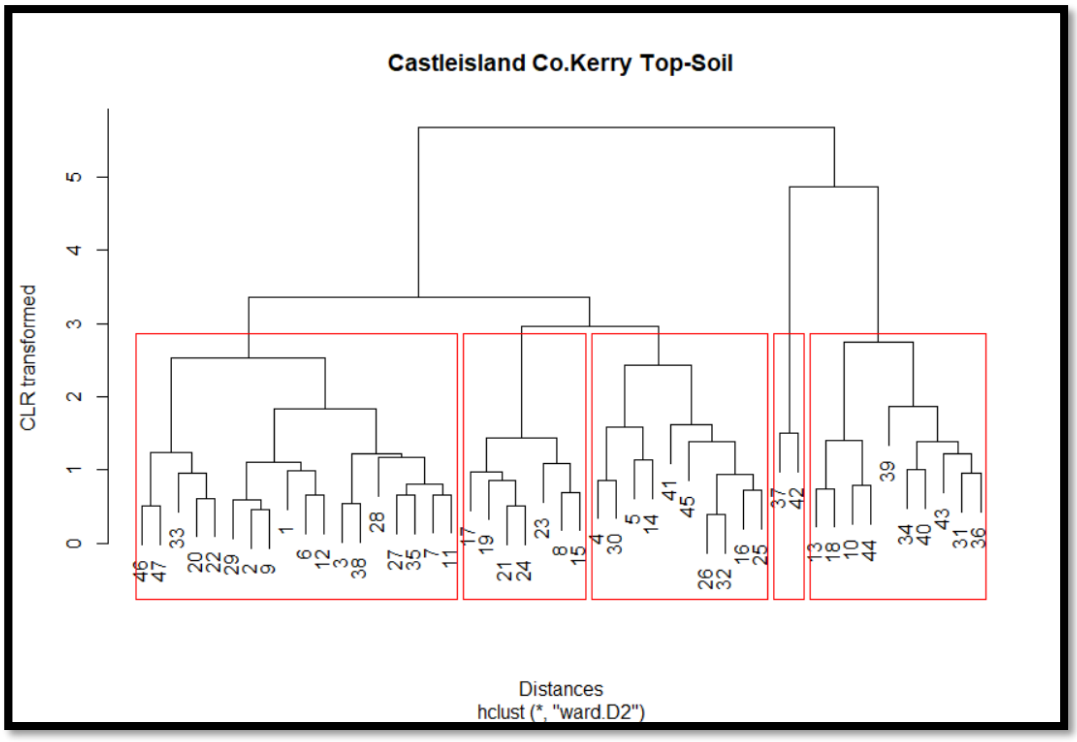

Figure 8.2.4 Cluster analysis of soil sample locations from Castleisland Co. Kerry.

Table 8.2.2 Index for cluster analysis results in figure above.

Index number	X. ITM	Y. ITM	sample	log10Rn Conc	Soil permeability	Rp class	Bedrock lithology	Quaternary Geology
34	499139	611189	004AL21	5.428135	Low	35+	ClareShales	Tillderivedfrom namuriansandstonessiltstonesandshales
36	499441	611393	S203AL59A	4.908485	Medium	35+	ClareShales	Tillderivedfrom namuriansandstonessiltstonesandshales
37	499886	611419	03AL60	5.594393	V.Low	35+	ClareShales	Tillderivedfromnamuriansandstonessiltstonesandshales

40	499208	611551	L70A010A	5.49693	ModeratelyLow	35+	ClareShales	TillderivedfromnamuriansandstonessiltstonesandshalesTillderivedfromnamuriansandstonessiltstonesandshales
42	499726	611673	002AL71A	6.156246	High	35+	ClareShales	TillderivedfromnamuriansandstonessiltstonesandshalesTillderivedfromnamuriansandstonessiltstonesandshales
43	500077	611689	L72AS213A	5.20412	Medium	35+	ClareShales	TillderivedfromnamuriansandstonessiltstonesandshalesTillderivedfromnamuriansandstonessiltstonesandshales
44	499405	611904	009AL66	5.545307	Low	35+	ClareShales	TillderivedfromnamuriansandstonessiltstonesandshalesTillderivedfromnamuriansandstonessiltstonesandshales
47	500327	611939	L68AS214A	4.799341	Low	22.5-35	ClareShales	TillderivedfromnamuriansandstonessiltstonesandshalesTillderivedfromnamuriansandstonessiltstonesandshales
46	499852	611939	L67AS221A	4.30103	Medium	22.5-35	ClooneFlagstones	TillderivedfromnamuriansandstonessiltstonesandshalesTillderivedfromnamuriansandstonessiltstonesandshales
27	500136	610766	L16AS237A	4.70757	Medium	35+	CracoeanReefMember	TillderivedfromnamuriansandstonessiltstonesandshalesTillderivedfromnamuriansandstonessiltstonesandshales
28	499956	610918	001AL53	4.414973	Medium	22.5-35	CracoeanReefMember	TillderivedfromnamuriansandstonessiltstonesandshalesTillderivedfromnamuriansandstonessiltstonesandshales
29	500481	610939	L54AS205A	4.80618	Medium	35+	CracoeanReefMember	TillderivedfromnamuriansandstonessiltstonesandshalesTillderivedfromnamuriansandstonessiltstonesandshales
30	499579	610965	L52AS207A	4.531479	ModeratelyLow	22.5-35	CracoeanReefMember	TillderivedfromnamuriansandstonessiltstonesandshalesTillderivedfromnamuriansandstonessiltstonesandshales
31	498874	610968	L20005A	5.469822	V.Low	35+	CracoeanReefMember	TillderivedfromLimestones
32	499039	610999	L51AS228A	5.170262	Low	35+	CracoeanReefMember	TillderivedfromLimestones
33	499811	611122	L22AS207A	4.944483	Medium	35+	CracoeanReefMember	TillderivedfromnamuriansandstonessiltstonesandshalesTillderivedfromnamuriansandstonessiltstonesandshales

35	500291	611248	L23AS206A	4.531479	Medium	22.5-35	DirtogeLimestones	Tillderivedfromnamuriansandstonessiltstonesandshales
38	500452	611439	L61A	4.431364	Medium	22.5-35	DirtogeLimestones	Tillderivedfromnamuriansandstonessiltstonesandshales
39	498498	611514	L57AS201A	5.320146	Low	35+	DirtogeLimestones	Tillderivedfromnamuriansandstonessiltstonesandshales
41	498681	611653	L69AS227A	5.673942	High	35+	DirtogeLimestones	Tillderivedfromnamuriansandstonessiltstonesandshales
45	498915	611909	L65AS202	4.361728	Medium	22.5-35	DirtogeLimestones	Tillderivedfromnamuriansandstonessiltstonesandshales
16	498714	610184	008AL9	4.880814	Medium	35+	RockfieldLimestones	TillderivedfromLimestones
17	499706	610203	L11AS230A	5.100371	V.Low	35+	RockfieldLimestones	TillderivedfromLimestones
18	499095	610262	L10AS232A	5.117271	Low	35+	RockfieldLimestones	TillderivedfromLimestones
19	498979	610434	L46A06A	5.283301	V.Low	35+	RockfieldLimestones	TillderivedfromLimestones
20	499967	610434	L48AS211A	4.826075	Low	22.5-35	RockfieldLimestones	TillderivedfromLimestones
21	499445	610436	S209L47A	4.361728	Low	10-22.5	RockfieldLimestones	TillderivedfromLimestones
22	500457	610437	S212AL49A	4.380211	ModeratelyLow	22.5-35	RockfieldLimestones	TillderivedfromLimestones
23	498441	610459	S233AL45A	4.755875	Medium	35+	RockfieldLimestones	TillderivedfromLimestones

24	499702	610679	L15AS210A	4.778151	V.Low	22.5-35	RockfieldLimestones	TillderivedfromLimestones
25	498681	610686	L13AS229A	4.690196	Medium	35+	RockfieldLimestones	TillderivedfromLimestones
26	499201	610705	007AL14A	5.017033	Medium	35+	RockfieldLimestones	TillderivedfromLimestones
1	498861	608891	L31AS223A	4.643453	Medium	35+	WaulsortianLimestones	TillderivedfromLimestones
2	499452	608950	L32AS222A	4.792392	Low	22.5-35	WaulsortianLimestones	TillderivedfromLimestones
3	498720	609181	L1AS225A	4.579784	Low	22.5-35	WaulsortianLimestones	TillderivedfromLimestones
4	499209	609183	L2AS219A	4.579784	Medium	22.5-35	WaulsortianLimestones	Alluvium
5	499697	609188	L3AS218A	4.724276	Medium	35+	WaulsortianLimestones	TillderivedfromLimestones
6	498643	609431	L36AS236A	4.934498	Medium	35+	WaulsortianLimestones	Alluvium
7	500218	609463	L4aS217A	4.886491	Low	22.5-35	WaulsortianLimestones	TillderivedfromLimestones
8	500537	609463	L34AS215A	4.556303	ModeratelyLow	22.5-35	WaulsortianLimestones	TillderivedfromLimestones
9	500537	609464	L39AS220A	4.977724	ModeratelyLow	22.5-35	WaulsortianLimestones	TillderivedfromLimestones
10	499203	609685	L6AS239A	4.60206	Medium	22.5-35	WaulsortianLimestones	Alluvium

11	**499 203**	**609 685**	**S239A L6A**	**4.60206**	**Medium**	**22.5 -35**	**WaulsortianLimestones**	**Alluvium**
12	**498 694**	**609 723**	**L51AS 235**	**4.875061**	**Medium**	**35+**	**WaulsortianLimestones**	**Alluvium**
13	**498 957**	**609 921**	**L41AS 238A**	**4.623249**	**Medium**	**22.5 -35**	**WaulsortianLimestones**	**TillderivedfromLimestones**
14	**498 457**	**609 929**	**L40AS 234A**	**4.113943**	**Medium**	**22.5 -35**	**WaulsortianLimestones**	**TillderivedfromLimestones**
15	**499 439**	**609 942**	**L42AS 231A**	**5.045323**	**Medium**	**35+**	**WaulsortianLimestones**	**TillderivedfromLimestones**

8.3 Topsoil factor scores Castleisland geochemistry (clr) ICPMS

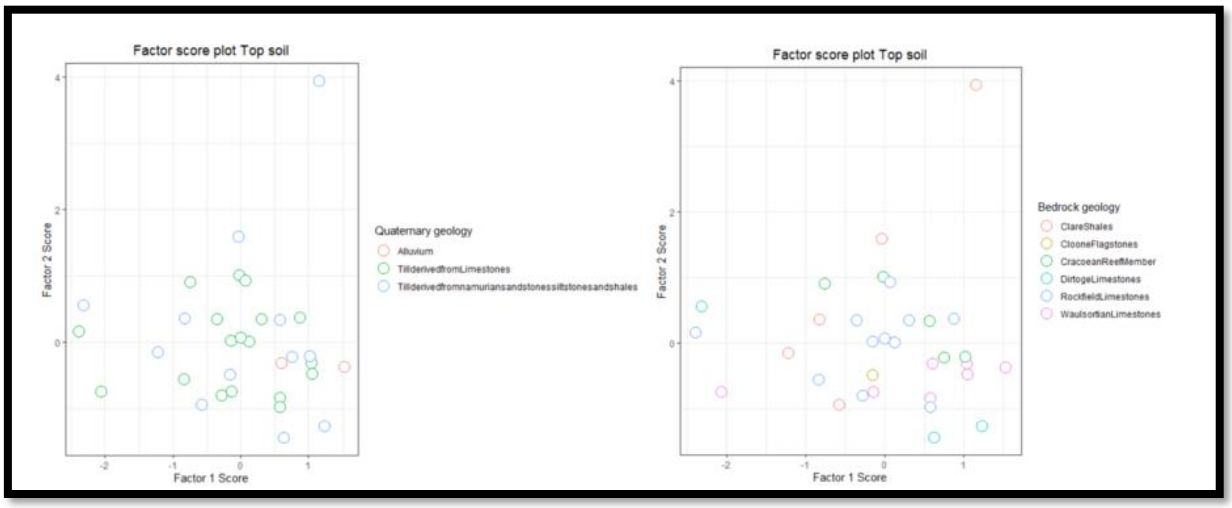

Figure 8.3.1 Factor score plot of clr transformed ICPMS results from Castleisland Co. Kerry shallow topsoil.

Table 8.3.1 Factor score results from clr transformed ICPMS results from Castleisland Co. Kerry shallow topsoil.

Rotated loadings	Factor1	Factor2	Factor3	Factor4	Factor5	communality
Mo	0.047707	-0.03325	0.499354	-0.18916	0.779711	0.876758
Cu	0.21675	-0.09229	0.744391	0.231771	-0.10536	0.754274
Pb	0.096408	0.101355	0.147293	0.446435	-0.13622	0.276964
Zn	0.898543	0.011209	0.265763	-0.06624	0.078407	0.94488
Ni	1.0241	-0.07348	-0.00319	0.053636	-0.07135	0.957866
Co	1.042259	-0.10816	-0.13595	0.096394	-0.01537	0.985169
Mn	0.965875	-0.30213	0.019492	-0.1867	0.171136	0.774746
Fe	0.610802	0.25472	-0.2585	-0.0052	0.413156	0.924843
As	0.497189	0.150892	0.047992	0.068884	0.568571	0.841816
U	-0.07287	-0.0836	0.338511	0.607306	0.113206	0.665529
Th	0.426074	0.50066	-0.00171	-0.33816	0.047258	0.820879

Sr	**-0.13242**	**-0.20063**	**0.930051**	**0.00408**	**-0.00704**	**0.913577**
Sb	**0.014419**	**-0.17766**	**0.691813**	**0.003882**	**0.19987**	**0.553551**
V	**-0.34263**	**0.205231**	**0.800596**	**0.12337**	**0.265713**	**0.875746**
Ca	**0.460951**	**-0.77907**	**0.127683**	**0.163419**	**-0.10053**	**0.523753**
P	**0.091404**	**-0.18904**	**0.713601**	**0.221536**	**0.216175**	**0.772987**
La	**-0.0107**	**0.425556**	**0.824309**	**-0.26171**	**-0.10511**	**0.852828**
Cr	**0.417319**	**0.59602**	**0.106869**	**0.308438**	**0.02673**	**0.923358**
Mg	**0.792151**	**0.221215**	**-0.20264**	**-0.09812**	**-0.0148**	**0.897663**
Ba	**0.059519**	**0.5805**	**0.568592**	**0.205217**	**-0.0122**	**0.829999**
Al	**0.225325**	**0.867371**	**-0.11093**	**0.158948**	**-0.00581**	**0.995**
Na	**0.219346**	**0.652113**	**0.053984**	**-0.08091**	**-0.20387**	**0.643669**
K	**0.109753**	**0.692646**	**0.240777**	**-0.54429**	**-0.03045**	**0.96041**
Hg	**0.017703**	**-0.21018**	**0.04252**	**0.677688**	**-0.1985**	**0.565877**
Sc	**0.618663**	**0.450225**	**-0.19746**	**0.036903**	**-0.0608**	**0.880793**
Ga	**-0.13159**	**0.986779**	**-0.10654**	**-0.08366**	**0.093876**	**0.909045**
port var	**0.247**	**0.193**	**0.184**	**0.074**	**0.056**	
cumul var	**0.247**	**0.44**	**0.624**	**0.699**	**0.755**	

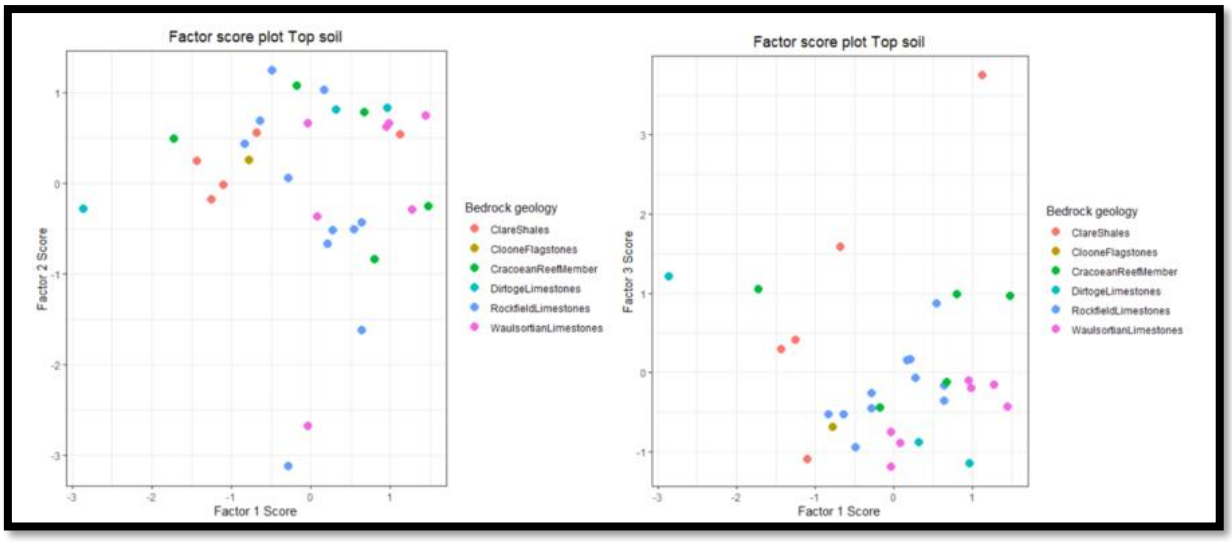

Figure 8.3.2 Factor score plots for ICPMS clr transformed shallow topsoil samples collected from Castleisland Co. Kerry. (Left) Factor score 1 vs factor score 2, (right) factor 1 vs factor 3 grouped according to bedrock geology type.

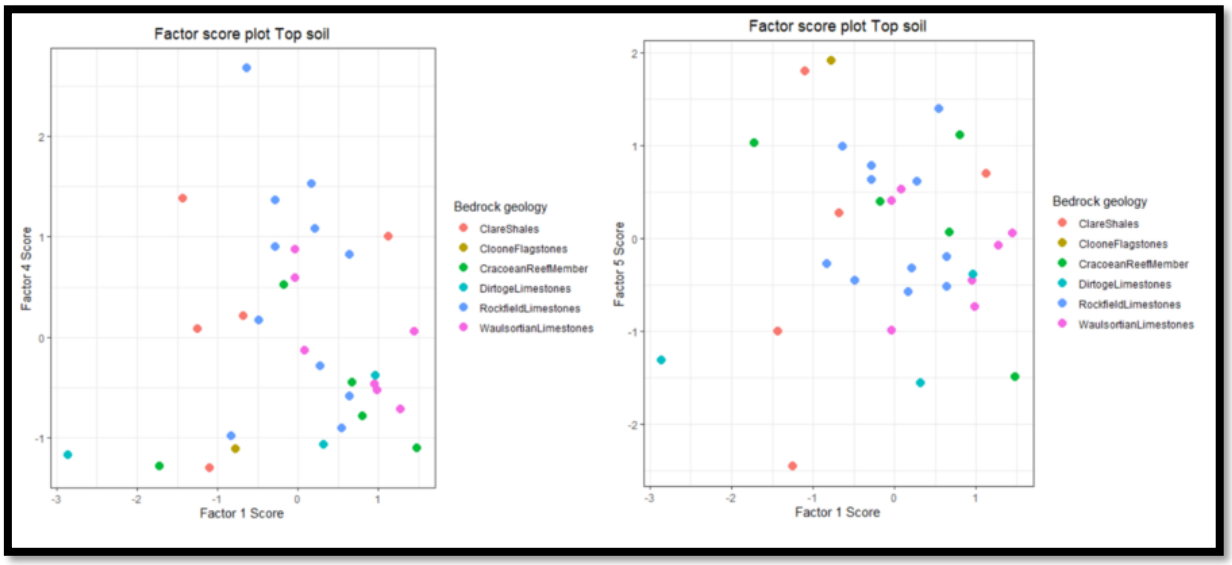

Figure 8.3.3 Factor score plots for ICPMS clr transformed shallow topsoil samples collected from Castleisland Co. Kerry. (Left) Factor score 1 vs factor score 4, (right) factor 1 vs factor 5 grouped according to bedrock geology type.

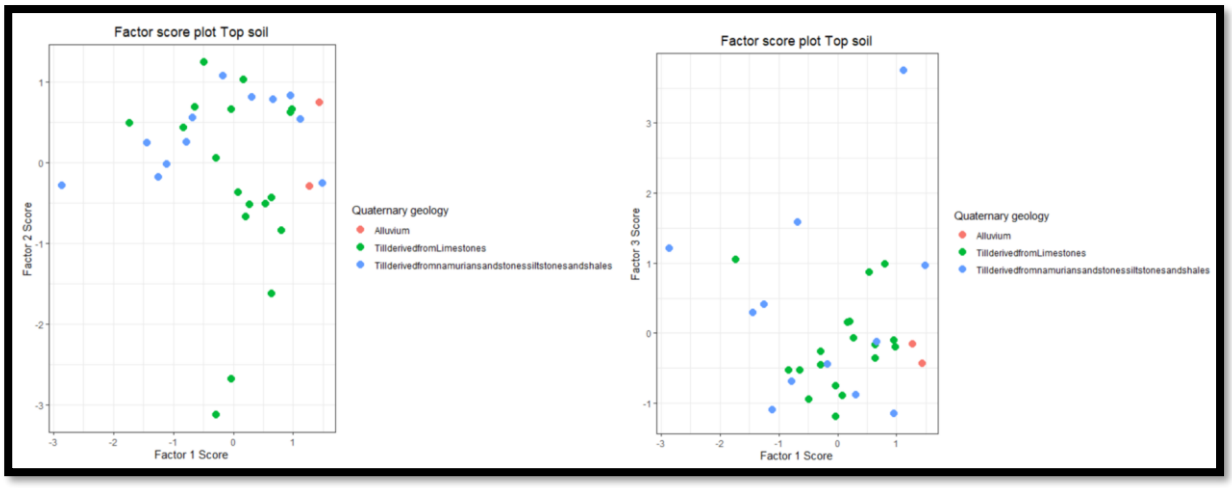

Figure 8.3.4 Factor score plots for ICPMS clr transformed shallow topsoil samples collected from Castleisland Co. Kerry. (Left) Factor score 1 vs factor score 2, (right) factor 1 vs factor 3 grouped according to Quaternary geology type.

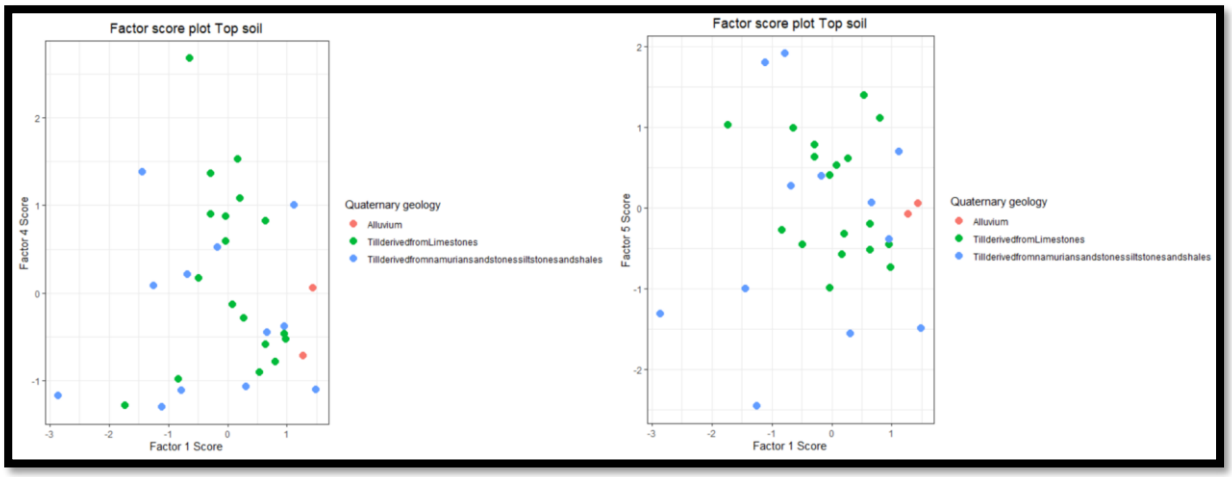

Figure 8.3.5 Factor score plots for ICPMS clr transformed shallow topsoil samples collected from Castleisland Co. Kerry. (Left) Factor score 1 vs factor score 4, (right) factor 1 vs factor 5 grouped according to Quaternary geology type.

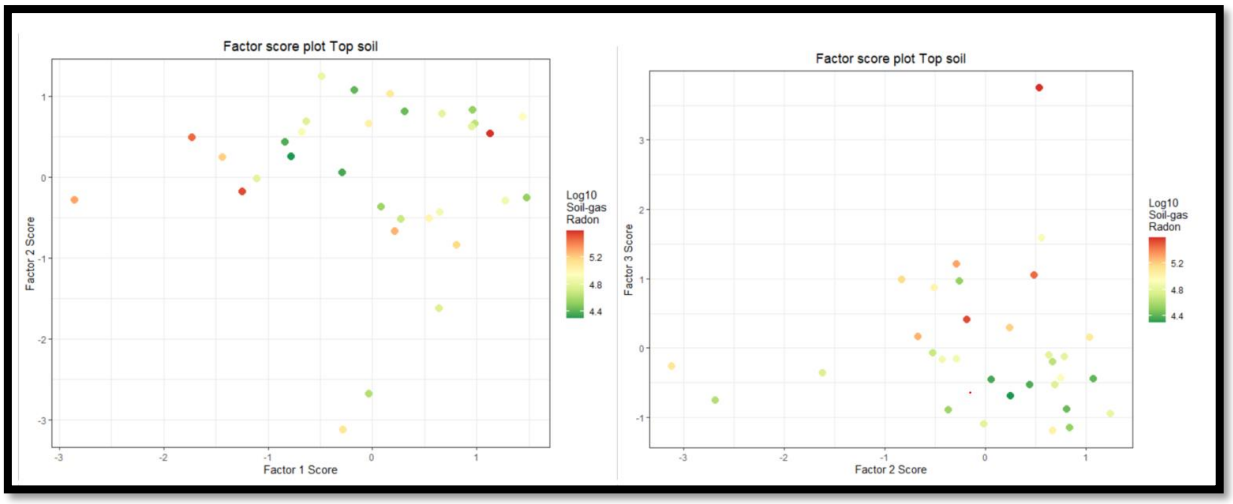

Figure 8.3.6 Factor score plots for ICPMS clr transformed shallow topsoil samples collected from Castleisland Co. Kerry. (Left) Factor score 1 vs factor score 2, (right) factor 2 vs factor 3 grouped according to log10 soil-gas radon.

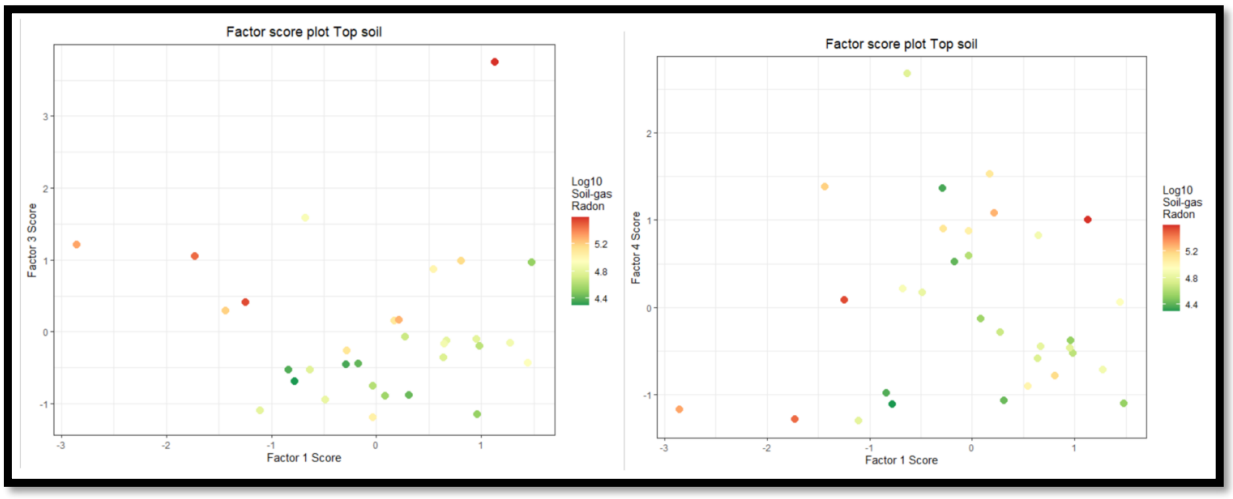

Figure 8.3.7 Factor score plots for ICPMS clr transformed shallow topsoil samples collected from Castleisland Co. Kerry. (Left) Factor score 1 vs factor score 3, (right) factor 1 vs factor 4 grouped according to log10 soil-gas radon concentration.

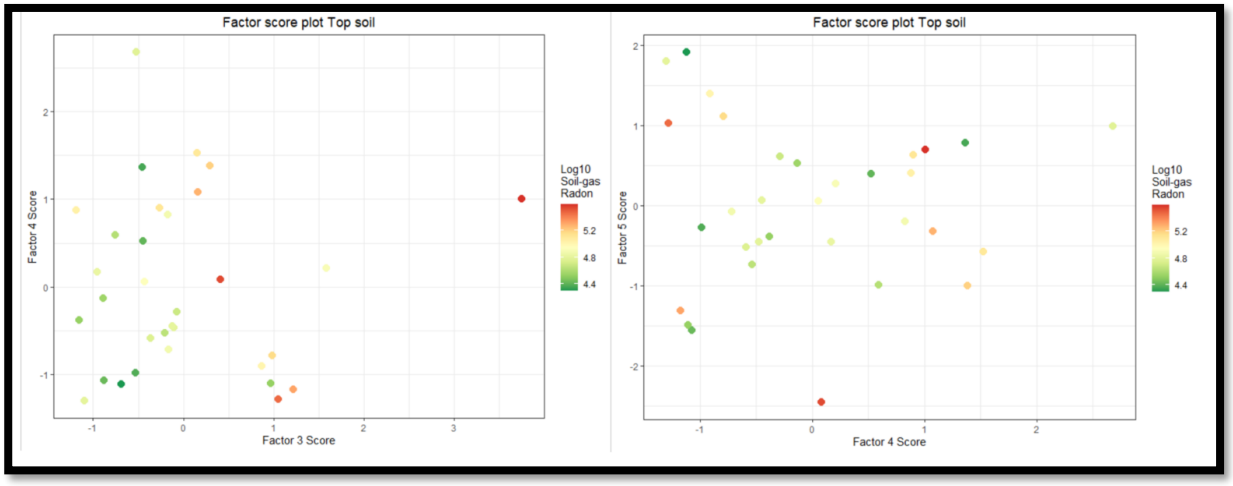

Figure 8.3.8 Factor score plots for ICPMS clr transformed shallow topsoil samples collected from Castleisland Co. Kerry. (Left) Factor score 3 vs factor score 4, (right) factor 4 vs factor 5 grouped according to log10 soil-gas radon concentration.

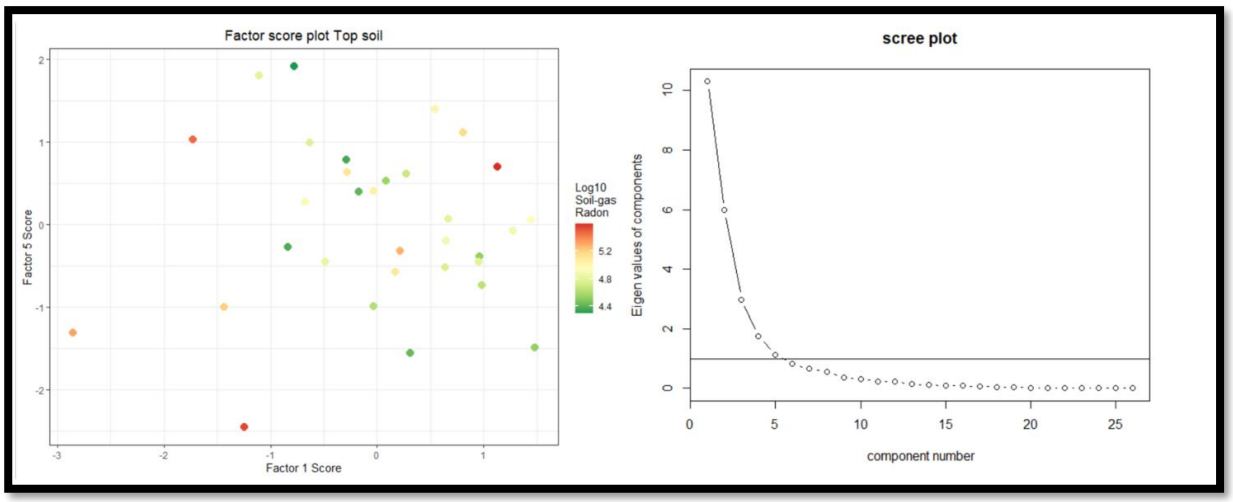

Figure 8.3.8 Factor score plots for ICPMS clr transformed shallow topsoil samples collected from Castleisland Co. Kerry. (Left) Factor score 1 vs factor score 5 grouped according to log10 soil-gas radon concentration, (right) scree plot from factor analysis.

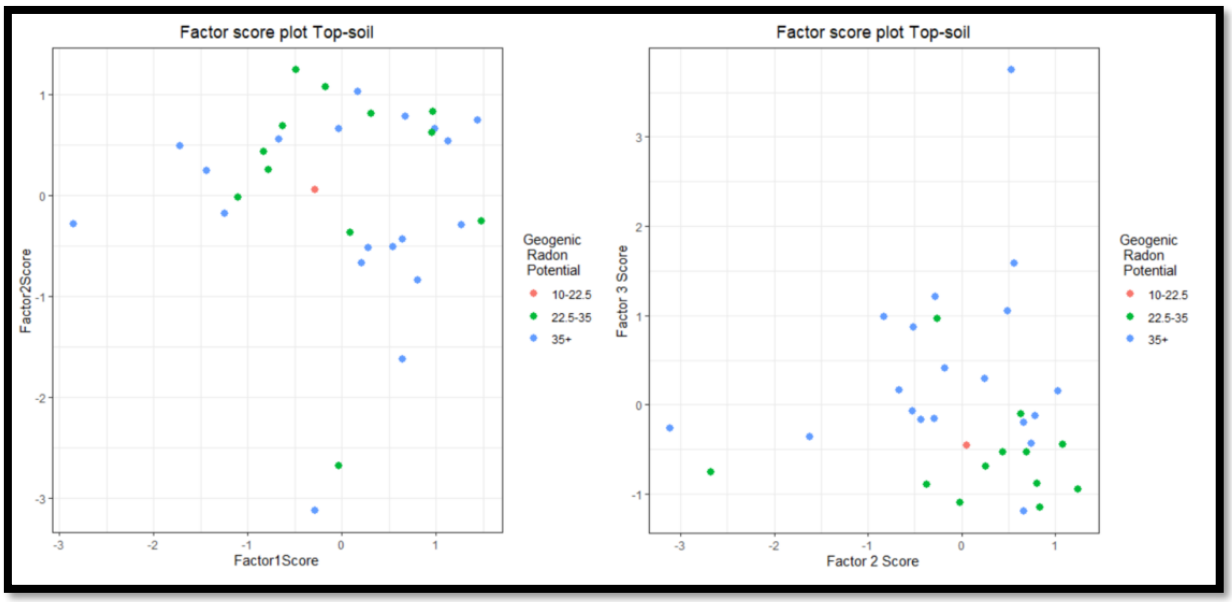

Figure 8.3.9 Factor score plots for ICPMS clr transformed shallow topsoil samples collected from Castleisland Co. Kerry. (Left) Factor score 1 vs factor score 2, (right) factor 2 vs factor 3 grouped according to geogenic radon potential.

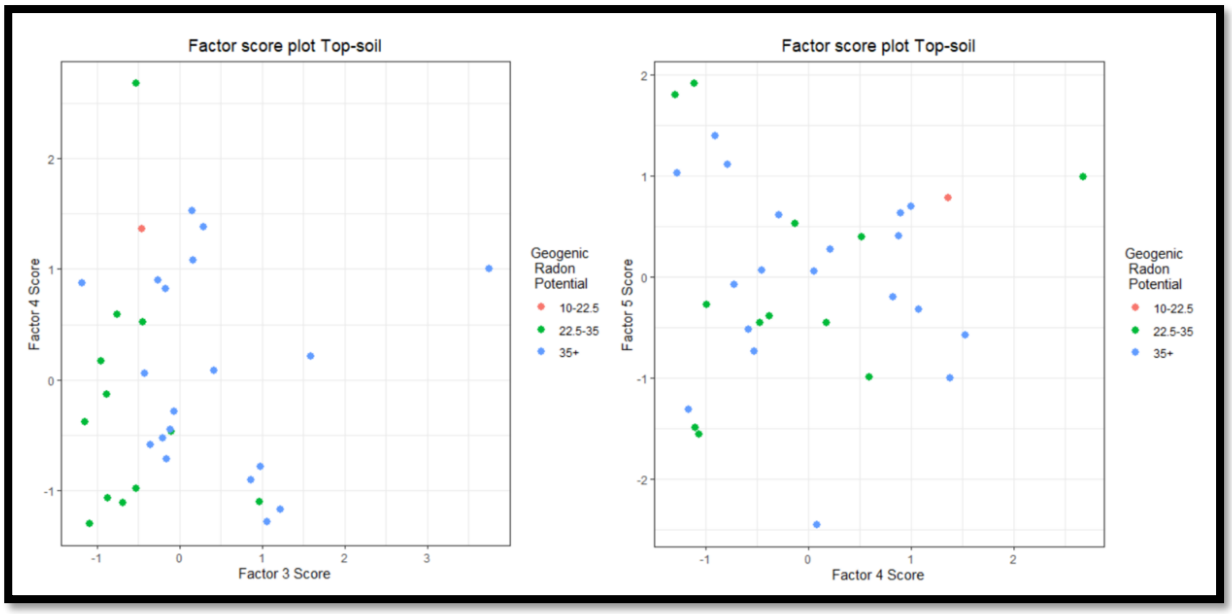

Figure 8.3.10 Factor score plots for ICPMS clr transformed shallow topsoil samples collected from Castleisland Co. Kerry. (Left) Factor score 3 vs factor score 4, (right) factor 4 vs factor 5 grouped according to geogenic radon potential.

8.4 Castleisland Co. Kerry shallow topsoil geochemistry

8.4.1 ANOVA of elements vs SGRn

The Castleisland shallow topsoil geochemical data was clr-transformed and one-way ANOVA was implimented for each elements vs each other element. The average effect-size caused by elements within the same cluster group is measured for each element and reported in the table below. The average effect-size caused by elements in another grouping is also reported. Only significant values measured here. The ANOVA results below show that elements which group together on the cluster analysis have significance effect size influence on other elements within the same cluster group. The anova results verify that the elements in the main cluster analysis groups and PC groups significanty explain variation of elements within the same cluster groups.

Appendix B

Table 8.4.1.1 ANOVA ICPMS geochemistry Castleisland, Co. Kerry

Element	Average SGRn effect-size of elements within same group (%)	Average effect-size of SGRn significant elements in other group (%)
Ca	0	22
V	53	12
P	48	13
La	32	16
Ba	42	18
Cu	37	10
Sr	50	14
U	40	15
Mo	34	19
Sb	34	14
Mn	36	9
Ni	51	9
Co	51	12
Fe	51	12
As	36	17
Zn	45	15
Mg	50	17
Th	41	10
Sc	53	11

K	28	18
Al	52	13
Ga	32	16
Cr	37	18
Na	31	10
Pb	40	0
Hg	25	17

The cluster analysis results show two main subgroups with further minor groups within them. The left subgroup is split into Ca to one side and the other is further split into two minor groups, containing (from left to right) V, P, La, Ba, Cu and Sr with U, Mo and Sb on the right minor group. The right subgroup is split with one element, Mn, to the left, with the right group further split into minor groups. The minor group on the right contains (from left to right) Ni and Co together on one branch with Fe, As, Zn, Mg, Th and Sc compiling the rest of this minor subgroup. The minor group to the right of the right subgroup contains (from left to right) K, Al, Ga, Cr and Na situated on a left branch with Pb and Hg grouped together on a right branch.

Neighbouring elements of the cluster analysis graph have a trend of explaining some of the highest variances resulting from ANOVA analysis; this is the case for the majority of elements besides Ca. The anova results show Ca only significantly associated with Ga and Hg which isn't interpretable from the cluster analysis. Overall, the anova results complement the cluster analysis in the sense that neighbouring elements in the cluster analysis explain the highest variances of each element. With few exceptions, the elements in each cluster group are significantly associated with one another. In some cases elements in different cluster groups explain some variances of certain elements but to a lesser degree.

However, V and P are significantly (P value < 0.05) associated with each other with an effect-size value of 73%. Similarly, La and Ba which are branched together share a significant effect-size value of 50%, which is the largest effect-size either elements share with another element. Cu and Sr are branched together on the cluster analysis and share a significant effect-size value of 53%. U, Mo and Sb are all significantly influenced by one another, U and Mo (31%), U and Sb (36%) and Mo and Sb (45%). Zn's highest variance (59%) is explained by it's neighbour Mg. However, Mg's highest variance is explained by Ni (73%). Th's highest variance is explained by Sc at 70%. Sc's highest variance isn't explained by it's neighbour K, instead Al, Mg, Ni and Th explain Sc's highest variances at 74%, 71%, 71% and 70% respectively. K's highest variance is explained by some of it's closest nieghbours Th, Ga and Al at 54%, 40% and 36% respectively. Similarly Al's highest variances aren't asociated with it's closest neighbours Ga (61%) and K (36%), instead other elements within the same cluster group Sc, Fe and Cr explain the highest variances (74%, 68% and 65% respectively). Ga's neighbours Al and Cr are amoung the highest which explain Ga's variance at 61% and 35% respectively, along with K (40%) and Fe (38%). Cr's highest variance isn't explained by it's neighbours on the cluster analysis but rather Al (65%) and Zn (50%) explain Cr's variance significantly. Na's variance isn't significantly associated with Pb, and it's highest variance is explained by other elements within the main grouping Al (46%) and Ga (43%). Lastly, Pb's only significant variance is explained by it's neighbour Hg (40%).

Table 8.4.1.2 Element variance ICPMS elements versus elements

Element	**Element (variance)**	**Element (variance)**	**Element (variance)**	**Element (variance)**
Ca	Hg (25%)	Ga (20%)	NA	NA
V	Sr (73%)	P (73%)	Ba (58%)	U (52%)

P	V (73%)	Sr (59%)	Ba (57%)	U (47%)
La	Ba (50%)	V (37%)	Sr (36%)	P (32%)
Ba	V (58%)	P (57%)	La (50%)	Cr (42%)
Cu	Sr (54%)	P (47%)	V (43%)	Ba (40%)
Sr	V (73%)	P (59%)	Cu (54%)	U (49%)
U	V (52%)	Sr (49%)	P (47%)	Sb (36%)
Mo	V(48%)	Sb (45%)	P (40%)	As (37%)
Sb	Sr (49%)	Mo (45%)	V (31%)	U (36%)
Mn	Co (67%)	Ni (58%)	Zn (53%)	Fe (41%)
Ni	Co (90%)	Mg (73%)	Sc (71%)	Zn (71%)
Co	Ni (90%)	Mg (71%)	Sc (69%)	Mn (67%)
Fe	Mg (69%)	Al (68%)	Co (67%)	Sc (66%)
As	Fe (62%)	Co (45%)	Sc (44%)	Al (41%)
Zn	Ni (71%)	Co (61%)	Mg (59%)	Sc (54%)
Mg	Ni (73%)	Sc (71%)	Co (71%)	Fe (69%)
Th	Sc (70%)	Mg (59%)	Fe (54%)	Al (54%)
Sc	Al (74%)	Mg (71%)	Ni (71%)	Th (70%)
K	Th (54%)	Ga (40%)	Al (36%)	Na (35%)
Al	Sc (74%)	Fe (68%)	Cr (65%)	Mg (62%)
Ga	Al (62%)	Ga (43%)	K (40%)	Fe (38%)
Cr	Al (65%)	Zn (50%)	Ba (42%)	Fe (42%)
Na	Al (46%)	Ga (43%)	K (35%)	Mg (34%)
Pb	Hg (40%)	NA	NA	NA

Hg	Pb (40%)	Ca (25%)	K (21%)	U (18%)

The major grouping to the right of the cluster analysis shows Mn branched by itsef. However, the anova results show that Mn shares significant effect-sizes with all elements in the right cluster grouping besides Ga, Na, Pb and Hg. Whereas, Mn does not show any significant influenece associated with elements grouped on the left of the cluster analysis. The highest effect-sizes associated with Mn are caused by its neighbours Ni and Co (58% and 67% respectively). Ni and Co have the highest effect-size (90%) in the dataset. Fe variance is explained by it's neighbour As by 62% which is the second highest explained variance after Co (67%).

The elements variations are signficantly explained by BG by 32%, SGRn 22%, SP 31% and QG 15%. Soil-gas radon explains the variance of the elements in the first cluster group over twice as much (29%) when compared to the second cluster group (11%). Furthermore, BG and QG explain the variance of the first cluster group slightly more (35% and 16%, respectively) than the second cluster group (28% and 13%, respectively). Specifically, from the first cluster group, the elements significally assocated with SGRn are P, V, Cu, Sr, Mo, Sb, Ba, La and U (i.e. all of the elements in cluster group 1 aside from Ca). In the second cluster group, the elements associated with SGRn are Mg, Fe, Co, Ni and Ga; elements within cluster group 2 not significantly associated with SGRn are Na, Al, K, Mn, Sc, Cr, Zn, As, Hg, Pb and Th.

There is only one element, Mn, which is signifcantly associated with soil-permeability variance. The only element associated with QG variance in cluster group 1 is Cu; the only sample in cluster group 2 associated with QG variation is Co. The elements from cluster group 1 associated with BG are P, V, Cu, Sr, Ba and U; elements in group 1 not associated with BG

variance are Mo, Sb, La and Ca. Elements from cluster group 2 explained by BG variation are Mg, Sc, Co and Ni; elements in group 2 with variation not significantly expained by BG are Na, Al, K, Mn, Fe, Cr, Zn, Ga, As, Hg, Pb and Th.

Table 8.4.1.3 ANOVA of elements in two main cluster analyis groups versus SGRn,soil permeability, BG and QG

Variable	Average effect-size of elements within Cluster group 1	Average effect-size of elements within Cluster group 2	Average effect-size of elements in dataset
Log10SGRn	29	11	22
Soil permeability	0	31 (1 sample)	31
BG	35	28	32
QG	15 (1 sample)	13 (1 sample)_	14

The elements which are significantly (P <0.05) associated with SGRn are U, Ba, Sr, Cu, Ni, Co, V, P, Mg, La, Sb, Mo, Ga and Fe. The elements which are significantly (P <0.05) associated with BG are U, Ba, Sr, Cu, Ni, Co, V, Sc, P and Mg.

There are 10/26 elements (U, Ba, Sr, Cu, Ni, Co, V, Sc, P and Mg) associated with BG. There are 14/26 elements (U, Ba, Sr, Cu, Ni, Co, V, P, Mg, **La, Sb, Mo, Ga and Fe**) associated with SGRn. Only 9 of the elements (U, Ba, Sr, Cu, Ni, Co, V, P, Mg) associated with SGRn are also associated with BG. To add, Sc is the only element that is associated with BG but not one of the elements associated with SGRn. There are 5 elements (**La, Sb, Mo, Ga and Fe**) associated with SGRn that are not associated with BG.

By visually comparing the Clr maps: Overall, Sc, Ni, Co and Fe are positively correlated with the Waulsortian limestones as well as samples collected above the Dirtoge limestones and

Cracoean reef member to the east of the study area. Sc, Ni, Co and Fe are all within the same cluster 2 subgroup. U, Ba, Sr, Cu, V, P, Mg, La, Sb and Mo are consistently high above the Clare Shales with some elevated samples collected in the Dirtoge limestones west of the Nw-Se fault, and in several samples in the Cracocean reef member and Rockfield limestones.

Ni and Co are positively correlated with the Waulsortian limestones. **Fe** is highest around the western Dirtoge limestones and Cracoean reef member, as well as the southern Waulsortian limestones. Fe shows a similar trend to Th, Co, Ni, Mn, Mg and Al.

Sr is hughest above the CS and elevated samples are observed in the DL and several RF west to the NW-SE fault. **V** is high above the CS with elevated samples seen in the DL west to the fault. Several samples collected above the Rf and CCRm are also elevated. **U** is highest above the Clare shales with several elevated samples Rockfield limestones. U concentrations are low in the WL and along the RL, CCRm and DL in the east of the study area. **La** is high above the CS and DL west to the fault as well as some samples above the WL collected in close proximity to the fault. **Ba** is high above the CS with some eleveated samoke in the RF and CCRm. **P** shows a similar trend to V, Sr, U, La and Ba. **Cu** is highest above the Clare shales. **Mo** is high in the Clare shales with several elevated samples above the Dirtoge limestones and Cracoean reef member loacted west to the NW-SE fault. Sb is high above the CS and DL west to the fault. The Mo concetrations in the Waulsortian limestones, Rockfield limestones are low. A similar trend is seen in the SGRn results.

Main points from results

- The ANOVA results show that elements in the same cluster group significantly explain more variance than elements in another group.
-
- PCA and cluster analysis results are complimentary i.e. same elements grouped on PCA and cluster analysis.

-
- The elements which are significantly (P <0.05) associated with SGRn are U, Ba, Sr, Cu, Ni, Co, V, P, Mg, La, Sb, Mo, Ga and Fe. The elements which are significantly (P <0.05) associated with BG are U, Ba, Sr, Cu, Ni, Co, V, Sc, P and Mg.
- Overall, Sc, Ni, Co and Fe are positively correlated with the Waulsortian limestones as well as samples collected above the Dirtoge limestones and Cracoean reef member to the east of the study area.
- U, Ba, Sr, Cu, V, P, Mg, La, Sb and Mo are consistently high above the Clare Shales with some elevated samples collected in the Dirtoge limestones west of the Nw-Se fault, and in several samples in the Cracocean reef member and Rockfield limestones.
- Lower PC2 correlates to higher SGRn.

8.4.2 PCA vs SGRn

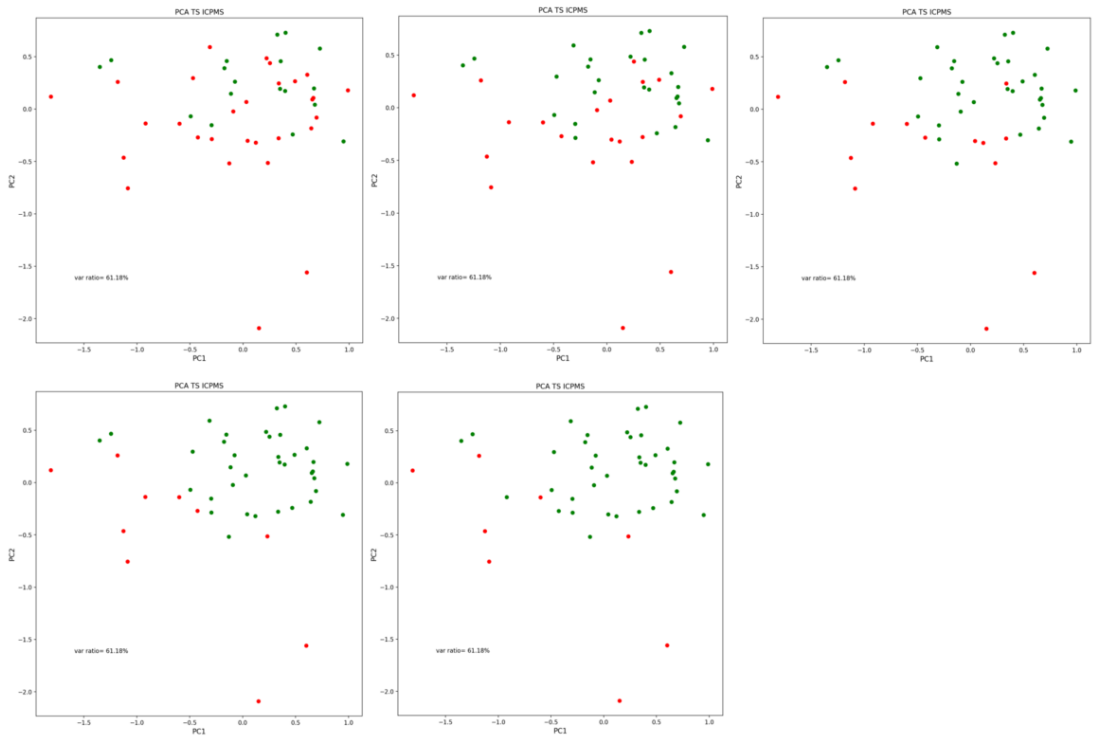

Figure 8.4.2.1 PCA of TS Clr-log transformed and scaled data colours denote SGRn concentrations. From top left to bottom right the PCA breaks of SGRn are red =: > 50, > 70, >100, >150 and >200.

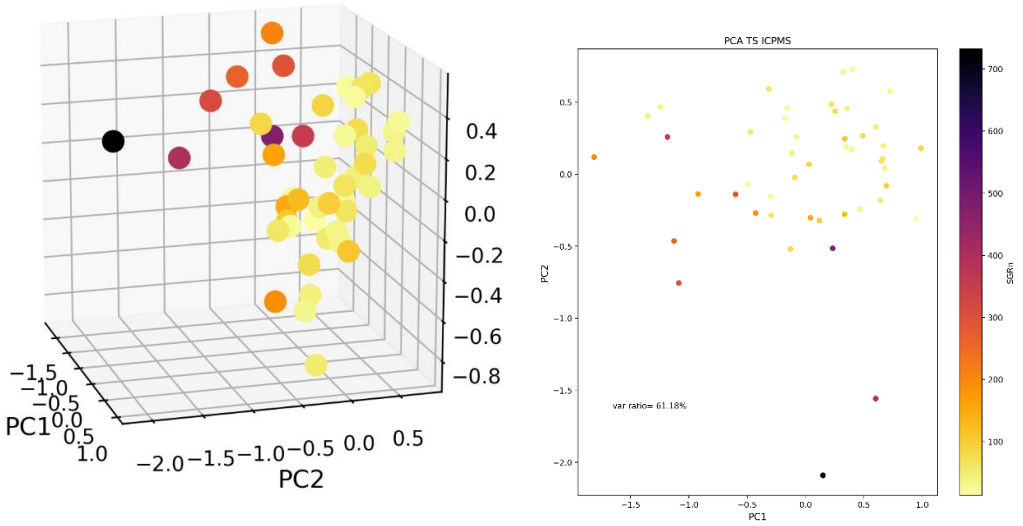

Figure 8.4.2.2 3D PCA (of PC1-3) of TS Clr-log transfromed and scaled data. Colours relate to SGRn (k Bq/m3)

8.5 Deeper topsoil Factor analysis ICPMS

Table 8.5.1 Factor score loadings table for ICPMS clr transformed shallow topsoil data from Castleisland, Co. Kerry.

Loadings	Factor1	Factor2	Factor3	Factor4	Factor5	Factor6	Communality
Mo	-0.2158	0.324672	-0.27769	0.149236	0.753119	0.151504	0.935866
Cu	0.153744	0.203555	-0.04015	0.089853	0.066635	0.610727	0.635482
Pb	0.072556	0.238341	0.262803	0.019821	-0.16665	0.532825	0.448714
Zn	0.913716	-0.06694	-0.06503	-0.009	0.069597	0.25376	0.96192
Ni	1.131577	0.221778	-0.05811	-0.02001	-0.17684	-0.0784	0.990631
Co	1.061826	-0.11254	-0.23439	0.056711	0.011573	-0.03579	0.954946
Mn	0.520178	-0.23224	-0.05163	-0.24695	0.190012	0.55991	0.713522
Fe	0.213874	-0.15888	0.300014	-0.16628	0.680054	0.053827	0.936474
As	0.105995	0.043638	-0.12957	0.047826	0.891388	0.067769	0.899105
U	0.086478	0.404463	-0.40015	0.89659	0.18664	-0.18385	0.995
Th	0.415364	0.019741	0.234153	0.171633	0.185789	-0.41948	0.564007
Sr	0.056011	0.903384	-0.06669	0.30134	-0.19503	0.092486	0.966478
Sb	0.093835	0.737261	-0.08571	-0.22246	0.160789	0.104947	0.755742
V	-0.24823	0.91105	0.291071	0.175771	0.238189	-0.04369	0.940194
Ca	-0.01075	-0.13429	-0.14741	0.649107	-0.31455	0.187835	0.57925
P	-0.13178	0.154746	0.054041	0.030872	0.117047	0.875483	0.980862
La	0.13193	0.792812	-0.11343	0.0109	-0.06968	0.114209	0.726477
Cr	0.375031	0.188824	0.628438	-0.05383	0.149845	0.03762	0.8768
Mg	0.776437	-0.01498	0.230263	-0.08273	-0.03181	-0.20211	0.860172
Ba	0.114795	0.485964	0.353651	0.468419	-0.01445	0.10529	0.63827
Al	0.364193	0.022486	0.784319	0.053486	-0.1512	-0.02528	0.988136
Na	-0.03702	-0.42736	0.366331	0.381992	0.018362	0.075638	0.572023
K	-0.10714	0.199749	0.911863	-0.41166	-0.07612	0.116777	0.726772
Hg	-0.20776	-0.05433	-0.06145	0.474403	0.167322	0.293432	0.437986
Sc	0.61179	-0.24549	0.084562	0.345355	0.135711	0.014384	0.836397
Ga	-0.20328	-0.14976	0.988902	-0.1641	-0.07336	0.00181	0.859362

SS loadings	**5.295**	**3.956**	**3.812**	**2.471**	**2.341**	**2.278**	
Proportion Var	**0.204**	**0.152**	**0.147**	**0.095**	**0.09**	**0.088**	
Cumulative Var	**0.204**	**0.356**	**0.502**	**0.597**	**0.687**	**0.775**	

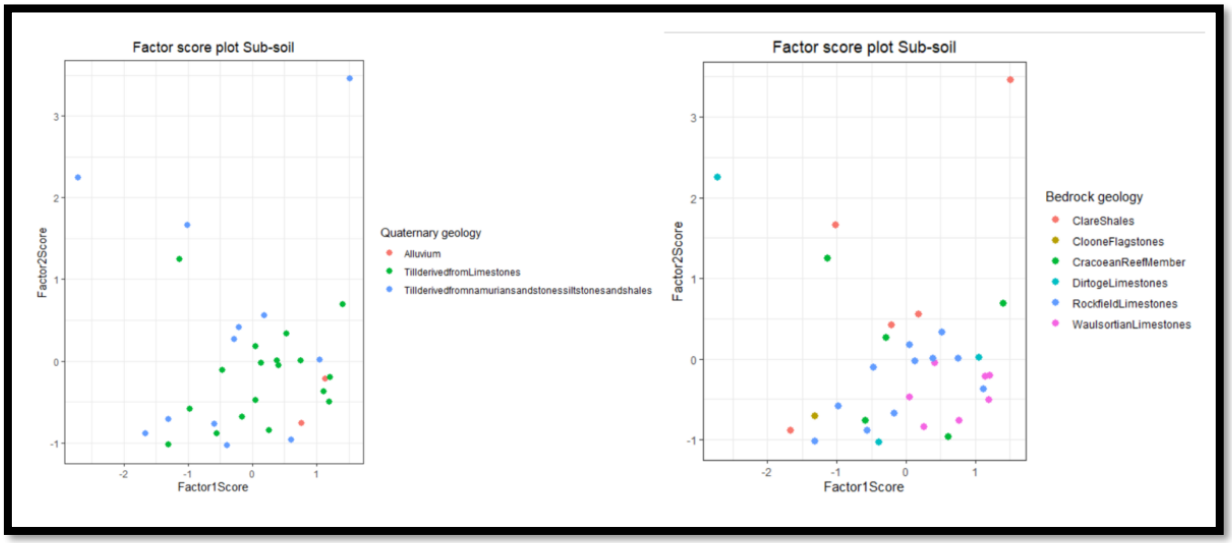

Figure 8.5.1 Factor score plots for ICPMS clr transformed deeper topsoil samples collected from Castleisland Co. Kerry. (Left) Factor score 1 vs factor score 2 grouped to Quaternary geology type, (right) factor 1 vs factor 2 grouped according to bedrock geology type.

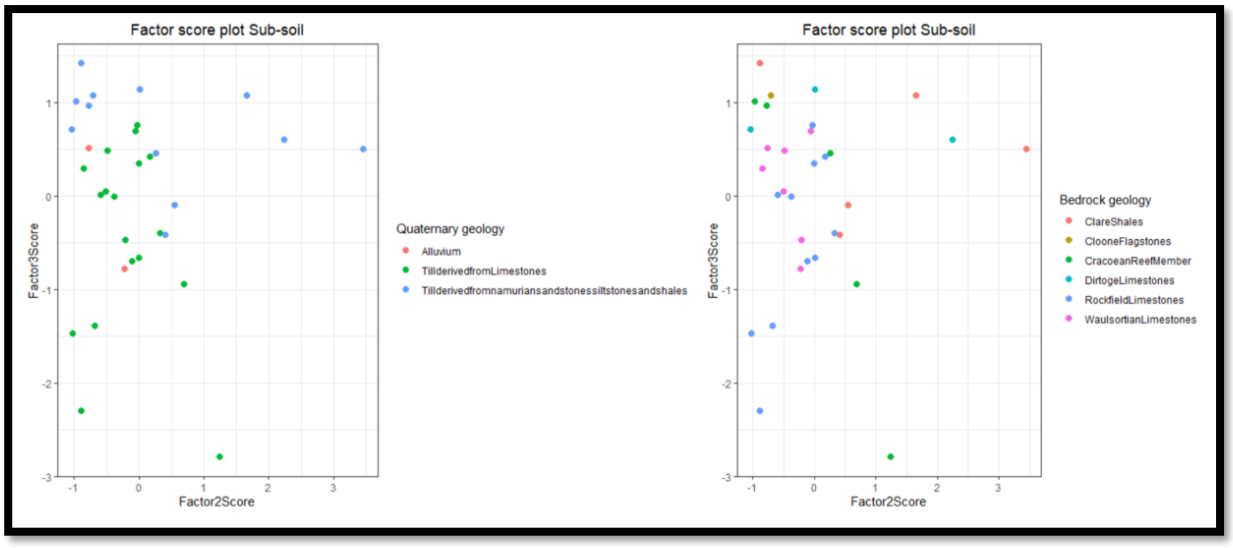

Figure 8.5.2 Factor score plots for ICPMS clr transformed deeper topsoil samples collected from Castleisland Co. Kerry. (Left) Factor score 2 vs factor score 3 grouped to Quaternary geology type, (right) factor 2 vs factor 3 grouped according to bedrock geology type.

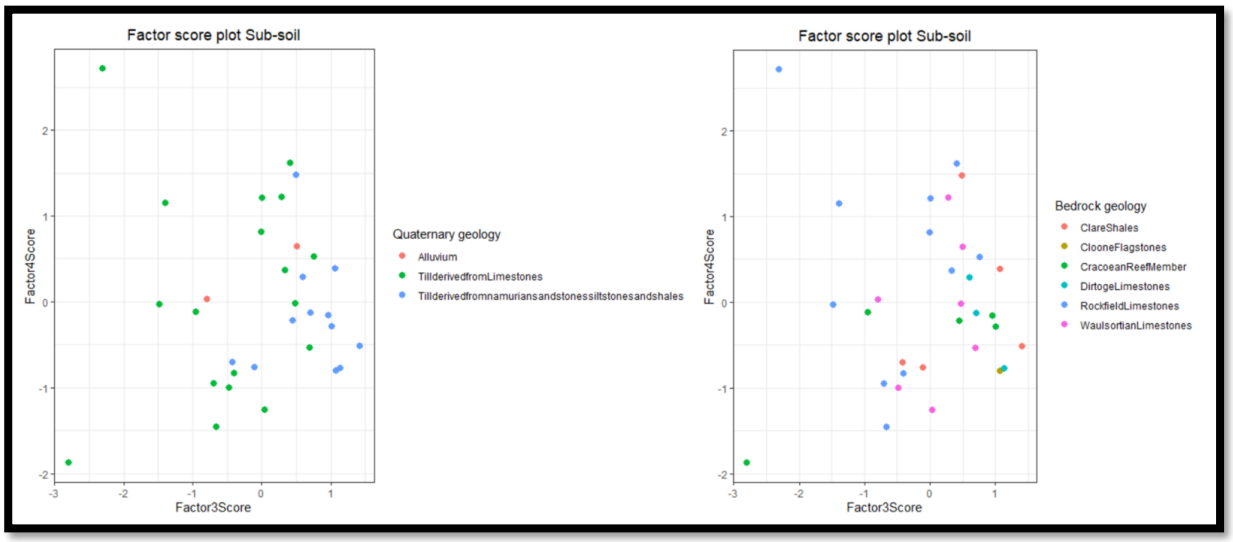

Figure 8.5.3 Factor score plots for ICPMS clr transformed deeper topsoil samples collected from Castleisland Co. Kerry. (Left) Factor score 3 vs factor score 4 grouped to Quaternary geology type, (right) factor 3 vs factor 4 grouped according to bedrock geology type.

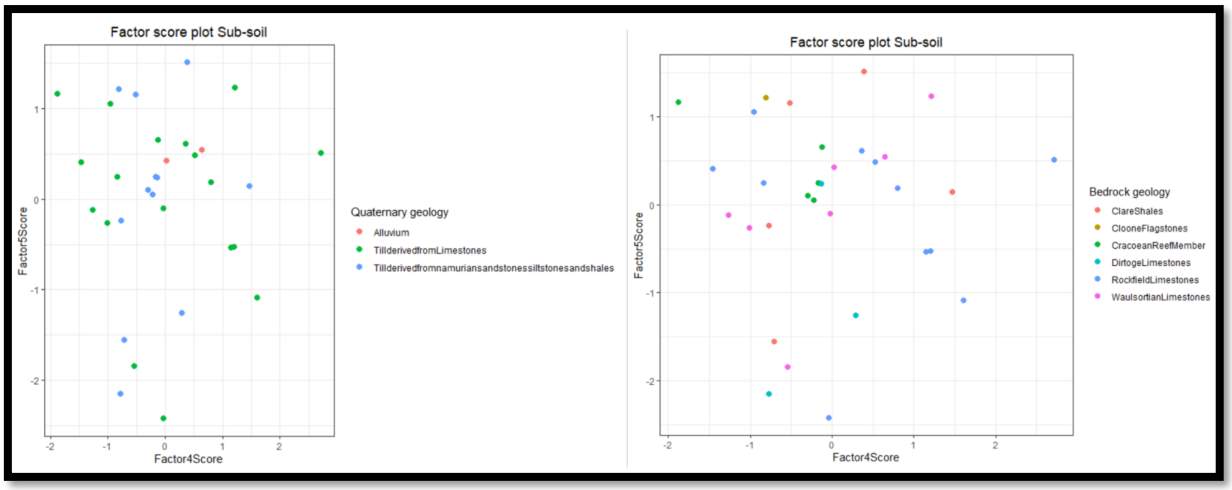

Figure 8.5.4 Factor score plots for ICPMS clr transformed deeper topsoil samples collected from Castleisland Co. Kerry. (Left) Factor score 4 vs factor score 5 grouped to Quaternary geology type, (right) factor 4 vs factor 5 grouped according to bedrock geology type.

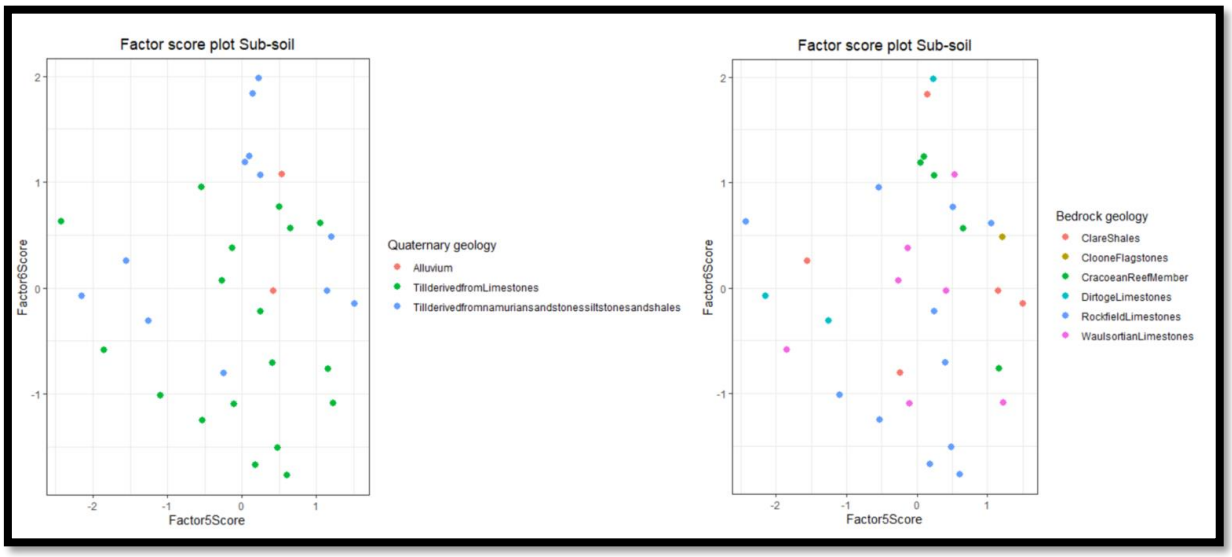

Figure 8.5.6 Factor score plots for ICPMS clr transformed deeper topsoil samples collected from Castleisland Co. Kerry. (Left) Factor score 5 vs factor score 6 grouped to Quaternary geology type, (right) factor 5 vs factor 6 grouped according to bedrock geology type.

Appendix B

8.6 Soil geochemistry statistics of raw data

1. XRF sample vs CRM
   (a) lab repeats
   (b) field repeats
2. ICPMS sample vs CRM
   (a) lab repeats
   (b) field duplicates

8.6.1. XRF

The XRF technique measured S, Cl, V, Cr, Co, Ni, Cu, Zn, Ga, As, Br, Rb, Y, Nb, Sn, Ba, Zr, Pb, U, Na2O, MgO, Al2O3, SiO2, K2O, CaO, TiO2, MnO, Fe2O3 and SrO. Elements (Ge, Se, Mo, Ag, Sb, Te, I, Hf, Ta, Bi, Cd, Th, W, Tl, Hg, Ce, La, Cs, In, Pd, Rh, Ru, Ir, Pt, Au, P205) which reported 5-100% below or above the detection limit were not included in the analysis. To validate the reliability of the results with regard to the analytical instrument used, two certified reference materials (Till-1 and GSJ JLk) were measured and compared to the certified values.

8.6.1.1 Lab measurement vs cert value: Till-1

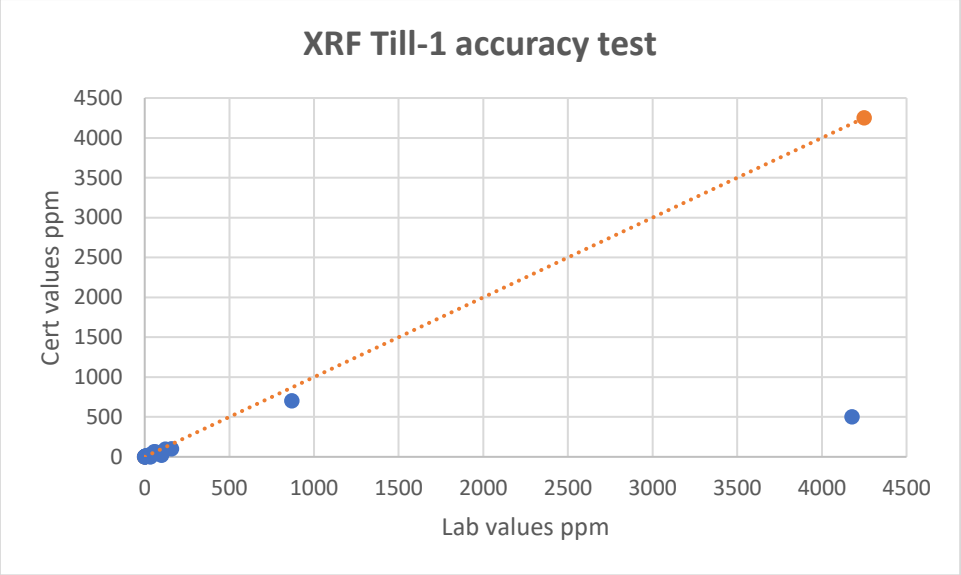

Figure 8.6.1.1.1 The lab value versus the certified value for the Till-1 CRM.

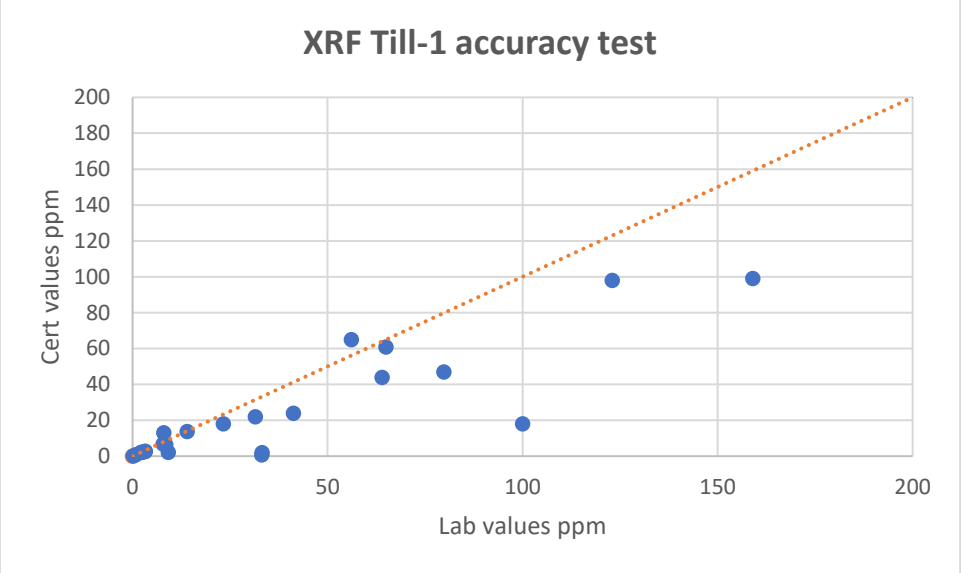

Figure 8.6.1.1.2 The lab value versus the certified value for the Till-1 CRM, zoomed in axis ((0, 200) (0,200)

Appendix B

Table 8.6.1.1.1 Tabulation showing results from the certified reference material laboratory value versus the certified value. The percentage (5) difference in accuracy is measured.

Element	TILL 1	TILL 1	Difference accuracy	Element	TILL 1	TILL 1	Difference accuracy
	Lab Value	Reference Value	%		Lab Value	Reference Value	%
Al2O3	14	13.7	2.14286	In	NA		NA
CaO	3.22	2.72	15.528	Ir	14.7		100
Fe2O3	7.9	6.82	13.6709	La	NA	28	NA
K2O	2.5	2.22	11.2	Mo	33.2	2	93.9759
MgO	2.18	2.15	1.37615	Nb	14.75	10	32.2034
MnO	0.2	0.18	10	Nd	NA	26	NA
Na2O	3.3	2.71	17.8788	Ni	41.34	24	41.9449
P2O5	NA	0.22	NA	Pb	31.54	22	30.2473
SiO2	64.96	60.9	6.25	Pr	NA		NA
TiO2	1	0.98	2	Rb	63.98	44	31.2285
Ag	11.2	0.2	98.2143	S	479.6	500	-4.2535
As	23.32	18	22.813	Sb	NA	7.8	NA
Au	8	13	-62.5	Sc	NA	13	NA
Ba	870	702	19.3103	Se	NA		NA
Bi	NA	5	NA	Sn	57.02		100
Br	8.52	6.4	24.8826	SrO	492.6	291	40.9257
Cd	NA	0.2	NA	Ta	33.14	0.7	97.8878
Ce	NA	71	NA	Te	39.2		100
Cl	280.4		100	Th	NA	5.6	NA
Co	99.88	18	81.9784	Tl	NA		NA
Cr	56.12	65	-15.823	U	9.18	2.2	76.0349

Cs	**NA**	**1**	**NA**	**V**	**159.2**	**99**	**37.8141**
Cu	**79.84**	**47**	**41.1323**	**W**	**NA**	**1**	**NA**
Ga	**16.96**		**100**	**Y**	**45.7**	**38**	**16.849**
Ge	**NA**		**NA**	**Zn**	**123.4**	**98**	**20.5835**
Hf	**NA**	**13**	**NA**	**Zr**	**4178**	**502**	**87.9847**
Hg	**NA**		**NA**	**I**	**NA**		**NA**

8.6.1.1.3 Lab measurement vs cert value - GSJJkI-1

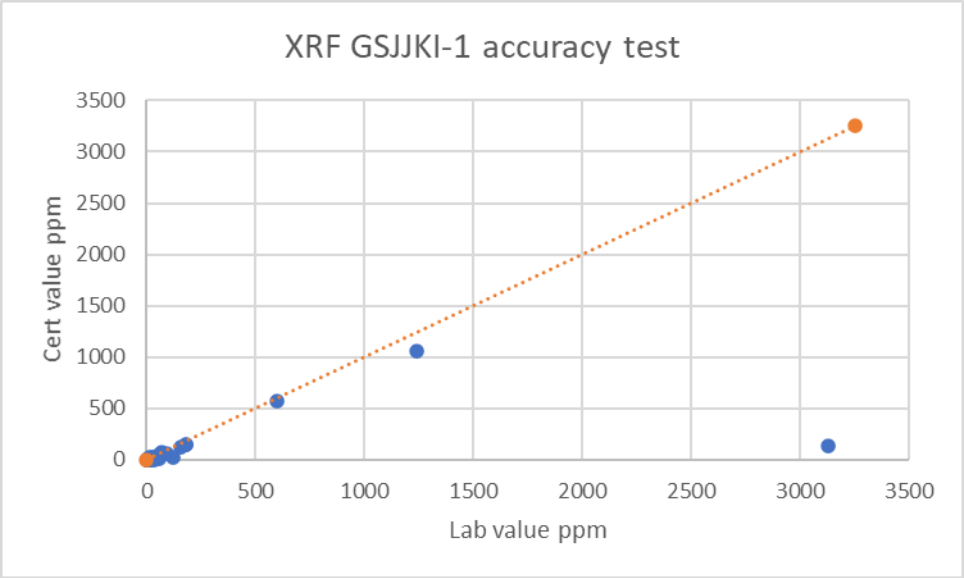

Figure 8.6.1.1.4 The lab value versus the certified value for the GSJJKl-1 CRM.

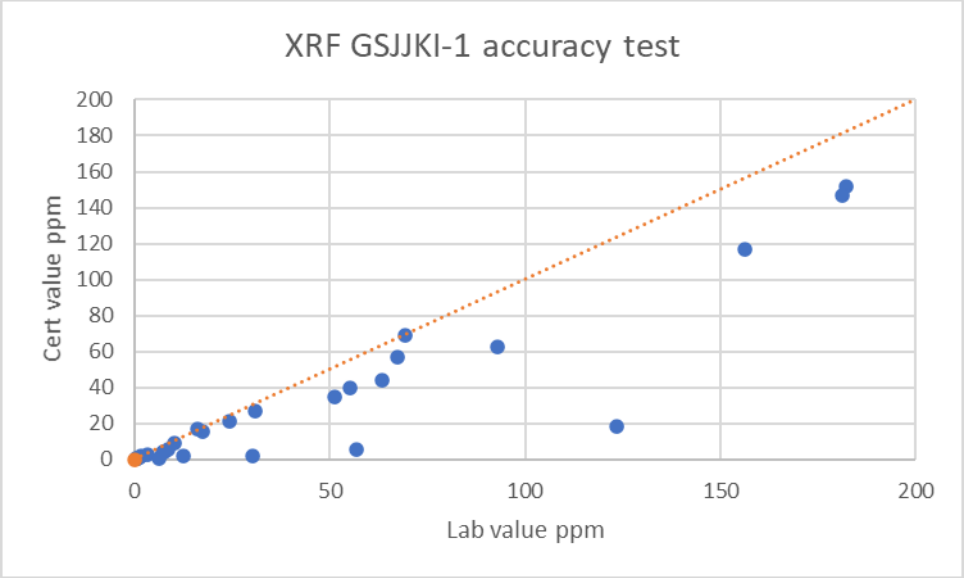

Figure 8.6.1.1.5 The lab value versus the certified value for the GSJJKl-1 CRM, zoomed in axis ((0, 200) (0,200)

Appendix B

Table 8.6.1.1.2 Tabulation showing results from the certified reference material laboratory value versus the certified value. The percentage (5) difference in accuracy is measured.

Element	***GSJ JLk 1***	***GSJ JLk 1***	**Difference accuracy**	***Element***	***GSJ JLk 1***	***GSJ JLk 1***	**Difference accuracy**
	Lab value	***Reference Value***	***%***		***Lab value***	***Reference Value***	***%***
Al2O3	16.2	***16.73***	**3.27161**	**La**	NA	***40.6***	**NA**
CaO	0.8	***0.686***	**14.25**	**Mo**	NA	***2.19***	**NA**
Fe2O3	7.6	***6.929***	**8.82895**	**Nb**	17.52	***15.8***	**9.81735**
K2O	3.34	***2.805***	**16.018**	**Nd**	NA	***35.7***	**NA**
MgO	1.6	***1.736***	**8.5**	**Ni**	51.16	***35***	**31.5872**
MnO	0.3	***0.266***	**11.3333**	**Pb**	63.42	***43.7***	**31.0943**
Na2O	1.32	***1.051***	**20.3788**	**Pr**	NA	***8.53***	**NA**
P2O5	NA	***0.208***	**NA**	**Rb**	181.2	***147***	**18.8742**
SiO2	67.46	***57.16***	**15.2683**	**S**	1236	***1052***	**14.8867**
TiO2	0.8	***0.668***	**16.5**	**Sb**	NA	***1.68***	**NA**
Ag	6.36667	***0.2***	**96.8586**	**Sc**	NA	***15.9***	**NA**
As	30.98	***26.8***	**13.4926**	**Se**	NA	***0.641***	**NA**
Au	8.63333	***5.42***	**37.2201**	**Sn**	56.84	***5.7***	**89.9719**
Ba	597.6	***574***	**3.94913**	**SrO**	105.2	***67.5***	**35.8365**
Bi	NA		**NA**	**Ta**	30.275	***1.57***	**94.8142**
Br	10.28	***8.7***	**15.3697**	**Te**	33.3		**100**
Cd	NA	***0.572***	**NA**	**Th**	NA	***19.5***	**NA**
Ce	NA	***87.9***	**NA**	**Tl**	NA	***1.17***	**NA**
Cl	109		**100**	**U**	7.38	***3.83***	**48.103**

Co	123.6	***18***	**85.4369**	**V**	156.2	***117***	**25.096**
Cr	69.44	***69***	**0.63364**	**W**	NA	***3.99***	**NA**
Cs	NA	***10.9***	**NA**	**Y**	55.04	***40***	**27.3256**
Cu	93.08	***62.9***	**32.4237**	**Zn**	182.2	***152***	**16.5752**
Ga	24.24	***21.4***	**11.7162**	**Zr**	3124	***137***	**95.6146**
Ge	NA		**NA**	**In**	NA		**NA**
Hf	NA	***3.78***	**NA**	**Ir**	10.5333		**100**
Hg	NA	***0.142***	**NA**	**I**	NA		**NA**

8.6.1.2 Accuracy analysis for lab repeat measurements

Three sample locations were chosen to study the uncertainty in lab preparation, i.e. measuring if a representative subsample was taken. The three locations chosen were L3a-S218a which is sampled above Till derived from limestone in the south of the Castleisland study area, L60a-03a which is sampled above till derived from Namurian sandstones, siltstones and shales in the north of the study area, and L54a-s205a sampled above the Cracoean reef member in the north east of the study area. The three samples were deliberately chosen to represent different soil types in order to not bias the results; furthermore, there may be some elements detected in a certain types and not in another, to ensure all elements have higher probability of being analysed, samples from three expectedly different soils were chosen.

For the L3a-218a sample, three subsamples (a, b and c) were made, each subsample was measured five times. The average element concentration of each subsample was used to compute overall mean values for which the standard deviation, absolute and relative uncertainty were derived.

Appendix B

Table 8.6.1.2.1 Tabulation showing results of the two standard deviation relative uncertainty (%) for three lab repeats.

(%) 2 stdev relative uncertainty					**SD (%) 2 stdev relative uncertainty**				
Sample ID		**MHL3A S218A**	**MHL60 A03A**	**MHL54 AS205a**	**Sample ID**		**MHL3A S218A**	**MHL60 A03A**	**MHL54 AS205a**
Date_time		11/21/2019 11:43 AM	11/28/2019 12:18 AM	11/27/2019 5:00 PM	Date_time		11/21/2019 11:43 AM	11/28/2019 12:18 AM	11/27/2019 5:00 PM
Major elements (wt %)	**Na2O**	6.81	11.09	2.02	**Minor elements (**	**Br**	1.8	6.02	8.36
	MgO	1.69	6.84	2.32		**Rb**	1.27	5.38	5.49
	Al2O3	2.22	5.74	2.29		**Y**	2.71	7.79	8.25
	SiO2	0.56	1.78	1.66		**Nb**	24.78	64.64	21.79
	P2O5	NA	5.04	11.86		**Mo**	NA	30.64	NA
	K2O	2.99	4.77	5.18		**Ag**	NA	NA	12.03
	CaO	7.57	4.37	6.38		**Sn**	45.22	6.73	6.32
	TiO2	6.35	4.38	6.21		**Sb**	NA	9.65	NA

	MnO	6.13	4.66	5.48	**ppm)**	**Te**	35.69	15.5	11.47
	Fe2O3	0.27	6.69	6.07		**Ba**	4.39	0.88	1.88
Minor elements (ppm)	**S**	20.32	19.93	27.7		**Hf**	NA	15.96	7.52
	Cl	14.5	6.76	1.83		**Ta**	11.92	10.31	4.56
	V	15.63	1.42	4.64		**Ir**	20.86	16.02	8.75
	Cr	53.19	11.99	10.08		**Au**	NA	6.58	NA
	Co	35.68	3.78	20.03		**Pb**	13.8	5.54	1.42
	Ni	2.44	5.45	4.51		**U**	55.19	4.41	10.14
	Cu	9.78	8.17	4.86		**SrO**	2.44	3.98	3.92
	Zn	3.2	12.7	7.65		**Zr**	4.56	3.54	3.29
	Ga	17.5	9.67	7.66		**As**	1.14	3.79	12.5
	Se	NA	3.02	NA					

8.6.1.3 Accuracy of field repeats XRF

Field repeats were collected following the TELLUS GSI protocol; where an extra field sample was collected 10 meters away from the original sample site, composed of five subsamples in a 20 m^2 area. Each sample was analysed five times using the XRF technique, taking the average of the five as the value for each element at each sample location. The average values were used to calculated the mean value, standard deviation absolute uncertainty and 2 standard deviation relative uncertainty (absolute uncertainty/mean value).

Table 8.6.1.3.1 Two0standard deviation of XRF Castleisland field repeats.

SampleID	2 stdev relative uncertainty (%)	2 stdev relative uncertainty (%)	2 stdev relative uncertainty (%)	2 stdev relative uncertainty (%)
SampleType	**L36A**	**L36S**	**AL66a**	**L66S**
Unit	**mg/kg**	**mg/kg**	**mg/kg**	**mg/kg**
Na2O	6.19	4.91	16.69	6.7
MgO	2.96	0.75	13.34	10.81
Al2O3	0.77	1.56	11.31	3.43
SiO2	0.51	1.13	3.94	2.02
K2O	4.18	3.31	20.17	4.21
CaO	0.24	84.26	39.72	12.65
TiO2	1.64	1.96	17.52	7.75
MnO	23.13	17.77	39.85	2.18
Fe2O3	5.19	2.54	27.19	38.26
SrO	3.06	6.79	18.15	5.46
Zr	0.17	7.01	8.64	3.23
S	6.34	22.94	72.07	13.26
Cl	51.84	17.59	33.29	6.23
V	1.55	16.4	7.35	10.89
Cr	6.6	12.11	26.33	23.23
Co	11.31	55.38	58.48	34.38

Ni	1.66	14.33	23.93	9.99
Cu	22.74	19.92	20.71	49.98
Zn	7.07	7.03	51.95	21.6
Ga	0.75	16.89	32.48	8.91
Ge	18.33	2.36	33.43	29.61
As	17.51	9.27	28.13	NA
Br	0.64	11.15	49.68	7.1
Rb	1.43	8.48	18.49	3.13
Y	4.12	5.83	21.13	14.18
Nb	22	8.15	31.52	26.97
Ag	8.3	NA	Na	NA
Sn	0.47	3.35	8.33	16.85
Te	11.04	2.29	4.83	15.41
Ba	8.64	4.46	12.87	3.06
Hf	26.74	0.65	7.58	9.55
Ta	22.41	51.6	22.7	20.69
Pb	22.2	4.51	24.57	2.72
U	1.34	95.67	61.75	24.21

8.6.2 AR ICPMS

8.6.2.1 Lab measurement vs certified reference values (a) STD DS11, (b) STD OREAS262 and (c) BVGE001.

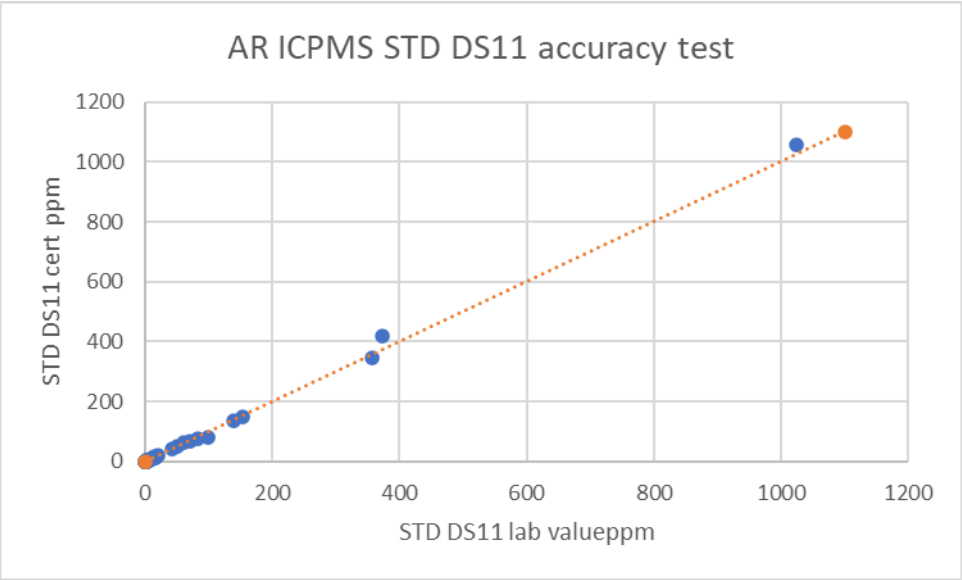

Figure 8.6.2.2 Lab value versus certified value of certified reference material STD DS 11.

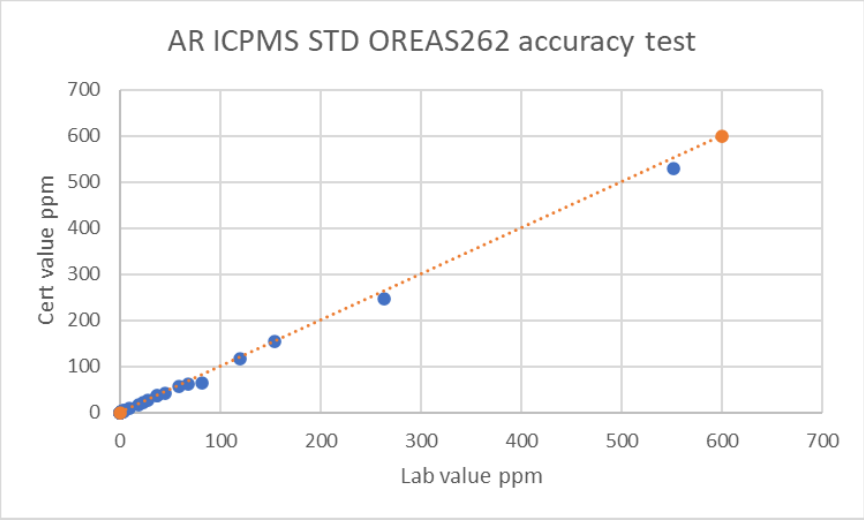

Figure 8.6.2.3 Lab value versus certified value of certified reference material STD OREAS262.

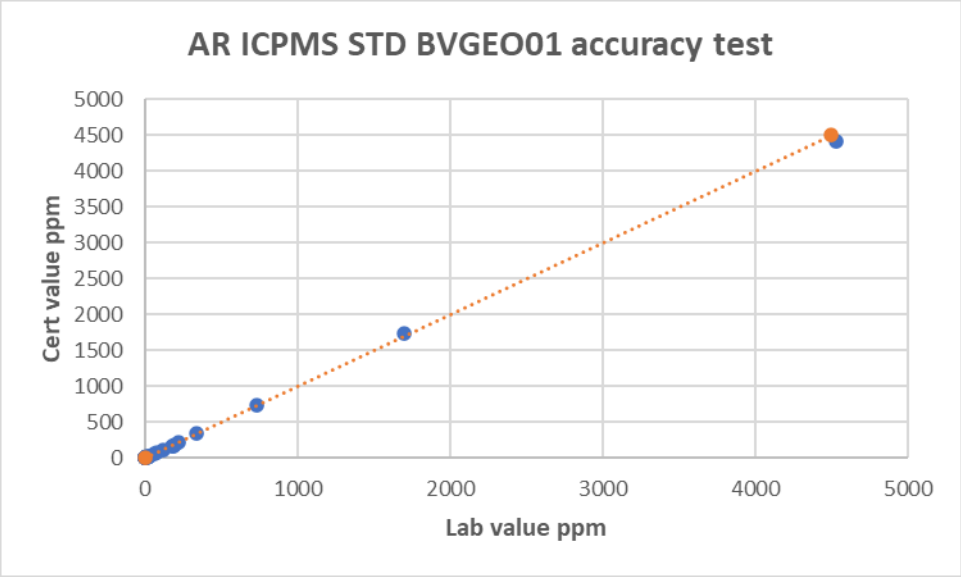

Figure 8.6.2.4 Lab value versus certified value of certified reference material STD BVGEO01.

Three certified reference materials were used prior to analysing the soil samples.

Table 8.6.2.1 The percentage difference accuracy between the lab values and certified values for the three stadards used during ICPMS anlaysis.

ICPMS	**% difference accuracy**	**% difference accuracy**	**% difference accuracy**
Analyte	**STD DS11**	**STD OREAS262**	**STD BVGEO01**
Mo	**8.63**	**2.94**	**0.93**
Cu	**2.92**	**1.78**	**2.71**
Pb	**1.38**	**4.82**	**3.58**
Zn	**3.33**	**0.22**	**2.41**
Ag	**0.58**	**3.7**	**1.19**

Ni	**6.82**	**10.27**	**8.65**
Co	**2.11**	**5.33**	**2.4**
Mn	**2.94**	**4.15**	**0.27**
Fe	**5.48**	**4.55**	**0.81**
As	**0.58**	**3.35**	**3.47**
U	**0.39**	**3.83**	**0.8**
Au	**25.63**	**25.79**	**0.59**
Th	**11.11**	**7.9**	**8.33**
Sr	**4.01**	**3.7**	**10.91**
Cd	**3.38**	**9.29**	**1.54**
Sb	**24.31**	**14.06**	**22.73**
Bi	**4.1**	**3.56**	**2.73**
V	**1**	**3.7**	**9.59**
Ca	**0.28**	**1.9**	**2.88**
P	**4.85**	**3.33**	**1.79**
La	**2.15**	**17.4**	**4.25**
Cr	**1.63**	**9.51**	**10.53**
Mg	**1.18**	**0.28**	**5.69**
Ba	**10.55**	**6.18**	**0**
Ti	**1.64**	**11.11**	**3.86**
B	**NA**	**NA**	**NA**
Al	**3.19**	**9.63**	**3.96**
Na	**10.23**	**8.92**	**4.99**

K	**1.25**	**4.7**	**8.99**
W	**0**	**53.85**	**5.71**
Hg	**9.62**	**7.84**	**20**
Sc	**22.58**	**13.17**	**5.53**
Tl	**2.04**	**6.38**	**3.23**
S	**11.82**	**10.41**	**3.83**
Ga	**6.38**	**7.24**	**8.55**
Se	**9.09**	**75**	**11.57**
Te	**3.07**	**15.94**	**1.96**

8.6.2.2 Accuracy analysis for lab repeat measurements

Table 8.6.2.2.13 The percentage two standard deviation between the samples which underwent repeat measurements in the lab.

Aqua Regia	**ICPMS**	**% 2std uncertainty**	**% 2std uncertainty**	**% 2std uncertainty**	**Average 2 stdev uncertainty (%)**
Unit	**Analyte**	**L72A S213A**	**L9S 008S**	**L13S S229S**	
PPM	**Mo**	**17.68**	**0**	**0**	5.89
PPM	**Cu**	**1.15**	**8.48**	**0.93**	3.52
PPM	**Pb**	**2.86**	**3.04**	**3.7**	3.2
PPM	**Zn**	**0**	**0**	**4.79**	1.6
PPM	**Ni**	**0**	**9.53**	**0.85**	0
PPM	**Co**	**5.14**	**0**	**6.9**	4.01

PPM	**Mn**	**2.55**	**4.69**	**2.56**	3.27
%	**Fe**	**12.18**	**10.29**	**1.36**	7.94
PPM	**As**	**5.05**	**32.64**	**0**	12.56
PPM	**U**	**0**	**9.75**	**0**	3.25
PPB	**Au**	**21.76**	**197.46**	**0**	73.07
PPM	**Th**	**61.49**	**56.57**	**14.89**	44.32
PPM	**Sr**	**4.22**	**0**	**6.29**	3.5
PPM	**Cd**	**0**	**25.71**	**0**	8.57
PPM	**Sb**	**31.43**	**0**	**56.57**	29.33
PPM	**Bi**	**0**	**0**	**94.28**	31.43
PPM	**V**	**2.98**	**13.47**	**7.64**	8.03
%	**Ca**	**0**	**17.04**	**12.3**	9.78
%	**P**	**4.6**	**14.5**	**3.33**	7.48
PPM	**La**	**16.64**	**0**	**14.89**	10.51
PPM	**Cr**	**0**	**0**	**5.55**	1.85
%	**Mg**	**14.89**	**18.86**	**0**	11.25
PPM	**Ba**	**0**	**4.1**	**6.43**	3.51
%	**Ti**	**0**	**NA**	**0**	0
PPM	**B**	**NA**	**NA**	**NA**	NA
%	**Al**	**1.06**	**1.41**	**3.37**	1.95
%	**Na**	**11.31**	**28.28**	**17.68**	19.09
%	**K**	**16.64**	**18.86**	**0**	11.83
PPM	**W**	**0**	**NA**	**NA**	0

PPM	**Hg**	**15.71**	**0**	**0**	5.24
PPM	**Sc**	**8.08**	**16.64**	**0**	8.24
PPM	**Tl**	**0**	**0**	**0**	0
PPM	**Ga**	**0**	**0**	**31.43**	10.48
PPM	**Se**	**49.19**	**80.81**	**14.89**	48.3

8.6.2.3 Accuracy of field repeats

Table 8.6.2.3.1 The percentage two standard deviation for each of the four field locations where repeat samples were collected.

AR ICPMS	**% 2std uncertainty**	**% 2std uncertainty**	**% 2std uncertainty**	**% 2std uncertainty**
Analyte	**L36A**	**L36S**	**L66A**	**L66S**
Mo	5.336654952	0	0	20.20305
Cu	79.14252994	13.51307852	2.262742	5.427685
Pb	25.42989525	0.701842959	6.133938	1.767767
Zn	0	7.252377243	32.6357	33.94113
Ag	NA	NA	0	NA
Ni	8.796543689	26.7599692	34.49301	20.39731
Co	11.12631788	14.4710225	23.57023	18.24792
Mn	24.24855729	19.54538447	22.0177	12.6646
Fe	7.362500108	9.60824501	1.950639	55.83626
As	3.108161676	1.075447576	4.09917	63.39578
U	12.29750924	21.75713173	35.35534	0

Au	14.88645855	NA	36.89253	149.7403
Th	0	17.31690076	18.85618	0
Sr	0	33.27561323	0	19.73321
Cd	16.63780662	28.28427125	40.4061	94.2809
Sb	94.28090416	56.56854249	0	121.2183
Bi	0	0	0	94.2809
V	0	14.50475449	0	12.29751
Ca	11.3137085	89.68183566	21.75713	9.123958
P	32.10647006	9.324485027	29.63114	20.69581
La	14.88645855	13.46870059	0	0
Cr	15.71348403	15.71348403	31.42697	0
Mg	12.29750924	9.428090416	18.85618	0
Ba	51.55261262	25.14157444	15.42778	32.6357
Ti	0	0	NA	0
B	NA	NA	NA	NA
Al	9.873359573	19.23330445	12.85649	21.75713
Na	0	49.19003695	12.29751	65.2714
K	9.753196982	47.14045208	14.88646	56.56854
W	NA	NA	94.2809	NA
Hg	31.42696805	47.14045208	40.4061	21.75713
Sc	6.428243465	22.18374215	0	26.9374
Tl	0	0	56.56854	56.56854
S	NA	NA	NA	NA

Ga	18.85618083	18.85618083	0	31.42697
Se	0	13.46870059	67.3435	NA
Te	NA	NA	NA	NA

Appendix B

Appendix C: Published papers in journal format.

ORIGINAL ARTICLE

9.1 A user's guide to radon priority areas, examples from Ireland

Méabh B. Hughes[1], Javier Elío[2] and Quentin G. Crowley[1*]

[1]Department of Geology, School of Natural Sciences, Trinity College, Dublin, Ireland; [2]Department of Planning, Aalborg University Copenhagen, Copenhagen, Denmark

Abstract

Exposure to radon over time has significant detrimental effects on human health. Approximately 226,000 annual radon-related deaths have been reported from 66 countries (1). Many countries have a radon action plan, in order to reduce the harmful effects of radon exposure on the general public. Maps are routinely used to assist with mitigation strategies and delineate areas of priority regulation. Standard regulations in the European Union include the requirement for workplaces to test and the requirement to have reduction methods in newly built homes. Such laws are assigned systematically to areas that are understood to have high values of indoor

radon. This article demonstrates that the boundaries of radon priority areas may vary, depending on the data set and methods used. We propose a table and a decision matrix to assist in choosing the most appropriate visual aid according to the purpose for which the map is to be used. We conclude that no single radon map is suitable to fit all objectives, and some maps are more suitable than others depending on the purpose.

Keywords: *indoor radon; radon maps; radon mapping objectives; spatial resolution; geogenic data.*

Citation: Journal of the European Radon Association 2022, **3**: 7586 http://dx.doi.org/10.35815/radon.v3.7586

Copyright: © 2022 M. Hughes et al. This is an Open Access article distributed under the terms of the Creative Commons Attribution-NonCommercial 4.0 International License (http://creativecommons.org/licenses/by-nc/4.0/), permitting all non-commercial use, distribution, and reproduction in any medium, provided the original work is properly cited.

Published: 04 March 2022

Competing interests and funding: The authors declare no potential conflicts of interest. This work has been financed by the Student Universal Support Ireland (SUSI) to MH.

*__Quentin G. Crowley__, Department of Geology, School of Natural Sciences, Trinity College, Dublin 2, Ireland. Email: crowleyq@tcd.ie

Mitigating the level of radioactive exposure to citizens has been the task of many countries for decades (2–4). The radioactive exposure mitigated against includes natural (e.g. radon) and anthropogenic (e.g. nuclear energy and medical x-rays) sources. This article focuses on the mapping and modelling of radon gas and its possible negative health effects on the general public, which accounts for approximately 50% of a person's radiation dose (5). Radon is a natural gas that poses a negligible health risk when outdoors, with radon concentrations in the order of 10's Bq m^{-3} (6). However, radon can accumulate inside dwellings and caves, typically from 100's Bq m^{-3} to 1,000's Bq m^{-3}, respectively (7, 8). Exposure to higher radon concentrations is linked to the development of health ailments, the most commonly recognized of which is lung cancer (9–14). Other diseases (e.g. skin cancer, non-Hodgkin's

lymphoma, stomach cancer and brain cancer) may be correlated with radon exposure, and any causative links are still under investigation (15–18).

Radon (Rn) is the largest contributor of natural radioactivity to the general public. The ^{222}Rn isotope is considered the primary radon risk source indoors (19–21) due to its relatively long half-life (i.e. 3.8 days). ^{222}Rn is commonly used indistinctly in the legislation, and the definitions of radon priority areas (RPAs) are based on this isotope. Therefore, we use this criterion in the text; however, another natural radon isotope that may pose a risk in particular circumstances is thoron (i.e. ^{220}Rn; half-life of 55.6 s), and it is attracting more attention with the development of the first thoron maps (22–24). ^{222}Rn, ^{220}Rn and their daughter products emit alpha particles, damaging lung tissue if inhaled (10, 25–27). ^{222}Rn and ^{220}Rn concentrations naturally vary geo-spatially, influenced by soil geochemistry, soil permeability and underlying geogenic factors (28–32). Furthermore, indoor radon (hereafter referred to as InRn) accumulation is also influenced by weather/climate, housing and occupancy characteristics (33–37).

The issue of radioactivity, including radon, is recognized by the European Union (EU), which has resulted in the development of an EU Directive (Basic

Safety Standards, BSS) that obliges member states to assign RPAs. The EU Directive aims to protect both individuals and the collective from radiation exposure (2). The aforementioned directive requires a National Radon Action Plan (NRAP) to be established, which addresses radon risk in water, domestic dwellings, public buildings and workplaces from radon ingress, whether from the soil, water or building materials. Furthermore, this directive requires that effective radon mitigation and prevention measures are established for new buildings. It legally binds the member states to identify areas where 'the radon concentration in a significant number of buildings is expected to exceed the relevant national reference level'. However, the definitions of 'a significant amount of buildings' and 'the reference level' are not clarified, allowing for different methods to be used. In turn, this can lead to radon risk maps, which are not directly comparable, and different evaluations needed to assess the success of each Action Plan (38).

Therefore, the Directive obligates EU member states to create radon maps where the spatial distribution of radon levels is presented. The radon maps are consequently useful for: (1) predicting regions with non-acceptable levels at home/workplace, (2) targeting public awareness, (3) estimating radiation

dose from radon and (4) studying the health effects of radon. The tools needed to achieve each objective may be different, and thus, different maps would be required simultaneously (39). The different types of radon hazard index maps should be distinguished to avoid confusion (40).

In Ireland, the 1997 Building Regulations state that high radon can occur in any part of the country (41). However, only buildings in high radon areas (HRA) are legally obliged to include mitigation measures in their construction, for example, a membrane and a subsurface radon extraction device (i.e. sump) should be provided. In other areas, a subsurface radon extraction device should be installed in case it needs to be activated at a future time. Other buildings do not have specific guidance in the 1997 regulations. In relation to gamma radiation for building materials, the Radiological Protection Act 1991 (42) states, in Regulation 67, that building materials should not emit more than 1 mSv of gamma radiation per year. Schedule 10 gives an indicative list of building materials with the potential to emit gamma radiation (42).

Building developers and employers in HRA are legally obliged to prevent, remediate and ensure that their buildings/workplaces are below the radon

reference level (hereafter referred to as RL). HRA receive priority regulation, which is necessary to reduce the harmful effects of natural radiation cost-effectively. The most recently established national RL decided by the EPA in Ireland should not exceed 300 Bq m^{-3} in homes as well as workplaces (42). Currently, the EPA decided a more conservative value, which, keeping with legislation, is 200 Bq m^{-3} for homes and 300 Bq m^{-3} for workplaces. As such, in Ireland, HRA for dwellings are defined as 'any area where it is predicted that 10% or more of homes will exceed the reference level of 200 Becquerels per cubic meter (Bq m^{-3})' (43). The initiatives to reduce radon from accumulating in a building could be considered a primary prevention method, whereas targeting public awareness and mitigation in HRA could be regarded as secondary and tertiary prevention measures.

Radon priority areas and mapping

RPAs signify areas that may have a higher radon risk than others. Such sites are prioritised for public awareness initiatives and are specially protected through the building regulations. RPAs are legally defined and can be determined using different data and criteria, which can lead to differing RPA boundaries in the same location (44). Without appropriate strategy and

communication, such discrepancies can lead to loss in fidelity of information, loss of credibility, and diminished public trust and interest.

Numerous methods have been used by different countries in Europe (Table 1). An in-depth report of natural radiation and the various techniques can be read in the European Atlas of Natural Radiation (45). The studies referred to in Table 1 utilize different concepts of radon risk, but all are valid. These concepts range from an area having a probability of InRn over the RL to the likelihood of developing lung cancer in a given region. In the following sections, we discuss the most relevant approaches.

Table 1. Various methods and resolutions of radon risk mapping seen from a selection of representative European countries

Country	Reference level	Objectives	Methods	Resolution	Reference
Austria	200 and 400 Bq m^{-3}	Divide the country into three classes,	Annual mean radon concentration	Administrative level (i.e. municipality)	(72)

Table 1. Various methods and resolutions of radon risk mapping seen from a selection of representative European countries

Country	Reference level	Objectives	Methods	Resolution	Reference
		that is, average annual concentration <200, 200–400 and > 400 Bq m^{-3}	in a standard situation Bayesian statistics, combining indoor radon measurements (standard situation) and geology	Geological classes (scale 1:500.000)	(73)
Belgium (Wallon region)	400 Bq m^{-3}	Percentage of dwellings above the RL taking into	Moving average between	1 km × 1 km	(74)

Table 1. Various methods and resolutions of radon risk mapping seen from a selection of representative European countries

Country	Reference level	Objectives	Methods	Resolution	Reference
United Kingdom	200 Bq m^{-3}	account geological information. Radon priority areas (RPA) when P[InRn > RL]≥1%	Percentage of houses above the RL taking into account geological information	Lognormal model, corrections to account for year-to-year and random variations (i.e. Bayesian statistics)	Grids 1 km × 1 km	(75–77)

Appendix C

Table 1. Various methods and resolutions of radon risk mapping seen from a selection of representative European countries

Country	Reference level	Objectives	Methods	Resolution	Reference
Norway	200 Bq m^{-3}	Percentage of houses above the RL based on indoor radon and geological information (bedrock and Quaternary geology). RPA when P[InRn > RL] ≥ 20%.	geological polygons according to local (polygon) statistics or national (class) statistics	Geological polygons	(51)
Ireland	200 Bq m^{-3}	Percentage of houses above	Lognormal model	Grids 10 × 10 km	(56)

Appendix C

Table 1. Various methods and resolutions of radon risk mapping seen from a selection of representative European countries

Country	Reference level	Objectives	Methods	Resolution	Reference
		the RL based solely on indoor radon measurements. RPA when P[InRn > R.L.] ≥ 10%			
	200 Bq m^{-3}	Percentage of houses above the RL based on indoor radon and geological information	Logistic regression model	Grids 1 × 1 km	(31)

Table 1. Various methods and resolutions of radon risk mapping seen from a selection of representative European countries

Country	Reference level	Objectives	Methods	Resolution	Reference
			(i.e. bedrock geology, Quaternary geology, subsoil permeability and soil permeability). RPA when P[lnRn > RL]≥10%		
-		Estimation of radon-related	Dose estimation based on	Administrative level (i.e.	(39)

Table 1. Various methods and resolutions of radon risk mapping seen from a selection of representative European countries

Country	Reference level	Objectives	Methods	Resolution	Reference
		lung cancer cases	average concentrations (i.e. block averages after ordinary kriging)	electoral division)	
Malta	100 Bq m^{-3}	Display the indoor radon concentration values	Average of geometric mean annual indoor radon gas concentration values for each	Grids 5 × 5 km	(78)

Table 1. Various methods and resolutions of radon risk mapping seen from a selection of representative European countries

Country	Reference level	Objectives	Methods	Resolution	Reference
			sampling point		

Average indoor radon values have been grouped to administrative levels, as seen for Austria and Ireland. Grids of 1 km^2 have been utilized in Belgium, the UK and Ireland. Austria and Norway used geological units. Several reference levels operate across the member states. These range from 100 Bq m^{-3} in Malta, 200 Bq m^{-3} in Ireland, Norway and the UK, and 400 Bq m^{-3} in Belgium. Adapted from Ref. (57).

Maps based on indoor radon measurements

Probabilistic map

This method uses the concept that a percentage of houses in a certain area does/does not exceed an RL. If more than a certain number (i.e. a threshold) of homes in the area are above the RL, then the site is deemed an RPA (44). For example, an InRn map of Switzerland assigned areas a percentage

representing the probability of exceeding the RL of 300 Bq m^{-3}, and the regions allocated with a higher rate are the RPAs (46).

Average concentration map

The concept of this method is that an area will have an average InRn value resulting from all of the InRn values for the zone. For example, Estonia averaged the InRn per administrative unit of communes to visualize the spatial distribution of InRn (47). Another example is Italy's map (48), which has determined the average InRn according to region. Austria and Switzerland have other examples where areas with a mean indoor value above the RL are deemed an RPA (44).

Radioactive dose map

This technique aims to map the distribution of the radioactive dose received by people in a zone. Furthermore, this approach seeks to correlate InRn exposure to the amount of radioactive exposure available to be received in an area. For example, the Slovak Republic deployed the method of converting the population-weighted arithmetic mean of the InRn measurements into an estimated radioactive dose for each district (49) and considered the different types of houses in this process.

Appendix C

Maps based solely on geogenic factors

Information on geogenic characteristics, such as geology, Quaternary geology, soil type, permeability, structural geology (faults and fractures) and aquifer type, has been utilized to improve the predictions of radon mapping (50, 51). Considering that radon arising from the earth is the primary source of InRn (4), understanding the spatial distribution and variation of geological factors is useful when mapping radon. Two main concepts are defined regarding the mapping of naturally available radon. The first concept is the Geogenic Radon Hazard Index (GRHI), which incorporates data of available geogenic entities. The second concept is the Geogenic Radon Potential (GRP), which is radon that is naturally available in an area and is mainly influenced by the soil properties, hydrology and geology (40). However, the use of GRP for radon mapping is more limited due to the availability of the necessary data; these concepts are discussed in detail in (40).

Radon potential maps

GRP mapping aims to define boundaries according to the availability of radon entering a building. The most commonly adopted method is the 'Czech method' (52), which collects *in situ* soil-gas radon and soil permeability

measurements. The combination of soil-gas radon information and soil permeability values results in a GRP, giving an index which represents the potential of finding elevated radon levels in a building on the surveyed site.

Spatial resolution of radon maps

Many different resolutions of radon maps have been used, each of which have their pros and cons.

Regular grids

Regular grids are used, for example 500 m^2 and 5 km^2 in Montenegro and 10 km^2 in Albania (53, 54). Many factors may be considered when deciding which size of a grid to use. For example, if creating a map using InRn data, the number of samples in a given area is incredibly relevant. Grids for rural areas may need to be larger to have a sufficient data set, whereas urban areas inherently have more InRn measurements, allowing for smaller grids to be used (53). Smaller grids are better at representing the high spatial variation of radon and should be preferentially used when the size of a data set allows it.

Administrative boundaries

In other cases, radon is mapped according to municipalities, counties or even electoral divisions (47–49, 55). In each case, the data for mapping radon risk are grouped within each boundary type. The chosen boundary type influences each map's outcome in a similar way that different grid sizes dictate the outcome. An advantage of this approach is that it is easier to engage the public to identify with an area. However, difficulties arise in mapping according to administrative boundaries, especially if using geogenic data. Using administrative boundaries for mapping makes it arduous to compare neighbouring countries when different methods and concepts are used, as is the case for all European countries (38).

Ireland as a case study

Maps based on indoor radon values

Probabilistic map

The legislative radon risk map in Ireland is a probabilistic map (56). It defines an area as radon prone if 10% or more of houses are above the RL (Fig. 1a). The probabilistic radon risk method is useful for defining areas that are generally more prone to radon. Since InRn measurements from private dwellings were used, it may be unsuitable for workplaces and other building

types due to the differences in radon behaviour in different building types (57). The advantage of using this mapping style is that measurements of InRn are used, allowing for a direct representation of an area's radon category status.

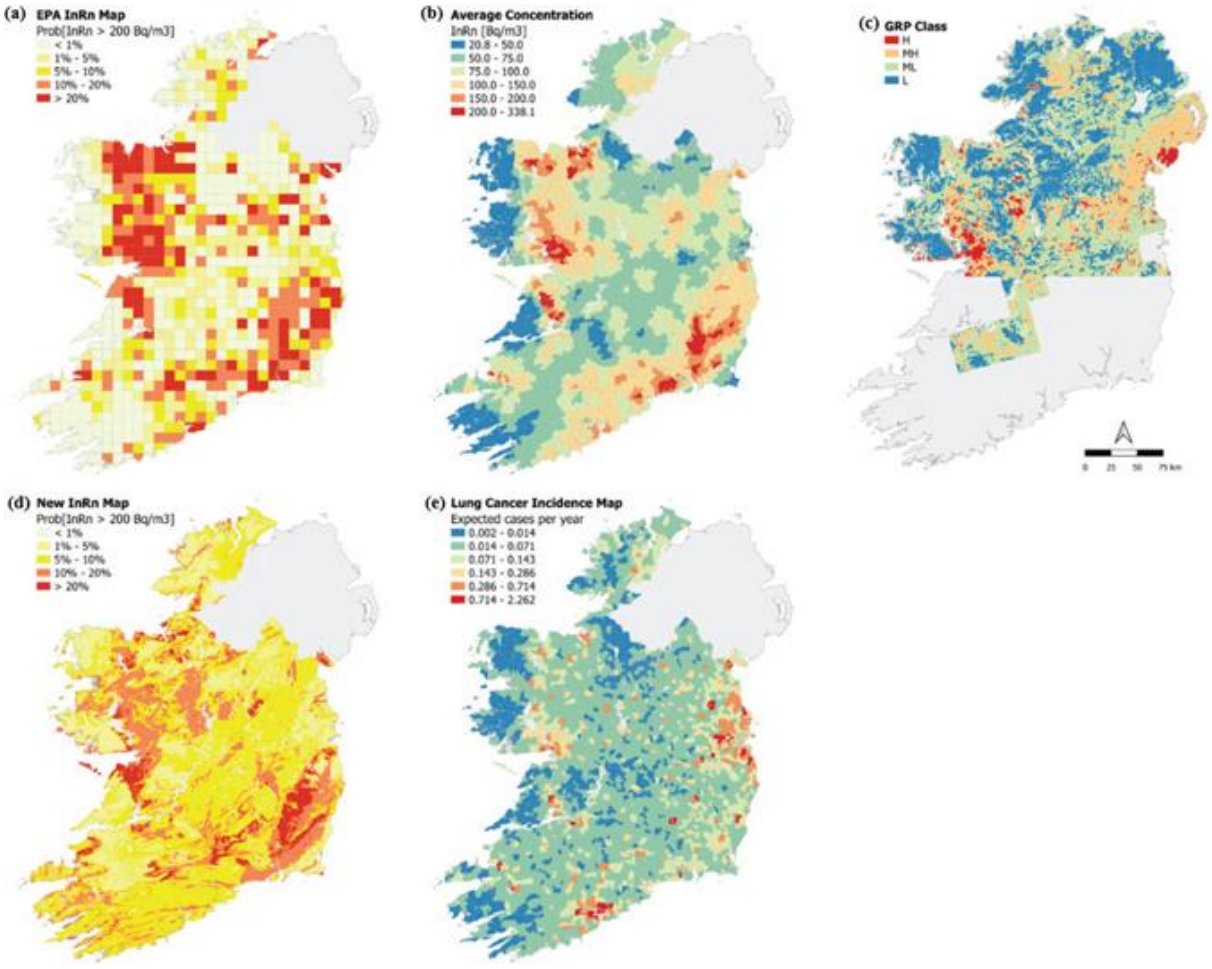

Fig. 1. (a) Legislative indoor radon probability map (56). (b) Indoor radon average concentration map (39). (c) Radon potential map (61). (d) Indoor radon probability map (31). (e) Radon-related modeled lung cancer incidence map (39).

Appendix C

The Irish Environmental Protection Agency (EPA) protocol for measuring indoor radon includes taking at least two measurements in two separate rooms of a house using a CR-39 detector over a 3-month measurement period. The results are then seasonally corrected to an annual average (58).

Average concentration map

The average concentration map illustrates the mean InRn level for an area [Fig. 1b (39)], allowing the map user to identify zones with higher radon levels. This helps to get an estimate of the typical InRn value for a specific area. Furthermore, this map is convenient for linking with health effects and epidemiological studies of lung cancer. An advantage of this map type is that it uses direct measurements of InRn, which allows for a true and accurate representation of the radon value in a given area. The mean InRn concentrations were collected from homes using the EPA protocol (58). Furthermore, the measurements were performed mainly from the ground floor of houses, and it is assumed that the results are representative of multistorey buildings (39).

Radon-related lung cancer cases

Appendix C

Maps made to include the radioactive dose due to radon allow for distinguishing areas based on the expected lung cancer incidence (39). In Ref. (39), two models were analysed, the first being a linear no-threshold model and the second being a dose-effect model, both of which resulted in similar numbers of estimated lung cancer cases (216–246, 257–249, 220–251 and 316–317 cases for the linear model and dose effect model, respectively). Comparable results, approximately 300 annual radon-related lung cancer cases were reported by presenters at Ireland's 14th and 15th National Radon Forum (59, 60). This mapping procedure targets the concept that lung cancer incident rates differ between areas. A map made using this method incorporated information on the population size and distribution [Fig. 1e (39)]. The resulting map may be useful for initiatives to reduce the long-term adverse health effects of radon exposure. Specifically, it could delineate areas designated as possessing a higher lung cancer incidence rate, therefore identifying where the collective population at a higher risk are situated. The main advantage is that the long-term aim of the radon action plan is targeted, which is to reduce the number of lung diseases resulting from Rn exposure. However, a disadvantage arises: high population areas are more likely to be designated as an RPA. As a result, this method would only be appropriate for

identifying larger populations at risk and is inappropriate for detecting individuals at high radon risk.

The radon-related lung cancer incidence was estimated over a lifetime of 70 years, and it is assumed that a person lives in the same place. Furthermore, the effect on smokers and non-smokers is assumed to be the same (39).

Adding geogenic data

Maps that integrate geological information utilize the fact that geology impacts radon values [Fig. 1d (31)]. Radon maps, which include geogenic data, are useful for improving mapping, especially in areas with a low amount of InRn data. Visual aids made using this methodology could also be practical for land redesignation in low populated areas. An advantage of this map type is that it employs information on the radon source and its pathway into a building. A drawback of using geogenic maps for radon mapping is that the geological maps scale may cause deviations of radon designation boundaries.

Maps based solely on geogenic factors

Radon potential map

Appendix C

The concept targeted by GRP maps is that the source and the pathway of radon gas determine the InRn risk. Such maps are useful for understanding the radon risk in any area. Advantages include that they are appropriate for any building type: workplace, public and domestic dwellings. These visual aids are also useful in low populated areas where there may be a lack of InRn data to make other radon risk map types. An example is shown in Fig. 1c (61).

Furthermore, *in situ* GRP surveys can be done rapidly at a local scale (62). It is important to note that the GRP map shown in Fig. 1c used a method that was created for a local scale and applied it to a regional/national scale, that is, the method was used differently from how it was designed. In theory, these maps are independent of building characteristics. However, the building characteristics do have an influence on the infiltration rate and behaviour of radon within a house (57, 63).

Spatial resolution

The boundaries of the radon risk categories on a map can change significantly depending on the spatial resolution used. Figure 2 demonstrates several probabilistic radon risk maps, with the only variable for sub-figures (a) to (f) being the spatial resolution. The probabilistic map is shown on the left side

of Fig. 2 [sourced from (31)]; it was created using lnRn data and several geogenic data sets. Distinctly, the addition of geogenic data reveals areas with higher radon, particularly in the southeast of County Dublin. The sub-figures (a) to (c) on Fig. 2 illustrate how different grid sizes (i.e. 1 km^2, 5 km^2 and 10 km^2, respectively) impact the radon categories despite the same input data lnRn being used. Noticeably, the 1 km^2 grid shows that there are areas in the north of County Dublin which have high lnRn values. The sub-figures (d) to (f) on Fig. 2 illustrate how radon categories for zones change according to spatial resolution (i.e. small areas, electoral divisions and county regions) despite the same input data (i.e. lnRn) being used. Importantly, smaller units allow for the spatial variability of radon be represented, which is essential for protecting individuals against high radon exposure.

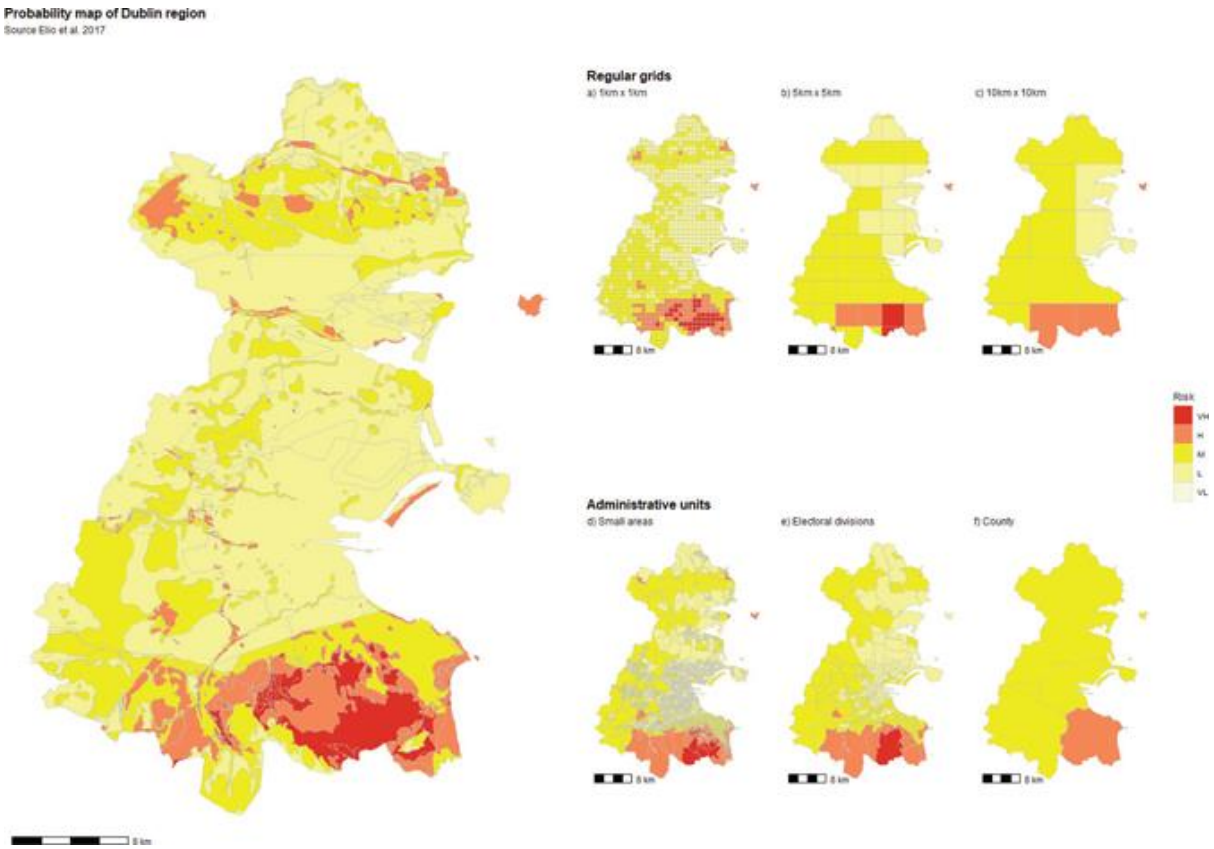

Fig. 2. Radon probabilistic map of County Dublin, Ireland. The various maps (a) to (f) in this figure have been made using the same input data. The spatial resolution varies between the maps. Maps (a) to (c) show how the radon probability boundaries change from grid sizes of 1 km^2, 5 km^2 and 10 km^2. Maps (d) to (f) show how the boundaries change depending on which administrative boundary is used, that is, small areas, electoral division and county region. For comparison, the large map of Dublin on the left is sourced from (31) and was created using both indoor radon data and several geogenic data types.

Appendix C

Regular boundaries

The benefit of using a 10 km^2 grid is that InRn data can be grouped, allowing for a more significant sample set, which is favourable for statistics. To elaborate, using larger grid sizes permits smaller areas with low-density data sets to be aggregated and assigned a category as opposed to being left blank. However, lower-resolution grids do not represent the high variability of radon within the area, that is, some parts of the grid may be more prone to radon. Even within a 10 km^2 area, radon concentrations can vary due to radon source variability and subsurface transportation routes (faults, fractures and soil permeability).

The use of smaller grids (i.e. 1 km^2) permits radon variability in any area to be represented more accurately. However, a high number of data points would be needed. This would be an issue in areas with a low population density. However, the need for large amounts of InRn data can be overcome by using alternative data sets, such as geogenic factors, for the models.

Administrative boundaries

Choosing to use administrative units for radon mapping makes it easier to link with other statistics (e.g. cancer registry and population density). This also

allows for better public awareness initiatives as it is easier to identify areas where people live.

As for the case with the gridded areas, larger administrative boundaries, such as municipalities or counties, make it easier to have a bigger sample set, which is more statistically favourable. In contrast, smaller areas (areas generally comprising between 80 and 120 dwellings) or Electoral Divisions in Ireland are better at representing the spatial variability of radon concentrations. However, in the latter, a higher density of data would be needed.

Overall, maps based on lnRn data are useful for targeting domestic dwellings that may be over the RL. Although the lnRn measurements taken decades ago may not still be representative of lnRn measures today, especially when the building style has changed, which impacts how radon accumulates inside. In contrast, radon maps based solely on geogenic data are more consistent through time because the geology in an area does not change for extended periods, although Geological Surveys may upgrade the geological maps when more information is available.

Discussion

Appendix C

It is important to mitigate against radon exposure, given that it accounts for the highest proportion of natural radioactivity to which the general public are exposed (5, 13). Maps as visual aids are a valuable resource and planning tool to prioritise certain areas to reduce radon exposure to citizens. However, choosing the most appropriate map is a complicated procedure that reflects the issues intricate nature. There are many factors to consider when deciding on a national or local radon mitigation strategy. These include if the purpose is to reduce Rn in workplaces, homes or public spaces, or if the aim is to reduce the resulting lung cancer incidence from Rn exposure. As well as considering the purpose of the strategy, the ease of using available data sets may be a determining factor on which map to use. Considering this intricacy, we attempt to make the decision process simpler by proposing a table (Table 2) and a decision matrix (Fig. 3) below.

Appendix C

Table 2. Summary of radon maps tabulated against several categories, including the cost-effectiveness and time efficiency, whether the variability of radon is captured at a local (<10 km^2) or large (≥10 km^2) scale, and if the radon map type considered the radon-induced lung-cancer incidence.

Map type	Cost-effective	Time effective	Captures Rn variability at a large scale (≥10 km^2)	Captures Rn variability at a local scale (<10 km^2)	Considers lung cancer incidence	Considers various lifestyles and building characteristics	Accurate individual measurements of indoor radon	Useful for protecting individuals	Useful for protected collective	Best suggest use
Indoor radon (Probability	N	N	Y	N	N	N	Y	Y depends on spatial	Y	(1) Identify people living

Appendix C

Table 2. Summary of radon maps tabulated against several categories, including the cost-effectiveness and time efficiency, whether the variability of radon is captured at a local (<10 km^2) or large (≥10 km^2) scale, and if the radon map type considered the radon-induced lung-cancer incidence.

Map type	Cost-effective	Time effective	Captures Rn variability at a large scale (≥10 km^2)	Captures Rn variability at a local scale (<10 km^2)	Considers lung cancer incidence	Considers various lifestyles and buildings characteristics	Accurate individual measurements of indoor radon	Useful for protecting individuals	Useful for protected collective	Best suggest use
reference level), for								resolution/data density		with high lnRn risk. (2)

Appendix C

Table 2. Summary of radon maps tabulated against several categories, including the cost-effectiveness and time efficiency, whether the variability of radon is captured at a local (<10 km^2) or large (≥10 km^2) scale, and if the radon map type considered the radon-induced lung-cancer incidence.

Map type	Cost-effective	Time effective	Captures Rn variability at a large scale (≥10 km^2)	Captures Rn variability at a local scale (<10 km^2)	Considers lung cancer incidence	Considers various lifestyles and buildings characteristics	Accurate individual measurements of indoor radon	Useful for protecting individuals	Useful for protected collective	Best suggested use
example, Fig. 1a										Assessment of remediation

Appendix C

Table 2. Summary of radon maps tabulated against several categories, including the cost-effectiveness and time efficiency, whether the variability of radon is captured at a local (<10 km^2) or large (≥10 km^2) scale, and if the radon map type considered the radon-induced lung-cancer incidence.

Map type	Cost-effective	Time effective	Captures Rn variability at a large scale (≥10 km^2)	Captures Rn variability at a local scale (<10 km^2)	Considers lung cancer incidence	Considers various lifestyles and buildings characteristics	Accurate individual measurements of indoor radon	Useful for protecting individuals	Useful for protected collective	Best suggest use effectiveness for homes. (3)

Appendix C

Table 2. Summary of radon maps tabulated against several categories, including the cost-effectiveness and time efficiency, whether the variability of radon is captured at a local (<10 km^2) or large (≥10 km^2) scale, and if the radon map type considered the radon-induced lung-cancer incidence.

Map type	Cost-effective	Time effective	Captures Rn variability at a large scale (≥10 km^2)	Captures Rn variability at a local scale (<10 km^2)	Considers lung cancer incidence	Considers various lifestyles and building characteristics	Accurate individual measurements of indoor radon	Useful for protecting individuals	Useful for protected collective	Best suggest ed use
Public communication										

Table 2. Summary of radon maps tabulated against several categories, including the cost-effectiveness and time efficiency, whether the variability of radon is captured at a local (<10 km^2) or large (≥10 km^2) scale, and if the radon map type considered the radon-induced lung-cancer incidence.

Map type	Cost-effective	Time effective	Captures Rn variability at a large scale (≥10 km^2)	Captures Rn variability at a local scale (<10 km^2)	Considers lung cancer incidence	Considers various lifestyles and building characteristics	Accurate individual measurements of indoor radon	Useful for protecting individuals	Useful for protected collective	Best suggested use initiatives.
Indoor radon	N	N	Y	Y dependent	N	N	Y	Y	Y	(1) Evaluate

Appendix C

Table 2. Summary of radon maps tabulated against several categories, including the cost-effectiveness and time efficiency, whether the variability of radon is captured at a local (<10 km^2) or large (≥10 km^2) scale, and if the radon map type considered the radon-induced lung-cancer incidence.

Map type	Cost-effective	Time effective	Captures Rn variability at a large scale (≥10 km^2)	Captures Rn variability at a local scale (<10 km^2)	Considers lung cancer incidence	Considers various lifestyles and buildings characteristics	Accurate individual measurements of indoor radon	Useful for protecting individuals	Useful for protecting collective	Best suggested use
(Annual average), for										health effects (e.g. lung

Appendix C

Table 2. Summary of radon maps tabulated against several categories, including the cost-effectiveness and time efficiency, whether the variability of radon is captured at a local (<10 km^2) or large (≥10 km^2) scale, and if the radon map type considered the radon-induced lung-cancer incidence.

Map type	Cost-effective	Time effective	Captures Rn variability at a large scale (≥10 km^2)	Captures Rn variability at a local scale (<10 km^2)	Considers lung cancer incidence	Considers various lifestyles and buildings characteristics	Accurate individual measurements of indoor radon	Useful for protecting individuals	Useful for protected collective	Best suggest use
example, Fig. 1b				set density						cancer) and detect potentia

Appendix C

Table 2. Summary of radon maps tabulated against several categories, including the cost-effectiveness and time efficiency, whether the variability of radon is captured at a local (<10 km^2) or large (≥10 km^2) scale, and if the radon map type considered the radon-induced lung-cancer incidence.

Map type	Cost-effective	Time effective	Captures Rn variability at a large scale (≥10 km^2)	Captures Rn variability at a local scale (<10 km^2)	Considers lung cancer incidence	Considers various lifestyles and building characteristics	Accurate individual measurements of indoor radon	Useful for protecting individuals	Useful for protected collective	Best suggest used areas with high collectiv

Appendix C

Table 2. Summary of radon maps tabulated against several categories, including the cost-effectiveness and time efficiency, whether the variability of radon is captured at a local (<10 km^2) or large (≥10 km^2) scale, and if the radon map type considered the radon-induced lung-cancer incidence.

Map type	Cost-effective	Time effective	Captures Rn variability at a large scale (≥10 km^2)	Captures Rn variability at a local scale (<10 km^2)	Considers lung cancer incidence	Considers various lifestyles and buildings characteristics	Accurate individual measurements of indoor radon	Useful for protecting individuals	Useful for protected collective	Best suggested use
										e doses. (2) Assessment of

Appendix C

Table 2. Summary of radon maps tabulated against several categories, including the cost-effectiveness and time efficiency, whether the variability of radon is captured at a local (<10 km^2) or large (≥10 km^2) scale, and if the radon map type considered the radon-induced lung-cancer incidence.

Map type	Cost-effective	Time effective	Captures Rn variability at a large scale (≥10 km^2)	Captures Rn variability at a local scale (<10 km^2)	Considers lung cancer incidence	Considers various lifestyles and building characteristics	Accurate individual measurements of indoor radon	Useful for protecting individuals	Useful for protected collective	Best suggested use
										remediation effectiveness for

Appendix C

Table 2. Summary of radon maps tabulated against several categories, including the cost-effectiveness and time efficiency, whether the variability of radon is captured at a local (<10 km^2) or large (≥10 km^2) scale, and if the radon map type considered the radon-induced lung-cancer incidence.

Map type	Cost-effective	Time effective	Captures Rn variability at a large scale (≥10 km^2)	Captures Rn variability at a local scale (<10 km^2)	Considers lung cancer incidence	Considers various lifestyles and buildings characteristics	Accurate individual measurements of indoor radon	Useful for protecting individuals	Useful for protected collective	Best suggest use
										homes. (3) Public commu

Appendix C

Table 2. Summary of radon maps tabulated against several categories, including the cost-effectiveness and time efficiency, whether the variability of radon is captured at a local (<10 km^2) or large (≥10 km^2) scale, and if the radon map type considered the radon-induced lung-cancer incidence.

Map type	Cost-effective	Time effective	Captures Rn variability at a large scale (≥10 km^2)	Captures Rn variability at a local scale (<10 km^2)	Considers lung cancer incidence	Considers various lifestyles and building characteristics	Accurate individual measurements of indoor radon	Useful for protecting individuals	Useful for protected collective	Best suggested use
										nication initiatives.

Appendix C

Table 2. Summary of radon maps tabulated against several categories, including the cost-effectiveness and time efficiency, whether the variability of radon is captured at a local (<10 km^2) or large (≥10 km^2) scale, and if the radon map type considered the radon-induced lung-cancer incidence.

Map type	Cost-effective	Time effective	Captures Rn variability at a large scale (≥10 km^2)	Captures Rn variability at a local scale (<10 km^2)	Considers lung cancer incidence	Considers various lifestyles and buildings characteristics	Accurate individual measurements of indoor radon	Useful for protecting individuals	Useful for protected collective	Best suggested use
Radon potential, for example	Y at local	Y at local	Y if data available	Y	N	N	N	Y depends on spatial	Y	(1) For Building regulations

Table 2. Summary of radon maps tabulated against several categories, including the cost-effectiveness and time efficiency, whether the variability of radon is captured at a local (<10 km^2) or large (≥10 km^2) scale, and if the radon map type considered the radon-induced lung-cancer incidence.

Map type	Cost-effective	Time effective	Captures Rn variability at a large scale (≥10 km^2)	Captures Rn variability at a local scale (<10 km^2)	Considers lung cancer incidence	Considers various lifestyles and building characteristics	Accurate individual measurements of indoor radon	Useful for protecting individuals	Useful for protecting collective	Best suggested use
e, Fig. 1c	scale	scale						resolution		reference. (2) Radon risk

Appendix C

Table 2. Summary of radon maps tabulated against several categories, including the cost-effectiveness and time efficiency, whether the variability of radon is captured at a local (<10 km^2) or large (≥10 km^2) scale, and if the radon map type considered the radon-induced lung-cancer incidence.

Map type	Cost-effective	Time effective	Captures Rn variability at a large scale (≥10 km^2)	Captures Rn variability at a local scale (<10 km^2)	Considers lung cancer incidence	Considers various lifestyles and buildings characteristics	Accurate individual measurements of indoor radon	Useful for protecting individuals	Useful for protecting collective	Best suggested use
										mapping regardless of

Appendix C

Table 2. Summary of radon maps tabulated against several categories, including the cost-effectiveness and time efficiency, whether the variability of radon is captured at a local (<10 km^2) or large (≥10 km^2) scale, and if the radon map type considered the radon-induced lung-cancer incidence.

Map type	Cost-effective	Time effective	Captures Rn variability at a large scale (≥10 km^2)	Captures Rn variability at a local scale (<10 km^2)	Considers lung cancer incidence	Considers various lifestyles and building characteristics	Accurate individual measurements of indoor radon	Useful for protecting individuals	Useful for protecting collective	Best suggested use
										building type. (3) Assessment of

Appendix C

Table 2. Summary of radon maps tabulated against several categories, including the cost-effectiveness and time efficiency, whether the variability of radon is captured at a local (<10 km^2) or large (≥10 km^2) scale, and if the radon map type considered the radon-induced lung-cancer incidence.

Map type	Cost-effective	Time effective	Captures Rn variability at a large scale (≥10 km^2)	Captures Rn variability at a local scale (<10 km^2)	Considers lung cancer incidence	Considers various lifestyles and buildings characteristics	Accurate individual measurements of indoor radon	Useful for protecting individuals	Useful for collective protecting	Best suggest used maps derived from

Appendix C

Table 2. Summary of radon maps tabulated against several categories, including the cost-effectiveness and time efficiency, whether the variability of radon is captured at a local (<10 km^2) or large (≥10 km^2) scale, and if the radon map type considered the radon-induced lung-cancer incidence.

Map type	Cost-effective	Time effective	Captures Rn variability at a large scale (≥10 km^2)	Captures Rn variability at a local scale (<10 km^2)	Considers lung cancer incidence	Considers various lifestyles and building characteristics	Accurate individual measurements of indoor radon	Useful for protecting individuals	Useful for protecting collective	Best suggested use
InRn and	Y if data	Y	Y	Y/N depe	N	N	Y	Y depend	Y	InRn data. (1) For Building

Table 2. Summary of radon maps tabulated against several categories, including the cost-effectiveness and time efficiency, whether the variability of radon is captured at a local (<10 km^2) or large (≥10 km^2) scale, and if the radon map type considered the radon-induced lung-cancer incidence.

Map type	Cost-effective	Time effective	Captures Rn variability at a large scale (≥10 km^2)	Captures Rn variability at a local scale (<10 km^2)	Considers lung cancer incidence	Considers various lifestyles and buildings characteristics	Accurate individual measurements of indoor radon	Useful for protecting individuals	Useful for protecting collective	Best suggested use
geogenic factors (bedro	available			nds				s on		regulations
				on				spatial		
				the				resoluti		referenc
				geolo				on		e. (2)

Appendix C

Table 2. Summary of radon maps tabulated against several categories, including the cost-effectiveness and time efficiency, whether the variability of radon is captured at a local (<10 km^2) or large (≥10 km^2) scale, and if the radon map type considered the radon-induced lung-cancer incidence.

Map type	Cost-effective	Time effective	Captures Rn variability at a large scale (≥10 km^2)	Captures Rn variability at a local scale (<10 km^2)	Considers lung cancer incidence	Considers various lifestyles and buildings characteristics	Accurate individual measurements of indoor radon	Useful for protecting individuals	Useful for protecting collective	Best suggested use
ck geology, aquifer				gical scale used.						Increase resolution of maps

Table 2. Summary of radon maps tabulated against several categories, including the cost-effectiveness and time efficiency, whether the variability of radon is captured at a local (<10 km^2) or large (≥10 km^2) scale, and if the radon map type considered the radon-induced lung-cancer incidence.

Map type	Cost-effective	Time effective	Captures Rn variability at a large scale (≥10 km^2)	Captures Rn variability at a local scale (<10 km^2)	Considers lung cancer incidence	Considers various lifestyles and buildings characteristics	Accurate individual measurements of indoor radon	Useful for protecting individuals	Useful for protecting collective	Best suggested use
types, E.U. airborne data										derived from InRn (i.e. probabil

Appendix C

Table 2. Summary of radon maps tabulated against several categories, including the cost-effectiveness and time efficiency, whether the variability of radon is captured at a local (<10 km^2) or large (≥10 km^2) scale, and if the radon map type considered the radon-induced lung-cancer incidence.

Map type	Cost-effective	Time effective	Captures Rn variability at a large scale (≥10 km^2)	Captures Rn variability at a local scale (<10 km^2)	Considers lung cancer incidence	Considers various lifestyles and building characteristics	Accurate individual measurements of indoor radon	Useful for protecting individuals	Useful for protecting collective	Best suggested use
– etc.), for example										ity and average InRn maps).

Table 2. Summary of radon maps tabulated against several categories, including the cost-effectiveness and time efficiency, whether the variability of radon is captured at a local (<10 km^2) or large (≥10 km^2) scale, and if the radon map type considered the radon-induced lung-cancer incidence.

Map type	Cost-effective	Time effective	Captures Rn variability at a large scale (≥10 km^2)	Captures Rn variability at a local scale (<10 km^2)	Considers lung cancer incidence	Considers various lifestyles and buildings characteristics	Accurate for individual measurements of indoor radon	Useful for protecting individuals	Useful for protected collective	Best suggest use
e, Fig. 1d										
Lung cancer	N	N	Y	Y	Y	N	Y	N	Y	(1) Long-

Appendix C

Table 2. Summary of radon maps tabulated against several categories, including the cost-effectiveness and time efficiency, whether the variability of radon is captured at a local (<10 km^2) or large (≥10 km^2) scale, and if the radon map type considered the radon-induced lung-cancer incidence.

Map type	Cost-effective	Time effective	Captures Rn variability at a large scale (≥10 km^2)	Captures Rn variability at a local scale (<10 km^2)	Considers lung cancer incidence	Considers various lifestyles and building characteristics	Accurate individual measurements of indoor radon	Useful for protecting individuals	Useful for protected collective	Best suggested use
incidence, for example										term radon action measure

Appendix C

Table 2. Summary of radon maps tabulated against several categories, including the cost-effectiveness and time efficiency, whether the variability of radon is captured at a local (<10 km^2) or large (≥10 km^2) scale, and if the radon map type considered the radon-induced lung-cancer incidence.

Map type	Cost-effective	Time effective	Captures Rn variability at a large scale (≥10 km^2)	Captures Rn variability at a local scale (<10 km^2)	Considers lung cancer incidence	Considers various lifestyles and buildings characteristics	Accurate individual measurements of indoor radon	Useful for protecting individuals	Useful for protecting collective	Best suggested use
e, Fig. 1e										s for reducing adverse

Appendix C

Table 2. Summary of radon maps tabulated against several categories, including the cost-effectiveness and time efficiency, whether the variability of radon is captured at a local (<10 km^2) or large (≥10 km^2) scale, and if the radon map type considered the radon-induced lung-cancer incidence.

Map type	Cost-effective	Time effective	Captures Rn variability at a large scale (≥10 km^2)	Captures Rn variability at a local scale (<10 km^2)	Considers lung cancer incidence	Considers various lifestyles and building characteristics	Accurate individual measurements of indoor radon	Useful for protecting individuals	Useful for protecting collective health effects (i.e. lung cancer).	Best suggested use

Appendix C

Table 2. Summary of radon maps tabulated against several categories, including the cost-effectiveness and time efficiency, whether the variability of radon is captured at a local (<10 km^2) or large (≥10 km^2) scale, and if the radon map type considered the radon-induced lung-cancer incidence.

Map type	Cost-effective	Time effective	Captures Rn variability at a large scale (≥10 km^2)	Captures Rn variability at a local scale (<10 km^2)	Considers lung cancer incidence	Considers various lifestyles and buildings characteristics	Accurate individual measurements of indoor radon	Useful for protecting individuals	Useful for protected collective	Best suggest use
(2) Public communication										

Appendix C

Table 2. Summary of radon maps tabulated against several categories, including the cost-effectiveness and time efficiency, whether the variability of radon is captured at a local (<10 km^2) or large (≥10 km^2) scale, and if the radon map type considered the radon-induced lung-cancer incidence.

Map type	Cost-effective	Time effective	Captures Rn variability at a large scale (≥10 km^2)	Captures Rn variability at a local scale (<10 km^2)	Considers lung cancer incidence	Considers various lifestyles and building characteristics	Accurate individual measurements of indoor radon	Useful for protecting individuals	Useful for protected collective initiatives	Best suggest use

Further, the maps are tabulated to highlight if building characteristics are considered and if indoor radon measurements are used to create the maps.

Appendix C

Table 2. Summary of radon maps tabulated against several categories, including the cost-effectiveness and time efficiency, whether the variability of radon is captured at a local (<10 km^2) or large (≥10 km^2) scale, and if the radon map type considered the radon-induced lung-cancer incidence.

Map type	Cost-effective	Time effective	Captures Rn variability at a large scale (≥10 km^2)	Captures Rn variability at a local scale (<10 km^2)	Considers lung cancer incidence	Considers various lifestyles and buildings characteristics	Accurate individual measurements of indoor radon	Useful for protecting individuals	Useful for protected collective	Best suggest use

The last several columns delineate if the maps are useful for protecting the collective. Lastly, the best-suggested use of each map is given in the final column. To clarify, the reference to 'spatial resolution' brings attention to how radon risk boundaries can change even if the grid size of the map

Appendix C

Table 2. Summary of radon maps tabulated against several categories, including the cost-effectiveness and time efficiency, whether the variability of radon is captured at a local (<10 km^2) or large (≥10 km^2) scale, and if the radon map type considered the radon-induced lung-cancer incidence.

Map type	Cost-effective	Time effective	Captures Rn variability at a large scale (≥10 km^2)	Captures Rn variability at a local scale (<10 km^2)	Considers lung cancer incidence	Considers various lifestyles and building characteristics	Accurate individual measurements of indoor radon	Useful for protecting individuals	Useful for protected collective	Best suggest use

changes. Reference to 'data density' highlights that there may be a lack of data for indoor radon at small scales, that is, in rural areas. Disclaimer: An example is given for each of the map types; however, the tabulation extends to other maps made with a similar process.

Appendix C

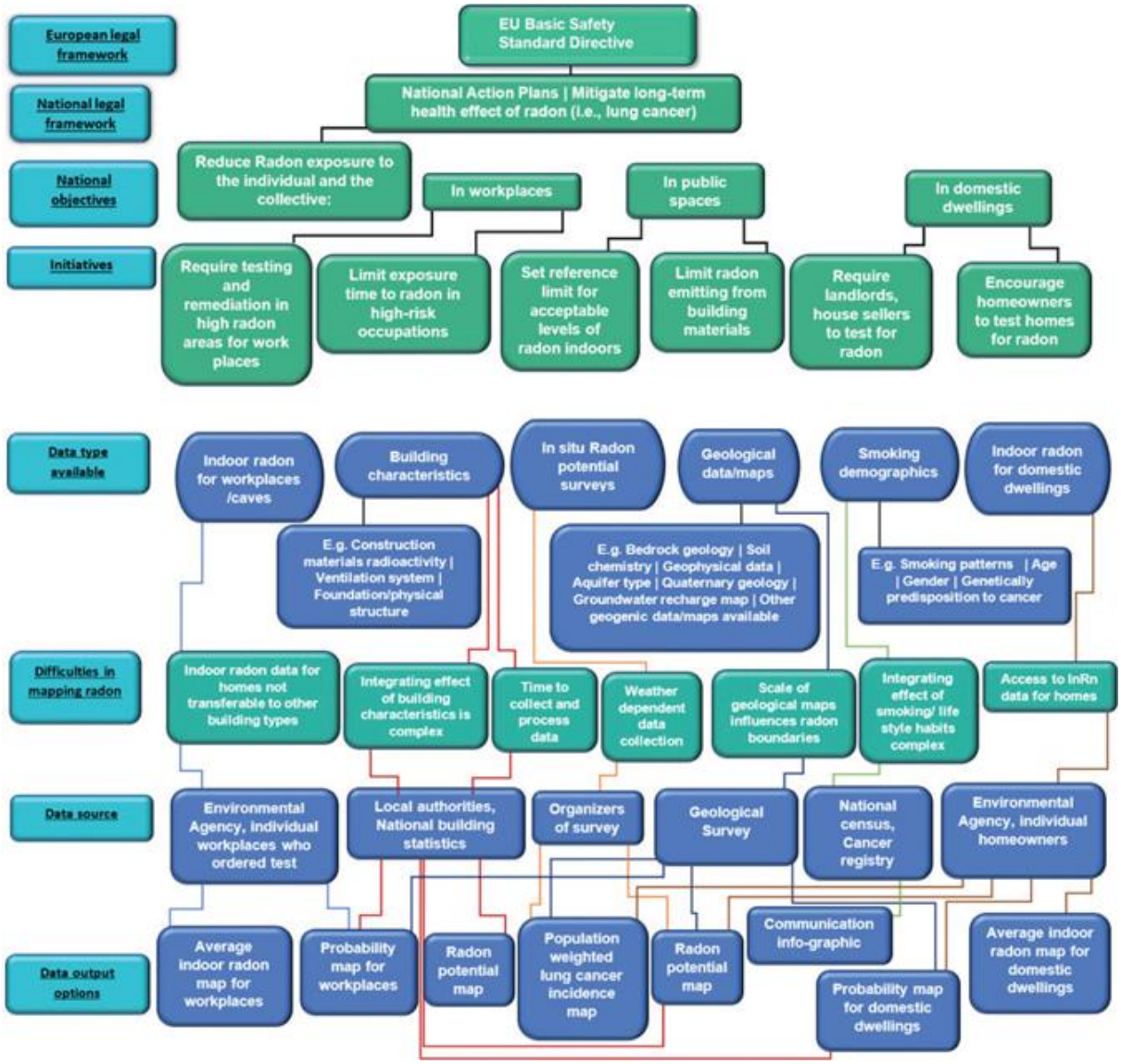

Fig. 3. Decision matrix to aid in choosing an appropriate radon map best suited to its purpose. Several frameworks and objectives, as well as initiatives, are indicated in the top half of the decision key. The bottom half gathers the range of data types available and how they are linked to the various data output options. Difficulties associated with and some potential sources of

each data group are given. The different coloured lines are simply to make the connections between categories easier to observe.

We propose a process, or method, to approach the task of deciding which visual aid to use based on (a) the purpose and (b) the available data.

In Table 2, the different Rn maps are tabulated according to time and cost-efficiency. We have indicated if each map type is representative at a local and large scale. Additionally, the suitability of the maps for protecting the collective or the individual is shown. The last column of Table 2 outlines the suggested use of each map type. The decision matrix (Fig. 3) simplifies the EU and national Rn mitigation objectives. These objectives are rationalized into several initiatives, available data sets and sources. Finally, considering the above counterparts, the output options are indicated for the data available.

The decision matrix, however, does not indicate the time and cost-efficiency of each option, although this is indicated in Table 2. Further difficulties are outlined in the decision matrix. Figure 3 does not capture that any data used may be updated over time, which could lead to discrepancies in the resulting maps. This issue could be accounted for by automating the process where the data set could be updated every few years or over a set amount of time.

Appendix C

Another disadvantage not depicted in Fig. 3 is that the accessibility to building characteristics may be difficult. The amount of time spent indoors and in different Rn areas has not been integrated into most of the reviewed maps. The exception is Fig. 1e, which assumes that the time spent indoors is 80% (39).

There is compelling evidence of a synergistic effect between radon and smoking in contributing to lung cancer development (64, 65). Smokers in high radon risk areas are more likely to develop lung cancer than smokers in low radon exposure areas (66, 67). Furthermore, (66) reported an 11% increase in lung cancer, with InRn increasing by 100 Bq m^{-3}. Hampson et al. (68) surveyed people regarding radon risk perception, noting that 32% of people knew little or nothing about radon. Butler et al. (69) suggested that people may perceive a higher risk of lung cancer when exposure to smoking and radon is combined. Such information (69) could prove vital in strategising more effective public outreach, engagement and respiratory health awareness programmes. Explicitly, it may be a practical approach to combine the public health initiative of smoking awareness with radon awareness.

Appendix C

Both smoking and radon exposure are systematic problems in respiratory health. However, the approaches for managing these two issues are compartmentalised. Public awareness regarding the risks related to tobacco smoking is extensive, whereas the risk awareness related to radon is relatively low. Considering that radon is the leading cause of lung cancer after smoking and the synergistic effect of developing lung cancer when smoking and radon exposure is combined, it may be beneficial to amalgamate these campaigns. Conceptualising smoking demographics onto a map may be challenging. However, it may be better to simultaneously communicate the effect of these two issues on respiratory health. Our lungs can be affected by radon as well as smoking. As such, incorporating this information would allow for a more holistic approach to combating respiratory health issues.

In some cases, this is starting to be done. For example, the World Health Organisation's International Agency for Research on Cancer (IARC) has developed an initiative implemented by the European Commission to inform people how to reduce cancer risk, which includes reducing exposure to radon (70). As part of the IARC initiative, the Irish Cancer Society has included radon on a public communication list of 12 ways to reduce cancer risk (71).

Appendix C

Conclusion

In this article, a review of some potential visual aids for radon mapping is made, focusing on Ireland's various radon maps already published. We have assumed that the indoor radon data were representative for mapping the target estimate (e.g. probability, average and collective dose) and that the maps were properly developed. In this sense, we do not discuss the methods of how maps are devised, but in how they are used.

Visual aids can make the decision process more manageable, considering where to target regulations or public awareness initiatives. The resources available and the radon map's purpose should be at the core of the decision process when deciding on a plan. Firstly, the spatial resolution can influence the map's outcome even if the same input data are used (Fig. 2). When considering spatial resolutions, a large scale is good for national-level initiatives, such as delineating RPAs for requiring workplaces to have radon barriers/sumps. A small/local spatial resolution would be useful for building developers or homeowners who want to remediate their homes.

Secondly, the different methods used do not map the same thing concerning radon exposure. For example, probabilistic maps aim to identify areas that

are more prone to InRn, while the average concentration radon maps aim to distinguish regions according to their mean concentration. These maps would help target radon awareness campaigns for individual homeowners. If the aim is to protect the collective and rank citizens' risk of developing radon-induced lung cancer, then choosing a lung cancer incidence map would be appropriate.

Finally, the GRP maps aim to provide information on the amount of soil-gas radon available to become InRn in the area, which is particularly useful for redesignating land or when constructing a new building. Depending on the purpose of which one wants a radon risk map to be used, one map type may be more favourable than the other, and one visual aid will not be appropriately suitable to fit all strategies.

References

1. Gaskin J, Coyle D, Whyte J, Krewksi D. Global estimate of lung cancer mortality attributable to residential radon. Environ Health Perspec 2018; 126: 057009. doi: 10.1289/EHP2503

2. European Commission. Council directive 2013/59/Euratom. Official Journal of the European Union 2013;2013/59/EURATOM. Publications Office of the European Union, Luxembourg.
3. United Nations Scientific Committee on the Effects of Atomic Radiation. Report of the United Nations Scientific Committee on the Effects of Atomic Radiation (UNSCEAR) 1958: Report to the General Assembly, with Scientific Annexes. 1958:229. United Nations, Vienna. https://doi.org/10.18356/0b0b1bc1-en.
4. World Health Organisation. International radon project survey on radon guidelines, programmes and activities. World Health Organisation, Geneva, 2007.
5. Monty C. UNSCEAR report 2000: sources and effects of ionizing radiation. J Radiol Protect 2000; 21. doi: 10.8/0952-4746/21/1/609
6. Gunning GA. Studies of radon in Ireland: Outdoor levels, detector intercomparison and school remediation methods, [thesis] Trinity College (Dublin, Ireland). School of Physics, 2016.
7. Darby S, Hill D, Auvinen A, Barros-Dios JM, Baysson H, Bochicchio F, et al. Radon in homes and risk of lung cancer: collaborative analysis of

individual data from 13 European case-control studies. BMJ 2005; 330: 223. doi: 10.1136/bmj.38308.477650.63

8. Duffy JT, Madden JS, Mackin GM, McGarry AT, Colgan PA. A reconnaissance survey of radon in show caves in Ireland. Environment International 1996; 22: 415–23. doi: 10.6/S0160-4120(96)00140-7
9. Kreuzer, M., Fenske, N., Schnelzer, M. and Walsh, L., Lung cancer risk at low radon exposure rates in German uranium miners. British journal of cancer 2015; 113: 1367–9. doi: 10.1038/bjc.2015.324
10. Lorenzo-González M, Torres-Durán M, Barbosa-Lorenzo R, Provencio-Pulla M, Barros-Dios JM, Ruano-Ravina A. Radon exposure: a major cause of lung cancer. Expert review of respiratory medicine 2019; 13: 839–50. doi: 10.1080/17476348.2019.1645599
11. Ludewig P, Lorenser E. Untersuchung der Grubenluft in den Schneeberger Gruben auf den Gehalt an Radiumemanation. Zeitschrift Für Physik 1924; 22: 178–85. doi: 10.1007/BF01328120
12. Vahakangas KH, Metcalf RA, Welsh JA, Bennett WP, Harris CC, Samet JM, et al. Mutations of p53 and ras genes in radon-associated lung cancer from uranium miners. The Lancet 1992; 339: 576–80. doi: 10.1016/0140-6736(92)90866-2

13. World Health Organisation. W.H.O Handbook on indoor radon: a public health perspective, World Health Organisation, Geneva, 2009.

14. Yarmoshenko IV, Malinovsky GP. Lung cancer mortality and radon exposure in Russia. Nukleonika 2016; 61: 263–8. doi: 10.1515/nuka-2016-0044

15. Ha M, Hwang S, Kang S, Park N-W, Chang B-U, Kim Y. Geographical correlations between indoor radon concentration and risks of lung cancer, non-Hodgkin's Lymphoma, and Leukemia during 1999–2008 in Korea. Int J Environ Res Public Health 2017; 14: 344. doi: 10.3390/ijerph14040344

16. López-Abente G, Núñez O, Fernández-Navarro P, Barros-Dios JM, Martín-Méndez I, Bel-Lan A, et al. Residential radon and cancer mortality in Galicia, Spain. Sci Total Environ 2018; 610–611: 1125–32. doi: 10.1016/j.scitotenv.2017.08.144

17. Monastero RN, Meliker JR. Incidence of brain and spinal cord cancer and county-level radon levels in New Jersey, Wisconsin, Minnesota, Pennsylvania, and Iowa, USA. Environ Geochem Health 2020; 42: 389–95. doi: 10.1007/s10653-019-00368-6

18. Ruano-Ravina A, Dacosta-Urbieta A, Miguel Barros-Dios J, T Kelsey K. Radon exposure and tumors of the central nervous system. Gaceta Sanitaria 2018; 32(6): 567–575. doi: 10.1016/j.gaceta.2017.01.002

19. Rosario AS, Wichmann H-E. Environmental pollutants | Radon. In: Laurent GJ, Shapiro SD, editors. Encyclopedia of respiratory medicine. Oxford: Academic Press, 2006, p. 120–5.

20. Schwela D. Pollution, indoor air. In: Wexler P, editor. Encyclopedia of toxicology. 3rd ed. Oxford: Academic Press, 2014; p. 1003–17.

21. Tommasino L. Radiochemical methods | Radon. In: Worsfold P, Townshend A, Poole C, editors. Encyclopedia of analytical science (2nd ed.). Oxford: Elsevier, 2005; p. 32–44.

22. Lucchetti C, Briganti A, Castelluccio M, Galli G, Santilli S, Soligo M, et al. Integrating radon and thoron flux data with gamma radiation mapping in radon-prone areas. The case of volcanic outcrops in a highly-urbanized city (Roma, Italy). J Environ Radioact 2019; 202: 41–50. doi: 10.1016/j.jenvrad.2019.02.004

23. Vuckovic B, Gulan L, Milenkovic B, Stajic JM, Milic G. Indoor radon and thoron concentrations in some towns of central and South Serbia. J

Environ Manage 2016; 183: 938–44. doi: 10.1016/j.jenvman.2016.09.053

24. Avinash PR, Rajesh S, Kerur BR, et al. Radon, thoron and their progeny concentration variations in dwellings of Gogi region, Yadgir district of Karnataka, India. J Radioanal Nucl Chem 302, 1321–1326, 2014. https://doi.org/10.1007/s10967-014-3608-x

25. Krewski D, Lubin JH, Zielinsk JM, Alavanja M, Catalan VS, Field RW, et al. Residential Radon and risk of lung cancer: a combined analysis of 7 North American case-control studies. Epidemiology 2019; 16(2): 137–45. doi: 10.1097/01.ede.0000152522.80261.e3

26. Samet JM. Radon and lung cancer. JNCI 1989; 81: 745–58. doi: 10.1093/jnci/81.10.745

27. Taylor JA, Watson MA, Devereux TR, Michels RY, Saccomanno G, Anderson M, et al. p53 mutation hotspot in radon-associated lung cancer. The Lancet 1994; 343: 86–7. doi: 10.1016/S0140-6736(94)90818-4

28. Je H-K, Kang C, Chon H-T. A preliminary study on soil–gas radon geochemistry according to different bedrock geology in Korea. Environ Geochem Health 1999; 21: 117–31. doi: 10.1023/A:1006613016217

29. Gallagher V, Knights KV, Carey S, Glennon M, Scanlon R. Atlas of topsoil geochemistry of the Northern Counties of Ireland: Data from the Tellus and Tellus border projects. Geological Survey of Ireland, Dublin, 2016.

30. Young ME, Knights KV, Smyth D, Glennon MM, Scanlon RP, Gallagher V. The Tellus geochemical surveys, results and applications. Unearthed: Impacts of the Tellus Surveys of the North of Ireland, Royal Irish Academy, Dublin, 2016; p. 33–52. doi: 10.3318/978-1-908996-88-6.ch3

31. Elío J, Crowley Q, Scanlon R, Hodgson J, Long S. Logistic regression model for detecting radon prone areas in Ireland. Sci Total Environ 2017; 181: 599–600. doi: 10.1016/j.scitotenv.2017.05.071

32. Ferreira A, Daraktchieva Z. Indoor radon measurements in south west England explained by topsoil and stream sediment geochemistry, airborne gamma-ray spectroscopy and geology. Elsevier J Environ Radioact 2018. doi: 10.1016/j.jenvrad.2016.05.007

33. Akbari K, Mahmoudi J, Ghanbari M. Influence of indoor air conditions on radon concentration in a detached house. J Environ Radioact 2013; 116: 166–73. doi: 10.1016/j.jenvrad.2012.08.013

34. Casal-Mouriño A, Ruano-Ravina A, Torres-Durán M, Parente-Lamelas I, Provencio-Pulla M, Castro-Añón O, et al. Lung cancer survival in never-

smokers and exposure to residential radon: results of the LCRINS study. Cancer Letters 2020; 487: 21–6. doi: 10.1016/j.canlet.2020.05.022

35. Lantz PM, Mendez D, Philbert MA. Radon, smoking, and lung cancer: the need to refocus radon control policy. Am J Publ Health 2013; 103: 443–7. doi: 10.2105/AJPH.2012.300926

36. Muntean LE, Cosma C, Cucos A, Dicu T, Moldovan DV. Assessment of annual and seasonal variation of indoor radon levels in dwelling houses from Alba County, Romania. Rom Journ Phys 2014; 59: 163–71.

37. Rigby JG, La Pointe DD. Wind and barometric pressure effects on radon in two mitigated houses. The 1993 international radon conference; p. 61–8, University of Nevada, Reno, 1993.

38. Tollefsen T, Cinelli G, Bossew P, Gruber V, De Cort M. From the European indoor radon map towards an atlas of natural radiation. Radiat Protect Dosim 2014; 162: 129–34. doi: 10.1093/rpd/ncu244

39. Elío J, Crowley Q, Scanlon R, Hodgson J, Zgaga L. Estimation of residential radon exposure and definition of Radon Priority Areas based on expected lung cancer incidence. Environ Int 2018; 114: 69–76. doi: 10.1016/j.envint.2018.02.025

40. Bossew P, Cinelli G, Ciotoli G, Crowley Q, Cort M, Elío J, et al. Development of a Geogenic Radon hazard index – concept, history, experiences. Int J Environ Res Publ Health 2020; 17: 4134. doi: 10.3390/ijerph17114134

41. Building Regulations. Building Regulations. Statutory Instruments No. 497 of 1997, Irish statute, Government of Ireland, Dublin, 1997.

42. Radiological Protection Act 1991 (Ionising Radiation) regulations. Statutory Instruments Ireland, S.I. No. 30 of 2019. Oireachtas, Government of Ireland, Dublin, 2019.

43. Environmental Protection Agency Ireland. Radon map: Environmental Protection Agency, Ireland. 2020. Available from: https://www.epa.ie/radiation/radonmap/ [cited 6 October 2021].

44. Bossew P. Radon Priority Areas – definition, estimation and uncertainty. Nucl Technol Radiat Protect 2018; 33: 11. doi: 10.2298/NTRP180515011B

45. Cinelli G, de C, Tollefsen T, (Eds.), European atlas of natural radiation, Publication Office of the European Union, Lexembourg, 2019.

46. Kropat G, Bochud F, Jaboyedoff M, Laedermann J-P, Murith C, Palacios M, et al. Major influencing factors of indoor radon concentrations in

Switzerland. J Environ Radioact 2014; 129: 7–22. doi: 10.1016/j.jenvrad.2013.11.010

47. Petersell V, Gustav Å. Radon risk Map of Estonia: explanatory text to the radon risk map set of Estonia at scale of 1: 500 000. Eesti Geoloogiakeskus, Tallinn, 2005

48. Bochicchio F, Campos-Venuti G, Piermattei S, Nuccetelli C, Risica S, Tommasino L, et al. Annual average and seasonal variations of residential radon concentration for all the Italian Regions. Radiat Meas 2005: 686–94. doi: 10.1016/j.radmeas.2004.12.023

49. Ministry of the Environment of Slovak Republic. State of the Environment. Report of the Slovak Republic, Bratislava, 2003.

50. Friedmann H, Baumgartner A, Bernreiter M, Gräser J, Gruber V, Kabrt F, et al. Indoor radon, geogenic radon surrogates and geology – investigations on their correlation. J Environ Radioact 2017; 166: 382–9. doi: 10.1016/j.jenvrad.2016.04.028

51. Watson RJ, Smethurst MA, Ganerød GV, Finne I, Rudjord AL. The use of mapped geology as a predictor of radon potential in Norway. J Environ Radioact 2017; 166: 341–54. doi: 10.1016/j.jenvrad.2016.05.031

52. Neznal M, Neznal M, Matolin M, Barnet I, Miksova J. The new method for assessing the radon risk of building sites. Czech Geological Institute, Prague, 2004.

53. Antovic N, Vukotic P, Zekic R, Svrkota R, Ilic R. Indoor radon concentrations in urban settlements on the Montenegrin Coast. Radiat Meas 2007; 42: 1573–9. doi: 10.1016/j.radmeas.2007.06.003

54. Tushe KB, Bylyku E, Xhixha G, Dhoqina P, Daci B, Cfarku F, et al. First step towards the geographical distribution of indoor radon in dwellings in Albania. Radiation protection dosimetry, Oxford University Press, Oxford, United Kingdom, 172, no. 4, 2016; p. 488–95.

55. Andersen CE, Ulbak K, Damkjær A, Gravesen P. Radon i danske boliger. Kortlægning Af Lands-, Amts-Og Kommuneværdier 2001. København : Sundhedsstyrelsen, Statens Institut for Strålehygiejne, 132 p.

56. Fennell SG, Mackin GM, Madden JS, McGarry AT, Duffy JT, O'colmain M, et al. Radon in dwellings: the Irish National Radon survey. Radiological Protection Institute of Ireland, Dublin, 2002.

57. Cinelli G, Tollefsen T, Bossew P, Gruber V, Bogucarskis K, De Felice L, et al. Digital version of the European Atlas of natural radiation. J Environ Radioact 2019; 196: 240–52. doi: 10.1016/j.jenvrad.2018.02.008

58. EPA. Environmental Protection Agency of Ireland Protocol for the measurement of radon in homes and workplaces, Environmental Protection Agency of Ireland, Wexford, 2019.

59. Hickey C. Setting the Scene. National Radon forum 2019. Department of Communications, Climate Action and Environment, Dublin, Ireland (DCCAE).

60. Walsh PM, National Cancer Registry, Environmental Protection Agency. A revision of the number of radon-related lung cancers in Ireland:National Radon Forum preliminary results, Wexford, 2017.

61. Elío J, Crowley Q, Scanlon R, Hodgson J, Long S, Cooper M, et al. Application of airborne radiometric surveys for large-scale geogenic radon potential classification. J Eur Radon Assoc 2020; 1. doi: 10.35815/radon.v1.4358

62. Elío J, Quentin C, Ray S, Jim H, Stephanie L. Rapid radon potential classification using soil-gas radon measurements in the Cooley Peninsula, County Louth, Ireland. Environmental Earth Sciences 2019; 78. doi: 10.1007/s12665-019-8339-4.1-16

63. Bossew P. Determination of radon prone areas by optimized binary classification. J Environ Radioact 2014; 129: 121–32. doi: 10.1016/j.jenvrad.2013.12.015

64. Leuraud K, Schnelzer M, Tomasek L, Hunter N, Timarche M, Grosche B, et al. Radon, smoking and lung cancer risk: results of a joint analysis of three European Case-control studies among Uranium miners. Radiat Res 2011; 176: 375–87. doi: 10.2307/41318201

65. Meenakshi C, Mohankumar MN. Synergistic effect of radon in blood cells of smokers – an in vitro study. Mutat Res: Genet Toxicol Environ Mutagen 2013; 757: 79–82. doi: 10.1016/j.mrgentox.2013.06.018

66. Li C, Wang C, Yu J, Fan Y, Liu D, Zhou W, et al. Residential Radon and histological types of lung cancer: a meta-analysis of case–control studies. Int J Environ Res Public Health 2020; 17: 1457. doi: 10.3390/ijerph17041457

67. Park EJ, Lee H, Kim HC, Sheen SS, Koh SB, Park KS, et al. Residential Radon exposure and cigarette smoking in association with lung cancer: a matched case-control study in Korea. Int J Environ Res Publ Health 2020; 17: 2946. doi: 10.3390/ijerph17082946

68. Hampson SE, Andrews JA, Lee ME, Foster LS, Glasgow RE, Liechtenstein E. Lay Understanding of synergistic risk: the case of Radon and cigarette smoking. Risk Analysis 1998; 18: 343–50. doi: 10.1111/j.1539-6924.1998.tb01300.x

69. Butler KM, Huntington-Moskos L, Rayens MK, Wiggins AT, Hahn EJ. Perceived synergistic risk for lung cancer after environmental report-back study on home exposure to tobacco smoke and Radon. Am J Health Promot 2018; 33: 597–600. doi: 10.1177/0890117118793886

70. World Health Organisation IA for R on C. The European Code Against Cancer, World Health Organisation, Geneva, Switzerland, 2016. https://www.europeancancerleagues.org/cancer-prevention-the-european-code-against-cancer/ [cited 6 October 2021].

71. Irish Cancer Society. 12 ways to reduce your risk of getting cancer 2016.

72. Friedmann H. Final results of the Austrian Radon Project. Health Physics 2005; 89: 339–48. doi: 10.1097/01.HP.0000167228.18113.27

73. Friedmann H, Gröller J. An approach to improve the Austrian Radon Potential Map by Bayesian statistics. Journal of Environmental Radioactivity 2010;101:804–8. doi: 10.1016/j.jenvrad.2009.11.008.

74. Cinelli G, Tondeur F, Dehandschutter B. Development of an indoor radon risk map of the Walloon region of Belgium, integrating geological information. Environ Earth Sci 2011; 62: 809–19. doi: 10.1007/s12665-010-0568-5

75. Daraktchieva Z, Appleton J, Reese D. Radon in Northern Ireland: indicative Atlas. Centre for Radiation, Chemical and Environmental Hazards, Public Health England, Oxfordshire, 2015.

76. Miles J. Calibration and standardisation of etched track detectors. Radon Measurements By Etched Track Detectors: Applications in Radiation Protection, Earth Sciences and the Environment, World Scientific, Singapore; 1997, p. 143–154. doi: 10.1142/9789812830197_0006

77. Miles JCH, Appleton JD, Rees DM, Green BMR, Adlam KAM, Myers AH. Indicative atlas of radon in England and Wales. Chilton, Oxon: Health Protection Agency, Government of the United Kingdom, Oxfordshire, 2007.

78. Baluci C, Vincenti K, Tilluck B, Conchin S, Formosa S, Grech D. National mapping survey of indoor radon levels in the Maltese Islands (2010–2011). Malta Medical Journal, Msida 2013.

Appendix C

Journal of Environmental Radioactivity

Volumes 251–252, October 2022, 106956

9.2 Using geogenic radon potential to assess radon priority area designation, a case study around Castleisland, Co. Kerry, Ireland

M.H.Banríon[a] J.Elío[b] Q.G.Crowley[a]

a Geology Department, School of Natural Sciences, Trinity College, Dublin 2, Ireland

b Department of Planning, Aalborg University Copenhagen, Copenhagen, Denmark

Received 16 February 2022, Revised 21 June 2022, Accepted 22 June 2022, Available online 30 June 2022, Version of Record 30 June 2022.

https://doi.org/10.1016/j.jenvrad.2022.106956Get rights and content

Under a Creative Commons license

Open access

Highlights

- Indoor radon risk can be rapidly modelled using geogenic radon mapping methods.
- Houses located near certain lithologies are susceptible to higher indoor radon.
- The methods in this study provide an alternative to modelling indoor radon risk.
- Geogenic data give insight to the source of Ireland's highest indoor radon value.

Abstract

Globally, indoor radon exposure is the leading cause of lung cancer in non-smokers and second most common cause after tobacco smoking. Soil-gas radon is the main contributor to indoor radon, but its spatial distribution is highly variable, which poses certain challenges for mapping and predicting radon anomalies. Measurement of indoor radon typically takes place over long periods of time (e.g. 3 months) and is seasonally adjusted to an annual

average concentration. In this article we investigate the suitability of using soil-gas radon and soil-permeability measurements for rapid radon risk assessments at local scale. The area of Castleisland, Co. Kerry was chosen as a case study due to availability of indoor radon data and the presence of significant radon anomalies. In total, 135 soil-gas and permeability measurements were collected and complemented with 180 indoor radon measurements for an identical 6 km^2 area. Both soil-gas and indoor radon concentrations ranged from very low (<10 $kBqm^{-3}$, 0.1 Bqm^{-3}) to anomalously high (>1433 $kBqm^{-3}$, 65,000 Bqm^{-3}) values. Our method classifies almost 50% of the area as a high radon potential area, and allows assessment of geogenic controls on radon distribution by including other geological variables. Cumulatively, the percentage of indoor radon variance explained by soil-gas radon concentration, bedrock geology, subsoil permeability and Quaternary geology is 34% (16%, 10%, 4% and 4% respectively). Soil-gas and indoor radon anomalies are associated with black shales, whereas the presence of karst and geological faults are other contributing factors. Sampling of radon soil-gas and soil permeability, used in conjunction with other geogenic data, can therefore facilitate rapid designation of radon priority areas. Such an approach demonstrates the usefulness of high-resolution geogenic maps in predicting indoor radon risk categories when compared to the application of indoor radon measurements alone. This method is particularly useful to assess radon potential in areas where indoor

radon measurements are sparse or lacking, with particular application to rural areas, land rezoned for residential use, or for sites prior to building construction.

Keywords

Radon

Geogenic radon map

Indoor radon

Soil-gas concentrations

Geology

Abbreviations

GRP

Geogenic Radon Potential

IRC

Indoor Radon Concentration

SGRn

Soil-Gas Radon

RPA

Radon Priority Area

1. Introduction

Appendix C

The global population receives its most significant proportion of natural ionizing radiation from radon exposure (Monty, 2000). The World Health Organization classifies radon as a class I carcinogen, and reports that it is the second leading cause of lung cancer after tobacco smoking, and the most common cause of lung cancer in non-smokers (World Health Organization, 2009). A study of 66 countries reported 226,057 total radon-attributed lung cancer deaths in 2012 (Gaskin et al., 2018). Annually in Ireland, approximately 350 people are estimated to develop radon-induced lung cancer (Fuente et al., 2020; Murphy et al., 2021). Typical 5-year survival rates from the time of diagnosis for lung cancer are 20% (National Cancer Registry Ireland, 2020). When identified, radon priority area (RPA) can be the focus for radon testing and remediation (Bossew, 2018), or they may be used as a geospatial parameter in targeted lung cancer screening programmes (Elío et al., 2018; Petermann et al., 2022). Any efforts which identify radon priority areas will help to reduce the lung cancer mortality in the general population.

Radon is a naturally occurring radioactive noble gas that emanates from rock, soil, and water. It is a dense, odourless and colourless gas. Radon (^{222}Rn) is an intermediate decay product in the ^{238}U decay chain. As uranium emits alpha particles, it transforms into a series of different isotopes before decaying to lead (^{206}Pb). The isotopes of ^{219}Rn (actinon) and ^{220}Rn (thoron) are

intermediate decay products of ^{235}U and ^{232}Th respectively. Radon concentrations in the atmosphere are generally low (typically 5 becquerels per cubic meter (Bqm^{-3})) (Barros et al., 2015; Gunning, 2016; Habib et al., 2018; Rafique et al., 2021). However, radon can occur at much higher concentrations in soil (typically 10's to 100's $kBqm^{-3}$) (Abdalla et al., 2021; Alonso et al., 2019), or enclosed spaces such as buildings and caves (typically 10's to 100's Bqm^{-3}) (Cucoş Dinu et al., 2017; Margineanu, 2019; Smith et al., 2019).

As radon decays over a short half-life (3.8 days), it emits alpha radiation (5.5909 MeV) as it transforms into polonium (^{218}Po and ^{214}Po). The short half-life of ^{218}Po and ^{214}Po (164.3µs and 3 min respectively) causes these isotopes to densely emit alpha radiation (energies of 6 MeV and 7.9 MeV respectively). The polonium isotopes, which are charged metal ions, can be inhaled either unattached or attached to airborne particulate matter. The polonium ions can become lodged in lung tissue and act as point sources of alpha radiation. For these reasons, there is a direct relationship between radon exposure and lung cancer (Marsh et al., 2021).

Globally, the detrimental health effects of radon exposure are recognized, and many countries have initiatives designed to mitigate these health issues (European Commission, 2013; Khan et al., 2019; United Nations Scientific

Committee on the Effects of Atomic Radiation, 2015). In Ireland, the national radon action plan is supported by the 'National Radon Control Strategy', 'Radon in workplaces', 'Gamma radiation from building materials', and 'Indoor exposure to radon in domestic dwellings' (Radiological Protection Act, 1991; Ionising Radiation Regulations, 2019). Of particular importance is the original radon risk map, which outlines areas of radon priority, with high radon areas defined as "any area where it is predicted that 10 percent or more of homes will exceed the reference level of 200 Becquerel per cubic metre (Bqm^{-3})" (Fennell et al., 2002). In high radon areas, new buildings are obliged to have preventative measures in place to reduce excessive radon accumulation. Furthermore, in areas deemed high radon risk, employers are obliged to measure for radon and if necessary, ensure that radon is below the reference level (Radiological Protection Act, 1991 (Ionizing Radiation) Regulations, 2019). Therefore, finding an effective method for defining high radon areas is crucial for radon mitigation (Bossew et al., 2020).

The original radon risk map of Ireland published by the Environmental Protection Agency (Fennell et al., 2002) has a 10 × 10 km^2 spatial resolution and is based exclusively on indoor radon concentration (IRC) (i.e. it does not contain any geological information). The Environmental Protection Agency in Ireland published an updated radon risk map in May 2022, which incorporates geogenic properties following the methodologies of Elío et al.

(2017), (Environmental Protection Agency, 2022). Importantly, the literature on radon and geology indicates a high spatial variability of soil-gas radon (SGRn), over areas far smaller than 10 × 10 km^2 (Duggal et al., 2014, Idriss et al., 2014; Ravikumar et al., 2015).

It is noteworthy that the greatest contributor to IRC is SGRn (Chen and Ford, 2017; World Health Organization, 2007). Porosity, soil permeability, structural geology and the pressure difference between the ground below the building and the indoor ground level, influences SGRn concentrations (Sun et al., 2004; Jelle 2012; Kulali et al., 2017; Laiolo et al., 2016). Both occupancy style, ventilation and building characteristics affect the radon concentrations within dwellings (Liping et al., 2016; Schubert et al., 2018). Additionally, the climatic and seasonal conditions affect the atmospheric pressure, wind speed, temperature, humidity and precipitation, which influence soil-gas radon accumulating indoors (Sundal et al., 2008; Xie et al., 2015).

Ireland's National Radon Control Strategy targets geographical regions deemed to be radon prone, i.e. High Radon Areas (HRA) or Radon Priority Areas (RPA). The National Radon Control Strategy second phase knowledge gaps report states that the national radon risk map may be improved by researching areas with anomalously high radon levels

associated with kartsified limestones particularly around Castleisland and Tralee in North Co. Kerry (National Radon Control Strategy, 2019). A specific area in Ireland was chosen as the focus of this study due to anomalous radon reported in the region, and the fact that it is underlain by karstified limestones. The study area is approximately 6 km^2 containing multiple geological units at a 1:100 K scale.

In this paper, the method of geogenic radon potential (GRP); a two-parameter method using SGRn and soil permeability measurements (Neznal et al., 2004), is assessed for suitability to identify radon-prone areas. Results are compared with the original radon map for Ireland (Fennell et al., 2002) and the updated EPA radon map of Ireland (Environmental Protection Agency, 2022). The approach for radon priority area assessment investigated in this study was tested for the townland of Castleisland, Co. Kerry, South-West Ireland (Fig. 1). This area was chosen considering one of Europe's highest, and Ireland's highest IRC measurement of 65,000 Bqm^{-3} was recorded here (seasonally adjusted average of multiple measurements of 49,000 Bqm^{-3}; Organo et al., 2004). Furthermore, the highest underground radon concentrations in Ireland were recorded in Crag Cave, Castleisland (11,285 Bqm^{-3}), during a reconnaissance survey of radon in three show caves in Ireland (Duffy et al., 1996). Approximately half of the study site is classified

as a high indoor radon area (Fig. 1) (Environmental Protection Agency, 2022; Fennell et al., 2002).

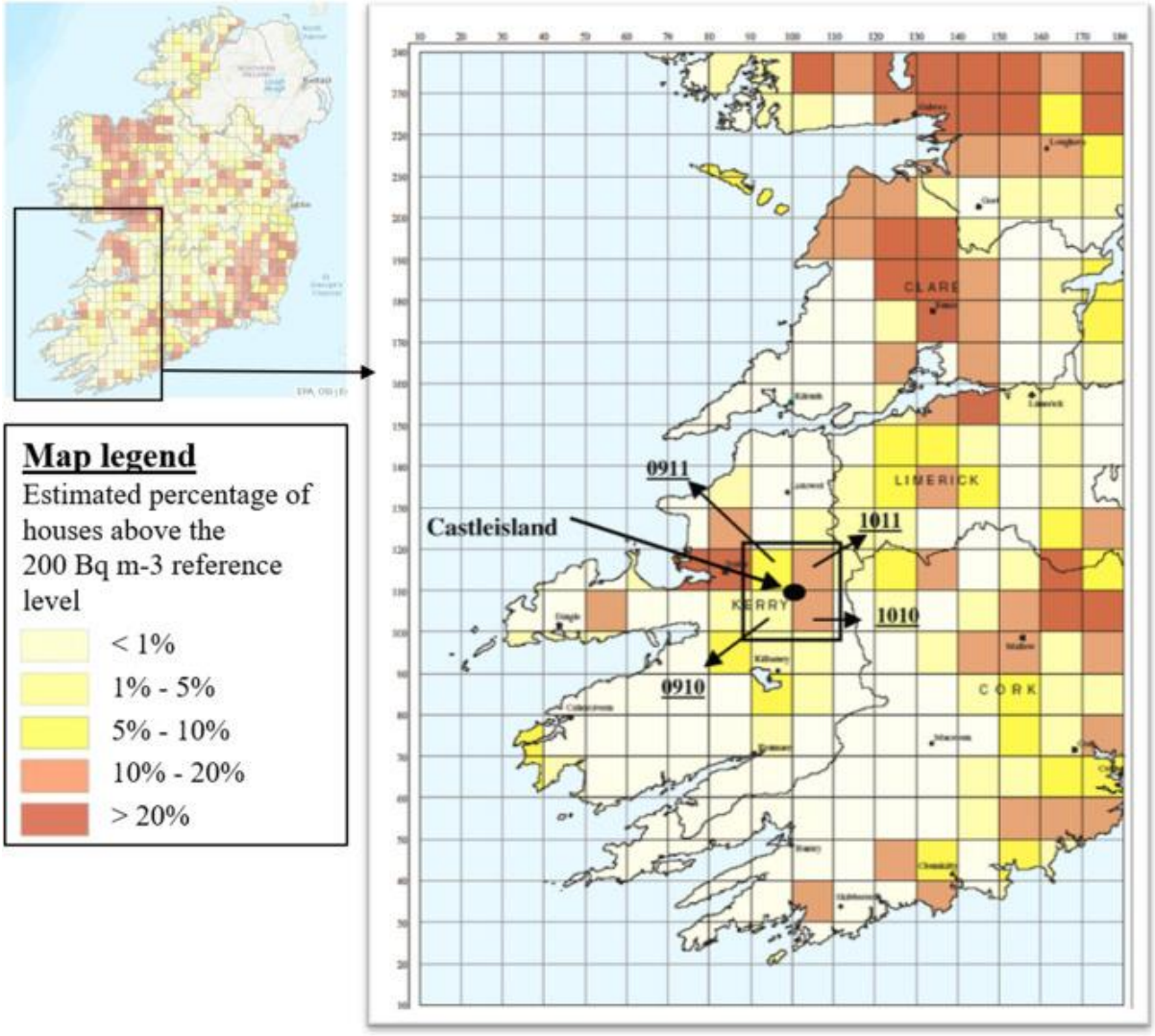

Fig. 1. Top left shows the Indoor radon map for Ireland (Fennell et al., 2002). The right map is adapted from (Organo and Murphy, 2007) which pinpoints the location of the Castleisland study area with consideration to Ireland's radon map. The grids are 10 × 10 km^2. The map legend shows the estimated percentage of homes likely to exceed the 200 Bqm^{-3} reference level.

Appendix C

The main aims of this study are to investigate the use of GRP as a means to assess radon risk and to compare the resultant risk maps with the original map which relies solely on IRC data (Fig. 1) and with the new EPA indoor radon map, which incorporates geological parameters (Environmental Protection Agency, 2022). The data analysis presented here illustrates strong evidence for the GRP method being a suitable process for estimating radon risk in this area. We present results that demonstrate a high spatial variability of radon and that a locally occurring lithology is a major contributor to the high IRC measurements in the Castleisland area. We suggest that radon gas utilizes faults and karst, and is transported from source to areas underlain by limestones. The scientific approach described in this study validates the feasibility for using geogenic data when assessing and defining radon priority areas, especially at local scales and in rural regions with a low population density and limited availability of indoor radon data.

2. Materials and methods

2.1. Study area

Upper Palaeozoic rocks form the bedrock geology of the Castleisland area (www.gsi.ie; Pracht, 1997). The primary bedrock type comprises various Dinantian (359 Ma – 326 Ma) limestones (un-bedded, bedded, bioclastic, argillaceous). The limestones formed in an open water sub-tidal

zone on the continental shelf (Sleeman et al., 2004). The north of the study area is dominated by carboniferous siltstones (Cloone Flagstones) and Namurian (326 Ma – 313 Ma) Clare Shales (Pracht, 1997).

The shales accumulated in deep basins which formed after faulting caused by the Variscan orogeny (Sleeman et al., 2004). The Clare Shales are black shales, formed in a deep water euxinic paleoenvironment 326 Ma to 313 Ma overlying Viséan (346.7 Ma to 330.9 Ma) limestones (Hodson, 1954; Rider, 1974; Wignall and Best, 2000). Substantial concentrations (mean 10's to 100's mg kg) of uranium are frequently reported to be contained within black shales (Lecomte et al., 2017; Soesoo et al., 2020). Elevated levels of uranium in organic rich black shales can be attributed to abiotic sequestering or symbiotic remediation processes, i.e. bacteria utilizing uranium for their growth while converting the mobile U(VI) to the immobile U(IV) (Anderson et al., 2003; Gadd, 2010; Koribanics et al., 2015; Min et al., 2005). In abiotic terms, uranium occurs in elevated concentrations in uranyl tricarbonate form, while anoxic conditions cause the uranium to present in higher concentrations as uranyl carbonate species, which allows for dissolved U(VI) to precipitate as U(IV) (Nagarajan et al., 2007; Hyun et al., 2014). It is important to note that not all shales are formed in anoxic environments, and that shales inherently vary in their uranium concentration.

Appendix C

Geologically, Castleisland is located at, what is conventionally considered, the northern edge of the Variscan orogeny in Ireland, which caused large-amplitude folds during the late Carboniferous and early Permian periods (Sleeman et al., 2004). Primary structural features of the study area resulted from the Variscan orogeny (Pracht, 1997; Thornton, 1966), including an east-west anticlinal axial plane approximately 1 km to the south. The main faults are directed NS and NW-SE (Fig. 3). The limestone is extensively karstified, exhibiting sinkholes, springs and dolines (www.gsi.ie) and resulting in caves spanning 100's m^2 (Gunn, 1982). Streams in Crag cave (200 m east of the study area) have a north to south flow direction (Tooth and Fairchild, 2003).

Quaternary glaciations affected the area resulting in predominantly locally derived glacial till (Sleeman et al., 2004). Quaternary sediments consist of till derived from Namurian sandstones, siltstones, and shales in the north of the area and till derived from limestones in the south, with alluvium also present in the south.

The exact location of the study area was decided utilizing available information on regional geology (www.gsi.ie). Fig. 2 depicts the study area sampling grid superimposed on geological maps for the area. The grid acted as an aid to collect samples in an equal spatial pattern as much as possible

(Fig. 2). In some scenarios it was not possible to collect data at certain locations due to a variety of reasons including the depth to bedrock being too shallow, or where the subsoil was too impermeable to obtain a measurement for GRP calculation. Furthermore, samples were not collected on artificial land (e.g. landscaped gardens). For these reasons, there are a lack of samples on the south-east of the map (Fig. 2) which correlates with the townland of Castleisland Co. Kerry.

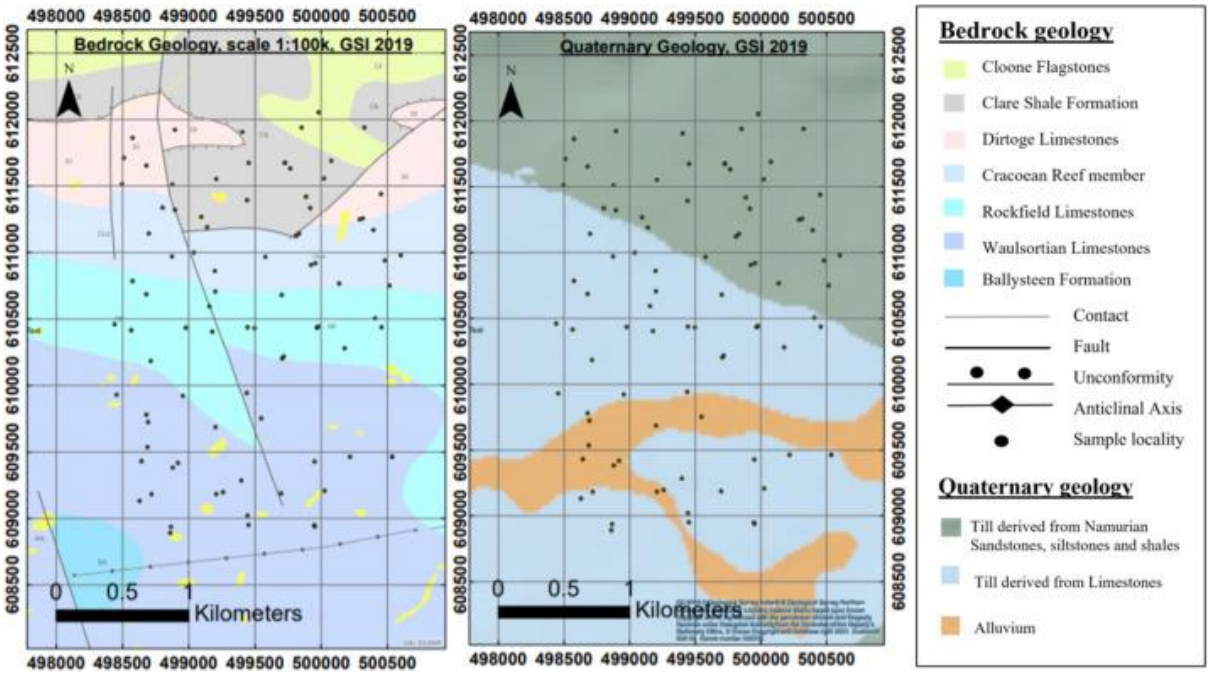

Fig. 2. Illustration of how the sample area was chosen to include a range of geogenic features. The coordinate system used is the Irish Time Mercator (ITM). (a) Bedrock geology 1:100 k scale G.S.I. 2019. (b) Quaternary geology map 1:50 k G.S.I. The points on each map represent the data sample collection locations. The small text at the bottom right side of the Quaternary map reads "CC-BY 4.0 Geological Survey Ireland & Geological Survey Northern Ireland. This publication contains material that is based upon Crown Copyright and is

reproduced with the permission of Land and Property Services under Delegated Authority from the Controller of Her Majesty's Stationary Office, © Crown Copyright and database right 2017. Customer ID4104. Permit number 100132.”.

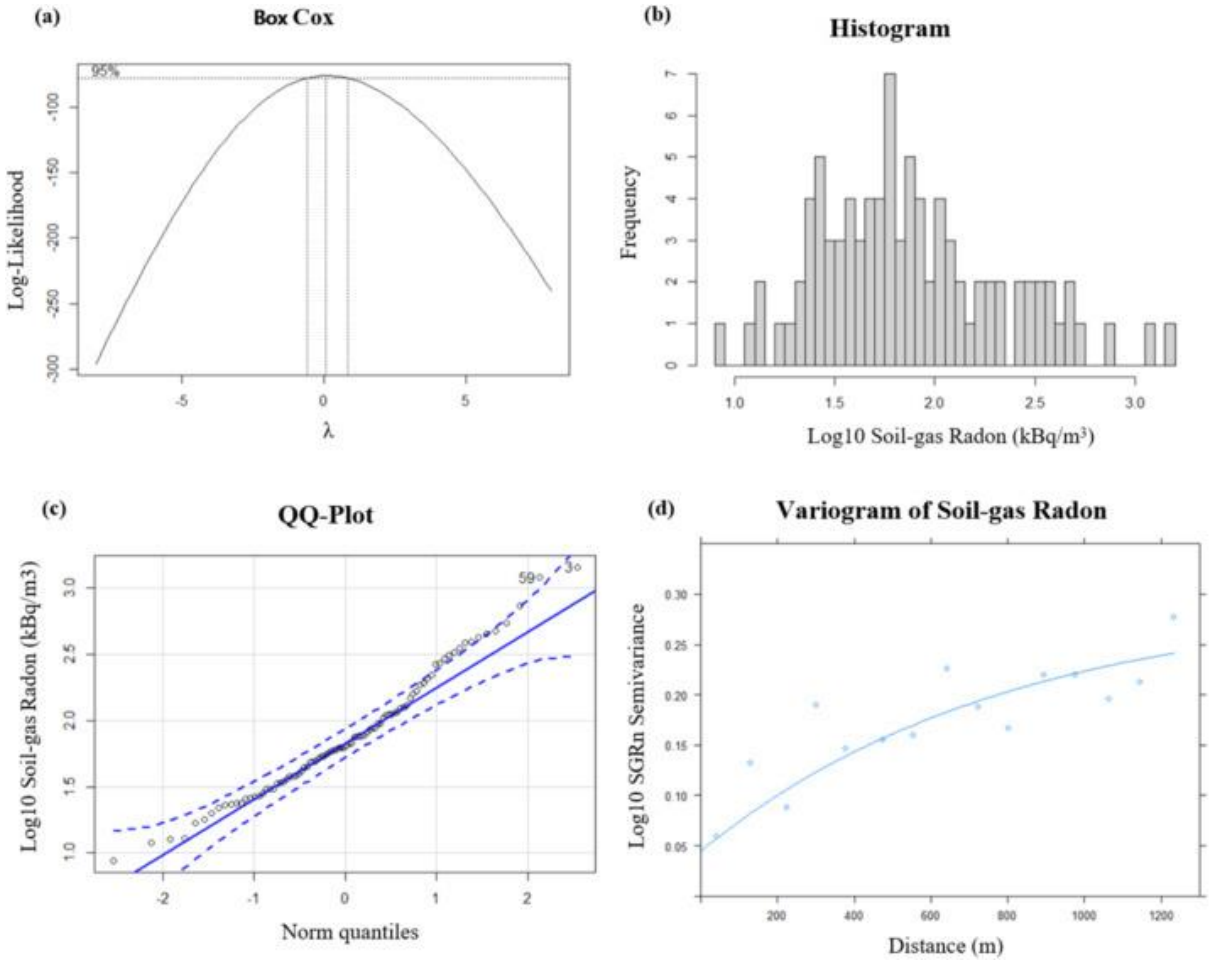

Fig. 3. (a) BoxCox (b) Histogram (c) QQ-Plot and (d) Variogram. The variogram (d) uses the “Exp” model with a nugget of 0.045, range of 800 m and psill of 0.25. of Log10 transformed soil-gas radon.

2.2. Subsoil permeability measurements

Subsoil permeability measurements were collected using a Radon-Jok device which forms part of the well-established, standardized method (Neznal et al., 2004). A 1-m hollow tube, with a ‘lost tip’ attached to the bottom, was

hammered vertically into the soil, and the tip was ejected at 80 cm to permit the extraction of a soil-gas sample. The hollow tube was connected to the Radon-Jok device using a rubber tube. The Radon-Jok device was activated, and the time to extract 2-L of air from the subsoil was recorded. In cases of lower permeability, one or two weights were attached to the Radon-Jok device in order to reduce the amount of time taken to extract an air sample from the subsurface. The theory of calculating permeability using the Radon-Jok instrument is derived from Darcy's equation:(1)$Q = F.\ (k\mu).\ \Delta p$, rearranged as $k = (Q.\ \mu)/(F.\ \Delta p)$Where: k is the permeability (in m^2), F is the shape factor (0.159 m for Radon-Jok), Q is the flow rate (m^3/s Δp is the pressure difference (Pa), and μ is the dynamic viscosity of air (1.75×10^{-5} Pa s @ 10C). Q is calculated from the time taken to fill the 2-L volume of the diaphragm. The pressure is provided by none, one or two weights, applying a pressure of 0, 2160 or 3750 Pa, respectively (Neznal et al., 2004).

2.3. Soil-gas measurements

In total, 135 SGRn samples were collected, including duplicate samples. Ninety-five of these were collected between the July 14, – July 22, 2018. The remaining 40 samples were collected between July 30, – August 2, 2019. In 2019, four samples were collected from control points over the collection period. In 2018, a total of 12 samples were collected from control points over the collection period. These duplicate samples were taken to assess any

change in measurement due to atmospheric variability or daily weather fluctuations. In the 2018 field survey, 23 extra samples were collected in the north of the field study, due to a significant radon anomaly. Eight samples were incomplete due to either failure in obtaining permeability readings or soil-gas to sample. These additional, failed and control samples were removed from the dataset for geostatistical analysis to avoid biasing of results. The data analysis included 88 samples in total.

Soil gas was extracted and soil radon concentrations were measured following the procedure of (Neznal et al., 2004). The same hollow tube set-up was used for the subsoil permeability samples to measure the SGRn. A 150 ml syringe was attached to the hollow tube to extract the soil-gas sample. The first two 150 ml samples were discarded to purge the pipe of any atmospheric air. The third sample was transferred into a 250 ml pre-vacuumed ionization chamber. The chamber pressure was equalised to the atmospheric pressure by introducing 100 ml of atmospheric air (atmospheric air contains negligible radon concentrations, typically less than 10 Bqm^{-3}) (Gunning, 2016). Variables of moisture content and particulate matter were mitigated by attaching an interface with a desiccant compartment (containing anhydrous calcium sulphate) and a 0.45 µm filter between the hollow tube and syringe. An RM-2 device was used

to measure radon concentration within the soil-gas, 15 min after the sample was introduced into the chamber.

The lower and upper detection limit of the RM-2 device is 3 $kBqm^{-3}$ and 1400 $kBqm^{-3}$, respectively. The radon concentration uncertainty is represented by sigma(σ), where sigma (σ) is 0.33 x(concentration of radon ($kBqm^{-3}$))$^{0.5}$, which results in the radon concentration being reported as concentration of radon±sigma. Therefore, the RM-2 device has a radon concentration measurement uncertainty of less than 20%. Elío et al. (2019) reported an average relative standard deviation of 15% for replicate samples and an average 5.75% uncertainty for the same RM-2 device.

2.4. Geogenic radon potential calculation

We used the geogenic radon potential G(RP) index as defined by (Neznal et al., 2004). The equation for which is:(2)GRP = *CRn* / (–log10 (*k*) – 10)Where *k* (m^2) is the soil permeability and CRn is the concentration of radon ($kBqm^{-3}$) in the soil-gas. This method uses both SGRn concentrations ($kBqm^{-3}$) and subsoil permeability measurements (m^2) and outputs a value representing GRP. The calculated GRP is conventionally reported without a unit because it is a categorical and relative value which represents the potential of radon gas entering a building. In order to facilitate comparison with other countries, GRP categories were chosen to reflect those

most commonly used, which are 0–10, 10–35 and 35+, corresponding to low, medium and high values respectively. The GRP method as originally defined (Neznal et al., 2004) utilizes at least 15 for a site less or equal to 800 m^2, otherwise individual SGRn and *k* samples are collected in a 10 × 10 m grid for a specific location (e.g. the area corresponding to a new building). The general GRP method of Neznal et al. (2004) has been adapted for different applications, for instance some studies in Germany use two measurements within a given sample site (Kemski et al., 1996), in other studies there is one sample per location (Singh et al., 2010). Additional differences in methodologies include some studies which use the maximum GRP and others use the median value (Günay et al., 2018; Kemski et al., 2001). In this study CRn and k measurements were taken at an approximate distribution every 250 m over a grid spacing, depending on subsoil depth and anthropogenic factors such as modification of soil profiles, or building developments. The GRP values derived from the in-situ measurements were interpolated using an inverse distance weighted kriging method with a resolution of 9 m in ArcGIS (Fig. 5b).

2.5. Indoor radon measurements

The Environmental Protection Agency (EPA) of Ireland provided the indoor radon measurements (IRC) under a specific data sharing agreement. The IRC measurements were collected between 1992 and 2017 by the

Radiological Protection Institute of Ireland; this was accomplished by placing two CR-39 detectors in separate ground floor rooms for a period between three and twelve months (Fennell et al., 2002). Measurements taken over a period less than twelve months were seasonally adjusted to give an average final measurement for each dwelling; this is necessary as radon concentrations vary seasonally (Muntean et al., 2014; Organo and Murphy, 2007). For the specific study site, an IRC of 49,000 Bqm^{-3} was added to the EPA dataset with the coordinates obtained from a now-demolished house during the field survey. The spatial distribution of IRC measurements was corrected by 40 m south and 30 m east to align with their actual geographical location (Dardac, 2022), due to a formatting error in the original dataset as supplied by the EPA.

3. Results

3.1. SGRn measurements

SGRn measurements from the study site range from 8.8 $kBqm^{-3}$ (s1031) to >1433 $kBqm^{-3}$ (s109). The highest measured value of >1433 $kBqm^{-3}$ is higher than the certified detection limit of the RM-2 device, so represents a minimum value. One percent of values are very low (<10 $kBqm^{-3}$), 17% of values are low (10–30 $kBqm^{-3}$), 18% of values are moderate (30–50 $kBqm^{-3}$), 15% of values are high (50–70 $kBqm^{-3}$), 13% of values are very high (70–100

kBqm^{-3}), and 36% of values are extremely high (+100 kBqm^{-3}) (Supplementary materials). The dataset used for analysis was log10 transformed (Fig. 3). The variogram (Fig. 3d) shows that the spatial variation at a local scale is very high, with the variation levelling at 700 m. The variogram model has a nugget effect of 0.001. The sill is 0.175, model "Sph" and range 800 m.

The daily repeats give an estimate of the cumulative measurement uncertainties plus the natural variability in soil-gas radon over relatively short time scales (i.e. days). The instrument is estimated to have a ± 20% uncertainty range, as previously determined by the manufacturer and by Elío et al. (2019). We measured between 2% and 6.8% variation from each of our four daily repeat sites, which is accounted for by the instrument measurement uncertainty (Table 1).

Table 1. Daily repeats of SGRn measurements in two localities in 2018 and 2019.

Locality ID	Date	Replica	Rn(kBqm^{-3})	Mean (kBqm^{-3})	RSD (%)	RM-2 uncertainty (%)
60	July 14, 2018	A	408	438.4	9.6	6.8
	July 15, 2018	B	462			
	July 19, 2018	C	460			
	July 20, 2018	D	488			

Appendix C

Locality ID	Date	Replica	Rn(kBqm^{-3})	Mean (kBqm^{-3})	RSD (%)	RM-2 uncertainty (%)
	July 21, 2018	E	374			
23	July 16, 2018	A	59.8	33.7	37.2	2.0
	July 17, 2018	B	22.2			
	July 18, 2018	C	27.6			
	July 19, 2018	D	27.4			
	July 20, 2018	E	37.6			
	July 21, 2018	F	27.7			
67a	July 30, 2019	A	50.6	55.6	12.7	2.5
67b	July 31, 2019	B	60.6	112	1.3	3.5
	August 01, 2019	A	111			
	August 02, 2019	B	113			

From 88 SGRn samples, 28 were collected above Waulsortian limestones, 2 above Cloone Flagstones, 19 above the Rockfield limestones, 16 above Cracoean Reef member, 8 above Dirtoge limestones, and 15 above Clare Shales. The box plot (Fig. 4) illustrates that samples collected above the Clare Shales contain higher SGRn values. The lowest values are included within the Cloone Flagstones, followed by the Waulsortian limestones, Rockfield limestones, Dirtoge limestones, and Cracoean Reef member. The majority (87%) of samples collected above the Clare Shales are exceptionally high (>100 kBqm^{-3}), whereas 86% of SGRn samples collected above the

Appendix C

Waulsortian limestones measured below 100 kBqm^{-3} (Supplementary data file).

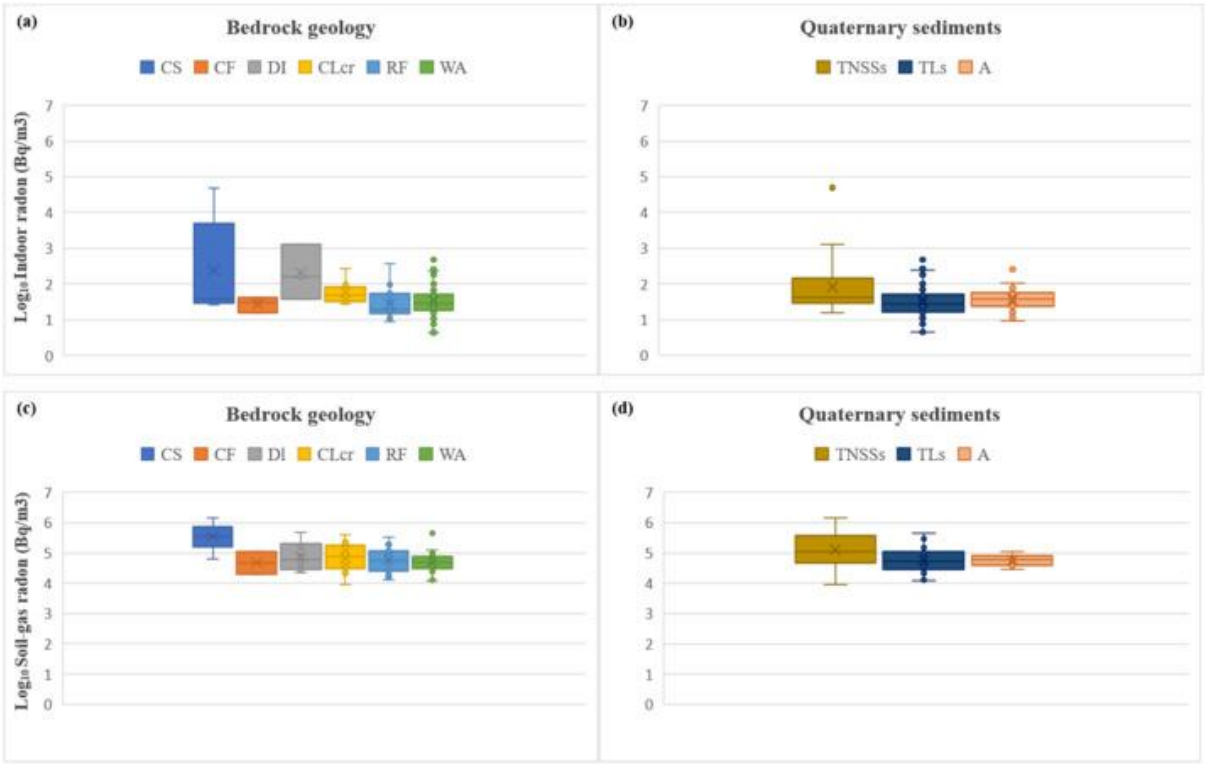

Fig. 4. Soil-gas radon results grouped to (a) bedrock geology unit. The Stratigraphic codes' full names on the plot are CS – Clare Shales, CF, Cloone Flagstones, Dl – Dirtoge limestones, CLcr – Cracoean reef member, RF – Rockfield limestone Formation, WA – Waulsortian limestones. And (b) Quaternary Sediments. The full names of the stratigraphic codes are TNSSs – Till derived from Namurian sandstones, siltstones, and shales, TLs – Till derived from limestones, A – Alluvium. Figures (c) and (d) Boxplot of Log_{10} normal Indoor radon data grouped to (c) Bedrock geology and (d) Quaternary Sediments.

Appendix C

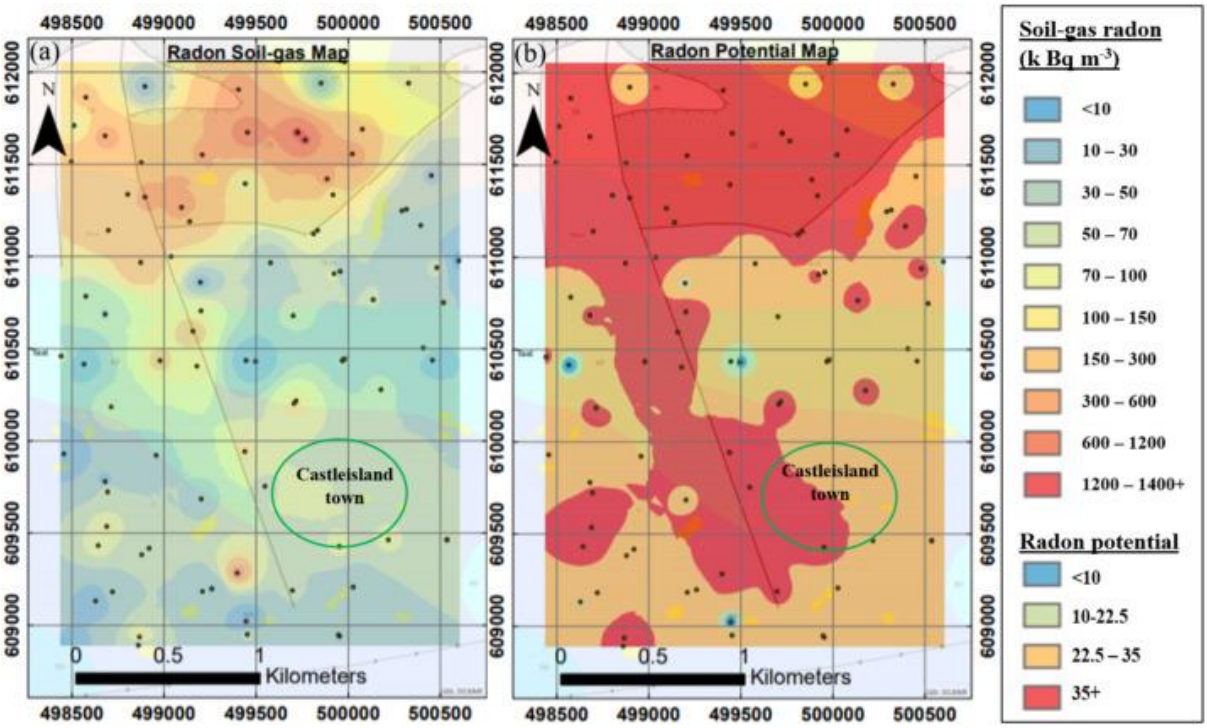

Fig. 5. (a) Soil-gas radon map and (b) radon potential map produced using Inverse distance weighted function in ArcGIS. The resulting maps have been superimposed on top of the bedrock geology 1:100 k G.S.I. map for the area. Points on the map signify where samples were collected.

Analysis of variance (ANOVA) is a method used to statistically analyse the similarity of data groups based on the variance between their means (Larson, 2008). The application of ANOVA in geogenic studies is commonly used (Domingos et al., 2020; Drolet et al., 2014; Tositti et al., 2017). For the present study, one-way ANOVA is used to determine the general variance that geological factors cause in relation to SGRn. The ANOVA is repeated in a similar manner to determine the degree of IRC variation caused by geological factors, which is reported further in the results section below. The

results of an ANOVA analysis statistically demonstrate a significant effect size variance of SGRn due to Quaternary geology and bedrock geology (Table 2).

Table 2. ANOVA table of soil-gas radon effect size due to subsoil permeability, Bedrock geology, and Quaternary geology. The Asterix symbols refer to the level of significance of the results. * equivalent to a p-value of 0.01, ** equivalent to a p-value of 0.001 and *** equivalent to a p-value of <0.001.

Factor	Df	Sum Sq.	Mean Sq.	F value	Pr (>F)
Subsoil permeability: variance explained 21%	4	4.327	1.082	5.578	0.000501***
Residuals	83	16.096	0.194		
Bedrock geology: variance explained 39%	5	7.728	1.546	9.983	1.74e-07 ***
Residuals	82	12.695	0.155		
Quaternary Sediments: Variance explained 13%	2	2.642	1.321	6.315	0.00726 **
Residuals	85	17.780	0.209		

Considering the Quaternary geology, 42 of the samples were collected above till derived from limestone, 37 above till derived from Namurian sandstones, siltstones, and shales, and nine were collected above alluvium (supplementary materials). The samples collected above till derived from Namurian sandstones, siltstones, and shales are mostly (59%) extremely high values. In contrast, 38% of samples collected above the till

derived from limestones are greater than 100 kBqm^{-3}. All of the extremely high (>100 kBqm^{-3}) SGRn values result in a high GRP (35+), although not all of the high GRP values are linked to extremely high SGRn concentrations.

Examining SGRn measurements in relation to bedrock geology (Fig. 5a) indicates higher concentrations above the Clare Shales in the north of the study area, with lower values generally above the limestones in the south of the study area. The map (Fig. 5a) reveals that higher SGRn concentrations occur above the limestones along a local NW-SE fault. Overall, 74% of the study area SGRn ranges from 8.8 k Bq m^{-3} to 100 kBqm^{-3}, with the most significant area (57%) equating to a moderate to high SGRn range (30 kBqm^{-3} – 70 kBqm^{-3}). Approximately 36% of the study area contains extremely high (100+ kBqm^{-3}) SGRn values.

3.2. Geogenic radon potential mapping

The GRP for the study area ranges from 5 to greater than 1200. Radon Potential values greater than 35 are considered exceptionally high (Neznal et al., 2004). The resulting map (Fig. 5b) shows 49% of the area has an GRP greater than 35, 50% is medium-high, with only 1% of the site being less than 10. The north of the study area featuring Clare Shales has a GRP ranging from 200 to a maximum value of 1778, while the lowest radon potential values occur over the Rockfield Limestones Formation with a minimum value of 5.

3.3. Indoor radon

IRC values within the study area range from 4.4 Bqm^{-3} to 49,000 Bqm^{-3}. Table 3 shows that the amount of variance explained by geogenic factors using one-way ANOVA tests are 34% (16% by SGRn, 10% by bedrock geology, 4% by subsoil permeability, and 4% by Quaternary geology).

Table 3. ANOVA table showing the variance of Indoor Radon measurements due to Bedrock geology, Quaternary geology, soil-gas radon, and subsoil permeability. The Asterix symbols refer to the level of significance of the results. * equivalent to a p-value of 0.01, ** equivalent to a p-value of 0.001 and *** equivalent to a p-value of <0.001.

Factor	Df	Sum Sq.	Mean Sq.	F value	Pr (>F)
Bedrock geology: variance explained 10%	**7**	3.202	0.457	2.779	0.00921**
Residuals	**172**	28.315	0.165		
Quaternary geology: variance explained 4%	**2**	1.222	0.611	3.571	0.0302*
Residuals	**177**	30.295	0.171		
Soil-gas radon: variance explained 16%	**5**	5.009	1.002	6.576	1.25e-05 ***
Residuals	**174**	26.508	0.152		
Subsoil permeability: Variance explained 4%	**4**	1.361	0.340	1.974	0.1
Residuals	**175**	30.157	0.172		

The IRC variogram (Fig. 6d) shows that the IRC measurements exhibit a relatively small degree of variation within a small spatial range (from approximately 100 m–700 m). The IRC values exhibit an increase in variation when the distance between the measurements is increased; this is reflected by the steep incline seen at approximately 800 m–1000 m on the variogram.

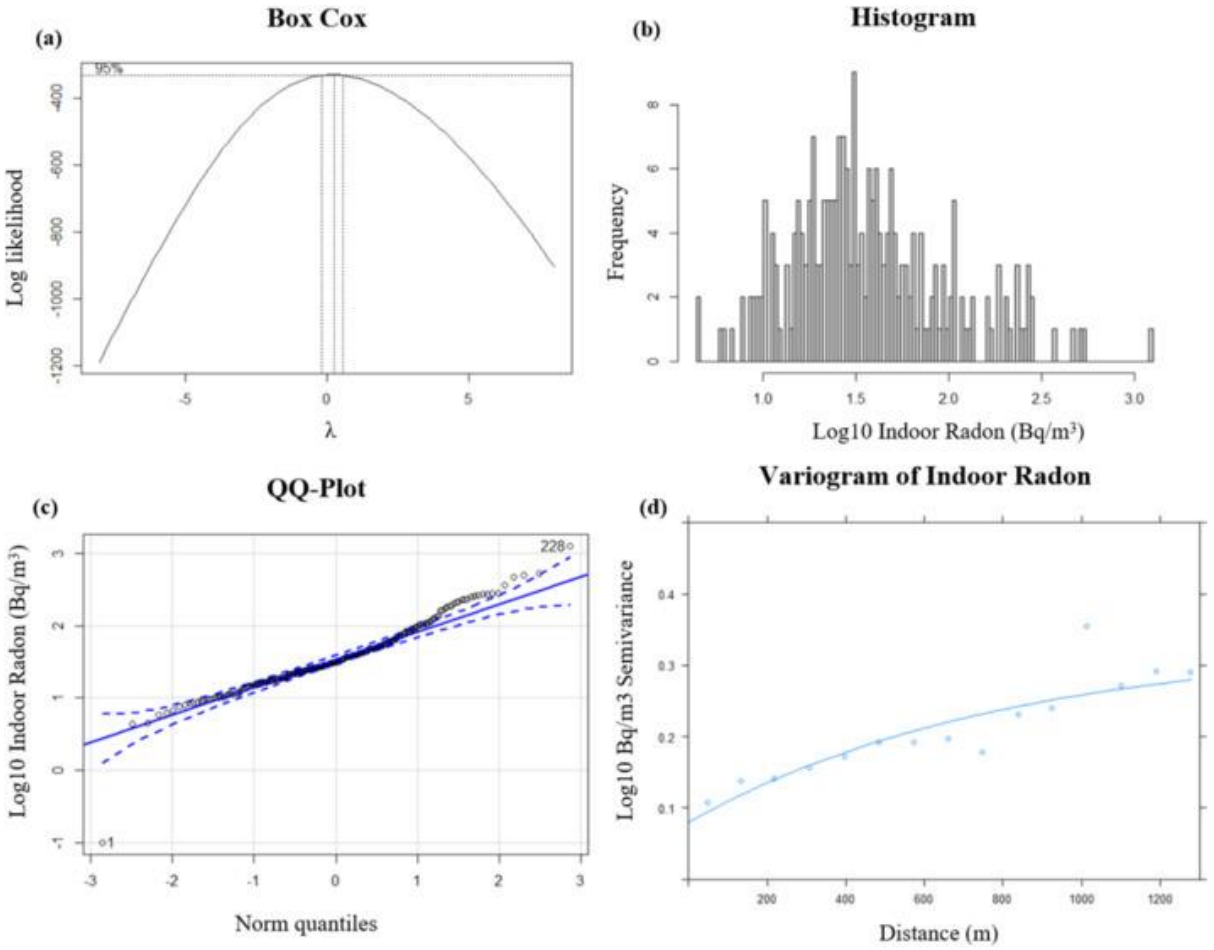

Fig. 6. Indoor radon log10 transformed data distribution. (a) BoxCox (b) Histogram (c) QQ-Plot and (d) Variogram. The variogram (d) uses the "Exp" model with a nugget of 0.08, range of 800 m and psill of 0.25.

3.3.1. Geogenic context of indoor radon results

Appendix C

A total of 180 houses were sampled in the area. Specifically, 144, 18, 8, 3, 4, and 3 indoor radon measurements were collected above several different bedrock lithologies (Waulsortian limestones, Rockfield limestones, Cracoean Reef member, Dirtoge limestones, Clare Shales, Cloone Flagstones, respectively) (table 6 supplementary materials). Fifteen houses (8%) have radon levels above the reference level. The probability of exceeding the reference level (table 6 supplementary material) is 8% (11 of 144 houses) for the Waulsortian limestones, 6% (1 of 18 houses) for Rockfield limestones, 12% (1 of 8 houses) for the Cracoean Reef member, 33% (1 of 3 houses) for the Dirtoge limestones, 25% (1 of 4 houses) for the Clare Shales and 0% (0 of 3 houses) for the Cloone Flagstones.

4. Discussion

Indoor radon concentrations from the study area in Castleisland, SW Ireland are amongst the highest recorded within Europe (Organo and Murphy, 2007), and are in the upper range of those recorded globally (World Health Organization, 2007). The SGRn, as might be expected from this context, are also high compared to the published literature. The median SGRn in Castleisland is ca. 66 $kBqm^{-3}$ compared to ranges typically between ca. 10–40 $kBqm^{-3}$ from other countries (Giustini et al., 2019; Kikaj et al., 2016; Mitra et al., 2021; Nuhu et al., 2021). In more detail, Table 4 summarizes SGRn concentrations which are typically associated with a range of different

lithologies. Analysis of SGRn from Castleisland indicates that 36% of the measured samples are greater than 100 kBqm^{-3}, compared to ca. 10% of samples from other representative studies (Elío et al., 2019; Haruna et al., 2020; O'Brien et al., 2011). Globally, and in general terms, very low to moderate (<10 to 70 kBqm^{-3}) SGRn values are associated with sedimentary lithologies (Fu et al., 2017; Khan et al., 2021; Kumar et al., 2014; Szabó et al., 2014). In comparison, the sedimentary lithologies in Castleisland are associated with extremely high SGRn values (with >46.7% of samples measuring >70 kBqm^{-3}). Although radon anomalies are sometimes associated with sedimentary rocks (not including placer deposits), most occurrences of SGRn anomalies (>70 to 4000 kBqm^{-3}) are associated with granites, gneiss, or uranium-bearing deposits (Esan et al., 2020; Kemski et al., 2001; Mitra et al., 2021; Pereira et al., 2010), which contrasts with the present study area.

Table 4. Summary of SGRn ranges associated with lithologies in selected regions globally.

Region	**Main lithologies in region**	**Range (kBqm^{-3})**	**Reference**
Perak state, Malaysia	Clays, granites	0.11 to 434.5	Nuhu et al. (2021)

Appendix C

Region	Main lithologies in region	Range ($kBqm^{-3}$)	Reference
Celleno municipality, Italy	Potassic lavas, travertine, clay-sandy clay, tuff-tuffite	6.4 to 253	Giustini et al. (2019)
Osun state, Nigeria	Gneisses and schists	0.04 to 190	Esan et al. (2020)
West Bengal, India	Granites and Gneisses	2.13 to 786	Mitra et al. (2021)
Iberian uranium province, Portugal	Granites, metasedimentary schists and greywackes	5 to 12,850	Pereira et al. (2010)
Northern Taiwan	Sandstones with silt alterations, sandstones with shales alteration	6.6 to 32.2	Fu et al. (2017)
Nova Scotia, Canada	Metasandstone, slate, granite	0.8 to 154.6	O'Brien et al. (2011)
Lesser Himalayas, Pakistan	Slate, quartzite, granite, gneiss, limestone, shale	2.3–20.1	Khan et al. (2021)
Cooley Peninsula Ireland	Sandstones, shales, granites, marine shelf facies	3.5 to 112	Elío et al. (2019)
Estonia	Sand, silt, gravel of Baltic sea deposits Glaciolacustrine clay	1 to 184 24 to 1801.6	Petersell et al. (2015)
Dharamshala, India	Sandstones	13 2 to 66.2	Kumar et al. (2014)
Central Hungary	Fluvial sand Loess (silt cemented by carbonate)	1.2 to 24.9 4.9 to 44.1	Szabó et al. (2014)

Appendix C

In relation to the GRP, several studies categorize 41% or less of an area/dataset as being in a high class (Elío et al., 2019; Giustini et al., 2019; Nuhu et al., 2021) which is lower than the 49% area (64% of samples) classified as high in this present study. The GRP in Castleisland reaches a maximum value of 1778, which is considerably higher than the limit of 35 which is conventionally considered to be high (Neznal et al., 2004). For comparison with other countries, "extreme" GRP values of ca. 40–280 have been reported elsewhere (Ciotoli et al., 2017; Pásztor et al., 2016; Szabó et al., 2014).

The original radon map of Ireland (Fig. 1) (Fennell et al., 2002) classifies the east, and south-east, of the study region as having high radon priority (with between 10% and 20% of houses above the reference level); this is in agreement with the GRP mapping carried out in this study. The NW and SW of the survey site are deemed as a high radon priority on the EPA map. The GRP (Fig. 5b) for the same sites is moderate to high with certain zones having a very high GRP. Although the EPA radon map of Ireland and the geogenic GRP map presented here are found to be in general agreement, the GRP map has higher spatial resolution and allows for more accurate representation of areas with lower population density where IRC measurements may be lacking.

Appendix C

The new EPA indoor radon (Environmental Protection Agency, 2022), has higher resolution and shows greater spatial variation of radon compared to the original radon map of Ireland (Fig. 1). The higher resolution in the new radon map arises from the inclusion of four geogenic parameters (bedrock geology, Quaternary geology, aquifer type and subsoil permeability) (Elío et al., 2017; Environmental Protection Agency, 2022). The new EPA map indicates houses above the Clare Shales north of Castleisland have a low probability of exceeding the 200 Bqm^{-3} IRC reference level in Ireland (https://www.epa.ie/environment-and-you/radon/). In contrast, the SGRn and GRP maps developed in this study (Fig. 5), depict the highly anomalous SGRn (greater than 1400 $kBqm^{-3}$) and GRP (up to 1778) occurring above the Clare Shales and in the vicinity of the demolished house which measured an average IRC of 49,000 Bqm^{-3}.

The difference in designation of radon risk between the new EPA radon map and the maps created in this study, likely signifies the anomalous nature of the Clare Shales in Castleisland. Carboniferous shales from other parts of Ireland are not necessarily associated with such elevated SGRn and IRC values. In this respect, our study demonstrates that small-scale studies are useful to examine local exceptions to national-scale models.

Appendix C

ANOVA tests illustrate that bedrock geology explains the highest portion of the SGRn variance (39%), followed by subsoil permeability (21%) and Quaternary geology (13%) (Table 2). It is possible to estimate the variance and concentration of SGRn with reference to bedrock geology and subsoil permeability. In particular, the Clare Shales have significantly high SGRn values compared to other bedrock geology types within the study area. SGRn values from samples collected over the Carboniferous limestones display higher than generally expected from such lithologies (range 9–472 kBqm^{-3}, median 57 kBqm^{-3}) with the highest values near local faults. More elevated SGRn and subsoil permeability measurements along fault zones are commonly reported elsewhere (Miklyaev et al., 2021; Xuan et al., 2020).

The IRC results (Fig. 4a and 4b) and SGRn results share a similar trend (Fig. 4c and 4d). Noticeably, IRC data for the study area are mostly (91%) less than 200 Bqm^{-3}, aside from a few anomalous results, whereas, the SGRn results are typically (90%) between 10,000 and 350,000 Bqm^{-3}. A similar relationship between SGRn and IRC is noted by Yalım et al. (2018).

4.1. Geogenic influence on indoor radon

The influence of geogenic factors on IRC concentrations is depicted in the ANOVA table (Table 3), which shows that bedrock geology (10%) explains over twice the variance of Quaternary geology (4%), both of which are

significant ($p < 0.01$); this could reflect the higher resolution/greater range of bedrock types (6) compared to Quaternary types (3).

SGRn has the most significant influence (16%) on IRC measurements. This result signifies that the greatest contributor to IRC is the radon coming from the soil-gas, which is an established concept within the literature (Åkerblom et al., 1984; Chen and Ford, 2017; World Health Organization, 2007). Since the SGRn ANOVA results (Table 2) show that bedrock geology has the most considerable influence (39%) on the SGRn concentrations, it can be argued that the bedrock geology impacts the IRC measurements indirectly by affecting the SGRn concentrations.

The combined effect of bedrock geology, Quaternary geology, SGRn and subsoil permeability for influencing indoor radon is 34% (Table 3) which compares to 30% reported for Cooley Peninsula in NE Ireland (Elío et al., 2019). Variance of indoor radon explained by bedrock geology is 10% which is in line with studies from Northern Ireland (12.1%) and SW England (10%) (Appleton et al., 2015; Ferreira et al., 2018). However, greater variance of up to 20% has been attributed to bedrock geology units in Norway, England and Wales (Appleton and Miles, 2010; Watson et al., 2017).

Appendix C

Considering houses with IRC above the reference level for Ireland, there is a clear difference between those located over different bedrock geology types (table 6 supplementary materials). Assigning each bedrock type an "EPA-type category" results in three units (Dirtoge limestones, Cracoean Reef member, Clare Shales) classified as high radon areas (i.e. greater than 10% of homes surpassing the reference level). The Waulsortian limestones and the Rockfield limestones would be classified as a medium radon area (between 5% and 10%). Lastly, the Cloone Flagstones would be in the lowest radon category (less than 1% of homes exceeding the reference level). Dwellings built above the Dirtoge limestones and the Clare Shales have significantly higher probability of exceeding the IRC reference level compared to other bedrock types. IRC samples which exceeded the reference level from houses built over the Dirtoge limestones were located along a fault and at the Clare Shales boundary, likely explained by their proximity to the Clare Shales and coupled with the fact that the houses are located in an area with higher radon exhalation rates due to their proximity to a fault.

Analysing the variation of IRC with reference to the Quaternary geology indicates that the till derived from Namurian siltstones, sandstones and shales contain a higher percentage of IRC exceeding the reference level (table supplementary materials). Precisely, 16% of houses located above the till derived from Namurian siltstones, sandstones and shales surpassed the

reference level, compared to 9% and 3% for till derived from limestones and Alluvium, respectively. This result reinforces that geogenic information influences IRC concentrations. In particular, houses above till derived from Namurian siltstones, sandstones and shales have higher probability of exceeding the reference level.

4.2. The use of geogenic data for mapping indoor radon

Geogenic data (i.e. SGRn, bedrock and subsoil permeability) sufficiently predict the IRC categories (i.e. low, moderate, high). Bedrock geology is the main contributor to SGRn (Table 2), whereas SGRn is most strongly associated with IRC (Table 3). As such, investigating geogenic maps of higher resolution (1:100 k) can quickly distinguish potential areas of elevated IRC. Precisely, pinpointing locations with radon source rocks and specific subsurface structures that enhance radon transportation to homes can be accomplished for regions with higher resolution geological maps which are generally publicly available. Utilizing geogenic maps for radon mapping can be extended to other bedrock units and validated by completing SGRn and subsoil permeability (i.e. GRP) surveys for representative geology types.

GRP surveys provide a substantially quicker alternative at approximately six to ten samples per day, compared to IRC surveys which requires a three-month measurement period (Elío et al., 2019; Environmental Protection

Agency, 2019). GRP surveys can be especially beneficial in areas rezoned for residential use where no previous IRC measurements exist. Another benefit to using this approach is that it assesses the amount of radon available to a building regardless of the building purpose or design (workplace or home), allowing the method to be applied to mapping both the radon risk of homes as well as workplaces.

Considering that geological information is freely available online for many countries, there are several potential benefits for integrating information from existing geological maps into radon surveys. Whereas SGRn surveys are weather-dependent, there are no such constraints on utilizing existing geological map data. Indoor radon measurements are useful for constructing radon hazard maps, however the measurements themselves are prone to human error (e.g., radon detectors must be installed in specific areas of a house with limited airflow), must take place over several months, are very costly and time-consuming, or simply may not be available. Using IRC data for mapping RPAs is increasingly complex and inefficient due to tighter regulations on General Data Protection Regulations (GDPR). Field surveys which utilize existing geological maps can specifically focus on areas where an elevated radon risk is suspected, based on the geological attributes. IRC measurements could then be collected to confirm the level of IRC in each workplace or home. Furthermore, for areas where there is a lack of IRC data,

it is practical to utilize the available geological data and radon-potential surveys for IRC risk mapping.

4.3. Limitations

Geogenic radon potential mapping is weather-dependent. Several days after rainfall should elapse before sampling to ensure that the soil is not water-saturated (Neznal et al., 2004). Due to weather conditions, atmospheric pressure, wind speed and temperature, SGRn varies on a daily basis (Arora et al., 2017; Kulali et al., 2017). Furthermore, SGRn varies on a seasonal basis; due to the overall mean differences in temperature and rainfall (Szabó et al., 2013). Considering these factors, it is important to ensure that soil gas samples are taken from a sufficient depth in the soil profile (usually 80–100 cm (Neznal et al., 2004)). Due to the high degree of spatial variation in SGRn concentrations, it is also important to collect several samples to obtain representative values for a given geology type, or region. Given that the original methodology of Neznal et al. (2004) has been adapted and used slightly differently in several studies, it is important to ensure different methodologies are taken into account when comparing GRP or RP from different study areas.

5. Conclusion

Appendix C

An approach to mapping radon-prone areas was investigated by collecting 135 soil-gas radon (SGRn) and subsoil permeability measurements across approximately 50 locations in a 6 km^2 region around Castleisland in Co. Kerry, SW Ireland. The area was chosen due to the extremely high indoor radon concentrations (average reading of 49,000 Bqm^{-3} from several measurements) previously reported from the region (Organo et al., 2004), and due to the fact that there was not a clear understanding of the source of such high values. The indoor radon concentration (IRC) variance explained by geogenic factors (bedrock geology, Quaternary geology, subsoil permeability, and SGRn) is 34%; with SGRn as the main contributor (16%). ANOVA tests illustrate that bedrock geology has the most substantial influence on SGRn concentrations (39%), although subsoil permeability (21%) and Quaternary geology (13%) also have significant effects. Results demonstrate that spatially restricted black shales, locally known as the Clare Shales, are spatially associated with both SGRn and IRC anomalies, and likely act as a radon source which may also be transported via enhanced permeability in non-mineralised fault zones and extensive subterranean karst systems which are prevalent in the region.

Geological factors (especially SGRn, bedrock geology, and subsoil permeability) sufficiently predict the IRC categories (i.e. low, moderate, high). Therefore, investigating the spatial variation and distribution of geological units in a given region can help to identify radon priority areas,

particularly if reliable high-resolution maps are available, relevant radon-related data (e.g. soil properties) exist and lithologies are assigned with accuracy regarding their potential for being a point source of radon. Such an approach could pinpoint high radon areas in a very cost-efficient and time-efficient manner. The radon priority area category assigned using geological attributes can be confirmed by carrying out a geogenic radon potential survey for smaller representative areas, such as that presented in this study. Geogenic radon potential mapping can verify if an area is susceptible to high IRC. Such an approach is especially useful for areas where population density is low, and where few IRC measurements already exist. The methodology presented in this study highlights the use of combined experimental and theoretical approaches in the study of radon as a natural hazard. The approach used in this study integrates both relevant field data and geostatistical modelling, and is demonstrated to be beneficial in efforts to predict radon anomalies. Such an approach ultimately leads to a better understanding of radon in both the natural and built environments. Radon potential or hazard maps constructed using this methodology add considerable value to existing legacy geological datasets. This research also highlights the importance of reliable digital geoscience data applied to environmental exposure, and when utilized to protect the general public from the harmful effects of ionizing radiation.

Role of the funding source

The funding source (SUSI) for Méabh Banríon's Ph.D. had no involvement or role in the study design, the collection, analysis and interpretation of data; in writing of the report; and in the decision to submit the article for publication.

Declaration of competing interest

The authors declare that they have no known competing financial interests or personal relationships that could have appeared to influence the work reported in this paper.

Acknowledgements

We would like to thank the EPA for providing the InRn dataset, Ryan O'Toole, Patricia McGuire, and Winifred Duncan for part-taking in the soil-gas radon and soil permeability measurement surveys. Méabh H. Banríon would like to thank Student Universal Support Ireland (SUSI) for helping to fund their Ph.D.

Appendix A. Supplementary data

The following is the supplementary data to this article:

Multimedia component 1.

References

Abdalla et al., 2021

A.M. Abdalla, A.M. Ismail, A.A. Al Madiy

Soil radon detection using active scintillation cell

J. Radiat. Res. Appl. Sci., 14 (2021), pp. 16-22, 10.1080/16878507.2020.1783631

ArticleDownload PDFView Record in ScopusGoogle Scholar

Åkerblom et al., 1984

G. Åkerblom, P. Andersson, B. Clevensjö

Soil gas radon - a source for indoor radon daughters

Radiat. Protect. Dosim., 7 (1984), pp. 49-54, 10.1093/oxfordjournals.rpd.a082961

View PDF

View Record in ScopusGoogle Scholar

Alonso et al., 2019

H. Alonso, J.G. Rubiano, J.G. Guerra, M.A. Arnedo, A. Tejera, P. Martel

Assessment of radon risk areas in the Eastern Canary Islands using soil radon gas concentration and gas permeability of soils

Sci. Total Environ., 664 (2019), pp. 449-460, 10.1016/j.scitotenv.2019.01.411

ArticleDownload PDFView Record in ScopusGoogle Scholar

Anderson et al., 2003

R.T. Anderson, H.A. Vrionis, I. Ortiz-

Bernad, C.T. Resch, P.E. Long, R. Dayvault, K. Karp, S. Marutzky, D.R. Metzler, A.

Peacock, D.C. White, M. Lowe, D.R. Lovley

Appendix C

Stimulating the in situ activity of geobacter species to remove uranium from the groundwater of a uranium-contaminated aquifer

Appl. Environ. Microbiol., 69 (2003), pp. 5884-5891, 10.1128/AEM.69.10.5884-5891.2003

View PDF

View Record in ScopusGoogle Scholar

Appleton et al., 2015

J.D. Appleton, Z. Daraktchieva, M.E. Young

Geological controls on radon potential in Northern Ireland

PGA (Proc. Geol. Assoc.), 126 (2015), pp. 328-345, 10.1016/j.pgeola.2014.07.001

ArticleDownload PDFView Record in ScopusGoogle Scholar

Appleton and Miles, 2010

J.D. Appleton, J.C.H. Miles

A statistical evaluation of the geogenic controls on indoor radon concentrations and radon risk

J. Environ. Radioact., 101 (2010), pp. 799-803, 10.1016/j.jenvrad.2009.06.002

ArticleDownload PDFView Record in ScopusGoogle Scholar

Arora et al., 2017

B.R. Arora, A. Kumar, V. Walia, T.F. Yang, C.-C. Fu, T.-K. Liu, K.-L. Wen, C.-H. Chen

Assesment of the response of the meteorological/hydrological parameters on the soil gas radon emission at Hsinchu, northern Taiwan: a prerequisite to identify earthquake precursors

J. Asian Earth Sci., 149 (2017), pp. 49-63, 10.1016/j.jseaes.2017.06.033

ArticleDownload PDFView Record in ScopusGoogle Scholar

Barros et al., 2015

N. Barros, D.W. Field, D.J. Steck, R.W. Field

Comparative survey of outdoor, residential and workplace radon concentrations

Radiat. Protect. Dosim., 163 (2015), pp. 325-332, 10.1093/rpd/ncu185

View PDF

Google Scholar

Bossew, 2018

P. Bossew

Radon priority areas - definition, estimation and uncertainty

Nucl. Technol. Radiat. Protect., 33 (2018), 10.2298/NTRP180515011B

11–11

View PDF

Google Scholar

Bossew et al., 2020

P. Bossew, G. Cinelli, G. Ciotoli, Q. Crowley, M. Cort, J. Elío, V. Gruber, E. Peterma nn, T. Tollefsen

Development of a geogenic radon hazard index—concept, history, experiences

Int. J. Environ. Res. Publ. Health, 17 (2020), p. 4134, 10.3390/ijerph17114134

View PDF

Google Scholar

Chen and Ford, 2017

Appendix C

J. Chen, K.L. Ford

A study on the correlation between soil radon potential and average indoor radon potential in Canadian cities

J. Environ. Radioact., 166 (2017), pp. 152-156, 10.1016/j.jenvrad.2016.01.018

ArticleDownload PDFView Record in ScopusGoogle Scholar

Ciotoli et al., 2017

G. Ciotoli, M. Voltaggio, P. Tuccimei, M. Soligo, A. Pasculli, S.E. Beaubien, S. Bigi

Geographically weighted regression and geostatistical techniques to construct the geogenic radon potential map of the Lazio region: a methodological proposal for the European Atlas of Natural Radiation

J. Environ. Radioact., 166 (2017), pp. 355-375, 10.1016/j.jenvrad.2016.05.010

ArticleDownload PDFView Record in ScopusGoogle Scholar

Cucoş Dinu et al., 2017

A. Cucoş Dinu, M.I. Călugăr, B.D. Burghele, O.A. Dumitru, C. Cosma, B.P. Onac

Radon levels in Romanian caves: an occupational exposure survey

Environ. Geochem. Health, 39 (2017), pp. 1085-1099, 10.1007/s10653-016-9878-1

View PDF

Google Scholar

Dardac, 2022

M. Dardac

Determining the Geogenic Influence for High Indoor Radon Areas in Ireland

(2022)

(submitted for publication)

Google Scholar

Domingos et al., 2020

F. Domingos, G. Cinelli, L. Neves, A. Pereira, R. Braga, P. Bossew, T. Tollefsen

Validation of a database of mean uranium, thorium and potassium concentrations in rock samples of Portuguese geological units, generated of literature data

J. Environ. Radioact., 222 (2020), Article 106338, 10.1016/j.jenvrad.2020.106338

ArticleDownload PDFView Record in ScopusGoogle Scholar

Drolet et al., 2014

J.-P. Drolet, R. Martel, P. Poulin, J.-C. Dessau

Methodology developed to make the Quebec indoor radon potential map

Sci. Total Environ., 473–474 (2014), pp. 372-380, 10.1016/j.scitotenv.2013.12.039

ArticleDownload PDFView Record in ScopusGoogle Scholar

Duffy et al., 1996

J.T. Duffy, J.S. Madden, G.M. Mackin, A.T. McGarry, P.A. Colgan

A reconnaissance survey of radon in show caves in Ireland

Environ. Int., 22 (1996), pp. 415-423, 10.1016/S0160-4120(96)00140-7

ArticleDownload PDFGoogle Scholar

Duggal et al., 2014

V. Duggal, A. Rani, R. Mehra

Measurement of soil-gas radon in some areas of northern Rajasthan, India

J. Earth Syst. Sci., 123 (2014), pp. 1241-1247

View PDF

CrossRefView Record in ScopusGoogle Scholar

Elío et al., 2019

J. Elío, Q. Crowley, R. Scanlon, J. Hodgson, S. Long

Rapid radon potential classification using SGRn measurements in the Cooley Peninsula, County Louth, Ireland

Environ. Earth Sci., 78 (2019), p. 359, 10.1007/s12665-019-8339-4

View PDF

View Record in ScopusGoogle Scholar

Elío et al., 2018

J. Elío, Q. Crowley, R. Scanlon, J. Hodgson, L. Zgaga

Estimation of residential radon exposure and definition of Radon Priority Areas based on expected lung cancer incidence

Environ. Int., 114 (2018), pp. 69-76, 10.1016/j.envint.2018.02.025

ArticleDownload PDFView Record in ScopusGoogle Scholar

Elío et al., 2017

Javier Elío, Q. Crowley, R. Scanlon, J. Hodgson, S. Long

Logistic regression model for detecting radon prone areas in Ireland

Sci. Total Environ. (2017), pp. 599-600, 10.1016/j.scitotenv.2017.05.071

View PDF

Google Scholar

Environmental Protection Agency, 2022

Environmental Protection Agency

New EPA Radon maps show more homes and workplaces at risk from cancer-causing gas

https://www.epa.ie/news-releases (2022)

Google Scholar

Environmental Protection Agency, 2019

Environmental Protection Agency

EPA Protocol for the Measurement of Radon in Homes and Workplaces

(2019)

Google Scholar

Esan et al., 2020

D.T. Esan, M.K.C. Sridhar, R. Obed, Y. Ajiboye, O. Afolabi, B. Olubodun, O.M. Oni

Determination of residential soil gas radon risk indices over the lithological units of a southwestern Nigeria university

Sci. Rep., 10 (2020), pp. 1-10

View PDF

CrossRefView Record in ScopusGoogle Scholar

European Commission, 2013

European Commission

Council directive 2013/59/Euratom

Off. J. Eur. Union 2013/59/EURATOM (2013), pp. 6-50

Google Scholar

Fennell et al., 2002,

S.G. Fennell, G.M. Mackin, A.T. McGarry, D. Pollard

Radon exposure in Ireland

Int. Congr., 1225 (2002, February), pp. 71-77

ArticleDownload PDFView Record in ScopusGoogle Scholar

Ferreira et al., 2018

A. Ferreira, Z. Daraktchieva, D. Beamish, C. Kirkwood, T.R. Lister, M. Cave, J. Wra gg, K. Lee

B. **Indoor radon measurements in south west England explained by topsoil and stream sediment geochemistry, airborne gamma-ray spectroscopy and geology**

J. Environ. Radioact., 181 (2018), pp. 152-171, 10.1016/j.jenvrad.2016.05.007

ArticleDownload PDFView Record in ScopusGoogle Scholar

Fu et al., 2017

C.-C. Fu, T.F. Yang, C.-H. Chen, L.-C. Lee, Y.-M. Wu, T.-

K. Liu, V. Walia, A. Kumar, T.-H. Lai

Spatial and temporal anomalies of soil gas in northern Taiwan and its tectonic and seismic implications

J. Asian Earth Sci., 149 (2017), pp. 64-77, 10.1016/j.jseaes.2017.02.032

ArticleDownload PDFView Record in ScopusGoogle Scholar

Fuente et al., 2020

M. Fuente, S. Long, D. Fenton, L.C. Hung, J. Goggins, M. Foley

Review of recent radon research in Ireland, OPTI-SDS project and its impact on the National Radon Control Strategy

Appl. Radiat. Isot., 163 (2020), Article 109210, 10.1016/j.apradiso.2020.109210

ArticleDownload PDFView Record in ScopusGoogle Scholar

Gadd, 2010

G.M. Gadd

Appendix C

Metals, minerals and microbes: geomicrobiology and bioremediation

Microbiology, 156 (2010), pp. 609-643

View PDF

CrossRefView Record in ScopusGoogle Scholar

Gaskin et al., 2018

J. Gaskin, D. Coyle, J. Whyte, D. Krewksi

Global estimate of lung cancer mortality attributable to residential radon

Environ. Health Perspect., 126 (2018), p. 57009, 10.1289/EHP2503

View PDF

Google Scholar

Appendix C

F. Giustini, G. Ciotoli, A. Rinaldini, L. Ruggiero, M. Voltaggio

Mapping the geogenic radon potential and radon risk by using Empirical Bayesian Kriging regression: a case study from a volcanic area of central Italy

Sci. Total Environ., 661 (2019), pp. 449-464

ArticleDownload PDFView Record in ScopusGoogle Scholar

Günay et al., 2018

O. Günay, M.M. Saç, M. İçhedef, C. Taşköprü

Soil gas radon concentrations along the Ganos Fault (GF)

Arabian J. Geosci., 11 (2018), p. 213, 10.1007/s12517-018-3542-2

View PDF

View Record in ScopusGoogle Scholar

Gunn, 1982

J. Gunn

Crag Cave, County Kerry, vol. 20, Irish Naturalists Journal Ltd (1982), pp. 445-449

View Record in Scopus

Gunning, 2016

G.A. Gunning

Studies of Radon in Ireland: Outdoor Levels, Detector Intercomparison and School Remediation Methods

School of Physics, Trinity College (Dublin, Ireland) (2016)

Google Scholar

Habib et al., 2018

R.R. Habib, R.Y. Nuwayhid, Z. Hamdan, I. Alameddine, G. Katul

Indoor and outdoor radon concentration levels in Lebanon

Health Phys., 115 (2018)

Google Scholar

Haruna et al., 2020

R. Haruna, M.A. Saleh, S. Hashim, K. Hamzah, J. Zainal, M.S.M. Sanusi

Assessment of geogenic radon potential in Johor Malaysia

J. Radioanal. Nucl. Chem., 326 (2020), pp. 1065-1074, 10.1007/s10967-020-07396-y

View PDF

View Record in ScopusGoogle Scholar

Hodson, 1954

F. Hodson

The Carboniferous rocks of Foynes island, county Limerick

Geol. Mag., 91 (1954), pp. 153-160

View Record in ScopusGoogle Scholar

Hyun et al., 2014

S.P. Hyun, J.A. Davis, K.F. Hayes

Appendix C

Abiotic U (VI) reduction by aqueous sulfide

Appl. Geochem., 50 (2014), pp. 7-15

ArticleDownload PDFView Record in ScopusGoogle Scholar

Idriss et al., 2014

H. Idriss, I. Salih, A.S. Alaamer, M. Abdelgalil, S.A. Salih, A.M. Hasan, M.A. ELtahir , M.M. Ahamed

Study of radon in soil gas, trace elements and climatic parameters around South Kordofan state, Sudan

Environ. Earth Sci., 72 (2014), pp. 335-339

View PDF

CrossRefView Record in ScopusGoogle Scholar

Jelle, 2012

B.P. Jelle

Development of a model for radon concentration in indoor air

Sci. Total Environ., 416 (2012), pp. 343-350, 10.1016/j.scitotenv.2011.11.052

ArticleDownload PDFView Record in ScopusGoogle Scholar

Kemski et al., 2001

J. Kemski, A. Siehl, R. Stegemann, M. Valdivia-Manchego

Mapping the geogenic radon potential in Germany

Sci. Total Environ., 272 (2001), pp. 217-230, 10.1016/S0048-9697(01)00696-9

ArticleDownload PDFView Record in ScopusGoogle Scholar

Kemski et al., 1996

J. Kemski, R. Klingel, A. Siehl

Classification and mapping of radon-affected areas in Germany

Environ. Int., 22 (1996), pp. 789-798

ArticleDownload PDFGoogle Scholar

Khan et al., 2019

S.M. Khan, J. Gomes, D.R. Krewski

Radon interventions around the globe: a systematic review

Heliyon, 5 (2019), Article e01737, 10.1016/j.heliyon.2019.e0173

ArticleDownload PDFView Record in ScopusGoogle Scholar

Khan et al., 2021

F. Khan, S.A. Khattak, Z. Wazir, M. Waqas

Spatial distribution of radon concentrations in balakot-bagh (B–B) fault line and adjoining areas, lesser himalayas, north Pakistan

Environ. Earth Sci., 80 (2021), p. 291, 10.1007/s12665-021-09569-8

View PDF

View Record in ScopusGoogle Scholar

Kikaj et al., 2016

D. Kikaj, Z. Jeran, M. Bahtijari, P. Stegnar

Radon in soil gas in Kosovo

J. Environ. Radioact., 164 (2016), pp. 245-252, 10.1016/j.jenvrad.2016.07.037

ArticleDownload PDFView Record in ScopusGoogle Scholar

N.M. Koribanics, S.J. Tuorto, N. Lopez-Chiaffarelli, L.R. McGuinness, M.M. Häggblom, K.H. Williams, P.E. Long, L.J. Kerkhof

Spatial distribution of an uranium-respiring betaproteobacterium at the rifle, CO field research site

PLoS One, 10 (2015), Article e0123378, 10.1371/journal.pone.0123378

View PDF

View Record in ScopusGoogle Scholar

F. Kulali, I. Akkurt, N. Özgür

The effect of meteorological parameters on radon concentration in soil gas

Acta Phys. Pol., A, 132 (2017), pp. 999-1001

View PDF

CrossRefView Record in ScopusGoogle Scholar

A. Kumar, V. Arora, V. Walia, B.S. Bajwa, S. Singh, T.F. Yang

Study of soil gas radon variations in the tectonically active Dharamshala and Chamba regions, Himachal Pradesh, India

Environ. Earth Sci., 72 (2014), pp. 2837-2847

View PDF

CrossRefView Record in ScopusGoogle Scholar

M. Laiolo, M. Ranaldi, L. Tarchini, M.L. Carapezza, D. Coppola, T. Ricci, C. Cigolini

Appendix C

The effects of environmental parameters on diffuse degassing at Stromboli volcano: insights from joint monitoring of soil CO2 flux and radon activity

J. Volcanol. Geoth. Res., 315 (2016), pp. 65-78, 10.1016/j.jvolgeores.2016.02.004

0377-0273

ArticleDownload PDFView Record in ScopusGoogle Scholar

M.G. Larson

Analysis of variance

Circulation, 117 (2008), pp. 115-121, 10.1161/CIRCULATIONAHA.107.654335

View PDF

View Record in ScopusGoogle Scholar

A. Lecomte, M. Cathelineau, R. Michels, C. Peiffert, M. Brouand

Uranium mineralization in the Alum Shale Formation (Sweden): evolution of a U-rich marine black shale from sedimentation to metamorphism

Ore Geol. Rev., 88 (2017), pp. 71-98, 10.1016/j.oregeorev.2017.04.021

ArticleDownload PDFView Record in ScopusGoogle Scholar

H.E. Liping, B. Chen, C. Zhao, W. Zhuo

The study on effects of indoor air filtration on radon exposure to residents

Chin. J. Radiol. Med. Protect., 36 (2016), pp. 688-693

View Record in ScopusGoogle Scholar

Appendix C

R.M. Margineanu

Radon measurements in underground mines and caves from several European countries

AIP Conference Proceedings, AIP Publishing LLC (2019), p. 50004

Google Scholar

J.W. Marsh, L. Tomášek, D. Laurier, J.D. Harrison

Effective dose coefficients for radon and progeny: a review of ICRP and UNSCEAR values

Radiat. Protect. Dosim., 195 (2021), pp. 1-20, 10.1093/rpd/ncab106

View PDF

View Record in ScopusGoogle Scholar

P.S. Miklyaev, T.B. Petrova, D.V. Shchitov, P.A. Sidyakin, M.A. Murzabekov, A.M. Marennyy, N.A. Nefedov, Y.A. Sapozhnikov

The results of long-term simultaneous measurements of radon exhalation rate, radon concentrations in soil gas and groundwater in the fault zone

Appl. Radiat. Isot., 167 (2021), Article 109460, 10.1016/j.apradiso.2020.109460

ArticleDownload PDFView Record in ScopusGoogle Scholar

M. Min, H. Xu, Mostafa Fayek, J. Chen

Evidence of uranium biomineralization in sandstone-hosted roll-front uranium deposits, northwestern China

Ore Geol. Rev., 26 (2005), 10.1016/j.oregeorev.2004.10.003

View PDF

Google Scholar

S. Mitra, S. Chowdhury, J. Mukherjee, S. Sutradhar, S. Mondal, C. Barman, A. Deb

Assessment of radon (222Rn) activity in groundwater and soil-gas in Purulia district, West Bengal, India

J. Radioanal. Nucl. Chem., 330 (2021), pp. 1331-1338

View PDF

CrossRefView Record in ScopusGoogle Scholar

C. Monty

UNSCEAR report 2000: sources and effects of ionizing radiation

J. Radiol. Prot., 21 (2000), 10.1088/0952-4746/21/1/609

View PDF

Google Scholar

L.E. Muntean, C. Cosma, A. Cucos, T. Dicu, D.V. Moldovan

Assessment of annual and seasonal variation of indoor radon levels in dwelling houses from Alba County, Romania

Rom. J. Phys., 59 (2014), pp. 163-171

View Record in ScopusGoogle Scholar

Murphy, Dowdall, Long, Curtin, Fenton

Estimating population lung cancer risk from radon using a resource efficient stratified population weighted sample survey protocol–Lessons and results from Ireland

J. Environ. Radioact., 233 (2021), 10.1016/j.jenvrad.2021.106582

View PDF

Google Scholar

R. Nagarajan, J. Madhavaraju, R. Nagendra, J.S. Armstrong-Altrin, J. Moutte

Geochemistry of neoproterozoic shales of the rabanpalli formation, bhima basin, northern Karnataka, southern India: implications for provenance and paleoredox conditions

Rev. Mex. Ciencias Geol., 24 (2007), pp. 150-160

View Record in ScopusGoogle Scholar

National Cancer Registry Ireland

Cancer in Ireland 1994-2018 with Estimates for 2018-2020: Annual Report of the National Cancer Registry

(2020)

Google Scholar

National Radon Control Strategy

NRCS Knowledge Gaps Phase 2

(2019)

Google Scholar

Matěj Neznal, Martin Neznal, M. Matolin, I. Barnet, J. Miksova

The New Method for Assessing the Radon Risk of Building Sites

Czech Geological Survey Prague (2004)

Google Scholar

H. Nuhu, S. Hashim, M. Aziz Saleh, M. Syazwan Mohd Sanusi, A. Hussein Alomari, M.H. Jamal, R.A. Abdullah, S.A. Hassan

Soil gas radon and soil permeability assessment: mapping radon risk areas in Perak State, Malaysia

PLoS One, 16 (2021), Article e0254099

View PDF

CrossRefView Record in ScopusGoogle Scholar

K. O'Brien, T. Goodwin, D. Risk

Radon soil gas in the halifax regional municipality, nova scotia, Canada

Atl. Geol., 47 (2011), pp. 112-124

View PDF

CrossRefView Record in ScopusGoogle Scholar

C. Organo, A. Ellard, D. Fenton, H. Synnott, M. O'Colmáin, S. Prenter, S. O'Reilly, P. Colgan

High radon concentrations in a house near Castleisland, County Kerry (Ireland)—identification, remediation and post-remediation

J. Radiol. Prot., 24 (2004), p. 107, 10.1088/0952-4746/24/2/001

View PDF

View Record in ScopusGoogle Scholar

C. Organo, P. Murphy

The Castleisland Radon Survey—follow-up to the discovery of a house with extremely high radon concentrations in County Kerry (SW Ireland)

J. Radiol. Prot., 27 (2007), 10.1088/0952-4746/27/3/002

View PDF

Google Scholar

L. Pásztor, K.Z. Szabó, G. Szatmári, A. Laborczi, Á. Horváth

Mapping geogenic radon potential by regression kriging

Sci. Total Environ., 544 (2016), pp. 883-891, 10.1016/j.scitotenv.2015.11.175

ArticleDownload PDFView Record in ScopusGoogle Scholar

E. Petermann, P. Bossew, B. Hoffmann

Radon hazard vs. radon risk - on the effectiveness of radon priority areas

J. Environ. Radioact., 244–245 (2022), Article 106833, 10.1016/j.jenvrad.2022.106833

ArticleDownload PDFView Record in ScopusGoogle Scholar

V. Petersell, K. Jüriado, A. Raukas, M. Shtokalenko, K. Täht-Kok

Quaternary deposits and weathered bedrock material as a source of dangerous radon emissions in Estonia

Geologos, 21 (2015)

Google Scholar

A. Pereira, M. Godinho, L. Neves

On the influence of faulting on small-scale soil-gas radon variability: a case study in the Iberian Uranium Province

J. Environ. Radioact., 101 (2010), pp. 875-882

ArticleDownload PDFView Record in ScopusGoogle Scholar

M. Pracht

Geology of Kerry - Cork: A Geological Description to Accompany the Bedrock Geology 1:100,000 Scale Map Series, Sheet 21

Kerry-Cork (1997)

Google Scholar

Radiological Protection Act

(Ionising Radiation) Regulations, 2019

(1991)

Statutory Instruments Ireland, S.I. No. 30 of 2019

Google Scholar

M. Rafique, S. Abbasi, C. Shahzadi, M. Basharat, A. Jabbar, S. Ur Rahman

Excessive lifetime cancer risk assessment due to short-term indoor/outdoor ambient radon and gamma dose rate exposures

Iran. J. Sci. Technol. Trans. A-Science, 45 (2021), pp. 2181-2190, 10.1007/s40995-021-01192-3

View PDF

View Record in ScopusGoogle Scholar

P. Ravikumar, D. Davis, R. Somashekar, K. Prakash

Measurement of radon activity in soil gas using RAD7 in the Environs of Chitradurga District, Karnataka, India

Elixir. Earth. Sci., 80 (2015), pp. 31078-31082

View Record in ScopusGoogle Scholar

M. Rider

The Namurian of West County Clare. Presented at the Proceedings of the Royal Irish Academy. Section B: Biological

Geological, and Chemical Science, JSTOR (1974), pp. 125-142

Google Scholar

M. Schubert, A. Musolff, H. Weiss

Influences of meteorological parameters on indoor radon concentrations (222Rn) excluding the effects of forced ventilation and radon exhalation from soil and building materials

J. Environ. Radioact., 192 (2018), pp. 81-85, 10.1016/j.jenvrad.2018.06.011

ArticleDownload PDFView Record in ScopusGoogle Scholar

J. Singh, H. Singh, S. Singh, B. Bajwa

Measurement of soil gas radon and its correlation with indoor radon around some areas of Upper Siwaliks, India

J. Radiol. Prot., 30 (2010), p. 63

View PDF

CrossRefGoogle Scholar

A. Sleeman, B. MacConnell, S. Gatley

Understanding Earth Processes, Rocks and the Geological History of Ireland: A Companion to the 1: 1.000. 000 Scale Bedrock Geological Map of Ireland

Geological Survey of Ireland (2004)

Google Scholar

M.E. Smith, O.A. Dumitru, B.D. Burghele, A. Cucoș, B.P. Onac

Radon concentration in three Florida caves: Florida, Jennings, and Ocala

Carbonates Evaporites, 34 (2019), pp. 433-439, 10.1007/s13146-018-0473-7

View PDF

View Record in ScopusGoogle Scholar

A. Soesoo, J. Vind, S. Hade

Uranium and thorium resources of Estonia

Minerals, 10 (2020), 10.3390/min10090798

View PDF

Google Scholar

K. Sun, Q. Guo, J.G. Cheng

The effect of some soil characteristics on soil radon concentration and radon exhalation from soil surface

J. Nucl. Sci. Technol., 41 (11) (2004), pp. 1113-1117, 10.1080/18811248.2004.9726337

View PDF

View Record in ScopusGoogle Scholar

A.V. Sundal, V. Valen, O. Soldal, T. Strand

The influence of meteorological parameters on soil radon levels in permeable glacial sediments

Sci. Total Environ., 389 (2008), pp. 418-428, 10.1016/j.scitotenv.2007.09.001

ArticleDownload PDFView Record in ScopusGoogle Scholar

Appendix C

K.Z. Szabó, G. Jordan, Á. Horváth, C. Szabó

Mapping the geogenic radon potential: methodology and spatial analysis for central Hungary

J. Environ. Radioact., 129 (2014), pp. 107-120

ArticleDownload PDFView Record in ScopusGoogle Scholar

K.Z. Szabó, G. Jordan, Á. Horváth, C. Szabó

Dynamics of soil gas radon concentration in a highly permeable soil based on a long-term high temporal resolution observation series

J. Environ. Radioact., 124 (2013), pp. 74-83, 10.1016/j.jenvrad.2013.04.004

ArticleDownload PDFView Record in ScopusGoogle Scholar

M.S. Thornton

The Lower Carboniferous Limestones of the Tralee Bay Area, Co. Kerry, Ireland

Unpublished PhD thesis, University of Cambridge (1966)

Google Scholar

Fairchild, 2003

A. Tooth, I. Fairchild

Soil and karst aquifer hydrological controls on the geochemical evolution of speleothem-forming drip waters, Crag Cave, Southwest Ireland

J. Hydrol., 273 (2003), pp. 51-68, 10.1016/S0022-1694(02)00349-9

ArticleDownload PDFView Record in ScopusGoogle Scholar

sitti et al., 2017

L. Tositti, G. Cinelli, E. Brattich, A. Galgaro, D. Mostacci, C. Mazzoli, M. Massironi, R. Sassi

Assessment of lithogenic radioactivity in the Euganean Hills magmatic district (NE Italy)

J. Environ. Radioact., 166 (2017), pp. 259-269, 10.1016/j.jenvrad.2016.07.011

ArticleDownload PDFView Record in ScopusGoogle Scholar

United Nations Scientific Committee on the Effects of Atomic Radiation, 2015

United Nations Scientific Committee on the Effects of Atomic Radiation

Report of the United Nations Scientific Committee on the Effects of Atomic Radiation to the General Assembly

(2015)

Google Scholar

Watson et al., 2017

R.J. Watson, M.A. Smethurst, G.V. Ganerød, I. Finne, A.L. Rudjord

The use of mapped geology as a predictor of radon potential in Norway

J. Environ. Radioact., 166 (2017), pp. 341-354, 10.1016/j.jenvrad.2016.05.031

ArticleDownload PDFView Record in ScopusGoogle Scholar

Wignall and Best, 2000

P. Wignall, J. Best

The western Irish Namurian basin reassessed

Basin Res., 12 (2000), pp. 59-78, 10.1046/j.1365-2117.2000.00113.x

View PDF

View Record in ScopusGoogle Scholar

World Health Organization, 2009

World Health Organization

WHO Handbook on Indoor Radon: a Public Health Perspective, World Health Organization (2009)

Google Scholar

World Health Organization, 2007

World Health Organization

International Radon Project: Survey on Radon Guidelines, Programmes and Activities (No

World Health Organization (2007)

WHO/HSE/RAD/07.01)

Google Scholar

Xuan et al., 2020

P. Xuan, N. Duong, V. Chinh, P. Dang, N. Qua, N. Pho

Soil gas radon measurement for identifying active faults in thua thien hue (vietnam)

J. Geosci. Environ. Protect., 8 (2020), 10.4236/gep.2020.87003

View PDF

Google Scholar

Xie et al., 2015

D. Xie, M. Liao, K.J. Kearfott

Appendix C

Influence of environmental factors on indoor radon concentration levels in the basement and ground floor of a building–A case study

Radiat. Meas., 82 (2015), pp. 52-58

ArticleDownload PDFView Record in ScopusGoogle Scholar

Yalım et al., 2018

H.A. Yalım, A. Gümüş, C. Başaran, M. Bağcı, A. Yıldız, D. Açil, M. Özçelik, M.Z. İl han, R. Ünal

Comparison of radon concentrations in soil gas and indoor environment of Afyonkarahisar Province

Arabian J. Geosci., 11 (2018), p. 246, 10.1007/s12517-018-3546-y

View PDF

View Record in ScopusGoogle Scholar

Extra statistical analysis of geochemical data: XRF CI stats

Appendix D

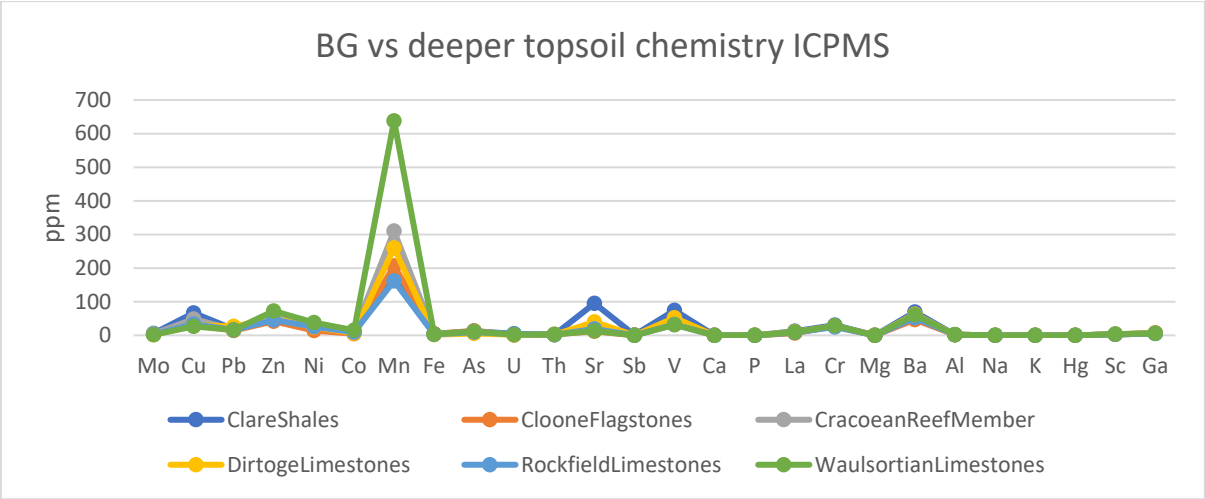
BG vs deeper topsoil chemistry ICPMS
ppm
700
600
500
400
300
200
100
0
Mo Cu Pb Zn Ni Co Mn Fe As U Th Sr Sb V Ca P La Cr Mg Ba Al Na K Hg Sc Ga
ClareShales
ClooneFlagstones
CracoeanReefMember
DirtogeLimestones
RockfieldLimestones
WaulsortianLimestones

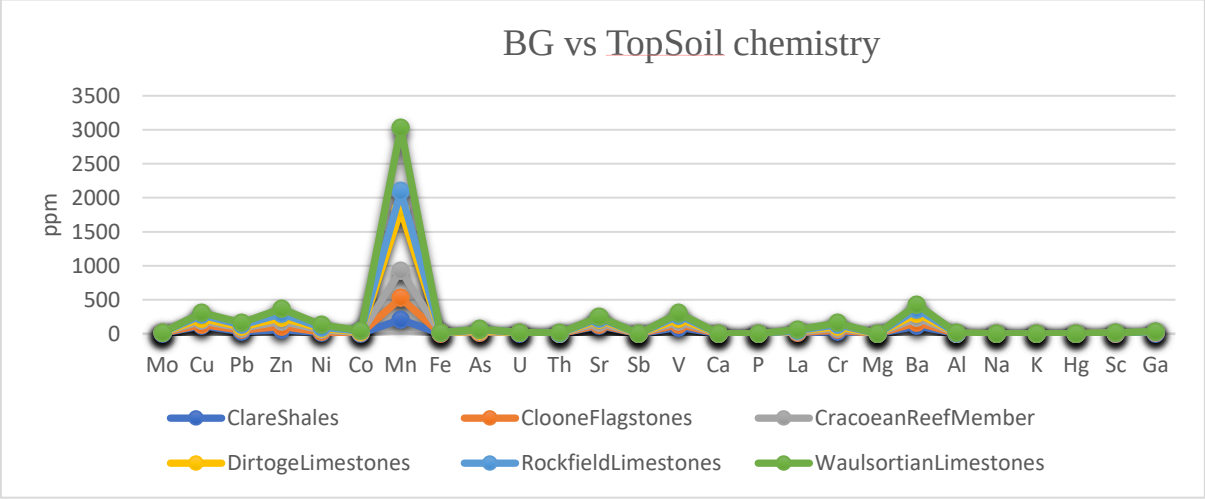
BG vs TopSoil chemistry
ppm
3500
3000
2500
2000
1500
1000
500
0
Mo Cu Pb Zn Ni Co Mn Fe As U Th Sr Sb V Ca P La Cr Mg Ba Al Na K Hg Sc Ga
ClareShales
ClooneFlagstones
CracoeanReefMember
DirtogeLimestones
RockfieldLimestones
WaulsortianLimestones

Appendix D

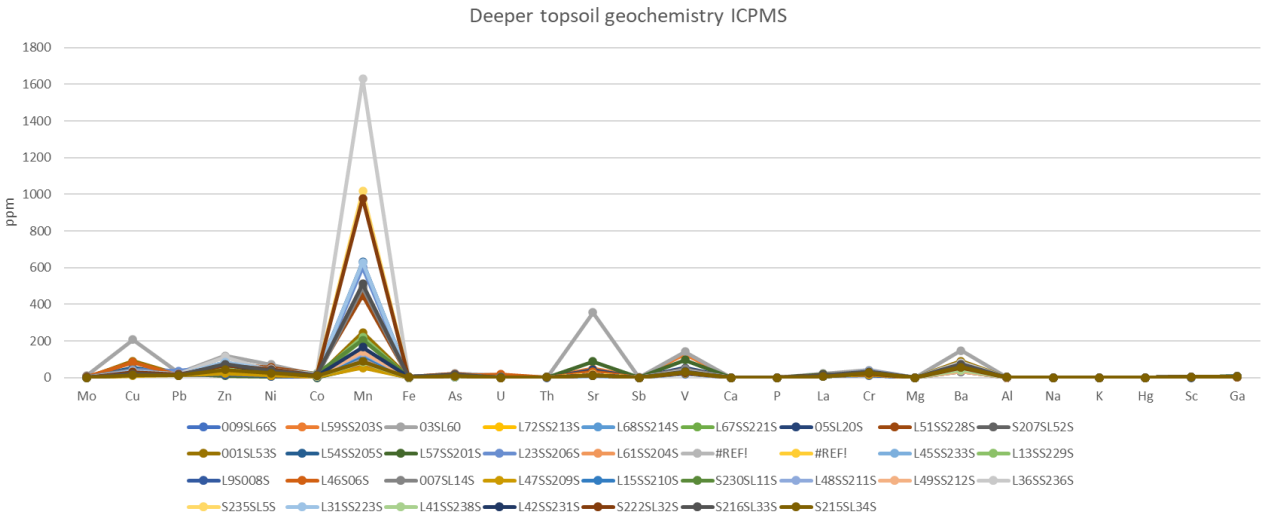
Deeper topsoil geochemistry ICPMS
ppm
1800
1600
1400
1200
1000
800
600
400
200
0
Mo Cu Pb Zn Ni Co Mn Fe As U Th Sr Sb V Ca P La Cr Mg Ba Al Na K Hg Sc Ga
009SL66S L59SS203S 03SL60 L72SS213S L68SS214S L67SS221S 05SL20S L51SS228S S207SL52S
001SL53S L54SS205S L57SS201S L23SS206S L61SS204S #REF! #REF! L45SS233S L13SS229S
L9S008S L46S06S 007SL14S L47SS209S L15SS210S S230SL11S L48SS211S L49SS212S L36SS236S
S235SL5S L31SS223S L41SS238S L42SS231S S222SL32S S216SL33S S215SL34S

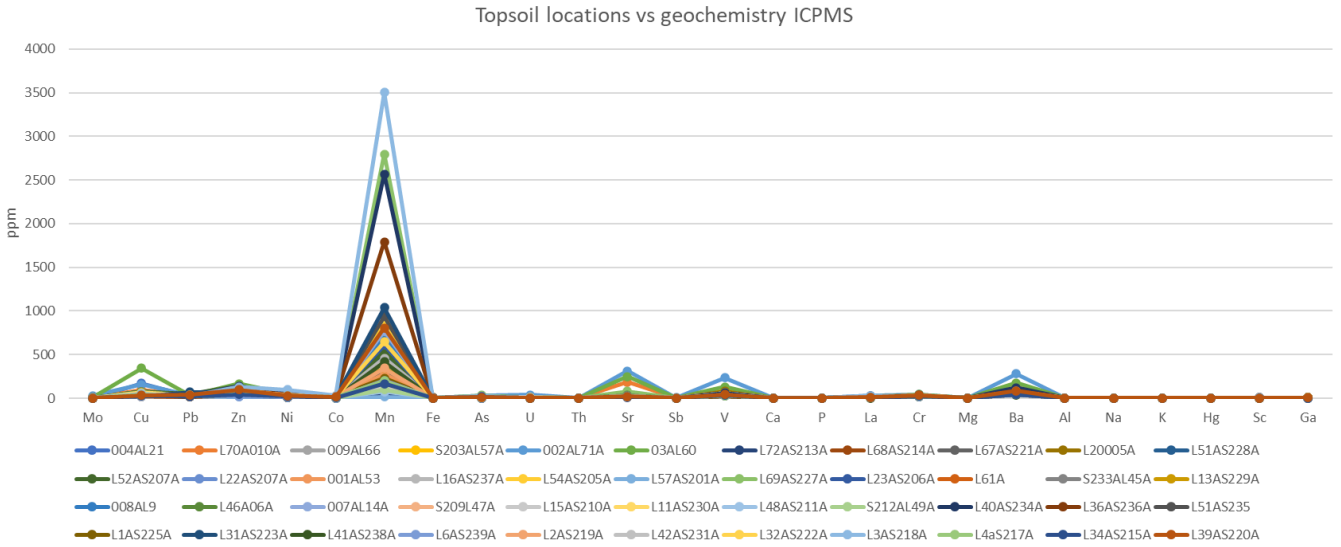
Topsoil locations vs geochemistry ICPMS
ppm
4000
3500
3000
2500
2000
1500
1000
500
0
Mo Cu Pb Zn Ni Co Mn Fe As U Th Sr Sb V Ca P La Cr Mg Ba Al Na K Hg Sc Ga
004AL21 L70A010A 009AL66 S203AL57A 002AL71A 03AL60 L72AS213A L68AS214A L67AS221A L20005A L51AS228A
L52AS207A L22AS207A 001AL53 L16AS237A L54AS205A L57AS201A L69AS227A L23AS206A L61A S233AL45A L13AS229A
008AL9 L46A06A 007AL14A S209L47A L15AS210A L11AS230A L48AS211A S212AL49A L40AS234A L36AS236A L51AS235
L1AS225A L31AS223A L41AS238A L6AS239A L2AS219A L42AS231A L32AS222A L3AS218A L4aS217A L34AS215A L39AS220A

Appendix D

Variograms ICPMS Aqua regia topsoil Castleisland, Co. Kerry.

Variograms compiled using ‘R’ software program, library ‘gstat’, r version 4.0.2.

```
TheVariogramModelxx <- vgm(psill= 0.015, #intersection at right yaxis
                           model="Sph", #curve type of model
                           nugget=0.001, #intersection with y axis
                           range=2000) #inflection point
```

ICPMS variograms

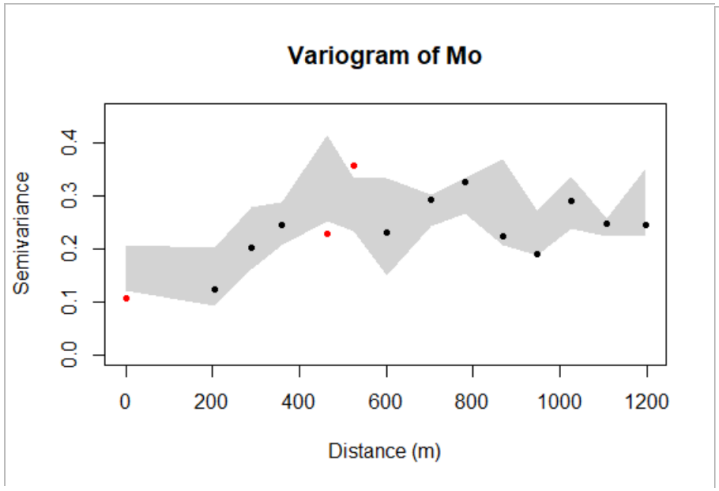

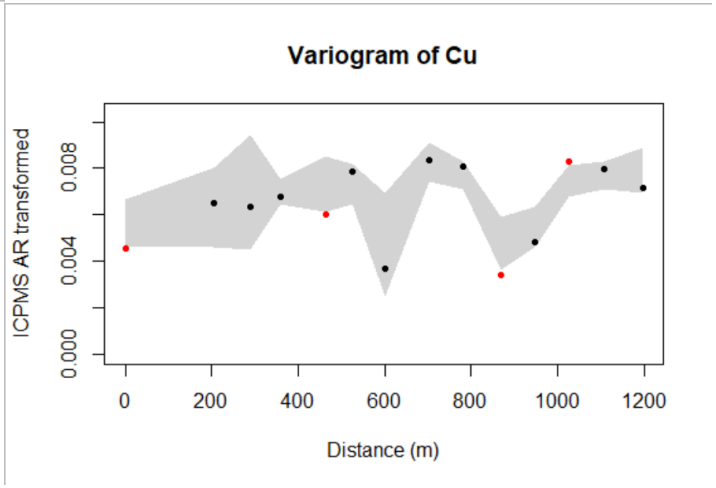

Appendix D

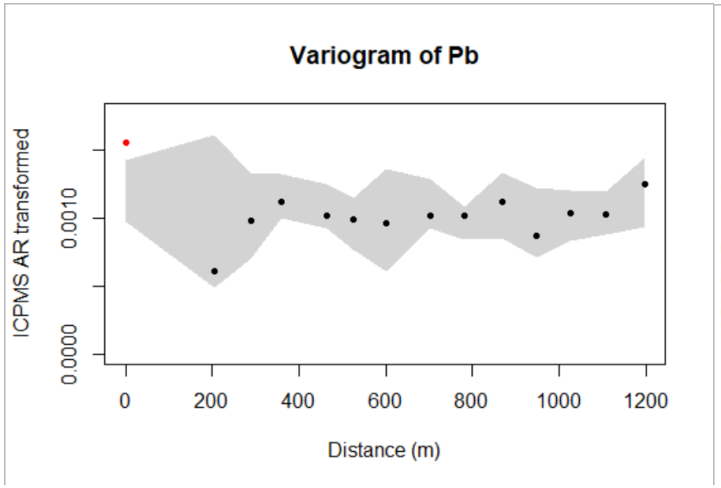
Variogram of Pb
ICPMS AR transformed
0.0000
0.0010
0
200
400
600
800
1000
1200
Distance (m)

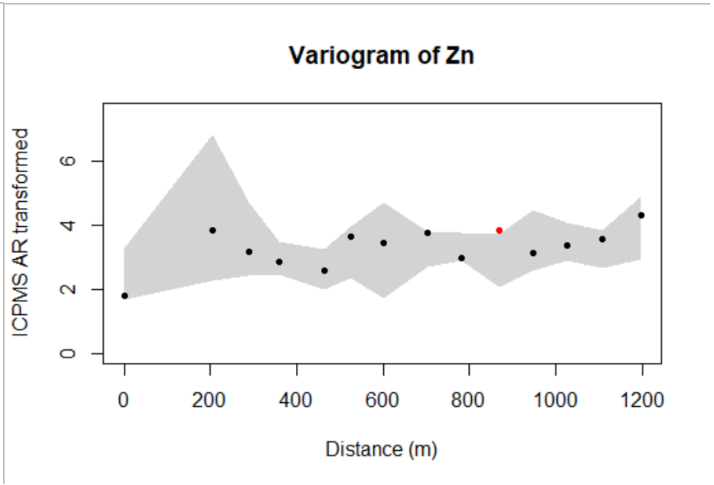
Variogram of Zn
ICPMS AR transformed
0
2
4
6
0
200
400
600
800
1000
1200
Distance (m)

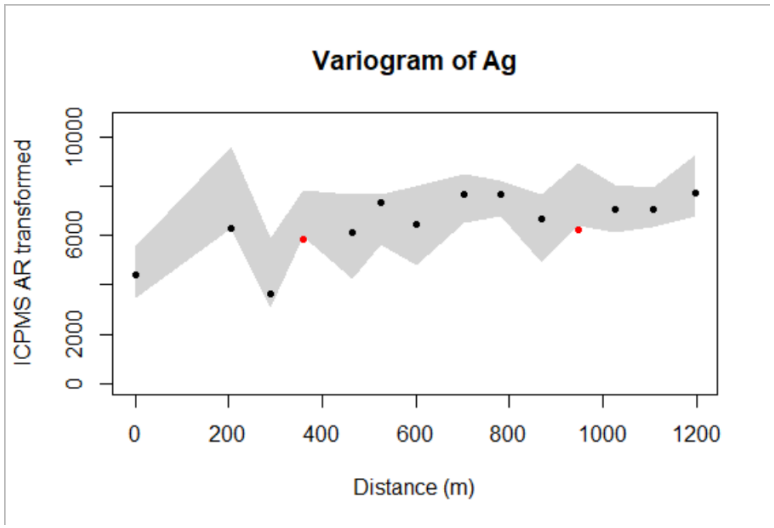
Variogram of Ag
ICPMS AR transformed
0
2000
6000
10000
0
200
400
600
800
1000
1200
Distance (m)

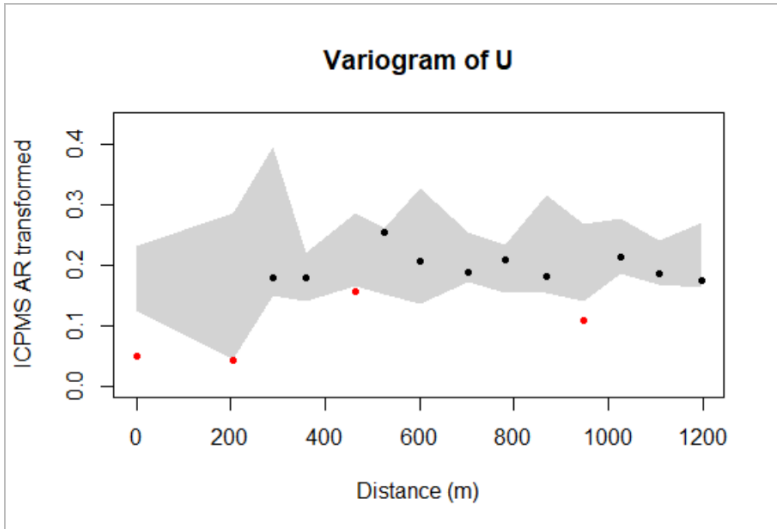
Variogram of U
ICPMS AR transformed
0.0
0.1
0.2
0.3
0.4
0
200
400
600
800
1000
1200
Distance (m)

Appendix D

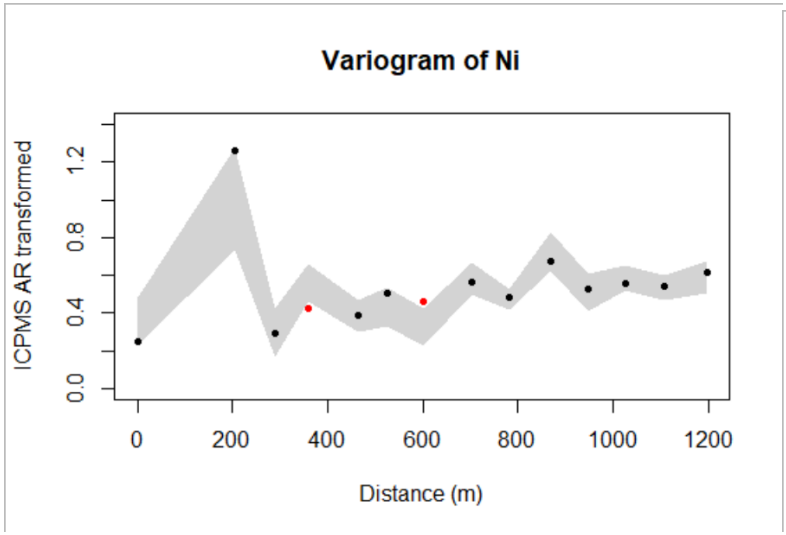
Variogram of Ni
ICPMS AR transformed
0.0
0.4
0.8
1.2
0
200
400
600
800
1000
1200
Distance (m)

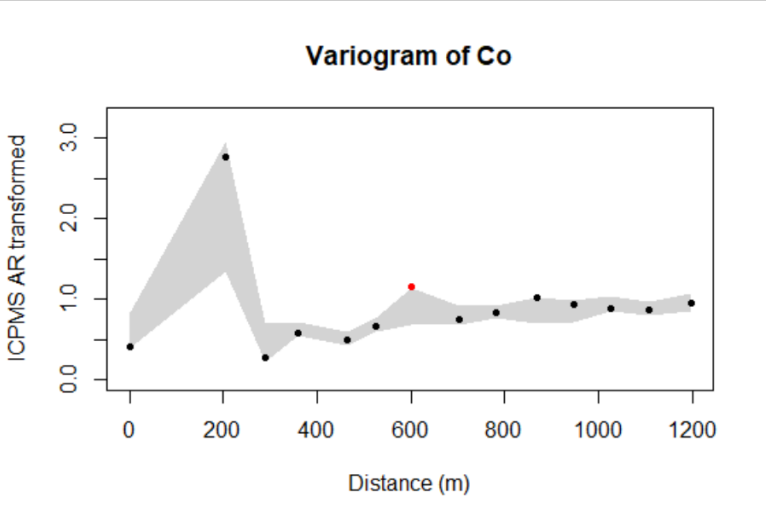
Variogram of Co
ICPMS AR transformed
0.0
1.0
2.0
3.0
0
200
400
600
800
1000
1200
Distance (m)

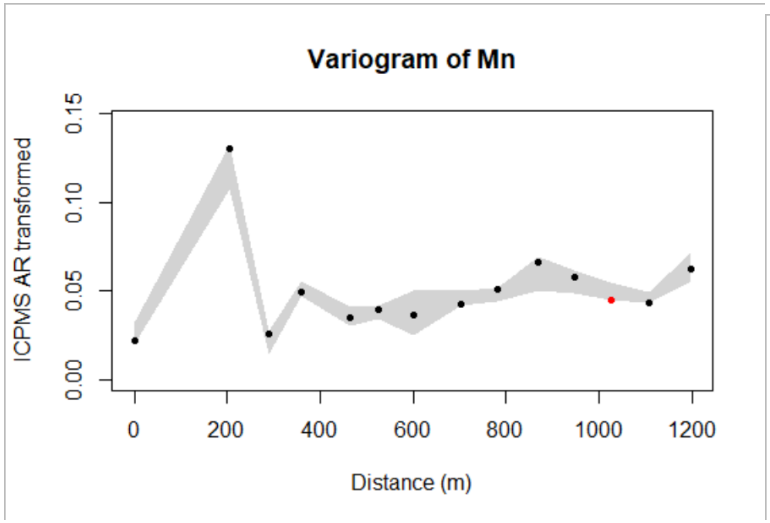
Variogram of Mn
ICPMS AR transformed
0.00
0.05
0.10
0.15
0
200
400
600
800
1000
1200
Distance (m)

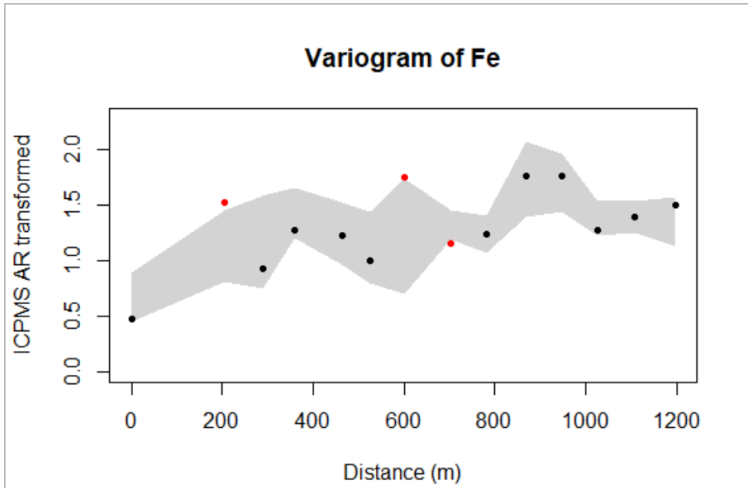
Variogram of Fe
ICPMS AR transformed
0.0
0.5
1.0
1.5
2.0
0
200
400
600
800
1000
1200
Distance (m)

Appendix D

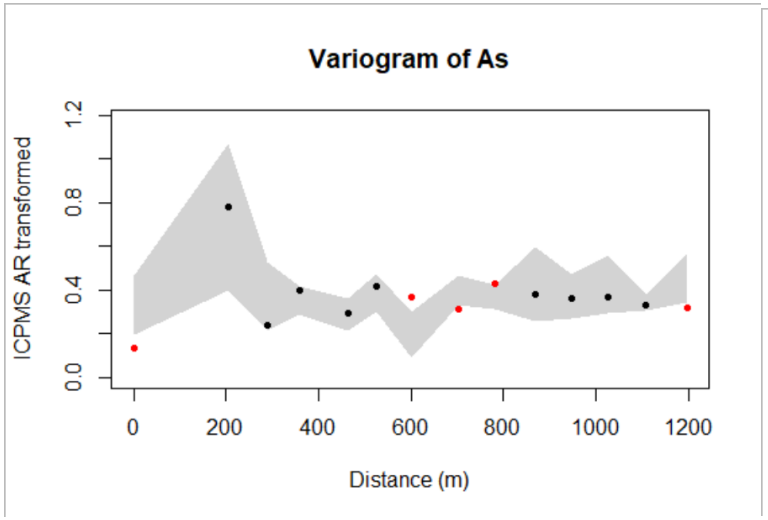
Variogram of As
ICPMS AR transformed
0.0
0.4
0.8
1.2
0
200
400
600
800
1000
1200
Distance (m)

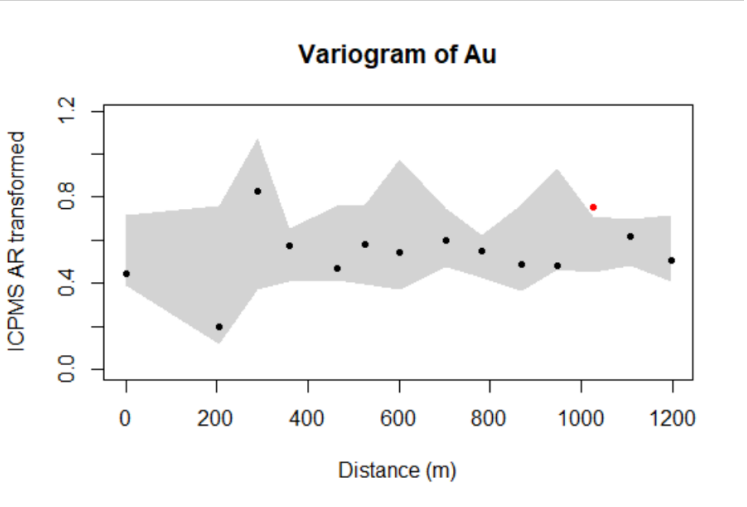
Variogram of Au
ICPMS AR transformed
0.0
0.4
0.8
1.2
0
200
400
600
800
1000
1200
Distance (m)

Appendix D

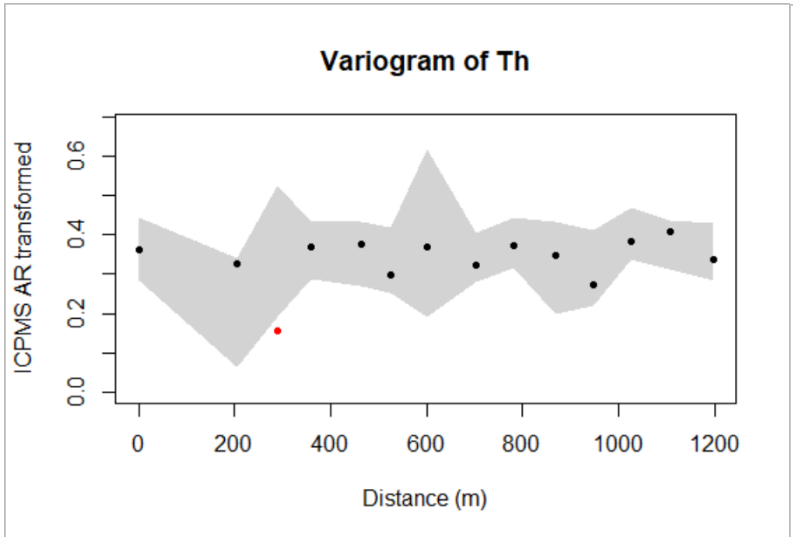
Variogram of Th
ICPMS AR transformed
0.0
0.2
0.4
0.6
0
200
400
600
800
1000
1200
Distance (m)

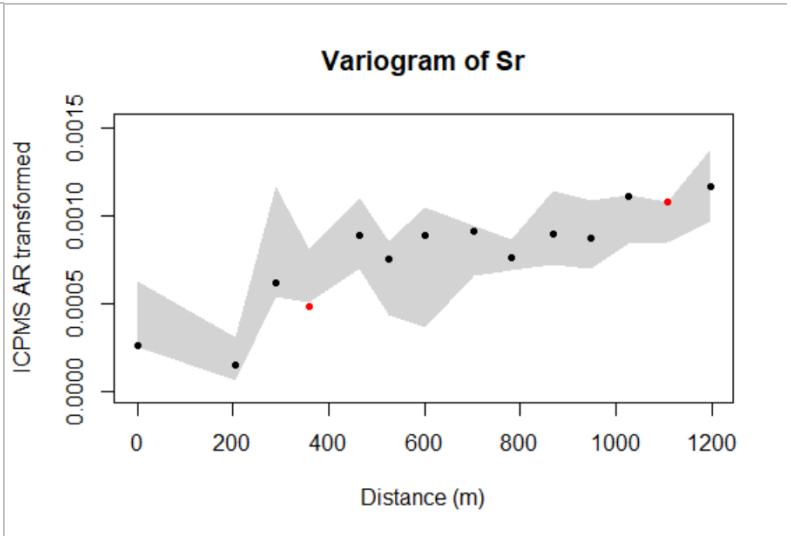
Variogram of Sr
ICPMS AR transformed
0.0000
0.0005
0.0010
0.0015
0
200
400
600
800
1000
1200
Distance (m)

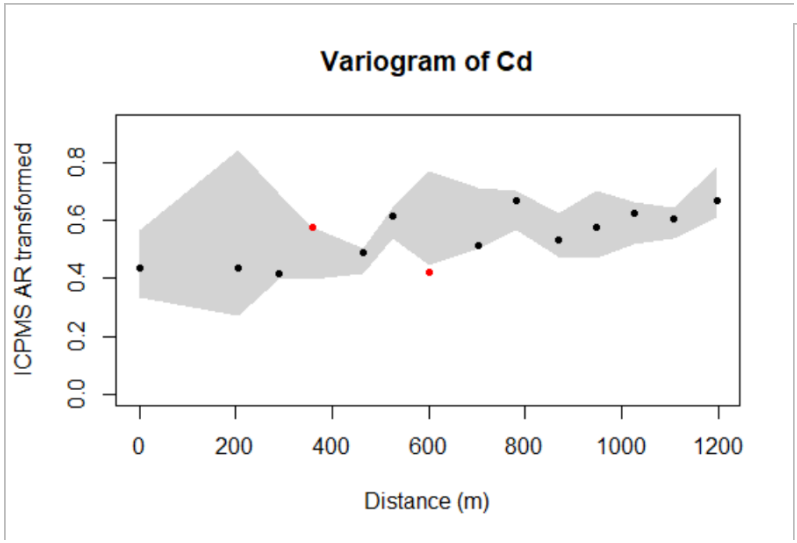
Variogram of Cd
ICPMS AR transformed
0.0
0.2
0.4
0.6
0.8
0
200
400
600
800
1000
1200
Distance (m)

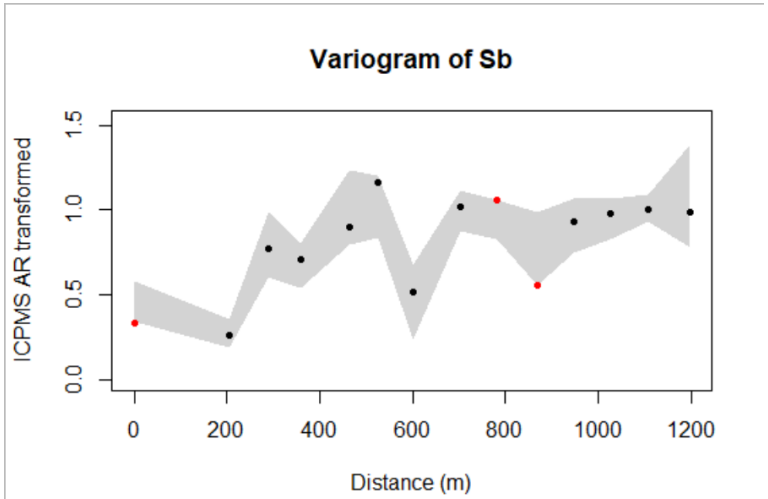
Variogram of Sb
ICPMS AR transformed
0.0
0.5
1.0
1.5
0
200
400
600
800
1000
1200
Distance (m)

Appendix D

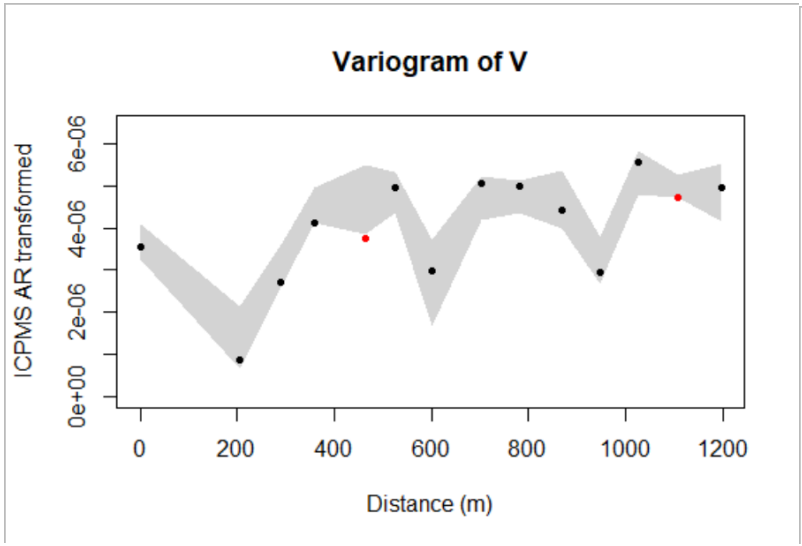
Variogram of V
ICPMS AR transformed
0e+00
2e-06
4e-06
6e-06
0
200
400
600
800
1000
1200
Distance (m)

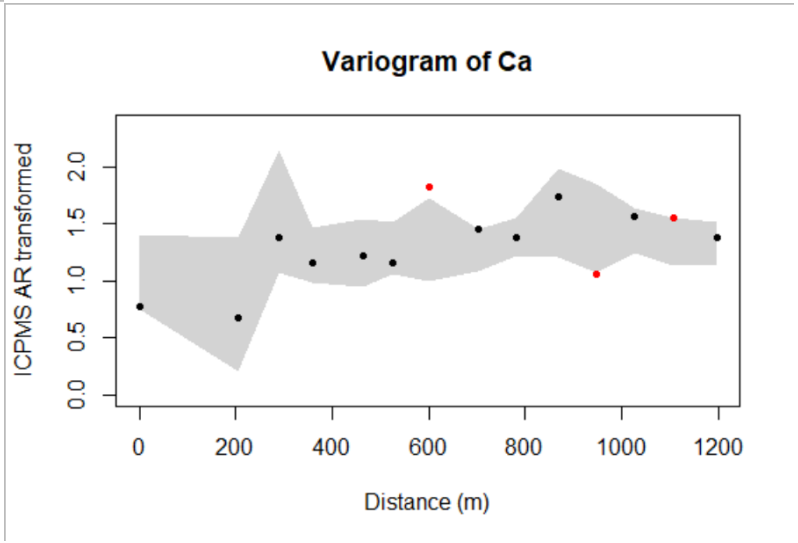
Variogram of Ca
ICPMS AR transformed
0.0
0.5
1.0
1.5
2.0
0
200
400
600
800
1000
1200
Distance (m)

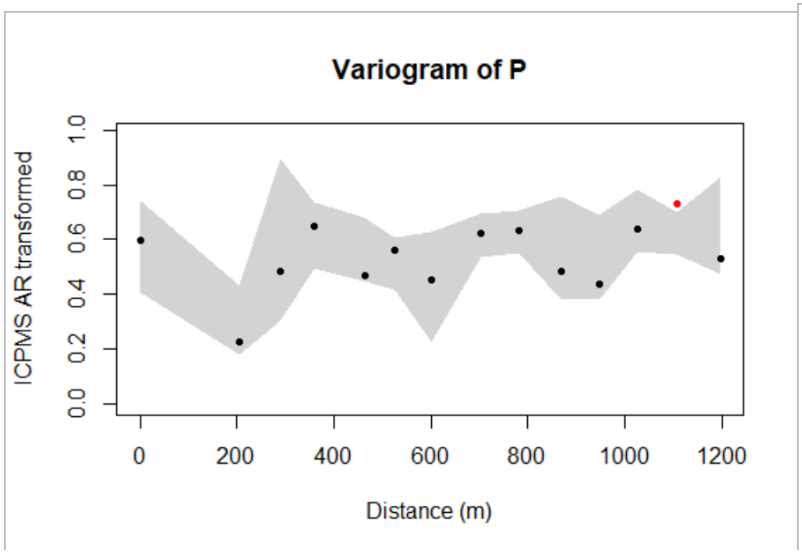
Variogram of P
ICPMS AR transformed
0.0
0.2
0.4
0.6
0.8
1.0
0
200
400
600
800
1000
1200
Distance (m)

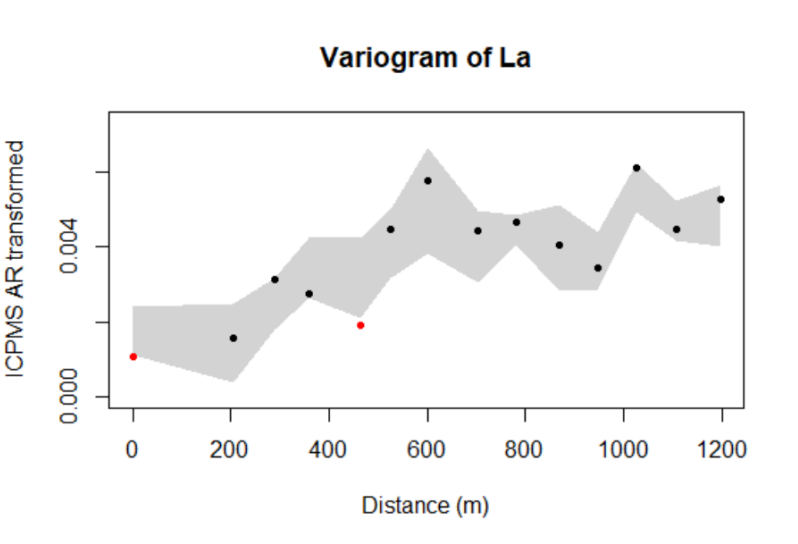
Variogram of La
ICPMS AR transformed
0.000
0.004
0
200
400
600
800
1000
1200
Distance (m)

Appendix D

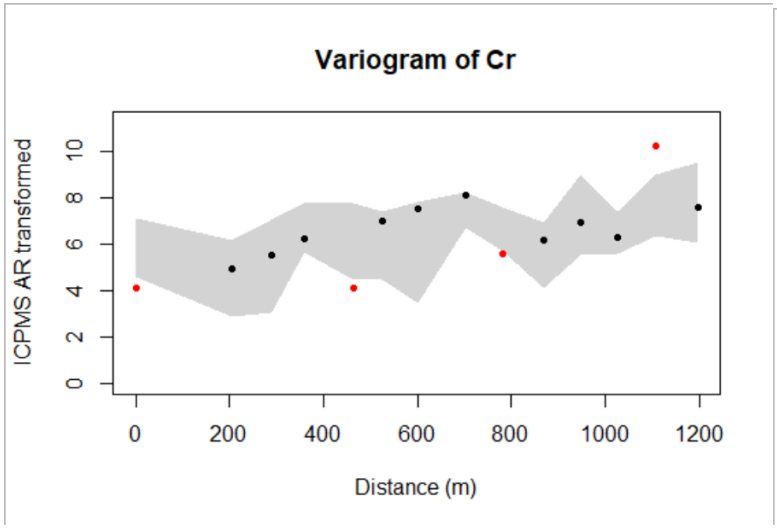
Variogram of Cr
ICPMS AR transformed
0
2
4
6
8
10
0
200
400
600
800
1000
1200
Distance (m)

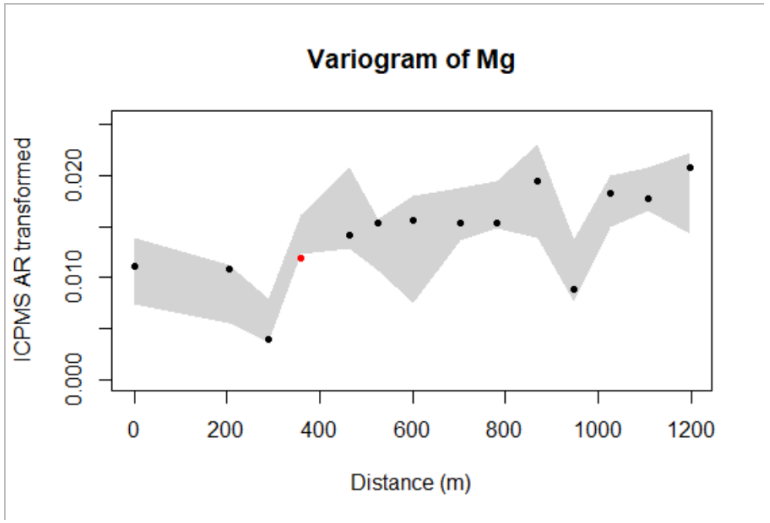
Variogram of Mg
ICPMS AR transformed
0.000
0.010
0.020
0
200
400
600
800
1000
1200
Distance (m)

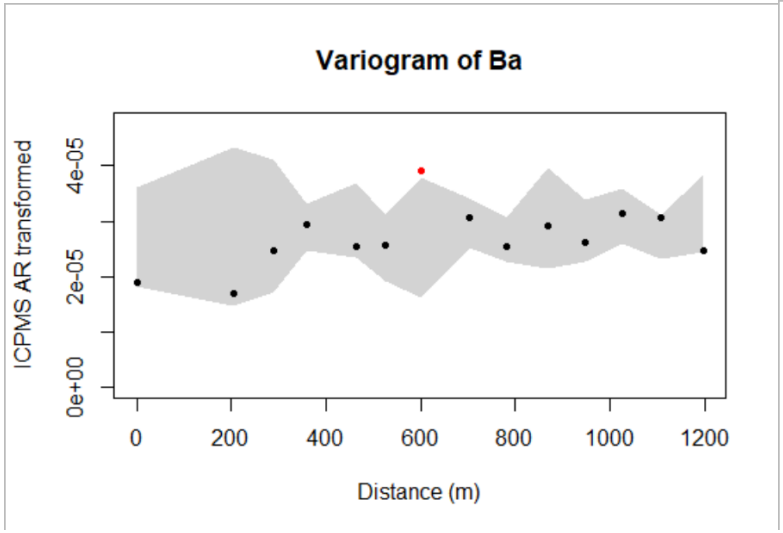
Variogram of Ba
ICPMS AR transformed
0e+00
2e-05
4e-05
0
200
400
600
800
1000
1200
Distance (m)

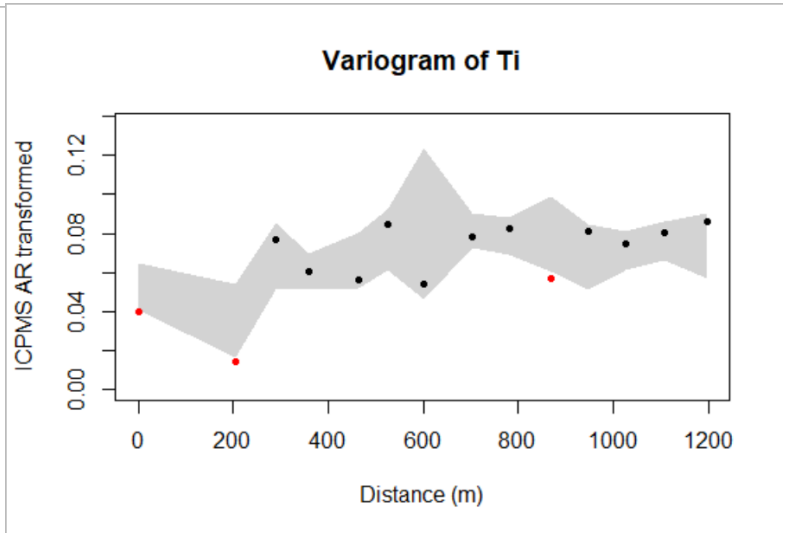
Variogram of Ti
ICPMS AR transformed
0.00
0.04
0.08
0.12
0
200
400
600
800
1000
1200
Distance (m)

Appendix D

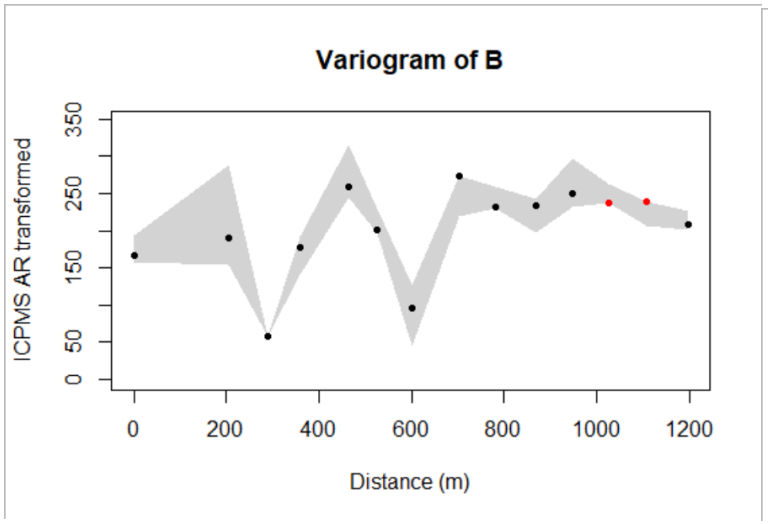
Variogram of B
ICPMS AR transformed
0
50
150
250
350
0
200
400
600
800
1000
1200
Distance (m)

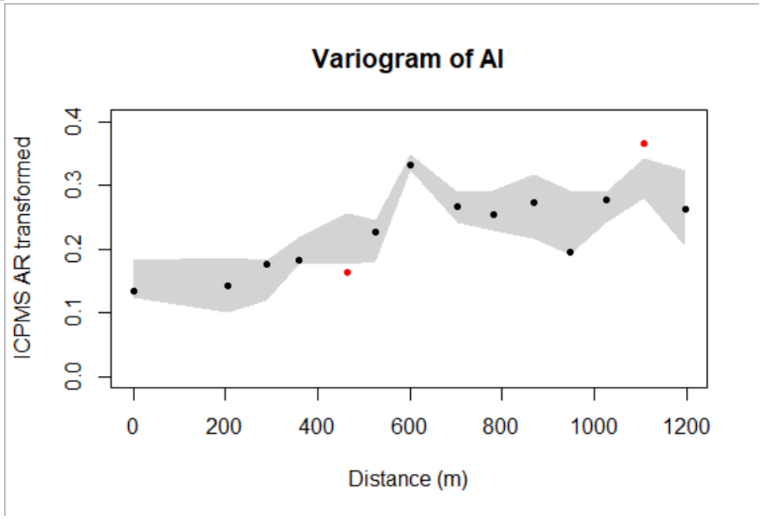
Variogram of Al
ICPMS AR transformed
0.0
0.1
0.2
0.3
0.4
0
200
400
600
800
1000
1200
Distance (m)

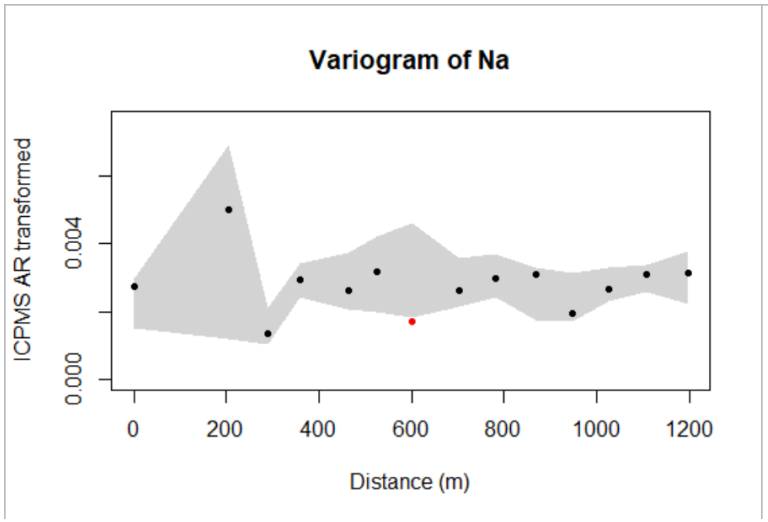
Variogram of Na
ICPMS AR transformed
0.000
0.004
0
200
400
600
800
1000
1200
Distance (m)

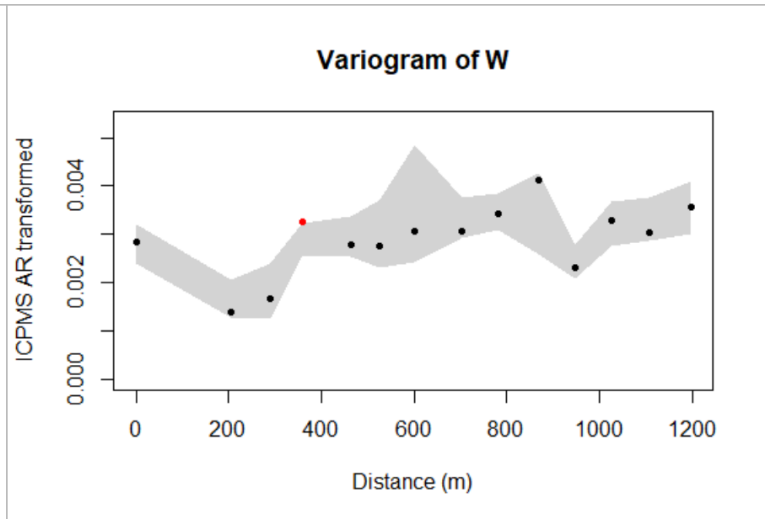
Variogram of W
ICPMS AR transformed
0.000
0.002
0.004
0
200
400
600
800
1000
1200
Distance (m)

Appendix D

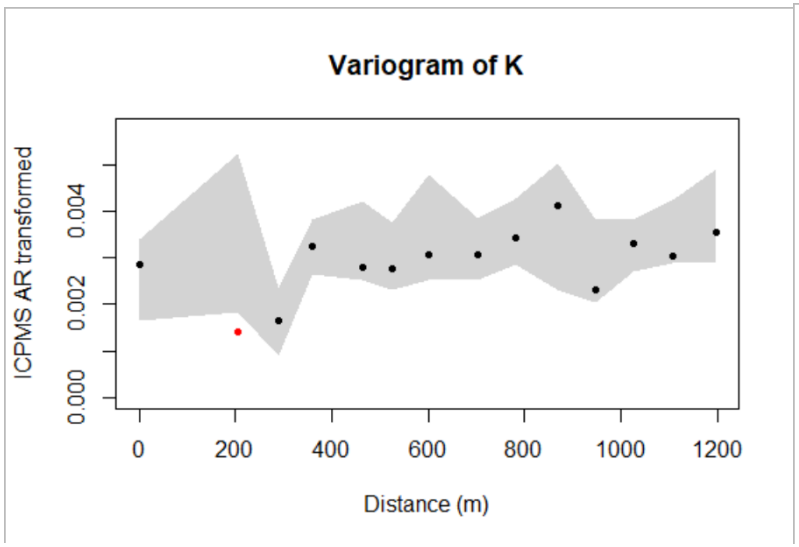
Variogram of K
ICPMS AR transformed
0.000
0.002
0.004
0
200
400
600
800
1000
1200
Distance (m)

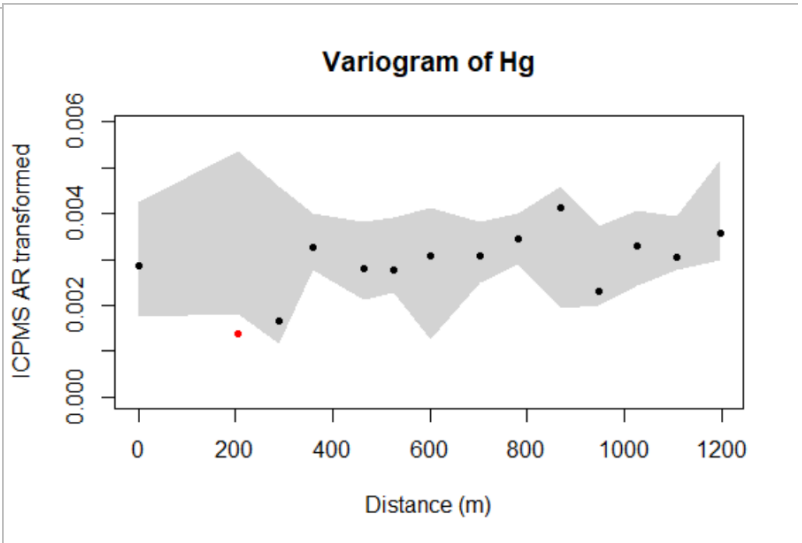
Variogram of Hg
ICPMS AR transformed
0.000
0.002
0.004
0.006
0
200
400
600
800
1000
1200
Distance (m)

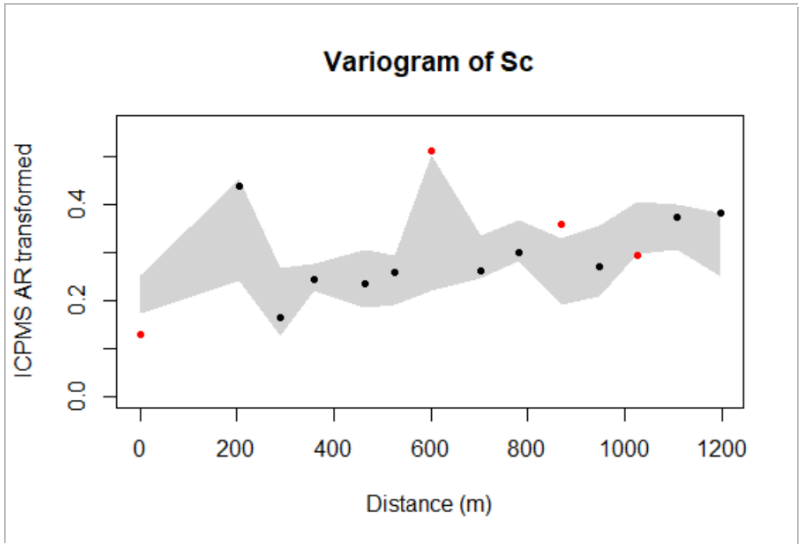
Variogram of Sc
ICPMS AR transformed
0.0
0.2
0.4
0
200
400
600
800
1000
1200
Distance (m)

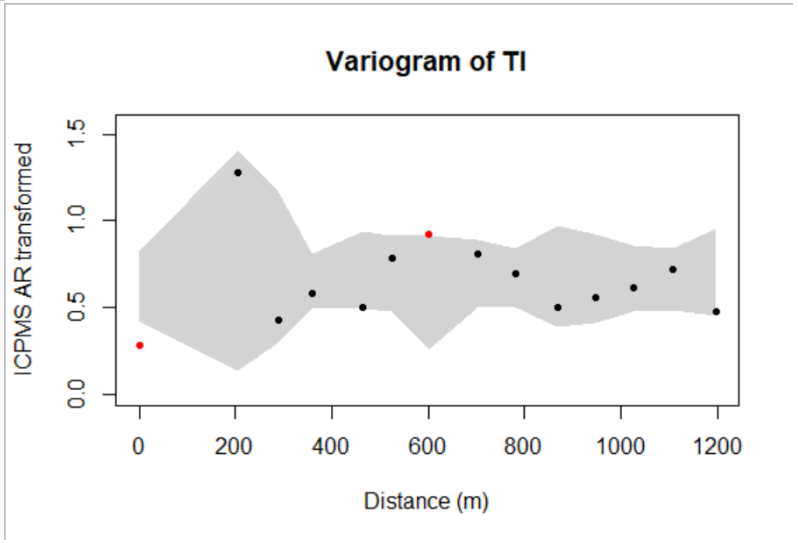
Variogram of Tl
ICPMS AR transformed
0.0
0.5
1.0
1.5
0
200
400
600
800
1000
1200
Distance (m)

Appendix D

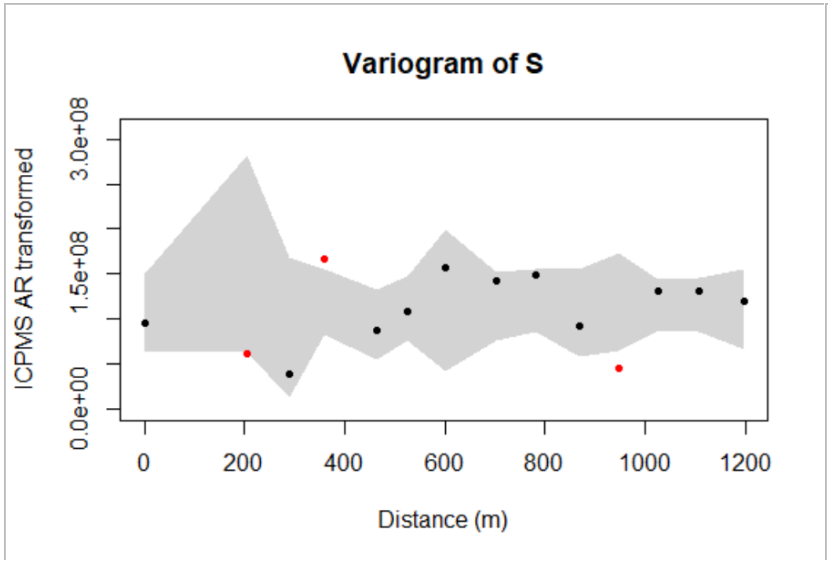
Variogram of S
ICPMS AR transformed
0.0e+00
1.5e+08
3.0e+08
0
200
400
600
800
1000
1200
Distance (m)

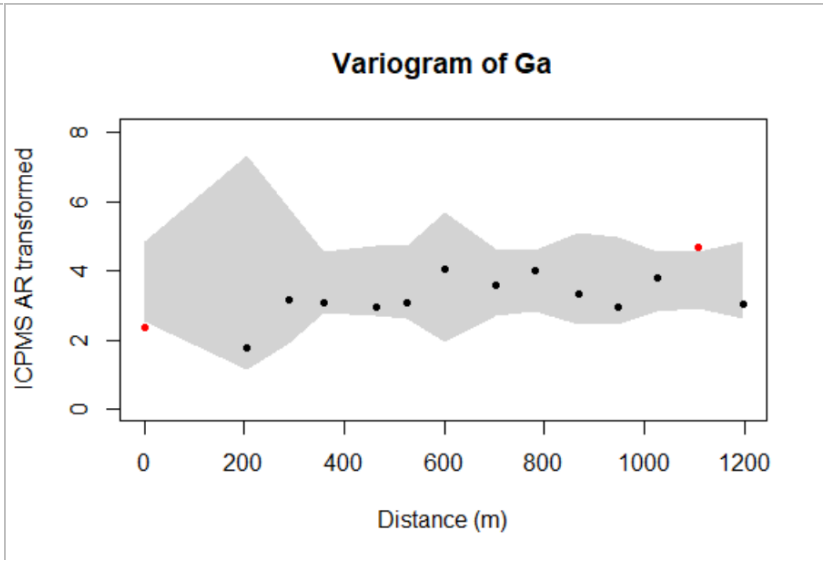
Variogram of Ga
ICPMS AR transformed
0
2
4
6
8
0
200
400
600
800
1000
1200
Distance (m)

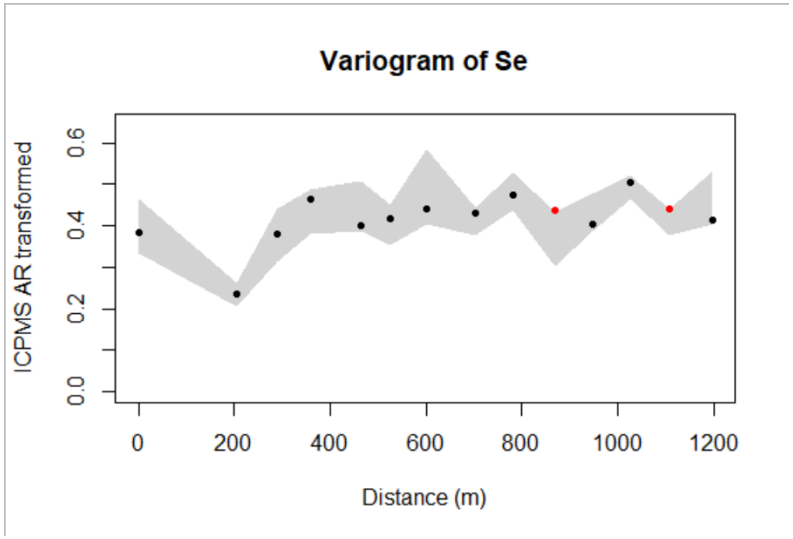
Variogram of Se
ICPMS AR transformed
0.0
0.2
0.4
0.6
0
200
400
600
800
1000
1200
Distance (m)

Appendix D

ICPES variograms

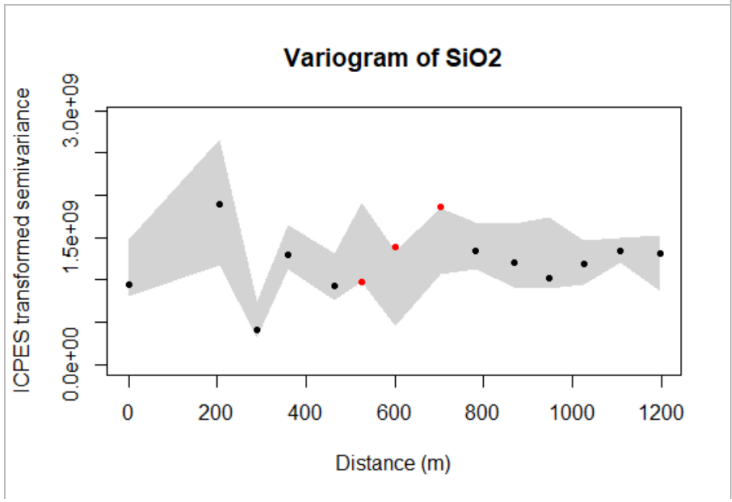

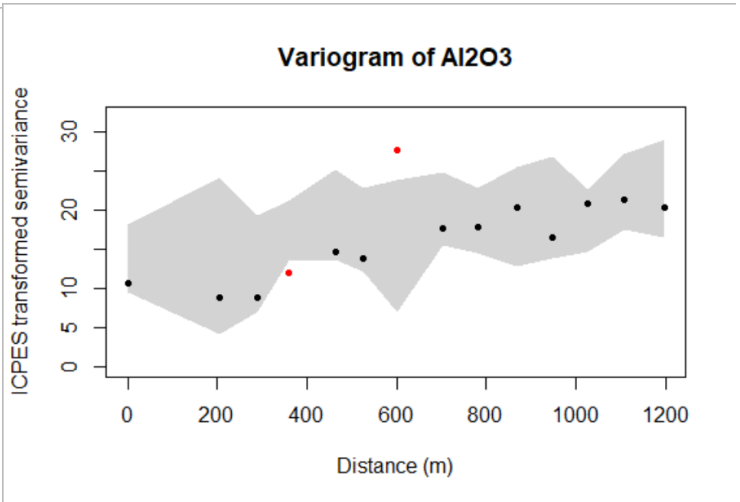

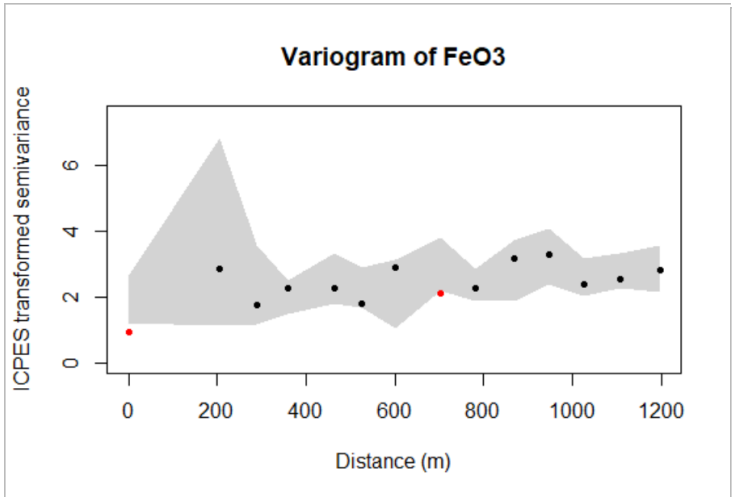

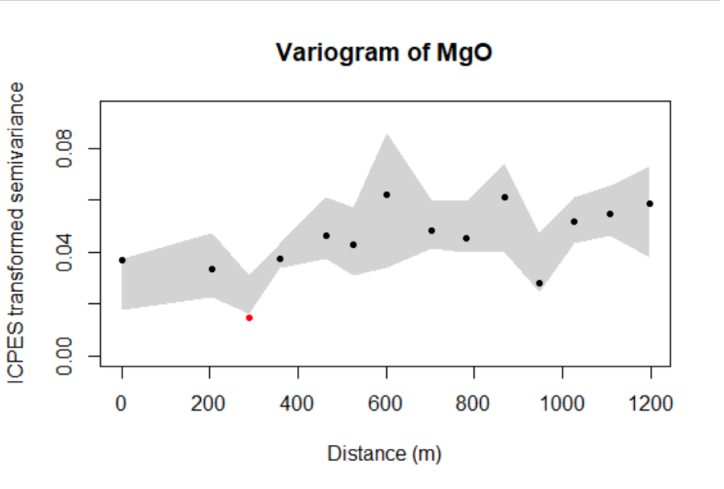

Appendix D

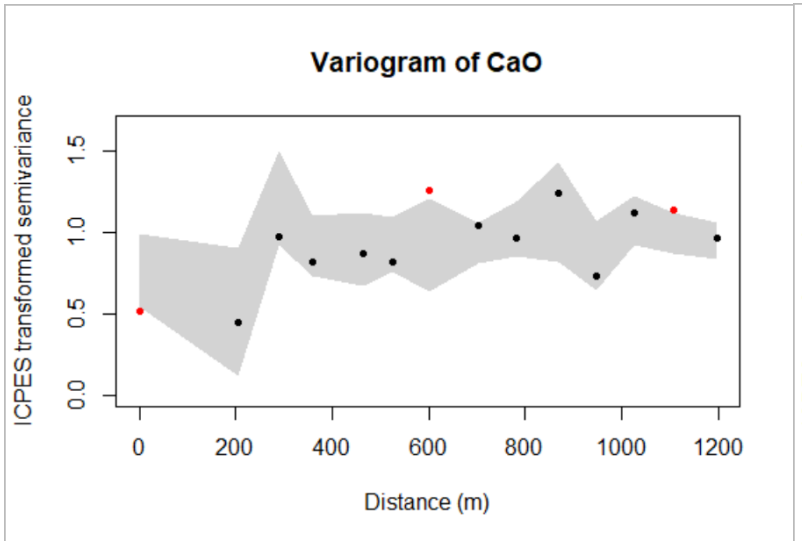
Variogram of CaO
ICPES transformed semivariance
0.0
0.5
1.0
1.5
0
200
400
600
800
1000
1200
Distance (m)

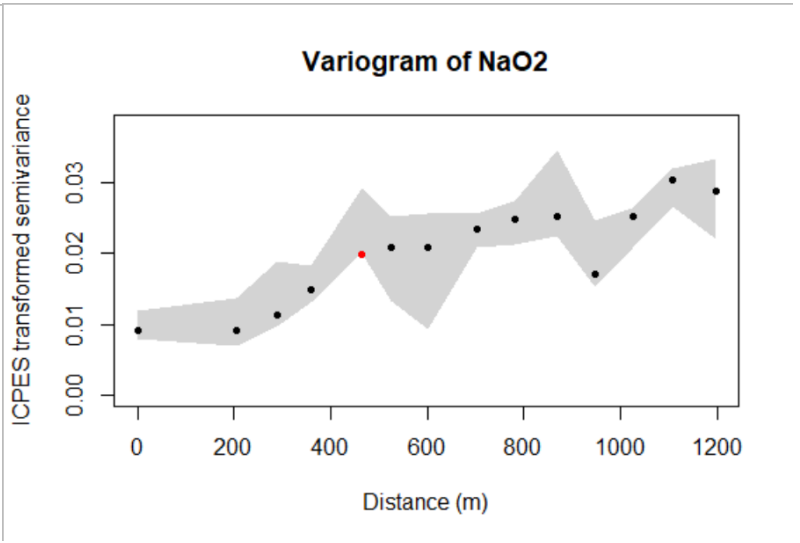
Variogram of NaO2
ICPES transformed semivariance
0.00
0.01
0.02
0.03
0
200
400
600
800
1000
1200
Distance (m)

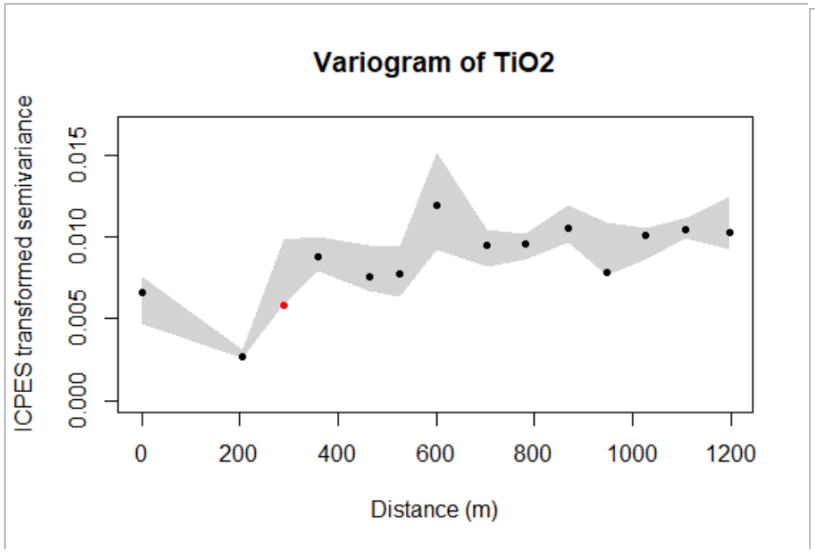
Variogram of TiO2
ICPES transformed semivariance
0.000
0.005
0.010
0.015
0
200
400
600
800
1000
1200
Distance (m)

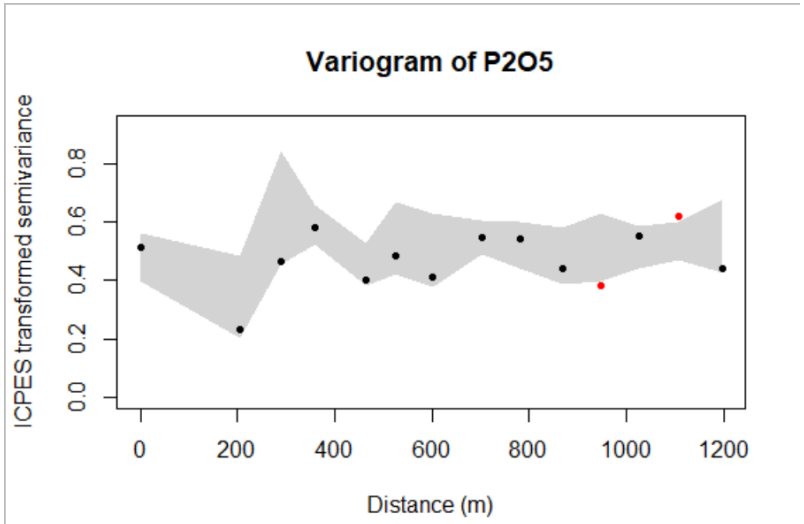
Variogram of P2O5
ICPES transformed semivariance
0.0
0.2
0.4
0.6
0.8
0
200
400
600
800
1000
1200
Distance (m)

Appendix D

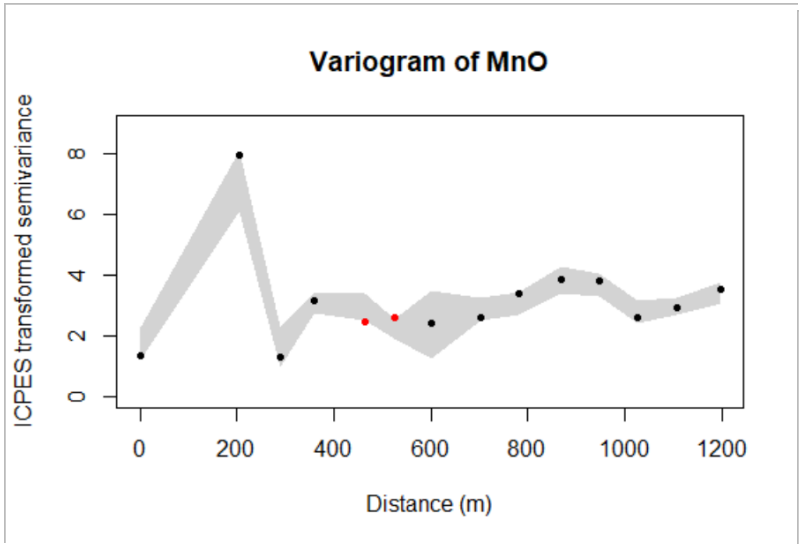
Variogram of MnO
ICPES transformed semivariance
0
2
4
6
8
0
200
400
600
800
1000
1200
Distance (m)

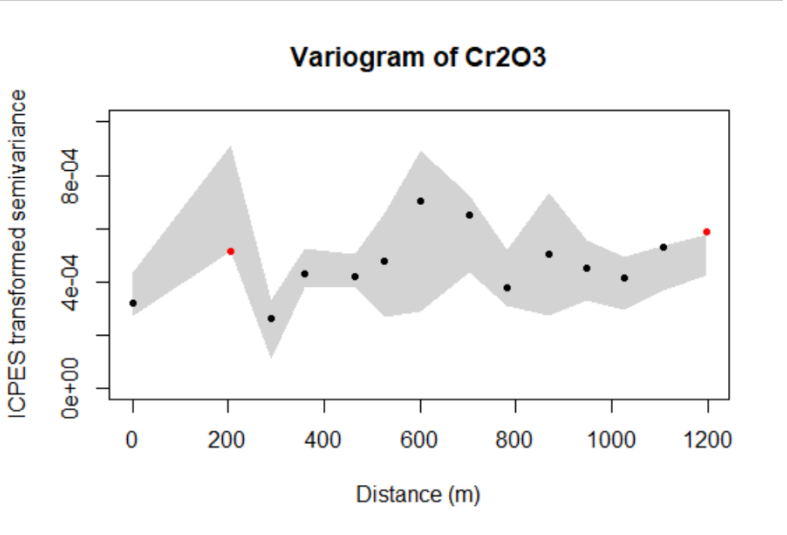
Variogram of Cr2O3
ICPES transformed semivariance
0e+00
4e-04
8e-04
0
200
400
600
800
1000
1200
Distance (m)

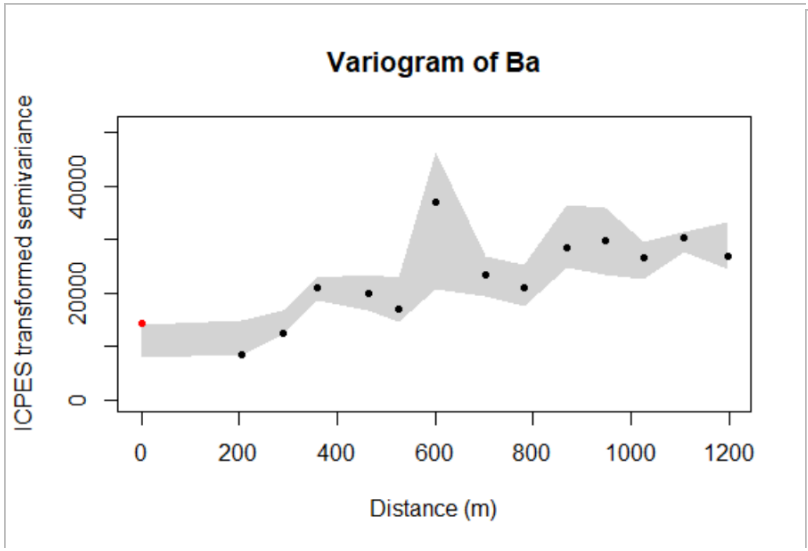
Variogram of Ba
ICPES transformed semivariance
0
20000
40000
0
200
400
600
800
1000
1200
Distance (m)

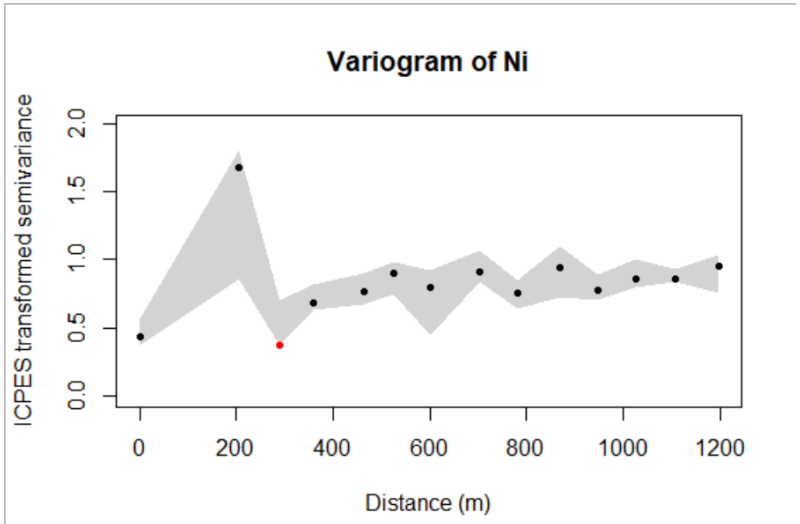
Variogram of Ni
ICPES transformed semivariance
0.0
0.5
1.0
1.5
2.0
0
200
400
600
800
1000
1200
Distance (m)

Appendix D

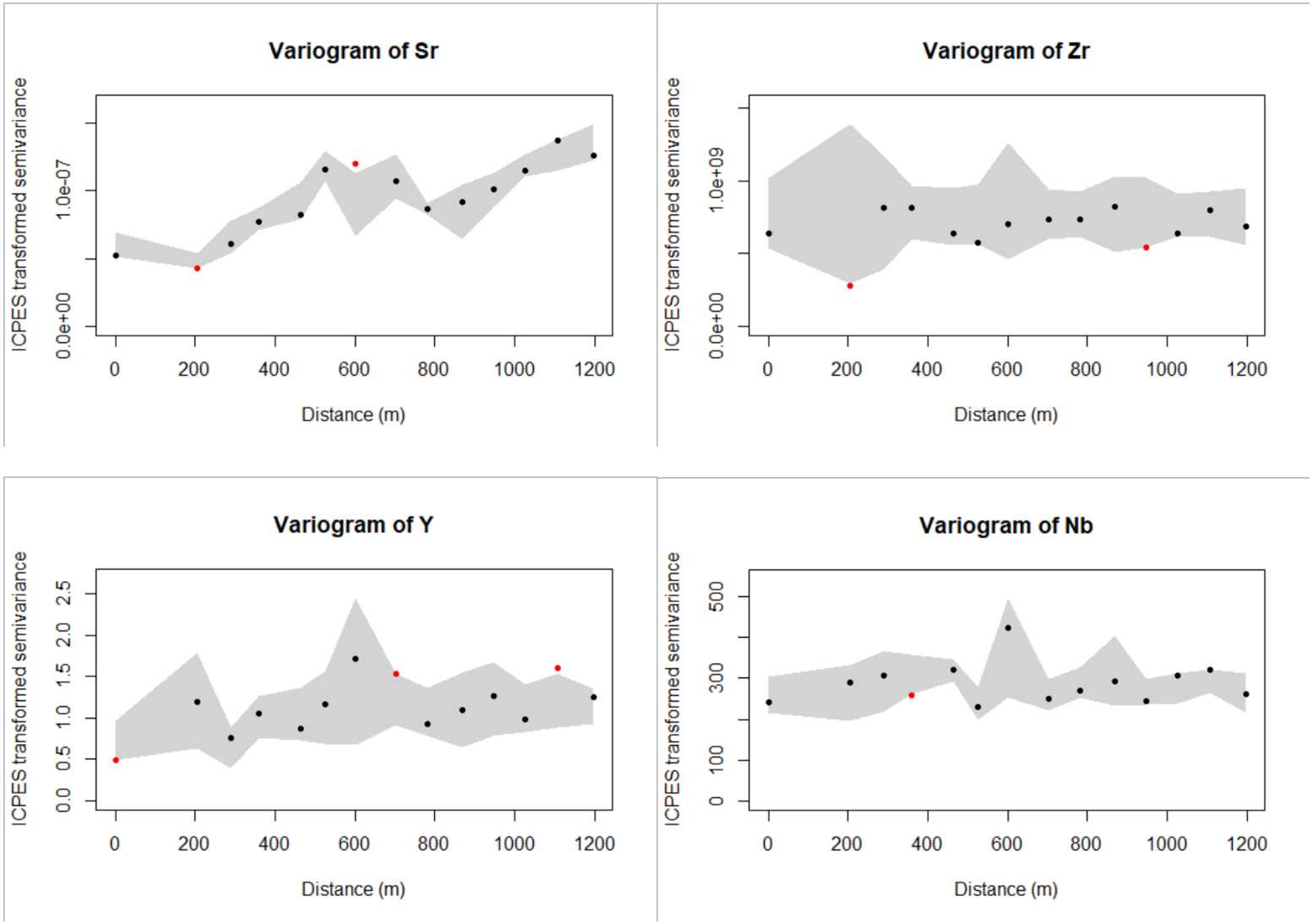
Variogram of Sr
ICPES transformed semivariance
0.0e+00
1.0e-07
0
200
400
600
800
1000
1200
Distance (m)
Variogram of Zr
ICPES transformed semivariance
0.0e+00
1.0e+09
0
200
400
600
800
1000
1200
Distance (m)
Variogram of Y
ICPES transformed semivariance
0.0
0.5
1.0
1.5
2.0
2.5
0
200
400
600
800
1000
1200
Distance (m)
Variogram of Nb
ICPES transformed semivariance
0
100
300
500
0
200
400
600
800
1000
1200
Distance (m)

Appendix D

XRF variograms

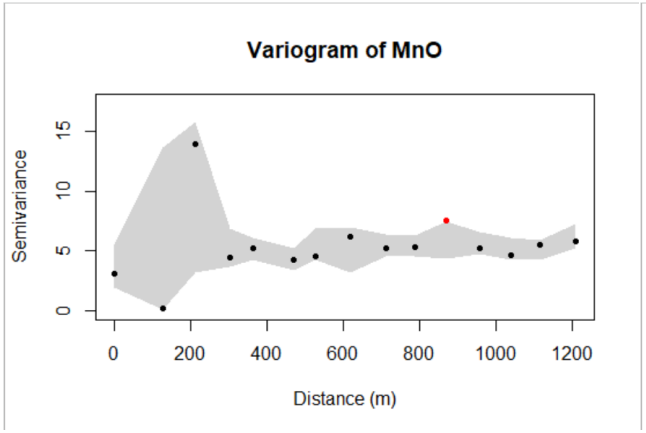

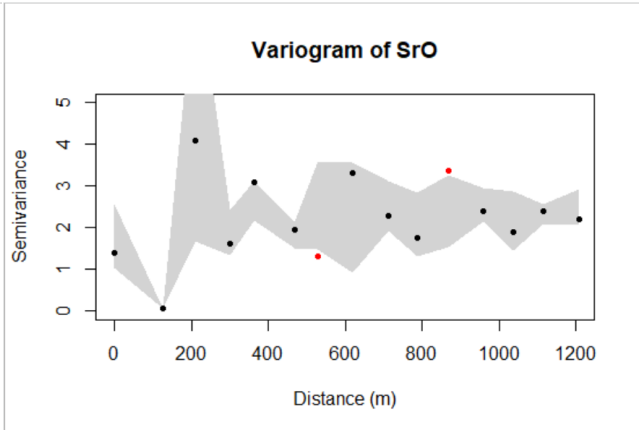

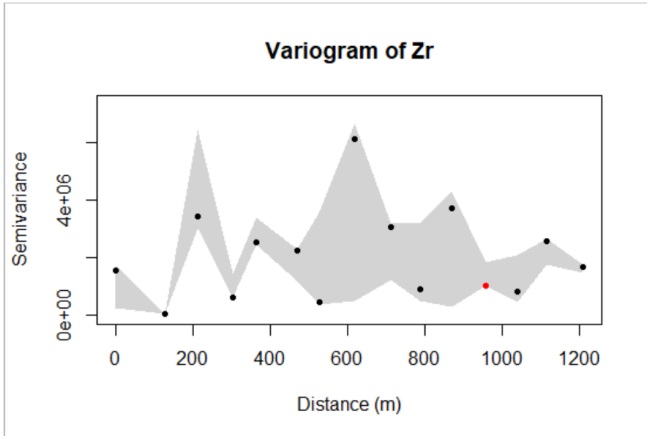

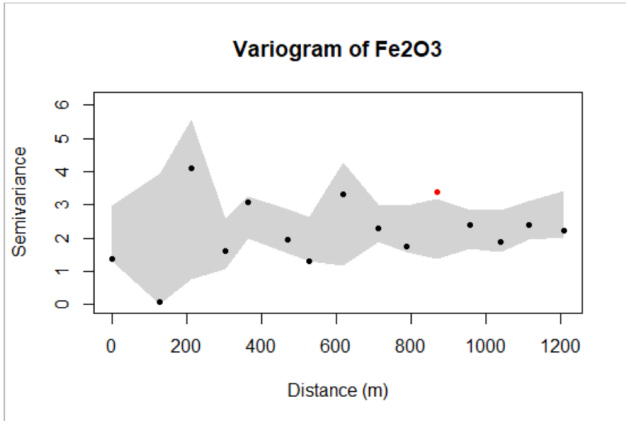

Appendix D

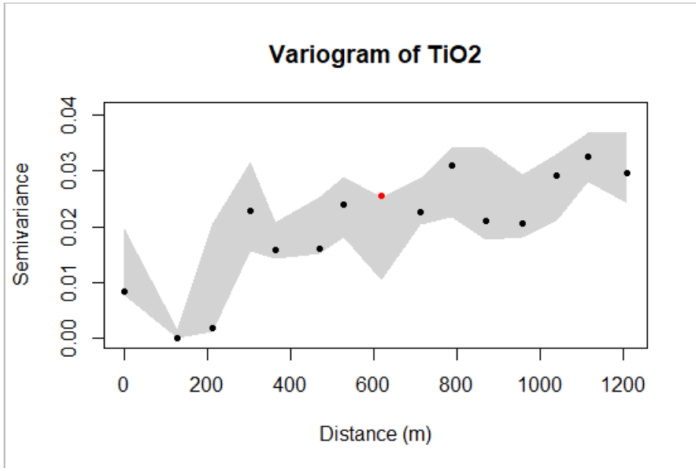
Variogram of TiO2
Semivariance
0.00
0.01
0.02
0.03
0.04
0
200
400
600
800
1000
1200
Distance (m)

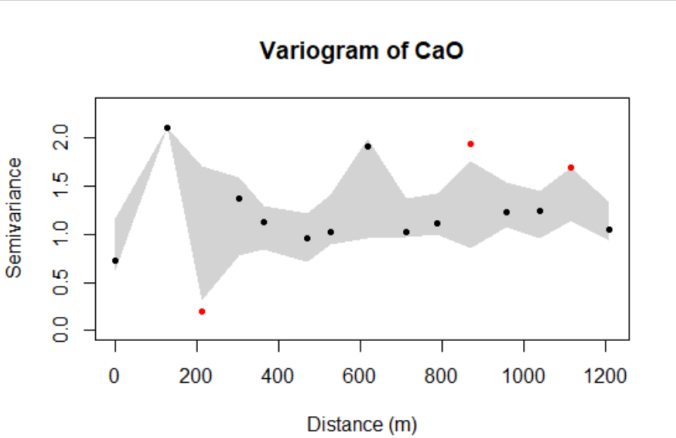
Variogram of CaO
Semivariance
0.0
0.5
1.0
1.5
2.0
0
200
400
600
800
1000
1200
Distance (m)

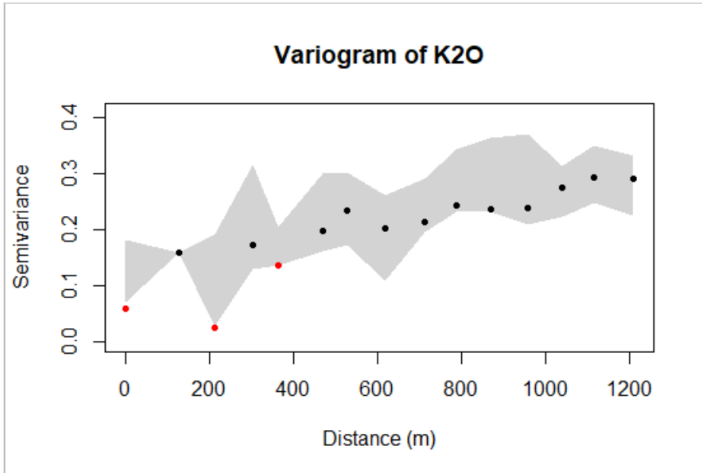
Variogram of K2O
Semivariance
0.0
0.1
0.2
0.3
0.4
0
200
400
600
800
1000
1200
Distance (m)

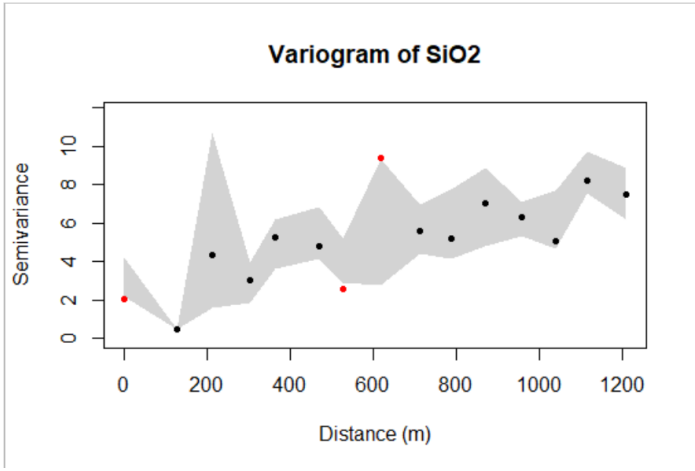
Variogram of SiO2
Semivariance
0
2
4
6
8
10
0
200
400
600
800
1000
1200
Distance (m)

Appendix D

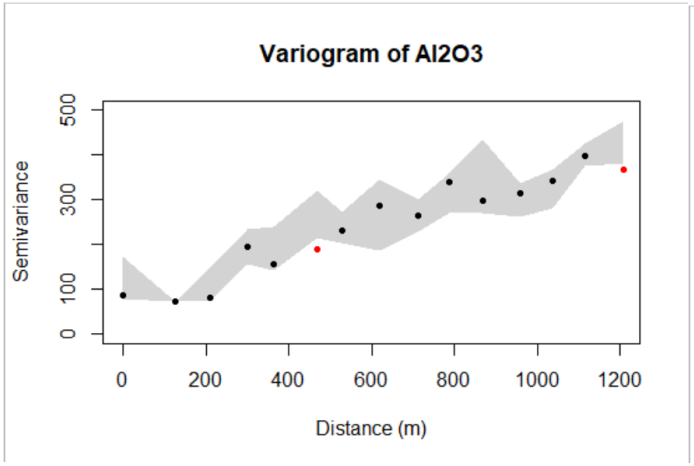
Variogram of Al2O3
Semivariance
0
100
300
500
0
200
400
600
800
1000
1200
Distance (m)

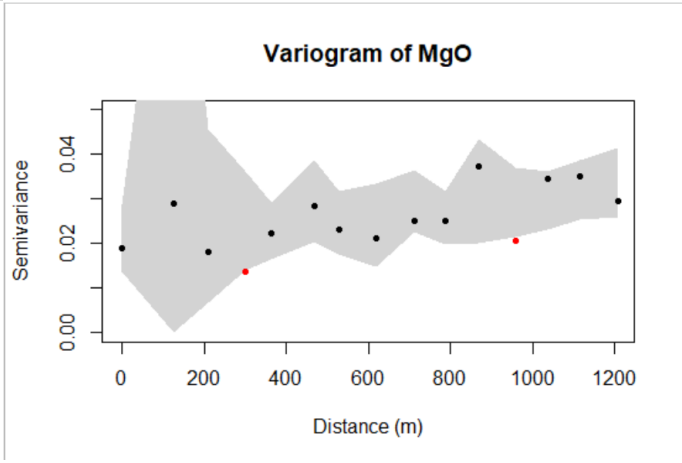
Variogram of MgO
Semivariance
0.00
0.02
0.04
0
200
400
600
800
1000
1200
Distance (m)

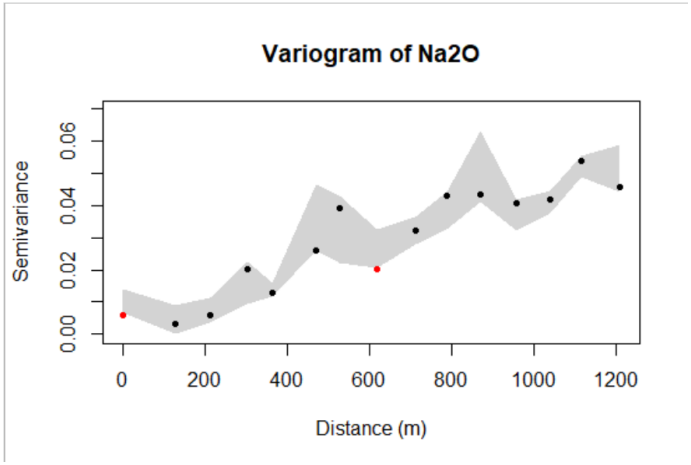
Variogram of Na2O
Semivariance
0.00
0.02
0.04
0.06
0
200
400
600
800
1000
1200
Distance (m)

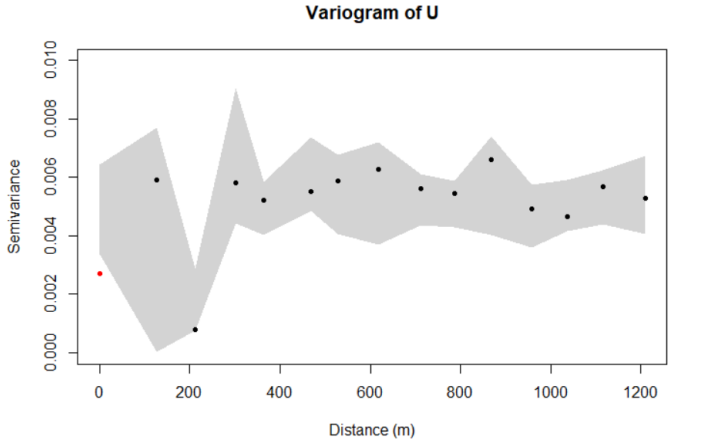
Variogram of U
Semivariance
0.000
0.002
0.004
0.006
0.008
0.010
0
200
400
600
800
1000
1200
Distance (m)

Appendix D

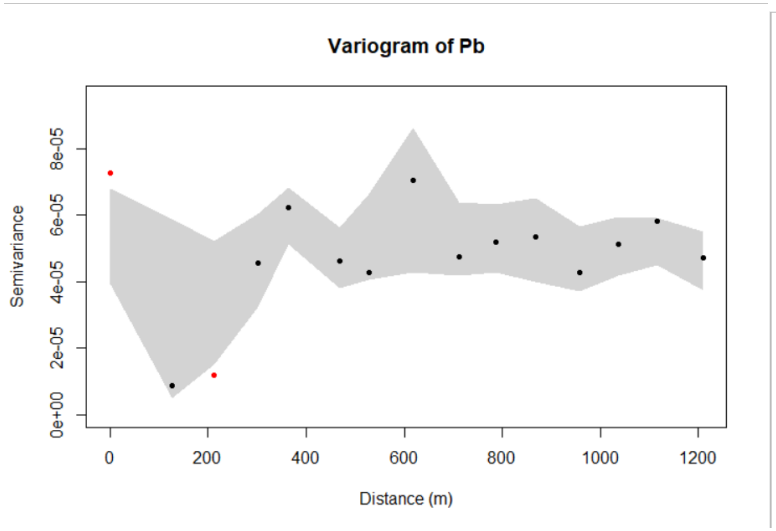
Variogram of Pb
Semivariance
0e+00
2e-05
4e-05
6e-05
8e-05
0
200
400
600
800
1000
1200
Distance (m)

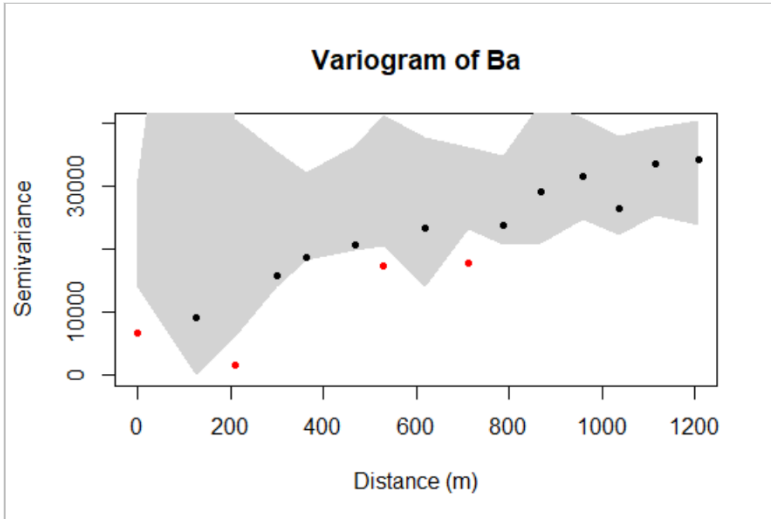
Variogram of Ba
Semivariance
0
10000
30000
0
200
400
600
800
1000
1200
Distance (m)

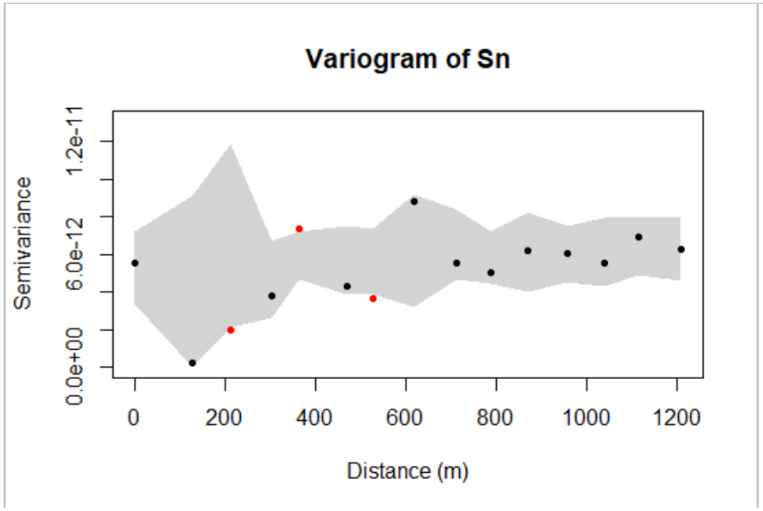
Variogram of Sn
Semivariance
0.0e+00
6.0e-12
1.2e-11
0
200
400
600
800
1000
1200
Distance (m)

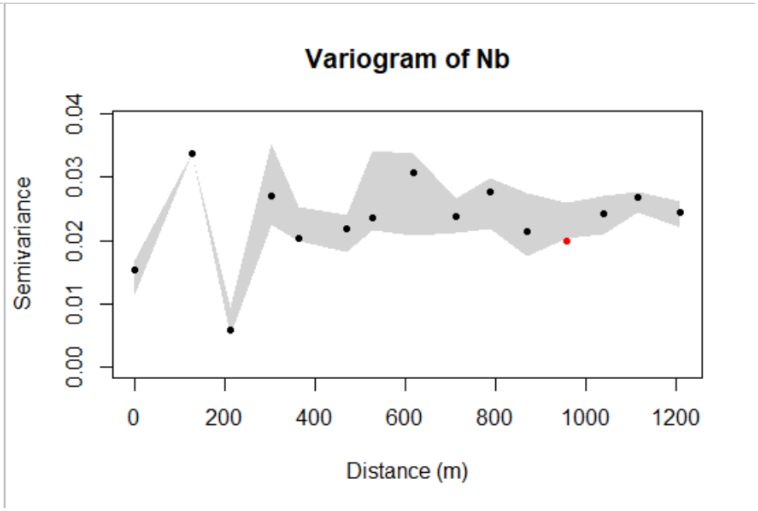
Variogram of Nb
Semivariance
0.00
0.01
0.02
0.03
0.04
0
200
400
600
800
1000
1200
Distance (m)

Appendix D

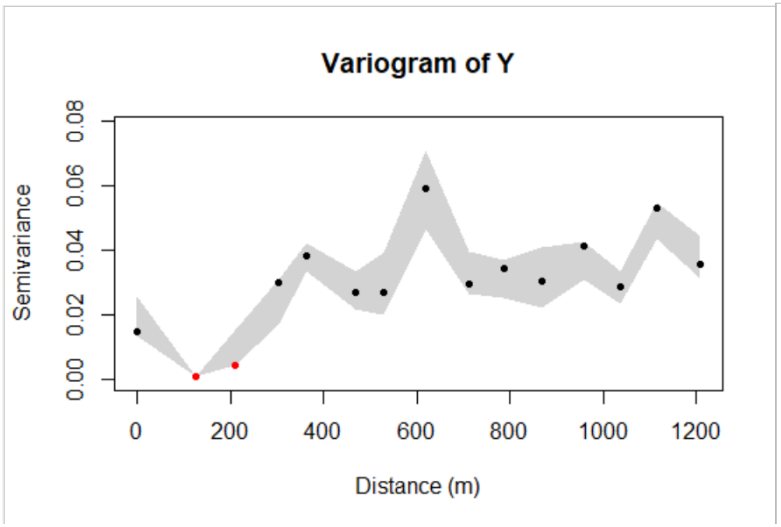
Variogram of Y
Semivariance
0.00
0.02
0.04
0.06
0.08
0
200
400
600
800
1000
1200
Distance (m)

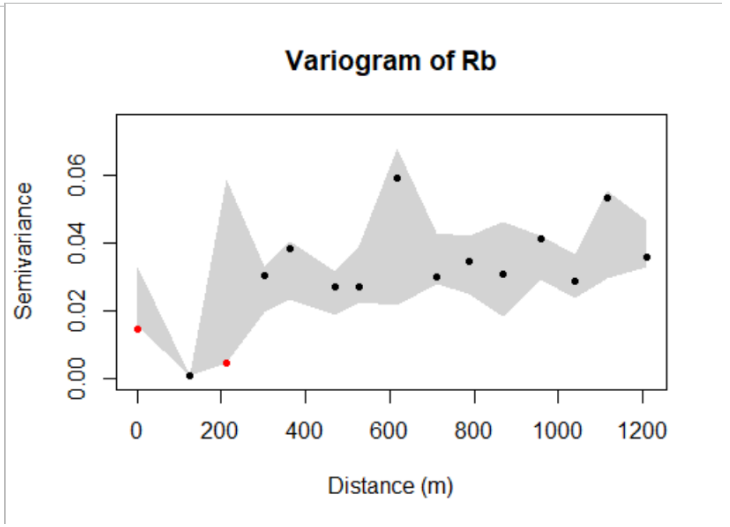
Variogram of Rb
Semivariance
0.00
0.02
0.04
0.06
0
200
400
600
800
1000
1200
Distance (m)

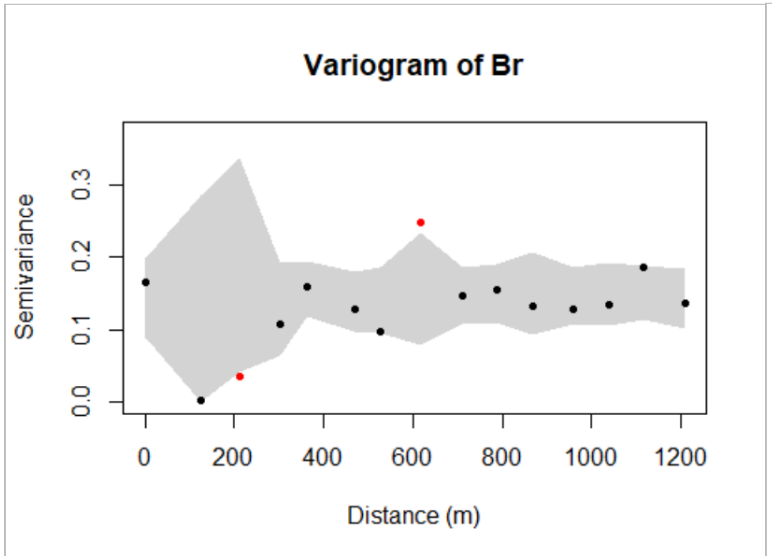
Variogram of Br
Semivariance
0.0
0.1
0.2
0.3
0
200
400
600
800
1000
1200
Distance (m)

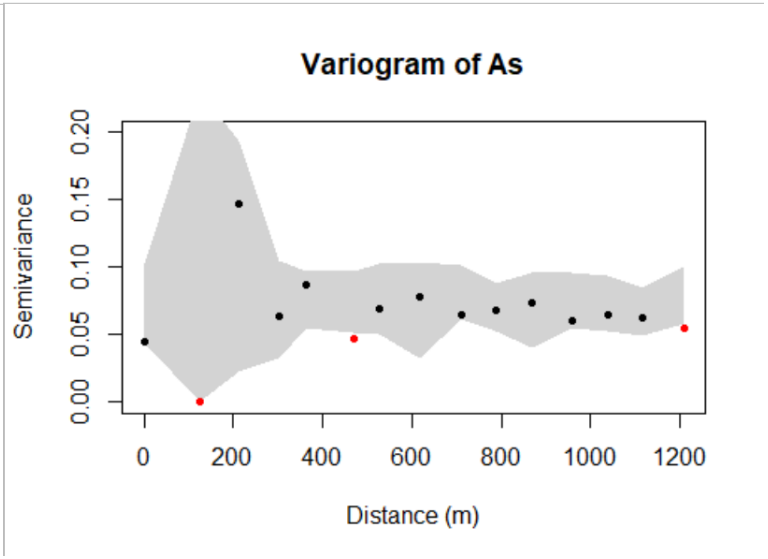
Variogram of As
Semivariance
0.00
0.05
0.10
0.15
0.20
0
200
400
600
800
1000
1200
Distance (m)

Appendix D

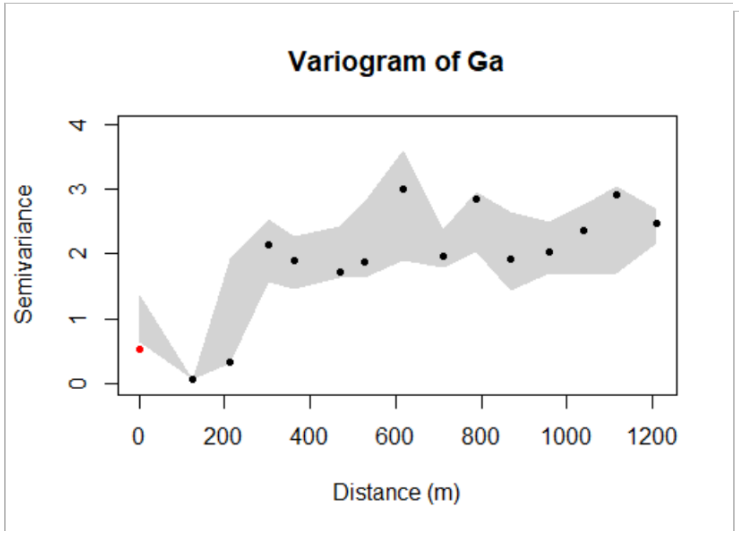
Variogram of Ga
Semivariance
0
1
2
3
4
0
200
400
600
800
1000
1200
Distance (m)

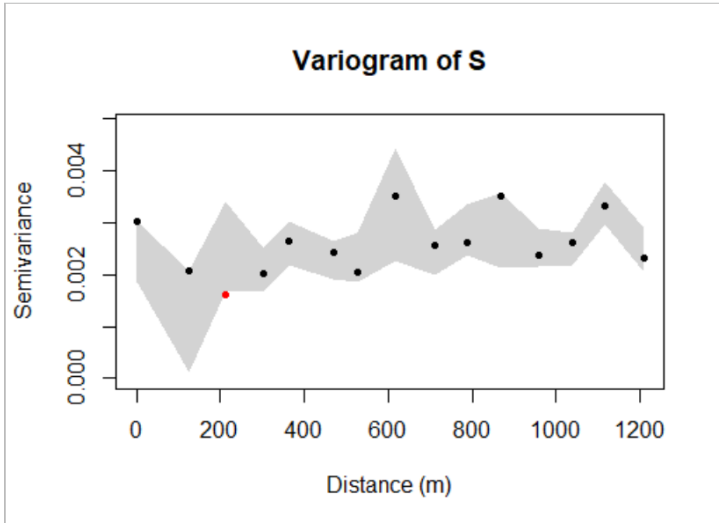
Variogram of S
Semivariance
0.000
0.002
0.004
0
200
400
600
800
1000
1200
Distance (m)

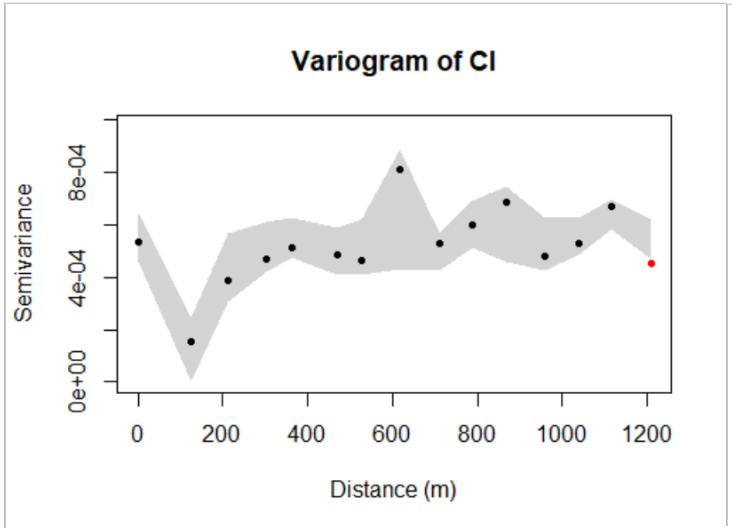
Variogram of Cl
Semivariance
0e+00
4e-04
8e-04
0
200
400
600
800
1000
1200
Distance (m)

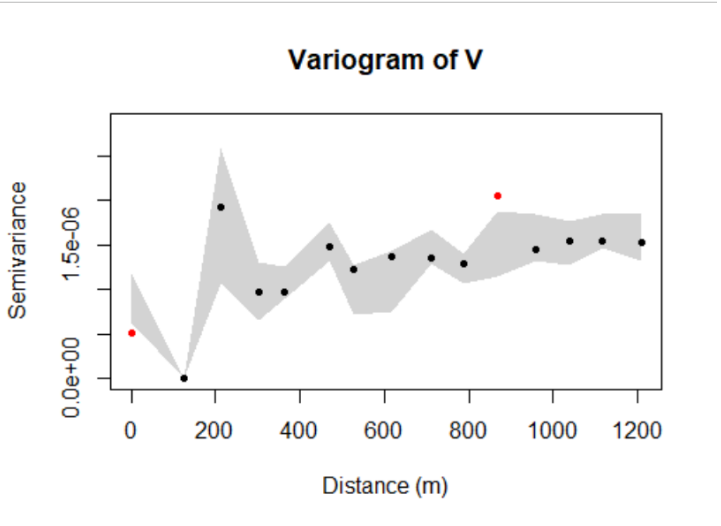
Variogram of V
Semivariance
0.0e+00
1.5e-06
0
200
400
600
800
1000
1200
Distance (m)

Appendix D

Variograms of major oxides from shallow topsoil samples from Castleisland Co. Kerry.

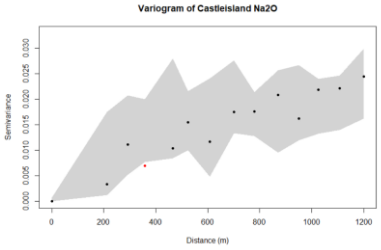

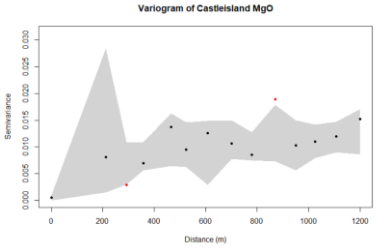

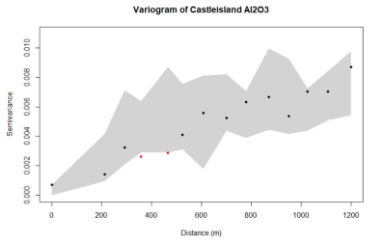

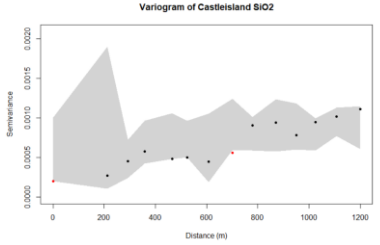

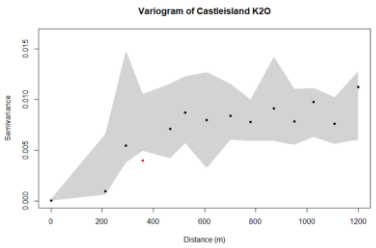

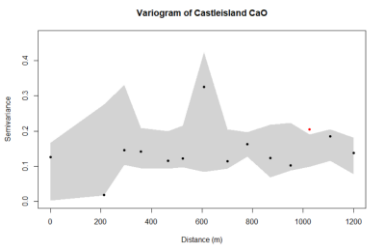

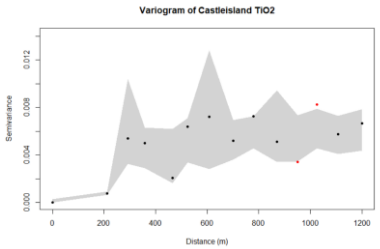

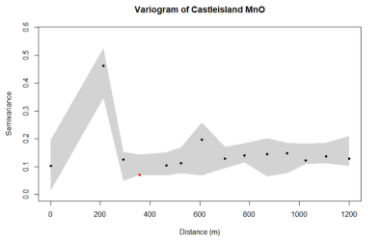

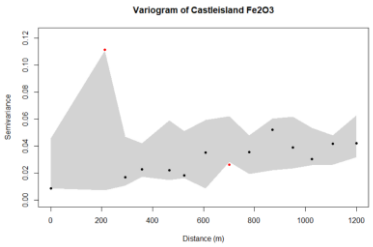

Histograms of ICPMS shallow topsoil (NA removed) Castleisland, Co. Kerry, SW Ireland.

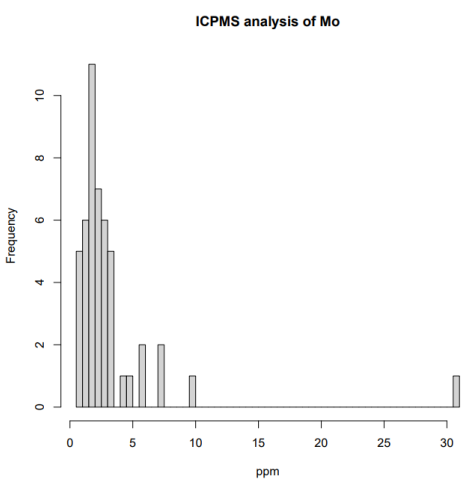

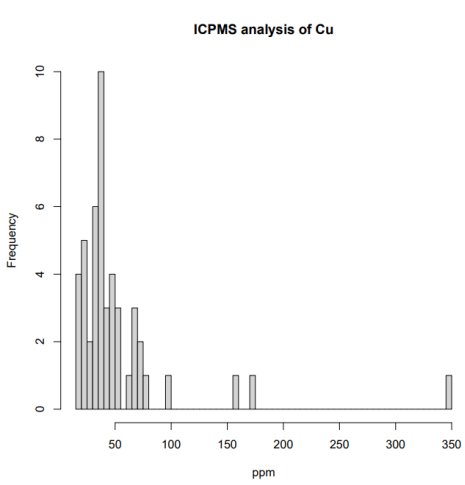

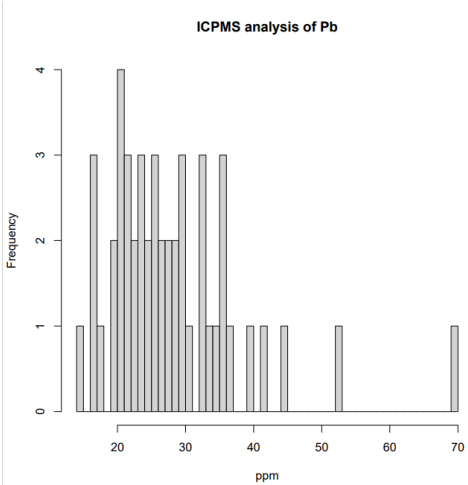

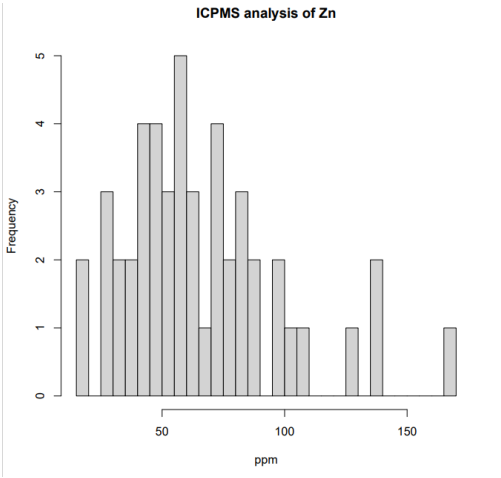

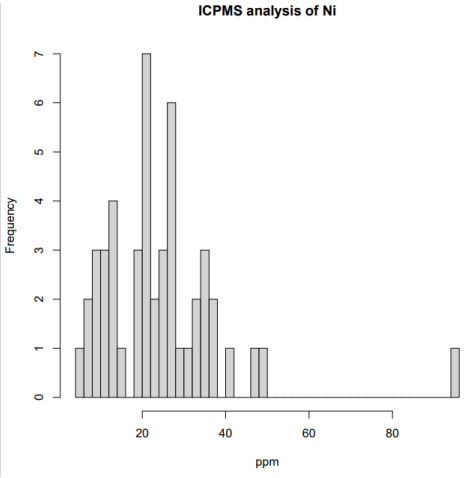

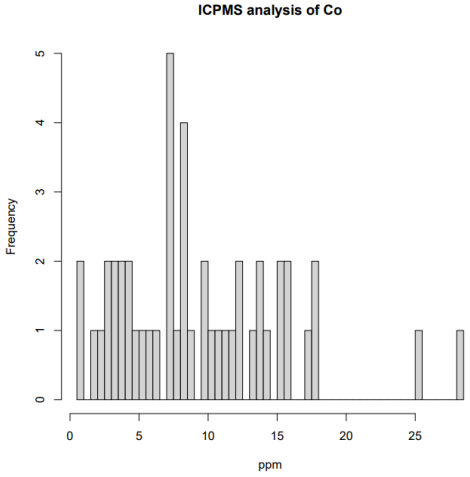

Appendix D

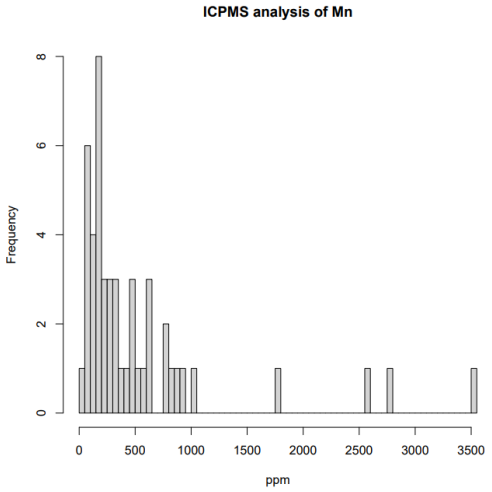
ICPMS analysis of Mn
Frequency
0
2
4
6
8
0
500
1000
1500
2000
2500
3000
3500
ppm

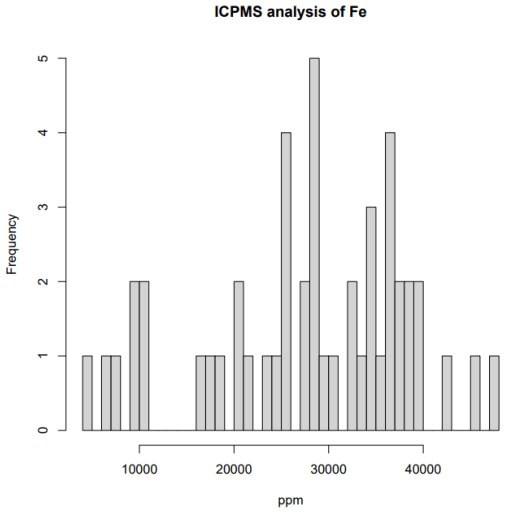
ICPMS analysis of Fe
Frequency
0
1
2
3
4
5
10000
20000
30000
40000
ppm

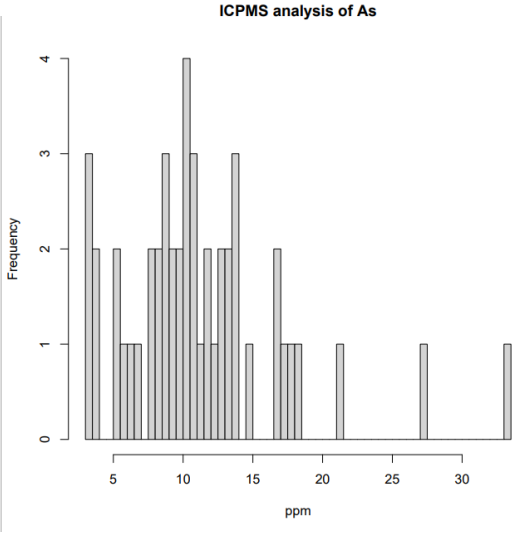
ICPMS analysis of As
Frequency
0
1
2
3
4
5
10
15
20
25
30
ppm

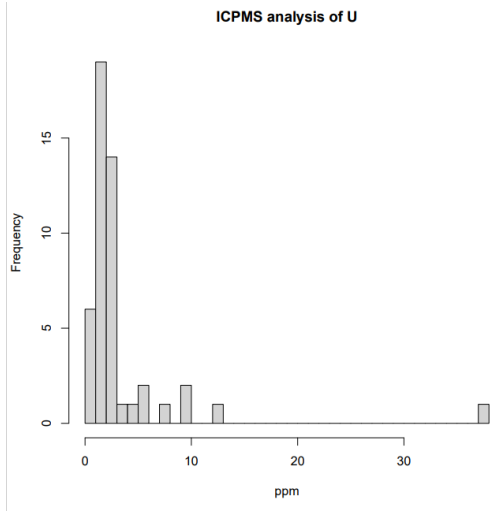
ICPMS analysis of U
Frequency
0
5
10
15
0
10
20
30
ppm

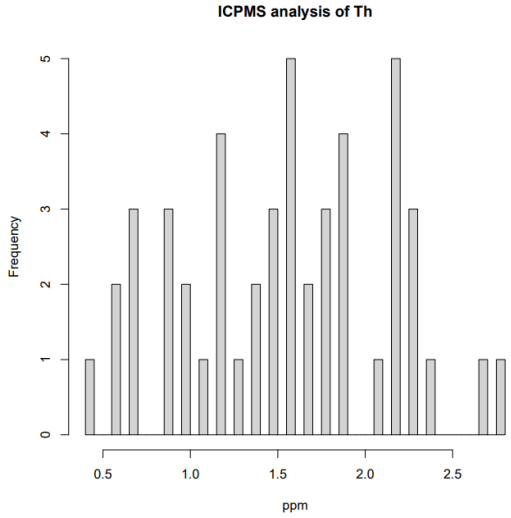
ICPMS analysis of Th
Frequency
0
1
2
3
4
5
0.5
1.0
1.5
2.0
2.5
ppm

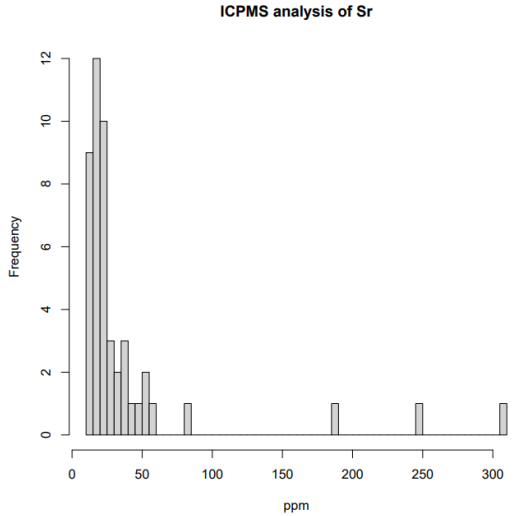
ICPMS analysis of Sr
Frequency
0
2
4
6
8
10
12
0
50
100
150
200
250
300
ppm

Appendix D

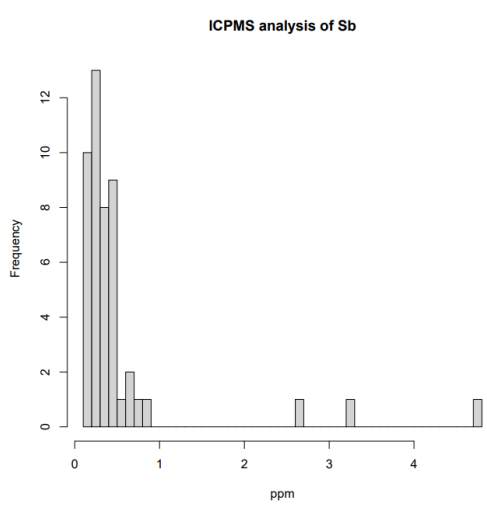
ICPMS analysis of Sb
Frequency
ppm

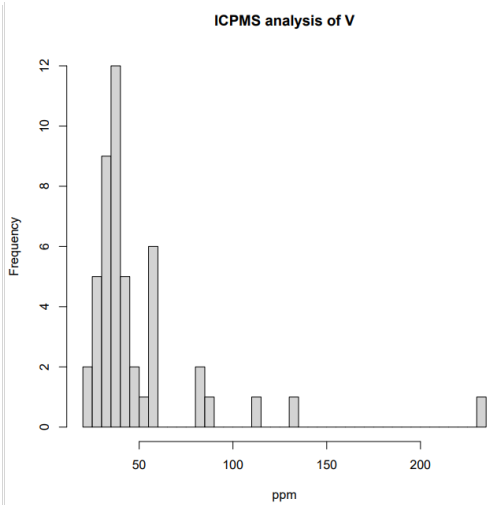
ICPMS analysis of V
Frequency
ppm

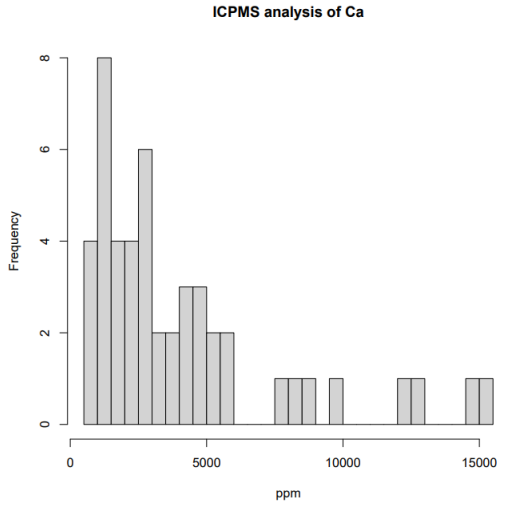
ICPMS analysis of Ca
Frequency
ppm

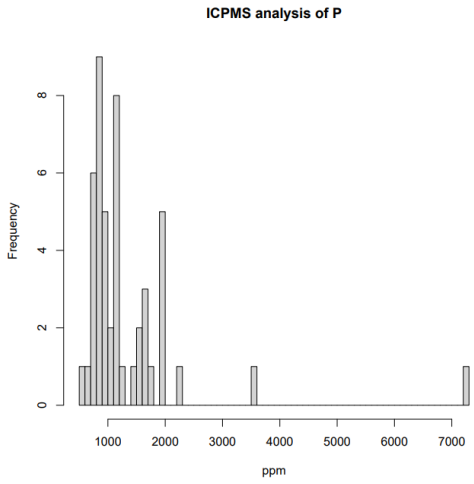
ICPMS analysis of P
Frequency
ppm

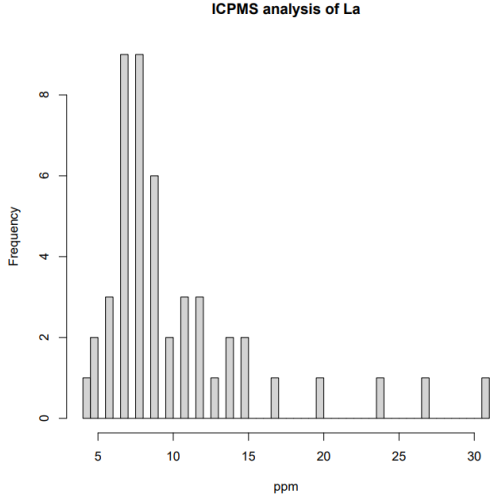
ICPMS analysis of La
Frequency
ppm

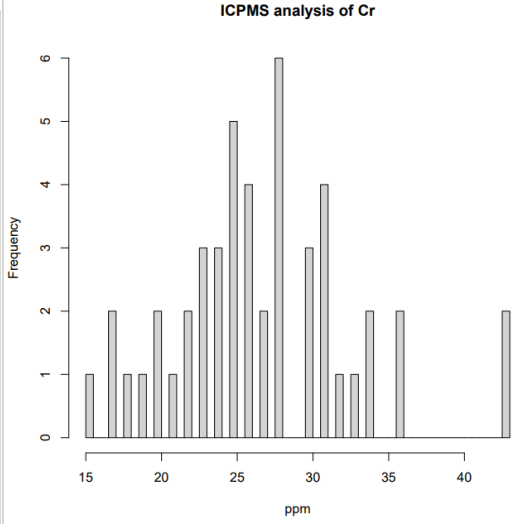
ICPMS analysis of Cr
Frequency
ppm

Appendix D

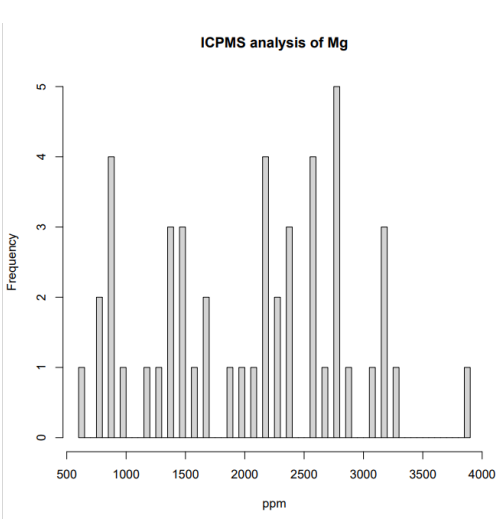
ICPMS analysis of Mg
Frequency
0
1
2
3
4
5
500
1000
1500
2000
2500
3000
3500
4000
ppm

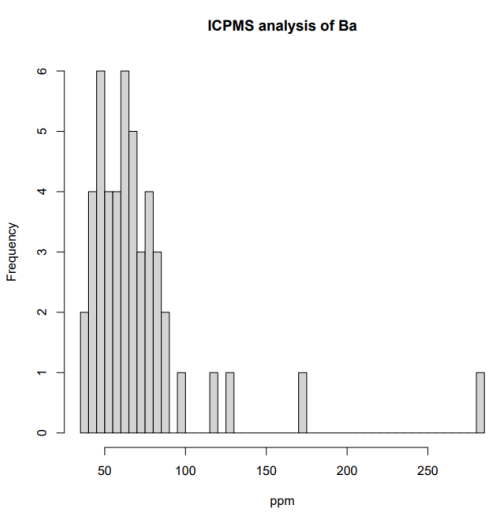
ICPMS analysis of Ba
Frequency
0
1
2
3
4
5
6
50
100
150
200
250
ppm

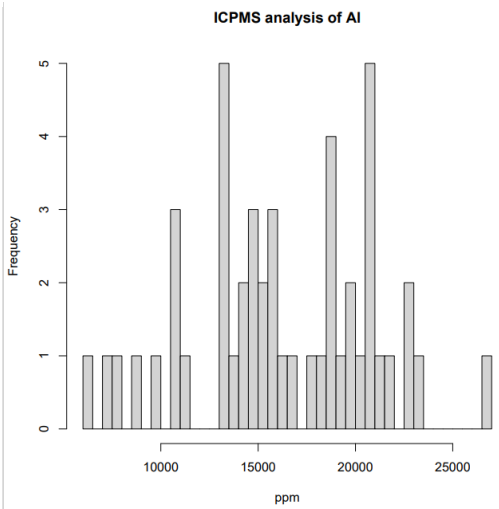
ICPMS analysis of Al
Frequency
0
1
2
3
4
5
10000
15000
20000
25000
ppm

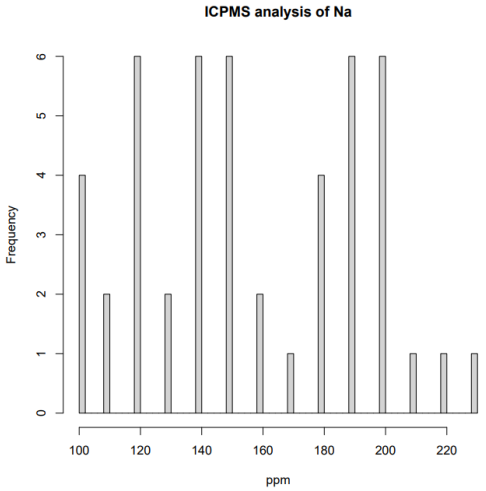
ICPMS analysis of Na
Frequency
0
1
2
3
4
5
6
100
120
140
160
180
200
220
ppm

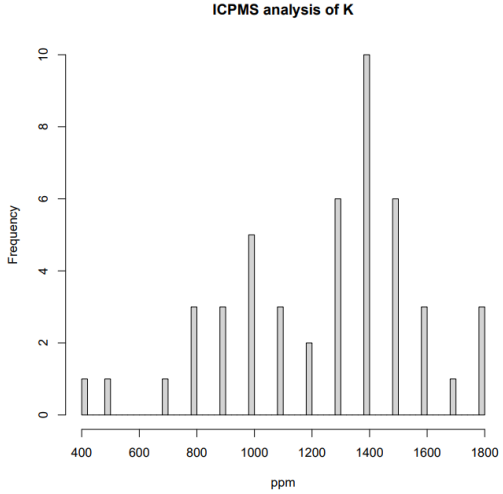
ICPMS analysis of K
Frequency
0
2
4
6
8
10
400
600
800
1000
1200
1400
1600
1800
ppm

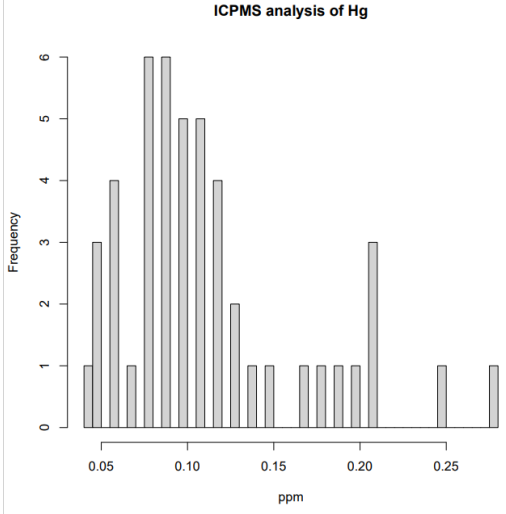
ICPMS analysis of Hg
Frequency
0
1
2
3
4
5
6
0.05
0.10
0.15
0.20
0.25
ppm

Appendix D

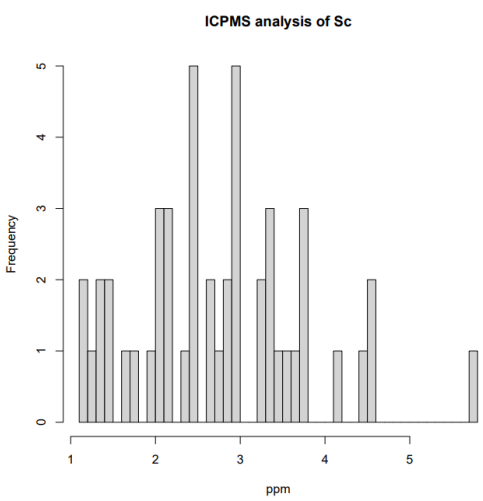
ICPMS analysis of Sc
Frequency
0
1
2
3
4
5
1
2
3
4
5
ppm

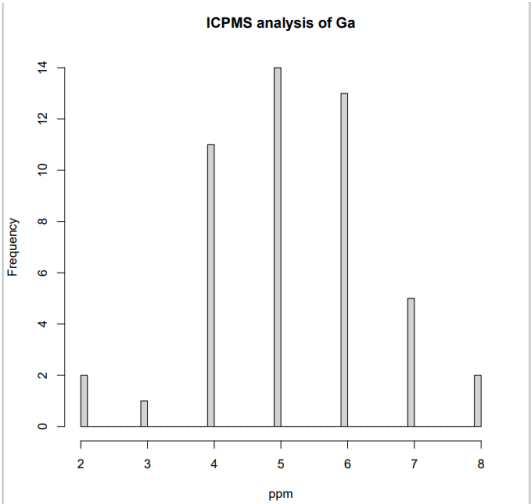
ICPMS analysis of Ga
Frequency
0
2
4
6
8
10
12
14
2
3
4
5
6
7
8
ppm

QQ-plots of ICPMS aqua regia shallow topsoil (NA removed) Castleisland, Co. Kerry, SW Ireland.

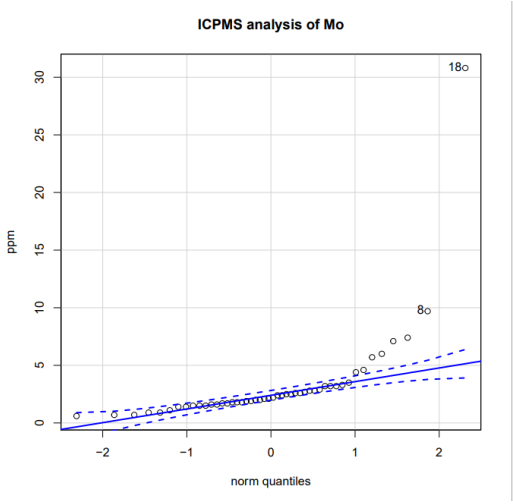

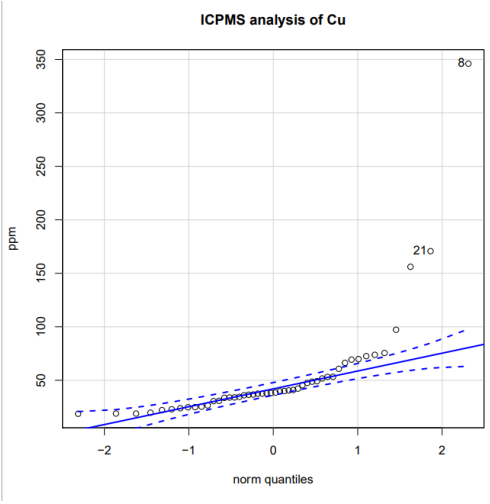

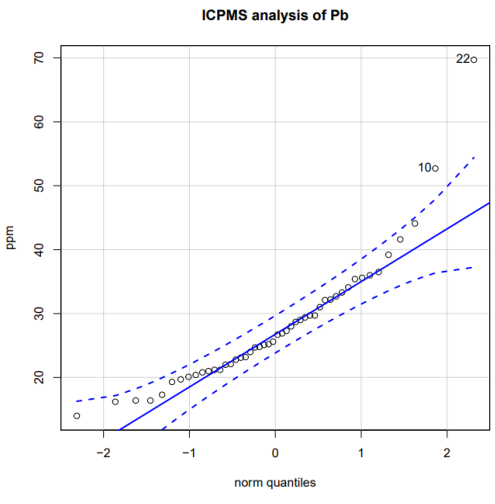

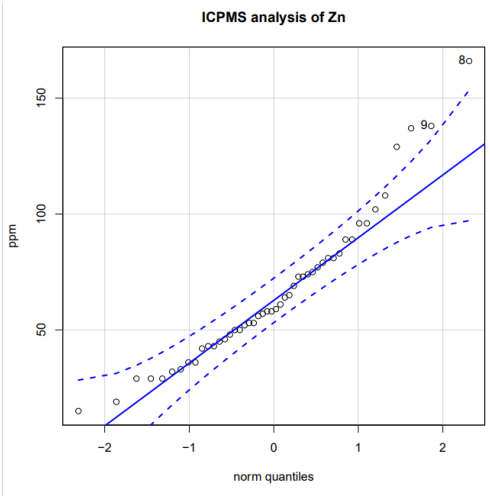

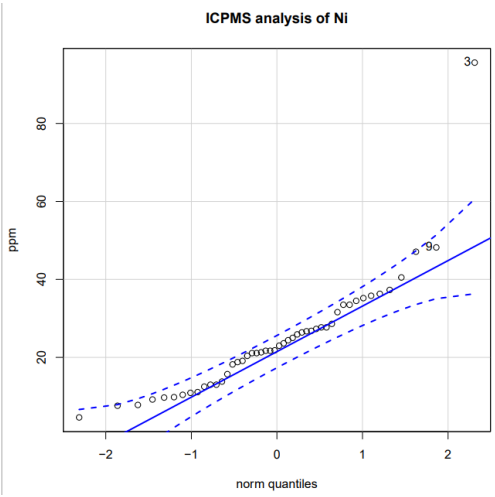

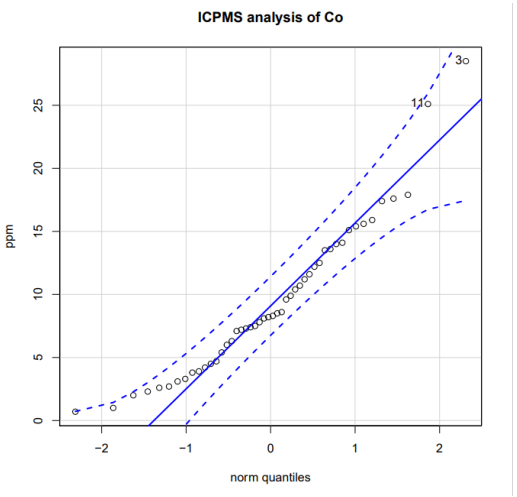

Appendix D

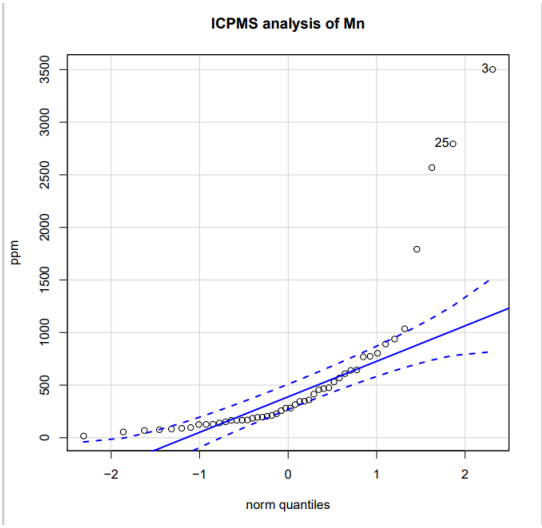
ICPMS analysis of Mn
ppm
norm quantiles
3
25

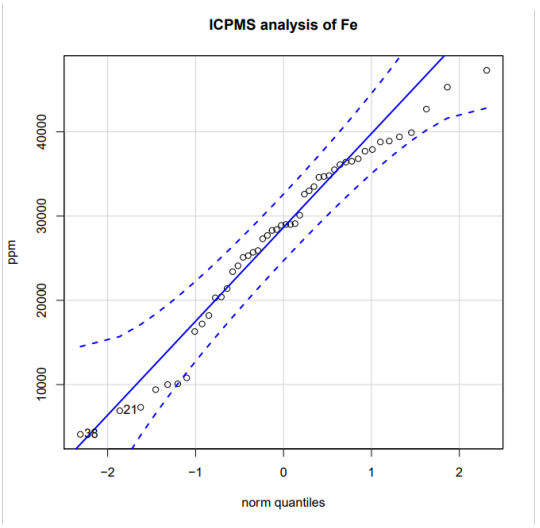
ICPMS analysis of Fe
ppm
norm quantiles
38
21

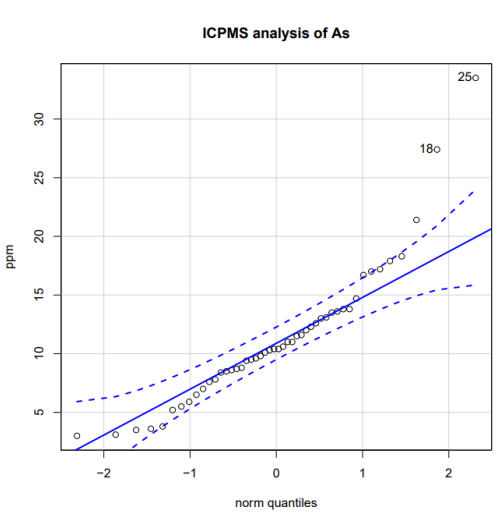
ICPMS analysis of As
ppm
norm quantiles
25
18

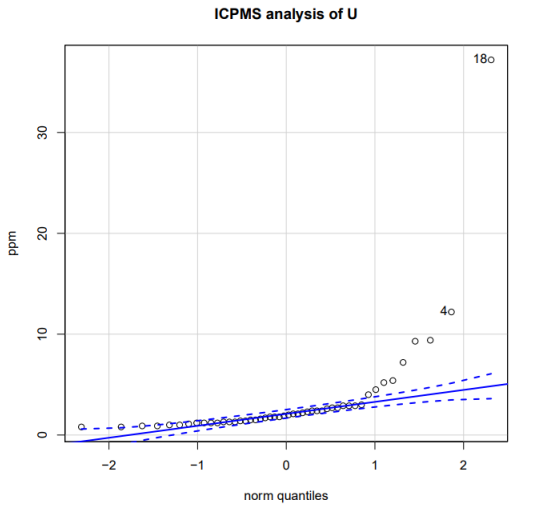
ICPMS analysis of U
ppm
norm quantiles
18
4

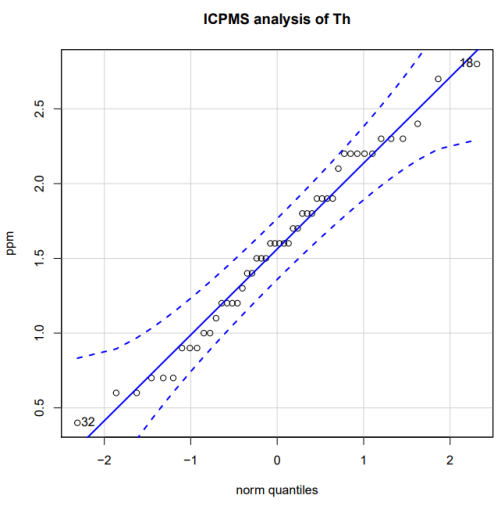
ICPMS analysis of Th
ppm
norm quantiles
18
32

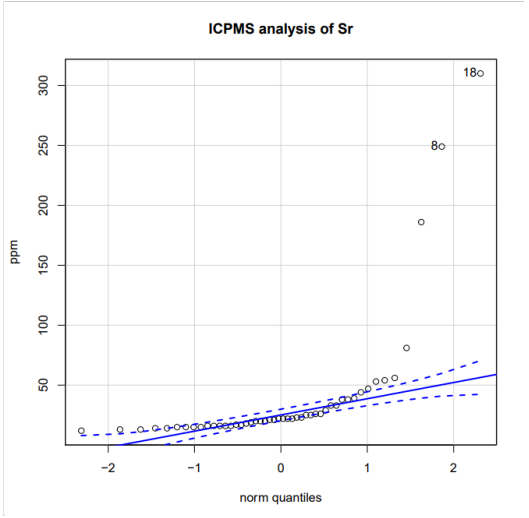
ICPMS analysis of Sr
ppm
norm quantiles
18
8

Appendix D

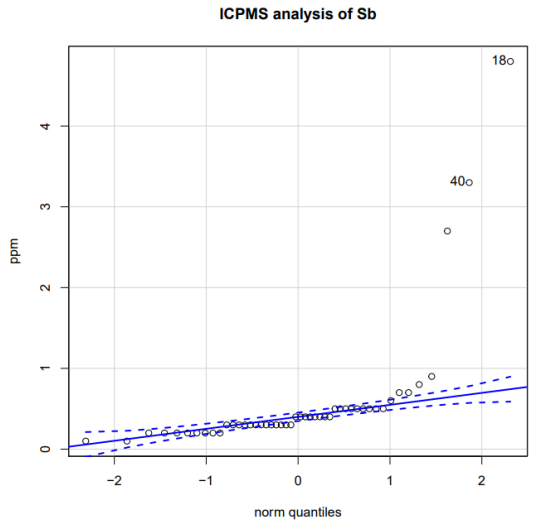
ICPMS analysis of Sb
ppm
norm quantiles
18
40

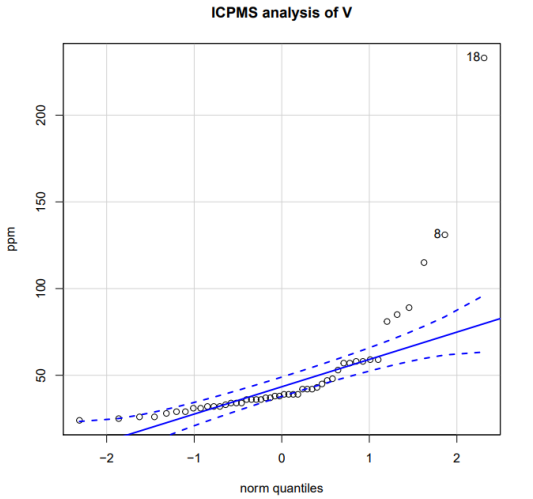
ICPMS analysis of V
ppm
norm quantiles
18
8

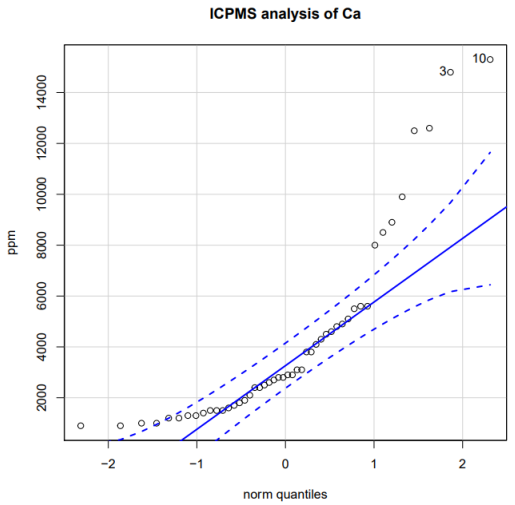
ICPMS analysis of Ca
ppm
norm quantiles
10
3

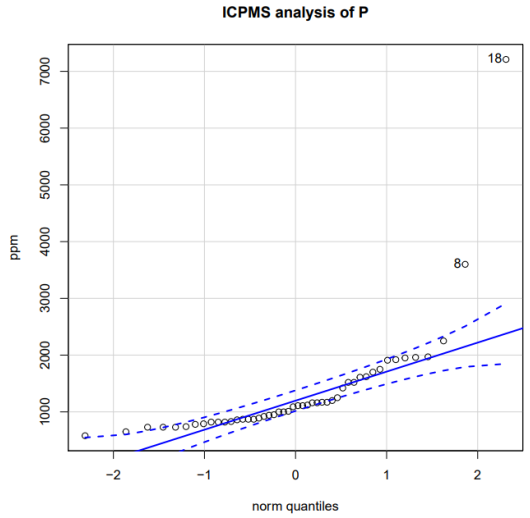
ICPMS analysis of P
ppm
norm quantiles
18
8

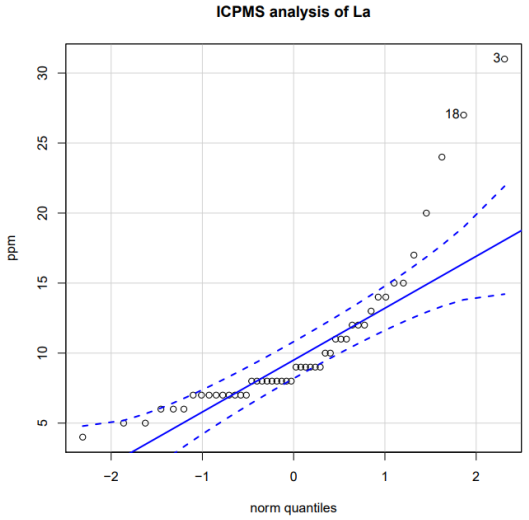
ICPMS analysis of La
ppm
norm quantiles
3
18

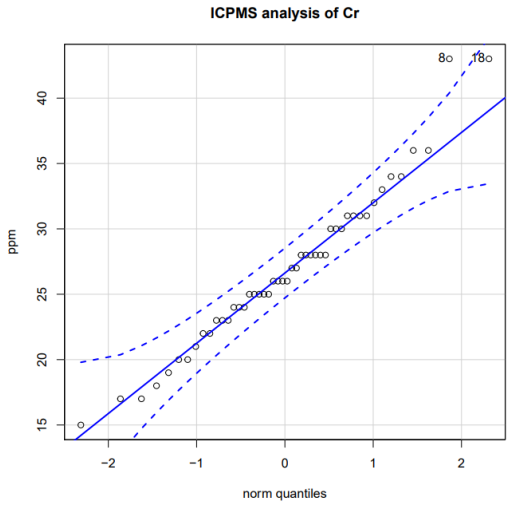
ICPMS analysis of Cr
ppm
norm quantiles
8
18

Appendix D

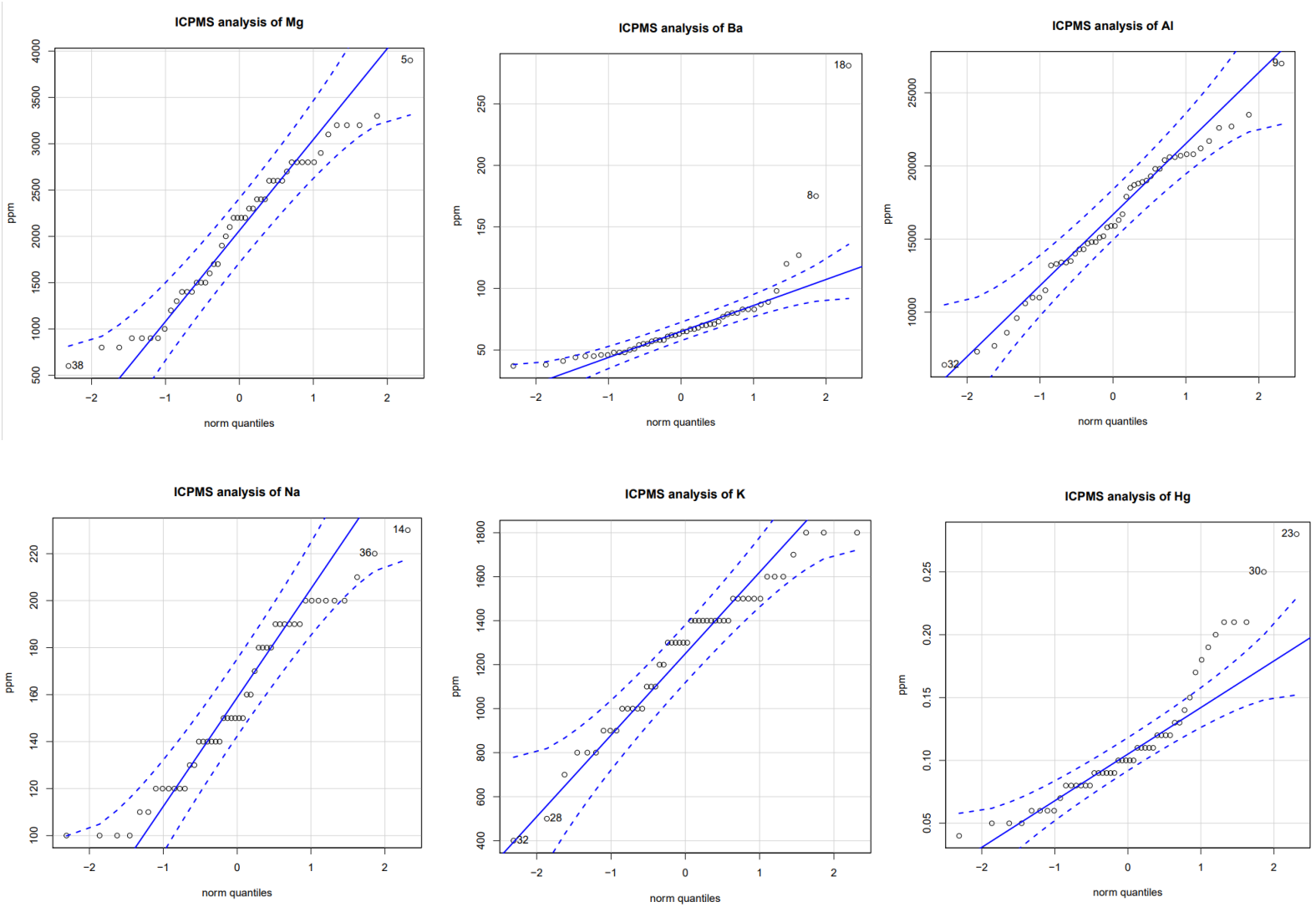
ICPMS analysis of Mg
ppm
norm quantiles
5
38
ICPMS analysis of Ba
ppm
norm quantiles
18
8
ICPMS analysis of Al
ppm
norm quantiles
9
32
ICPMS analysis of Na
ppm
norm quantiles
14
36
ICPMS analysis of K
ppm
norm quantiles
28
32
ICPMS analysis of Hg
ppm
norm quantiles
23
30

Appendix D

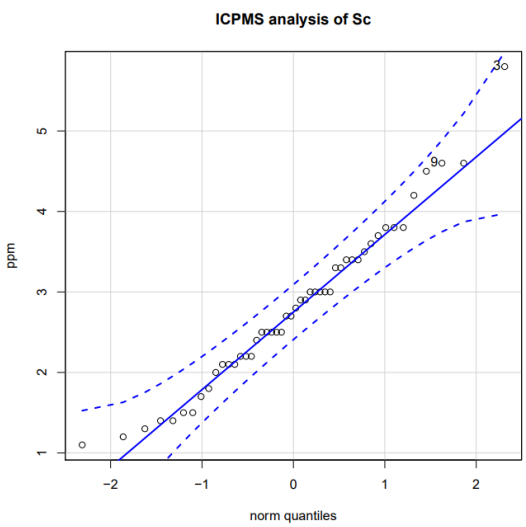
ICPMS analysis of Sc
ppm
norm quantiles
−2
−1
0
1
2
1
2
3
4
5
30
9

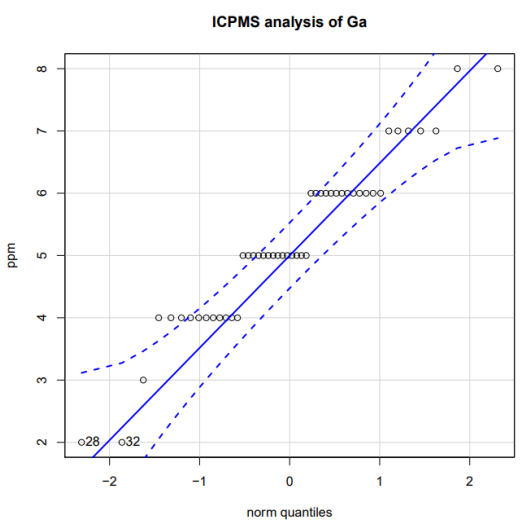
ICPMS analysis of Ga
ppm
norm quantiles
−2
−1
0
1
2
2
3
4
5
6
7
8
28
32

QQ-plots of ICPES shallow topsoil (NA removed) Castleisland, Co. Kerry, SW Ireland.

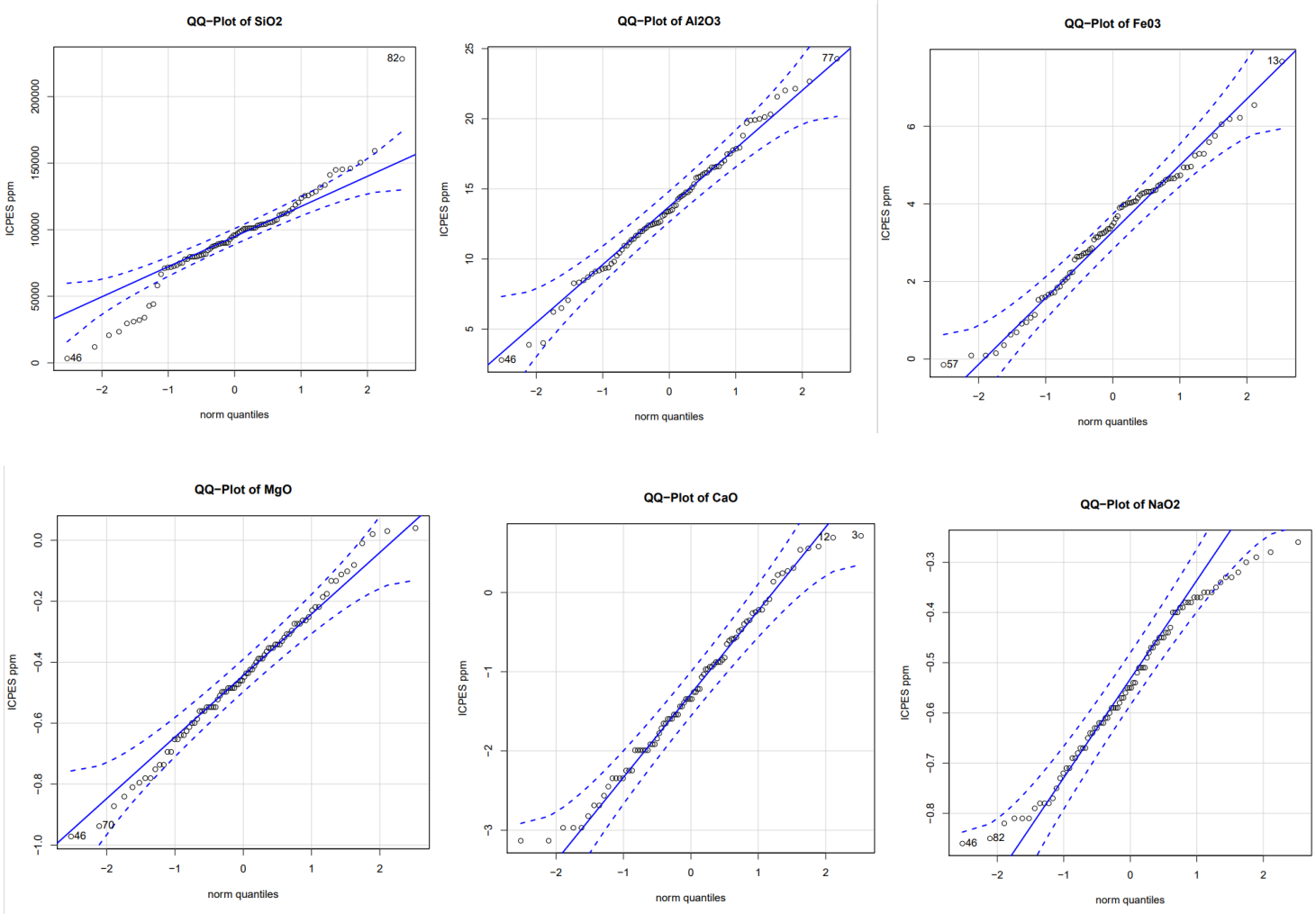

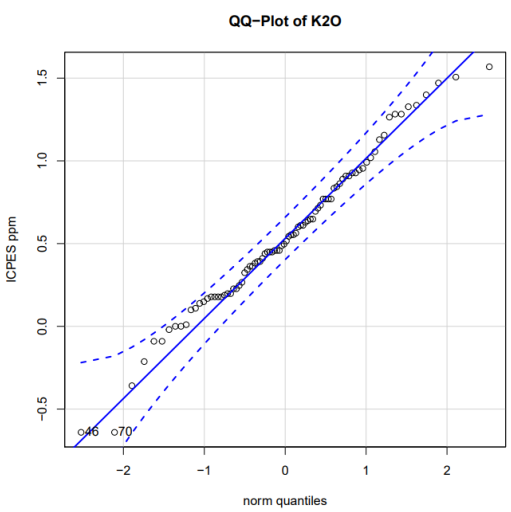
QQ−Plot of K2O
ICPES ppm
norm quantiles
46
70

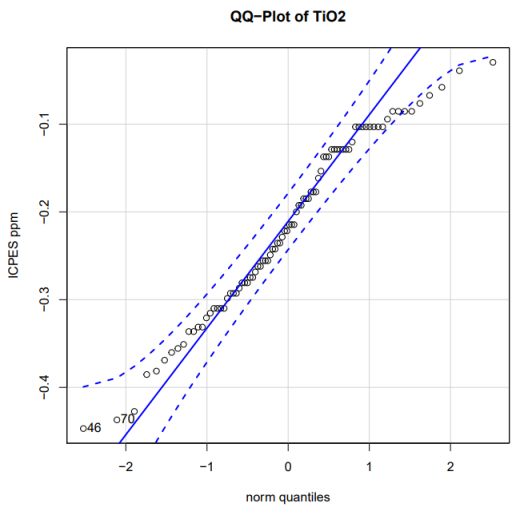
QQ−Plot of TiO2
ICPES ppm
norm quantiles
46
70

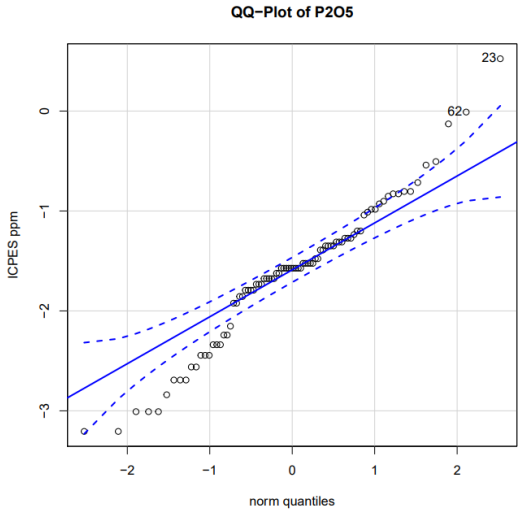
QQ−Plot of P2O5
ICPES ppm
norm quantiles
23
62

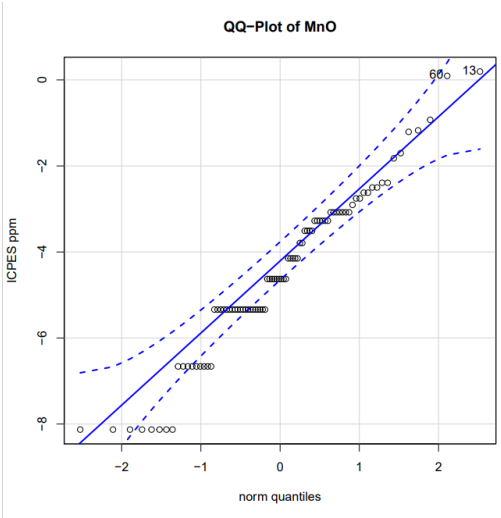
QQ−Plot of MnO
ICPES ppm
norm quantiles
60
13

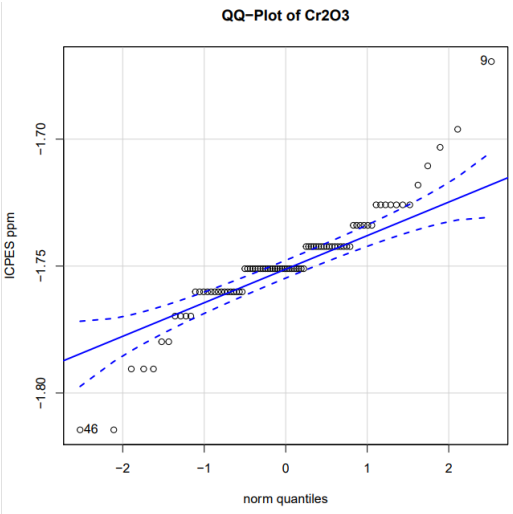
QQ−Plot of Cr2O3
ICPES ppm
norm quantiles
9
46

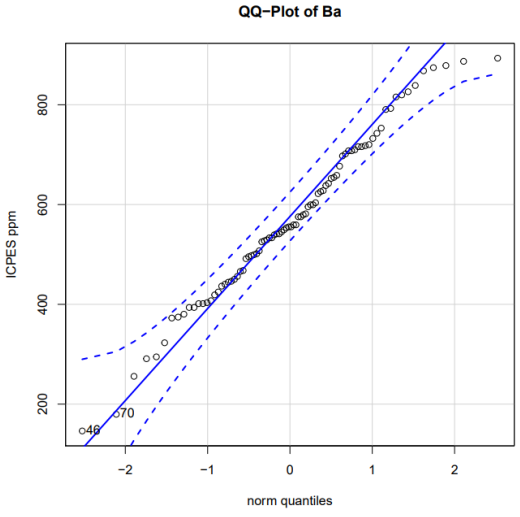
QQ−Plot of Ba
ICPES ppm
norm quantiles
46
70

Appendix D

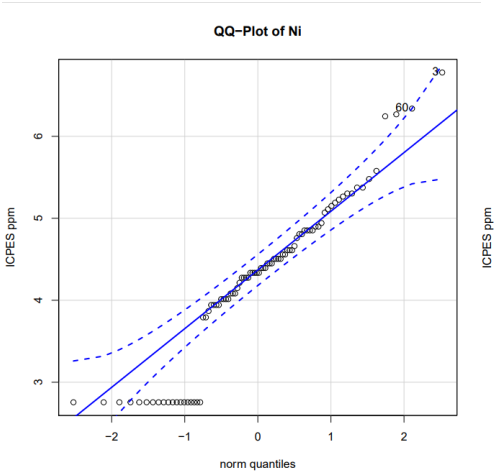
QQ−Plot of Ni
ICPES ppm
norm quantiles
3
60

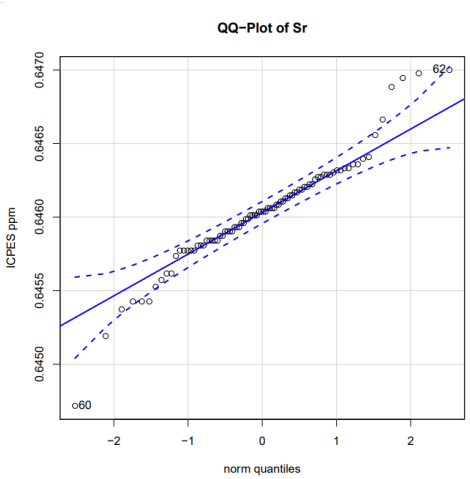
QQ−Plot of Sr
ICPES ppm
norm quantiles
62
60

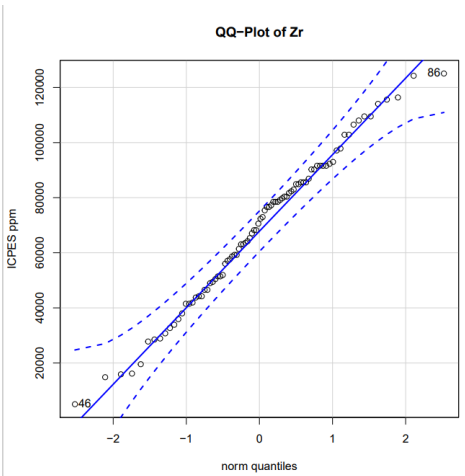
QQ−Plot of Zr
ICPES ppm
norm quantiles
86
46

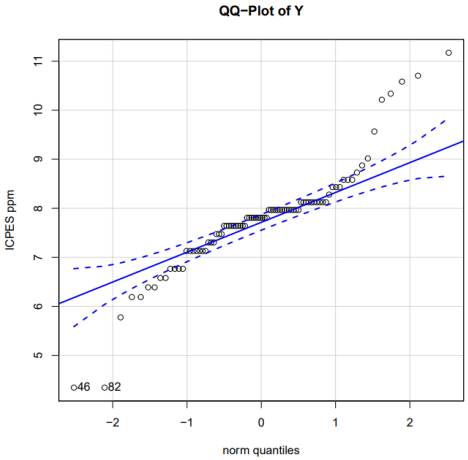
QQ−Plot of Y
ICPES ppm
norm quantiles
46
82

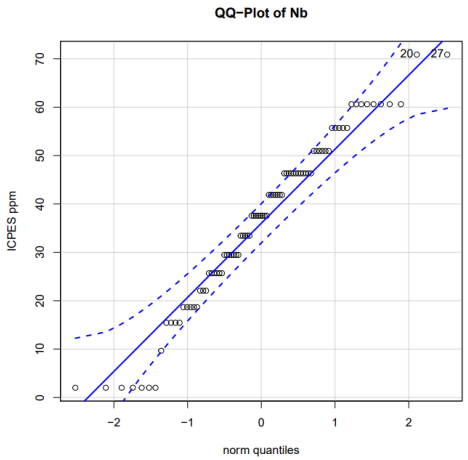
QQ−Plot of Nb
ICPES ppm
norm quantiles
20
27

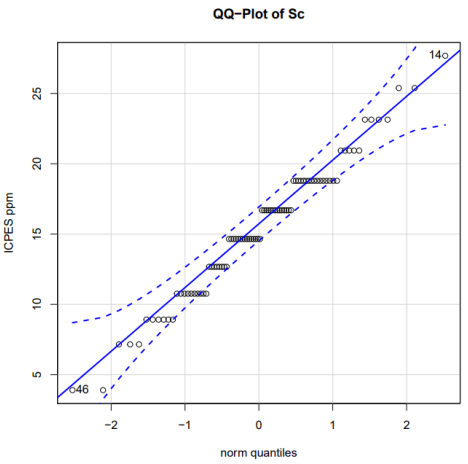
QQ−Plot of Sc
ICPES ppm
norm quantiles
14
46

Histogram plots of XRF topsoil data fromCastleisland, Co. Kerry, SW Ireland.

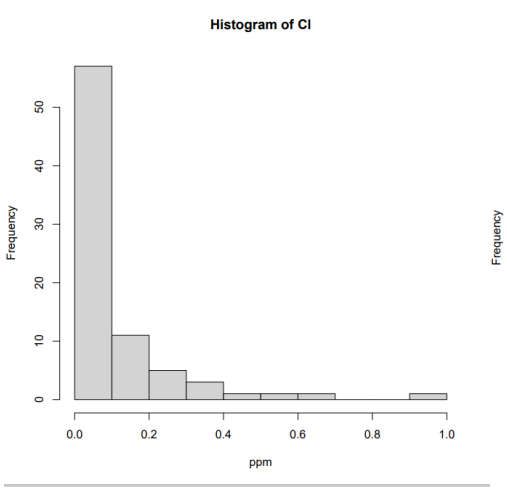

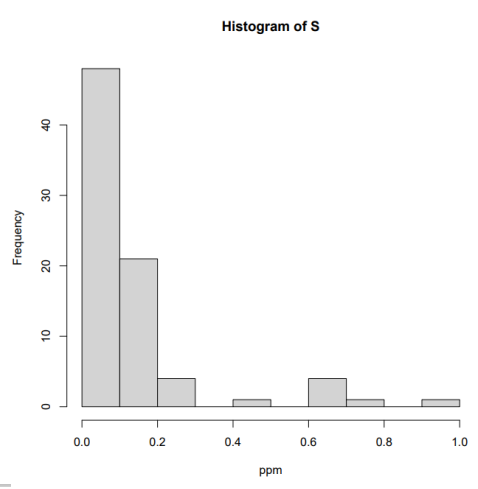

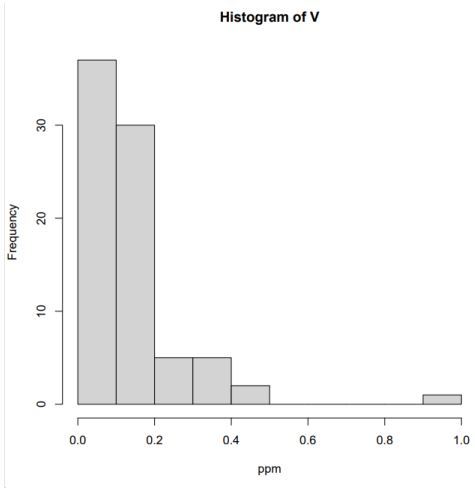

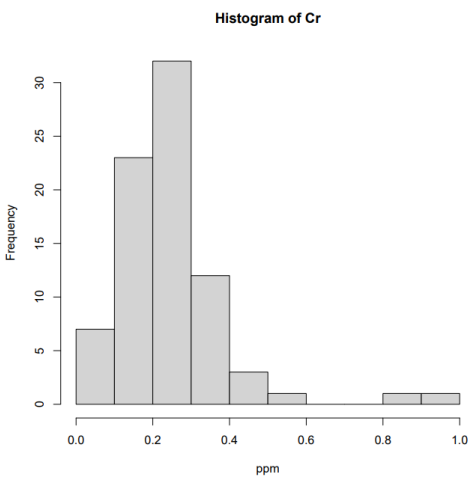

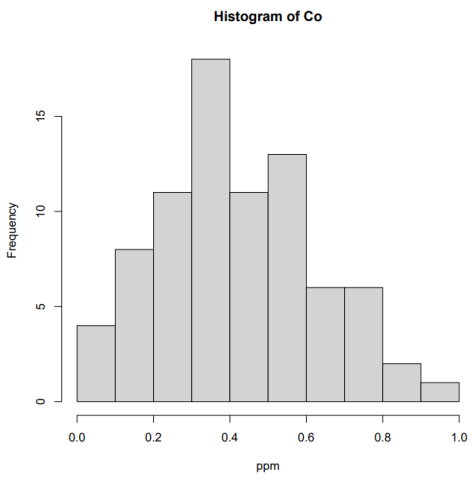

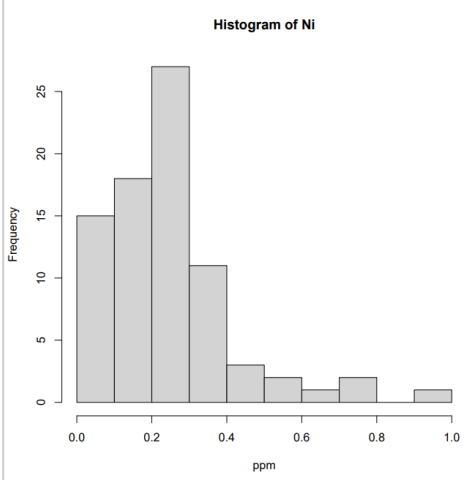

Appendix D

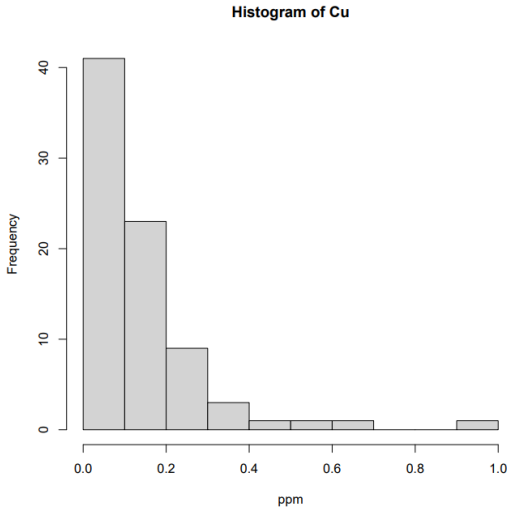
Histogram of Cu
Frequency
0
10
20
30
40
0.0
0.2
0.4
0.6
0.8
1.0
ppm

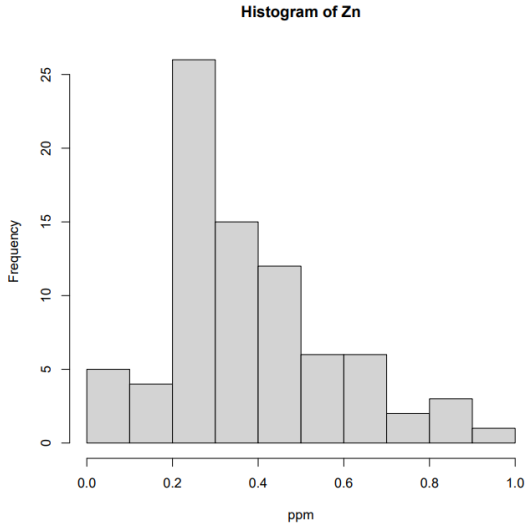
Histogram of Zn
Frequency
0
5
10
15
20
25
0.0
0.2
0.4
0.6
0.8
1.0
ppm

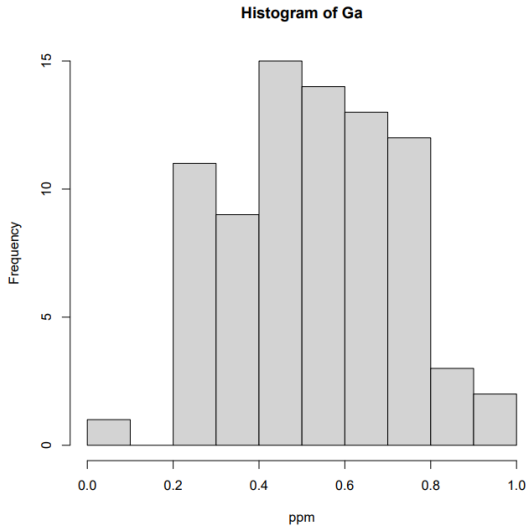
Histogram of Ga
Frequency
0
5
10
15
0.0
0.2
0.4
0.6
0.8
1.0
ppm

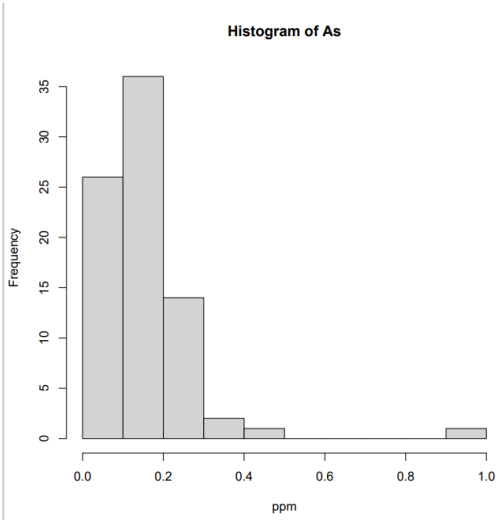
Histogram of As
Frequency
0
5
10
15
20
25
30
35
0.0
0.2
0.4
0.6
0.8
1.0
ppm

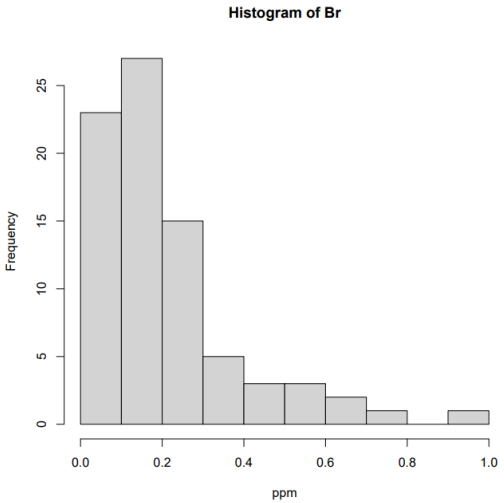
Histogram of Br
Frequency
0
5
10
15
20
25
0.0
0.2
0.4
0.6
0.8
1.0
ppm

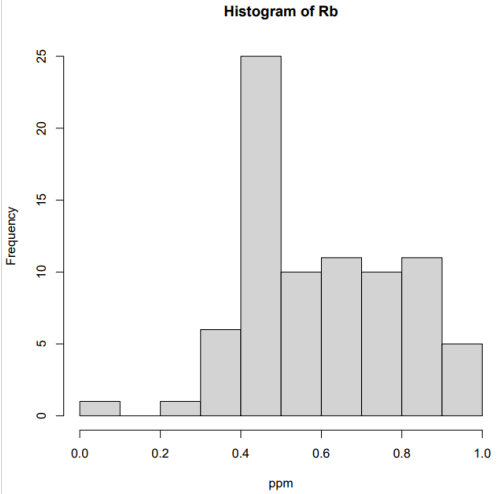
Histogram of Rb
Frequency
0
5
10
15
20
25
0.0
0.2
0.4
0.6
0.8
1.0
ppm

Appendix D

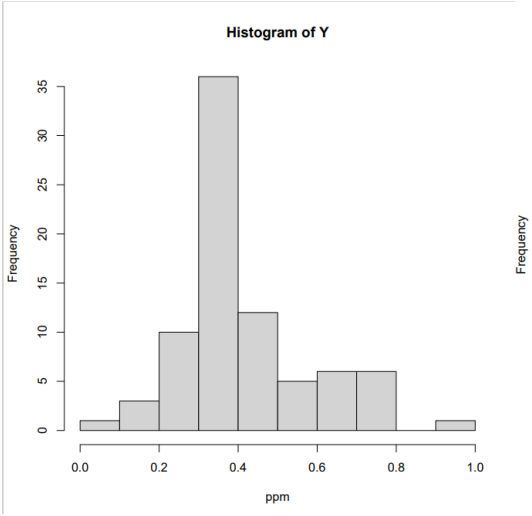
Histogram of Y
Frequency
ppm

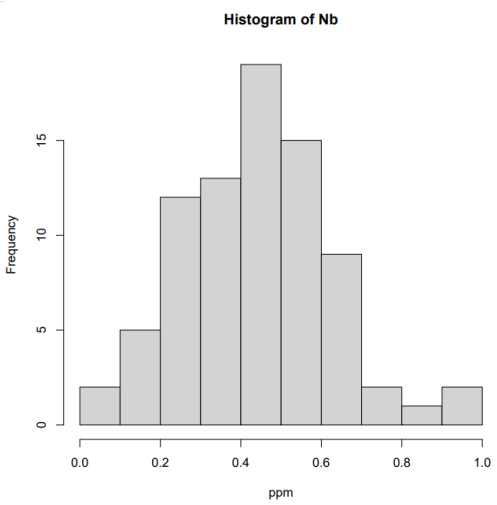
Histogram of Nb
Frequency
ppm

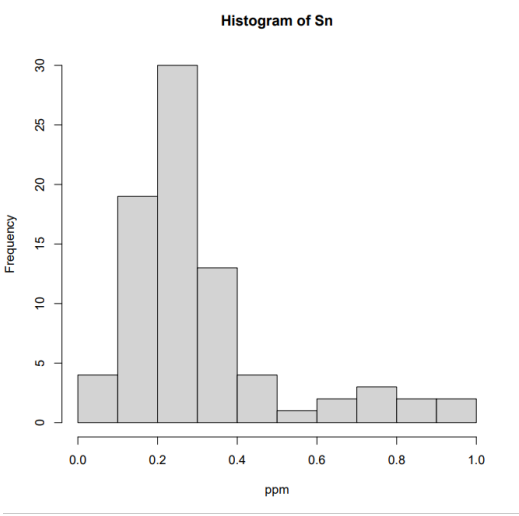
Histogram of Sn
Frequency
ppm

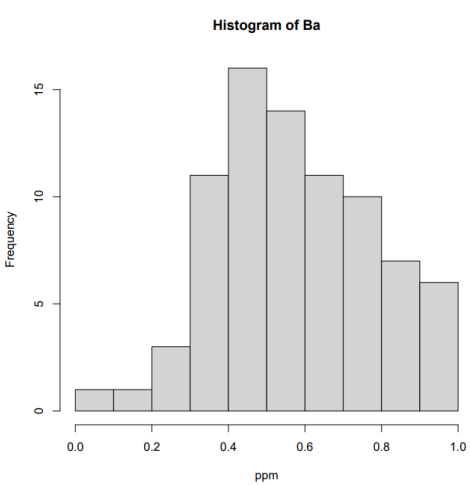
Histogram of Ba
Frequency
ppm

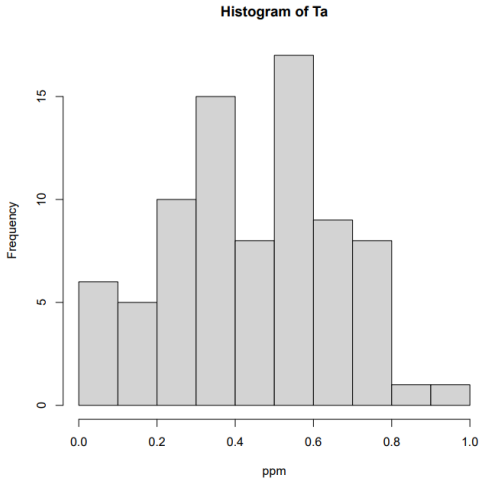
Histogram of Ta
Frequency
ppm

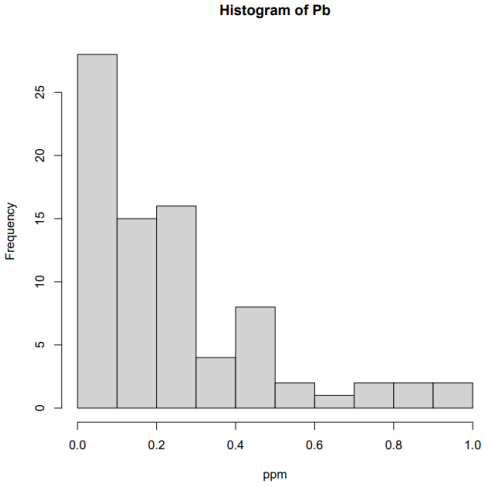
Histogram of Pb
Frequency
ppm

Appendix D

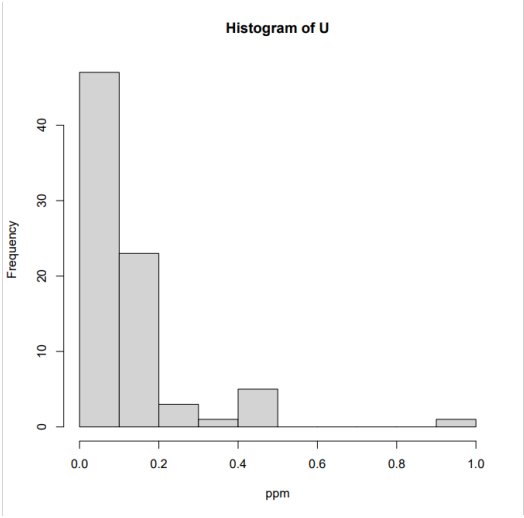
Histogram of U
Frequency
0
10
20
30
40
0.0
0.2
0.4
0.6
0.8
1.0
ppm

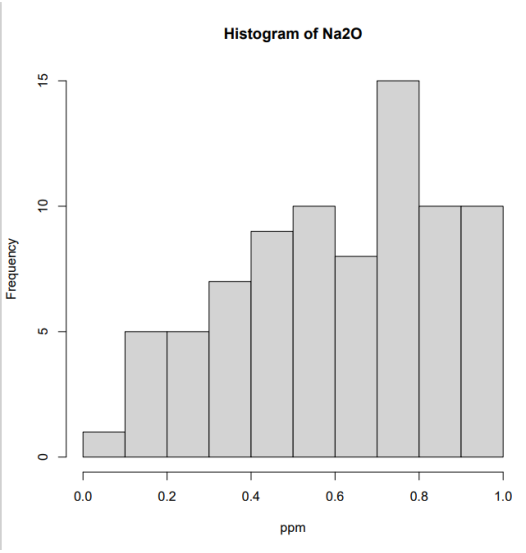
Histogram of Na2O
Frequency
0
5
10
15
0.0
0.2
0.4
0.6
0.8
1.0
ppm

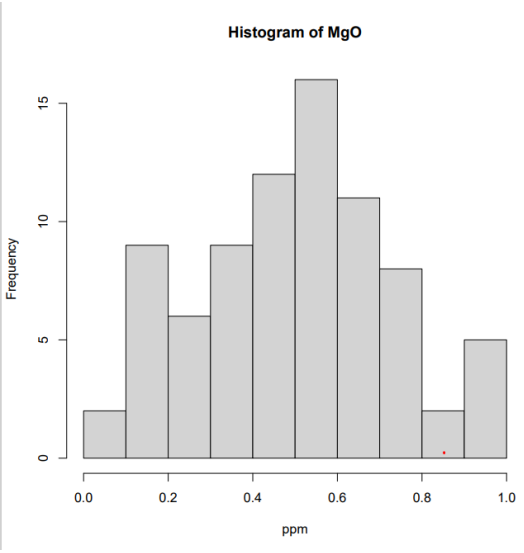
Histogram of MgO
Frequency
0
5
10
15
0.0
0.2
0.4
0.6
0.8
1.0
ppm

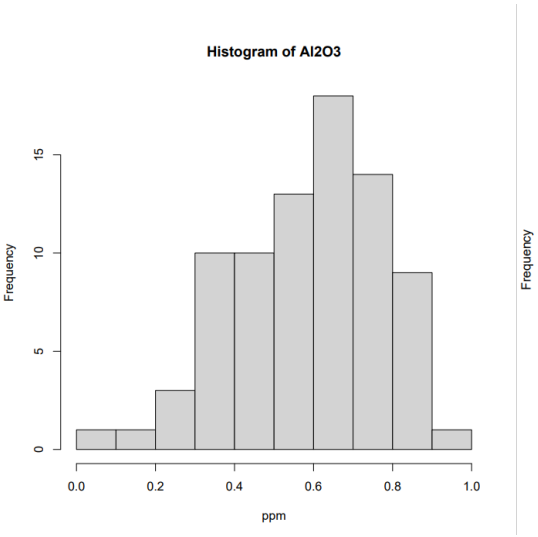
Histogram of Al2O3
Frequency
0
5
10
15
0.0
0.2
0.4
0.6
0.8
1.0
ppm

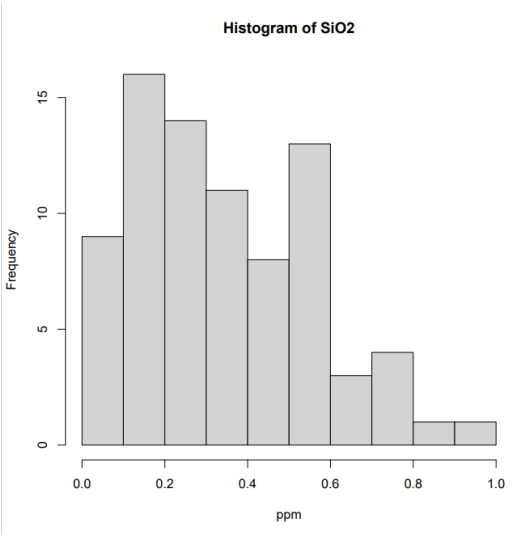
Histogram of SiO2
Frequency
0
5
10
15
0.0
0.2
0.4
0.6
0.8
1.0
ppm

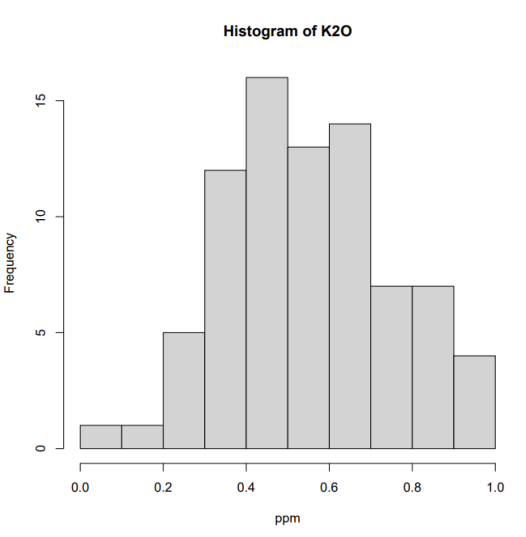
Histogram of K2O
Frequency
0
5
10
15
0.0
0.2
0.4
0.6
0.8
1.0
ppm

Appendix D

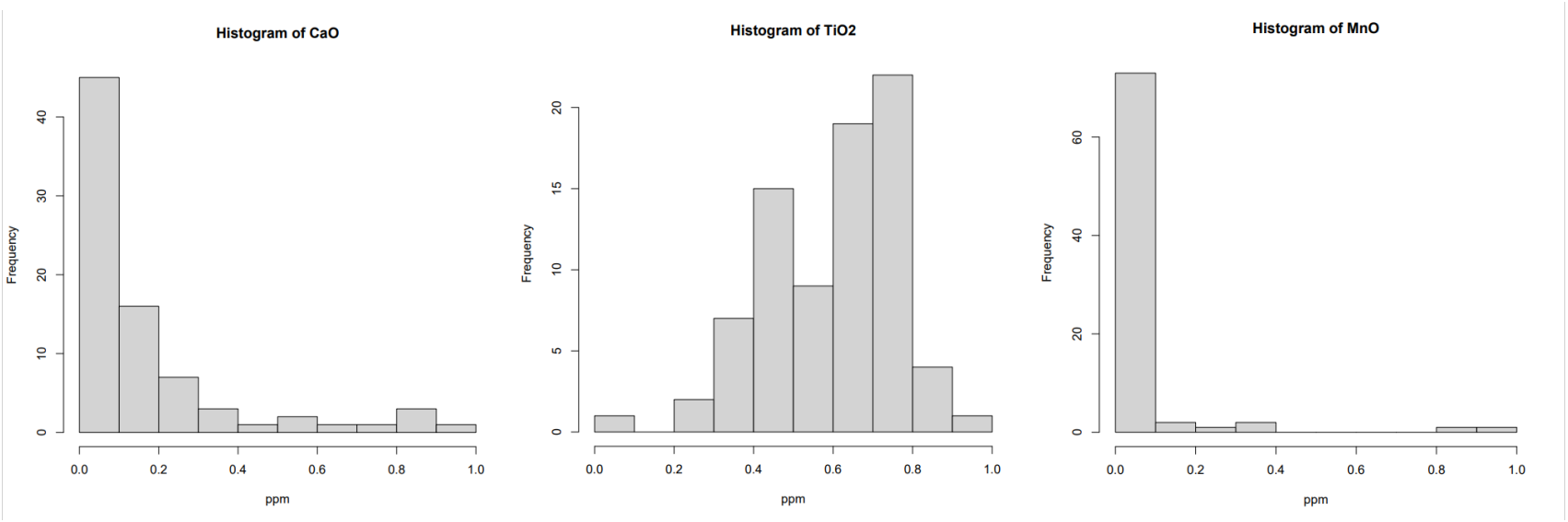
Histogram of CaO
Frequency
0
10
20
30
40
0.0
0.2
0.4
0.6
0.8
1.0
ppm
Histogram of TiO2
Frequency
0
5
10
15
20
0.0
0.2
0.4
0.6
0.8
1.0
ppm
Histogram of MnO
Frequency
0
20
40
60
0.0
0.2
0.4
0.6
0.8
1.0
ppm

Appendix D

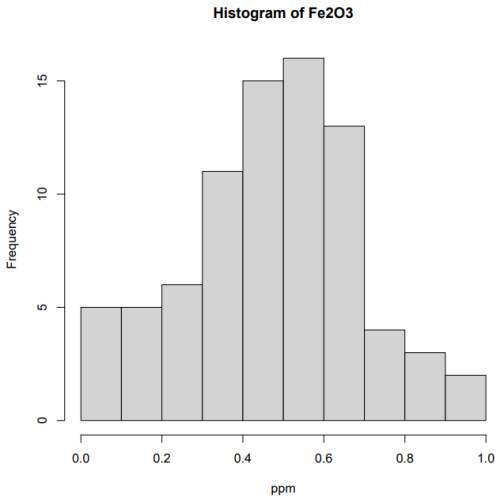
Histogram of Fe2O3
Frequency
0
5
10
15
0.0
0.2
0.4
0.6
0.8
1.0
ppm

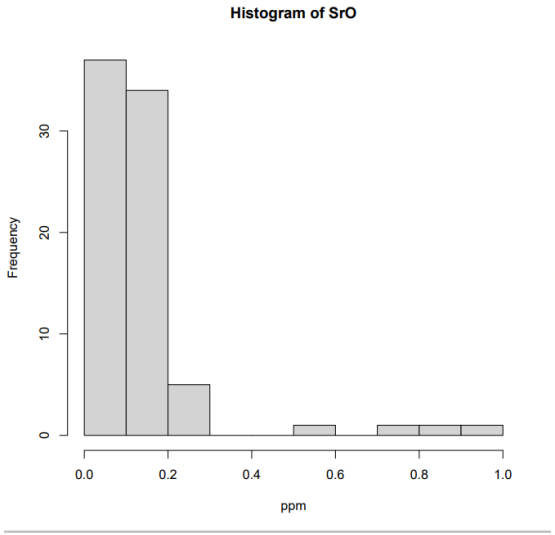
Histogram of SrO
Frequency
0
10
20
30
0.0
0.2
0.4
0.6
0.8
1.0
ppm

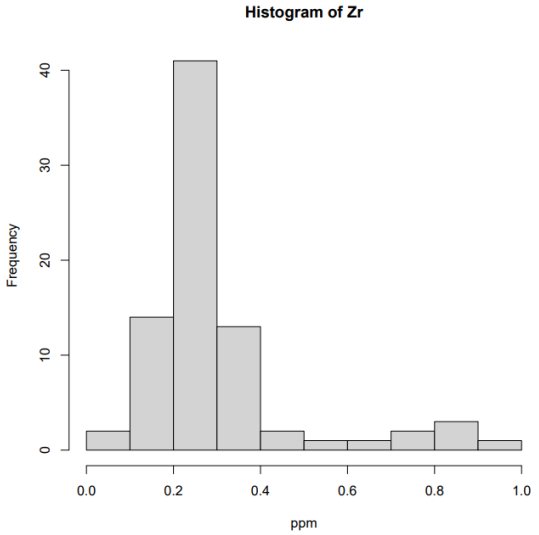
Histogram of Zr
Frequency
0
10
20
30
40
0.0
0.2
0.4
0.6
0.8
1.0
ppm

QQ-plots plots of XRF topsoil data fromCastleisland, Co. Kerry, SW Ireland.

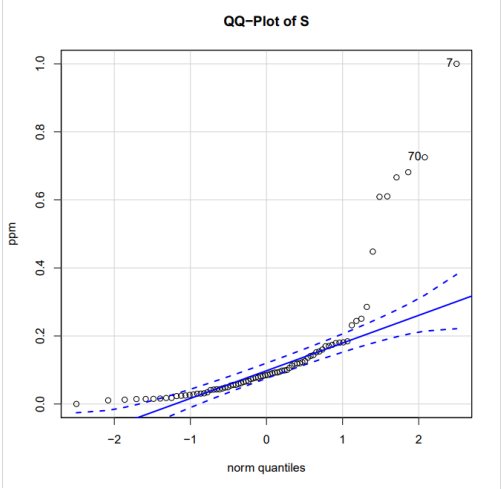

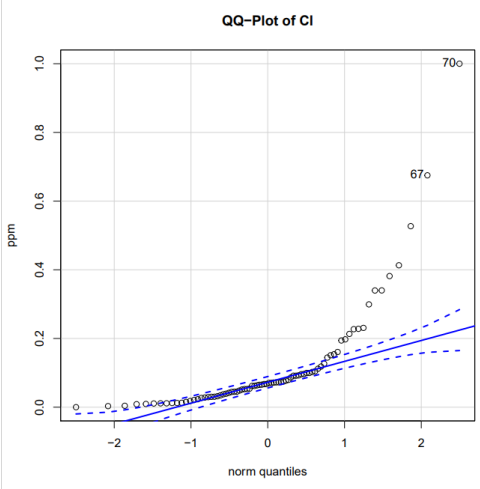

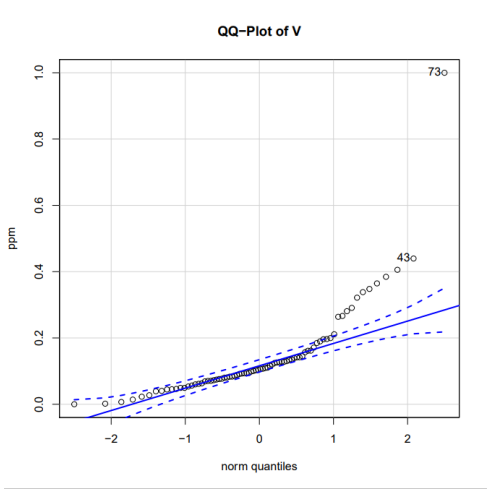

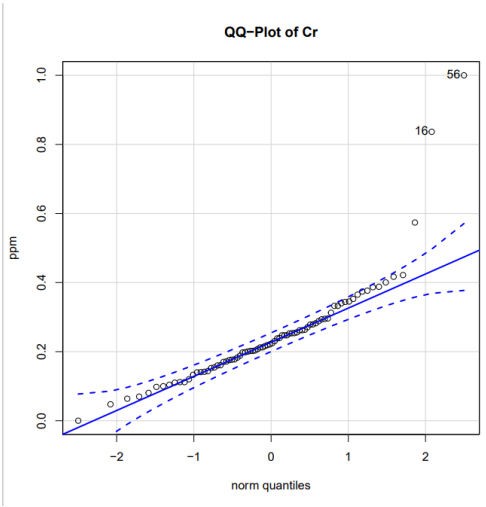

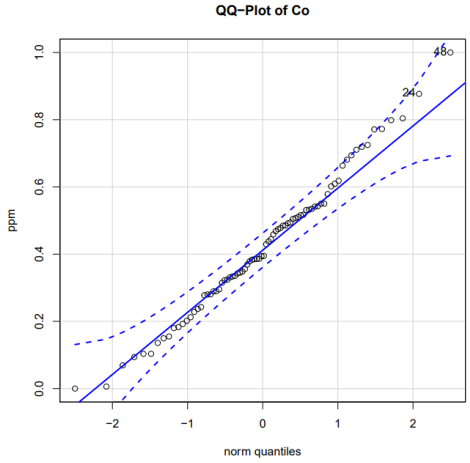

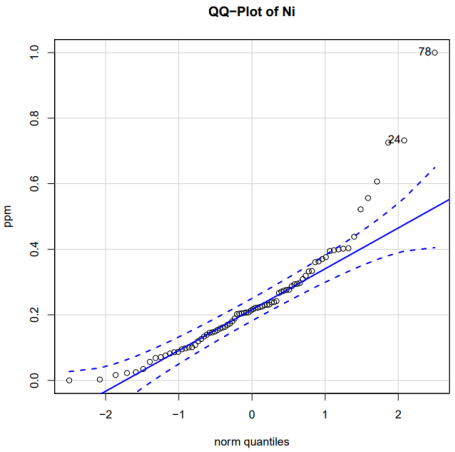

Appendix D

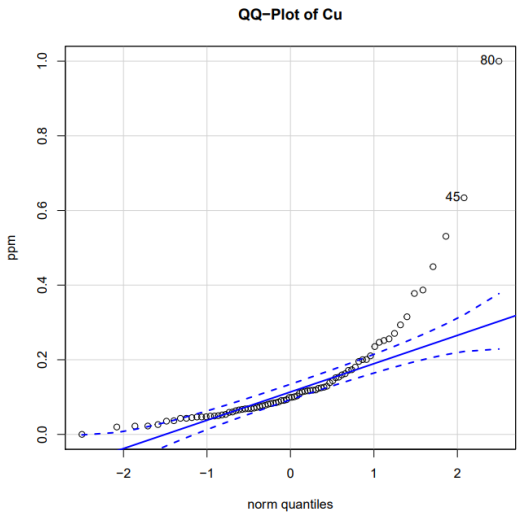
QQ−Plot of Cu
ppm
norm quantiles
80
45

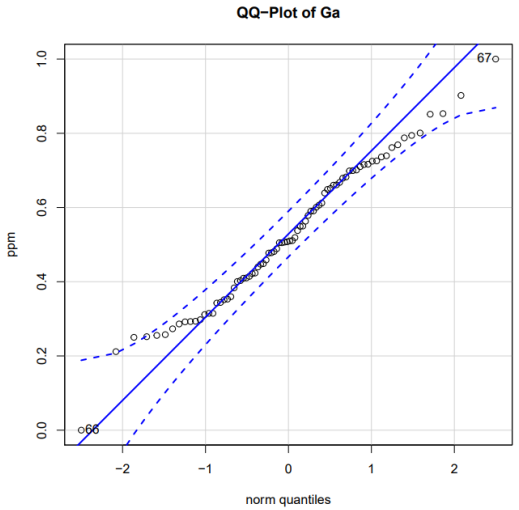
QQ−Plot of Ga
ppm
norm quantiles
67
66

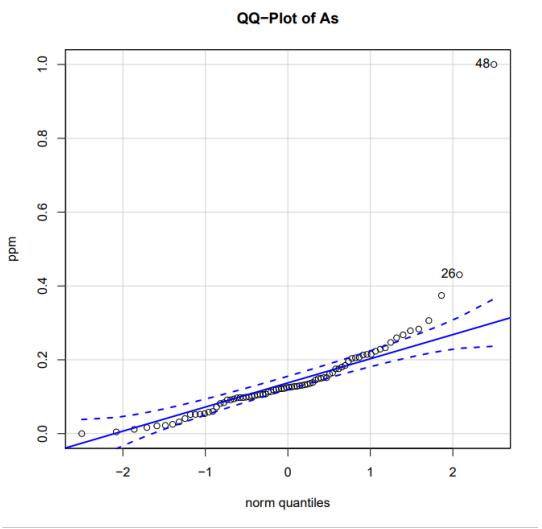
QQ−Plot of As
ppm
norm quantiles
48
26

Appendix D

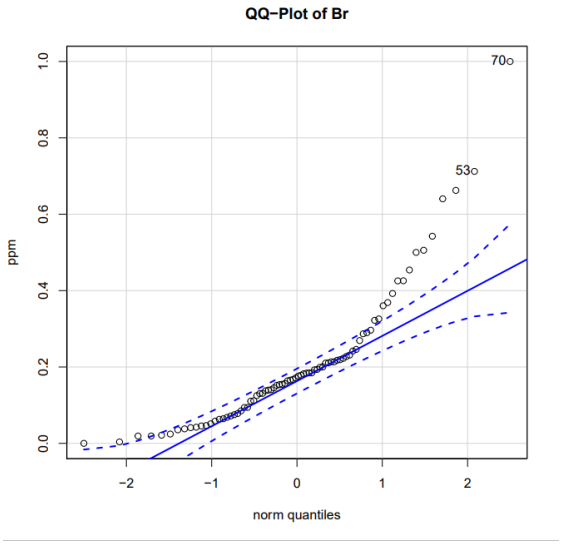
QQ−Plot of Br
ppm
norm quantiles
70
53

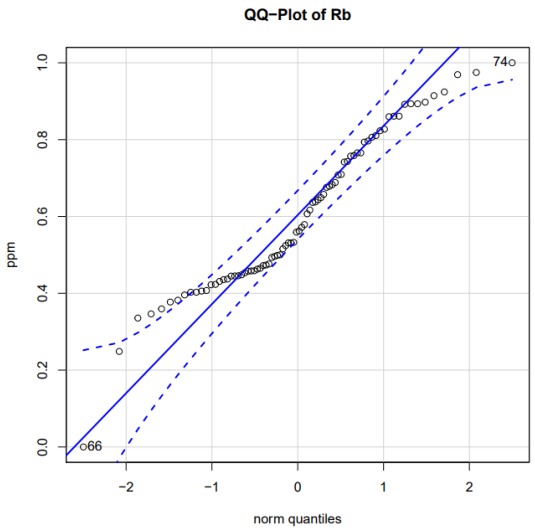
QQ−Plot of Rb
ppm
norm quantiles
74
66

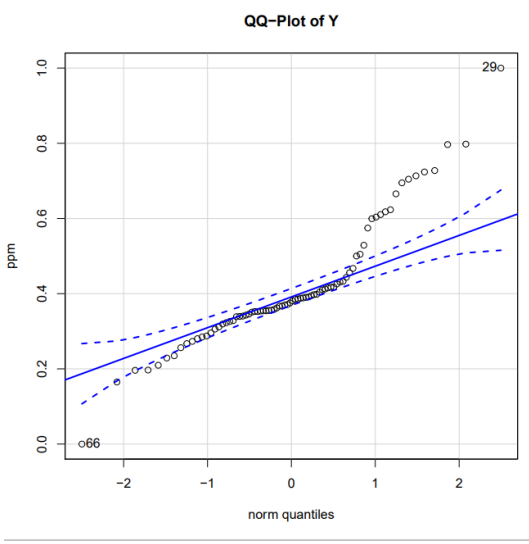
QQ−Plot of Y
ppm
norm quantiles
29
66

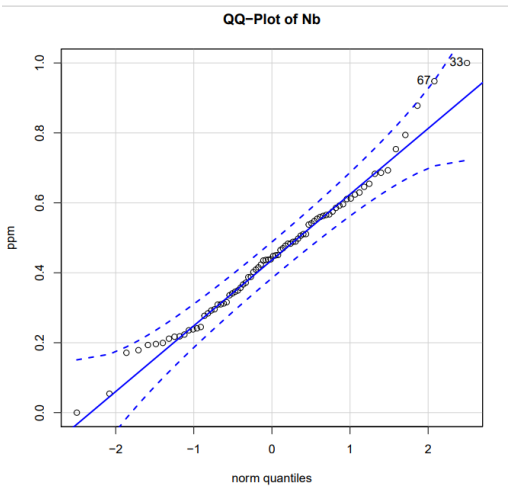
QQ−Plot of Nb
ppm
norm quantiles
33
67

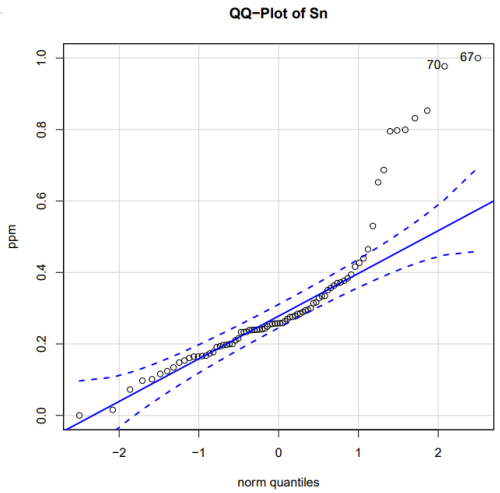
QQ−Plot of Sn
ppm
norm quantiles
70
67

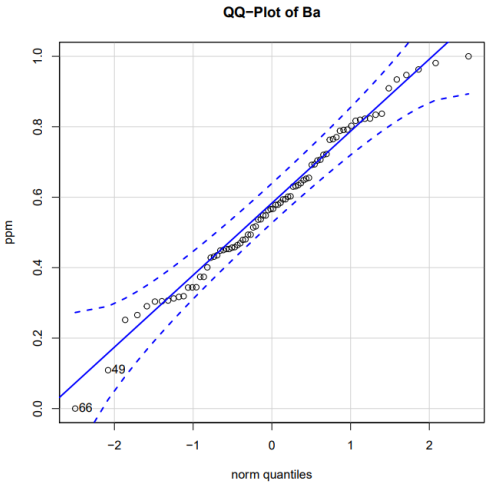
QQ−Plot of Ba
ppm
norm quantiles
49
66

Appendix D

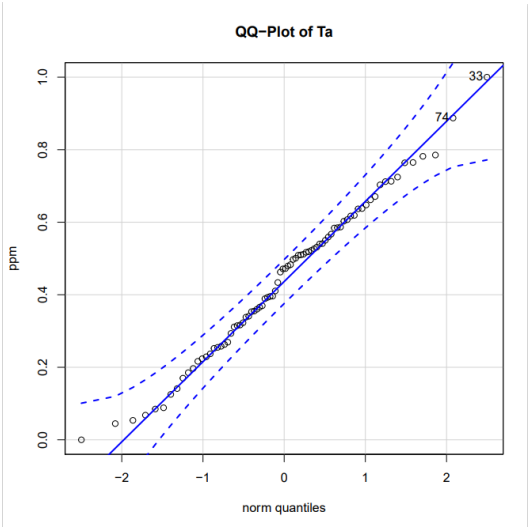
QQ−Plot of Ta
ppm
norm quantiles
33
74

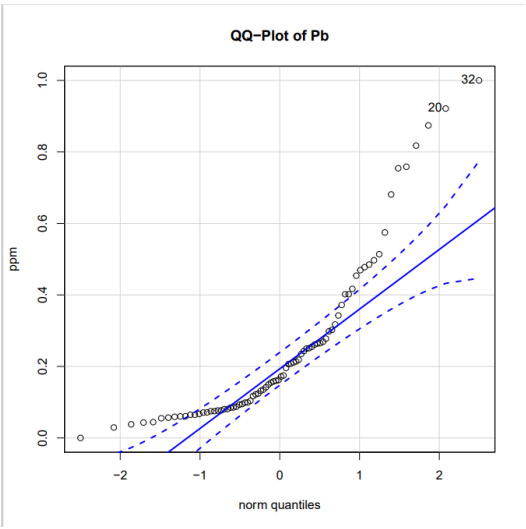
QQ−Plot of Pb
ppm
norm quantiles
32
20

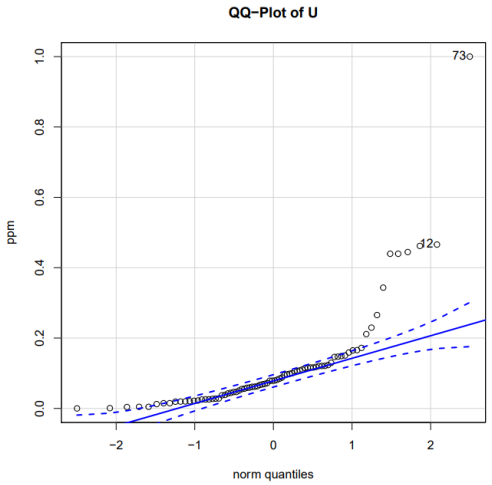
QQ−Plot of U
ppm
norm quantiles
73
12

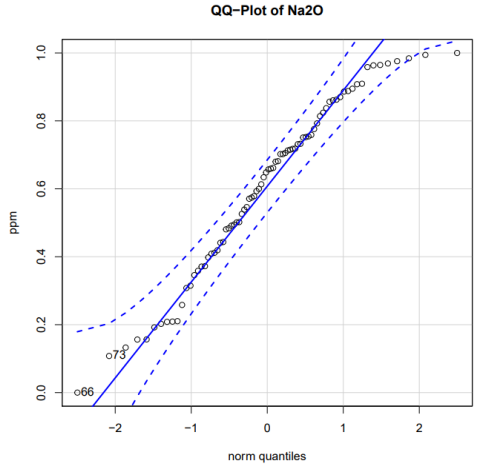
QQ−Plot of Na2O
ppm
norm quantiles
73
66

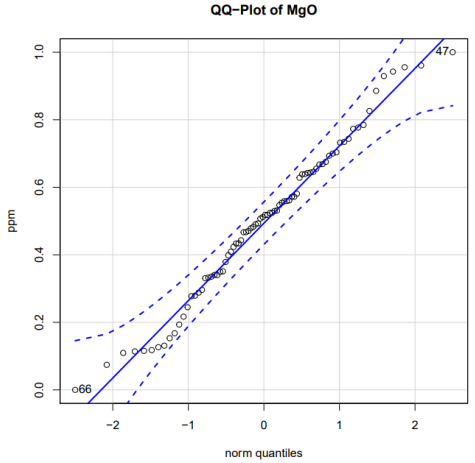
QQ−Plot of MgO
ppm
norm quantiles
47
66

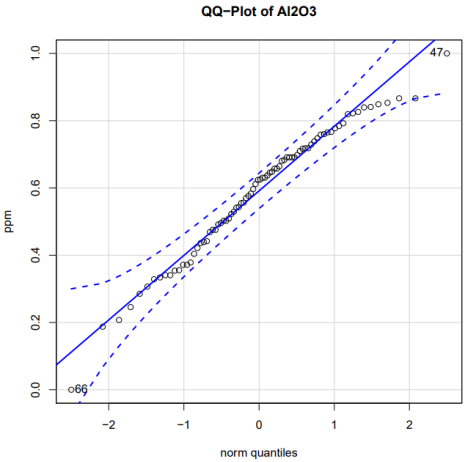
QQ−Plot of Al2O3
ppm
norm quantiles
47
66

Appendix D

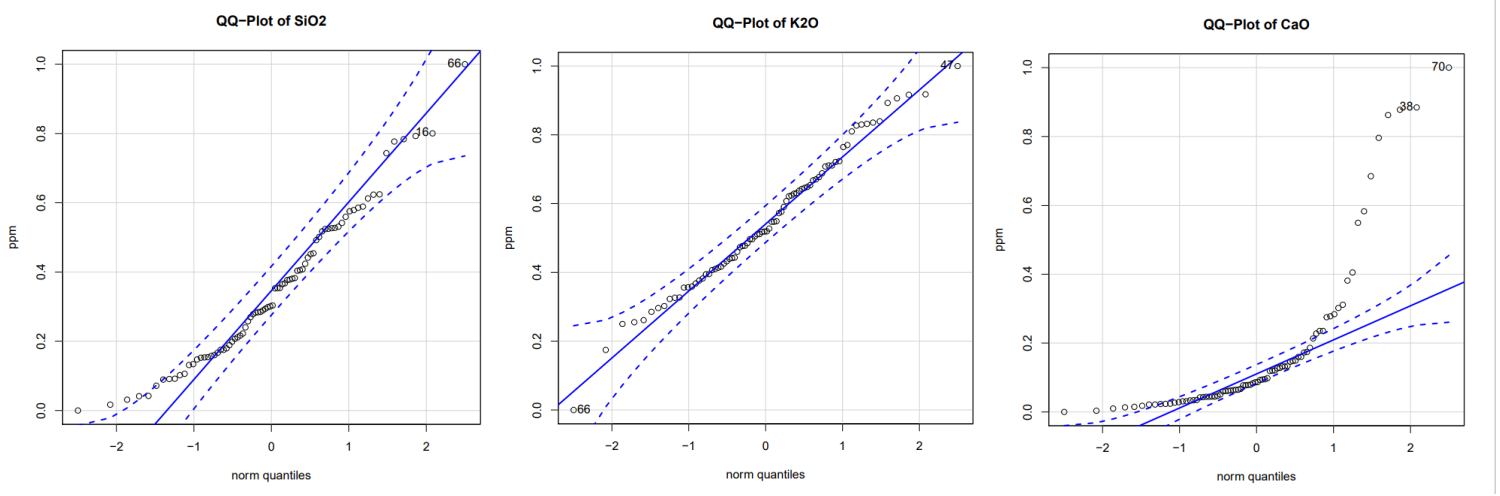
QQ−Plot of SiO2
QQ−Plot of K2O
QQ−Plot of CaO
ppm
norm quantiles
66
16
47
66
70
38

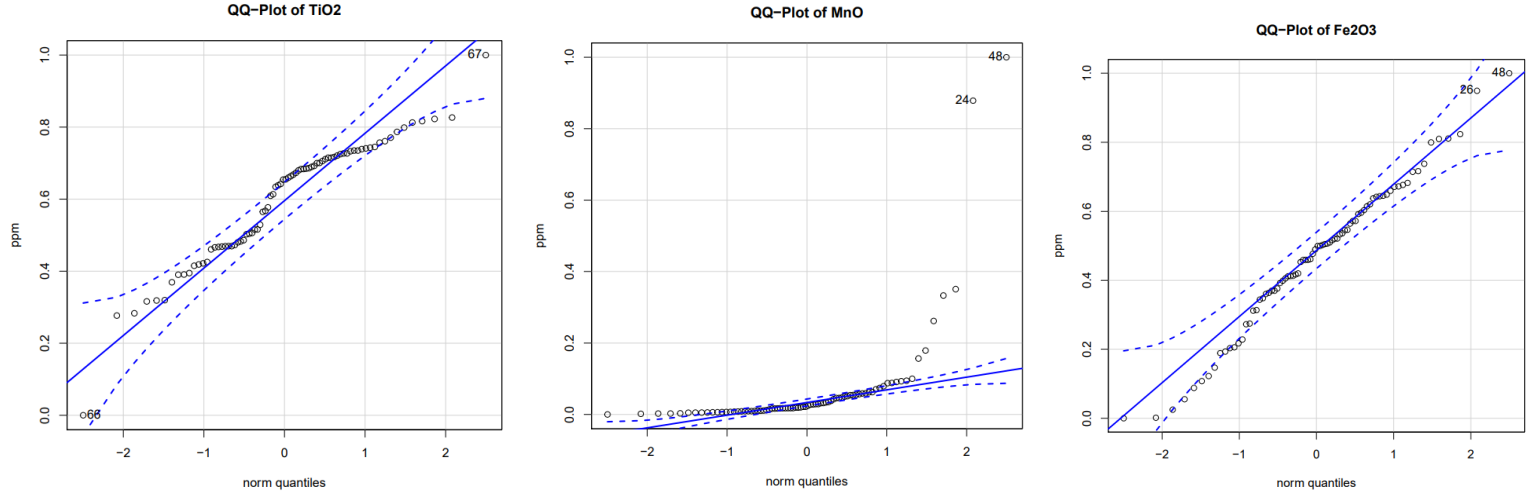
QQ−Plot of TiO2
QQ−Plot of MnO
QQ−Plot of Fe2O3
ppm
norm quantiles
67
66
48
24
48
26

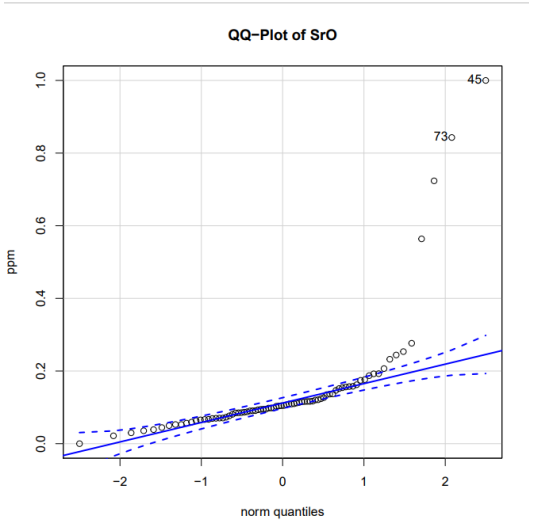
QQ−Plot of SrO
45
73
ppm
norm quantiles
0.0
0.2
0.4
0.6
0.8
1.0
−2
−1
0
1
2

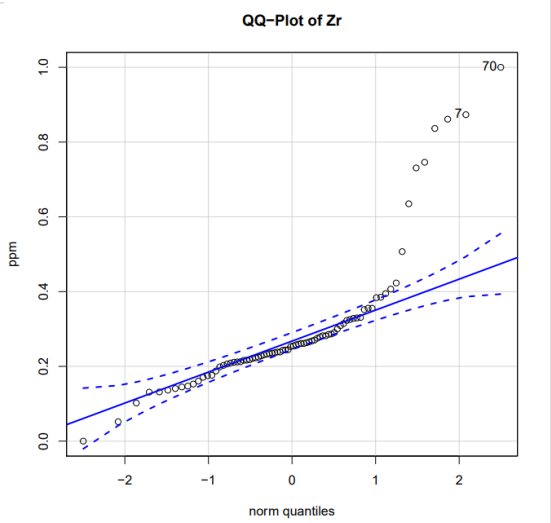
QQ−Plot of Zr
70
7
ppm
norm quantiles
0.0
0.2
0.4
0.6
0.8
1.0
−2
−1
0
1
2

QQ-plots of ICPMS aqua regia shallow topsoil (NA removed) CLR-transformed Castleisland, Co. Kerry, SW Ireland.

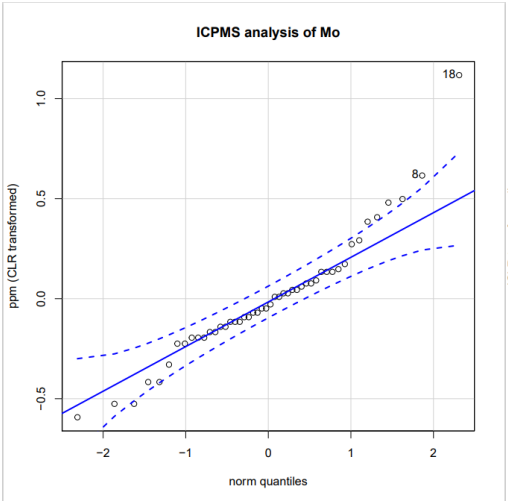

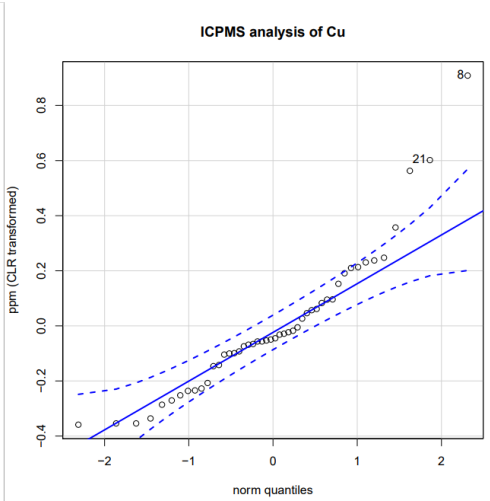

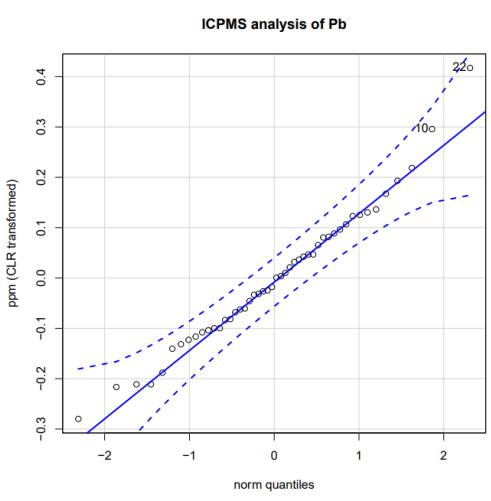

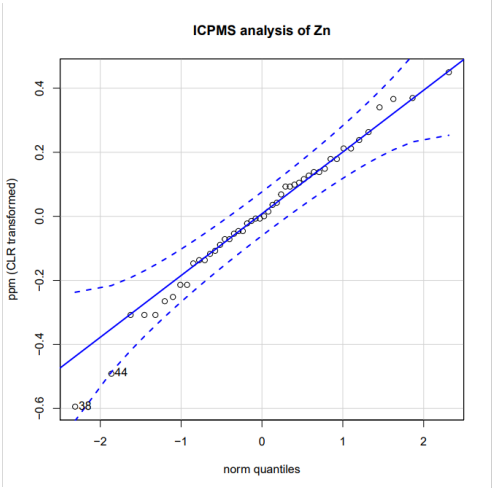

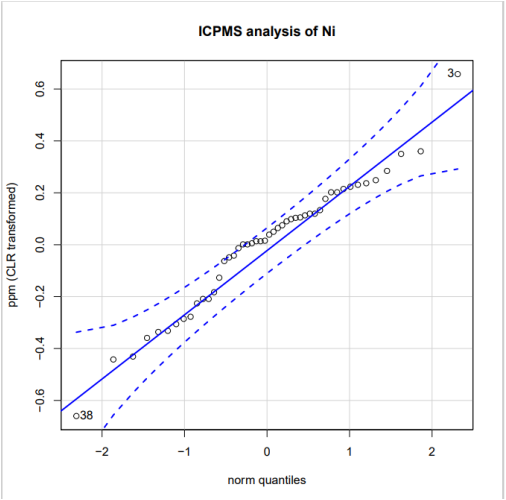

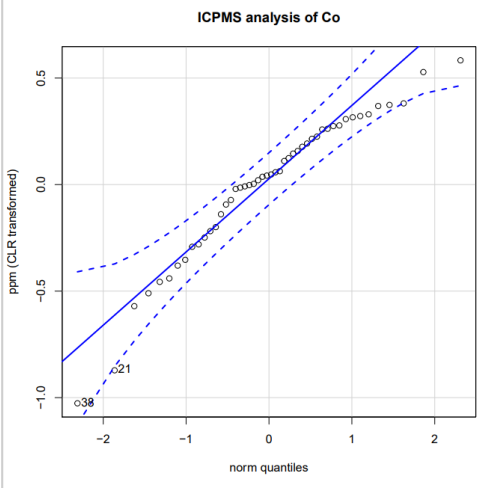

Appendix D

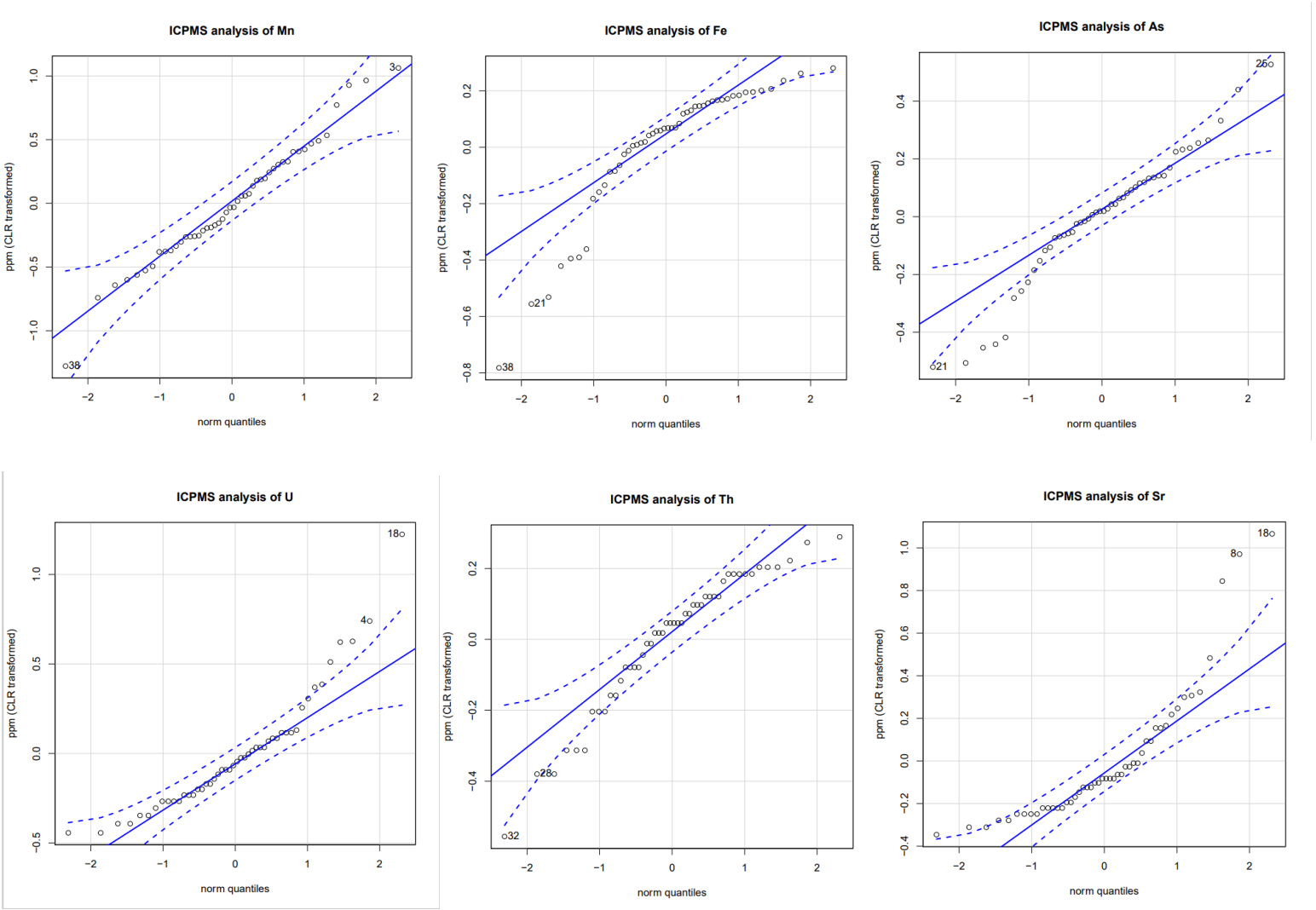
ICPMS analysis of Mn
ICPMS analysis of Fe
ICPMS analysis of As
ICPMS analysis of U
ICPMS analysis of Th
ICPMS analysis of Sr
ppm (CLR transformed)
norm quantiles

Appendix D

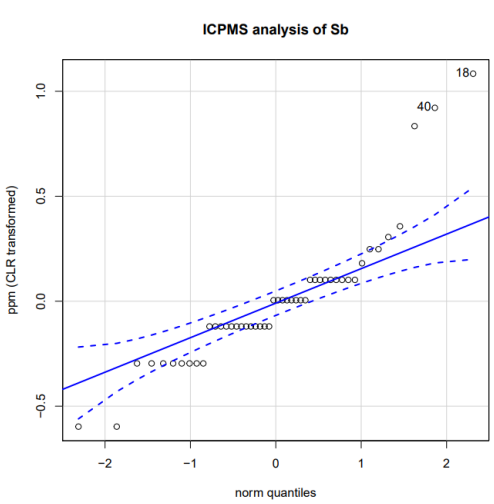
ICPMS analysis of Sb
ppm (CLR transformed)
norm quantiles
18
40

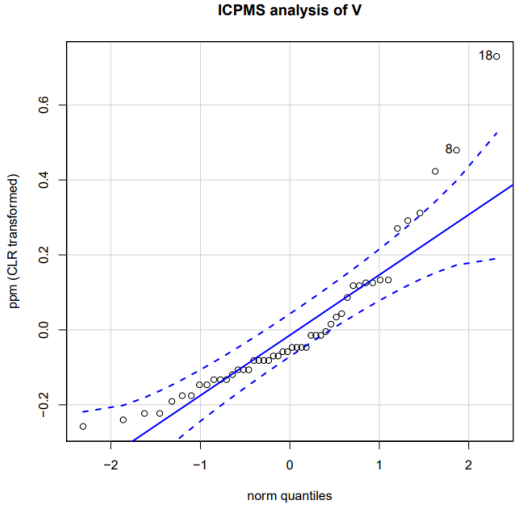
ICPMS analysis of V
ppm (CLR transformed)
norm quantiles
18
8

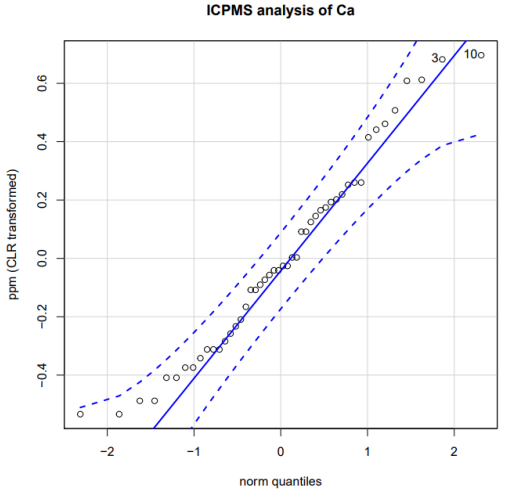
ICPMS analysis of Ca
ppm (CLR transformed)
norm quantiles
3
10

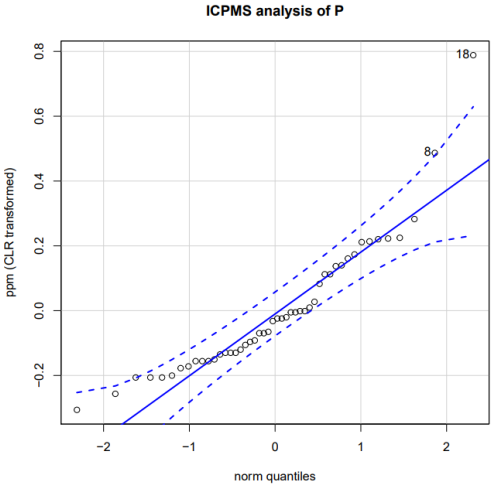
ICPMS analysis of P
ppm (CLR transformed)
norm quantiles
18
8

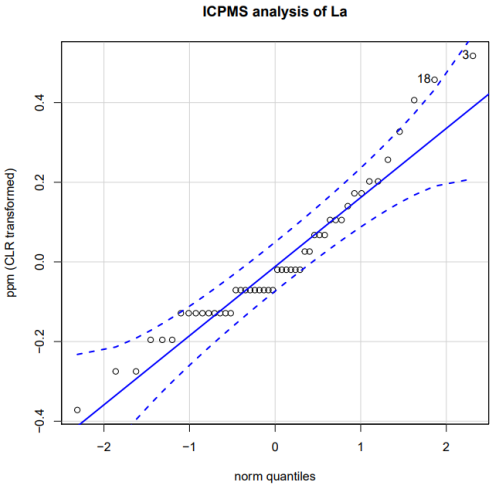
ICPMS analysis of La
ppm (CLR transformed)
norm quantiles
3
18

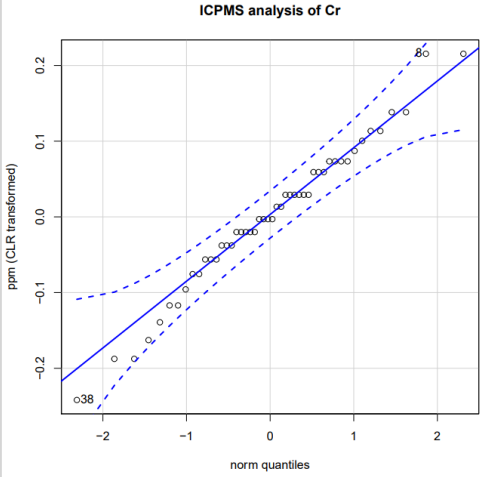
ICPMS analysis of Cr
ppm (CLR transformed)
norm quantiles
8
38

Appendix D

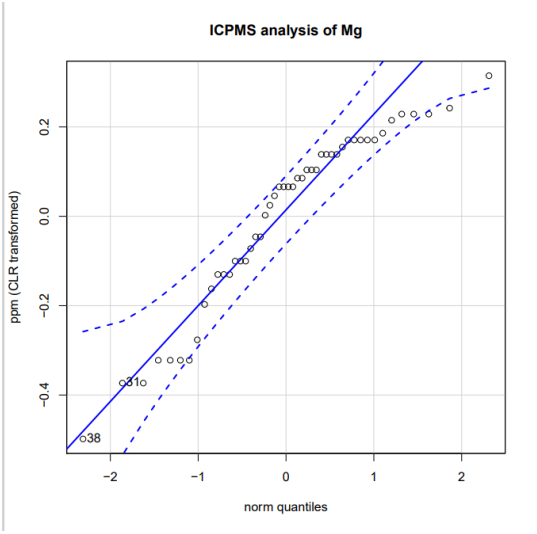
ICPMS analysis of Mg
ppm (CLR transformed)
norm quantiles
38
31

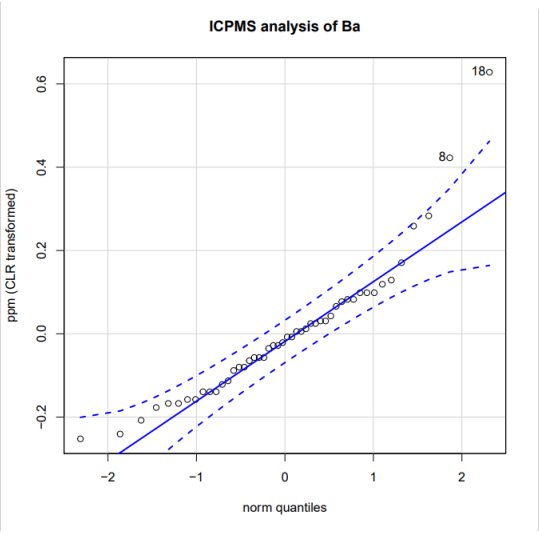
ICPMS analysis of Ba
ppm (CLR transformed)
norm quantiles
18
8

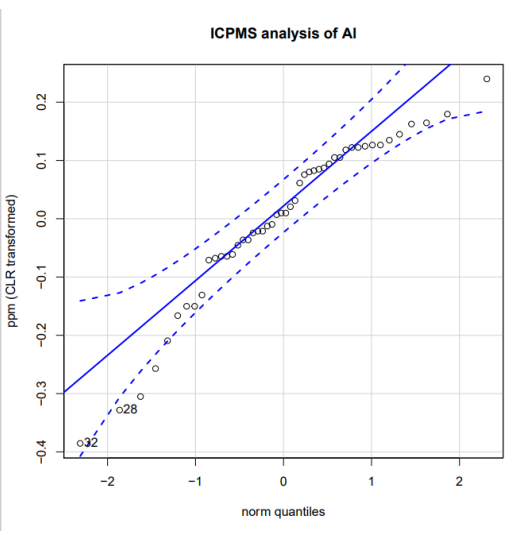
ICPMS analysis of Al
ppm (CLR transformed)
norm quantiles
32
28

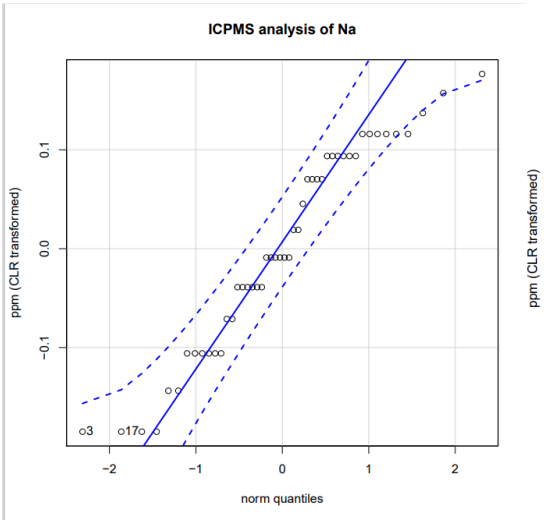
ICPMS analysis of Na
ppm (CLR transformed)
norm quantiles
3
17

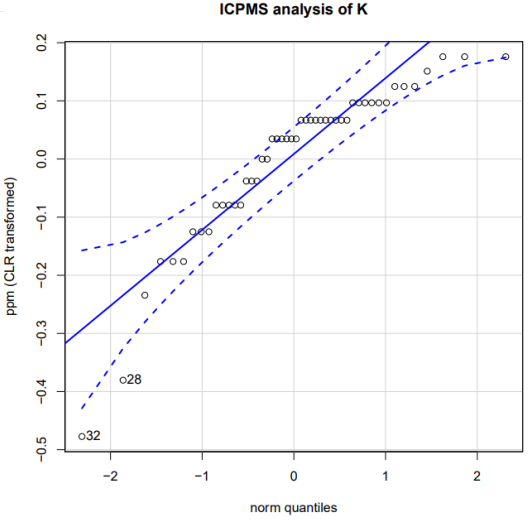
ICPMS analysis of K
ppm (CLR transformed)
norm quantiles
32
28

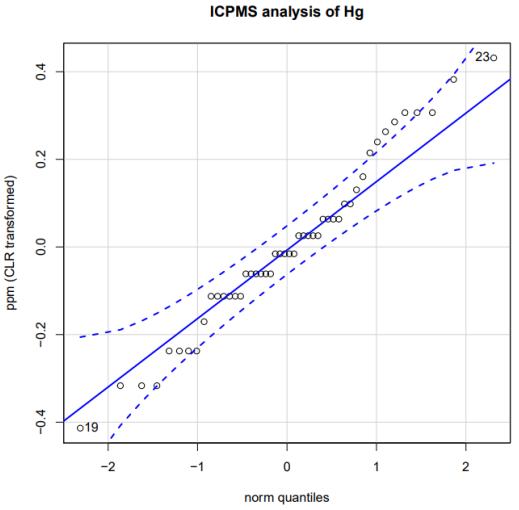
ICPMS analysis of Hg
ppm (CLR transformed)
norm quantiles
19
23

Appendix D

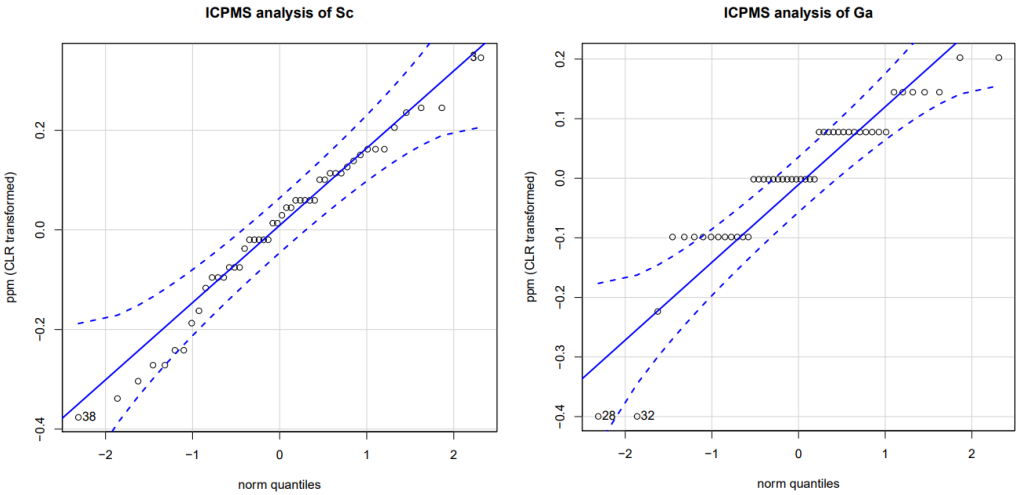
ICPMS analysis of Sc
ppm (CLR transformed)
norm quantiles
38
ICPMS analysis of Ga
ppm (CLR transformed)
norm quantiles
28
32

Appendix D

Appendix D

ICPMS transformed shallow topsoil Castleisland, Co. Kerry, SW Ireland dot concentration plots.

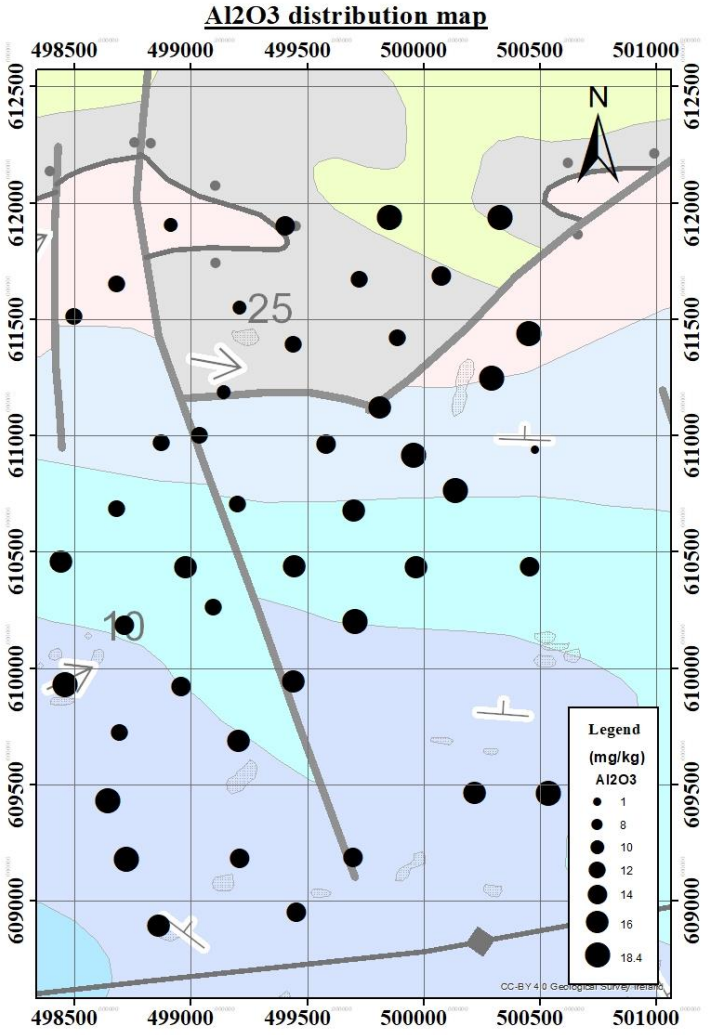

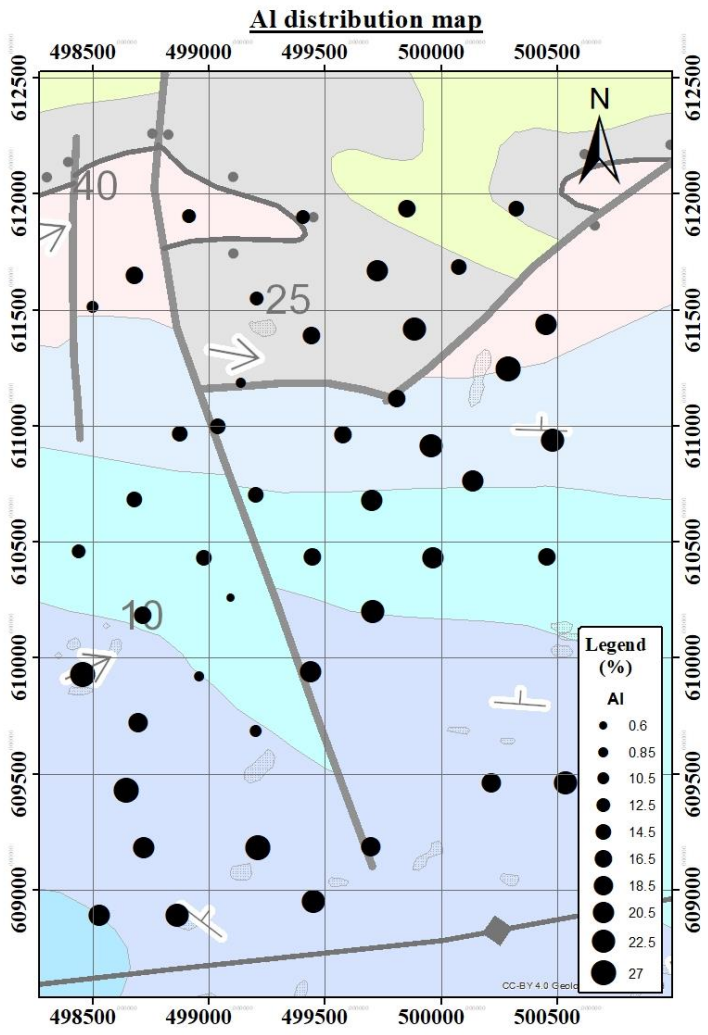

Appendix D

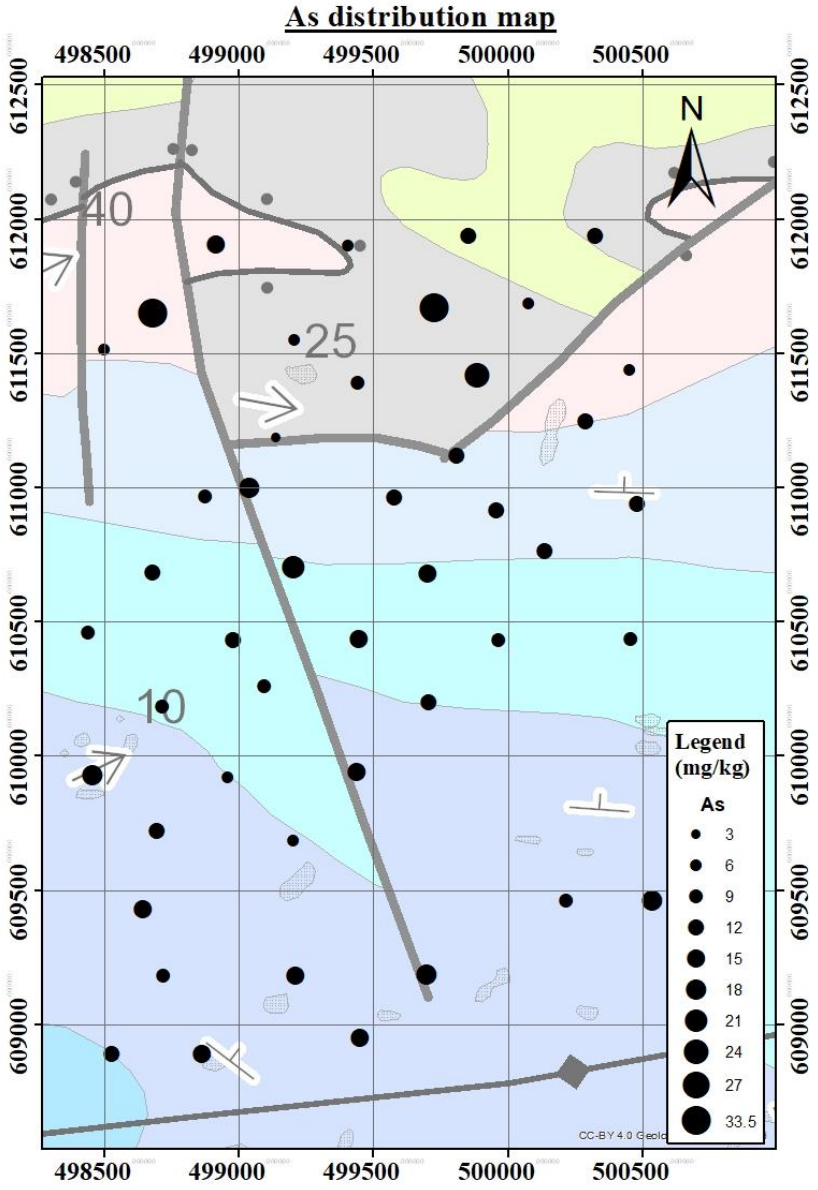
As distribution map
498500
499000
499500
500000
500500
612500
612000
611500
611000
610500
610000
609500
609000
N
40
25
10
Legend
(mg/kg)
As
3
6
9
12
15
18
21
24
27
33.5

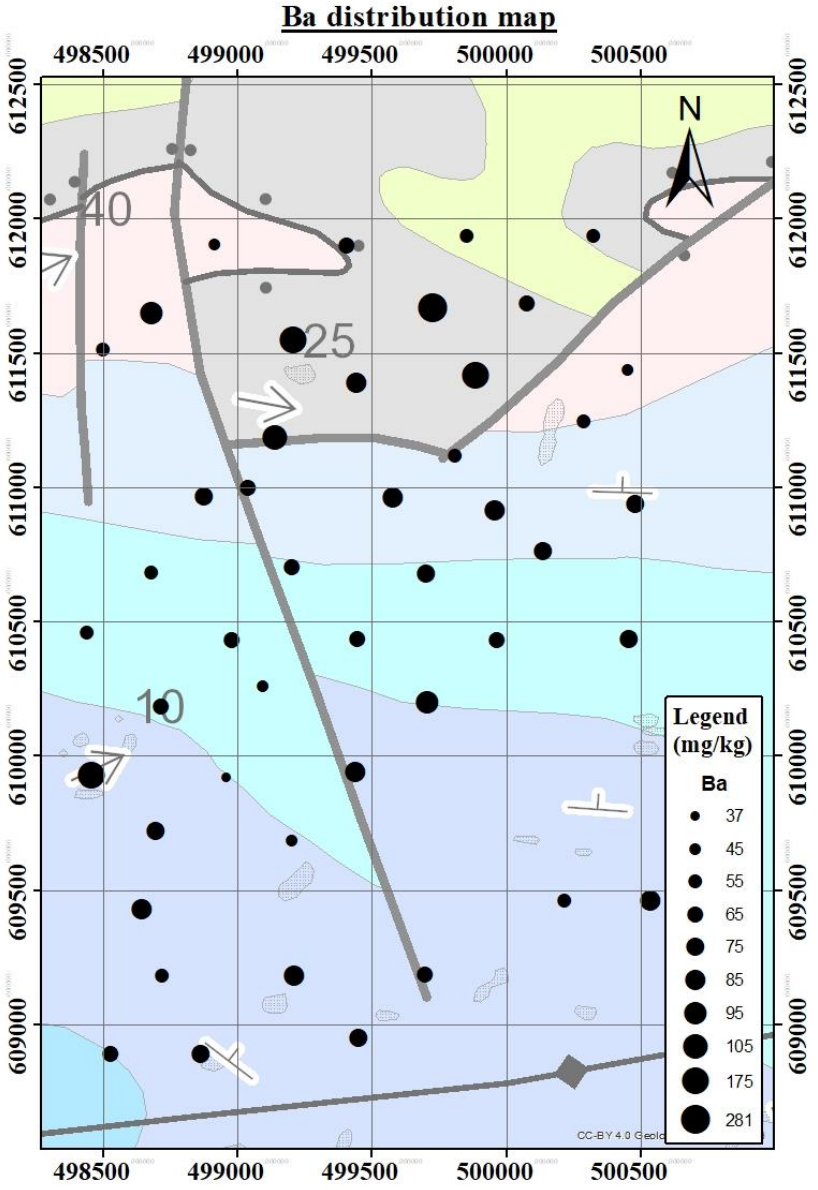
Ba distribution map
498500
499000
499500
500000
500500
612500
612000
611500
611000
610500
610000
609500
609000
N
40
25
10
Legend
(mg/kg)
Ba
37
45
55
65
75
85
95
105
175
281

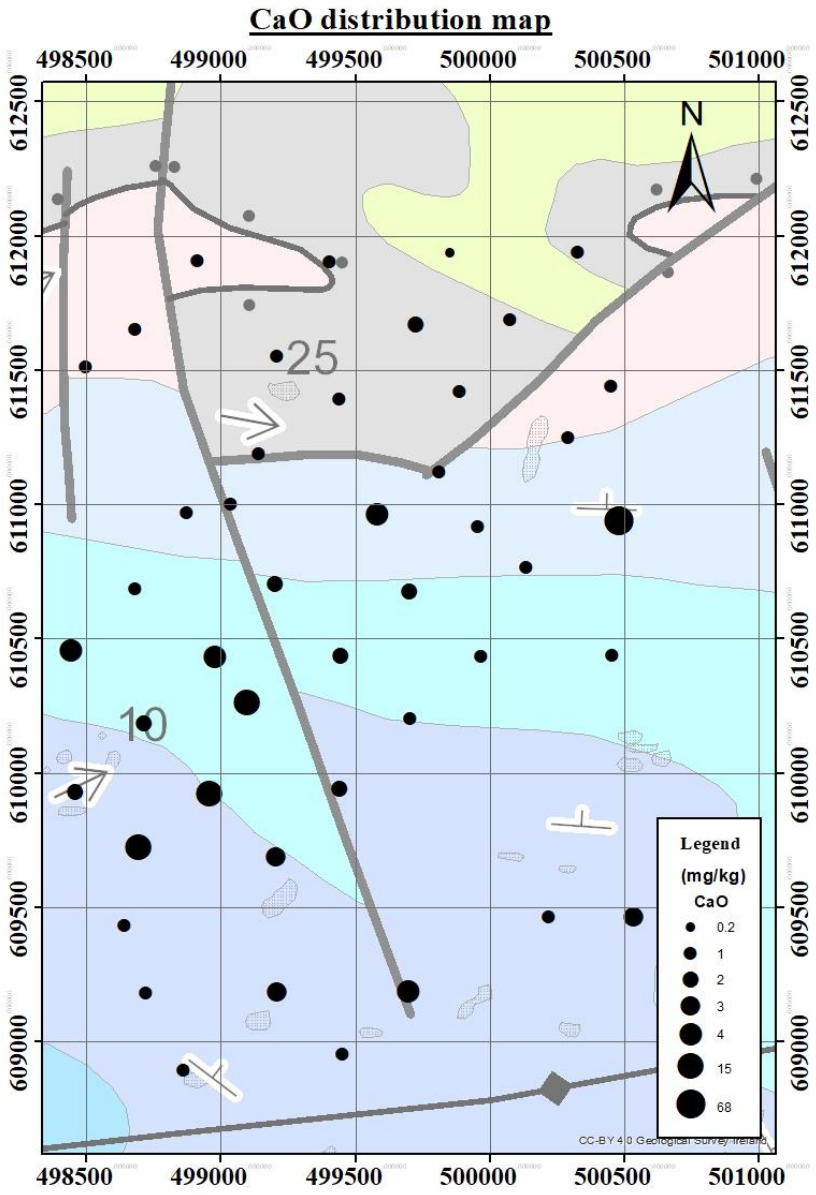
CaO distribution map
498500
499000
499500
500000
500500
501000
612500
612000
611500
611000
610500
610000
609500
609000
N
25
10
Legend
(mg/kg)
CaO
0.2
1
2
3
4
15
68
CC-BY 4.0 Geological Survey Ireland

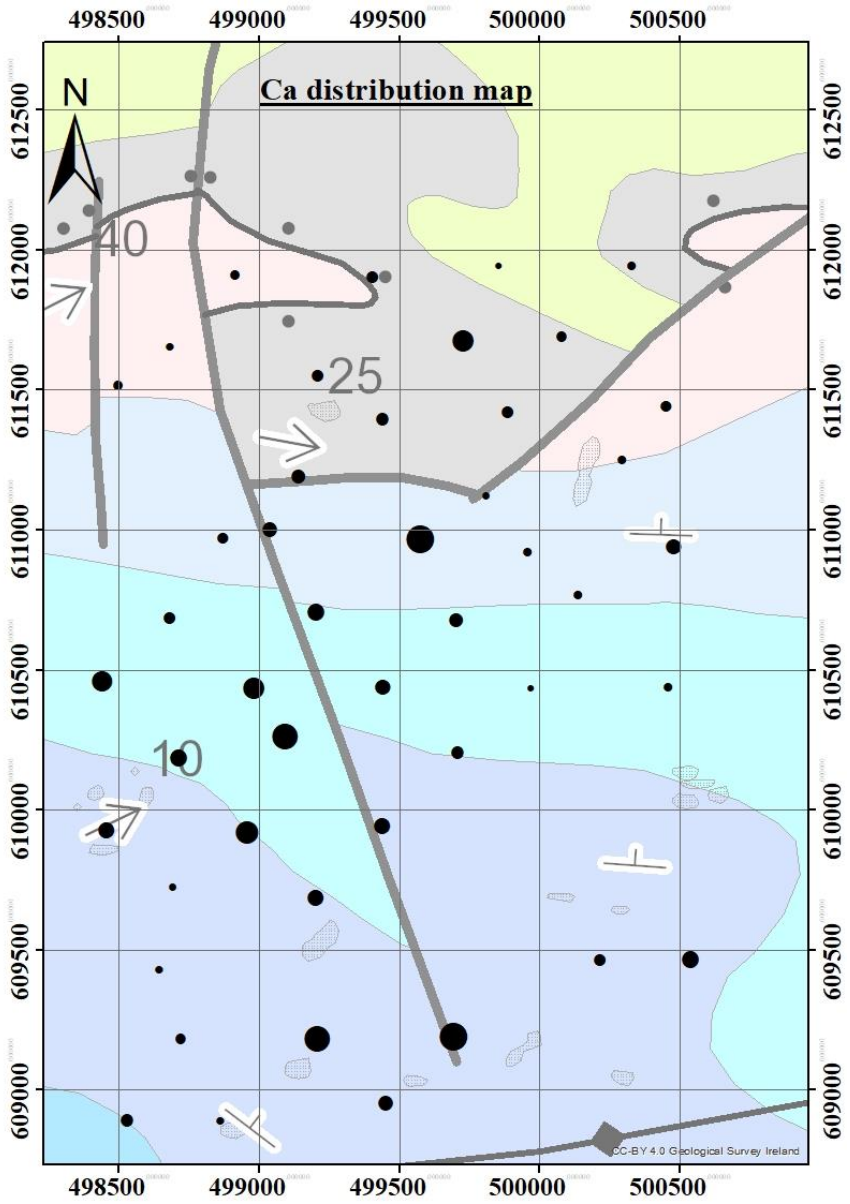
498500
499000
499500
500000
500500
612500
612000
611500
611000
610500
610000
609500
609000
N
Ca distribution map
40
25
10
CC-BY 4.0 Geological Survey Ireland

Appendix D

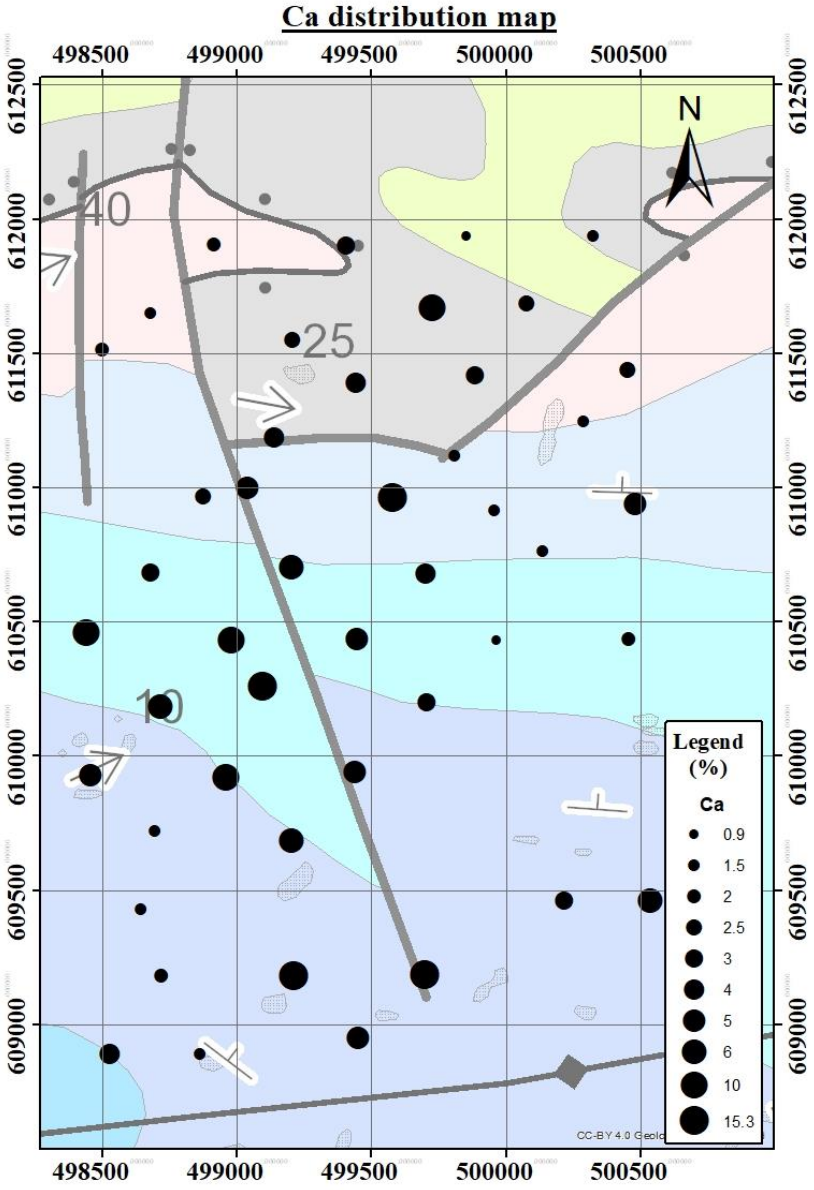
Ca distribution map
498500
499000
499500
500000
500500
612500
612000
611500
611000
610500
610000
609500
609000
N
40
25
10
Legend
(%)
Ca
0.9
1.5
2
2.5
3
4
5
6
10
15.3
CC-BY 4.0 Geolo

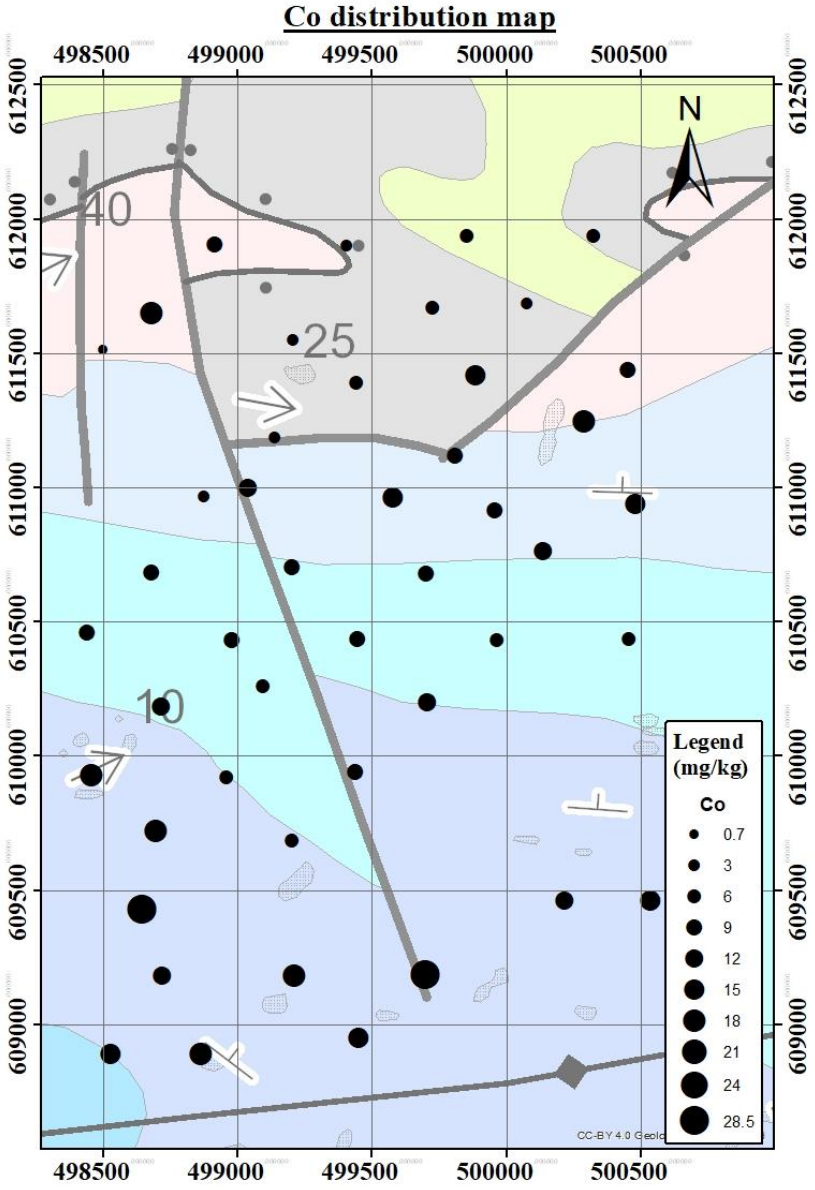
Co distribution map
498500
499000
499500
500000
500500
612500
612000
611500
611000
610500
610000
609500
609000
N
40
25
10
Legend
(mg/kg)
Co
0.7
3
6
9
12
15
18
21
24
28.5
CC-BY 4.0 Geolo

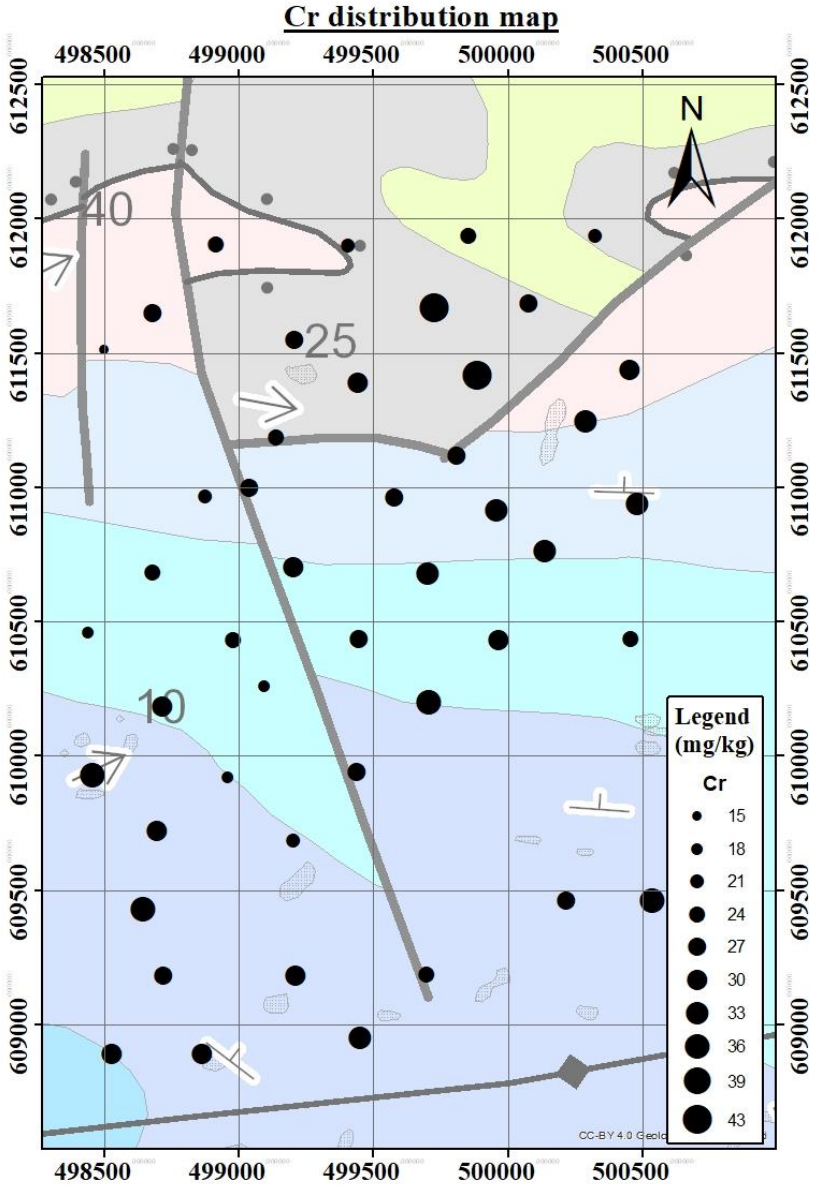
Cr distribution map
498500
499000
499500
500000
500500
612500
612000
611500
611000
610500
610000
609500
609000
N
40
25
10
Legend
(mg/kg)
Cr
15
18
21
24
27
30
33
36
39
43
CC-BY 4.0 Geolo

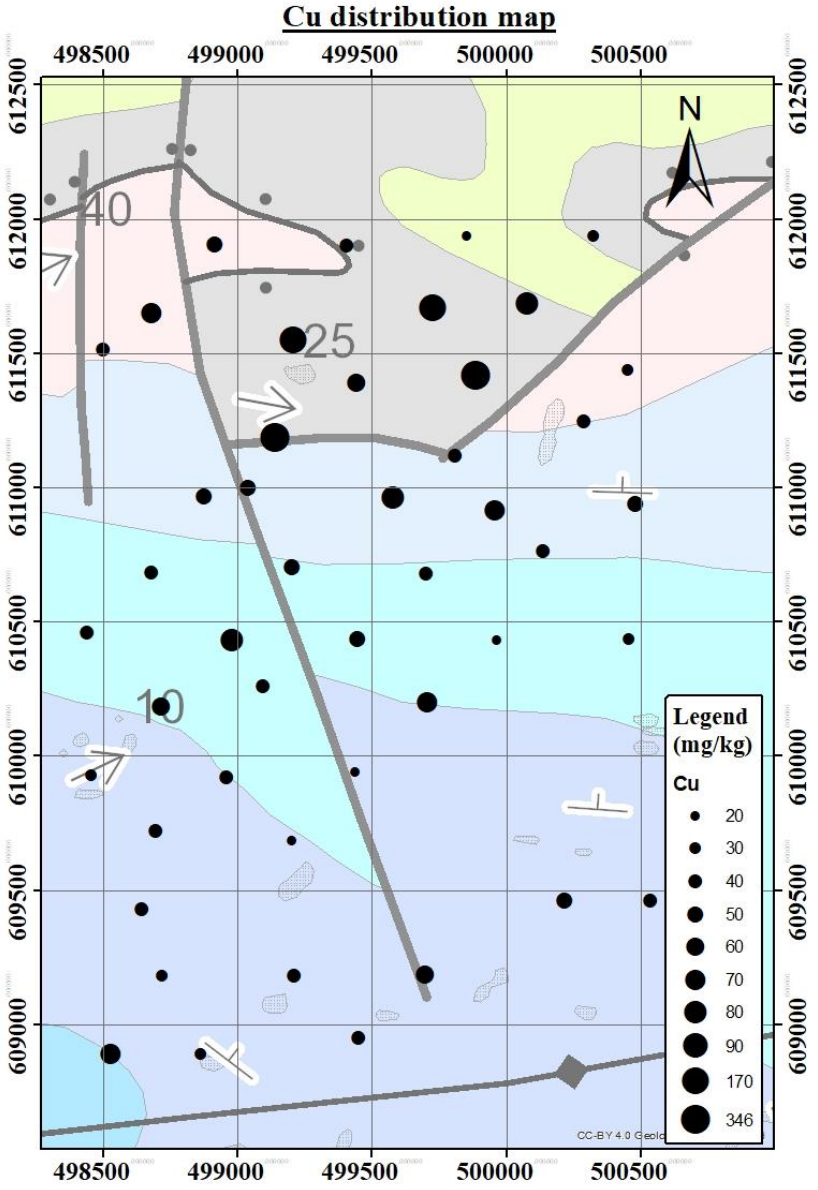
Cu distribution map
498500
499000
499500
500000
500500
612500
612000
611500
611000
610500
610000
609500
609000
N
40
25
10
Legend
(mg/kg)
Cu
20
30
40
50
60
70
80
90
170
346
CC-BY 4.0 Geolo

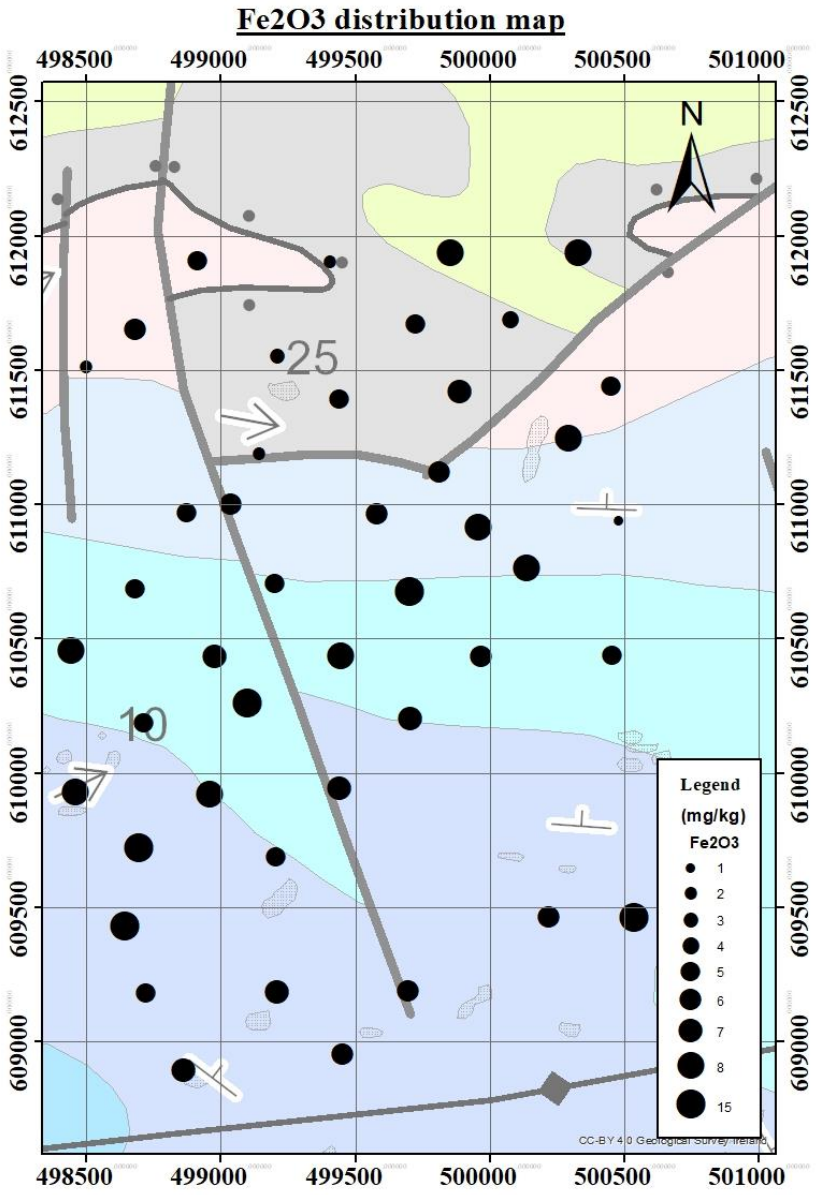
Fe2O3 distribution map
498500
499000
499500
500000
500500
501000
612500
612000
611500
611000
610500
610000
609500
609000
N
25
10
Legend
(mg/kg)
Fe2O3
1
2
3
4
5
6
7
8
15
CC-BY 4.0 Geological Survey Ireland

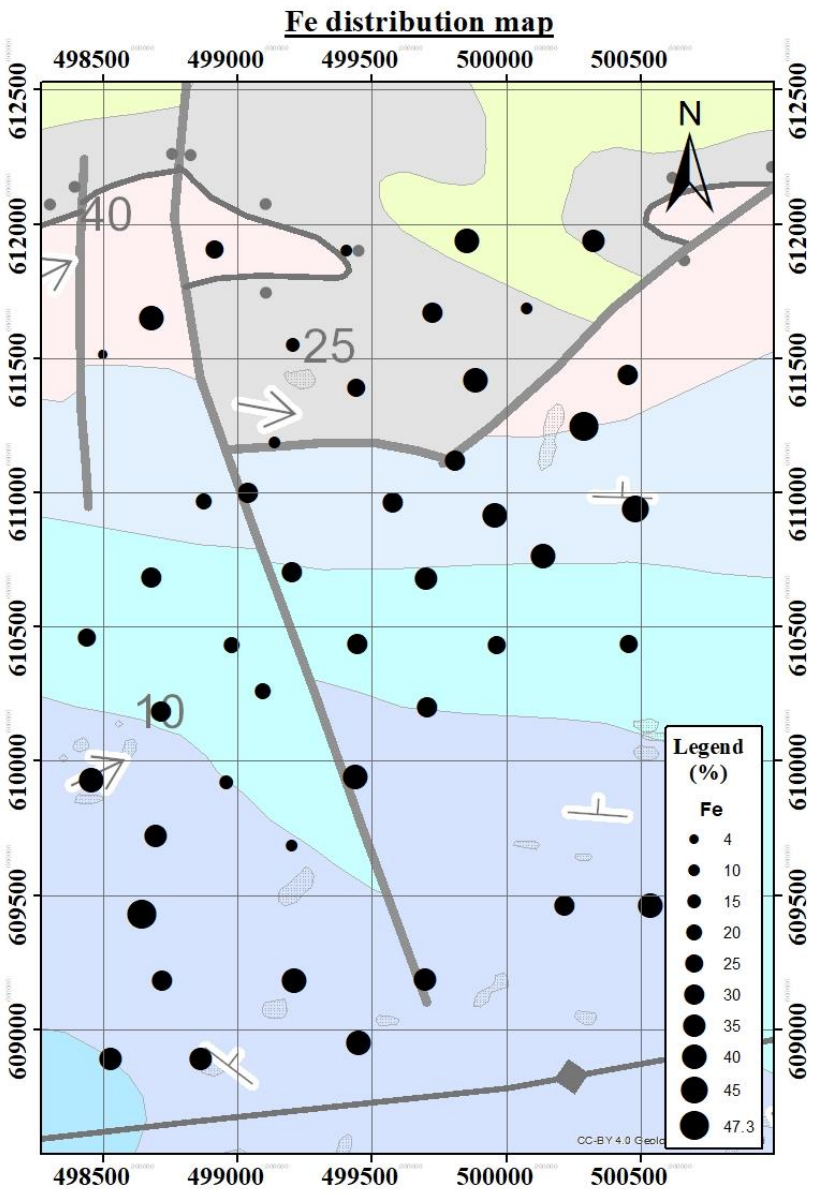
Fe distribution map
498500
499000
499500
500000
500500
612500
612000
611500
611000
610500
610000
609500
609000
N
40
25
10
Legend
(%)
Fe
4
10
15
20
25
30
35
40
45
47.3
CC-BY 4.0 Geolo

Appendix D

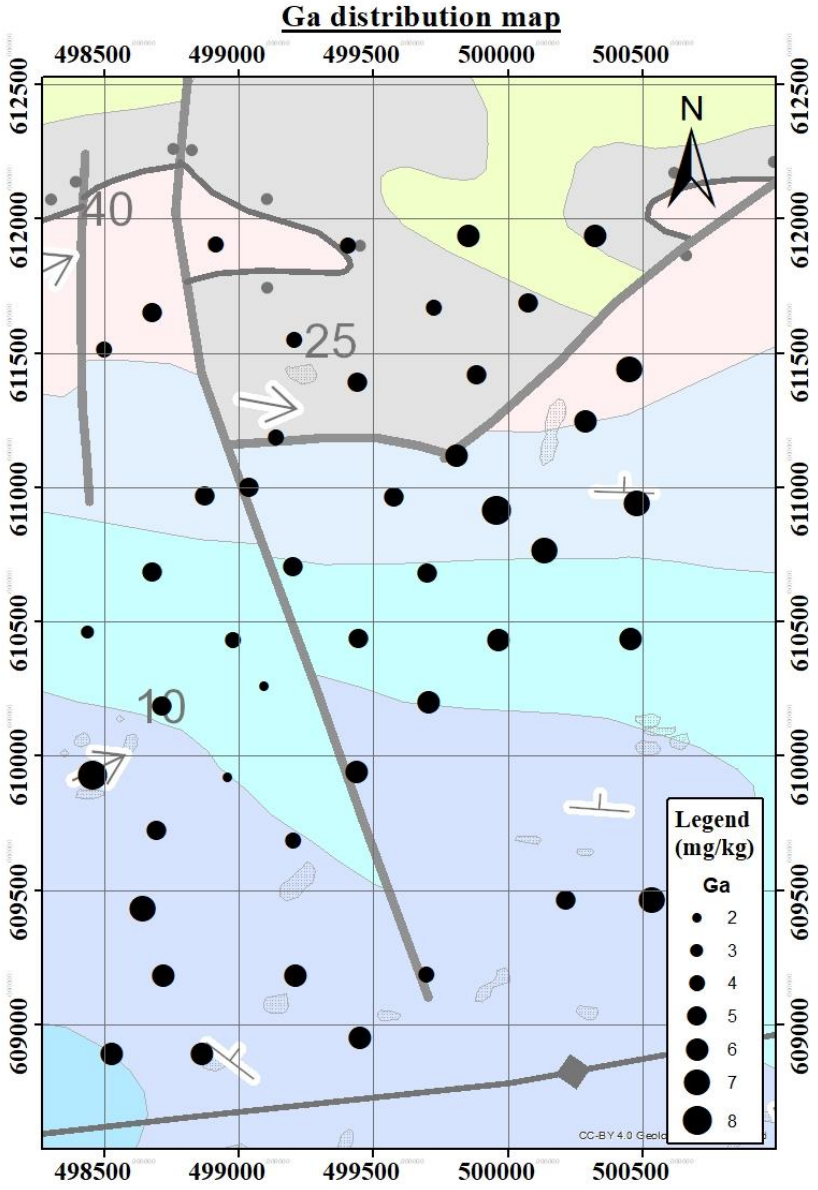
Ga distribution map
498500
499000
499500
500000
500500
612500
612000
611500
611000
610500
610000
609500
609000
N
40
25
10
Legend
(mg/kg)
Ga
2
3
4
5
6
7
8

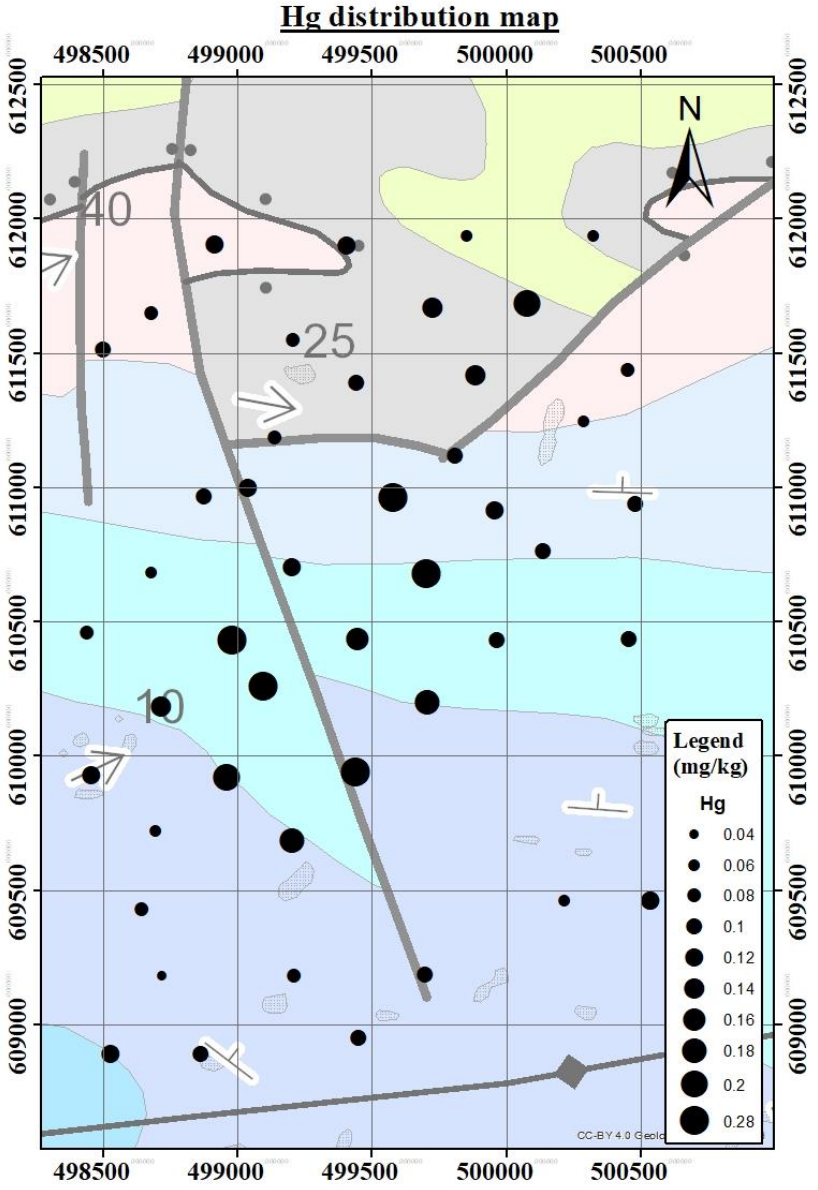
Hg distribution map
498500
499000
499500
500000
500500
612500
612000
611500
611000
610500
610000
609500
609000
N
40
25
10
Legend
(mg/kg)
Hg
0.04
0.06
0.08
0.1
0.12
0.14
0.16
0.18
0.2
0.28

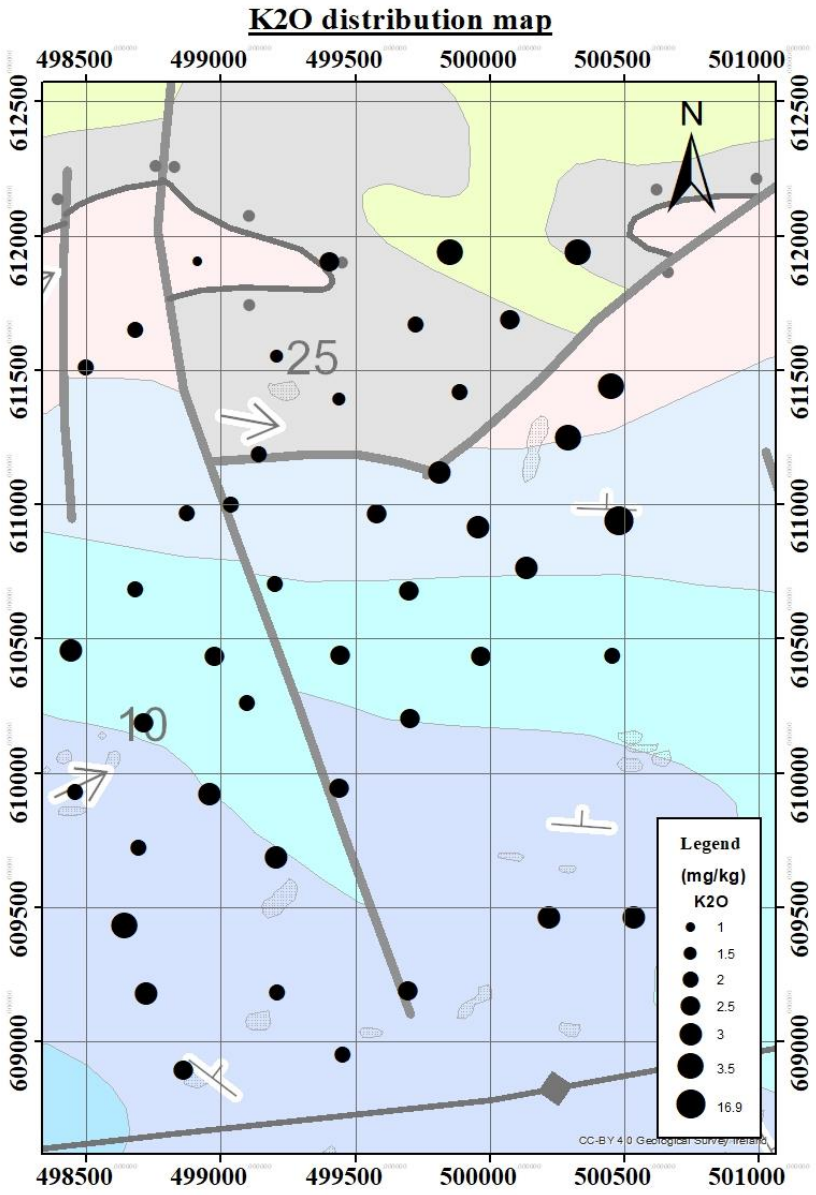
K2O distribution map
498500
499000
499500
500000
500500
501000
612500
612000
611500
611000
610500
610000
609500
609000
N
25
10
Legend
(mg/kg)
K2O
1
1.5
2
2.5
3
3.5
16.9
CC-BY 4.0 Geological Survey Ireland

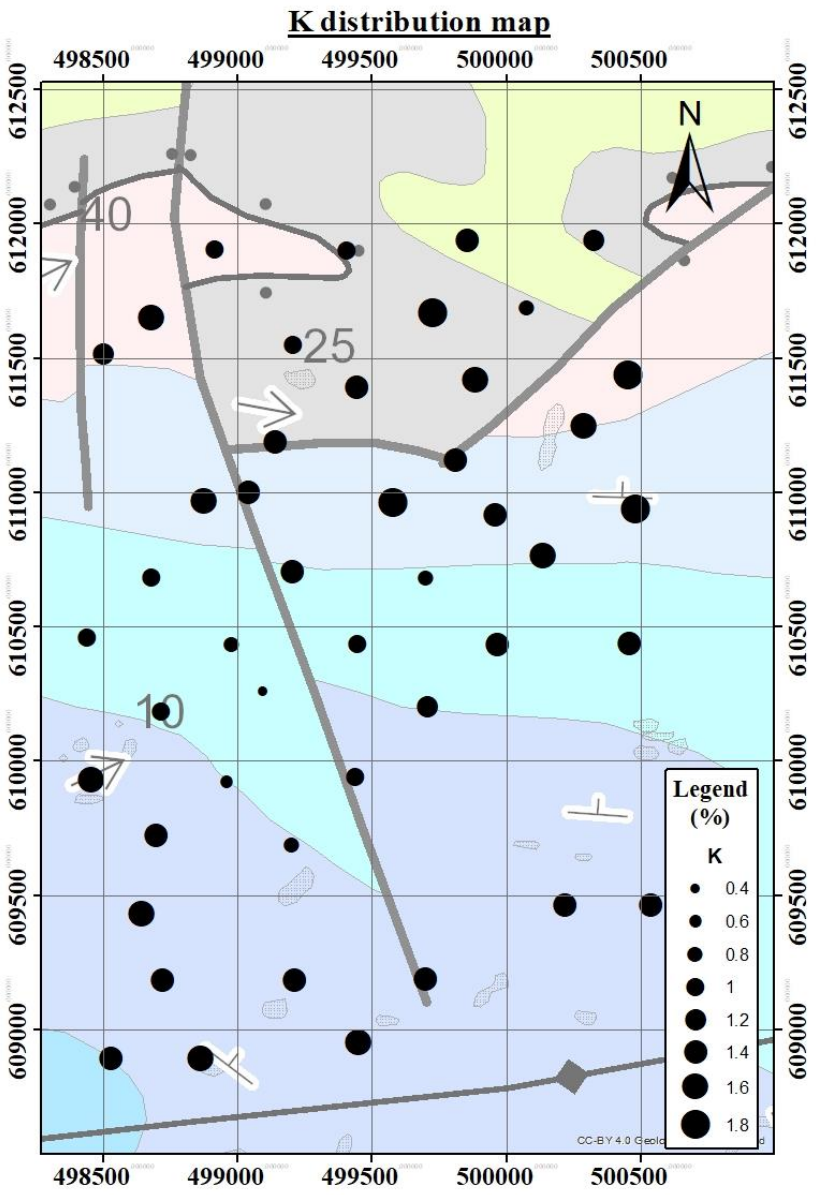
K distribution map
498500
499000
499500
500000
500500
612500
612000
611500
611000
610500
610000
609500
609000
N
40
25
10
Legend
(%)
K
0.4
0.6
0.8
1
1.2
1.4
1.6
1.8

Appendix D

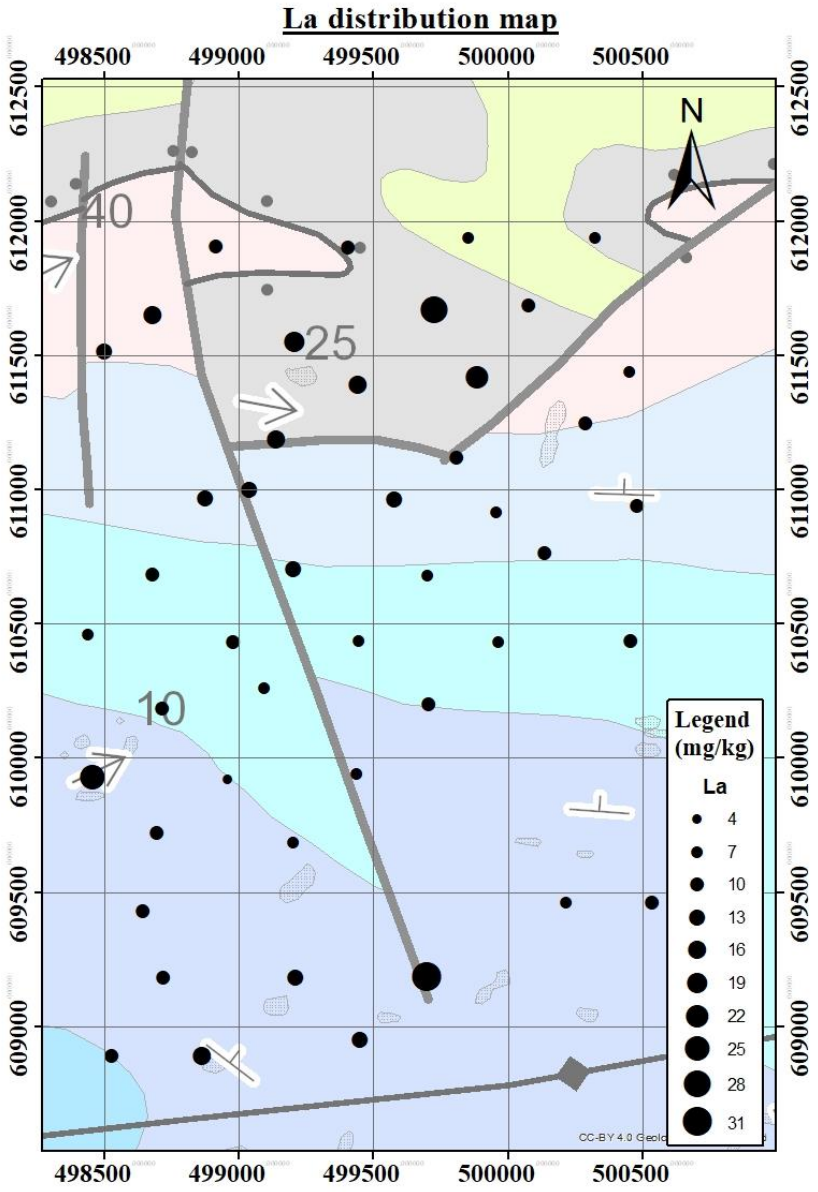
La distribution map
498500
499000
499500
500000
500500
612500
612000
611500
611000
610500
610000
609500
609000
N
40
25
10
Legend
(mg/kg)
La
4
7
10
13
16
19
22
25
28
31
CC-BY 4.0 Geolo

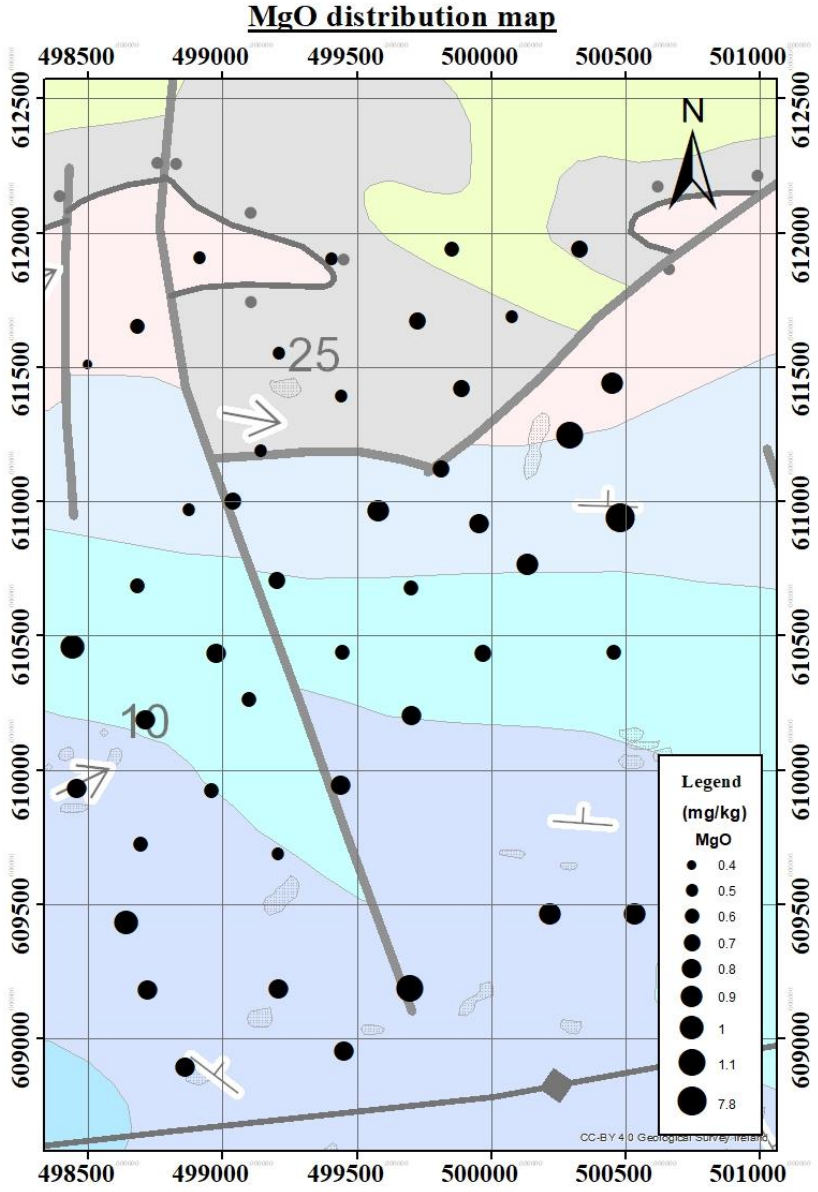
MgO distribution map
498500
499000
499500
500000
500500
501000
612500
612000
611500
611000
610500
610000
609500
609000
N
25
10
Legend
(mg/kg)
MgO
0.4
0.5
0.6
0.7
0.8
0.9
1
1.1
7.8
CC-BY 4.0 Geological Survey Ireland

Appendix D

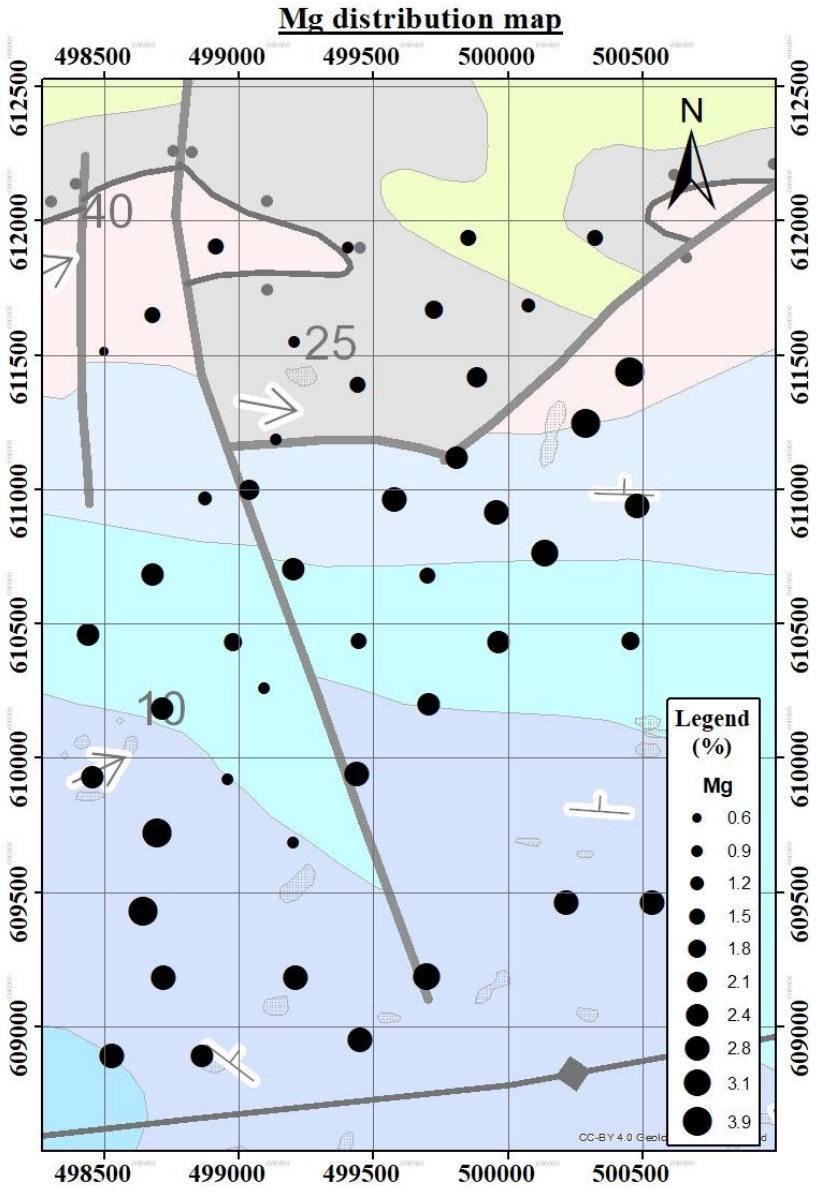
Mg distribution map
498500
499000
499500
500000
500500
612500
612000
611500
611000
610500
610000
609500
609000
N
40
25
10
Legend
(%)
Mg
0.6
0.9
1.2
1.5
1.8
2.1
2.4
2.8
3.1
3.9

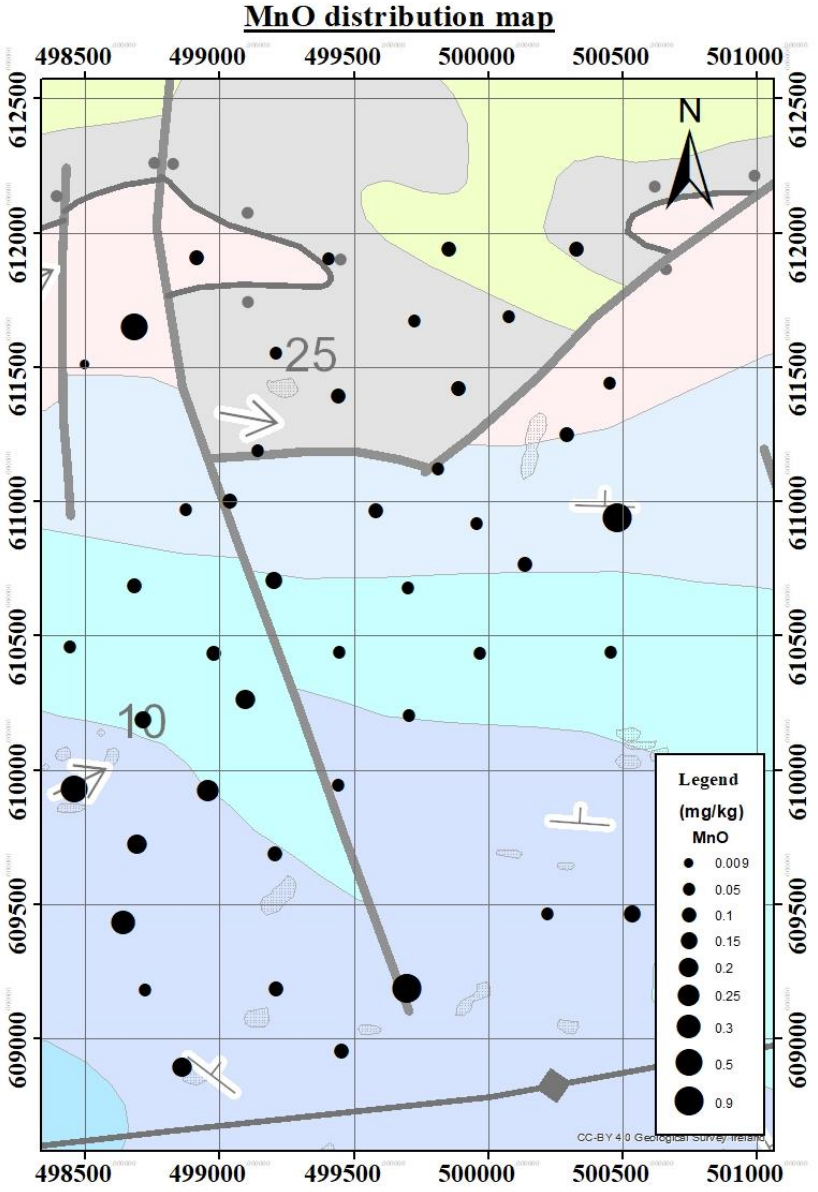
MnO distribution map
498500
499000
499500
500000
500500
501000
612500
612000
611500
611000
610500
610000
609500
609000
N
25
10
Legend
(mg/kg)
MnO
0.009
0.05
0.1
0.15
0.2
0.25
0.3
0.5
0.9

Appendix D

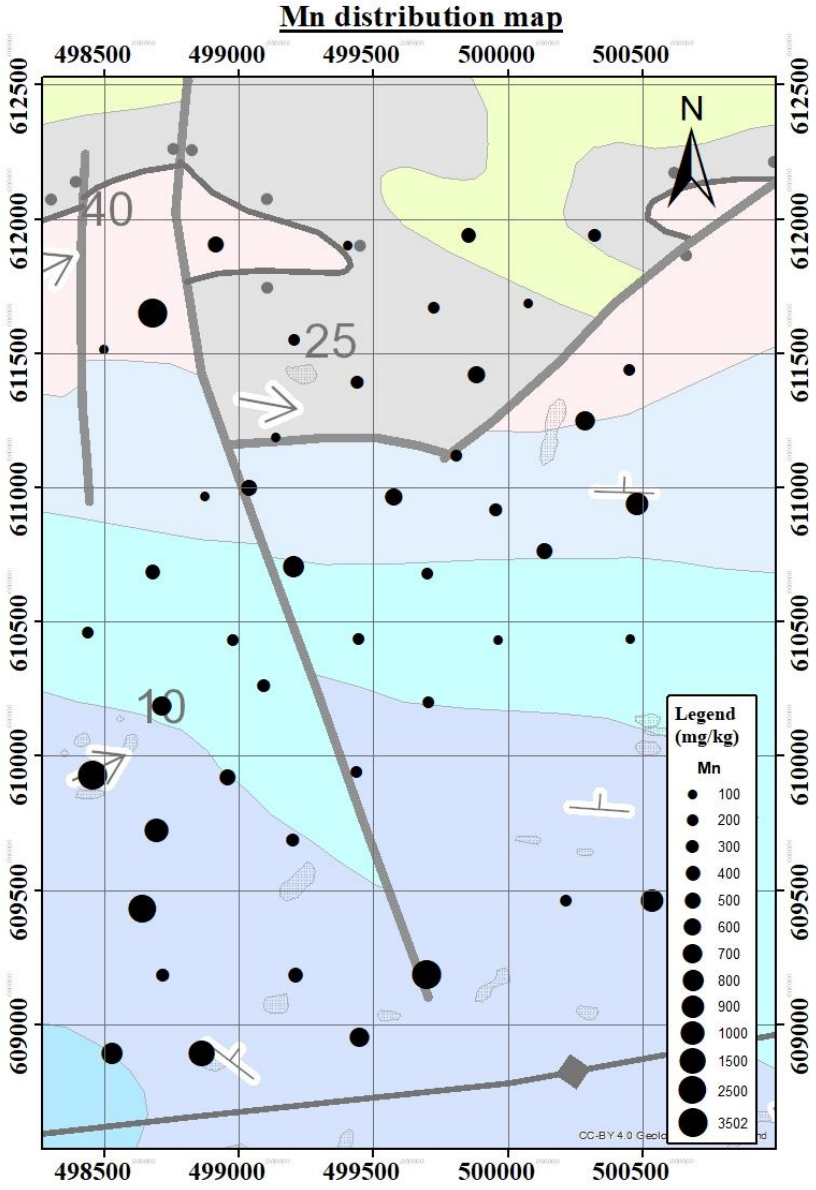
Mn distribution map
498500
499000
499500
500000
500500
612500
612000
611500
611000
610500
610000
609500
609000
N
40
25
10
Legend
(mg/kg)
Mn
100
200
300
400
500
600
700
800
900
1000
1500
2500
3502
CC-BY 4.0 Geolo

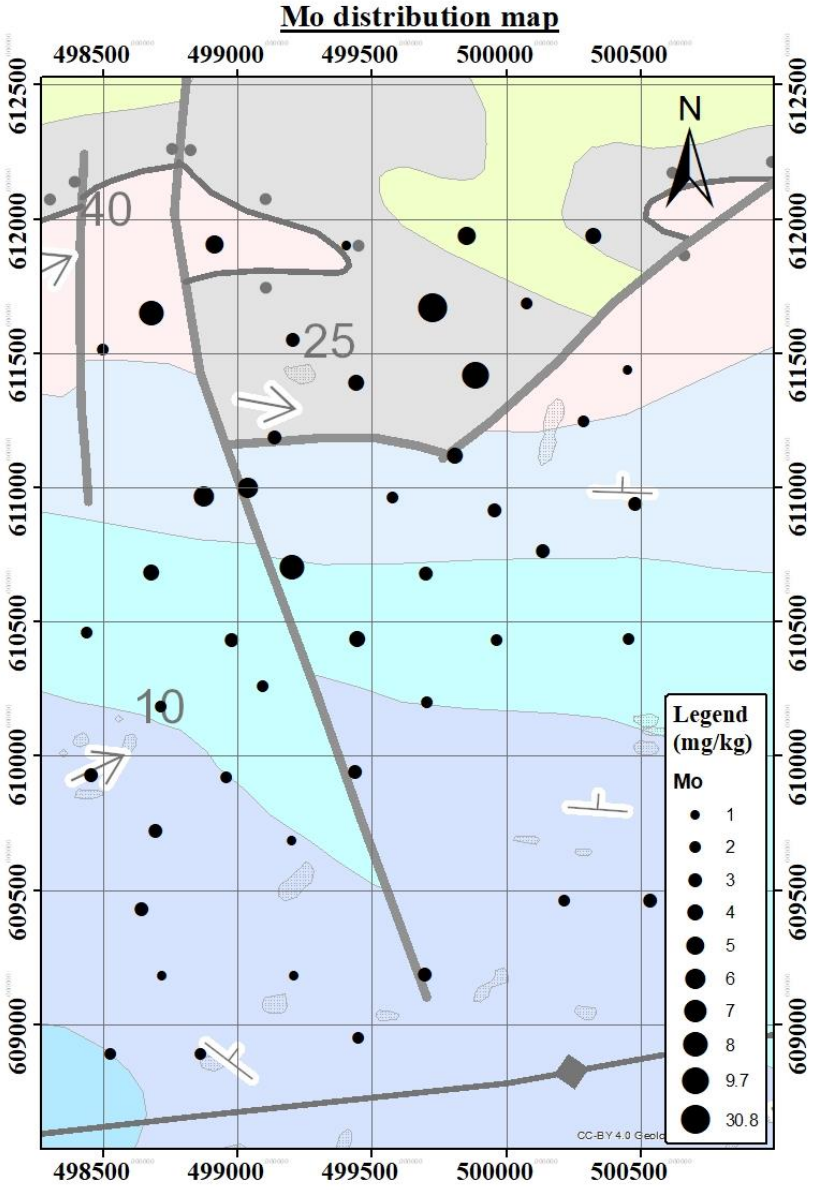
Mo distribution map
498500
499000
499500
500000
500500
612500
612000
611500
611000
610500
610000
609500
609000
N
40
25
10
Legend
(mg/kg)
Mo
1
2
3
4
5
6
7
8
9.7
30.8
CC-BY 4.0 Geolo

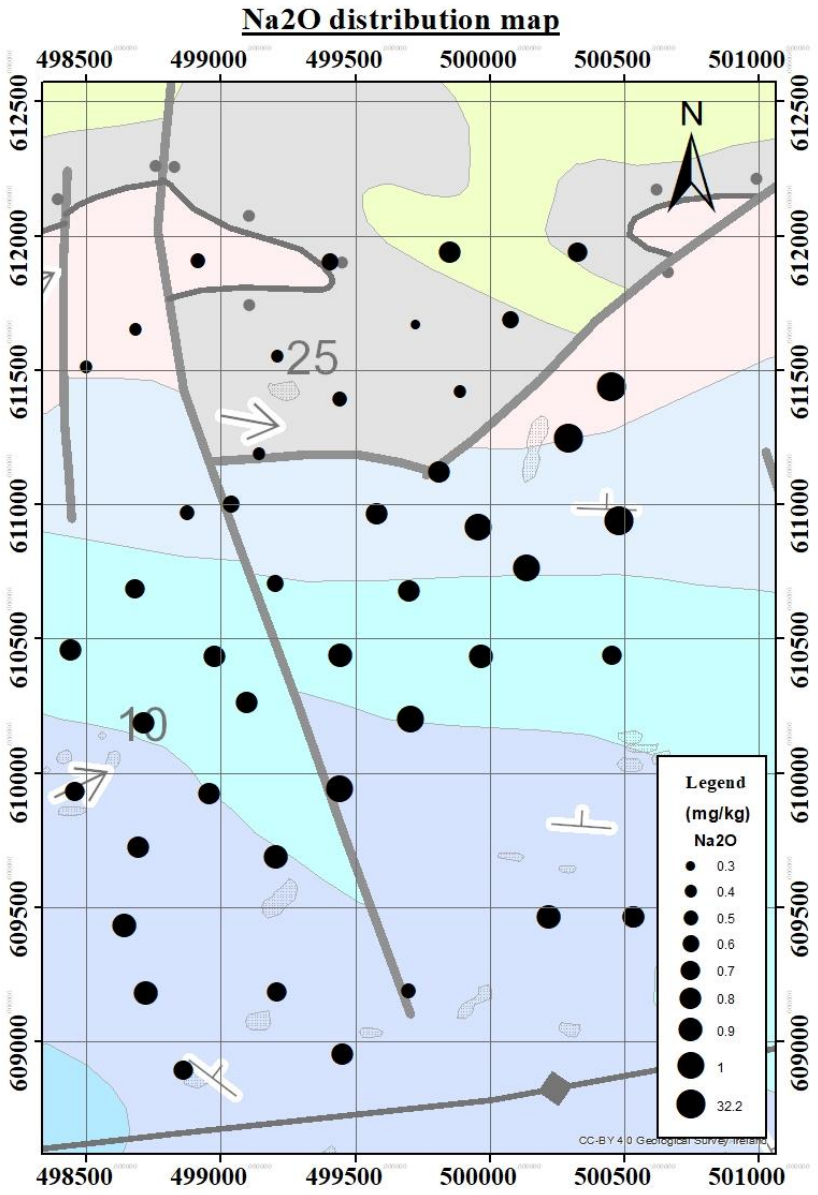
Na2O distribution map
498500
499000
499500
500000
500500
501000
612500
612000
611500
611000
610500
610000
609500
609000
N
25
10
Legend
(mg/kg)
Na2O
0.3
0.4
0.5
0.6
0.7
0.8
0.9
1
32.2
CC-BY 4.0 Geological Survey Ireland

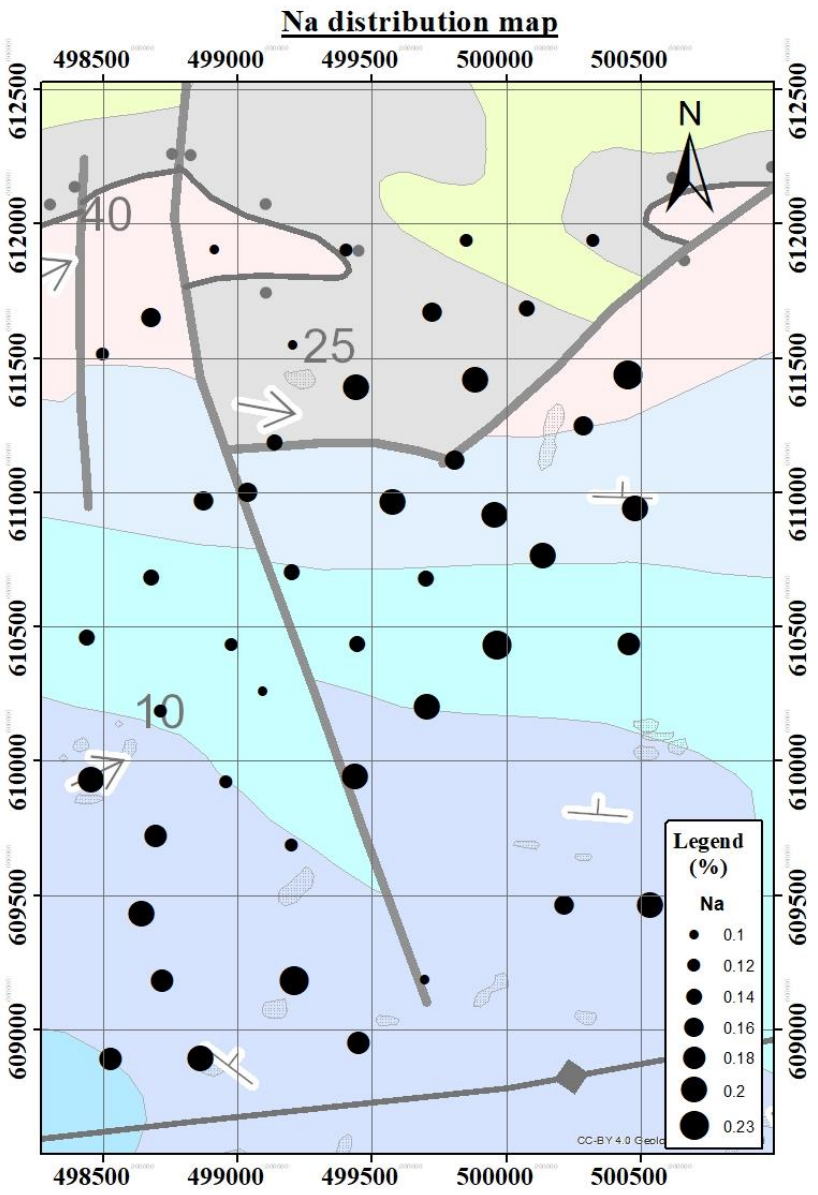
Na distribution map
498500
499000
499500
500000
500500
612500
612000
611500
611000
610500
610000
609500
609000
N
40
25
10
Legend
(%)
Na
0.1
0.12
0.14
0.16
0.18
0.2
0.23
CC-BY 4.0 Geolo

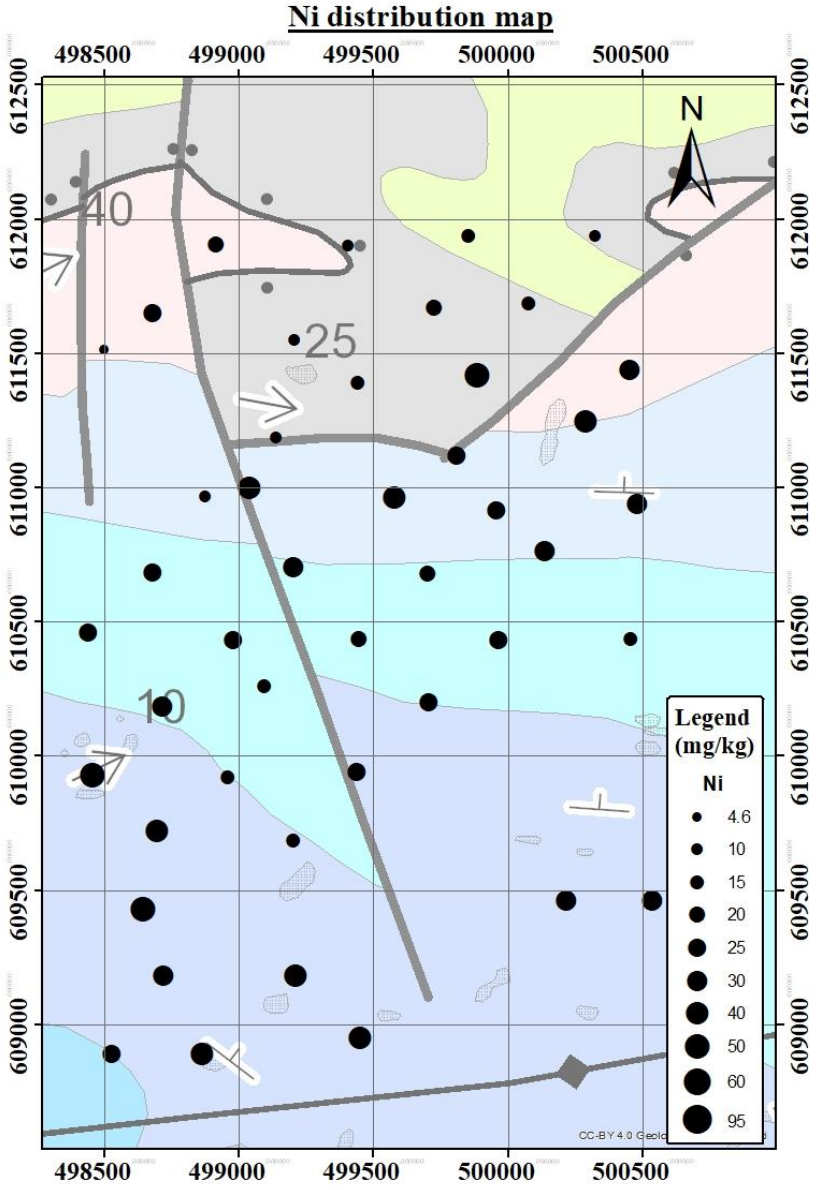
Ni distribution map
498500
499000
499500
500000
500500
612500
612000
611500
611000
610500
610000
609500
609000
N
40
25
10
Legend
(mg/kg)
Ni
4.6
10
15
20
25
30
40
50
60
95

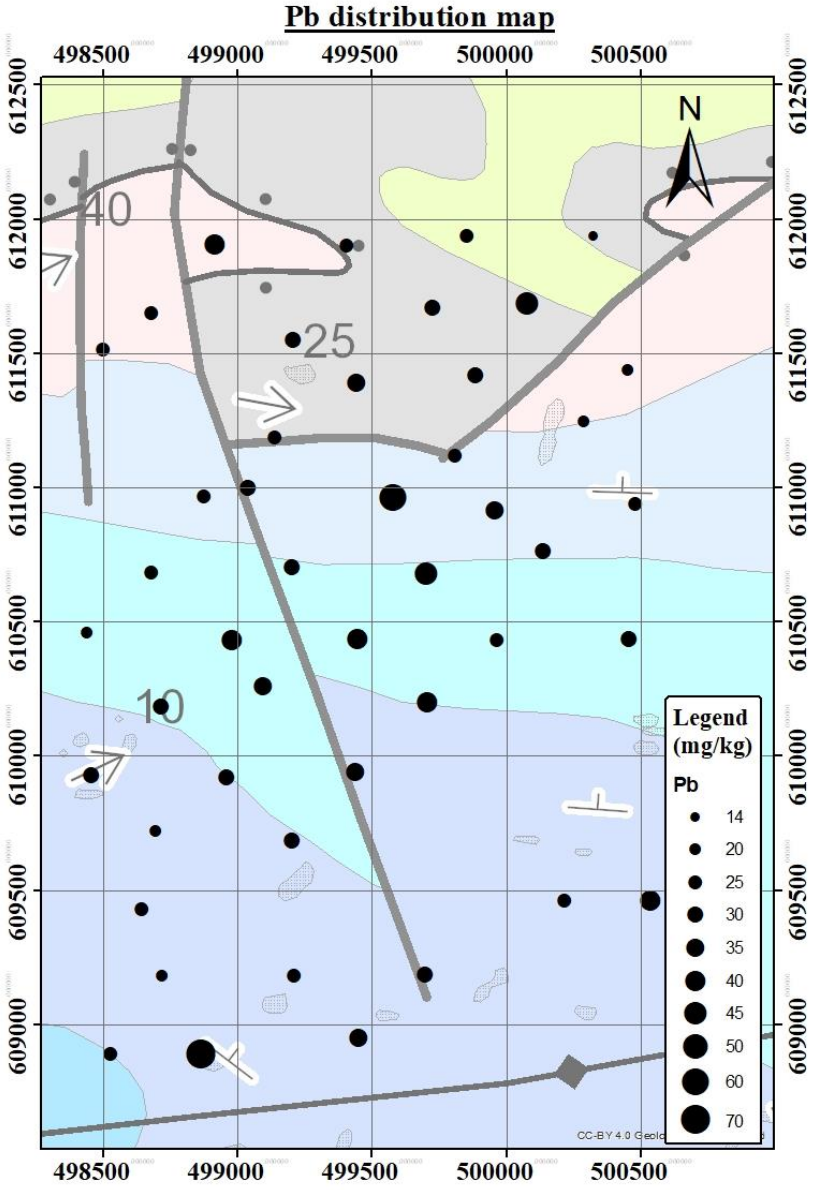
Pb distribution map
498500
499000
499500
500000
500500
612500
612000
611500
611000
610500
610000
609500
609000
N
40
25
10
Legend
(mg/kg)
Pb
14
20
25
30
35
40
45
50
60
70

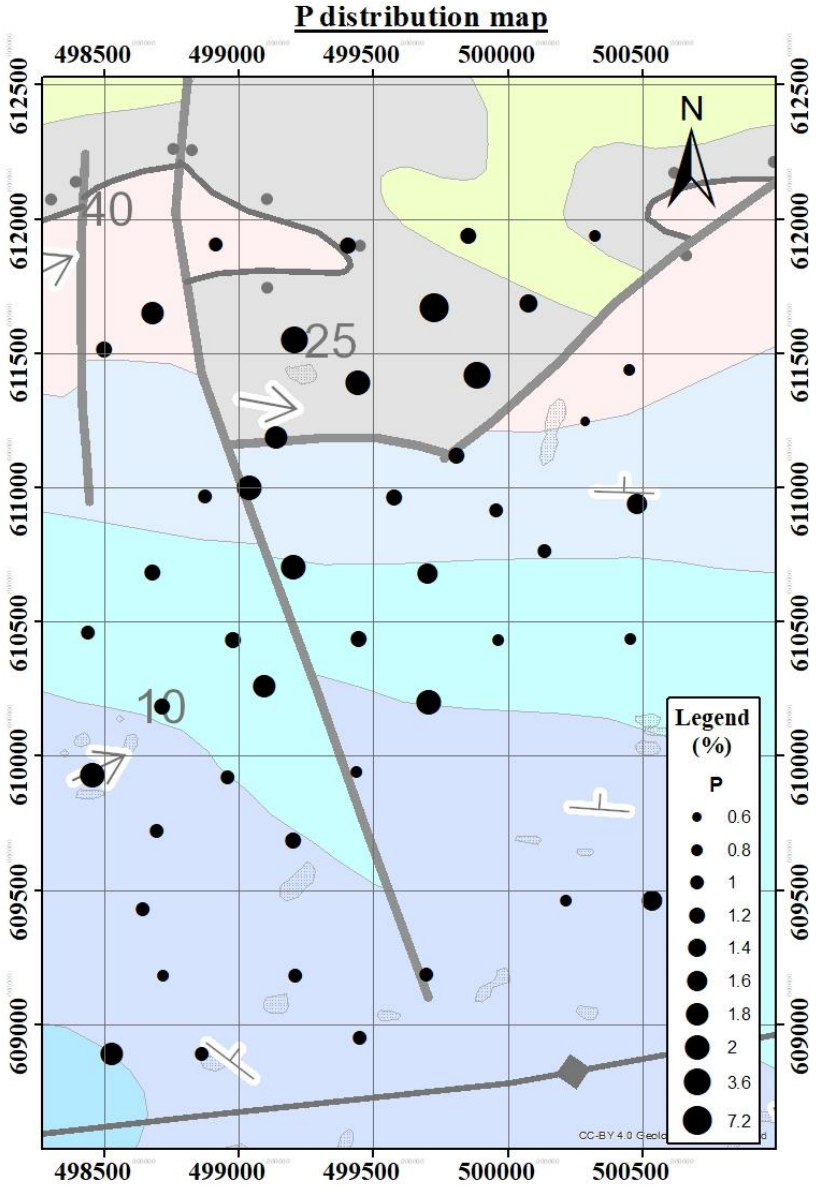
P distribution map
498500
499000
499500
500000
500500
612500
612000
611500
611000
610500
610000
609500
609000
N
40
25
10
Legend
(%)
P
0.6
0.8
1
1.2
1.4
1.6
1.8
2
3.6
7.2
CC-BY 4.0 Geolo

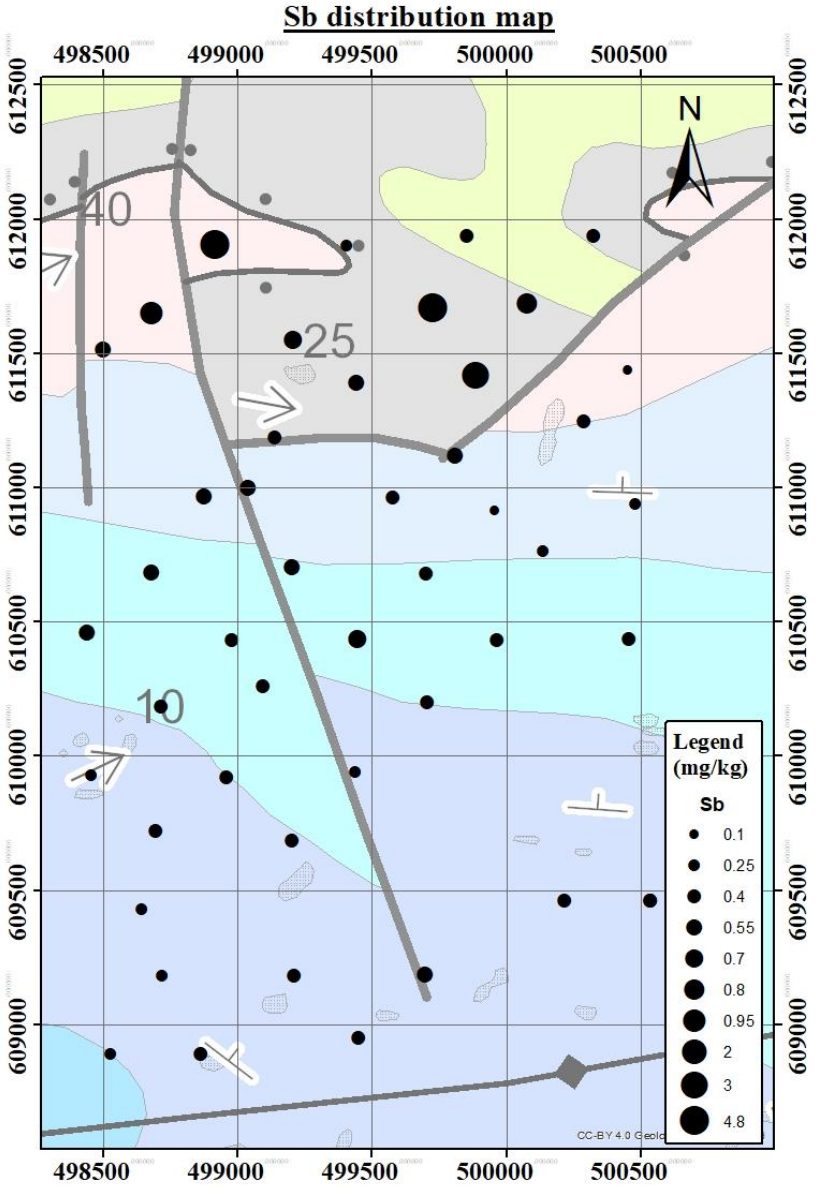
Sb distribution map
498500
499000
499500
500000
500500
612500
612000
611500
611000
610500
610000
609500
609000
N
40
25
10
Legend
(mg/kg)
Sb
0.1
0.25
0.4
0.55
0.7
0.8
0.95
2
3
4.8
CC-BY 4.0 Geolo

Appendix D

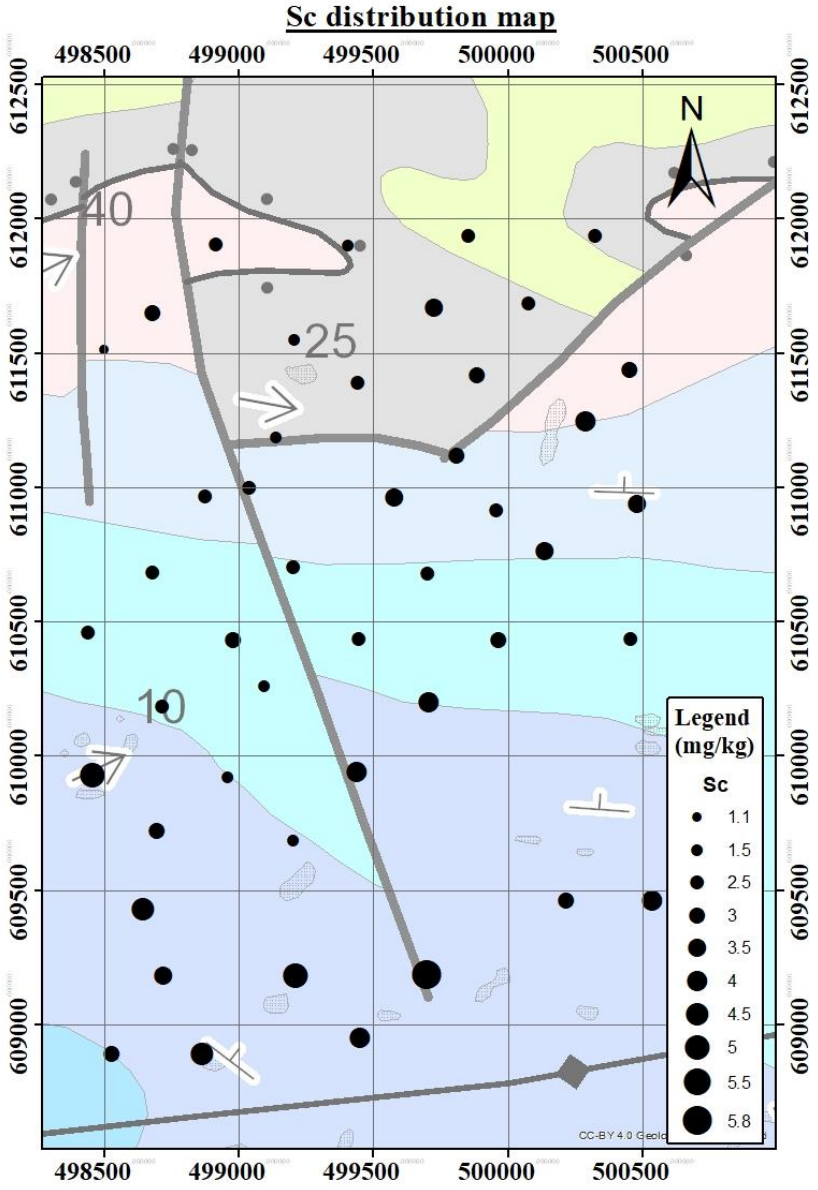
Sc distribution map
498500
499000
499500
500000
500500
612500
612000
611500
611000
610500
610000
609500
609000
N
40
25
10
Legend
(mg/kg)
Sc
1.1
1.5
2.5
3
3.5
4
4.5
5
5.5
5.8

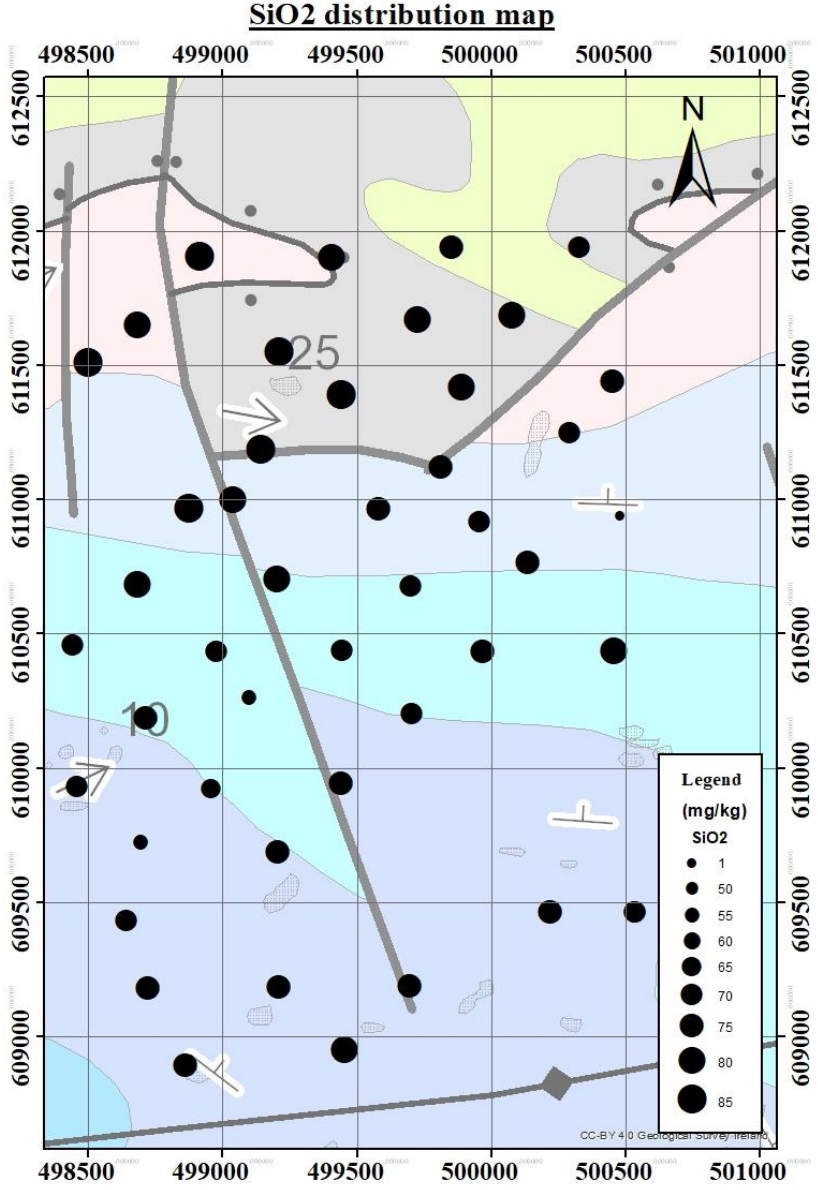
SiO2 distribution map
498500
499000
499500
500000
500500
501000
612500
612000
611500
611000
610500
610000
609500
609000
N
25
10
Legend
(mg/kg)
SiO2
1
50
55
60
65
70
75
80
85

Appendix D

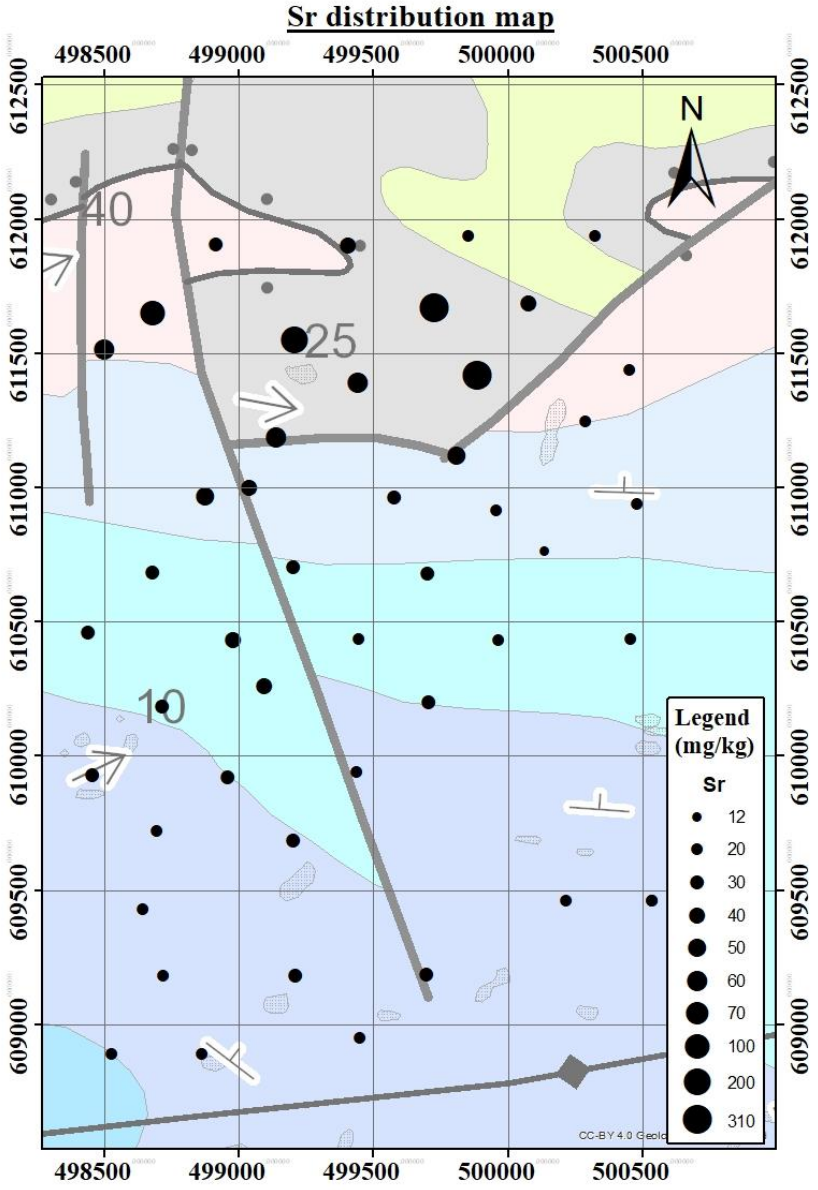
Sr distribution map
498500
499000
499500
500000
500500
612500
612000
611500
611000
610500
610000
609500
609000
N
40
25
10
Legend
(mg/kg)
Sr
12
20
30
40
50
60
70
100
200
310

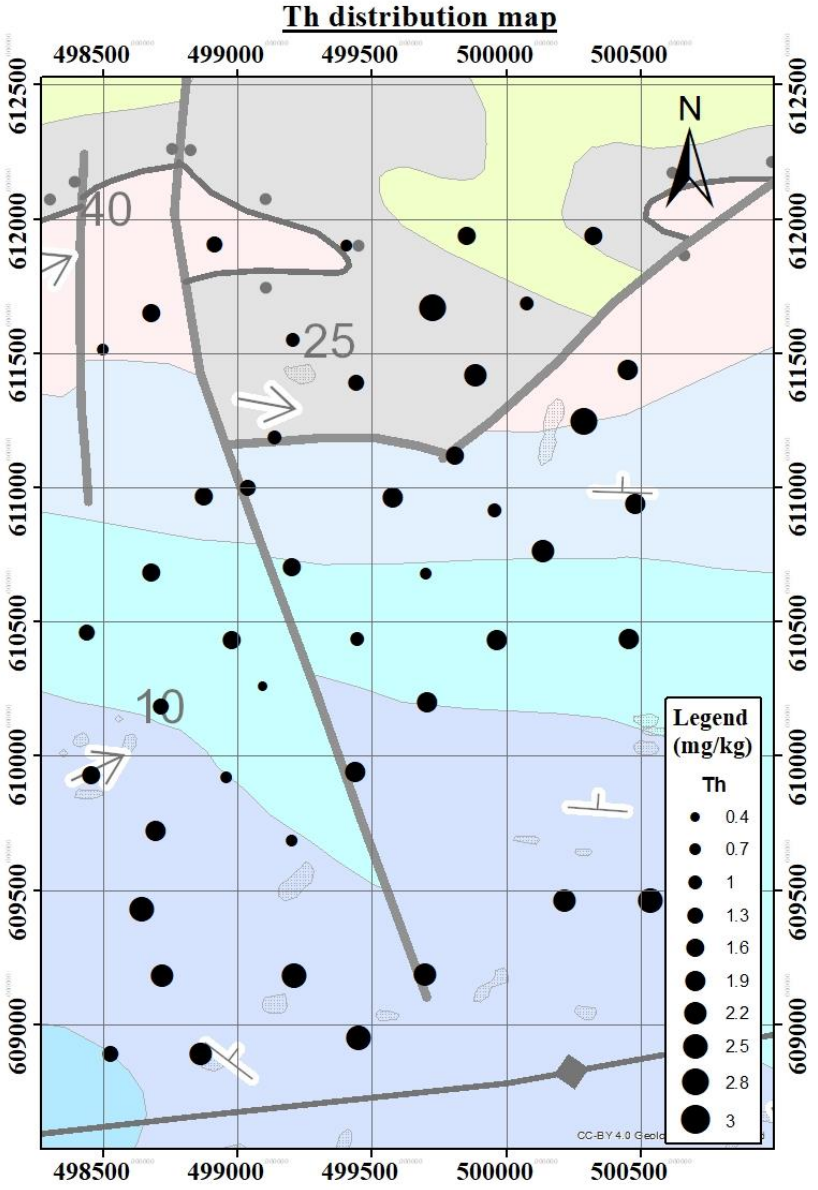
Th distribution map
498500
499000
499500
500000
500500
612500
612000
611500
611000
610500
610000
609500
609000
N
40
25
10
Legend
(mg/kg)
Th
0.4
0.7
1
1.3
1.6
1.9
2.2
2.5
2.8
3

Appendix D

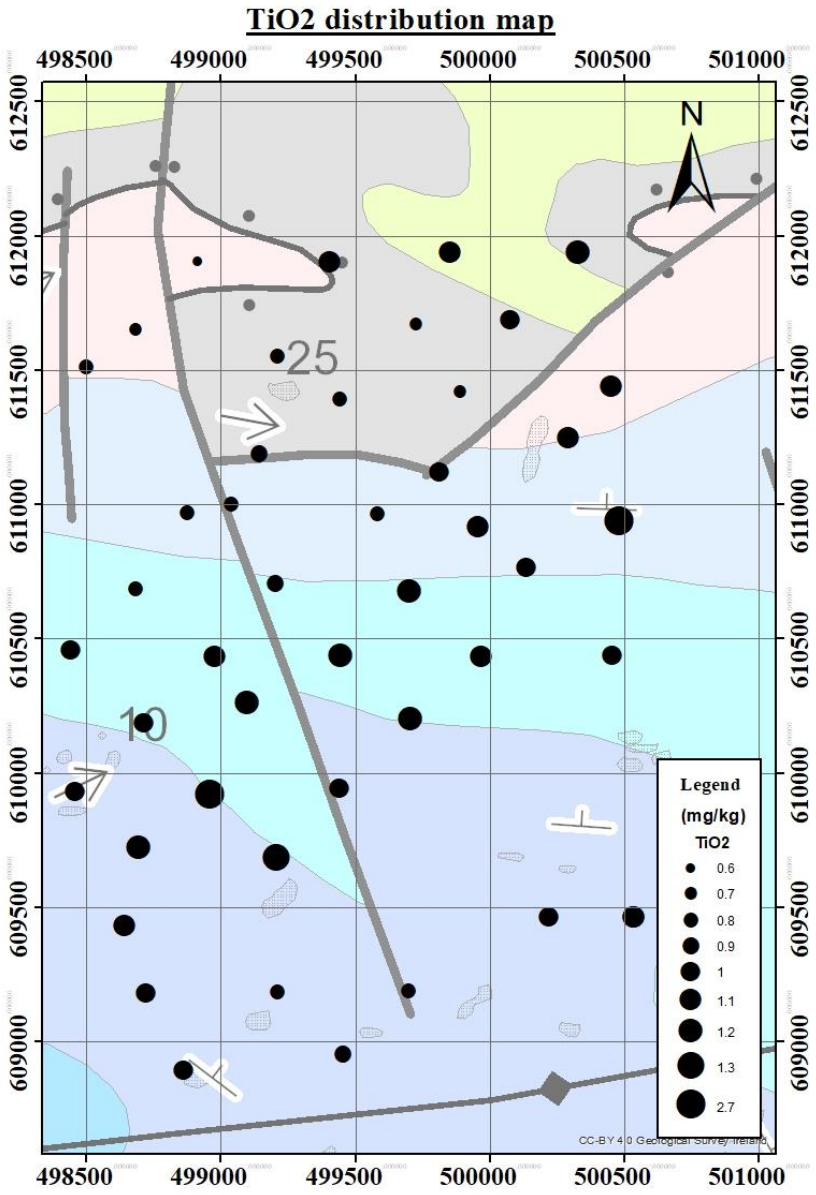
TiO2 distribution map
498500
499000
499500
500000
500500
501000
612500
612000
611500
611000
610500
610000
609500
609000
N
25
10
Legend
(mg/kg)
TiO2
0.6
0.7
0.8
0.9
1
1.1
1.2
1.3
2.7

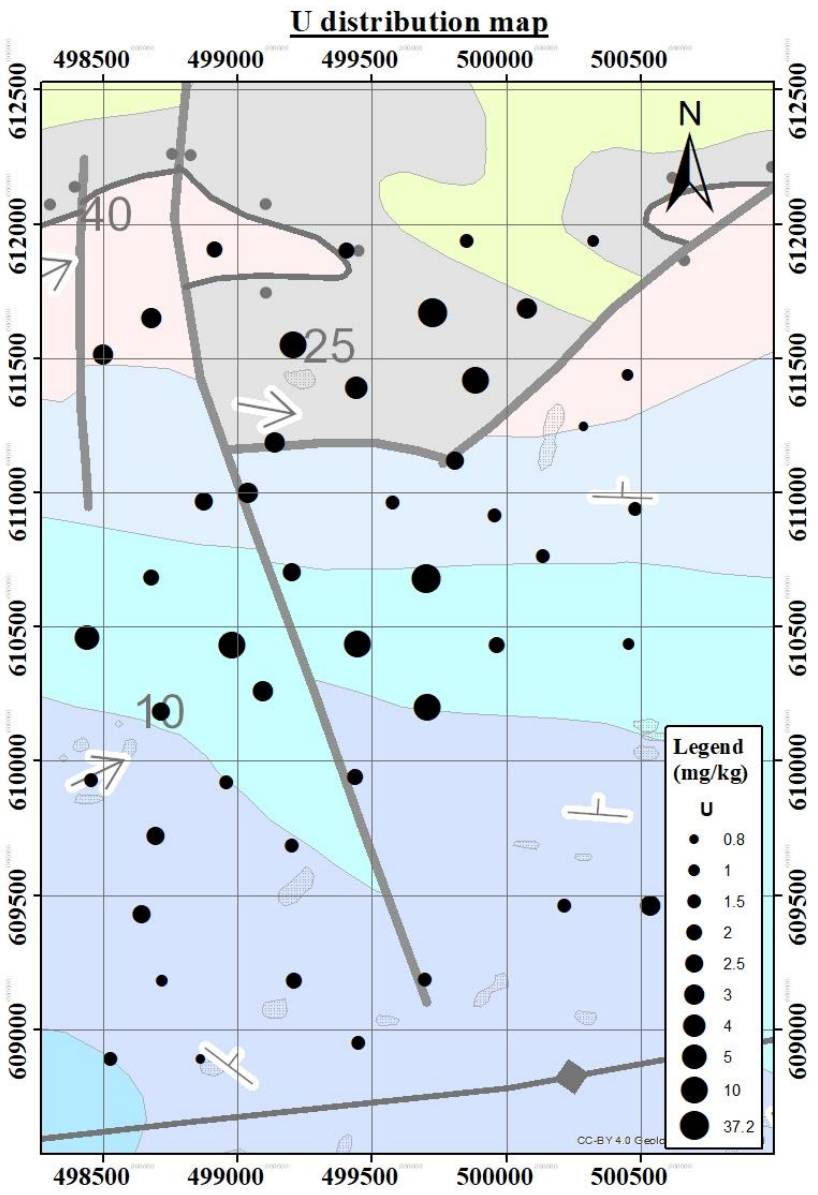
U distribution map
498500
499000
499500
500000
500500
612500
612000
611500
611000
610500
610000
609500
609000
N
40
25
10
Legend
(mg/kg)
U
0.8
1
1.5
2
2.5
3
4
5
10
37.2

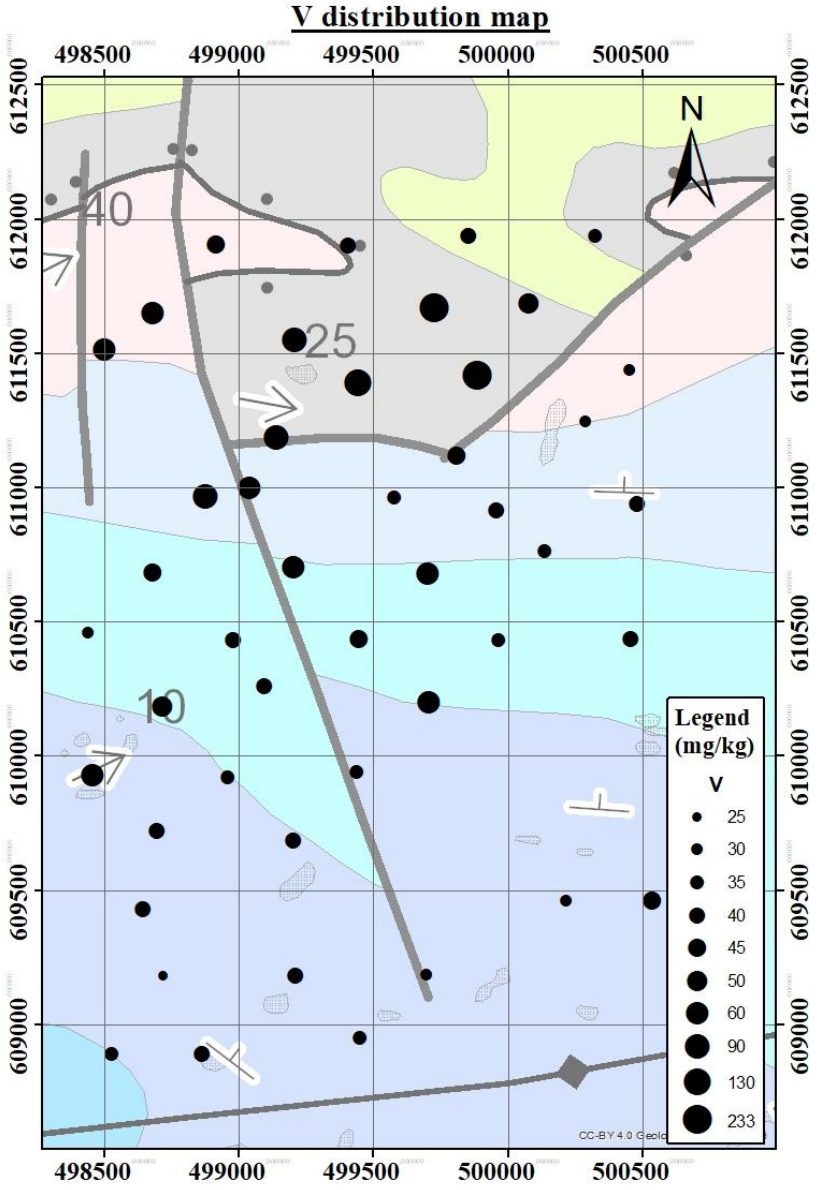
V distribution map
498500
499000
499500
500000
500500
612500
612000
611500
611000
610500
610000
609500
609000
N
40
25
10
Legend
(mg/kg)
V
25
30
35
40
45
50
60
90
130
233
CC-BY 4.0 Geolo

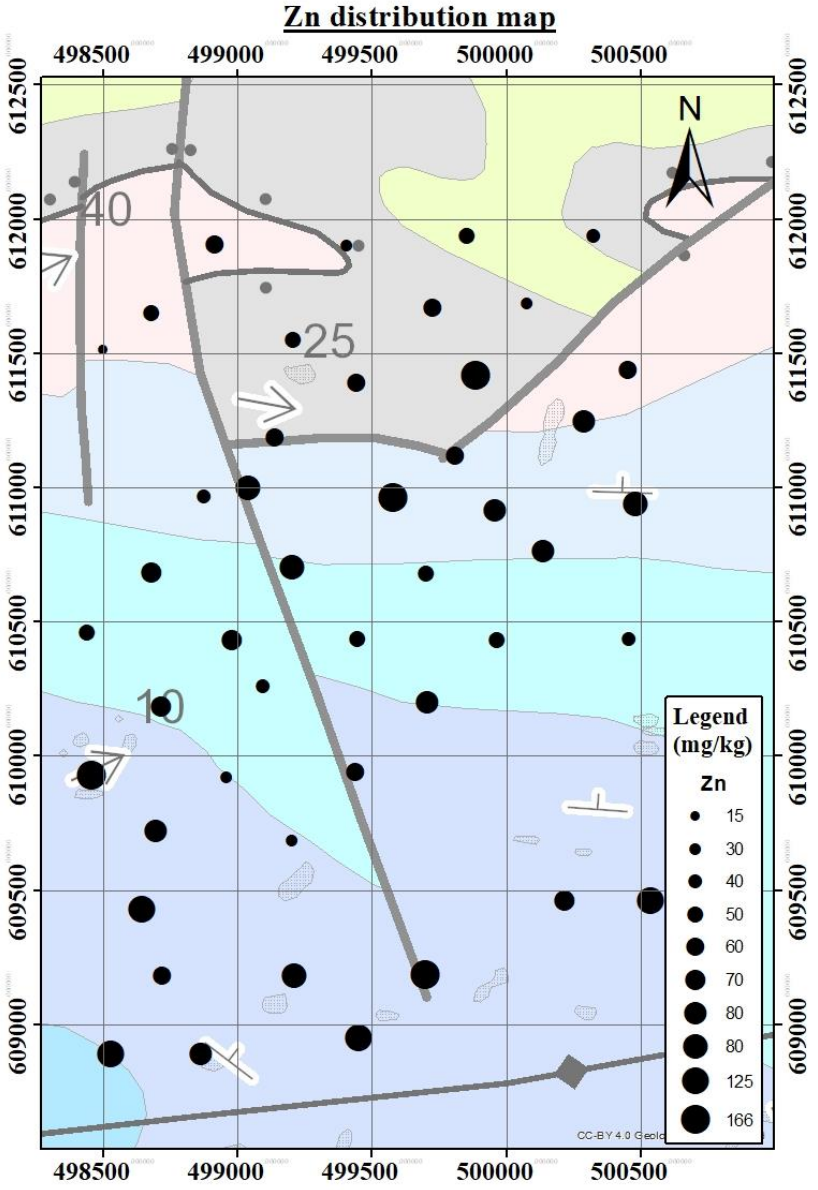
Zn distribution map
498500
499000
499500
500000
500500
612500
612000
611500
611000
610500
610000
609500
609000
N
40
25
10
Legend
(mg/kg)
Zn
15
30
40
50
60
70
80
80
125
166
CC-BY 4.0 Geolo

Appendix D